



Radiolytic Degradation of Organic Pesticides: A Pulse Radiolysis and Steady State Study.



The University of Adelaide
Department of Chemistry
July 1998

A research report submitted by
Karl Cornelius
in partial fulfilment of the requirements for the
Degree of Doctor of Philosophy

ABSTRACT

Developing an understanding of the degradation of organic pesticides, herbicides and fungicides in natural systems is an essential component in the environmental management of our agricultural activities. Free radicals are being increasingly recognised as having importance in environmental chemistry, particularly of aqueous systems. For example the hydroxyl radical and the superoxide radical anion are believed to be relevant to the degradation of organic molecules in the environment. This thesis reports the results of a comprehensive study into the reactions of radicals commonly formed in aqueous systems with a variety of commercially available pesticides.

Gamma and pulse radiolysis techniques have been used to initiate reactions and determine relevant kinetic data such as rate constants. Products generated have been characterised by HPLC and mass spectrometric techniques. *Ab initio* calculations have been employed to gain insight into the transient species formed.

Nine pesticides currently in use in Australia were studied and include Acifluofen, Chlorsulfuron, Cyromazine, Dichlorophen, Dimethrimol, Hexazinone, Ioxynil, MCPA and Napropamide.

ACKNOWLEDGEMENTS

This thesis would not have been possible without the help and support of the following people:

The guidance of my supervisor, A/Prof. Gerald Laurence, throughout this project has been never-failing. Without Gerald's suggestions and help this thesis would never have come to fruition. Gerald's enthusiastic input continued following his retirement from the university. I would also like to thank my "on paper only supervisor", Dr Mark Buntine, who looked after my welfare upon Gerald's retirement.

I also wish to express my deep gratification to all the past and present members of the Department of Chemistry who helped with the project or made life interesting. Special thanks go to Paul Wabnitz (LC-MS), Bruce May (HPLC), Mark Tattersall (Cobalt-60), Ella Robinson (thesis editing) and the past and present members of the MAB and GSL research groups.

The pulse radiolysis work would not have been possible without the help and guidance of the following people: Dr Wayne Garrett, A/Prof. Ron Cooper, Dr Bob Anderson and Dr David Webb. Particular thanks go to Gerald Laurence and Ron Cooper who were instrumental in establishing the pulse radiolysis facility at Australian Radiation Laboratories. Special thanks also go to all the friends who made my stays at the Australian Radiation Laboratories, the Australian Nuclear Science and Technology Organisation, and the University of Auckland, fun and productive.

Thanks must also go to my past and present flatmates who have endured me for the duration of my Ph.D., along with all my "non-chemistry" friends. Mum and Dad also deserve particular thanks for the encouragement that they have always shown me throughout every aspect of my life.

Finally I cannot express enough appreciation to my girlfriend Christine Daly who has been a pillar of support and love for the entire duration of my Ph.D. Thank you!

Financial support in the form of an Australian Postgraduate Award and an Australian Institute of Nuclear Science and Engineering supplemental scholarship are gratefully acknowledged.

This thesis is dedicated to my memories of Granddad Cornelius and Grandpa Heaven, both who past away during my time as a Ph.D. student. R.I.P.

This work contains no material which has been accepted for the award of any other degree or diploma in any university or other tertiary institution and, to the best of my knowledge and belief, contains no material previously published or written by another person, except where due reference has been made in the text.

I give consent to copy my thesis, when deposited in the University Library, being available for loan and photocopying.

Karl Cornelius

10/7/1998

ABBREVIATIONS

BFA	Heptafluoro butyric acid
CB	Conduction Band
DTA	Delta Transient Absorbance
esr	electron spin resonance
H-adduct	Hydrogen atom adduct
HPLC	High Performance Liquid Chromatography
HOMO	Highest Occupied Molecular Orbital
IR	Infra Red
LC-MS	Liquid Chromatography-Mass Spectrometry
LUMO	Lowest Unoccupied Molecular Orbital
NMR	Nuclear Magnetic Resonance
NPA	Natural Population Analysis
OH-adduct	hydroxyl radical adduct
TFA	Trifluoro Acetic Acid
TLC	Thin Layer Chromatography
VB	Valance Band
U.V.	Ultra-Violet

Addendum

In the abbreviations, DTA should be replaced with TDA.

Page 5, line 3, should have the word powerful omitted.

Page 11, Section 2.1.5, should read, Hydrated electrons are generated by irradiation of water, t-butyl alcohol is used to scavenge the hydroxyl radicals generated by the irradiation.

Page 15, Section 2.2.2, line 4, should read, This is because superoxide is not scavenged by other molecules other than the target molecule, while the hydroxyl radical is scavenged.

Page 24, Section 3.3.2, line 2 should contain Sangster and O'Donnell, not Sangster and O'Donnell.

Page 25, Section 3.3.2, paragraph 2, last line should read value not valve.

Page 26, Section 3.3.5, paragraph 2, line 6, should read Tripropylamine not Tripropylamine.

Page 30, Section 3.5.1, line 3, should read Beer's Law, not Bragg's Law.

Page 31, last line, factor should read $[S_2]/[S_1]$, not $k_2[S_2]/k_1[S_1]$.

Page 38, Paragraph 2, line 5, should read HCCH_3 not HCH_3 .

Page 39, Figure 4.08, Caption, Symbol for product F should be \blacksquare not \square .

Page 48, Table 7.01 should read Table 4.01.

Page 54, Line 7, should read $e^-_{(aq)}$ may add to carbonyl, not carboxyl.

Page 57, Line 3 should read slightly, not slightLY.

Page 63, Paragraph 1, should read bromine atom not bromide atom.

Page 82, Section 5.6, line 1, should read, Absorbance of the hydrated electron at 640 nm was observed to decrease in the presence of small amounts of Ioxynil ($1 \times 10^{-4} \text{M}$) at pH 7.0 (phosphate buffer).

Page 83, Section 5.6, Paragraph 2, line 2, should read, Time resolved studies out to 1000 μs produced only a minimal decrease in the absorbance at 290 nm, suggesting the transient does not react or reacts to products within the irradiation pulse.

Page 96, Section 6.2, Paragraph 2, line 2, should read, This suggests that the transient formed by reaction of the hydroxyl radical with Chlorsulfuron possesses a charge since it has been previously been shown since the transient reacts with itself (through second order kinetics).

Page 102, Paragraph 1, line 6-8, Should read there is no detectable reaction between oxygen and the transient. The back reaction can not be commented on.

Page 111, Paragraph 1, line 4, should read OH-adduct, not H-adduct.

Page 126, Section 7.4, line 6, should read, A deviation from second order kinetics indicates that transients produced by the reaction of Dichlorophen with the hydroxyl radicals reacts with oxygen.

Page 137, Figure 137, the left structure in the third row needs a radical dot on the “phenoxy” oxygen, while the neighbouring carbonylic oxygen carries a superfluous radical dot.

Page 149, Paragraph 1, the abstraction from the weaker N-H bond is not considered because the mass spectral data indicates that the product has not increased in bond saturation. Abstraction from the N-H bond would increase the saturation of the molecule.

Page 180, Section 9.4, line 3, should read, The TDA spectrum is different from that observed in Figure 9.02; the absorbance bands at 330 nm and the maximum at 490 nm are significantly reduced.

Page 181, Paragraph 1, Figure 9.15 should be Figure 9.14.

Page 186, Table 9.02, footnote in table should read Dimethrimiol, not Ioxynil.

Page 189, Section 9.6, line 1, should read, Absorbance of the hydrated electron at 640 nm was observed to decrease in the presence of small amounts of Dimethrimiol ($1 \times 10^{-4} \text{M}$) at pH 7.0 (phosphate buffer).

Page 203, Last line, should read, because of the substituents, not because of the rest of the molecule.

Page 204, Section 10.2, lines 7-9, should read, Experiments performed by Mabury and Crosby to compare their reported value with pulse radiolysis indicated that the steady state method produced results that are up to five time slower.

Page 223 Radical dot on the H-abstraction production radical (from the hydroxyl radical reaction) is missing.

Page 230, Figure 11.05, Product A should have the symbol ■ not ▲.

Page 232/3, should have figure 11.17(a) present. See below.

Common errors through-out the thesis

The double isotope pattern of chlorine should be 9.8:6.3:1, not 4:3:1.

∴ Frickie should be replaced with Fricke.

∴ Through out the thesis a conclusion is reached to the charge of the transient by use of the addition of 1 M NaClO_4 . In all cases, the charge of the transient was concluded not only from the effect of the salt on the decay rate, but the fact that the decay had previously been shown to be second order by the decreased pulse method.

1.0 INTRODUCTION.....	1
1.1 BACKGROUND.....	1
1.2 PHOTOCHEMISTRY AND PHOTOCHEMICAL DEGRADATION.....	1
1.2.1 Natural system photochemistry	1
1.2.2 Photochemical treatment for industrial discharge water.....	2
1.3 PRODUCTION OF FREE RADICALS IN AQUEOUS SOLUTION.....	3
1.3.1 Production of radicals in natural water	3
1.3.2 Production of radicals for industrial discharge water treatment	5
1.3.3 Radiolytic soil decontamination	6
1.3.4 Radiolytic aqueous degradation	6
1.4 OUTLINE AND SCOPE OF THESIS	7
2.0 RADIATION CHEMISTRY.....	9
2.1 RADIOLYTIC RADICAL PRODUCTION.....	9
2.1.1 Hydroxyl radicals	9
2.1.2 Perhydroxyl and superoxide radical anions	9
2.1.3 Hydrogen atoms	10
2.1.4 Dihalogen radical anions	11
2.1.5 Hydrated electrons.....	11
2.1.6 Oxide radicals.....	11
2.1.7 Azide radicals	12
2.1.8 Sulfate radical anions	12
2.1.9 Carbon dioxide radical anions	12
2.2 PROPERTIES OF RADICALS.....	12
2.2.1 Hydroxyl radicals (OH [•]).....	13
2.2.2 Superoxide radical anions (O ₂ ^{•-}).....	13
2.2.3 Perhydroxyl radicals (HO ₂ [•])	15
2.2.4 Hydrated electrons (e _(aq) ⁻).....	16
2.2.5 Hydrogen atoms (H [•]).....	16
2.2.6 Oxide anions (O ⁻)	17
2.2.7 Dihalogen radical anions (X ₂ ^{•-}).....	18
2.2.8 Azide radicals (N ₃ [•])	18
2.2.9 Sulfate radical anion (SO ₄ ^{•-})	18
2.2.10 Carbon dioxide radical anion (CO ₂ ^{•-})	19
3.0 EXPERIMENTAL.....	21
3.1 MATERIALS	21
3.2 PESTICIDES.....	21
3.2.1 Acifluorfen	21
3.2.2 Chlorsulfuron	22
3.2.3 Cyromazine	22
3.2.4 Dichlorophen	22
3.2.5 Dimethrimiol	22
3.2.6 Hexazinone	22
3.2.7 Ioxynil	23
3.2.8 MCPA (Methyl Chloro Phenoxy Acetic acid).....	24
3.2.9 Napropamide	24

3.3 STEADY STATE IRRADIATION (COBALT 60).....	24
3.3.1 Source Set-up.....	24
3.3.2 Calibration.....	24
3.3.3 Steady State investigation.....	25
3.3.4 High Performance Liquid Chromatography (HPLC).....	25
3.3.5 Mass Spectra.....	26
3.3.6 Ultra-Violet Spectra.....	27
3.4 PULSED IRRADIATION (HIGH ENERGY ELECTRONS).....	27
3.4.1 Accelerator Set up.....	27
3.4.2 Pulse Radiolysis Studies.....	28
3.5 MATHEMATICAL TREATMENT OF DATA.....	30
3.5.1 Dosimetry.....	30
3.5.2 Competition Kinetics.....	31
3.5.3 Molar Absorbance of transient species produced by Pulse Radiolysis.....	32
3.6 COMPUTATIONAL CHEMISTRY METHODS.....	32
4.0 RADIATION CHEMISTRY OF AQUEOUS NAPROPAMIDE SOLUTION.....	33
4.1 NAPROPAMIDE.....	33
4.2 REACTION OF NAPROPAMIDE WITH THE HYDROXYL RADICAL.....	33
4.3 REACTION OF NAPROPAMIDE WITH THE HYDROXYL RADICAL IN ACIDIC SOLUTION.....	40
4.4 REACTION OF NAPROPAMIDE WITH THE HYDROXYL RADICAL IN THE PRESENCE OF OXYGEN.....	43
4.5 REACTION OF NAPROPAMIDE WITH ONE ELECTRON OXIDANTS.....	46
4.6 REACTION OF NAPROPAMIDE WITH THE HYDRATED ELECTRON.....	53
4.7 REACTION OF NAPROPAMIDE WITH THE HYDROGEN ATOM.....	56
4.8 REACTION OF NAPROPAMIDE WITH REDUCING RADICALS.....	59
4.9 OVERVIEW OF THE RADIATION CHEMISTRY OF NAPROPAMIDE.....	60
5.0 RADIATION CHEMISTRY OF AQUEOUS IOXYNIL SOLUTION.....	65
5.1 IOXYNIL.....	65
5.2 REACTION OF IOXYNIL WITH THE HYDROXYL RADICAL.....	65
5.3 REACTION OF IOXYNIL WITH THE HYDROXYL RADICAL IN ACIDIC SOLUTION.....	71
5.4 REACTION OF IOXYNIL WITH THE HYDROXYLRADICAL IN THE PRESENCE OF OXYGEN.....	73
5.5 REACTION OF IOXYNIL WITH ONE ELECTRON OXIDANTS.....	75

5.6 REACTION OF IOXYNIL WITH THE HYDRATED ELECTRON.....	82
5.7 REACTION OF IOXYNIL WITH THE HYDROGEN ATOM.....	85
5.8 REACTION OF IOXYNIL WITH REDUCING RADICALS.....	87
5.9 OVERVIEW OF THE RADIATION CHEMISTRY OF IOXYNIL.....	87
6.0 RADIATION CHEMISTRY OF AQUEOUS CHLORSULFURON SOLUTION.....	93
6.1 CHLORSULFURON	93
6.2 REACTION OF CHLORSULFURON WITH THE HYDROXYL RADICAL.....	94
6.3 REACTION OF CHLORSULFURON WITH THE HYDROXYL RADICAL IN ACIDIC SOLUTION	101
6.4 REACTION OF CHLORSULFURON WITH THE HYDROXYL RADICAL IN THE PRESENCE OF OXYGEN	102
6.5 REACTION OF CHLORSULFURON WITH ONE ELECTRON OXIDANTS.....	103
6.6 REACTION OF CHLORSULFURON WITH THE HYDRATED ELECTRON.....	107
6.7 REACTION OF CHLORSULFURON WITH THE HYDROGEN ATOM.....	111
6.8 REACTION OF CHLORSULFURON WITH REDUCING RADICALS.....	112
6.9 OVERVIEW OF THE RADIATION CHEMISTRY OF CHLORSULFURON.....	112
7.0 RADIATION CHEMISTRY OF AQUEOUS DICHLOROPHEN SOLUTION.....	117
7.1 DICHLOROPHEN.....	117
7.2 REACTION OF DICHLOROPHEN WITH THE HYDROXYL RADICAL.....	118
7.3 REACTION OF DICHLOROPHEN WITH THE HYDROXYL RADICAL IN ACIDIC SOLUTION	124
7.4 REACTION OF DICHLOROPHEN WITH THE HYDROXYL RADICAL IN THE PRESENCE OF OXYGEN	126
7.5 REACTION OF DICHLOROPHEN WITH ONE ELECTRON OXIDANTS.....	129
7.6 REACTION OF DICHLOROPHEN WITH THE HYDRATED ELECTRON.....	137
7.7 REACTION OF DICHLOROPHEN WITH THE HYDROGEN ATOM.....	141
7.8 REACTION OF DICHLOROPHEN WITH REDUCING RADICALS.....	142
7.9 OVERVIEW OF THE RADIATION CHEMISTRY OF DICHLOROPHEN.....	142

8.0 RADIATION CHEMISTRY OF AQUEOUS CYROMAZINE SOLUTION	147
8.1 CYROMAZINE	147
8.2 REACTION OF CYROMAZINE WITH THE HYDROXYL RADICAL.....	148
8.3 REACTION OF CYROMAZINE WITH THE OXIDE RADICAL.....	153
8.4 REACTION OF CYROMAZINE WITH THE HYDROXYL RADICAL IN ACIDIC SOLUTION	154
8.5 REACTION OF CYROMAZINE WITH THE HYDROXYL RADICAL IN THE PRESENCE OF OXYGEN.....	155
8.6 REACTION OF CYROMAZINE WITH ONE ELECTRON OXIDANTS.....	158
8.7 REACTION OF CYROMAZINE WITH THE HYDRATED ELECTRON.....	162
8.8 OVERVIEW OF THE RADIATION CHEMISTRY OF CYROMAZINE.....	163
9.0 RADIATION CHEMISTRY OF AQUEOUS DIMETHRIMIOL SOLUTION	167
9.1 DIMETHRIMIOL	167
9.2 REACTION OF DIMETHRIMIOL WITH THE HYDROXYL RADICAL.....	167
9.3 REACTION OF DIMETHRIMIOL WITH THE HYDROXYL RADICAL IN ACIDIC SOLUTION	175
9.4 REACTION OF DIMETHRIMIOL WITH THE HYDROXYL RADICAL IN THE PRESENCE OF OXYGEN.....	180
9.5 REACTION OF DIMETHRIMIOL WITH ONE ELECTRON OXIDANTS.....	183
9.6 REACTION OF DIMETHRIMIOL WITH THE HYDRATED ELECTRON.....	189
9.7 REACTION OF DIMETHRIMIOL WITH THE HYDROGEN ATOM.....	193
9.8 REACTION OF DIMETHRIMIOL WITH REDUCING RADICALS.....	195
9.9 OVERVIEW OF THE RADIATION CHEMISTRY OF DIMETHRIMIOL.....	195
10.0 RADIATION CHEMISTRY OF AQUEOUS HEXAZINONE SOLUTION	201
10.1 HEXAZINONE	201
10.2 REACTION OF HEXAZINONE WITH THE HYDROXYL RADICAL.....	202
10.3 REACTION OF HEXAZINONE WITH THE HYDROXYL RADICAL IN ACIDIC SOLUTION.....	208

10.4 REACTION OF HEXAZINONE WITH THE HYDROXYL RADICAL IN THE PRESENCE OF OXYGEN.....	209
10.5 REACTION OF HEXAZINONE WITH ONE ELECTRON OXIDANTS.....	213
10.6 REACTION OF HEXAZINONE WITH THE HYDRATED ELECTRON.....	217
10.7 REACTION OF HEXAZINONE WITH THE HYDROGEN ATOM.....	221
10.8 REACTION OF HEXAZINONE WITH REDUCING RADICALS.....	221
10.8 OVERVIEW OF THE RADIATION CHEMISTRY OF HEXAZINONE.....	222
11.0 RADIATION CHEMISTRY OF AQUEOUS MCPA SOLUTION...	225
11.1 METHYL CHLORO PHENOXY ACETIC ACID.....	225
11.2 REACTION OF MCPA WITH THE HYDROXYL RADICAL.....	226
11.3 REACTION OF MCPA WITH THE HYDROXYL RADICAL IN ACIDIC SOLUTION	231
11.4 REACTION OF MCPA WITH THE HYDROXYL RADICAL IN THE PRESENCE OF OXYGEN	232
11.5 REACTION OF MCPA WITH OXIDISING RADICALS.....	234
11.6 REACTION OF MCPA WITH THE HYDRATED ELECTRON.....	239
11.7 REACTION OF MCPA WITH THE HYDROGEN ATOM.....	243
11.8 REACTION OF MCPA WITH REDUCING RADICALS.....	245
11.9 OVERVIEW OF THE RADIATION CHEMISTRY OF MCPA.....	245
12.0 RADIATION CHEMISTRY OF AQUEOUS ACIFLUORFEN SOLUTION.....	249
12.0 ACIFLUORFEN.....	249
12.2 REACTION OF ACIFLUORFEN WITH THE HYDROXYL RADICAL.....	250
12.3 REACTION OF ACIFLUORFEN WITH THE HYDROXYL RADICAL IN ACIDIC SOLUTION	256
12.4 REACTION OF ACIFLUORFEN WITH THE HYDROXYL RADICAL IN THE PRESENCE OF OXYGEN	256
12.5 REACTION OF ACIFLUORFEN WITH ONE ELECTRON OXIDANTS.....	258
12.6 REACTION OF ACIFLUORFEN WITH THE HYDRATED ELECTRON.....	261
12.7 REACTION OF ACIFLUORFEN WITH THE HYDROGEN ATOM.....	264
12.8 REACTION OF ACIFLUORFEN WITH REDUCING RADICALS.....	265

12.9 OVERVIEW OF THE RADIATION CHEMISTRY OF ACIFLUORFEN.....	267
13.0 APPENDIX 1.....	271
14.0 BIBLIOGRAPHY	283

1.0 Introduction

1.1 BACKGROUND

The use of organic pesticides in modern agricultural practices is now standard procedure. However, history has shown that the use of such chemicals can produce environmentally unfavourable results [1-6]. Accumulation of agricultural chemicals in any ecosystem can cause irreparable damage. In recent years this has led to the development of more environmentally friendly pesticides which require smaller application rates and degrade more rapidly in the environment after application [1].

Loss of a pesticide after application through environmental degradation means that reapplication of the pesticide is required each rotational year. There are two mechanisms for the degradation of pesticides in the environment, chemical and microbiological. Chemical degradation can be divided into two separate subgroups: photochemical degradation and hydrolysis [7-9]. The mechanism of photochemically induced degradation of organic pesticides in aqueous media is the primary research interest of this project. A particular focus is placed upon investigating the rates, mechanisms and products of reactions of free radicals derived from photochemical processes with pesticides.

1.2 PHOTOCHEMISTRY AND PHOTOCHEMICAL DEGRADATION

1.2.1 Natural system photochemistry

Environmental conditions (such as pH, oxygen content etc.) do not always favour the hydrolysis and microbiological degradation of organic compounds that enter an aquatic ecosystem. The degradation of these chemicals may then occur through photochemically mediated pathways. Photochemical degradation can be considered to occur via one of two mechanisms: either direct or indirect photolysis.

1.2.1.1 Direct Photolysis

Conditions that control the rate of direct photolysis are; solar flux, quantum yield and molar absorbance. There are a number of compounds that are known to undergo direct photolysis in sunlight. Known inorganic chromophores are nitrates, hydrogen peroxide and ferrous ions [7]. These compounds exhibit absorption greater than the 290 nm cut off line for solar radiation. Whether or not a particular organic pesticide is susceptible to direct photolysis depends on its ability to absorb wavelengths longer than 290 nm.

1.2.1.2 Indirect Photolysis

Indirect photolysis is the reaction of reactive species produced by direct photolysis (such as radicals) with other compound (the substrate).

Indirect photolysis is a means of degradation for pesticides whose degradation via other mechanisms (chemical or microbial) is hindered. While direct photolysis can occur in distilled water, indirect photolysis can only occur in water where there is at least one absorbing species and another compound for the absorbing species to react with [7]. Natural water has these conditions [10].

Prediction of pesticide degradation rates through indirect photolysis are almost impossible due to the large number of variables involved. It is known that the rate of indirect photolysis is dependent on such variables as the attenuation coefficient, water depth, rate of direct photolysis of the precursor to the reactive species and the number of competing reactions for the activated species [11].

Indirect photolysis pathways in aquatic systems are especially abundant [7, 12]. Pesticides that show no degradation in distilled water when irradiated with wavelength greater than 290 nm can show significant degradation when irradiated with the same light in natural water [11, 13]. The increased degradation in natural water is due to the indirect photolysis of the pesticide through radical initiated degradation.

1.2.2 Photochemical treatment for industrial discharge water

As well as being involved in pesticide degradation in natural water, direct and indirect photolysis are also employed in the purification treatment of industrial discharge water which contain organic contaminants. In the industrial scenario (unlike the natural situation) conditions experienced are such that the water body can be manipulated to optimise the degradation of the organic contaminant [14].

The sun is not the only source of radiation that can be used to initiate direct photolysis. Ultra-Violet (U.V.) light, which can possess wavelengths shorter than solar radiation is often used to induce the direct photolysis of organic compounds that would not undergo direct photolysis in normal sunlight [14].

Indirect photolysis can also be optimised for compounds that do not absorb U.V. light. The addition of reagents to the solution that do absorb U.V. light are used to produce highly reactive free radicals. These free radicals then react with the organic contaminant.

The two methods employed by industry frequently for the decontamination of organic polluted discharge water are the addition of the reagent Titanium dioxide (TiO_2) or Ozone (O_3), both of which are coupled with U.V. light [14].

1.3 PRODUCTION OF FREE RADICALS IN AQUEOUS SOLUTION

1.3.1 Production of radicals in natural water

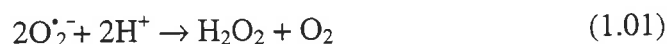
Free radicals and other reactive species produced from the photochemical reactions of organic and inorganic solutes may initiate the degradation of organic pesticides. The formation of these radicals are as follows.

1.3.1.1 Superoxide radical anions ($\text{O}_2^{\bullet -}$)

Humic acids are the product of the decay of organic matter. The structure of a humic acid varies widely with its origin. Humic acids absorb solar radiation to become electronically excited. It is thought that the excited humic acid reacts with dissolved oxygen (O_2) reducing the oxygen by energy transfer from its excited state (the mechanism of this process is not completely understood). The end result is the production of the superoxide radical anion ($\text{O}_2^{\bullet -}$) [15]. Other mechanisms postulated for the production of superoxide radical anion is the one electron transfer from reduced metals, and the heterogeneous photocatalysed reaction of semi-conductors (ie. TiO_2) [16].

1.3.1.2 Hydrogen Peroxide

The superoxide radical anion reacts with itself to form hydrogen peroxide (H_2O_2) [16-25] (reaction 1.01).



Though humic acids are essential for radical production, it should be recognised that as the concentration of humic acid in water rises, the ability of light to penetrate the water decreases, therefore decreasing the amount of photolysis that can occur. Humic acids can also react with the newly formed radical, therefore prohibiting any reaction between the radical and a pesticide [22].

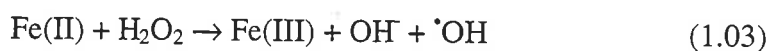
1.3.1.3 Hydroxyl radicals

Hydrogen peroxide absorbs slightly at wavelengths longer than 290 nm and therefore can undergo direct photolysis when irradiated with solar radiation, forming hydroxyl radicals (OH^{\bullet}).

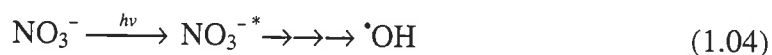


The absorption coefficient of hydrogen peroxide at 300 nm is less than $1 \text{ M}^{-1}\text{cm}^{-1}$, showing the photolysis of hydrogen peroxide is inefficient. It has been estimated that to destroy 37% of Chlorobutane (initial concentration $2 \mu\text{M}$) through the photolysis of hydrogen peroxide alone in natural water would require eight years [19, 24, 26].

It can therefore be observed that the photolysis of hydrogen peroxide to form hydroxyl radicals is not likely to be a main source of free radicals. Hydrogen peroxide, however, can also react with iron (II) in aqueous solution to form hydroxyl radicals by a Fenton type reaction (reaction 1.03). This method of generating hydroxyl radicals in natural water is greatly dependent on the amount of iron (II) in the water [27-29].



Another mechanism for the formation of hydroxyl radicals in natural water is through the photolysis of nitrate ions. Nitrate ions can be found in most natural waters in concentrations between 1 and 25 ppm [30]. The amount of hydroxyl radicals formed through the photolysis depends greatly on the concentration of nitrate ion in the water. It has been observed that an increase in nitrate concentration of 1.4 to 25 ppm only produces a 7 fold increase in the concentration of hydroxyl radicals [26]. This non proportional rise is thought to occur because of the nitrate ion self quenching effects [13, 31].



The quantum yield of the photolysis of nitrate to produce hydroxyl radicals is 0.002 at 20°C in the pH range 6.2 to 8.2 [26].

1.3.1.4 Radical Concentration

Studies have been conducted to determine the concentration of the hydroxyl radical and the superoxide radical anion reactive species in natural water. Measurements of the rate of auto-oxidation of cumene, along with kinetic models have been used to estimate the steady state concentration of hydroxyl radicals in natural waters. Most papers have reported the steady state concentration of hydroxyl radicals to be between 10^{-15} to 10^{-17} M. This concentration varies because of the variations in the amount of iron and nitrate ion between different natural waters [7].

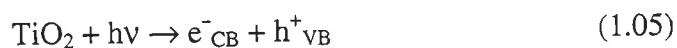
The concentration of hydrogen peroxide and superoxide radical anions in natural water must be determined together. The method used involves monitoring the fluorometric depletion of an enzyme through its reaction with hydrogen peroxide. An assumption is made that the only mechanism for formation of hydrogen peroxide is through the disproportionation of superoxide radical ions (reaction 1.01). This type of measurement allows for upper estimates of the concentration of superoxide radical anion. The upper limit to superoxide concentration in natural water is 10^{-8} M [7].

1.3.2 Production of radicals for industrial discharge water treatment

A review emphasising the number of techniques available for industrial discharge water containing organic pollutants has been published by Lengrini *et al.* [14]. The two most popular methods at the present time are the use of titanium dioxide, and ozone coupled with U.V. light [32-38]. Both methods use indirect photolysis by the generation of free radical species to react with the contaminant.

1.3.2.1 Titanium Dioxide

Titanium Dioxide is a semi-conductor thus there is only a small difference in energy between the valance band (VB) and the conduction band (CB). The energy difference between the two bands is such that radiation with wavelengths less than 387.5 nm has ^Senough energy to promote an electron from the valance band to the conduction band [37, 39].



It is the production of the electron in the conduction band (e^-_{CB}) and the hole in the valance band (h^+_{VB}) which provide the site for the reactions of the waste compounds. This is because h^+_{VB} is a powerful oxidant while e^-_{CB} is a powerful reductant. The degradation of waste compounds occurs through one of two mechanisms. The first involves the absorbance of the compound onto the titanium dioxide where the pollutant reacts with the oxidising and reducing e^-_{CB} and h^+_{VB} bands [13]. Waste chemicals that do not absorb onto the titanium dioxide, degrade because hydrogen ions and oxygen react with the e^-_{CB} and h^+_{VB} resulting in the formation of hydrogen peroxide and hydroxyl radicals [40]. It is the production of hydroxyl radicals that will cause the majority of the degradation, though reaction with other radicals could potentially induce degradation of the pollutant [36-38].

1.3.2.2 Ozone

Ozone is itself a very powerful oxidant ($\epsilon = 2.07$ V versus the Normal Hydrogen Electrode (NHE)) [32], but when ozone is coupled with U.V. light the full potential of the technique can be observed. Ozone when irradiated produces perhydroxyl radicals (HO_2^\bullet), superoxide radicals and hydroxyl radicals, through a series of cyclic reactions described by Lengrini *et al.* [14, 32]. These radicals are responsible for the degradation of the organic contaminants in the discharge water.

1.3.3 Radiolytic soil decontamination

Ionising radiation can be used to generate radicals in aqueous solution. This knowledge has been used previously by Hilarides *et al.* [41, 42] to decontaminate soils containing the pesticide dioxin. In this experiment soils were artificially contaminated with dioxin (100 ppb). The soils were then irradiated with gamma rays using cobalt 60 (this technique will be discussed later) with doses up to 450 kGy. This method proved effective in removing 60 to 70 % of the pesticide.

In an attempt to determine the individual effect of the active species involved (ie. superoxide radical anions, hydroxyl radicals and hydrated electrons) on the degradation of dioxin, single reactive species were singled out for examination by similar methods employed in section 2.1. It was observed that there were only minor effects in changing the radical type on the amount of degradation of dioxin.

The economical viability of cobalt 60 radiation technique to detoxify contaminated soils was also evaluated against other known methods for pesticide decontamination. It was estimated (not including the capital costs needed for initial set up) that to purge soil of organic contaminants would cost between (US) \$100 to \$200 per ton of soil. When compared to other accepted methods of soil decontamination (ie. high temperature furnaces), this method is the cheapest on the market. The only negative aspect of the process is the initial capital cost involved with setting up a reactor capable of performing cobalt 60 irradiations. An estimated (US) \$275 000 would be required every five years. When the capital costs are included this method is still competitive with existing techniques.

1.3.4 Radiolytic aqueous degradation

No attempts at a commercial decontamination plant for polluted water using radiative techniques could be found by the author in the literature. There have, however, been numerous studies conducted observing the reaction between organic compounds and

radiolytically generated radicals. These studies were recently reviewed by Buxton *et al.*, Neta *et al.* and Bielski *et al.* [43-45]. Studies of the reaction of radicals with organic pesticides have not been so prevalent. The first investigation into the effects of radiation induced radicals was attempted by Buxcholtz *et al.* in 1977 [46]. This study involved the steady state irradiation of aqueous pesticides and analysis of the formation of products by Thin Layer Chromatography (TLC). The study did not investigate any possible reaction mechanisms. Initial interest in examining the mechanisms of these type of reactions was shown by Getoff and Solar [47]. In this paper the rates and reaction mechanisms were investigated for the ortho, meta and para of the pesticide chlorophenol with $\cdot\text{OH}$ and H^{\cdot} and $e_{(\text{aq})}^{-}$ generated using dynamic and steady state methods.

The number of papers investigating the reactions of radiolytically generated radicals with organic pesticides have been relatively few. Papers recently published include Fox 1993 [48], Gierer *et al.* 1994 [25], Terzain *et al.* 1995 [49], Quaint *et al.* [50] and Merga 1996 [66].

1.4 OUTLINE AND SCOPE OF THESIS

The work in this thesis is the accumulation of the work completed on nine separate pesticides. The pesticides were chosen with varying functionality to be representative of a number of pesticides widely available in Australia. The reaction rates, reaction pathways, properties of radical intermediates and radical final products of the reaction were measured in aqueous solution using steady state and dynamic methods. The data allowed for the determination of free radical mechanisms with the organic pesticides studied as well as the initial products of the reaction. This data can be used to predict the fate of these pesticides if radical mediated degradation occurs (through natural or artificial methods), specifically through ionising radiation methods such as described by Hilarides *et al.* [41, 42].

Following this introductory chapter is a section summarising the literature of the radicals used in this report. It includes the radiolytic generation of radicals in aqueous solution as well as the types of reactions that these radicals undergo with specific organic functional groups.

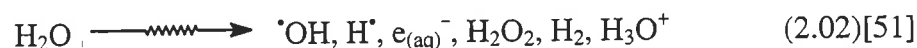
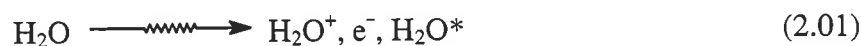
Chapter 3 describes in detail the experiment procedure that was used throughout the rest of the thesis. Included is the detailed report of the pulse radiolysis, steady state and theoretical calculations undertaken.

Chapters 4 to 12 are self contained sections detailing the results of the experiments for each of the specific pesticides studied. The results obtained from the pulse radiolysis, steady state and theoretical studies are discussed in relation to the mechanism of the reaction of the radical with the pesticide.

2.0 Radiation Chemistry

2.1 RADIOLYTIC RADICAL PRODUCTION

A convenient method for the generation of radicals is through the use of ionising radiation. When water is irradiated with ionising radiation, energy is deposited into the solution causing chemical changes that results in the formation of ions, excited molecules and free radicals along the path of the radiation. The end result of this energy deposition into liquid water is the formation of the following radicals and molecular products described in equation 2.02.



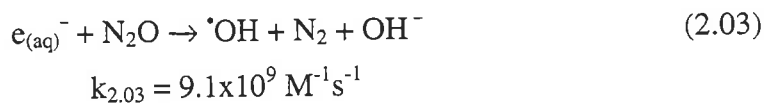
The G values¹ for reaction 2.02 are $G(\cdot\text{OH})=2.8$, $G(e_{(\text{aq})}^-)=2.7$, $G(\text{H}^{\cdot})=0.55$, $G(\text{H}_2)=0.45$, $G(\text{H}_2\text{O}_2)=0.7$ and $G(\text{H}^+)=3.6$ for pH values between 4 and 10 [51, 52]. The G values of the irradiation of water remains relatively constant between the pH values of 4 and 10. Outside of this pH range the G values exhibit a strong pH dependence [53]. *But here radical yield this is not relevant*

By variation of the pH and the species present in the irradiated aqueous solution, one radical can be selectively generated in excess. This allows for the reaction between a pesticide and a single radical of choice.

The conditions required to form radicals selectively are stated below.

2.1.1 Hydroxyl radicals

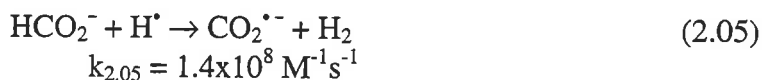
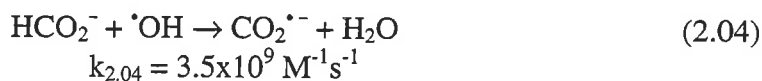
Hydroxyl radicals are selectively created by saturating the solution with nitrous oxide (N_2O). This converts all hydrated electrons to hydroxyl radicals by reaction 2.03 [51, 52].



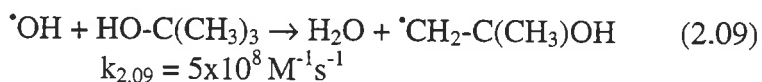
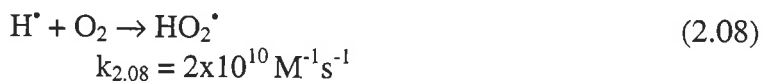
2.1.2 Perhydroxyl and superoxide radical anions

Perhydroxyl and superoxide radical anions can be produced through three different mechanisms. The first involves the addition of sodium formate (HCO_2Na) [45].

¹ G Value is defined as the number of molecules formed for every 100eV deposited.



The second reaction involves the use of *t*-butyl alcohol in an oxygenated solution. The *t*-butyl alcohol effectively scavenges the hydroxyl radicals [45].



The last method involves the addition of hydrogen peroxide. This method, unlike the previous ones, does not require the presence of oxygen in solution [45].



Superoxide radical anions and perhydroxyl radicals are in an acid-base equilibrium, with a $\text{p}K_a$ of 4.8 [45].



At low pH the perhydroxyl radical predominates, while at neutral and high pH the superoxide radical anion predominates.

2.1.3 Hydrogen atoms

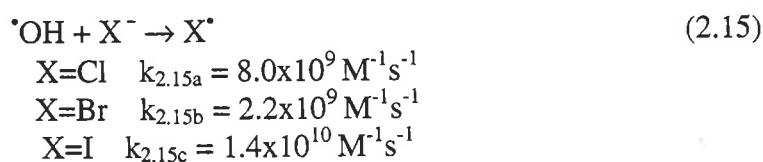
Hydrogen atoms are formed at low pH by the addition of perchloric acid. Addition of *t*-butyl alcohol to water eliminates hydroxyl radicals by reaction 2.09 [45]. Saturating the

solution with nitrogen or argon eliminates oxygen from the system and therefore stops the formation of the perhydroxyl radicals by stopping reaction 2.08.



2.1.4 Dihalogen radical anions

Dihalogen radical anions are formed by the one electron oxidation reaction of the hydroxyl radical with a halide [43]. The halide must be in excess to ensure that the hydroxyl radical reacts with the halide and not the compound being studied.



The addition of nitrous oxide doubles the yield of hydroxyl radicals (reaction 2.03) and therefore doubles the yield of the dihalogen radical ion.

For the formation of the dichloride radical anion, the pH must also be lowered as the formation of the dichloride radical anion is thermodynamically unfavourable at neutral to high pH. The pH is generally lower with the perchloric acid due to its low reactivity with any of the radical products generated through radiolysis [43].

2.1.5 Hydrated electrons

Hydrated electrons are ^{NO} generated by the addition of excess *t*-butyl alcohol to scavenge the hydroxyl radicals (reaction 2.09). The solution is saturated with nitrogen or argon gas to stop the formation of the superoxide radical anion by excluding oxygen from the solution (reaction 2.07) [44, 54].

2.1.6 Oxide radicals

Oxide radicals are formed by deprotonating the hydroxyl radical. This requires an increase of the pH of the system above 13. The solution is also saturated with nitrous oxide to ensure all the hydrated electrons are converted into hydroxyl radicals for deprotonation.

2.1.7 Azide radicals

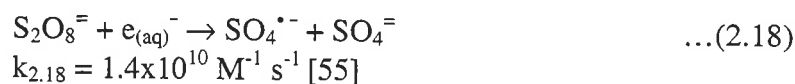
Azide radicals are generated by the one electron oxidation reaction of the azide ion with the hydroxyl radical (reaction 2.17) and the hydrogen atom. The azide ion must be in excess to ensure that the hydroxyl radical reacts with it and not the compound being studied.



The yield of azide radicals can be nearly doubled by the saturation of the solution with nitrous oxide to convert all the hydrated electrons into hydroxyl radicals (reaction 2.03). Hydrogen atoms also react with the azide anion to form azide radicals.

2.1.8 Sulfate radical anions

Sulfate radical anions are generated by the one electron reduction of the persulfate ion by the hydrated electron (reaction 2.18). The persulfate ion must be in excess to ensure that the hydrated electron reacts with it and not the compound being studied.



The solution is saturated with nitrogen or argon to stop the competing reaction of the formation of the superoxide radical anion (reaction 2.07). The solution also has the addition of excess *t*-butyl alcohol to ensure that the hydroxyl radical does not react with the solute (reaction 2.09).

2.1.9 Carbon dioxide radical anions

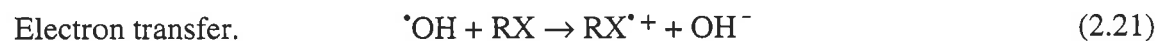
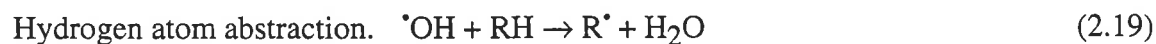
Carbon dioxide radical anions are formed by the reaction of hydroxyl radicals and hydrogen atoms with the formate ion as observed in reactions 2.04 and 2.05. The solution is also saturated with nitrous oxide to convert the hydrated electron into hydroxyl radicals, therefore doubling the yield (reaction 2.03). It is also used to stop the formation of the superoxide radical anion by excluding oxygen from the solution and stopping reaction 2.06.

2.2 PROPERTIES OF RADICALS

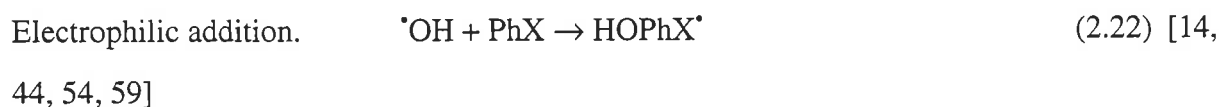
Reactions of radicals with organic solutes in aqueous solution has previously been reviewed by several authors [43-45, 56] and the typical reactions of radicals used within this study are summarised below.

2.2.1 Hydroxyl radicals (OH^\bullet)

The oxidising potential of the hydroxyl radical is 2.7 V ($\text{OH}^\bullet/\text{OH}^-$ versus NHE) in acidic solution and 1.8 V in neutral solution where the free energy of neutralisation of OH^- by H^+ is less [44, 51, 57, 58]. As well as oxidation by electron transfer (reaction 2.21), hydroxyl radicals are potent at hydrogen atom abstraction from organic molecules (reaction 2.19).



Another reaction possible with hydroxyl radicals in the presence of unsaturated organic compounds, especially aromatics is electrophilic addition.



2.2.2 Superoxide radical anions ($\text{O}_2^{\bullet-}$)

As the name suggests has a dual nature. It is a negatively charged species which allows it to react as a Bronsted base and a nucleophile. A superoxide radical anion also has an unpaired electron, making it a free radical. Overall, five types of reactions are possible for superoxide radical anion:

Basicity. Superoxide radical anion is in equilibrium with its protonated form the perhydroxyl radical (HO_2^\bullet). The pK_a of this equilibrium is 4.75 ± 0.08 , implying that superoxide is a relatively weak base [40].




Superoxide is a relatively weak base because it is a small non-polarisable anion which is stable in aqueous media due to a tightly bound solvation sphere. The ability of superoxide to act as a base is increased by the dismutase reaction of the perhydroxyl radical (formed when superoxide extracts a hydrogen ion) which drives the equilibrium to the right.



Therefore the effective basicity is actually more than the Bronsted basicity. Ultimately, however, superoxide only has a short lifetime in water and kinetic factors, not thermodynamic factors determine its activity. This means that only acid-base reactions that are of similar rate of reaction (reaction 2.24) to the dismutase of superoxide will be of importance [60].

Nucleophilicity. A superoxide radical anion is expected to be a poor nucleophile because of its strong hydrogen bonding to the solvent. Any nucleophilicity reaction must again compete with the disproportionation reaction (reaction 2.25). It can therefore be postulated that superoxide radical anion will not possess any nucleophilic properties in water [60].

Free radical character. Superoxide's free radical reactions can be grouped into one of two different types of reactions. It can either add to a double bond or it can abstract a labile hydrogen atom.

Both of these types of reactions have been examined thermodynamically. Addition to double bonds has been shown to be thermodynamically unfavourable [60]. This has also been observed experimentally with no reactions being recorded with many different types of unsaturated compounds and superoxide. Reactions via hydrogen abstraction proceed, but only with molecules that have extremely labile hydrogen [60]. *e.g's ?* 

Though both of these free radical reactions seem unlikely, the reaction of superoxide with other free radicals does occur. These reactions occur at diffusion controlled rates and are important in free radical chemistry [60].



One electron oxidation. Due to the stability of oxygen, the loss of the electron from the superoxide radical anion to a substrate should be a thermodynamically favourable process.



The reduction potential ($O_2/O_2^{\bullet -}$, versus NHE) is -0.33 V in water [60].

One electron reduction. Superoxide radical anions in the presence of hydrogen ions, can accept an electron to form hydrogen peroxide [60]. The reduction potential of this reaction ($O_2^{\bullet -}/H_2O_2$, versus NHE) is + 0.88 V.



It can therefore be concluded that superoxide will be a reasonable oxidant if hydrogen ions are available to be consumed.

From the mechanisms of superoxide radical anion reactions, it can be observed that it is not an extremely reactive species. Its importance however, in free radical mediated degradation cannot be overlooked. The upper limit for the concentration of superoxide is approximately 10^{-8} M and concentrations are even higher in discharge water. The environmental importance of superoxide has been acknowledged, but no direct studies have been conducted to clarify this importance [7].

Most reactions with superoxide have been carried out using biologically significant compounds. Mathematical models using these compounds have shown that when comparing the reactivity of hydroxyl radicals to superoxide radical anions, the superoxide is actually more effective at attacking the target molecule. This is because superoxide is considerably less reactive than hydroxyl radicals and therefore superoxide tends not to be consumed by scavenger molecules, unlike hydroxyl radicals which react with most scavenger molecules [61].

2.2.3 Perhydroxyl radicals (HO_2^{\bullet})

As stated earlier, perhydroxyl radicals are in equilibrium with superoxide radicals (reaction 2.23). Perhydroxyl radicals can act as either oxidising or reducing agents, depending on the solute involved. Reduction potentials suggest that perhydroxyl radicals are stronger oxidising agents while superoxide is a stronger reducing agent [52].

Hydrogen abstraction from an organic compound will only occur when weakly bonded hydrogen atoms are attacked by perhydroxyl radicals [52]. A complete review of the reactions of both superoxide and perhydroxyl radicals has been compiled by Bielski *et al.* [45].

2.2.4 Hydrated electrons ($e_{(aq)}^-$)

The hydrated electron can be considered as an electron trapped by a small group of water molecules.



The hydrated electron can be visualised as a singularly charged anion of approximately the same size as an iodide ion. It possesses a large absorption in the visible region with a maximum molar absorption coefficient of approximately $18\,000\text{ M}^{-1}\text{cm}^{-1}$ at approximately 700 nm [44, 51]. *ϵ for e_{aq}^- is known very accurately, so why the approx.?*

The hydrated electron has a standard reduction potential (versus NHE) of -2.9 V [51, 52], and therefore reacts rapidly with species with a more positive reduction potential. The reaction can generally be represented as shown in reaction 2.30 [44, 51, 62].



The reactions of hydrated electrons with organic compounds can be characterised by those expected for a nucleophilic reagent, [51, 52, 55, 62] including:

- Singly bonded compounds are unreactive (ie. carbon).
- Halogen groups react rapidly (except fluorine).
- Aliphatic halogens react quantitatively with dehalogenation the result.
- Reactions are greatly enhanced by the presence of electron withdrawing groups.
- Attack on double bonds is accelerated by the presence of an electron withdrawing group.

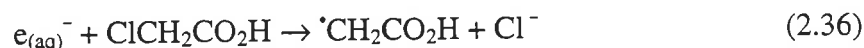
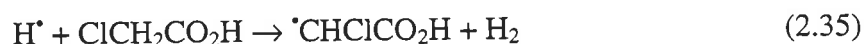
2.2.5 Hydrogen atoms (H^\bullet)

The smallest and simplest chemical known. It consists of a single proton and an electron. The hydrogen atom is the conjugate acid to the hydrated electron (reaction 2.31). When formed, the hydrogen atom reacts in a similar way to hydroxyl radicals. That is, hydrogen atoms react through mechanisms such as hydrogen atom abstraction (reaction 2.32) and addition to double bonds and aromatic systems (reaction 2.33) [63].

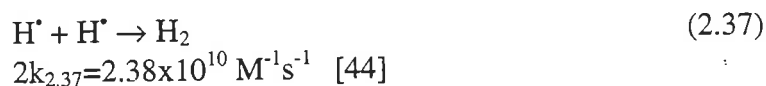




Charge transfer reactions involving hydrogen atoms (unlike, hydroxyl radicals which are oxidising species) proceed through an oxidation process (reaction 2.34). This is because the reduction potential of Hydrogen ($\text{H}^+_{(\text{aq})}/\text{H}^{\bullet}$ versus NHE) is -2.31 V [44]. The hydrogen atom is therefore a moderately less powerful reducing agent than the hydrated electron. When hydrogen atoms react with organic compounds they tend to behave more like the hydroxyl radical rather than the hydrated electron [44]. A good example of this is the reactions of the hydrated electron and hydrogen atom with chloroacetic acid (reactions 2.35 and 2.36) [44].



Though the reaction mechanisms of hydrogen atoms are similar to hydroxyl radicals, the reactivity of the hydrogen atom is significantly less when compared with hydroxyl radicals. Addition reactions tend to have rate constants an order of magnitude lower than the corresponding hydroxyl radical reaction [44, 63-66]. Hydrogen atoms also have a competing reaction with themselves resulting in the formation of molecular hydrogen.



2.2.6 Oxide anions ($\text{O}^{\bullet -}$)

The oxide anion is the deprotonated form of the hydroxyl radical with the deprotonation having a pK_a of 11.9. The oxide anion differs greatly in its reactions with organic molecules from that of the hydroxyl radical. The hydroxyl radical tends to react with organic molecules as an electrophile, while the oxide ion reacts like a nucleophile [59]. While the hydroxyl radical readily adds to double bonds, the oxide ion reacts via hydrogen abstraction from C-H bonds. If for example an aromatic compound contains an aliphatic side chain, the hydroxyl radical will add to the ring while the oxide ion will abstract a hydrogen from the carbon chain [44].



2.2.7 Dihalogen radical anions ($X_2^{\bullet -}$)

($X_2^{\bullet -}$) ($X = \text{Cl, Br, I}$) have both radical and redox properties. As radicals they react with each other and have the potential to start polymeric reactions. Often dihalogen radical ions are generated to replace hydroxyl radicals in experiments because dihalogen radical ions are often less likely to undergo hydrogen atom abstraction and more likely to undergo redox reactions [43]. All dihalogen radical ions are strong oxidising agents with reduction potential (versus NHE) of 2.09 V, 1.77 V, 1.03 V for chloride, bromide and iodide respectively [43, 58, 67]. They react with the substrate by one electron transfer.



A number of reactions of dihalogen radical anions have been summarised by Neta *et al.* [43]

2.2.8 Azide radicals ($N_3^{\bullet -}$)

The azide radical is a strong one electron oxidant, having a reduction potential of 1.4 Volts [$(N_3^-/N_3^{\bullet -})$ versus NHE]. Reactions involving the azide radicals are generally faster than the corresponding dihalogen radical anion. Azide reacts faster than the dibromide radical anion even though the reduction potential of the bromide radical anion is greater. Azide generally reacts with phenoxide ions and aniline at diffusion controlled rates [43].

2.2.9 Sulfate radical anion ($SO_4^{\bullet -}$)

The sulfate radical anion is a very strong one electron oxidant with a reduction potential estimated to be between 2.5 and 3.1 V ($SO_4^-/SO_4^{\bullet -}$ versus NHE) [43]. It is a more selective oxidant than the hydroxyl radical but its reactions are generally slower than the corresponding hydroxyl reaction [68]. The sulfate radical will react at diffusion controlled rates with compounds such as phenol and aniline, it will also oxidise compounds such as benzene. The product of the last reaction is a radical cation which quickly reacts with water to form hydroxycyclohexadienyl radical, the same species made by the reaction of hydroxyl radicals with benzene. Reactions with compounds like toluene also result in the formation of the radical cation, however this then rapidly deprotonates to give the more stable phenyl radical. Hydrogen abstraction also takes place from aliphatic compounds [43].

2.2.10 Carbon dioxide radical anion ($\text{CO}_2^{\bullet-}$)

The carbon dioxide radical anion is a strong reducing species with a redox potential of -2.0 V ($\text{CO}_2^{\bullet-}/\text{CO}_2$ versus NHE). It will transfer an electron very rapidly to compounds containing functional groups such as nitro, quinone and pyridiniums [43].

3.0 Experimental

3.1 MATERIALS

The chemicals used throughout this report are phosphoric acid (88%), potassium dihydrogen phosphate, di-potassium hydrogen orthophosphates, tripotassium orthophosphate, sodium chloride, sodium bromide, sodium iodide, potassium ferrocyanide, ammonium ferric sulfate, ammonium ferrous sulfate, sodium azide, sodium formate, di-potassium persulfate, sodium hydroxide (BDH A.R.), spectroscopic grade *t*-butyl alcohol (Fulka) and 70% perchloric acid (Prolabo). All gases used [oxygen, nitrogen, nitrous oxide and nitrous oxide : oxygen (4:1 v/v)] were of instrument grade or higher and used as purchased from BOC. Organic solvent such as methanol, dichloromethane, hexane and ethyl acetate were received as bulk solvents (CRC) and re-distilled before use. HPLC ion pairing reagents such as trifluoro acetic acid (TFA) and heptafluoro butyric acid (BFA) were analytical grade and used as received from Aldrich. Acetonitrile and isopropanol were HPLC grade and filtered through a 0.22 μm filter before use. Silica used in all flash columns was normal phase and purchased from Merck. Water used in all experiments was deionised and purified through a Milli-Q purification system (Millipore). NMR experiments were conducted in deuterated chloroform (unless otherwise stated) purchased from Aldrich.

3.2 PESTICIDES

The purification technique for each pesticide is described below:

3.2.1 Acifluorfen

Acifluorfen was received from Rhone-Poulenc as a water soluble salt of unknown concentration. The following procedure was used for its purification.

To a clean dry 250 mL separating funnel approximately 75 mL of water and 75 mL of dichloromethane were added. Two grams of the Acifluorfen solution was added. The resulting mixture had a small amount of dilute sulphuric acid added and was then shaken for approximately one minute. The resulting solution was allowed to settle for one hour into the organic and aqueous layers. The organic layer was then collected and the solvent removed under reduced pressure to yield a brown oil. The sample crystallised upon seeding.

The sample was then washed with a small amount of hexane before being recrystallised from hexane. $^1\text{H NMR}$ δ 8.8 (s), δ 8.0 (d), δ 7.8 (m), δ 7.6 (dd), δ 7.0 (dd), δ 3.7 (dm), δ 3.5 (t), δ 1.5 (dq), δ 0.9 (t), LC-MS (M-H) $^-$ 360/362 (3:1).

3.2.2 Chlorsulfuron

Chlorsulfuron was received from Du Pont in a formulated mixture containing 75% Chlorsulfuron and other ingredients such as fillers. The following procedure was used for its purification.

To a clean dry 250 mL separating funnel approximately 75 mL of water and 75 mL of dichloromethane were added. Two grams of the formulated mixture was then added and the resulting mixture shaken for approximately 1 minute. The organic layer was separated from the aqueous layer and dried over anhydrous magnesium sulfate. The organic layer was then filtered and the solvent removed under reduced pressure to yield a white solid. The solid was recrystallised from methanol. Overall yield was 56%. $^1\text{H NMR}$ δ 2.5 (s), δ 4:1 v/v (s), δ 7.3 (s), δ 7.5 (m), δ 8.3 (dd) LC-MS (M+H) $^-$ 358/360. (3:1).

3.2.3 Cyromazine

Cyromazine was received from Ciba-Giegy as a technical grade mixture (96%). This was recrystallised from water. $^1\text{H NMR}$ (D_2O) δ 2.4 (m), δ 0.4 (dm), LC-MS (M+H) $^+$ 167.

3.2.4 Dichlorophen

Dichlorophen was purchased from Aldrich as a 95% pure sample. This was recrystallised from hexane. $^1\text{H NMR}$ δ 7.2 (d), δ 7.0 (dd), δ 6.7 (d), δ 3.9 (s), LC-MS (M-H) $^-$ 267/269/271 (4:3:1).

3.2.5 Dimethrimiol

Dimethrimiol was received from ICI as an analytical standard (99.3%). No further purification was required. $^1\text{H NMR}$ δ 3.1 (s), δ 2.4 (t), δ 2.2 (s), δ 1.5 (s), δ 1.3 (m), δ 0.9 (s), LC-MS (M+H) $^+$ 210.

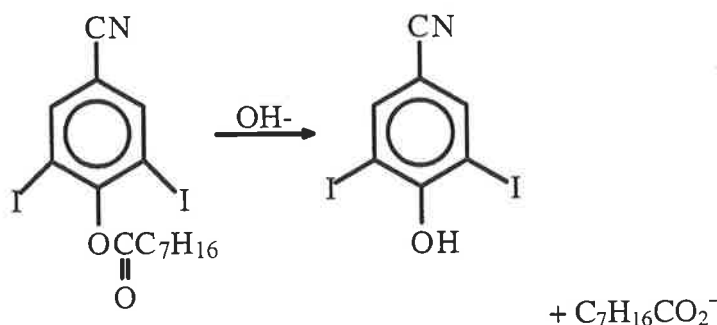
3.2.6 Hexazinone

Hexazinone was received from Du Pont as a formulated mixture containing 75% Hexazinone and other chemicals as fillers. The following procedure was used for the purification of Hexazinone.

To a clean dry 250 mL separating funnel approximately 75 mL of water and 75 mL of dichloromethane were added. Two grams of the formulated mixture was then added and the resulting mixture shaken for approximately 1 minute. The organic layer was separated from the aqueous layer and dried over anhydrous magnesium sulfate. The organic layer was then filtered and the solvent removed under reduced pressure to yield an orange oil. The oil was dissolved in the minimum amount of dichloromethane and passed down a silica flash column with 75% ethyl acetate / 25% hexane solvent mix, working through to 100% ethyl acetate. The fractions containing Hexazinone were identified by thin layer chromatography (TLC) and U.V. light, combined and their solvent removed under reduced pressure to yield a white solid. The solid was recrystallised from hexane. The overall yield was 20%. $^1\text{H NMR}$ δ 4.5 (tt), δ 3.3 (s), δ 2.9 (s), δ 2.3 (dq), δ 1.6 (dd), δ 1.2 (m), LC-MS (M+H)⁺ 253.

3.2.7 Ioxynil

Ioxynil was received from Rhone-Poulenc in the ester form of Ioxynil octanate. Base hydrolysis was used to convert the ester into the desired alcohol.



Scheme 2.01. Base hydrolysis of Ioxynil octanate.

To a clean dry 500 mL round bottom flask was added approximately 200 mL of methanol, 2 gm of Ioxynil octanate (0.004 moles) and 0.1700 gm of sodium hydroxide (0.0043 moles). The resultant mixture was gently refluxed for 2 hours, allowed to cool and then acidified with 1 M HCl. The solvent was removed under reduced pressure. The residue was redissolved in dichloromethane and shaken in a separating funnel with saturated sodium bicarbonate. The organic layer was separated from the aqueous phase and dried over anhydrous magnesium sulfate, filtered and the solvent removed under reduced pressure to yield a yellow solid. The resulting solid was recrystallised from carbon tetrachloride to yield a white solid. Overall yield was 15%. $^1\text{H NMR}$ δ 8.0 (s), IR (all cm^{-1}) 3400, 3058 (OH (s)), 2226 (CN(s)), 1534, 1575 (aromatic), 1245 (OH(b)), 1142 (CO), 481 (C-I), LC-MS (M-H)⁻ 370.

3.2.8 MCPA (Methyl Chloro Phenoxy Acetic acid)

MCPA was received from Nu Farm as a technical formulation. This was recrystallised from water using hot filtration to remove any insoluble impurities. ^1H NMR δ 7.2 (m), δ 7.1(d), δ 6.5 (d), δ 4.7 (s), δ 2.2 (s), LC-MS (M-H) $^-$ 199.6/201.6 (3/1).

3.2.9 Napropamide

Napropamide was received from ICI in the formulated mixture containing 50% Napropamide and other chemicals such as fillers. The following procedure was used for the purification of Napropamide.

To a clean dry 250 mL separating funnel approximately 75 mL of water and 75 mL of dichloromethane were added. Two grams of the formulated mixture was then added and the resulting mixture shaken for approximately 1 minute. The organic layer was separated from the aqueous layer and dried over anhydrous magnesium sulfate. The organic layer was then filtered and the solvent removed under reduced pressure to yield an orange oil. The oil was dissolved in the minimum amount of dichloromethane and passed down a silica flash column with 75% hexane / 25% ethyl acetate mixture, working through to 100% ethyl acetate. The fractions containing Napropamide were identified using TLC and U.V. light. The fractions were combined and the solvent removed under reduced pressure to yield a white solid. This was recrystallised from hexane. Overall yield 50%. ^1H NMR δ 0.9 (t), δ 1.1 (t), δ 1.6 (d), δ 3.3 (m), δ 3.5 (m), δ 5.1 (q), δ 6.8 (d), δ 7.4 (m), δ 7.6 (t), δ 7.8 (m), δ 8.3 (m) LC-MS (M+H) $^+$ 272.

3.3 STEADY STATE IRRADIATION (COBALT 60)

All steady state irradiations in this report used the cobalt 60 source at the University of Adelaide.

3.3.1 Source Set-up

The cobalt 60 source was set up so that six 25 mL volumetric flasks (used in all irradiations unless otherwise stated) could be irradiated at once. The positions of the flasks were marked so that the position of the flasks could be kept constant.

3.3.2 Calibration

The cobalt 60 source was calibrated using the Frickie Dosimeter. The Frickie solution was prepared by using the procedure below which was published in Sangaster and O'Donnell [51].

Concentrated (95-98%) analytical (A.R.) quality sulphuric acid (22 mL) was added to 600 mL of Milli-Q water in a 1 L Volumetric flask. When the solution had cooled, A.R. ammonium ferrous sulfate (0.56g) and A.R. sodium chloride (0.06g) were dissolved into solution and the volume made up to 1 L. The resulting solution was used to fill six volumetric flasks. The flasks were placed into position and irradiated for two and a half hours. Once irradiation was complete, the absorption of each solution at 304 nm was determined on a Hewlett Packard Diode Array U.V.-Visible Spectrometer, using an unirradiated Frickie solution as the blank. The absorption value of each solution was used to determine the dose rate of the cobalt 60 source at that position.

Dose rate calculations rely on the molar absorptivity of the ferric ion at 304 nm. To ensure that the correct molar absorptivity was being used, a range of standard solutions were made up using ammonium ferric sulfate.

3.3.3 Steady State investigation

The exact preparation of the solution varied slightly according to the desired radical that was to be studied. Reagents added were as stated in section 2.1.

To a clean dry 200 mL volumetric flask an appropriate amount of pesticide was added. The flask was filled with approximately 150 mL of Milli-Q reagent water and the resulting solution was sonicated until the pesticide dissolved. Once all the pesticide had dissolved, the additional reagents (if any) were added along with buffer (Phosphate $1 \times 10^{-3} \text{M}$), filled to the mark with Milli-Q water, separated into six 25 mL volumetric flasks, saturated with the appropriate gas and sealed. Irradiation times varied with the pesticide concentration and the G value of the radical being reacted.

Experiments were repeated exactly, except HClO_4 was added to adjust the pH to 2 instead of the phosphate buffer.

3.3.4 High Performance Liquid Chromatography (HPLC)

After irradiation, the rate of formation of the degraded products, and the rate of loss of the pesticide was followed by High Performance Liquid Chromatography (HPLC). The HPLC system used contained a Reodyne injector, Waters Model 481 Variable Wavelength U.V.-Visible detector, Waters Model 510 and 501 Solvent Delivery Units, ICI Data Interface, Waters Automated Gradient Controller, ICI DP 700 Data Processing Software and a Waters Symmetry C_8 Reverse Phase Steel Column (3.9x150 mm). The mobile phase varied depending on the compound used in the experiment (Table 2.01). All solutions were filtered

through either a 0.22 μm nylon or a 0.45 μm Polypropylene membrane before 80 μL of sample was injected.

Once the major products of the degradation were determined, they were collected. The 1mL loop on the injector was flushed with 3 mL of sample and then loaded onto the HPLC column. The major products were collected in clean eppendorf vials as they eluted off the column. This process was repeated 2 or 3 times until enough sample had been collected.

Some samples collected also had their U.V.-Visible spectra recorded as well their mass spectra.

COMPOUND	Detection (nm)	Solvent A	Solvent B	Starting Ratio A:B	Finishing Ratio A:B	Gradient Start Time	Retention Time (min)
Acifluorfen	228	.1%TFA/ H ₂ O	CH ₃ CN	70:30	40:60	8	24
Chlorsulfuron	236	.1%TFA/ H ₂ O	CH ₃ CN	70:30	70:30	-	21
Cyromazine	236	.1%BFA/ H ₂ O	CH ₃ CN	90:10	90:10	-	19
Dichlorophen	254	.1%TFA/ H ₂ O	CH ₃ CN	70:30	40:60	8	19.5
Dimethrimiol	236	H ₂ O	CH ₃ CN	80:20	80:20	-	20
Hexazinone	246	H ₂ O	CH ₃ CN	80:20	50:50	15	12
Ioxynil	238	.1%TFA/ H ₂ O	CH ₃ CN	70:30	40:60	8	16
MCPA	232	.1%TFA/ H ₂ O	CH ₃ CN	70:30	40:60	8	16
Napropamide	288 & 254	H ₂ O	CH ₃ CN	65:35	40:60	8	18

Table 3.01. HPLC condition for pesticides.

3.3.5 Mass Spectra

Reaction products collected by HPLC had their masses determined by electrospray mass spectrometry. The electrospray system used was a Finnigan LC-Q Mass Spectrometer.

Reaction products were introduced into the LC-Q by infusion at flow rates of 10 to 20 μL per minute. Positive ion mode was used for the neutral pesticides Chlorsulfuron, Cyromazine, Dimethrimiol, Hexazinone and Napropamide, while negative ion mode was selected for the negatively charged compounds Acifluorfen, Dichlorophen, Ioxynil and MCPA. To ensure good detection limits in negative ion mode, either an equimolar amount of Tripropylamine was added post separation to the collected products or the products were extracted with Dichloromethane. This has the effect of neutralising the acid essential for good chromatographic separation of negatively charged compounds [69].

Once the mass of the compound had been determined, further structural information was obtained by performing MS^n experiments². MS^2 scans involve all but the selected parent ion being ejected from the ion trap. The selected parent ion is then fragmented into daughter ions by reacting it with a collision gas (Helium) and the newly formed ions are then mass analysed. This process can be repeated on the daughter ions several times and is known as MS^n . The advantage of this type of fragmentation pattern is that the step in the breakdown of the molecule can be followed consecutively [70].

3.3.6 Ultra-Violet Spectra

Some reaction products collected by HPLC had their U.V.-Vis. spectra recorded. The U.V.-Vis. spectrum was recorded on a Hewlett-Packard Diode Array Spectrophotometer.

The reaction products collected were placed into a special U.V.-Vis. Silica cell with a path length of 1cm and a width of 3mm. The blank used was a solution collected from the HPLC (running the gradient) at the same time as the product without any sample present.

3.4 PULSED IRRADIATION (HIGH ENERGY ELECTRONS)

Three types of accelerators were used throughout this report, a 1.3 MeV Van de Graaff accelerator located at the Australian Nuclear Science and Technology Organisation (ANSTO) scientific laboratories, a 4 MeV Linear Accelerator (LINAC) located at the Department of Chemistry, University of Auckland and a 20 MeV Linear Accelerator located at the Australian Radiation laboratory (ARL), Melbourne.

The Accelerator used for the majority of this work was the 1.3MeV Van de Graaff. This was retired towards the end of this project and the two LINAC's were used to complete the work.

3.4.1 Accelerator Set up

A schematic diagram of the apparatus used in the experiments is shown in Figure 3.01. The 1.3 MeV Van de Graaff accelerator was used to deliver an approximate 2.5 microsecond pulse of ionising radiation while the 4 MeV LINAC accelerator delivered a 200 ns pulse and the 20 MeV a 500 ns pulse. The electron beam was directed at a fused silica cell. A U.V.-Visible detector was set up perpendicular to the direction of the ionising radiation. The signal from the photomultiplier was passed to an electronic digitiser, providing the data in digital

² The number n, was dependent on the sample's signal to noise ratio as well as the amount of product collected. The term MS^n fragmentation is used throughout this report where multiple fragmentation steps were used.

form which was stored in the computer. The computer program "ELACC" was used to view the resultant data. Due to variations in the dose delivered between pulses, the error in all measurements is estimated to be 10%.

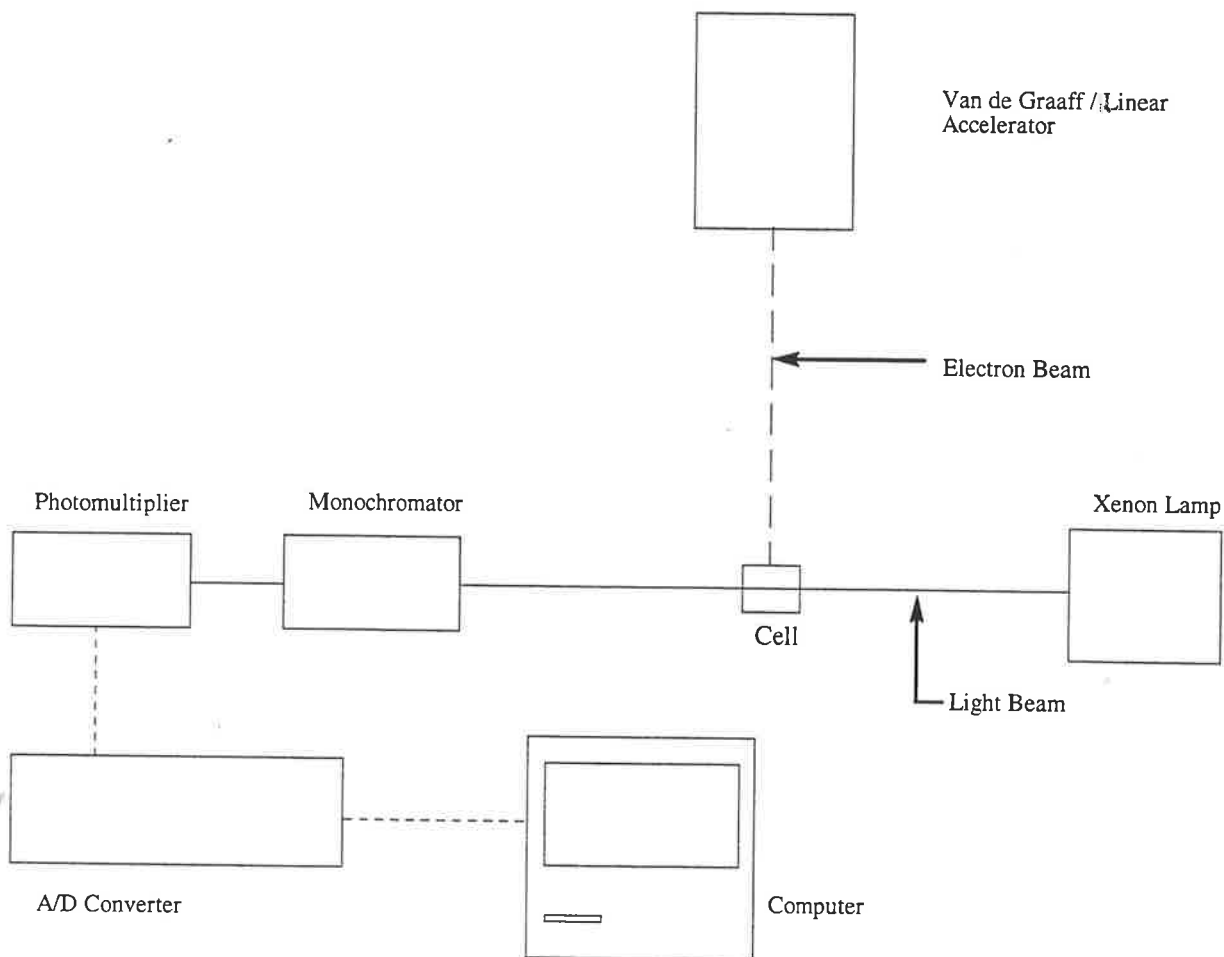


Figure 3.01. Schematic diagram of the apparatus used in the pulse radiolysis experiments used at ANSTO and ARL.

3.4.2 Pulse Radiolysis Studies

3.4.2.1 Transient Delta Absorbance spectra

To a clean dry 250 mL volumetric flask an appropriate amount of pesticide was added from a pre-dissolved stock solution. The flask was filled with approximately 150 mL of Milli-Q water. Additional reagents (if any) were added along with buffer (Phosphate 1×10^{-3} M), filled to the mark with Milli-Q water, saturated with the appropriate gas, and placed in the irradiation cell. The dose per pulse was varied between 10 to 23 Gray.

Experiments at low pH were repeated exactly, except HClO_4 was added to adjust the pH to 2.

3.4.2.2 Competition Kinetics

A series of solutions were prepared in which pesticide concentration was varied such that the ratio of the pesticide concentration to the SCN^- concentration ranged between 10 : 1 to 0.1 : 1 (the SCN^- concentration was kept constant throughout). These solutions were saturated with nitrous oxide and buffered with phosphate (pH 6.8) ($1 \times 10^{-3} \text{M}$) and the magnitude of absorption (due to $\text{SCN}_2^{\bullet -}$) measured at 480 nm. Dose rates employed were kept between 3.5 and 4 Gray per pulse (all data normalised to 4 Gray) to avoid the effect of secondary reactions.

The experiment was repeated at pH 2 using HClO_4 , the absorbance of $\text{SCN}_2^{\bullet -}$ was also redetermined at this wavelength, because of the lower G value of the hydroxyl radical formed due to the competing reaction of the hydrated electron with the hydrogen ion.

3.4.2.3 Determination of the pK_a of the transient radical

Buffered pesticide solutions were made up at different pH values using H_3PO_4 , KH_2PO_4 and K_2HPO_4 as the buffering reagents. An appropriate amount of stock pesticide was pipetted into a volumetric flask. This flask was filled to the mark with a buffer of appropriate pH. That solution was then saturated with N_2O and the magnitude of the absorption measured at a predetermined wavelength (Section 3.4.4.1). Small adjustments to pH were made using NaOH or HClO_4 with the final pH recorded using a pH meter. Dose rates employed were kept between 3.5 and 4 Gray per pulse (all data normalised to 4 Gray) to avoid the effect of secondary reactions.

3.4.2.4 Formation Kinetics

From a stock solution of pesticide a series of dilute solutions of the pesticide were made (1 to $10 \times 10^{-5} \text{M}$). Using the 200 ns pulse of the LINAC, the rate of formation of the radical being studied was monitored at a predetermined wavelength. The bimolecular rate constant was determined from the slope of a plot of the resulting pseudo first order rate constant against the concentration of the pesticide. Dose rates employed were kept between 3.5 and 4 Gray per pulse (all data normalised to 4 Gray) to avoid the effect of secondary reactions.

3.4.2.5 Decay Kinetics

Using a pesticide solution made up from section 3.4.2.1, the decay of the trace was fitted to both first and second order kinetics using the equations 3.01 and 3.02 respectively

[71]. Dose rates employed were kept between 3.5 and 4 Gray per pulse (all data normalised to 4 Gray) to avoid the effect of secondary reactions.

$$\ln \frac{A_0}{A} = kt \quad (3.01)$$

$$\frac{1}{A} = \frac{1}{A_0} + kt \quad (3.02)$$

t = time

A₀ = Absorbance at t=0

A = Absorption at t=x

k = rate constant

3.5 MATHEMATICAL TREATMENT OF DATA

3.5.1 Dosimetry

The following equations were used to determine the dose of the Cobalt 60 source and the Pulse Radiolysis apparatus. The concentration of the species was determined by ultra-violet spectrometry and Bragg's Law at the appropriate wavelength (Fe³⁺ at 304 nm for Cobalt 60 and (SCN)₂^{•-} at 480 nm for pulse radiolysis) after irradiation [51].

$$\text{Abs}_{(\text{Fe}^{3+} \text{ 304 nm}) / (\text{SCN}_2^{\bullet-} \text{ 480 nm})} = \epsilon_{(\text{Fe}^{3+} \text{ 304 nm}) / (\text{SCN}_2^{\bullet-} \text{ 480 nm})} * l * ([\text{Fe}^{3+}] / [\text{SCN}_2^{\bullet-}]) \quad (3.03)$$

The concentration of the ferric ion / SCN₂^{•-} was then used to determine the dose using equation 3.04.

The dose of radiation delivered can be determined by using equation 3.04.

$$\text{Dose (krad)} = \frac{1000 * [X] (mM)}{G(X) * \rho * 1.024} \quad (3.04)$$

where X = either Fe³⁺ or SCN₂^{•-}

G(X) = G Value of X (= 15.5 for the Frickie dosimetry)

ρ = density of the solution

The dose is converted into Grays by multiplying the dose (in krad) by ten.

$$\text{Dose (Gray)} = \text{Dose (krad)} * 10 \quad [52]$$

3.5.2 Competition Kinetics

The reaction of X^* with two compounds S_1 and S_2 can be summarised by the following equations (3.05 and 3.06).



The rates of formation of the P_1 and P_2 can be written as

$$\frac{d[P_1]}{dt} = k_1[X^*][S_1] \quad (3.07)$$

$$\frac{d[P_2]}{dt} = k_2[X^*][S_2] \quad (3.08)$$

Therefore

$$\frac{[P_2]}{[P_1]} = \frac{K_2[X^*][S_2]}{K_1[X^*][S_1]} \quad (3.09)$$

$$[X^*]_{\text{total}} = [P_1] + [P_2] \quad (3.10)$$

$$= [P_1]_0 \quad [P_1]_0 \text{ when } S_1 \text{ is present only}$$

Therefore

$$\frac{[P_1]_0 - [P_1]}{[P_1]} = \frac{k_2[S_2]}{k_1[S_1]}$$

and

$$\frac{1}{[P_1]} = \frac{1}{[P_1]_0} + \frac{k_2[S_2]}{k_1[S_1][P_1]_0} \quad (3.11)$$

and

$$\frac{[P_1]_0}{[P_1]} = 1 + \frac{k_2[S_2]}{K_1[S_1]} \quad (3.12)$$

Now

$$[P_1] = \frac{Abs_{[P_1]}}{\epsilon P_1} \quad \text{and} \quad [P_1]_0 = \frac{Abs_{[P_1]_0}}{\epsilon P_1}$$

Therefore

$$\frac{Abs_{[P_1]_0}}{Abs_{[P_1]}} = 1 + \frac{k_2[S_2]}{k_1[S_1]} \quad (3.13)$$

By varying the concentration ratio of S_1 to S_2 over a suitable range and monitoring the absorbance of P_1 , a plot of $\frac{Abs_{[P_1]_0}}{Abs_{[P_1]}}$ versus $\frac{k_2[S_2]}{k_1[S_1]}$ can be generated. The slope of the resulting

graph is $\frac{k_2}{k_1}$. If the rate constant of reaction 3.05 (k_1) is known, then the rate constant of reaction 3.06 (k_6) can be determined using the slope of the graph.

3.5.3 Molar Absorbance of transient species produced by Pulse Radiolysis

In pulse radiolysis there is no blank cell for the U.V.-Visible light. The blank instead is considered the ground state of the compound that is about to be irradiated. When determining the molar absorptivity of the transient species this absorbance of the ground state compound must be included in the calculation.

$$\epsilon_B = (\Delta\text{Abs}_t / Y_{bt}) + \epsilon_A \quad (3.14)$$

where ϵ_A is the molar absorbance of the parent compound

Y_{bt} is the yield of the radical (determined using the SCN^- dosimeter)

ΔAbs_t is the absorbance measured in pulse radiolysis.

3.6 COMPUTATIONAL CHEMISTRY METHODS

Compounds that were studied using this method had their structure generated using the MOLGEN program [72]. The structure was then optimised using the Gaussian 94 [73] suite of programs at the Hartree Fock level of theory with the basis set 6-31G**. The optimised structure of the starting compound was then submitted for a natural [74] population analysis. This type of analysis computes the charge distribution for the molecule. Since atomic charge indicates the estimate of total charge on each atom in the molecule, it should be considered arbitrary and not extrapolated from one molecule to another.

The optimised radical and the starting compound were submitted to the Spartan program [75] and a single point energy calculation run, followed by the generation of the *i*) Highest Occupied Molecular Orbital (HOMO), *ii*) Lowest Occupied Molecular Orbital (LUMO) or, *iii*) a spin density surface. The spin density surfaces can be used to describe the imbalance between the spin-up (α spin) and the spin down (β spin) electron distribution in open shell molecules. They provide information concerning the location of the unpaired electron in free radicals.

4.0 Radiation Chemistry of Aqueous Napropamide Solution

4.1 NAPROPAMIDE

Napropamide ((R,S)-N,N diethyl-2-(1-naphthyloxy) propionamide) (Figure 4.01) was initially developed at Western Research Centre of the Stauffer Chemical Company [76]. It is a white solid with a melting point of 74.8-75.7 °C. The maximum solubility of Napropamide in water is 73 mg/L [77].

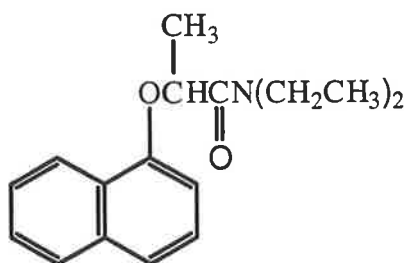


Figure 4.01. Chemical Structure of Napropamide.

Napropamide was released by ICI Crop Care as a herbicide for broad leaf and pre-emergence weed control. It is a selective herbicide which works by absorption into the roots inhibiting root development and growth. Napropamide consists of two optically active isomers. The D(-) isomer is used in the herbicide as it is 8 times more active than the L(+) isomer [78].

Napropamide is stable to both acidic and alkaline conditions. Photodegradation by direct photolysis has been shown to be the most important degradation pathway, with the products of this degradation being fully characterised [79]. Microbial degradation is limited in normal conditions [80].

4.2 REACTION OF NAPROPAMIDE WITH THE HYDROXYL RADICAL

Figure 4.02 shows the time resolved transient delta absorption (TDA) spectra obtained upon the pulse radiolysis of an aqueous Napropamide solution (1×10^{-4} M) saturated with nitrous oxide (pH 6.8, phosphate buffer). It exhibits an absorption band with a maximum at 330 nm. In the presence of *t*-butyl alcohol (0.1 M), an effective hydroxyl radical scavenger but a weak hydrogen atom scavenger, the absorption spectrum was considerably reduced. The high $G(\cdot\text{OH})$ yield and appreciable decrease in the transient absorption suggests that the

transient absorption spectrum in Figure 4.02 is due mainly to the reaction of the hydroxyl radical with Napropamide.

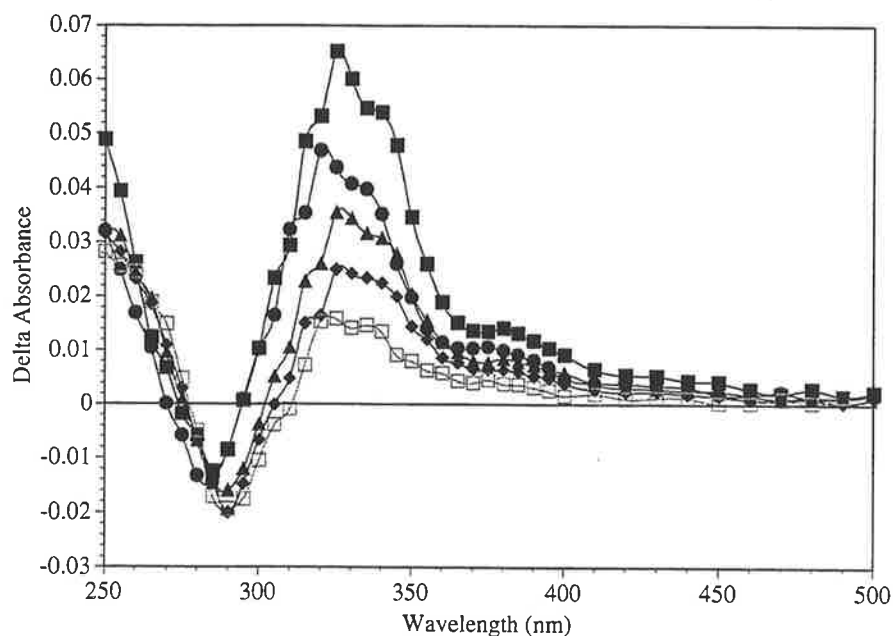


Figure 4.02. Time resolved transient delta absorbance (TDA) spectra obtained upon the pulse radiolysis of an aqueous Napropamide solution (1×10^{-4} M) saturated with nitrous oxide (pH 6.8, phosphate buffer). (■ Directly, ● 10 μ s, ▲ 20 μ s, ◆ 100 μ s and □ 500 μ s after the pulse).

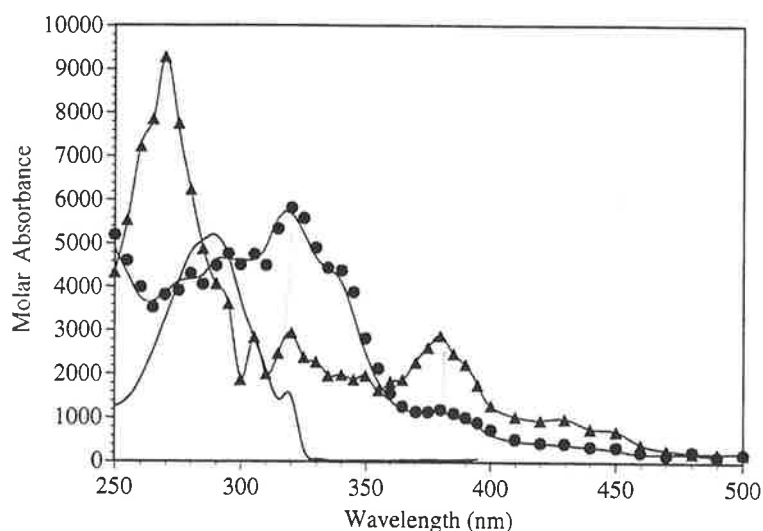


Figure 4.03. Molar absorbance spectra of Napropamide (solid line), and the transients arising from the reaction of Napropamide with hydroxyl radicals (● pH 6.8, ▲ pH 2).

As well as a maximum, the spectrum in Figure 4.02 possesses a minimum which contains a negative region between 270 to 290 nm. The negative absorption is due to Napropamide having a large ground state absorbance in this region (Figure 4.03). The TDA spectrum is corrected using equation 3.14 in chapter 3 and the assumption that the yield of hydroxyl radicals is equal to the yield of the transient radical (Figure 4.02). Since the yield of transient radicals is not known for certain, our results should not be over interpreted.

Reducing the radiation dose (and hence the amount of radical and transient) produced an increased half life of the transient species. The radical therefore decays by second order kinetics. When the curve was fitted to second order kinetics a decay rate of $2k/\epsilon l = 1.1 \times 10^5 \text{ s}^{-1}$ was obtained. Using the molar absorbance value given in Figure 4.03, it was determined that $2k = 6.6 \times 10^8 \text{ M}^{-1} \text{ s}^{-1}$. The transient therefore decays by a radical-radical mechanism to form products.

The ground state corrected spectrum (Figure 4.03) exhibits the same absorption maximum at 330 nm. The extinction coefficient of this maximum is $6000 \text{ M}^{-1} \text{ cm}^{-1}$.

The transient species arising from the reaction of Napropamide with hydroxyl radicals may be formed by one of three ways.

- 1) One electron oxidation to yield a radical cation $\text{Nap}^{\bullet+}$.
- 2) Hydroxyl radical addition to the aromatic rings.
- 3) Abstraction of a hydrogen atom from Napropamide.

The reaction of benzene and similar aromatic derivatives with hydroxyl radicals have characteristic absorbance in the region of 300 to 340 nm [81-94]. This reaction has been extensively studied and the resulting radical has been determined to be the OH-adduct. The transient produced by the reaction of Napropamide with the hydroxyl radical absorbs in the same region as the cyclohexadienyl type radicals, therefore the transient is assigned as a OH-adduct.

Adjustment of the ionic strength of the solution by addition of NaClO_4 (1 M) produces no change in the observed rate of decay of the transient. This implies the transient is neutral, as an increase in ionic strength would affect the rate of decay of a charged transient [95-97]. This is consistent with the OH-adduct, which would be neutral.

Competition kinetics produced a bimolecular rate constant determined for the reaction of the hydroxyl radical with Napropamide of $7.5 \times 10^9 \text{ M}^{-1} \text{ s}^{-1}$ (pH 6.8, phosphate buffer). The competitor chosen for the kinetic study was SCN^- ($k_{\text{OH}\cdot} + k_{\text{SCN}^-} = 1.1 \times 10^{10} \text{ M}^{-1} \text{ s}^{-1}$) [98]. The rate constant indicates that Napropamide reacts with hydroxyl radicals at close to diffusion controlled rates. The rate constant for the addition of the hydroxyl radical to Napropamide is similar to that observed for the addition of the hydroxyl radical to a Naphthalene ring, which has been reported as $9.4 \times 10^9 \text{ M}^{-1} \text{ s}^{-1}$ [99]. The similar rate constants obtained for the two compounds further supports the hypothesis that the reaction of the hydroxyl radical with

Napropamide results in a OH-adduct, since it is known that Naphthalene reacts with hydroxyl radicals to form this type of transient.

Steady state irradiation of an aqueous Napropamide solution (1.1×10^{-4} M) saturated with nitrous oxide using cobalt 60 produced a decrease in the absorbance due to Napropamide at 288 nm (Figure 4.04). The decrease of the absorbance at 288 nm was less than expected for the dose of radiation. Therefore the compounds produced by this reaction must also absorb in the 288 nm region. Likewise it can also be observed that the products absorb in the region around 254 nm.

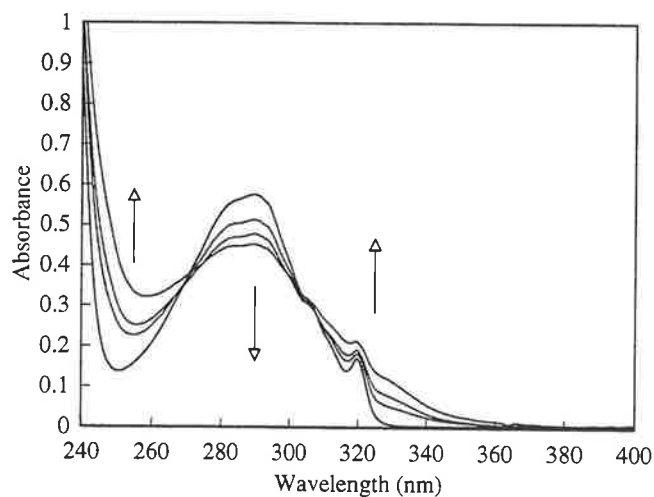


Figure 4.04. Observed change in the optical absorbance of an aqueous Napropamide solution (1.1×10^{-4} M) saturated with nitrous oxide and irradiated with gamma irradiation (0 to 200 Gray). Arrows indicate the direction of absorbance change with radiation dose. Dose rate 80 Gray/hr.

High Performance Liquid Chromatography (HPLC) of the resulting irradiated solution revealed the formation of new products and the decrease in the concentration of Napropamide (Figure 4.05). The products showed small absorbance at 288 nm and larger absorbance at 254 nm. Eight major products (A to H) were observed in the chromatogram, along with other minor products, all of which except one had retention time less than that of Napropamide. This makes the products more polar than Napropamide, since the C_8 column releases compounds according to their polarity. This result is consistent with the addition of a hydroxyl group to the parent compound as the products of this type of reaction are expected to be more polar. Re-running the solution using a steep acetonitrile gradient to ensure any non-polar compounds are eluted off the column produced no other peaks in the HPLC trace, suggesting dimer formation was not occurring. Merga *et al.* [100] reported that the formation of hydroxylated products was not as favourable as dimer formation for chlorobenzene. This phenomenon is not observed in our experiments. The discrepancy in our results may be due

to the low dose rate employed in the experiment when compared to Merga *et al.* (one tenth the dose rate) [100].

The area of the products formed at 254 nm does not equal the decrease in Napropamide concentration. The G value for the loss of Napropamide (after 20% of Napropamide had reacted) is 6.1. This value is greater than the G value of the hydroxyl radical. If second order reaction kinetics are controlling the decay of the OH-adduct to form hydroxylated derivatives then a G value of approximately 2.8 would be expected for the loss of Napropamide. The result suggests that the transient formed is reacting through a pseudo first order mechanism with Napropamide. This reaction transpires because steady state irradiation produces a concentration of the transient that is many orders of magnitude less than the pulse radiolysis study. This effectively allows the pseudo first order reaction between the transient and Napropamide to compete with the second order radical-radical reaction. The result of the pseudo first order reaction is high molecular weight compounds that do not elute off the column readily.

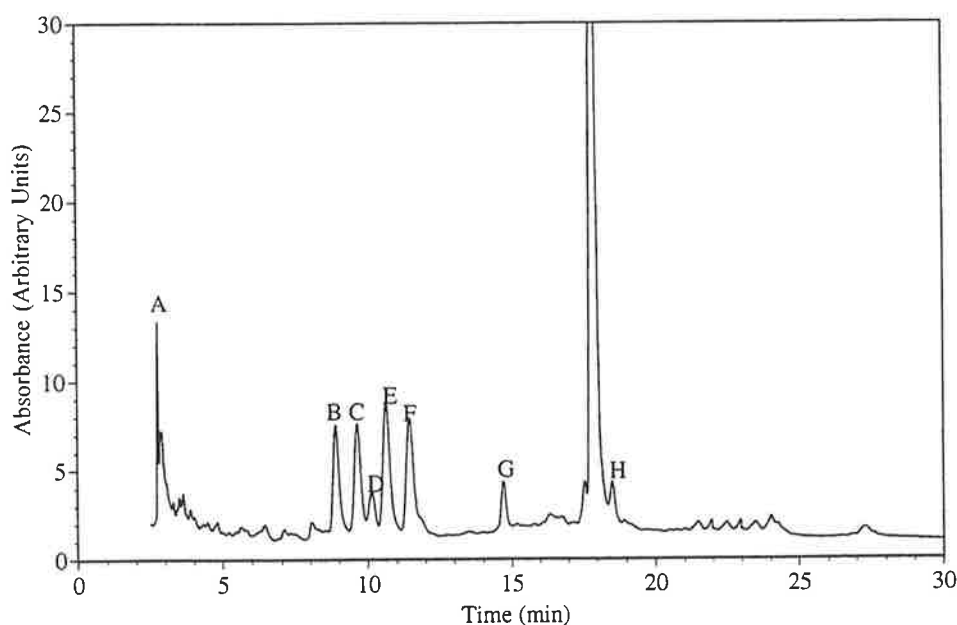


Figure 4.05. HPLC analysis following the gamma irradiation of a Napropamide (1×10^{-4} M) solution saturated with nitrous oxide. The trace displays the products formed from the reaction of Napropamide with hydroxyl radicals (A to H). See Figure 4.07 for compound identification.

The rate of Napropamide loss was linear against the concentration of hydroxyl radicals added to the system (calculated using Frickie Dosimetry) until approximately 30% of Napropamide had reacted (Figure 4.08). The appearance of the products (Figure 4.08) was also observed to be linear. The loss of linearity after approximately 30% of the Napropamide had disappeared indicates that products of the first reaction also react with the hydroxyl

radical. This information is important when considering the practical applications of radiation mediated decay. To ensure recently formed compounds do not inflict more damage than the original pesticide the reaction must continue until base compounds are formed. The reaction of the initial products confirms that the degradation process is continuing.

The structures of the products observed in this trace were determined by electrospray mass spectrometry and are recorded in Figure 4.07. When Napropamide is fragmented with a collision gas inside the ion trap of the electrospray (MS^2) it showed a loss of 73 Daltons (NEt_2), further collisions (MS^3) with this daughter ion produce another loss of 28 Daltons (CO), and then a further loss of 28 Daltons (HCH_3) (Figure 4.06). The radiation products B to F all produced the same 288 Daltons parent ion. This corresponds to the addition of an oxygen atom to the parent molecule Napropamide. Fragmentation of the parent ion produced the same loss of 73, followed by 28, then another 28 Daltons, as Napropamide. Since the Napropamide fragmentation resulted in the loss of the chain attached to the aromatic ring, the addition of the oxygen in the steady state irradiation must be attached to the ring since it produced the same loss of the chain.

The compound G showed a mass to charge ratio ($M+H$) of 244 Daltons. This mass to charge ratio is effectively the replacement of one ethyl group with a hydrogen atom from the starting compound Napropamide. MS^2 fragmentation of this compound produced daughter ions at 199 and 171 Daltons, the same as the fragmentation products as observed for Napropamide. This product must be Napropamide with a hydrogen replacing an ethyl group on the amide.

Formation of the compounds B to F would occur through the disproportionation reaction of the cyclohexadienyl transients to generate the observed product and a Napropamide molecule. Compound G's formation will be discussed in section 4.3.

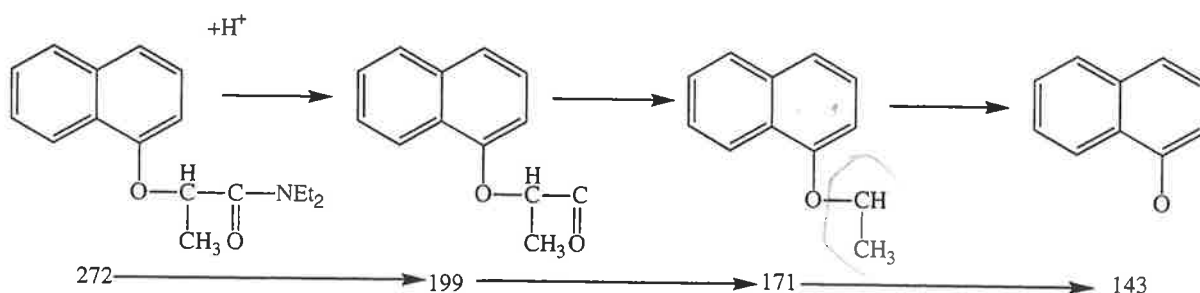


Figure 4.06. MS^4 fragmentation of Napropamide using an electrospray mass spectrometer.

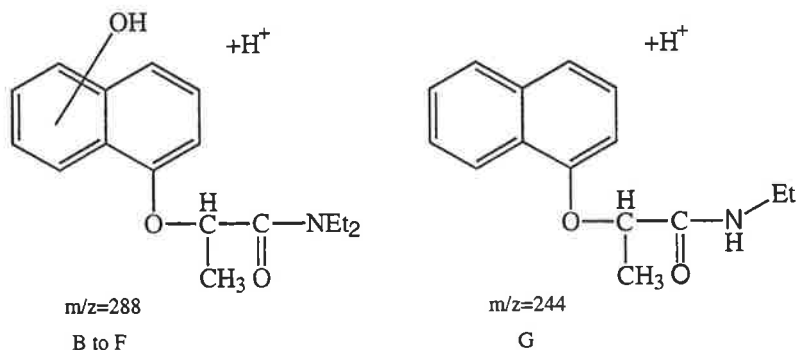


Figure 4.07. Products (B to G) of the gamma radiolysis of an aqueous Napropamide in nitrous oxide saturated solution as determined by the analysis of electrospray mass spectrometric fragmentation data. Location of the hydroxyl groups are not unambiguously assignable in structures B to F. See text for discussion.

The exact position of the addition of the hydroxyl radical to the naphthalene ring could not be determined from the mass spectral data. The hydroxyl radical is electrophilic in nature and therefore will react at the site of greatest electron density in the ring. Schuler *et al.* [101] observed that hydroxyl radicals react with biphenyl at the electron rich ortho and para sites in preference to the electron poor meta site. *Ab initio* calculations were used to analyse the structure of the Napropamide molecule using natural population analysis. The calculations assign a charge to each atom in the molecule relative to every other atom in the system. The full results of these calculations are recorded in appendix 1. As would be expected, the smallest electron density on the ring carbons is on the carbons next to the oxygen. The most electron dense carbons are those which are ortho or para to the electron donating oxygen. It is suspected that the hydroxyl addition will occur here.

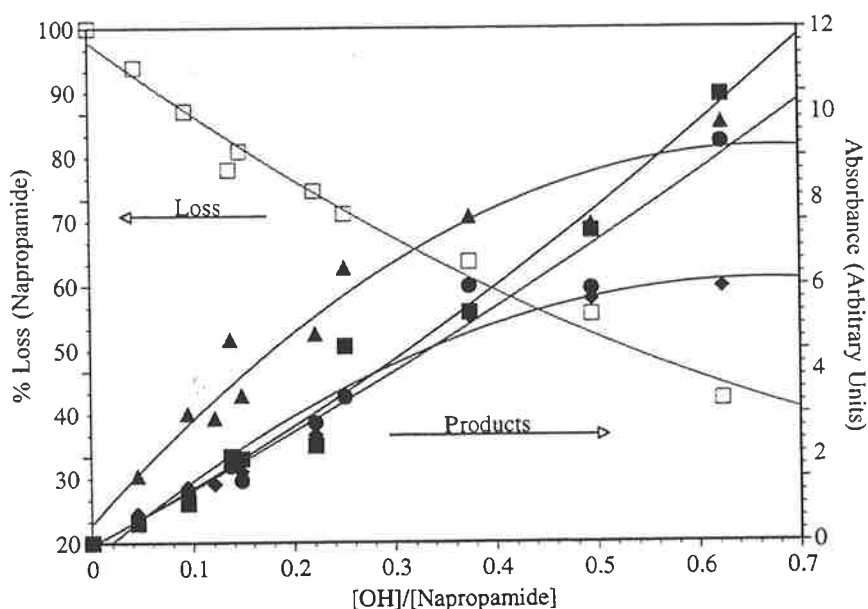


Figure 4.08. Loss of Napropamide (left axis) and the formation of products (right axis) from the gamma irradiation of aqueous Napropamide solution (1×10^{-4} M) saturated with nitrous oxide, determined by HPLC. Products are B=■, C=●, E=◆, F=□. *solid*

4.3 REACTION OF NAPROPAMIDE WITH THE HYDROXYL RADICAL IN ACIDIC SOLUTION

The TDA spectrum obtained from the pulse radiolysis of Napropamide (1×10^{-4} M) in acidic solution (pH 2, HClO_4) saturated with nitrous oxide can be observed to be different from the spectrum recorded at neutral pH (Figure 4.09). Displayed also is the spectrum after the contributing effects of the hydrogen atom are subtracted. Comparison of the effect of pH on the transient species is shown more effectively in the molar absorbance spectra (Figure 4.03) because it takes into account the lower G value of the hydroxyl radical at pH 2 and the effect of the hydrogen atom. From these figures the transient produced by the reaction of Napropamide with hydroxyl radical at pH 2 cannot be assigned to the same transient produced by the neutral pH reaction.

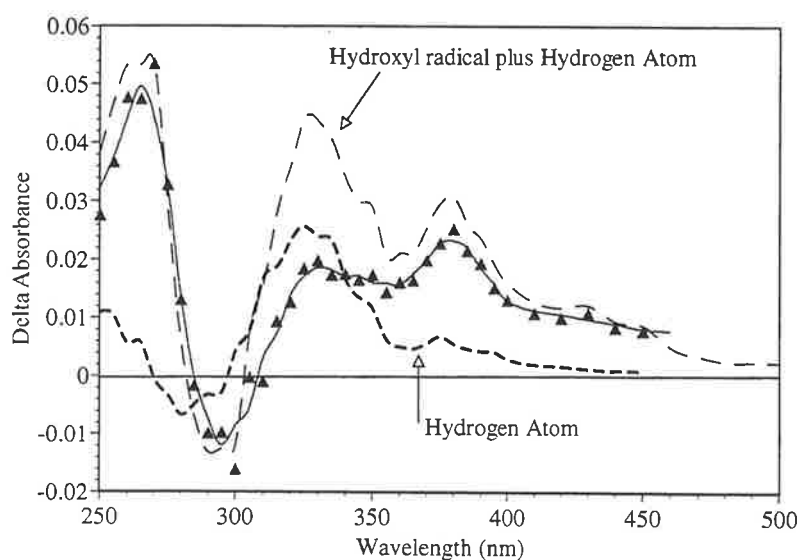


Figure 4.09. TDA spectra obtained upon the pulse radiolysis of an aqueous Napropamide solution (1×10^{-4} M) saturated with nitrous oxide (pH 2, HClO_4). (\blacktriangle Directly after the pulse and corrected for the absorbance of the hydrogen atoms absorbance). Dotted lines are of the absorbance of the hydrogen atom (see figure 4.27) and the combined absorbance of the hydroxyl radical and the hydrogen atom.

A plot of absorbance versus pH at 375 nm is shown in Figure 4.10. This gives a pK_a for the radical of 2.2. The behaviour of the absorbance at 375 nm indicates the transient can be protonated at low pH. Since this acid-base equilibria does not occur for Napropamide, it can be concluded that this is a property of the radical. The differences in the TDA spectra observed could be due to the rapid transformation of this transient species to a radical cation. This reaction requires a large concentration of hydrogen ions to be present and results in the addition of a hydrogen atom and the elimination of a water molecule from the transient species.

The rate constant for the reaction of Napropamide with the hydroxyl radical at pH 2 was determined using the competition kinetics technique to be $7.5 \times 10^9 \text{ M}^{-1} \text{ s}^{-1}$. This is the same rate constant reported at neutral pH. This was expected since Napropamide remains neutral at pH 2. The absence of any change in the rate constant for the reaction is consistent with the hydroxyl radical adding to the ring, and the resulting transient undergoing protonation to produce the spectrum shown in Figure 4.09.

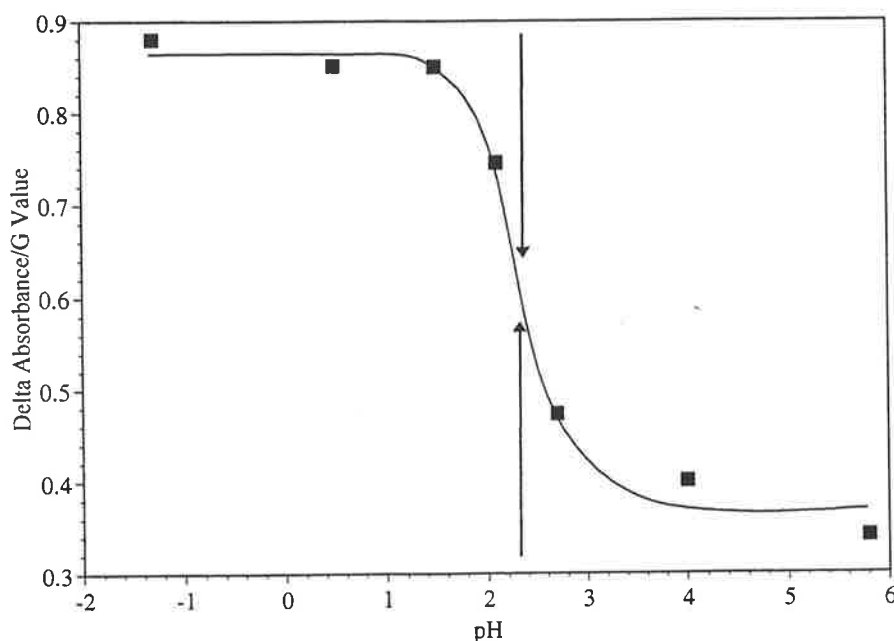


Figure 4.10. Variation of the transient absorbance with solution pH of aqueous Napropamide solution ($1 \times 10^{-4} \text{ M}$) saturated with nitrous oxide (pH adjusted using phosphate buffers and HClO_4). Data is fitted with a curve of best fit. Data were measured at 375 nm. $\text{pK}_a(375 \text{ nm}) = 2.2$. Arrows indicate the inflection point.

Gamma irradiation coupled with HPLC of a Napropamide ($1 \times 10^{-4} \text{ M}$) solution saturated with nitrous oxide at pH 2 (HClO_4) revealed that only one compound was formed, when Napropamide was reacted at low pH (pH 2, HClO_4) (Figure 4.12). This product is one of the minor species (G, Figure 4.05) formed in the reaction of hydroxyl radicals with Napropamide at neutral pH. The same retention time of the compound in this reaction suggests that it is the same as compound G of Figure 4.05. Electrospray mass spectrometry confirms that the two products are the same by producing the same mass to charge ratio and fragmentation pattern.

The product formed by the reaction of the hydroxyl radical at pH 2 would suggest that the electrophilic addition of the hydroxyl radical to the aromatic ring is not as favourable as the abstraction of hydrogen from the CH_2 group on the amide. Considering the previous evidence of similar rate constants for the reaction of the hydroxyl radical with Napropamide at neutral and low pH, the hydroxyl radical must react to form a OH-adduct which then forms a

radical cation and then the observed product. Radical cations have previously been studied using halogenated benzene compounds. It is known from these studies that radical cations are powerful one electron oxidants, removing electrons from halide ions [86-88, 90]. Without the presence of any other compounds it is possible that intramolecular electron transfer takes place, leading to the formation of the species observed in the HPLC chromatogram (Figure 4.11).

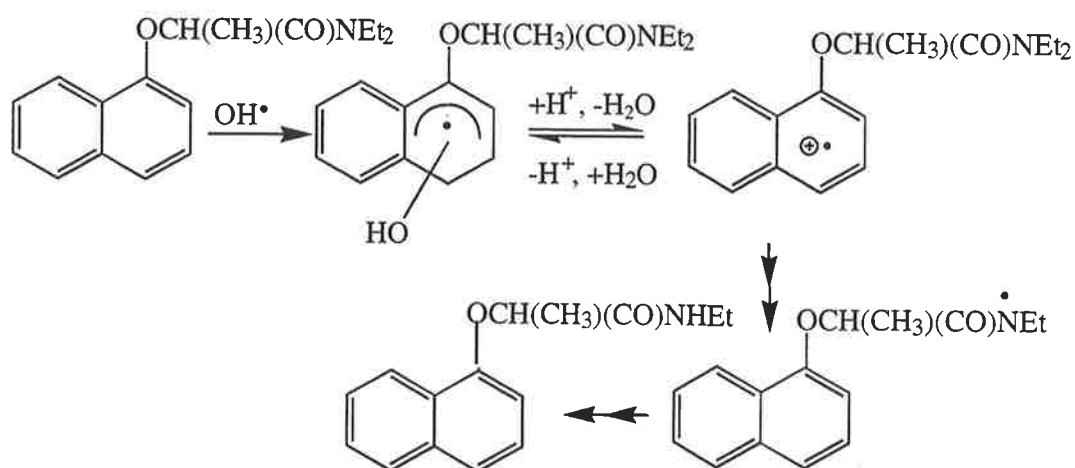


Figure 4.11. Proposed scheme for the reaction of hydroxyl radicals with Napropamide at pH 2. See text for discussion.

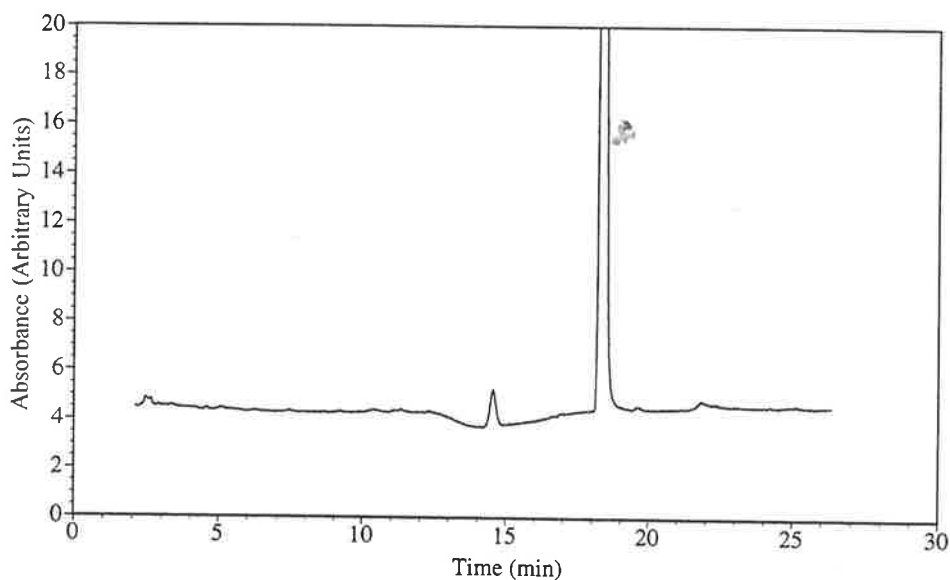


Figure 4.12. HPLC analysis following the gamma irradiation of a Napropamide (1×10^{-4} M) solution saturated with nitrous oxide at pH 2 (HClO_4). The trace displays the product formed from the reaction of Napropamide with hydroxyl radicals at pH 2. See Figure 4.07 for the compound identification.

A plot of the peak area at 15 minutes versus the pH was attempted between the pH values of 1.4 and 6. The results of this experiment indicated that the product had not fully

formed at the lowest pH, with a sharp increase in the area starting at pH 2.5. The increase in pH had not levelled off by pH 1.4 and lower pH values could not be tested due to the damage a solution of this type would inflict on the HPLC column. While this experiment failed to produce a result which could be compared to the pulse radiolysis pK_a , it does indicate that the pK_a of the product is in the same region.

4.4 REACTION OF NAPROPAMIDE WITH THE HYDROXYL RADICAL IN THE PRESENCE OF OXYGEN

The TDA spectrum obtained upon the pulse radiolysis of Napropamide (1×10^{-4} M) saturated with nitrous oxide/oxygen (4:1 v/v) is shown in Figure 4.13. The TDA spectrum appears similar to that observed in Figure 4.02, except that the absorbance was approximately half. Comparison of the decay rates of the transient species indicated a change from second order kinetics to initial first order kinetics (Figure 4.14). This indicates that transients produced by the reaction of Napropamide with the hydroxyl radical react with oxygen through initial pseudo first order kinetics. This is consistent with the OH-adduct mechanism as carbon centred radicals are known to react rapidly with oxygen [48, 82, 84, 102, 103]. The transient produced by the reaction of hydroxyl radicals with Naphthalene has also been observed to undergo a reaction with oxygen. The transient produced a similar TDA spectrum to that of the de-oxygenated solution.

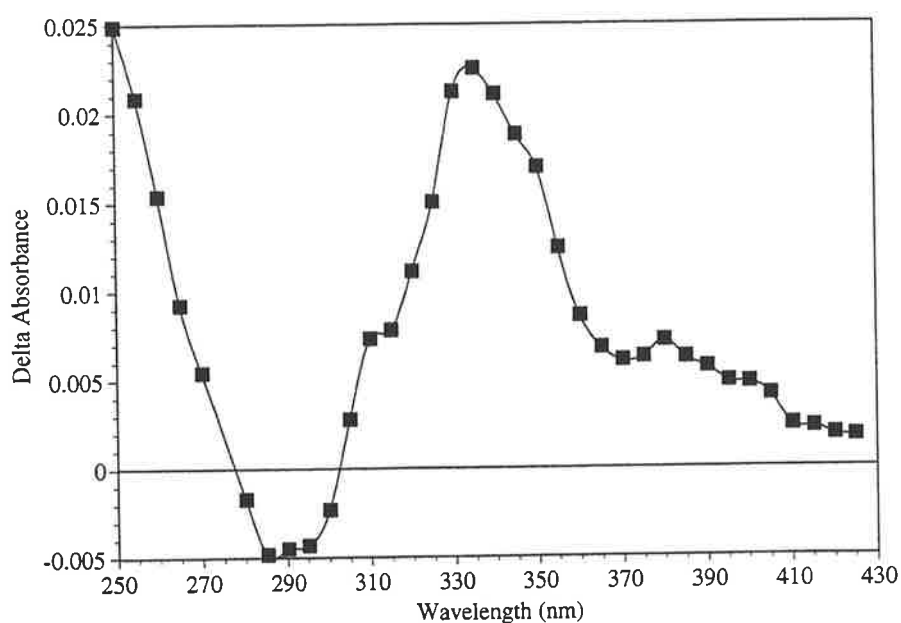


Figure 4.13. TDA spectrum obtained from the pulse radiolysis of an aqueous Napropamide (1×10^{-4} M) solution saturated with nitrous oxide/oxygen (4:1 v/v) at pH 6.8 (phosphate buffer). Spectrum recorded 10 μ s after the pulse.

The inset of Figure 4.15 shows the change in the ultra violet spectrum obtained upon gamma irradiation of an aqueous nitrous oxide/oxygen saturated solution containing Napropamide (1×10^{-4} M). The change in spectra can be observed to be different from that observed for the de-oxygenated system. This spectrum indicates a large loss at 288 nm and a large increase in absorption at 250 nm. The HPLC chromatogram of the same solution was observed to be different from the trace for the de-oxygenated solution (Figure 4.15).

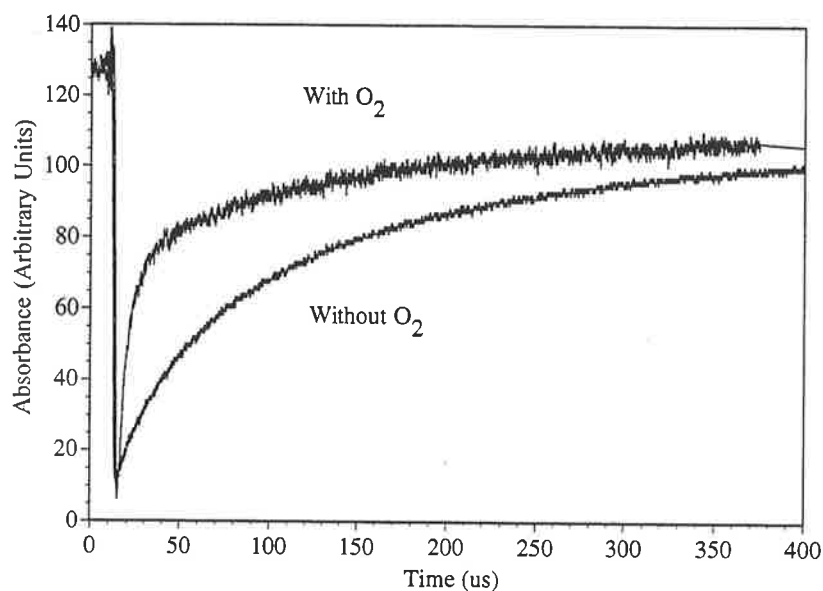


Figure 4.14. Comparison of the pulse radiolysis traces obtained from a solution of Napropamide (1×10^{-4} M) saturated with nitrous oxide and nitrous oxide/oxygen (4:1 v/v). Absorbance data were collected at 330 nm. Traces are normalised. Both radiation pulses are $2.5 \mu\text{s}$ long with dose of 10.4 Grays per pulse.

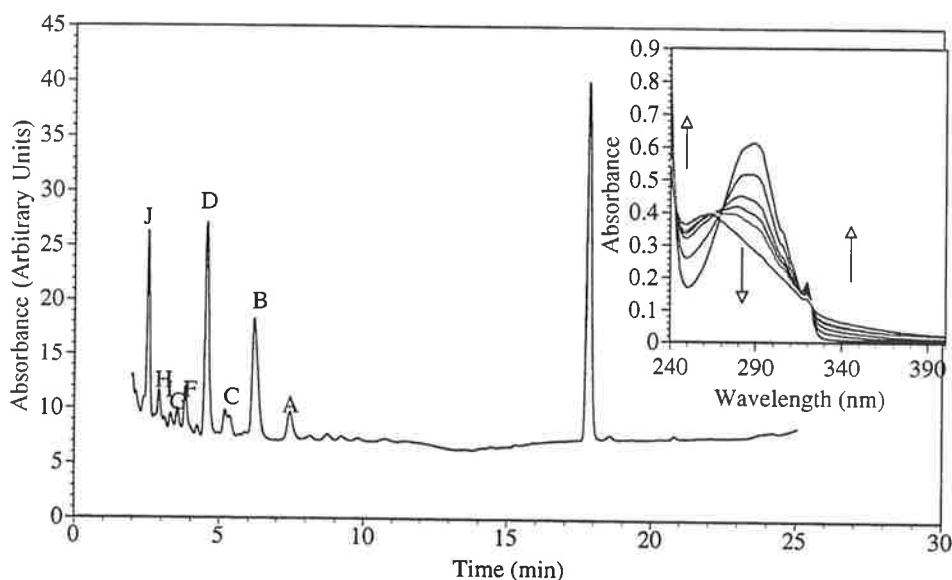


Figure 4.15. HPLC analysis following gamma irradiation of an aqueous nitrous oxide/oxygen saturated solution containing Napropamide (1×10^{-4} M). Product's identity displayed in Figure 4.16. Inset shows the observed change in absorbance of the same solution (0 to 240 Gray). Arrows indicate the direction of absorbance change with radiation dose. Dose rate 80 Gray/hr.

The area for the products is consistent with the observed change for the U.V. spectrum at 254 nm. This result is in agreement with the hypothesis postulated in section 4.2, that is, a pseudo first order reaction is transpiring between the OH-adduct and Napropamide in deoxygenated solution. The transient reacts faster with oxygen than it does with Napropamide to form compounds which are more polar than those postulated in section 4.2 for the pseudo first order reaction between the OH-adduct and Napropamide, thus all the products are detected in this trace.

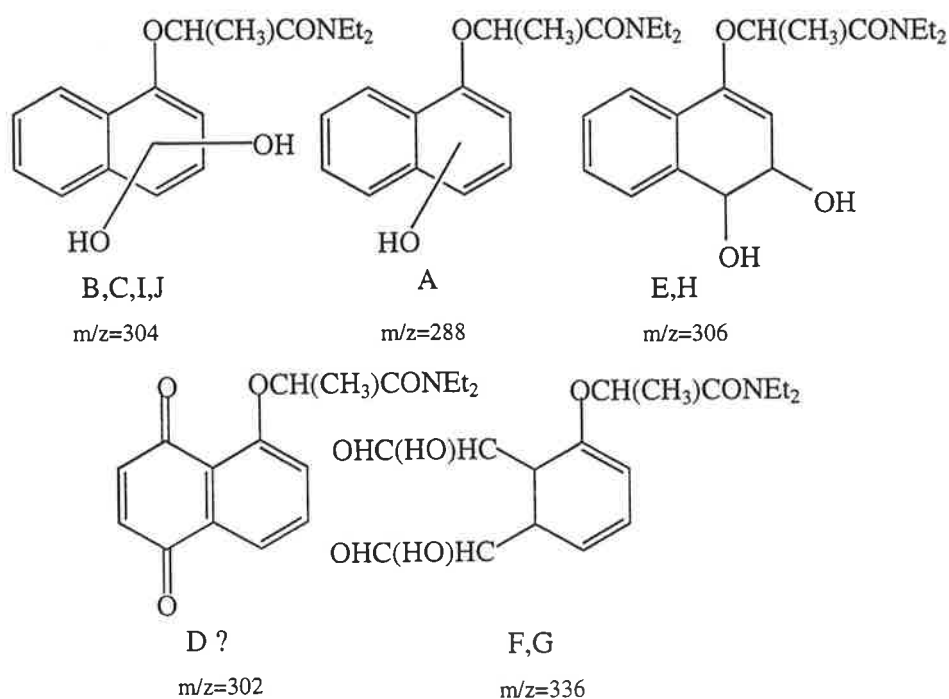


Figure 4.16. Compounds (A to J) of the gamma radiolysis of an aqueous Napropamide (1×10^{-4} M) solution saturated with nitrous oxide/oxygen as determined by the analysis of electrospray mass spectrometric fragmentation data. Location of the new functional groups are not unambiguously assignable in structures A to J. See text for discussion.

Collection of the products allowed for determination of the compounds observed in Figure 4.16 using electrospray mass spectrometry and the MS^n techniques.

Products of the reaction of benzene with hydroxyl radicals in the presence of oxygen have been studied previously by Pan *et al.* [82]. Compounds A To C and E to J are derivatives similar to those observed in the Pan *et al.* study. Product D's mass to charge ratio (302 Daltons) equated to the addition of two oxygen atoms and the loss of two hydrogen atoms from the starting compound Napropamide. This type of compound has not previously been observed, possibly equating to either epoxide or carbonyl formation. Mass spectral data did not allow for exact determination. The Pan *et al.* study also showed a number of compounds which resulted in fragmentation of the ring. This was not observed to the same

extent in the current study. Two reasons for the observed difference in the results is postulated. The first is that the fused ring system of the Naphthalene does not allow for the correct positioning for the attachment of the second O₂ such that the ring can fragment. Secondly, it is also possible that these fragmentation products are forming, but do not absorb at 254 nm, and are therefore are not detected by the HPLC detector.

4.5 REACTION OF NAPROPAMIDE WITH ONE ELECTRON OXIDANTS

The dichloride radical anion formed in the pulse radiolysis of oxygen saturated sodium chloride (0.02 M), Napropamide solution (2×10^{-4} M) at pH 2 (HClO₄) reacts as a strong one electron oxidant with a redox potential of 2.09 V (versus NHE) [43]. The reaction of the dichloride radical anion with Napropamide was studied by following the decay of the dichloride radical anion absorption band at 340 nm. It was observed that in the presence of Napropamide (2×10^{-4} M) this band decayed faster and by first order kinetics instead of second order kinetics (Figure 4.17).

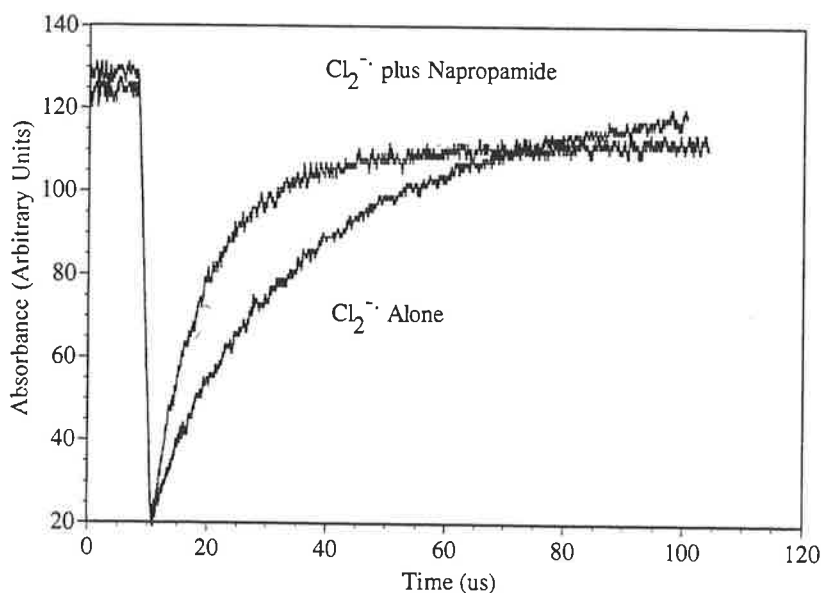
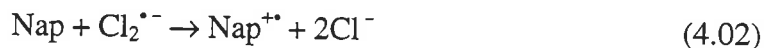


Figure 4.17. Comparison of the pulse radiolysis traces produced at 340 nm, with and without the presence of Napropamide (2×10^{-4} M) in an oxygen saturated solution of NaCl (0.02 M) solution (pH 2, HClO₄), indicating that a reaction between the dichloride radical anion and Napropamide had occurred.

This indicates that the following reaction has taken place.



The bimolecular rate constant was determined to be $8.3 \times 10^8 \text{ M}^{-1}\text{s}^{-1}$ from the slope of a plot of the pseudo first order rate constant against the concentration of Napropamide (5 to

20×10^{-5} M). Time resolved studies initially produced a broad absorption with λ_{\max} at 340 nm due to the formation of the dichloride radical anion. Using the pseudo first order rate constant it was determined that twenty microseconds after the pulse more than 90% of the dichloride radical anion had reacted with the Napropamide, and thus the spectrum showed is mainly due to the transient of this reaction. The spectrum exhibited a peak at 380 nm (Figure 4.18) and while different to that observed in Figure 4.09, does produce the same maximum for the transient produced by the hydroxyl radicals reaction with Napropamide. It is therefore possible to assign the spectrum to the same transient produced by the hydroxyl radical and Napropamide at pH 2. The spectrum must therefore be due to the radical cation.

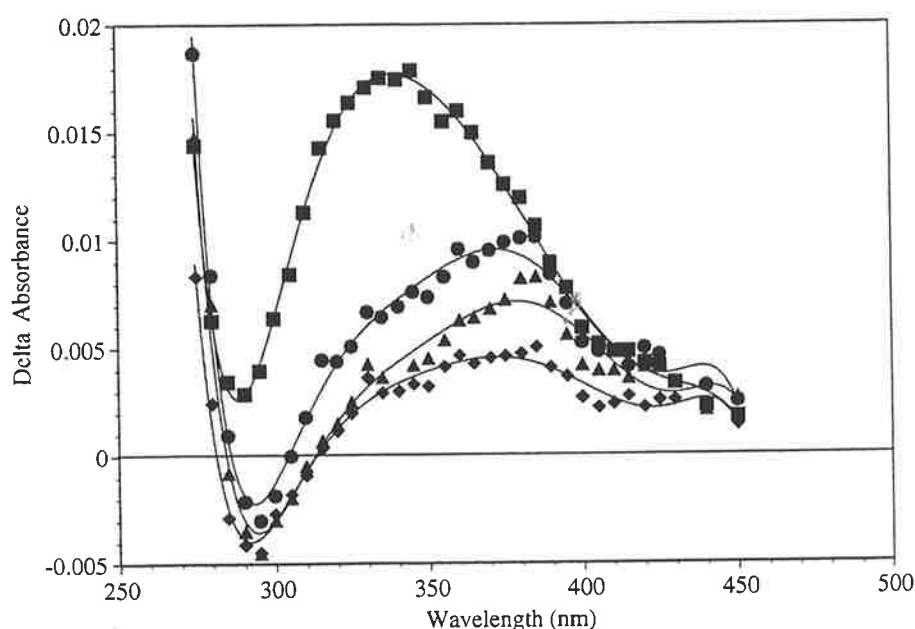


Figure 4.18. Time resolved TDA spectra obtained upon pulse radiolysis of an aqueous Napropamide solution (2×10^{-4} M), with 0.02 M Chloride ion, saturated with oxygen at pH 2 (HClO_4). (■ Directly after the pulse, ● $10 \mu\text{s}$, ▲ $20 \mu\text{s}$, ◆ $50 \mu\text{s}$).

A HPLC chromatogram of the steady state irradiated solution of Napropamide (1×10^{-4} M) and sodium chloride (0.02 M) at pH 2 saturated with nitrous oxide showed the formation of several compounds (Figure 4.20). One compound is detected at 14.5 minutes, the same retention time as observed for the hydroxyl radical's major product at low pH.

Studies of the reactions of other radical anions such as the sulfate, dibromide, thiosulfate radical anions with Napropamide were also conducted. The transient absorption spectra resulting from these reactions is shown in Figure 4.19. The graphs display the spectra recorded after at least 90% of the radical anion has reacted (determined from the pseudo first order decay rate). It is observed that the spectra resulting from the reaction with the dichloride and sulfate radical anions appear similar. The dichloride radical anion shows an absorbance

less than the sulfate radical anion. This is due to a lower G value for dichloride radical anion (2.8) [52] than the sulfate radical anion (3.3) [43]. This suggests the two transient species are similar. The dibromide radical anion produced a TDA spectrum different to that shown by the other two radicals, suggesting the formation of another radical species. The reaction of the dibromide radical anions is a lot slower than the other two radical reactions (Table 4.01). The transients produced may be decaying while the reaction with the dibromide radical anion is still occurring. This would lead to a situation where the full absorbance of the transient is not observed. The bimolecular rate constant for each of the other reactions of the radical anions was determined by a plot of the pseudo first order rate constant against the concentration of Napropamide. As expected the bimolecular rate constant decreases with the oxidising power of the radical anion.

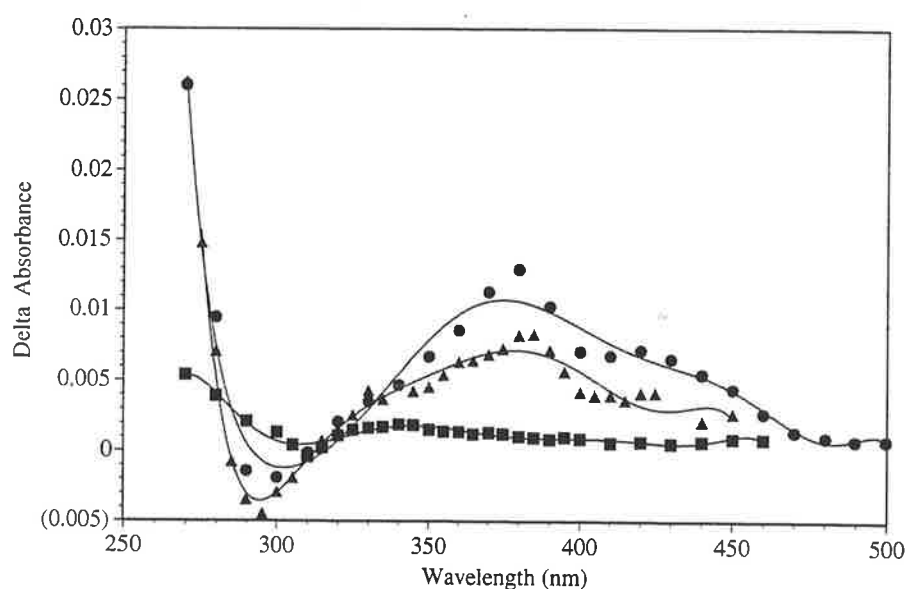


Figure 4.19. TDA spectra recorded for the reaction of Napropamide (2×10^{-4} M) with \blacksquare $\text{Br}_2^{\bullet-}$ (150 μs), \bullet $\text{SO}_4^{\bullet-}$ (10 μs), \blacktriangle $\text{Cl}_2^{\bullet-}$ (20 μs). Experimental conditions are as follows: $\text{Br}_2^{\bullet-}$; pH 6.8, 0.02 M NaBr, oxygen saturated. $\text{SO}_4^{\bullet-}$; pH 6.8, 0.02 M $\text{S}_2\text{O}_8^{2-}$, 0.1 M *t*-butyl alcohol, nitrogen saturated. $\text{Cl}_2^{\bullet-}$; pH 2, 0.02 M NaCl, oxygen saturated.

Radical	pH	Rate of reaction with Napropamide ($\text{M}^{-1}\text{s}^{-1}$)	Wavelength of Determination (nm)
$\text{Cl}_2^{\bullet-}$	2.0	8.3×10^8	340
$\text{SO}_4^{\bullet-}$	6.8	1.9×10^9	460
$\text{Br}_2^{\bullet-}$	6.8	7.2×10^7	360

Table 7.01. Bimolecular rate constants determined for the reaction of Napropamide with one electron oxidants. Rates were determined from the slope of a plot of the pseudo first order rate constant against the concentration of Napropamide (50 to 200 μM).

Unlike the dichloride radical anion the sulfate and dibromide radical anion can both be readily formed at neutral pH. The TDA spectra of both radicals at pH 2 (HClO_4) correlated with their spectra recorded at neutral pH. This implies that the one electron transfer reaction from the radical anions to Napropamide is pH independent between pH 2 and pH 7.

Napropamide was also reacted with the thiosulfate radical anion, azide radical and the diiodide radical anions but no increase in the decay rates of these radicals was observed. Time resolved studies indicated that there were no new absorbance maxima present between 250 nm and 500 nm. The dibromide radical anion has a redox potential of 1.77 V (versus NHE) [43] while the thiosulfate radical anion and the azide radical anion have redox potential's of 1.3 and 1.4 V respectively [67, 104, 105]. Since Napropamide reacts with the dibromide radical anion and not the thiosulfate radical anion or the azide radical anion the redox potential for the $\text{Nap}^{\bullet+}/\text{Nap}$ couple in reaction 4.03 must be between 1.77 and 1.4 V (versus NHE).



HPLC traces resulting from the reactions of the dibromide radical anion and sulfate radical anion with Napropamide after gamma irradiation are recorded in Figure 4.20.

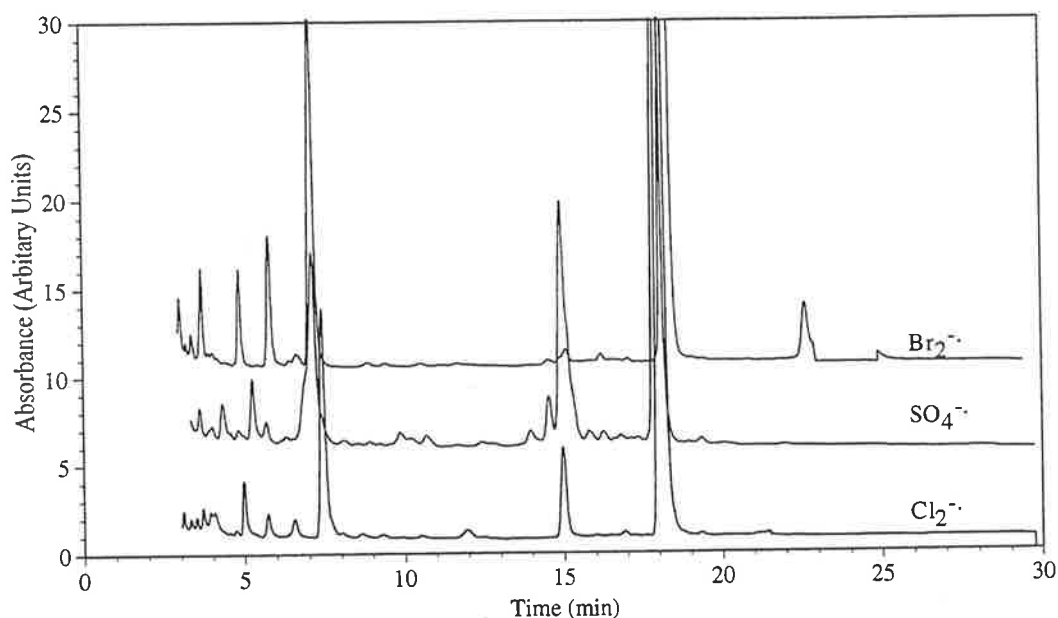


Figure 4.20. HPLC chromatograms recorded for the reaction of dichloride, dibromide and the sulfate radical anions with Napropamide (1×10^{-4} M). Experimental conditions are as follows: $\text{Br}_2^{\bullet-}$; pH 6.8, 0.02 M NaBr, oxygen saturated. $\text{SO}_4^{\bullet-}$; pH 6.8, 0.02 M $\text{S}_2\text{O}_8^=$, 0.1 M *t*-butyl alcohol, nitrogen saturated. $\text{Cl}_2^{\bullet-}$; pH 2, 0.02 M NaCl, oxygen saturated. The traces display the compounds formed from the reaction of Napropamide with the radical anions. See text for discussion on the identification of specific products.

The product distribution of the dichloride and sulfate radical anions produce two compounds of similar retention time. The dibromide radical anion, however, produces one species which corresponds to the dichloride and sulfate radical anions, but the other major product (15 minutes) is missing. In its place several other compounds are observed, including one at a retention time longer than that of Napropamide.

Mass spectral analysis of the compounds produced in the one electron oxidation reaction indicates that the sulfate radical anion's and dichloride radical anion's peak at 15 minutes were two different compounds. The 15 minute compound for the dichloride radical anion had a parent ion of 244, while the sulfate radical anion had a parent ion of 326 Daltons. The dichloride radical anion produced the compound observed at 15 minutes from the hydroxyl radical at low pH. The fragmentation pattern of the parent ion also produced the same daughter ions as the pH 2 hydroxyl radical experiment. Since it was postulated that this transient proceeded through a radical cation to form the end species and dichloride radical anions initially form this transient anyway, the formation of this compound is not surprising. The major product in the dichloride radical anion reaction at 7.5 minutes had a parent ion of 226 Daltons which is 46 Daltons less than the starting compound. No fragmentation could be obtained on this compound and a structure could not be assigned. The minor peak at 5 minutes did not produce a parent ion that could be distinguished from the base line.

The major peak in the HPLC trace for the reaction of the dibromide radical anion was observed at 7 minutes and had a parent ion of 226 Daltons suggesting that it was a similar (or the same) compound as that observed for the equivalent peak in the dichloride radical anion. The compounds at 4.5 and 6 minutes had parent ions of 226 and 324 Daltons respectively. While the compound with the parent ion of 226 Daltons did not undergo any observable fragmentation, the 324 Daltons parent ion did. Two daughter ions were observed using MS² fragmentation at 237 and 197 Daltons. Since the parent ion is 54 Daltons more than the starting compound it is likely that dimerisation followed by the breakdown of the resulting product occurred to form the observed compound. The compound which is at the longest retention time in this HPLC trace had two parent ions of equal intensity at 350 and 352 Daltons. The isotope pattern suggests the addition of bromine atom to the molecule. The parent ion equates to addition of the a bromine atom and the loss of a hydrogen atom from Napropamide. Fragmentation of the 350 Daltons parent ion produced a daughter ion at 276 Daltons (minus NMe₂), further fragmentation produced another daughter ion at 198 Daltons (minus Br⁷⁹). The fragmentation data suggests that the bromine atom is located on the naphthalene ring since fragmentation of Napropamide did not lead to the formation of

daughter ion of 199 Daltons. This ion consists of the naphthalene ring and the chain up to the carbonyl group. The 198 Daltons peak is produced by the loss of the bromine atom from the bromine substituted equivalent ion of the Napropamide ion. If the loss of the bromine atom was to come from the chain, the ion would have a mass of 199 Daltons since it is now equivalent to the Napropamide ion, however, if the bromine atom was on the ring and was lost, then the daughter ion would be one Dalton less because the ion is missing one hydrogen when compared to the equivalent Napropamide ion. The observed 198 Daltons daughter ion in the fragmentation pattern confirms that the bromine atom is attached to the ring. The exact position of the bromine atom in the ring could not be determined from the mass spectrometry. The formation of this compound must result from the addition of the bromine atom from the dibromide radical anion. This type of reaction has been observed before by Cruco *et al.* [106] and can be summarised by the following reaction.



The resulting transient from reaction 4.04 must then proceed to react with another radical to reform Napropamide and the species observed.

The compound observed at 7 minutes in the HPLC trace between the reaction of the sulfate radical with Napropamide was determined to have a parent ion of mass to charge ratio of 227 Daltons. This is one Dalton greater than the corresponding peaks in the dibromide and dichloride radical anions. Unlike those parent ions, the sulfate radical anion's parent ion did fragment to produce daughter ions at 209, 199, 185 and 171 Daltons. The presence of the 199 and 171 Daltons daughter ions indicates the ring structure of the compound is still intact. No structure could be assigned to this compound from the data obtained. It is possible however that the 227 peak is not the parent ion and the actual parent ion breaks down during the ionisation process and is therefore not observed as the base peak. The other major product observed in the HPLC trace produced a parent ion with a mass to charge ratio of 344 Daltons. Fragmentation of the parent ion produced a daughter ion at 326 Daltons (minus 18, OH₂). Fragmentation of the daughter ion produced a grand-daughter ion at 253 Daltons (minus 73, NEt₂). Further fragmentation produced a great grand-daughter ion at 225 Daltons (minus 48, CO) followed by another at 183 Daltons (minus 42, OCCH₂). The fragmentation pattern of this compound indicates the ring is still intact but with an additional 72 Daltons. This suggests the addition of a group with a mass to charge ratio of 72 Daltons to the ring. *Tertiary*-butyl alcohol has a mass to charge ratio of 74 Daltons, the loss of one hydrogen from the Napropamide and another from the *t*-butyl alcohol would produce a molecule with mass to

charge ratio of 344 Daltons. The compound at 15 minutes is therefore assigned to the addition of a *t*-butyl alcohol to the Napropamide. The initial radical cation formed from the reaction of Napropamide with the sulfate radical anion reacted with the *t*-butyl alcohol in a similar way as was reported in the acid generated radical cation intramolecular reaction.

Compounds at 15 minutes for the dichloride and sulfate radical anions both have similar retention times but the mass spectral data has revealed the two as completely different species.

Ab initio calculations were performed on Napropamide minus one electron from its full electron set at HF/6-31G** (with a doublet multiplicity) to determine the spin surface. A spin calculation indicated the difference in alpha and beta spin orbitals and is reported in Figure 4.21 (a). This shows the unpaired electron is stabilised over the ring as would be expected, and can be described by the resonance stabilisation as observed in Figure 4.22. Calculations indicate that the electron taken by the one electron oxidants comes from the ring. The optimised structure of Napropamide was calculated in the gas phase and therefore any direct comparison to the aqueous phase should be done with appropriate caution. Figure 4.21 (b) displays the HOMO for Napropamide in the gas phase. It can be observed from this illustration that the HOMO is also on the ring and therefore it is probable that the electron was initially removed from this orbital. This is to be expected since the HOMO would be the first orbital the one electron oxidant encounters.

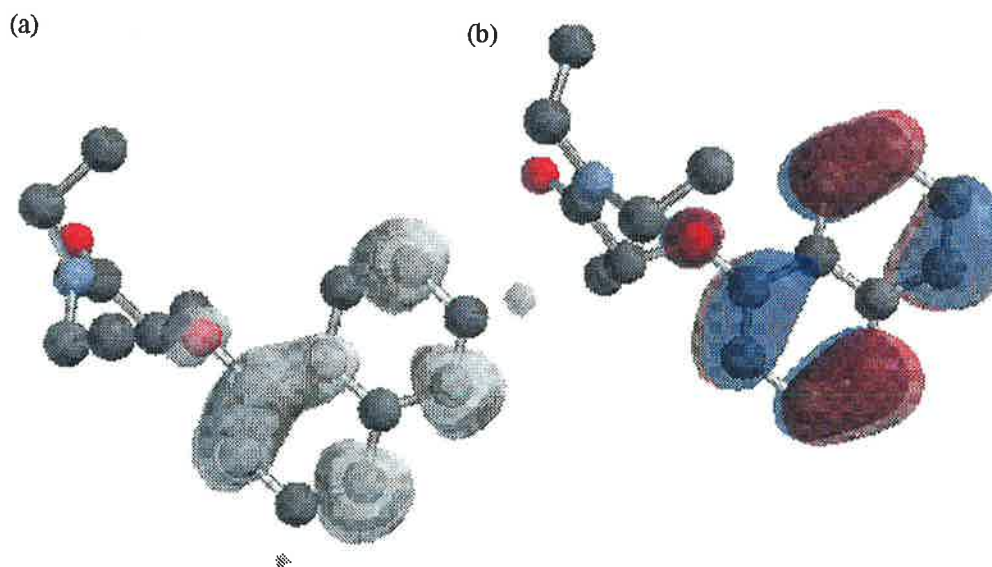


Figure 4.21. Plots of the electron spin density surface (a), and highest occupied molecular orbital (HOMO) (b), of Napropamide as determined by *ab initio* molecular orbital theory. Calculations were performed at the HF/6-31G** level of theory. The electron spin density surface represents the difference in overall electron density between α and β (ie. Spin up versus spin down) electrons. Plot (a) was determined with a molecular charge of +1 and a multiplicity of 2. Plot (b) was determined for the neutral molecule possessing a corresponding multiplicity of +1.

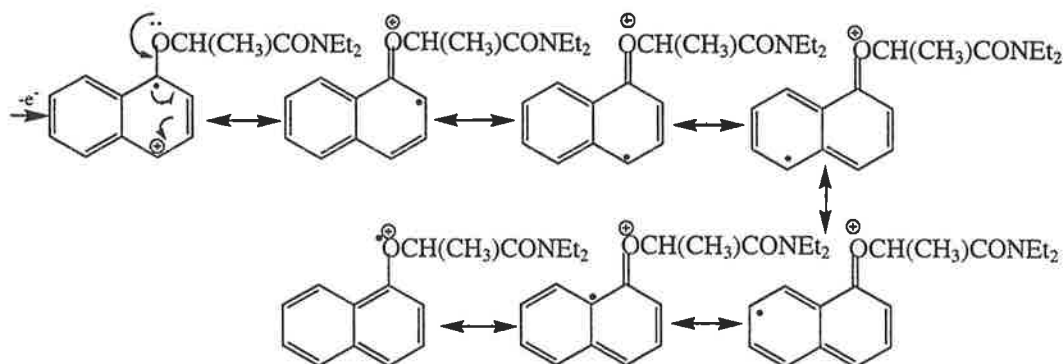


Figure 4.22. Resonance structures accounting for calculated difference in electron spin density for α and β electrons in the Napropamide radical cation. The difference in electron was illustrated in Figure 4.21.

4.6 REACTION OF NAPROPAMIDE WITH THE HYDRATED ELECTRON

The absorbance of the hydrated electron at 640 nm was observed to increase in the presence of small amounts of Napropamide (1×10^{-4} M). This indicates a reaction between the hydrated electron and Napropamide has occurred. The time resolved TDA spectra obtained on the pulse radiolysis of an aqueous Napropamide (1×10^{-4} M) solution containing *t*-butyl alcohol (0.1 M) saturated with nitrogen (pH 6.8, phosphate buffer) is shown in Figure 4.23. This exhibits an absorbance peak at 330 nm.

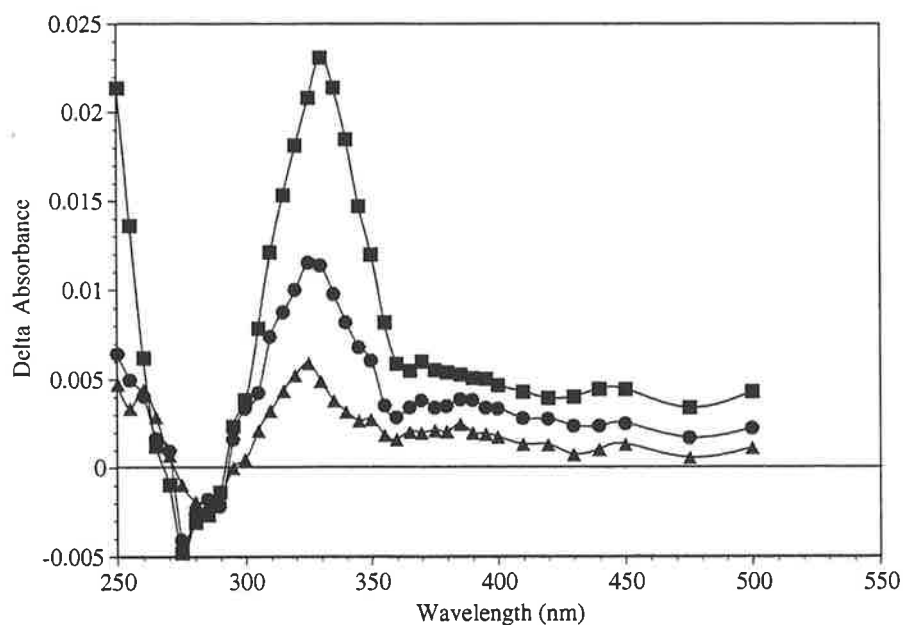


Figure 4.23. Time resolved TDA spectra obtained on the pulse radiolysis of an aqueous Napropamide (1×10^{-4} M) solution containing, *t*-butyl alcohol (0.1 M) saturated with nitrogen (pH 6.8, phosphate buffer). (■ Directly after, ● 20 μ s, and ▲ 100 μ s after the pulse).

Though this spectrum appears similar to that observed for the reaction of the hydroxyl radical with Napropamide, the size of the absorbance is significantly lower than that of the

hydroxyl radical adduct. Even when the G value for the hydrated electron is taken into account (2.7 versus 5.5) the absorbance of the hydrated electron adduct at the maximum of 330 nm is significantly lower (0.048 versus 0.076 for the OH-adduct).

The reaction of the hydrated electron with Napropamide should initially result in the addition of an electron to Napropamide (ie. $\text{Nap}^{\bullet-}$). The site of the radical attack cannot be determined by pulse radiolysis. Potential sites for radical addition in the molecule include the carboxyl group on the side chain and the naphthalene ring, as these functional groups are both known to react with hydrated electrons.

The bimolecular rate constant for the reaction of Napropamide with the hydrated electron was determined at pH 7.0 (phosphate buffer and NaOH) from the slope of a plot of the observed pseudo first order rate constant against the concentration of Napropamide. The method produced a rate constant of $8.6 \times 10^9 \text{ M}^{-1} \text{ s}^{-1}$. Rate constants for the reaction of the hydrated electron for naphthalene, acetone and N-Ethylacetamide are recorded below.

Naphthalene	$k=6.3 \times 10^9 \text{ M}^{-1} \text{ s}^{-1}$ [107]
N-Ethylacetamide	$k=1.4 \times 10^7 \text{ M}^{-1} \text{ s}^{-1}$ [108]
Acetone	$k=7.7 \times 10^9 \text{ M}^{-1} \text{ s}^{-1}$ [109]

The rate constant information contained above indicates that the reaction of the hydrated electron with the naphthalene ring is rapid while reactions with a simple amide is slow in comparison to other molecules containing carbonyl groups like acetone. Presumably this is due to the resonance stability the carbonyl provides to the nitrogen group of the amide. It is therefore likely that the hydrated electron reacts with the naphthalene ring of Napropamide since it has a similar rate constant to Naphthalene.

The maximum at 330 nm was observed to decay by second order kinetics with $2k/\epsilon l = 4.4 \times 10^5 \text{ s}^{-1}$. This indicates the transient decays to products by radical-radical mechanisms.

Gamma irradiation of an aqueous Napropamide ($1 \times 10^{-4} \text{ M}$) solution, containing *t*-butyl alcohol (0.1 M) saturated with nitrogen (pH 6.8, phosphate buffer) produced the HPLC chromatogram shown in Figure 4.24. It indicates the formation of one major product at a retention time of 10.5 minutes.

Electrospray mass spectral analysis of the major product shows a parent ion mass to charge ratio of 545 Daltons. MS^2 experiments showed that the parent ion produced a daughter ion at 418 Daltons. A MS^3 experiment produced a peak at 274 Daltons. This compound

corresponds to the singularly hydrogenated dimerised form of Napropamide (Figure 4.25). This suggests the hydrated electron attaches to the naphthalene ring of the Napropamide molecule. The transient produced by this reaction then reacts to add a hydrogen atom to form the hydrogen radical adduct of Napropamide. The species then reacts with itself to form the final product. The absence of other compounds in the HPLC trace suggests there is one site which is preferential for attachment of the hydrogen ion. This site cannot be determined using mass spectral data obtained.

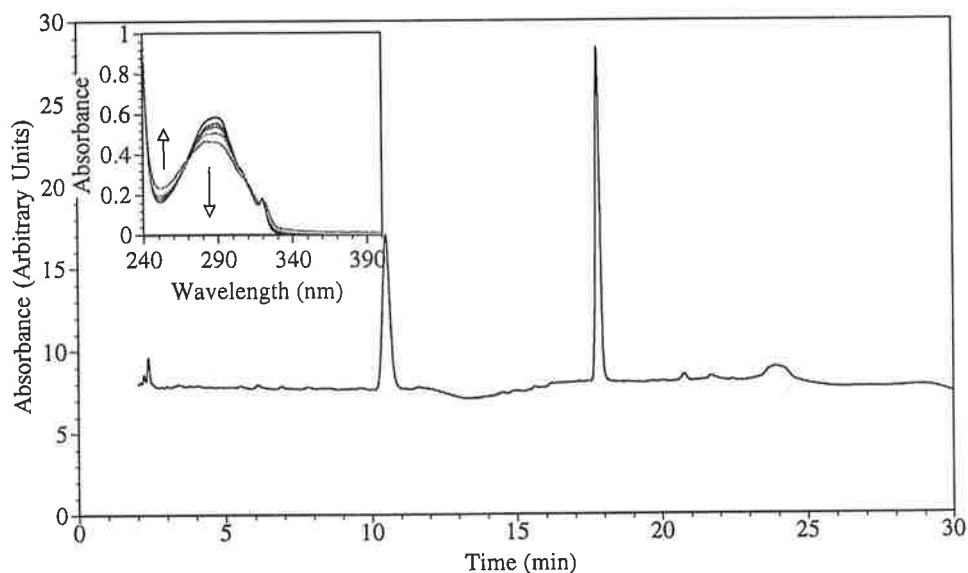


Figure 4.24. HPLC analysis following the gamma irradiation of an aqueous Napropamide (1×10^{-4} M) solution, containing *t*-butyl alcohol (0.1 M) saturated with nitrogen (pH 6.8, phosphate buffer). The trace displays the product formed from the reaction of Napropamide with the hydrated electron (10.5 minutes). See Figure 4.25 for product identification. Inset. Observed change in optical absorbance of the same solution (0 to 350 Gray). Arrows indicate the direction of absorbance change with radiation dose. Dose rate 80 Gray/hr.

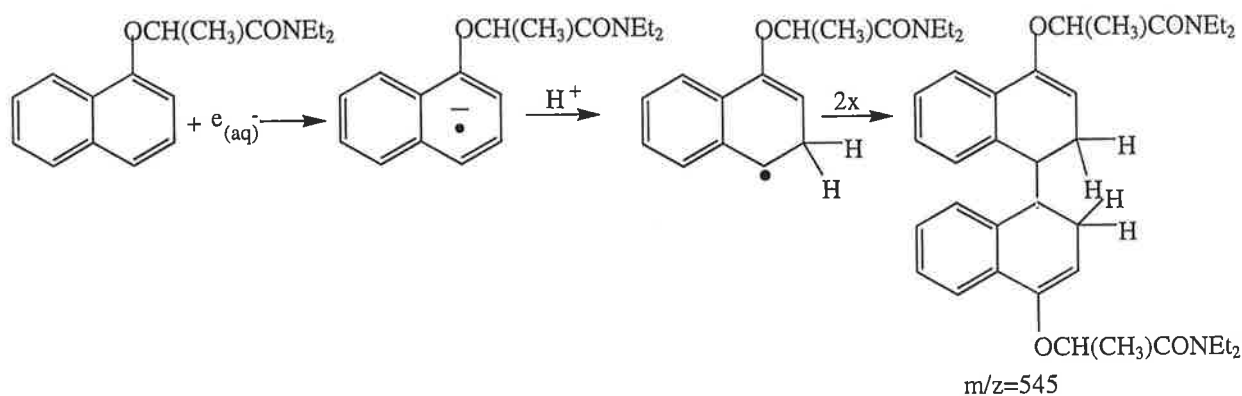


Figure 4.25. Reaction pathway for the reaction of the hydrated electron with Napropamide. The location of the hydrogen in the above scheme is arbitrary as the mass spectral data is unable to determine the exact site of attack.

Ab initio calculations were performed on Napropamide plus one electron in its full electron set at HF/6-31G** (with a doublet multiplicity) to determine the spin surface (Figure 4.26 (a)). This shows location of the unpaired electron over the ring as expected from experimental results. The optimised structure of Napropamide was calculated in the gas phase and therefore any direct comparison to the aqueous phase should be performed with appropriate caution. Figure 4.21 (b) displays the LUMO for Napropamide in the gas phase. It can be observed from this illustration that the LUMO is also on the ring and therefore it is probable that the electron was initially added from this orbital. This is to be expected since the LUMO would be the first orbital the nucleophilic hydrated electron would encounter.

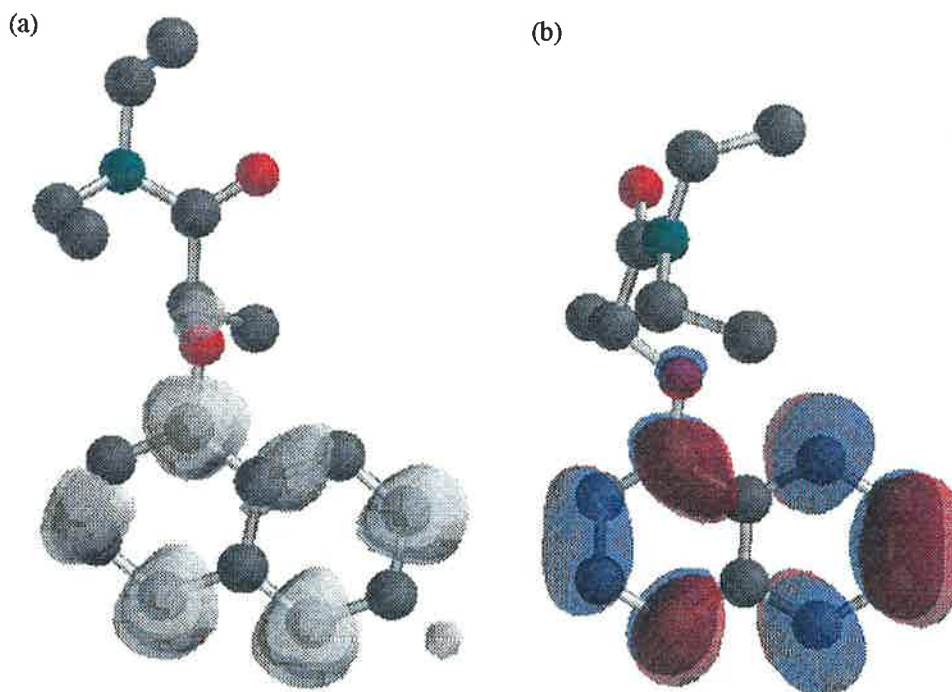


Figure 4.26. Plots of the electron spin density surface (a), and lowest unoccupied molecular orbital (LUMO) (b), of Napropamide as determined by *ab initio* molecular orbital theory. Calculations were performed at the HF/6-31G** level of theory. Plot (a) was determined with a molecular charge of -1 and a multiplicity of 2. Plot (b) was determined for the neutral molecule possessing a corresponding multiplicity of 1.

4.7 REACTION OF NAPROPAMIDE WITH THE HYDROGEN ATOM

Figure 4.27 shows the time resolved TDA spectra obtained upon the pulse radiolysis of an aqueous Napropamide (1×10^{-4} M) solution containing, *t*-butyl alcohol (0.1 M) saturated with nitrogen (pH 2, HClO_4). It exhibits an absorption peak with a maximum at 325 nm. This spectrum appears similar to that observed for the reaction of the hydrated electron with Napropamide. From the proposed mechanism for the reaction of the hydrated electron with

Napropamide the observed spectra is to be expected. The magnitude of the peak at 330 nm is slightly higher than that observed for the hydrated electron because the G value of the hydrogen atom is slight greater than that of the hydrated electron (3.1 versus 2.7).

Formation kinetics conducted on the maximum at 325 nm produced a bimolecular rate constant for the reaction of Napropamide with hydrogen atoms of $4.9 \times 10^9 \text{ M}^{-1} \text{ s}^{-1}$. Comparison of the rate constant for Naphthalene with the hydrogen atom ($3.4 \times 10^9 \text{ M}^{-1} \text{ s}^{-1}$) [110], indicates a similar magnitude to that recorded for the reaction with Napropamide. The similarity in the rate constants would suggest Napropamide proceeds through a similar reaction mechanism to naphthalene.

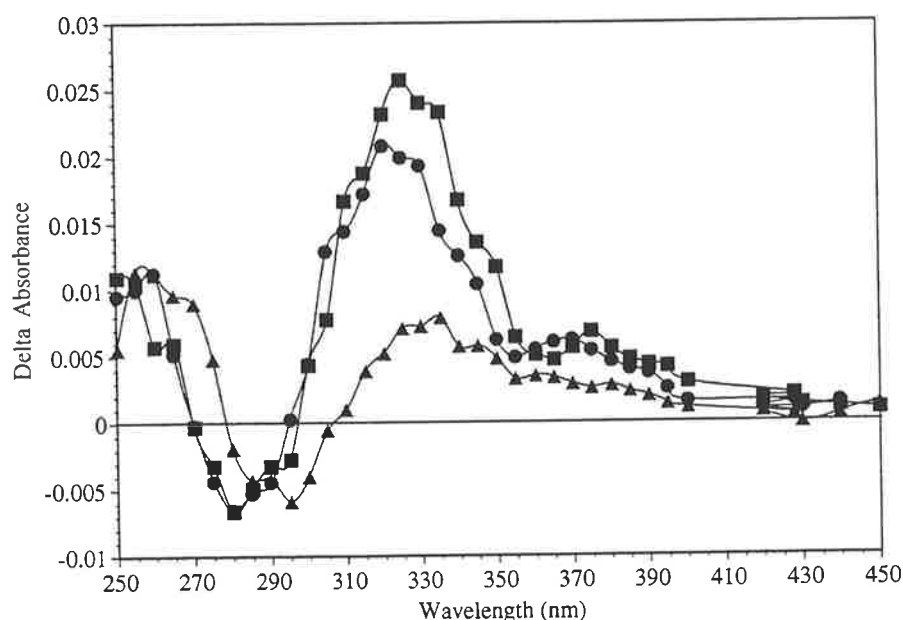


Figure 4.27. Time resolved TDA spectra obtained upon the pulse radiolysis of an aqueous Napropamide ($1 \times 10^{-4} \text{ M}$) solution containing, *t*-butyl alcohol (0.1 M) saturated with nitrogen (pH 2, HClO_4). (■ Directly after, ● 20 μs , and ▲ 100 μs after the pulse)

Transient species arising from the reaction of Napropamide with hydrogen atoms may result from three potential mechanisms

- 1) Hydrogen atom addition to a double bond,
- 2) One electron reduction to yield a radical anion ($\text{Nap}^{\bullet -}$)
- 3) Abstraction of a hydrogen from Napropamide. [63]

Since the TDA spectrum is similar in shape to that of a H-adduct obtained for the addition of the hydrogen atom to naphthalene, the addition of the hydrogen atom to Napropamide is probably principally responsible for the spectrum observed. This reaction has been studied extensively in the past and the reaction mechanism established, as shown in

Figure 4.28 [49, 64, 66, 83, 86-88, 92]. The HPLC trace (Figure 4.29) following gamma irradiation of an aqueous Napropamide (1×10^{-4} M) solution containing *t*-butyl alcohol (0.1 M) saturated with nitrogen (pH 2, HClO_4) showed the presence of three compounds which absorb at 254 nm. One of these species (product C) absorbs at 288 nm and has a very similar absorption spectrum to that of Napropamide. This compound is also at the same retention time as the only product produced in the hydrated electron reaction. The electrospray mass spectral data of this compound exhibits the same mass to charge ratio as well as the same fragmentation pattern of the major product from the hydrated electron reaction. This compound can therefore be assigned as the result of the hydrogen atom addition to the aromatic ring, followed by the reaction of the transient with itself to form the dimer observed in the reaction with the hydrated electron. The parent ion indicates no loss of molecular hydrogen to reform the more thermodynamically stable aromatic compound.

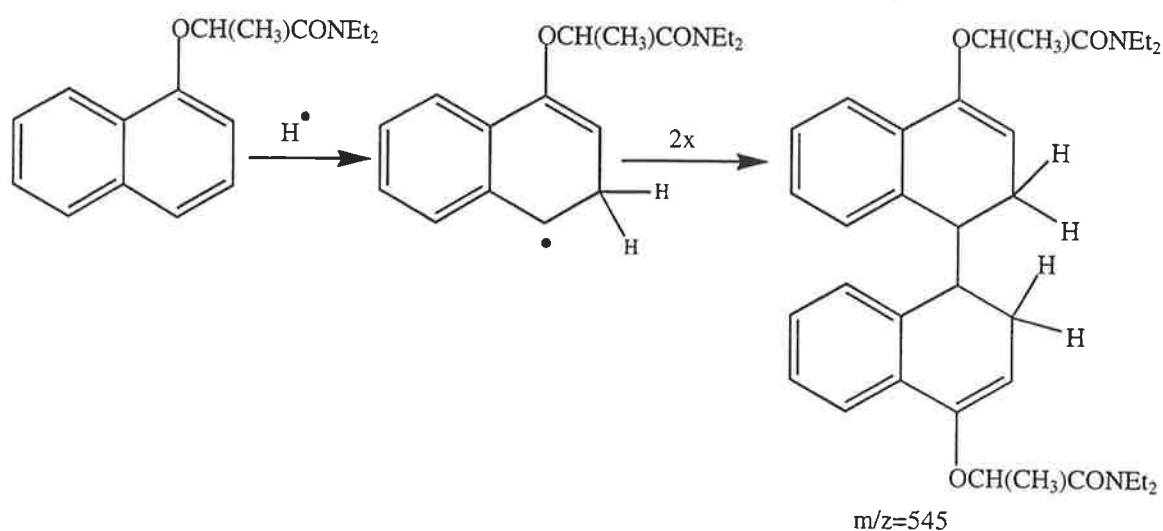


Figure 4.28. Reaction pathway for the reaction of the hydrogen atom with Napropamide. The position of the hydrogen in the above scheme is arbitrary as the mass spectral data is unable to determine the exact site of attack.

Product distribution for the reaction of the hydrogen atom with Napropamide shows the formation of numerous and small peaks in the HPLC chromatogram when compared to that observed for the equivalent HPLC trace involving the hydrated electron. Most of these peaks were too small for any confident mass spectral results to be obtained, with only two peaks producing positive results. These were compounds A and B which both produced a mass to charge ratio of 274 Daltons, corresponding to addition of two hydrogen atoms to Napropamide. Fragmentation data using the MS^2 techniques showed formation of a daughter ion at 201 Daltons. The MS^3 experiment produced daughter ions at 145 and 130 Daltons. The data indicates that the addition of hydrogen occurs on the ring, as the fragmentation pattern indicates that the side chain has remained at the same mass to charge ratio while the

naphthalene ring is two Daltons above that of the corresponding fragmentation in Napropamide. The mass spectral data does not indicate the position of attachment to the ring by the hydrogens.

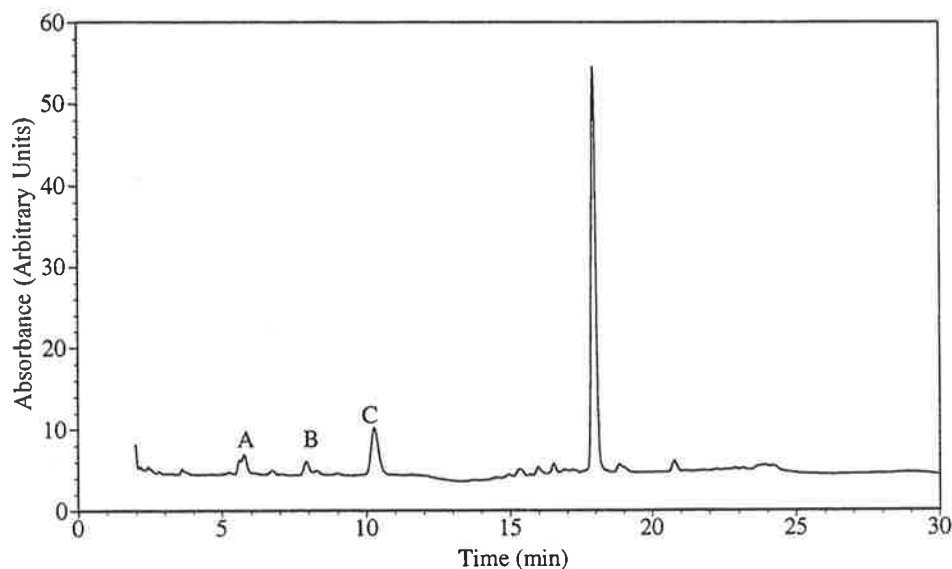


Figure 4.29. HPLC chromatogram following the gamma irradiation of an aqueous Napropamide (1×10^{-4} M) solution containing *t*-butyl alcohol (0.1 M) saturated with nitrogen (pH 2, HClO_4). The trace displays the products formed from the reaction of Napropamide with the hydrogen atom (A to C). See Figures 4.28 and 2.30 for product identification.

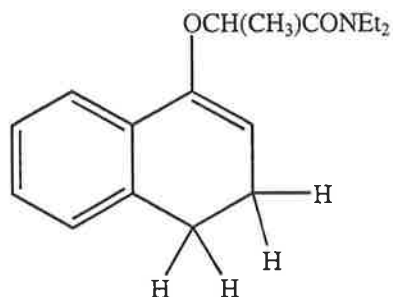


Figure 4.30. Compounds A and B of the gamma irradiation of a Napropamide (1×10^{-4} M) solution containing 0.1 M *t*-butyl alcohol, saturated with nitrogen (pH 2, HClO_4) as determined by the analysis of electrospray mass spectrometric fragmentation data. Location of the hydrogen atoms are not ambiguously assignable in structures A and B. See text for details.

4.8 REACTION OF NAPROPAMIDE WITH REDUCING RADICALS.

Pulse radiolysis of a nitrous oxide saturated solution containing sodium formate (0.02 M) and Napropamide (1×10^{-4} M) produced a maximum below 250 nm with no other absorbance maximum observed. Absorbance detected was due to formation of the carbon dioxide radical. Time resolved studies indicated the presence of no new absorption in the range of 250 to 600 nm. This suggests the carbon dioxide radical does not react with

Napropamide. The redox potential of the carbon dioxide radical has been determined to be -2.0 V (versus NHE) [43, 111]. This suggests that the redox potential for the Nap/Nap $^{\bullet-}$ is more negative than -2.0 V. Therefore, Nap $^{\bullet-}$ is a strong reducing agent with a reduction potential between -2.0 and -2.9 V (versus NHE).

4.9 OVERVIEW OF THE RADIATION CHEMISTRY OF NAPROPAMIDE

For the first time this study has allowed the elucidation of the radiation chemistry of aqueous Napropamide. The new chemistry for Napropamide is summarised in Figure 4.31.

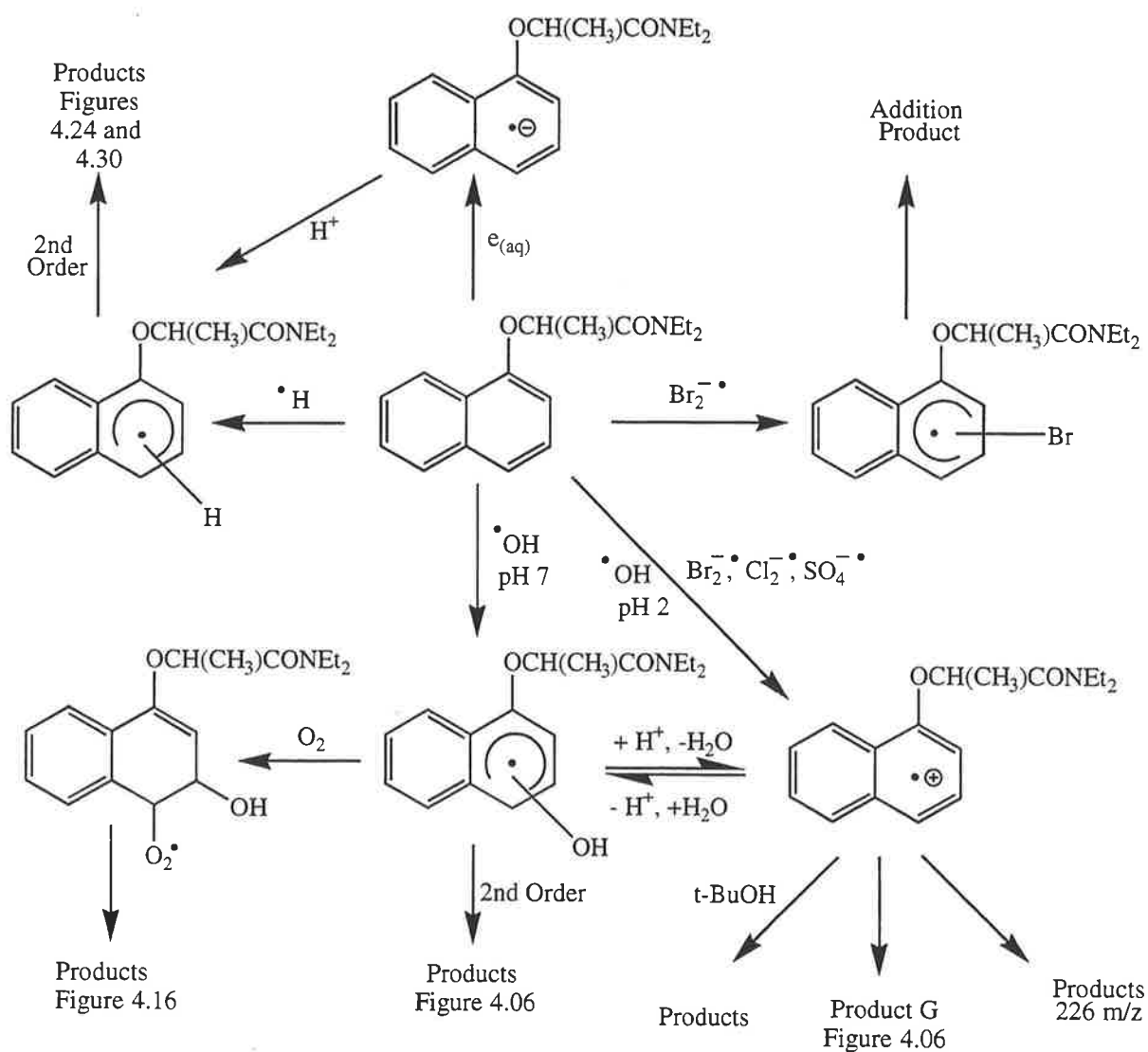


Figure 4.31. Overview of the radiation chemistry discovered in this study.

The TDA spectrum obtained from the reaction of Napropamide with hydroxyl radicals suggests the formation of a OH-adduct as an intermediate. The rate constant obtained for the reaction of Napropamide with the hydroxyl radical is similar to that of naphthalene's reaction

with the hydroxyl radical. Reaction of naphthalene with the hydroxyl radical is known to proceed through a OH-adduct intermediate, supporting our hypothesis.

The decay rate of the OH-adduct shows no dependence on the ionic strength of the solution, therefore the transient is neutral. The transient decays by second order kinetics, indicating that degradation products are formed by radical-radical reactions. HPLC characterisation of compounds formed by reactions of Napropamide with the hydroxyl radical showed that these compounds have a retention time less than Napropamide. This suggests that the degradation products are more polar than Napropamide. Mass spectrometric studies have determined that the five major products each have masses equivalent to the addition of one oxygen atom to the Napropamide molecule. Comparison of the mass spectrometric fragmentation data collected for Napropamide with that of the newly formed compounds indicate that the oxygen is attached to the naphthalene ring. This is in agreement with what we have determined through the pulse radiolysis studies. The rate of Napropamide loss and the formation of products from the reaction of Napropamide with the hydroxyl radical is initially linear under steady state irradiation. As the amount of hydroxyl radicals is increased past 30% of Napropamide's concentration, the loss of Napropamide and the formation of products follows a higher order kinetic mechanism. This result suggests that the products of the initial reaction also reacts with the hydroxyl radical to form (uncharacterised) compounds.

TDA spectrum obtained upon reaction of the hydroxyl radical with Napropamide at pH 2 differs from that obtained for the same reaction at neutral pH. As such, transients formed from the two reactions could not be assigned as the same species. The rate constant for the reaction of Napropamide with the hydroxyl radical at pH 2 is not markedly different to that obtained from the addition of the hydroxyl radical to Napropamide at neutral pH. The similarity in rate constants suggests that the hydroxyl radical adds to the naphthalene ring at pH 2 and the transient formed then reacts with hydrogen atoms producing a radical cation. Transient absorbance at 375 nm for the reaction of the hydroxyl radical with Napropamide showed a pH dependence typical of an acid-base equilibria. Gamma irradiation coupled with HPLC of Napropamide at pH 2, has shown that the compounds observed for the reaction of Napropamide with the hydroxyl radical at neutral pH are no longer formed. Instead, a single product is observed. Mass spectral fragmentation data indicate that this compound is, in fact, Napropamide with a hydrogen atom replacing one ethyl group. The exact mechanism for the formation of the observed product could not be determined from the data collected.

The transient produced from the reaction of Napropamide with the hydroxyl radical has been shown to be reactive with oxygen. Gamma irradiation coupled with HPLC shows formation of different compounds than those obtained for the de-oxygenated experiment. Mass spectral fragmentation data indicates that the products result from the addition of molecular oxygen to the transient. The newly produced transient then reacts to form the observed products. A previous study found that addition of a single oxygen atom to the starting compound was the most prevalent product for the reaction of benzene with the hydroxyl radical in the presence of oxygen [82]. Napropamide reacts to produce compounds with the addition of two oxygen atoms. It has also been observed that fragmentation of the ring structure seen for benzene is not occurring for the equivalent Napropamide reaction. The difference in results arise because the naphthalene ring of Napropamide reduces the chance for the correct positioning of the second oxygen molecule which is required for the ring fragmentation.

TDA spectra obtained from the reaction of Napropamide with one electron oxidants differs from that obtained for the OH-adduct of Napropamide. The spectra obtained for the dichloride and sulfate radical anions are similar to the radical cation spectrum for the reaction of Napropamide with hydroxyl radicals at pH 2. The dibromide radical spectrum is different to all other previously recorded TDA spectra. It is suspected that the difference in spectral appearance might be caused by the slower rate constant for the reaction of Napropamide with the dibromide radical anion. Rate constants for the bimolecular reaction of Napropamide with one electron oxidising agents decreased as expected with the redox potential of the oxidising agents. Napropamide is not observed to react with the azide radical and therefore the radical cation of Napropamide is a powerful one electron oxidant with a redox potential between 1.7 V and 1.4 V. This suggests that in natural and industrial waste water, if the Napropamide anion was formed, it could react as an oxidising agent with electron donating compounds present to reform Napropamide.

Gamma irradiation coupled with HPLC for the one electron oxidising agents indicated the product distribution varied with the oxidant used, however, a common product is observed between the oxidising agents. The structure of this compound cannot be determined from the mass spectrometric data obtained. We have determined that one of the products formed from the reaction of Napropamide with the sulfate radical anion, arises following the reaction of the transient with the *t*-butyl alcohol required for the study. The dichloride radical anion's reaction produces a compound that is formed from the radical cation of Napropamide and therefore is in agreement with the putative notion that transient spectrum produced is in part

made up from the radical cation. This indicates that formation of the radical cation can only be stabilised to form products at this low pH. Napropamide's reaction with the dibromide radical anion produces a product which results in the addition of a bromide atom to Napropamide.

Ab initio calculations indicates that the HOMO of Napropamide is located over the naphthalene ring. It is suspected that the electron lost to the oxidant occurs from this orbital, which is in agreement with the experimental results. The spin density surface is also located on the ring, and can be accounted for by resonance theory.

TDA spectrum obtained for the reaction of Napropamide with the hydrated electron suggests formation of a H-adduct as the transient. The rate constant obtained for the reaction of Napropamide with the hydrated electron is similar to that of naphthalene. It is known that the naphthalene reacts with the hydrated electron by addition to the aromatic ring, followed by the addition of a hydrogen ion to form a H-adduct. The decay of the radical is second order and thus the intermediate reacts through radical-radical mechanisms to form products. Gamma irradiation coupled with HPLC found the formation of one major product. Using mass spectral fragmentation data we have determined that the product is a dimer of Napropamide. The radical anion of Napropamide has been shown to be a strong reducing agent with a redox potential of between -2.0 and -2.9 V, however, in natural and industrial waste water, if the Napropamide anion is formed it would react rapidly to form a H-adduct instead of via electron transfer with other compounds to reform Napropamide. This would lead to the break down of Napropamide.

Ab initio calculations indicate that the LUMO of Napropamide is located over the naphthalene ring. It is suspected that the electron gain would initially occur in this orbital, which is in agreement with the experimental results. The spin density surface is also located on the ring.

The TDA spectrum for the reaction of Napropamide with hydrogen atoms is similar to the TDA spectrum obtained for Napropamide's reaction with the hydrated electron, supporting the hypothesis that the hydrated electron adds to the naphthalene ring. Gamma irradiation coupled with HPLC shows the formation of one major product. Using mass spectral fragmentation data the product was determined to be the same compound as determined for the hydrated electron. Minor products have also been detected and characterised as a mono-saturated form of Napropamide.

Napropamide will degrade upon the reaction with a number of free radicals produced in natural and treated industrial discharge water, however, upon the formation of the radical cation of Napropamide, this radical could also act as an oxidant with other compounds to regenerate Napropamide.

5.0 Radiation Chemistry of Aqueous Ioxynil Solution

5.1 IOXYNIL

Ioxynil (4 hydroxy-3,5-di-iodobenzonitrile) (Figure 5.01) is a white solid with a melting point of 212-213 °C. The maximum solubility of Ioxynil in water is 50 mg/L [112]. Ioxynil has a pK_a of 4.0, therefore at a pH of 5.0 and above Ioxynil will be predominantly in its anionic form, while at a pH below 3.0 the neutral form will predominate [113]. The solubility of the anion is substantially greater than the neutral form.

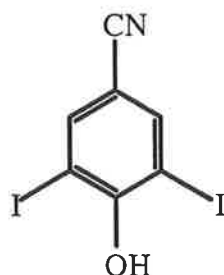


Figure 5.01. Chemical structure of Ioxynil.

Ioxynil was released by Rhone-Poulenc for broad leaf weed control as a post-emergent herbicide [114]. Ioxynil is normally used in combination with other pesticides to provide better crop protection. When higher application rates are used, it can control total plant growth [113]. Ioxynil works to inhibit photosynthesis by the uncoupling of oxidative phosphorylation [112].

Ioxynil has been reported to be stable in both alkaline and acidic environments. Degradation has been reported through direct photolysis of Ioxynil [115]. Another process that may degrade Ioxynil is the deiodination to less toxic substances such as hydrobenzoic acid through micro-organisms such as *Agrobacterium radiobacter* 8/4 [112, 114]. A less important factor in the degradation of Ioxynil was found to be volatilisation.

5.2 REACTION OF IOXYNIL WITH THE HYDROXYL RADICAL

Figure 5.02 shows the time resolved TDA spectra obtained upon the pulse radiolysis of a nitrous oxide saturated solution of Ioxynil (1×10^{-4} M) at pH 6.8 (phosphate buffer). It exhibits an absorption band with a maximum at 360 nm. In the presence of *t*-butyl alcohol (0.1 M), an effective hydroxyl radical scavenger but a weak hydrogen atom scavenger, the absorption spectrum was considerably reduced. The high $G(^{\bullet}\text{OH})$ yield and appreciable

decrease in the transient absorption suggests the transient absorption spectrum in Figure 5.02 is due mainly to the reaction of the hydroxyl radicals with Ioxynil.

As well as a maximum, the spectrum in Figure 5.02 possesses a minimum that contains a negative region between 280 to 330 nm. The negative absorption is due to the Ioxynil anion having a large absorbance in this region (Figure 5.03). The TDA spectrum is corrected by using the formula given in equation 3.14 and the assumption that the yield of hydroxyl radicals is equal to the yield of the transient radicals (Figure 5.04). Since the yield of transient radicals is not known for certain the result should not be over interpreted.

The corrected spectrum (Figure 5.03) exhibits the absorption maxima at 280 and 360 nm. The extinction coefficients of these maxima are approximately 8000 and 2000 $M^{-1}cm^{-1}$ respectively.

Reducing the dose (and hence the amount of transient radical) produced an increased half life of the transient species at 360 nm. The radical therefore decays by second order kinetics to products via radical-radical mechanisms. When fitted to second order kinetics, the curve produced a decay rate of $2k/\epsilon l = 2.0 \times 10^6 s^{-1}$. Using the molar absorbance value in Figure 5.03, it was determined that $2k = 4 \times 10^9 M^{-1}s^{-1}$.

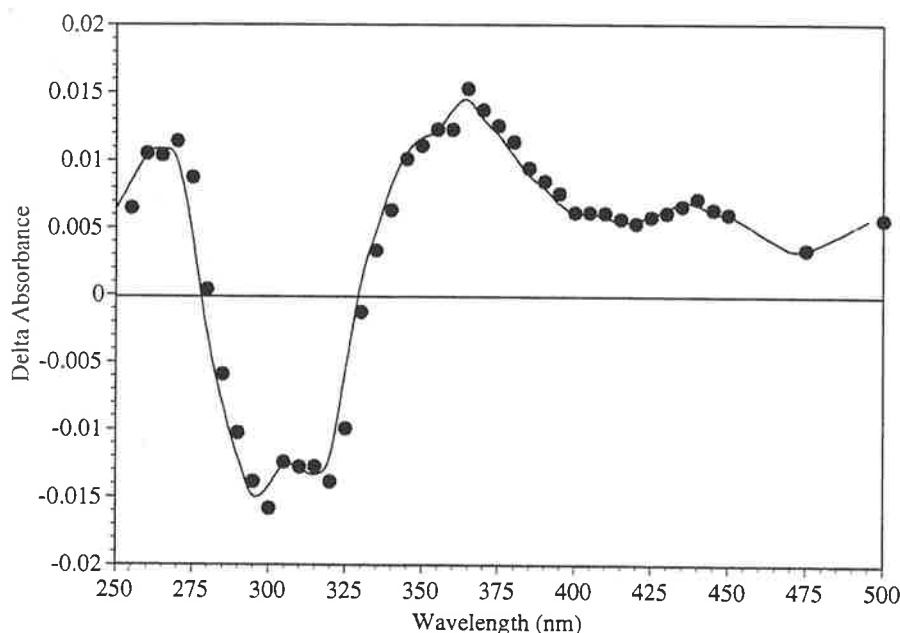


Figure 5.02. TDA spectrum obtained upon the pulse radiolysis of an aqueous Ioxynil ($1 \times 10^{-4} M$) solution saturated with nitrous oxide saturated (pH 6.8, phosphate buffer). (• Directly after the pulse).

The reactions of phenoxide anion, iodobenzene and benzonitrile have been studied previously [49, 116, 117]. All of the above compounds react through the addition of the hydroxyl radical to the aromatic ring to form the OH-adduct. The cyclohexadienyl type

transients then react with each other to form the original and hydroxylated products as well as dimers. Phenoxide anion derivatives have however been observed to react through a different mechanism, resulting in the production of a phenoxyl radical [118, 119].

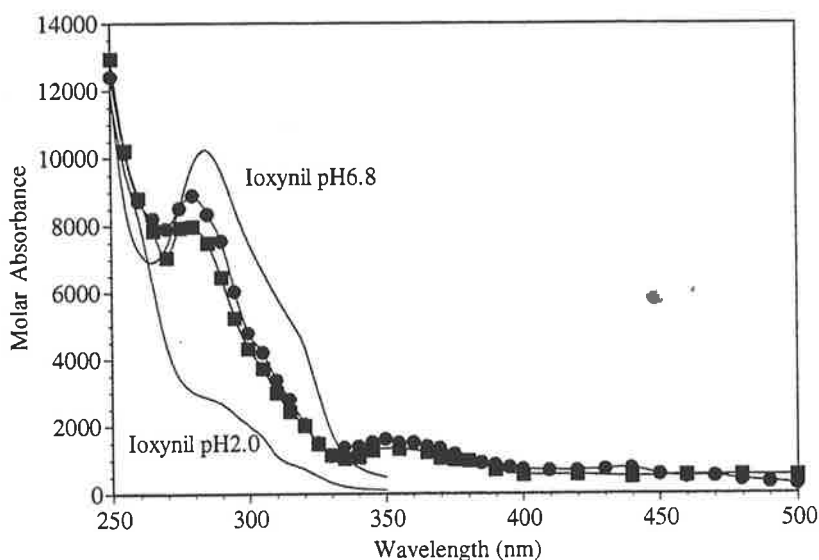


Figure 5.03. Molar Absorbance spectra of Ioxynil at pH 2 and 6.8 (solid lines), and the transients arising from the reaction of Ioxynil with hydroxyl radicals (pH 2.0 ■, pH 6.8 ●). Spectra recorded directly after the pulse.

The phenoxyl radical produced by the reaction of the hydroxyl radical with phenoxide anion produces a U.V. spectrum with a maximum at 380 nm (molar absorbance $2200 \text{ M}^{-1}\text{cm}^{-1}$) with a sharp peak at 400 nm [119]. The transient produced by the reaction of the Ioxynil anion with hydroxyl radicals has a TDA spectrum with a maximum at 360 nm with a molar absorbance of a similar order of magnitude. The sharp spike at 400 nm observed in the phenoxyl radical spectrum is not detected in the equivalent spectrum for Ioxynil. The evidence presented allows for the tentative assignment of the transient produced by the reaction of hydroxyl radicals with the Ioxynil anion as a phenoxyl type radical.

Changing the ionic strength of the solution by addition of NaClO_4 (1 M) at pH 6.8, produced no change in the observed rate of decay of the transient. This implies that the transient is neutral as an increase in ionic strength would effect the rate of decay of a charged transient [120]. This is consistent with the formation of the phenoxyl radical which has no charge.

Competition kinetics produced a bimolecular rate constant for the reaction of the hydroxyl radical with the Ioxynil anion of $1.5 \times 10^{10} \text{ M}^{-1}\text{s}^{-1}$. The rate constant indicates that the Ioxynil anion reacts with hydroxyl radicals at near diffusion controlled rates.

Though this is the first reported rate constant for the reaction of the hydroxyl radical with the Ioxynil anion, rate constants for molecules that contain similar functional groups have been studied with the hydroxyl radical. These rate constants are:

Phenoxide anion	$k=9.6 \times 10^9 \text{ M}^{-1} \text{ s}^{-1}$ [117]
Iodobenzene	$k=5.6 \times 10^9 \text{ M}^{-1} \text{ s}^{-1}$ [116]
Benzonitrile	$k=4.9 \times 10^9 \text{ M}^{-1} \text{ s}^{-1}$ [121]
3,5-Diiodotyrosine	$k=2.3 \times 10^{10} \text{ M}^{-1} \text{ s}^{-1}$ [122]

From the values presented above it is observed that the phenoxide anion reacts with the hydroxyl radical at a similar rate to the Ioxynil anion. A molecule which is structurally similar to Ioxynil is 3,5-Diiodotyrosine. The study with the 3,5-Diiodotyrosine molecule also concluded that hydroxyl radicals react to produce a phenoxyl radical as the resulting transient. This is consistent with our hypothesis for a phenoxyl type radical resulting from the reaction of hydroxyl radicals with the Ioxynil anion. In this molecule the electron withdrawing cyano group is replaced with an electron donating CH_2 group. It is observed that the rate constant reported for the reaction of 3,5-Diiodotyrosine is slightly higher than for the value we have reported. This is most likely due to the strong electron withdrawing effects of the cyano group. Hydroxyl radicals are electrophilic and therefore the electron donating CH_2 group on the diiodobenzene increases the rate of reaction with the hydroxyl radical, while the electron withdrawing cyano group decreases the reaction rate.

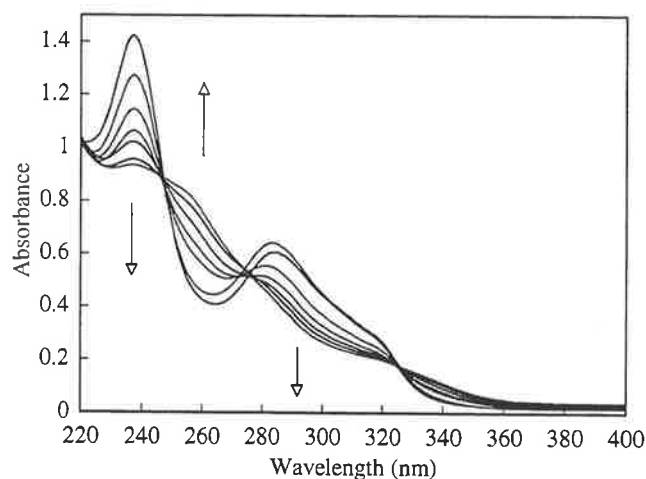


Figure 5.04. Observed change in the optical absorbance of an aqueous Ioxynil (60 μM) solution saturated with nitrous oxide (pH 6.8, phosphate buffer) and irradiated with gamma irradiation (0 to 120 Gray). Arrows indicate the direction of absorbance change with radiation dose. Dose rate 80 Gray/hr.

Steady state irradiation of an aqueous Ioxynil (60 μM) solution saturated with nitrous oxide (pH 6.8, phosphate buffer) using cobalt 60 (80 Grays per hour) produced a decrease in

the absorbance due to Ioxynil at 280 nm (Figure 5.04). The decrease in absorbance was less than expected by the dosimetry. The products must therefore absorb in this region, or the transient formed by the reaction of the hydroxyl radical with the Ioxynil anion reacts to reform the starting compound.

HPLC of an aqueous Ioxynil (1×10^{-4} M) solution saturated with nitrous oxide (pH 6.8, phosphate buffer) and irradiated with gamma irradiation produced the formation of new compounds and a decrease in the concentration of Ioxynil (Figure 5.05) at 232 nm. No change in the product distribution was observed when the detection wavelength was changed to 280 nm. One predominate compound was detected in this trace (Product A). Three other minor products were also formed. Since the C_8 column separates species on their polarity, and all the compounds were at longer retention times than Ioxynil, the products of the reaction are therefore less polar than the starting compound. Again this is consistent with the formation of the phenoxyl radical as the transient because the products resulting from the addition of hydroxyl radicals alone would be expected to be more polar than the starting compound and therefore have a shorter retention time.

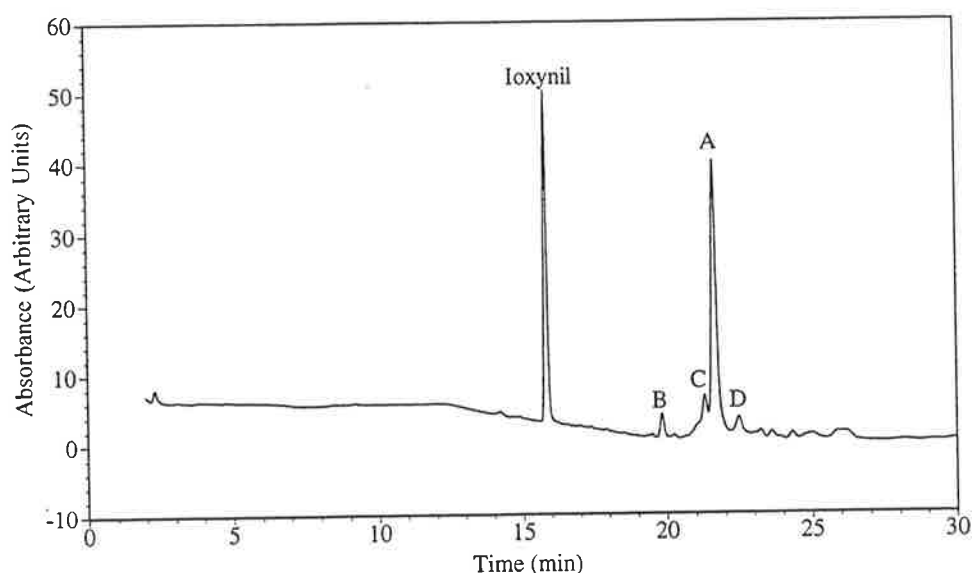


Figure 5.05. HPLC analysis following the gamma irradiation of a Ioxynil (1×10^{-4} M) solution saturated with nitrous oxide (pH 6.8, phosphate buffer). The trace displays the products formed from the reaction of Ioxynil with hydroxyl radicals (A to D). See text for details for product identification.

Structures of the compounds observed in this trace were determined by electrospray mass spectrometry. Ioxynil produced a parent ion at 370 (M-H) Daltons and a fragmentation pattern using MS^2 experiment that consisted of daughter ions at 127 and 243 Daltons. The ions correspond to an iodine atom and Ioxynil minus iodine atom respectively. The major compound (A) produced a parent ion of 487 Daltons. This mass corresponds to the formation

of a dimer from the phenoxyl radical, minus two iodine atoms. The fragmentation pattern of compound A (using MS² experiments), showed two sequential losses of iodine (127 Daltons). This was followed by a loss of 28 Daltons (CO) and finally the loss of 39 Daltons (C₂NH). The exact mechanism for the formation of this compound is unknown. The dimerisation of two phenoxyl radicals should result in the formation of a compound with a parent ion of 741 Daltons. Elimination of I₂ would result in the formation of a bicarbonyl compound with a parent ion of 485 Daltons (observed for compound B). The mechanism for the addition of two hydrogen atoms to the compound remains unsolved.

Mass spectra of the other minor compounds was also determined. Compound B was determined to have a parent ion of 485 Daltons. This corresponds to the major product minus two hydrogen atoms. This compound produced a fragmentation pattern that included the loss of iodine, followed by a CO group. An MS⁴ experiment exhibited the loss of a further iodine.

Compound C produced a parent ion with a mass to charge ratio of 730 Daltons. The MSⁿ fragmentation showed the loss of 3 consecutive Iodine atoms. Further MS⁵ experiments produced the loss of another 28 Daltons (CO) and 84 Daltons. The structure of this product could not be determined from the mass spectral data. Compound D's parent ion mass to charge ratio could not be differentiated from the base line signal because of interference from the TFA required as an ion pairing reagent for good separation of the products.

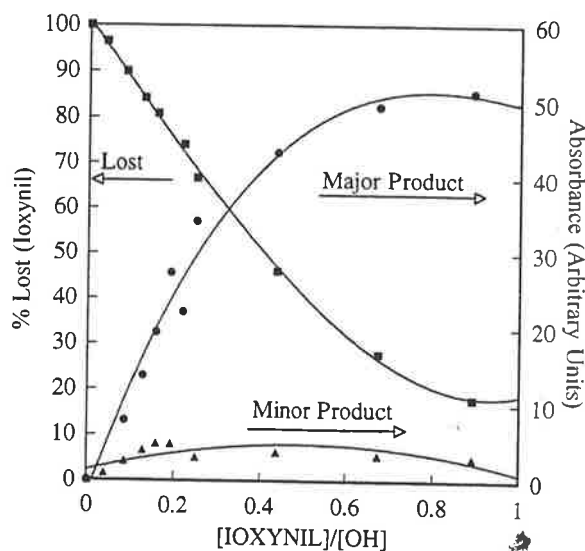


Figure 5.06. The loss of the Ioxynil anion (left axis) and the formation of the products (right axis) from the gamma irradiation of aqueous Ioxynil (1×10^{-4} M) solution saturated with nitrous oxide (pH 6.8, phosphate buffer), determined by HPLC. The products are A=●, B=◆.

A linear rate of Ioxynil anion loss against the concentration of the hydroxyl radical added to the system (calculated using Frickie Dosimetry) was observed until approximately

50% of the Ioxynil anion had reacted. The rate of appearance of the products, followed by HPLC, was also observed to be linear over this period. After this the production rate of these compounds decreased, suggesting products of the initial reaction also reacted with the hydroxyl radical.

5.3 REACTION OF IOXYNIL WITH THE HYDROXYL RADICAL IN ACIDIC SOLUTION

Time resolved TDA spectrum obtained upon the pulse radiolysis of Ioxynil (1×10^{-4} M) in acidic solution (pH 2, HClO_4) saturated with nitrous oxide can be observed to be different from the spectrum recorded at neutral pH (Figure 5.07). The spectrum has a maxima at 280 and 360 nm. Reducing the dose produced an increase in the half life of the transient at 360 nm. The radical therefore decays by second order kinetics. When the curves were fitted to second order kinetics they produced decay rates of $2k/\epsilon l = 1.5$ and $21.0 \times 10^5 \text{ s}^{-1}$ for 280 nm and 360 nm respectively. The rate constant measured for the 360 nm absorbance is similar to that recorded for the same absorbance at pH 6.8. This suggests the absorbance at 360 nm is due to the same species.

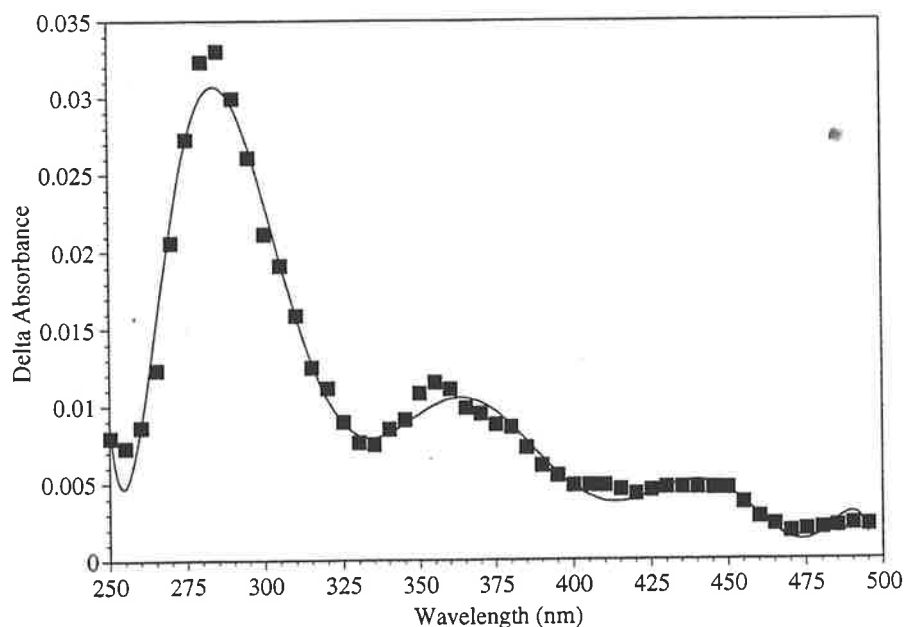


Figure 5.07. TDA spectrum obtained upon the pulse radiolysis of an aqueous Ioxynil (1×10^{-4} M) solution saturated with nitrous oxide (pH 2, HClO_4). Spectrum recorded directly after the pulse (■).

The effect of pH on the TDA spectrum can be observed more clearly in the molar absorbance spectra (Figure 5.03) because it takes into account the lower G value of the

hydroxyl radical and the difference in ground state absorbance between Ioxynil and the Ioxynil anion. Since neutral Ioxynil has a protonated hydroxyl group, the electron density it has available to donate into the ring is less than the deprotonated form. The U.V. absorbance maximum of the neutral form therefore moves to a lower wavelength. This is observed in Figure 5.03 with the ground state absorbance of the phenoxide form of Ioxynil being at 280 nm while the phenolic form of Ioxynil is below 250 nm [123].

For reasons described in section 3.5.3 any change in the ground state absorbance will effect the resulting TDA spectrum. It is therefore necessary to make a correction for this effect. The result of this correction for the change in ground state absorbance and lower G value of the hydroxyl radical at low pH is the formation of two molar absorbance spectra for the reaction of the anionic and neutral forms. A comparison of these spectra is observed in Figure 5.03. From the spectra, the two transients, within experimental error are similar. Therefore the anionic and neutral Ioxynil react to form the same transient species. Since it was determined in section 5.2 that the transient observed for the reaction of the hydroxyl radical with the Ioxynil anion was a phenoxyl radical, the transient produced by the reaction with neutral Ioxynil must also be the phenoxyl radical.

Like the reaction of the hydroxyl radical with the phenoxide anion, the reaction with phenol has also been extensively studied [119]. The hydroxyl radical initially reacts by addition to the aromatic ring of the phenol. After the formation of the dihydroxycyclohexadienyl radical differences in the literature are reported. Fields *et al.* [119] report the dihydroxycyclohexadienyl radical undergoes an acid catalysed elimination of water to form the phenoxyl radical. This type of mechanism is consistent with the result observed for Ioxynil. The dihydroxycyclohexadienyl radical has a reported maximum in the region of 300 to 340 nm [119, 124], the absence of any absorbance in this region and the maximum at 360 nm from the transient produced by the reaction of hydroxyl radicals with Ioxynil suggests that the phenoxyl type radical is the transient produced. The spectrum also matches that of the phenoxyl radical for 3,5-diiodotyrosine generated by photolysis at 248 nm [122].

The bimolecular rate constant determined using competition kinetics for the reaction of hydroxyl radicals with Ioxynil (pH 2, HClO₄) was $9.4 \times 10^9 \text{ M}^{-1}\text{s}^{-1}$. The rate constant indicates that Ioxynil reacts with hydroxyl radicals slightly slower than its anionic form. This effect has also been observed for the phenol/phenoxide anion system [119]. A decrease in the rate of addition of the hydroxyl radical occurs because the phenol is protonated, reducing the amount of electron density donated to the aromatic ring. This therefore effects the rate at

which the electrophilic hydroxyl radical adds to the aromatic ring. The rate constant for the addition of a hydroxyl radical to a phenol has been measured to be $6.6 \times 10^9 \text{ M}^{-1}\text{s}^{-1}$ [119].

Gamma irradiation coupled with HPLC of an aqueous Ioxynil ($1 \times 10^{-4} \text{ M}$) solution saturated with nitrous oxide (pH 2, HClO_4) revealed only one major product was formed when Ioxynil was reacted with hydroxyl radicals at pH 2 (HClO_4). This compound was at the same retention time as the product observed in the neutral pH experiment. Electrospray mass spectrometry on this compound revealed it was the same product observed in the neutral pH experiment. The major compound also had the same mass to charge ratio and fragmentation pattern (using MS^n) as the neutral pH experiment's major product. It is therefore assigned as the same product. This observation is consistent with the pulse radiolysis data.

5.4 REACTION OF IOXYNIL WITH THE HYDROXYL RADICAL IN THE PRESENCE OF OXYGEN

Comparison of the pulse radiolysis traces obtained from a solution of Ioxynil ($1 \times 10^{-4} \text{ M}$) saturated with nitrous oxide and nitrous oxide / oxygen (4:1 v/v), produced no observable change in the rate of decay of the transient at 360 nm. This observation is consistent with the transient being a phenoxyl type radical. It is known that while carbon centred radicals react quickly with oxygen, oxygen centred radicals do not [122]. The consistent decay rates between the de-oxygenated and oxygenated system suggests that a non carbon centred radical is forming. This experiment was repeated at low pH (pH 2, HClO_4) with the same result as the Ioxynil anion being observed.

Steady state irradiation of a solution of Ioxynil ($1 \times 10^{-4} \text{ M}$) saturated with nitrous oxide / oxygen produced no change in product distribution from that observed for the de-oxygenated solution (neutral and low pH). The presence of oxygen does not have any effect on the reaction of Ioxynil with hydroxyl radicals from the initial reaction to the final products.

Reaction of hydroxyl radicals with Ioxynil under steady state conditions was repeated, with the solution saturated with oxygen only. The change in experimental method affected the type of radicals produced by the radiation of the aqueous solution. The hydrated electron no longer reacted with nitrous oxide to form hydroxyl radicals (reaction 2.03), but instead reacted with oxygen to form the superoxide radical anion (reaction 2.07). The presence of the superoxide radical anion did not affect the formation of the initial phenoxyl radical (with the same initial spectrum that was observed in Figure 5.02 being formed), but it did however react with the phenoxyl radical once formed. Steady state irradiation of the above solution

produced a G value near zero for the loss of the Ioxynil anion at pH 6.8 (phosphate buffer). This was due to the reaction of the superoxide radical anion transferring an electron to the phenoxyl radical reforming the original Ioxynil anion. This type of reaction has been observed before by Jin *et al.* [125] who reported the reaction of a superoxide radical anion with the phenoxyl radical. Jin *et al.* [125] found that superoxide reacts with the phenoxyl radical to reform the phenoxide anion. Jin *et al.* [125] also observed the addition of the superoxide radical to the ring by the mechanism given in Figure 5.08. The addition reaction was not detected with the Ioxynil anion to any significant extent, with nearly all the reaction occurring through electron transfer to reform the starting compound (from the zero loss of the Ioxynil anion). A possible explanation for this difference in observations is that it is favourable for the superoxide radical anion to add to either the ortho or para positions on the ring for a phenoxyl radical. For the phenoxyl type radical of Ioxynil, in both the ortho positions there is a large iodine atom. This could provide enough steric hindrance such that addition to this position is unfavourable. In the para position, a CN functional group provides the steric hindrance. Jonsson *et al.* [103] studied the reaction of 15 phenoxyl radicals with superoxide, reaching an opposite conclusion to the Jin *et al.* [125] study, with electron transfer being as high as 94% for some phenoxyl radicals.

A solution saturated with oxygen at pH 2 (HClO₄) irradiated under steady state conditions, did not produce the same ability to regenerate Ioxynil as the neutral pH solution. The G value for the loss of Ioxynil was the same as reported for the de-oxygenated solution. Change in chemical behaviour should not be affected by the initial form of Ioxynil, since both react with hydroxyl radicals to form the same transient species. The change in pH does not only affect the protonation state of Ioxynil, it also affects the superoxide radical anion concentration as it has a pK_a of 4.8 [45]. At pH 2 superoxide is present as the perhydroxyl radical. This result implies that reaction of the perhydroxyl radical with the phenoxyl radical does not occur at an appreciable rate. Variation of the loss of Ioxynil (1×10^{-4} M) with solution pH saturated with oxygen and irradiated under steady state conditions can be observed in Figure 5.09. The plot produces an inflection point at approximately 4.8, the same pK_a as observed for superoxide and perhydroxyl radical, therefore indicating that superoxide radical anion is responsible for the regeneration of Ioxynil in oxygenated solution at neutral pH.

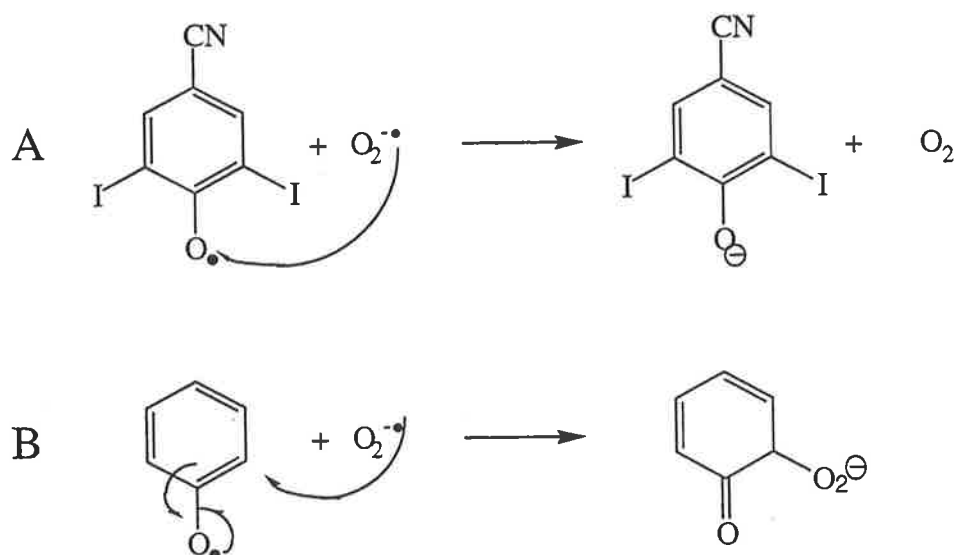


Figure 5.08. Proposed scheme for the reaction of phenoxyl type radical of Ioxynil with the superoxide radical anion (A), and the scheme determined by Jin *et al.* [125] for the reaction of the phenoxyl radical with the superoxide radical anion (B).

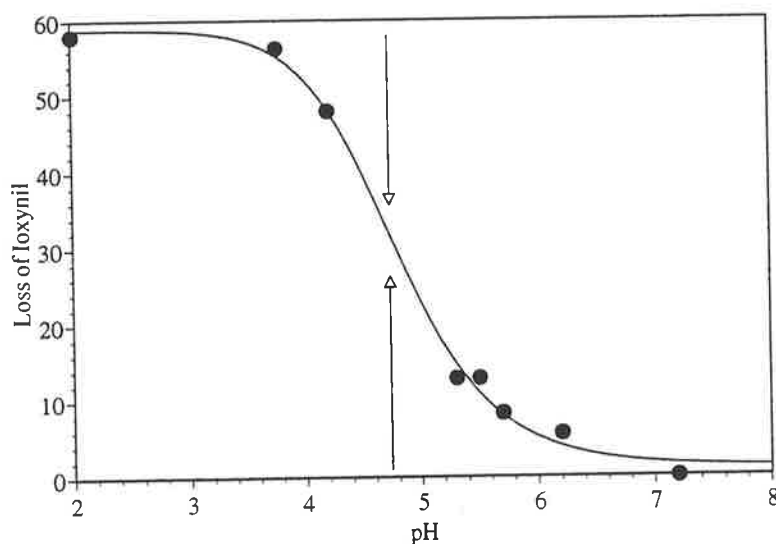


Figure 5.09. Variation of the loss of Ioxynil (1×10^{-4} M) with solution pH saturated with oxygen and irradiated under steady state conditions. Data were determined by HPLC at an analysis wavelength of 232 nm.

5.5 REACTION OF IOXYNIL WITH ONE ELECTRON OXIDANTS

The dichloride radical anion formed in the pulse radiolysis of oxygen saturated sodium chloride (0.02 M) Ioxynil solution (1×10^{-4} M) at pH 2 (HClO_4) reacts as a strong one electron oxidant with a potential of 2.09 V (versus NHE) [43]. Reaction of the dichloride radical anion with Ioxynil was studied by following the decay of the dichloride radical anion absorption band at 340 nm. It was observed that in the presence of Ioxynil (1×10^{-4} M) this band decayed faster and by first order kinetics instead of second order kinetics (Figure 5.10), indicating that a reaction between Ioxynil and the dichloride radical anion had resulted.



The bimolecular rate constant was determined to be $1.2 \times 10^9 \text{ M}^{-1} \text{ s}^{-1}$ from the slope of a plot of the pseudo first order rate constant against the concentration of Ioxynil (5 to $10 \times 10^{-5} \text{ M}$). Time resolved studies initially showed a broad absorbance with λ_{max} at 340 nm due to the formation of the dichloride radical anion. Using the pseudo first order rate constant it was determined that more than 90% of the dichloride radical anion had reacted $20 \mu\text{s}$ after the pulse. The spectrum at $20 \mu\text{s}$ is similar to that recorded for Ioxynil's reaction with hydroxyl radicals at pH 2, with absorbance maxima at 280 nm and 360 nm . Since the dichloride radical anion is a specific one electron oxidant, it should react by electron transfer. The resulting species must then undergo rapid hydrogen ion loss to form the phenoxyl type radical observed in the reaction with the hydroxyl radical. TDA spectra cannot be recorded at neutral pH because the dichloride radical anion cannot form readily at this pH.

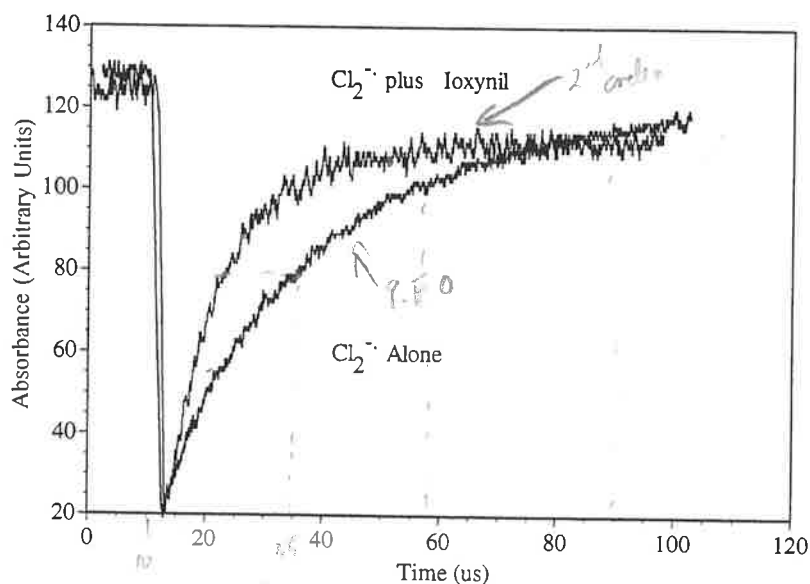


Figure 5.10. Comparison of the pulse radiolysis traces produced at 340 nm , with and without the presence of Ioxynil ($1 \times 10^{-4} \text{ M}$) in oxygen saturated, NaCl (0.02 M) ($\text{pH } 2, \text{HClO}_4$) solution, indicating that a reaction between the dichloride radical anion and Ioxynil had occurred.

Steady state irradiation of a sodium chloride (0.02 M), oxygen saturated solution containing Ioxynil ($1 \times 10^{-4} \text{ M}$) at $\text{pH } 2$ (HClO_4) produced a HPLC trace which showed the formation of one predominate compound (Figure 5.12). This compound appeared at the same retention time as that observed for the major hydroxyl radical reaction product. Electrospray mass spectrometry revealed this was the same product with an identical parent ion and mass fragmentation pattern as that reported in section 5.2. Formation of indistinguishable compounds is consistent with the pulse radiolysis data, since if the same transient species were observed the same final compounds should result.

Studies of the reactions of other specific one electron oxidants such as the sulfate, dibromide, diiodide radical anions and the azide radical with Ioxynil were also conducted. The TDA spectra that resulted from these reactions can be observed in Figure 5.11. Data indicates the spectra recorded following 90% completion of the reaction between Ioxynil and the one electron oxidants (determined from the resulting pseudo first order rate constants).

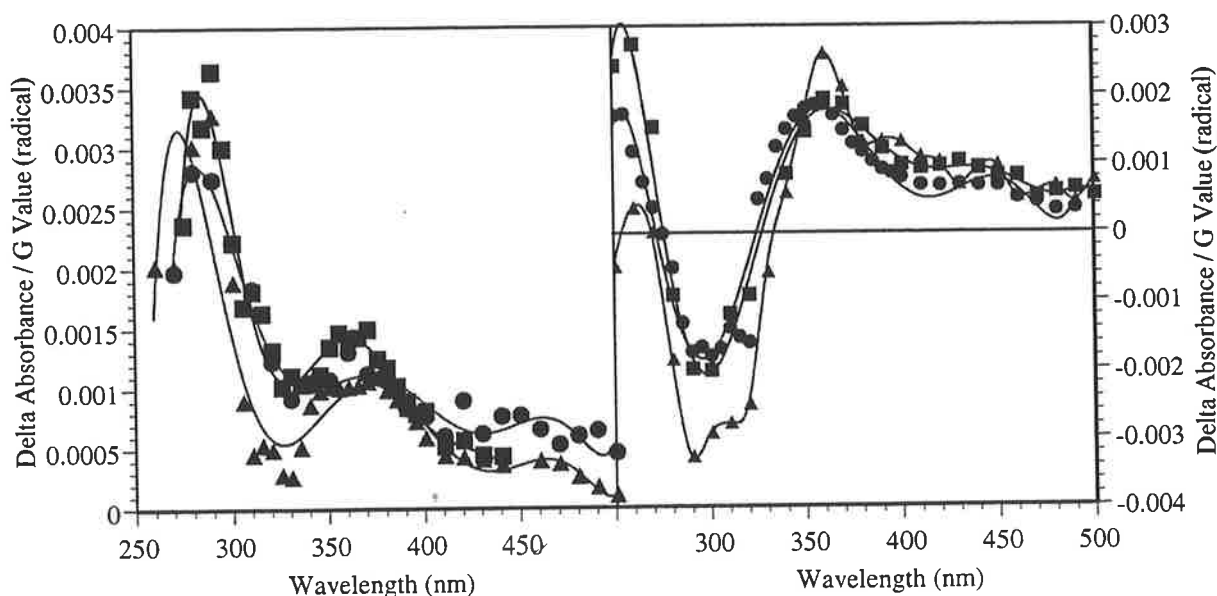


Figure 5.11. TDA spectra recorded for the reaction of Ioxynil (1×10^{-4} M) with left hand side, pH 2 (HClO_4) \blacksquare $\text{Cl}_2^{\bullet-}$, \bullet $\text{SO}_4^{\bullet-}$, \blacktriangle $\text{Br}_2^{\bullet-}$ and right hand side, pH 6.8 (phosphate buffer) \blacksquare N_3^{\bullet} , \bullet $\text{SO}_4^{\bullet-}$, \blacktriangle $\text{Br}_2^{\bullet-}$. Experimental conditions are as follows; $\text{Br}_2^{\bullet-}$; 0.02 M NaBr, oxygen saturated. $\text{SO}_4^{\bullet-}$; 0.02 M $\text{S}_2\text{O}_8^{2-}$, 0.1 M *t*-butyl alcohol, nitrogen saturated. $\text{Cl}_2^{\bullet-}$; pH 2, 0.02 M NaCl, oxygen saturated. N_3^{\bullet} ; 0.02 M NaN_3 , nitrous oxide saturated.

TDA spectrum of the sulfate radical anion appeared similar to the dichloride radical anion and hydroxyl radical TDA spectra. This is consistent with the one electron transfer hypothesis proposed earlier in this section. The dibromide radical anion spectrum also appears similar, however it is not within experimental error of the two previous spectra, suggesting formation of another transient species when Ioxynil is reacted with the bromide radical anion.

The transients formed at pH 6.8 by the azide radical, dibromide and the sulfate radical anion, again produced a similar spectra to that determined for the hydroxyl radical at this pH. Previous studies have determined that the azide radical reacts with a phenoxide anion to form phenoxyl radicals. The similarity between these two spectra confirm that the transient observed in the hydroxyl radical reaction is the phenoxyl radical.

The rate constant determined from the slope of a plot of the pseudo first order decay rate (formation for N_3^{\bullet}) against the concentration of Ioxynil (50 to 100 μM) for the reactions with the specific one electron oxidants can be observed in Table 5.01.

Radical	pH	Rate of reaction with Ioxynil ($M^{-1}s^{-1}$)	Wavelength of Determination (nm)
$Cl_2^{\bullet-}$	2.0	1.2×10^9	340
$Br_2^{\bullet-}$	2.0	1.5×10^8	360
$Br_2^{\bullet-}$	6.8	1.7×10^8	360
$SO_4^{\bullet-}$	2.0	3.7×10^9	460
$SO_4^{\bullet-}$	6.8	5.4×10^9	460
N_3^{\bullet}	6.8	6.9×10^9	360

Table 5.01. Bimolecular rate constants determined for the reaction of Ioxynil with one electron oxidants. Rates were determined from the slope of a plot of the pseudo first order rate constant against the concentration of Ioxynil (50 to 100 μ M).

The rate constants decrease with the strength of the corresponding one electron oxidant's redox potential of the radical, with the exception of the azide radical. The azide radical reacts at close to a diffusion controlled rate. This phenomenon has been observed previously between the reaction of the phenoxide anion and the azide radical. Two possible reasons have been postulated for this phenomenon. The azide radical has no charge while the phenoxide anion possesses a single negative charge. The electrostatic repulsion between the negative charge of the phenoxide anion and the radical anions is thought to slow the reaction rates down. The self exchange rate between the azide radical and the azide anion is also considerably faster than the corresponding self exchange rate for the radical anions [43]. Reactions of the radical anions with neutral Ioxynil produced a slower rate constant than for the corresponding anion because the electron density available for the one electron transfer is less due to the protonation of the oxygen.

A literature search found that reactions of specific one electron oxidants were of a similar order of magnitude as those recorded in table 5.01 when reacted in with phenol, phenoxide and cyanophenoxide anion [68, 126-128].

The diiodide radical anion formed on the pulse radiolysis of an oxygen saturated solution containing Iodide (0.02 M) was not observed to decay faster in the presence of small amounts of Ioxynil (1×10^{-4} M). The diiodide radical anion is a one electron oxidant with redox potential of 1.0 V (versus NHE) [44] while the azide radical has a redox potential of 1.4 V (versus NHE) [44]. Since Ioxynil reacts with the azide radical and not the diiodide radical

anion the redox potential of the Iox^+/Iox ($\text{Iox}^{\bullet}/\text{Iox}^-$) couple in reaction 5.02 must be between 1.4 and 1.0 Volts (versus NHE).



HPLC traces obtained from reactions of the sulfate, dichloride, and dibromide radical anions generated by steady state gamma irradiation with Ioxynil are recorded in Figure 5.12.

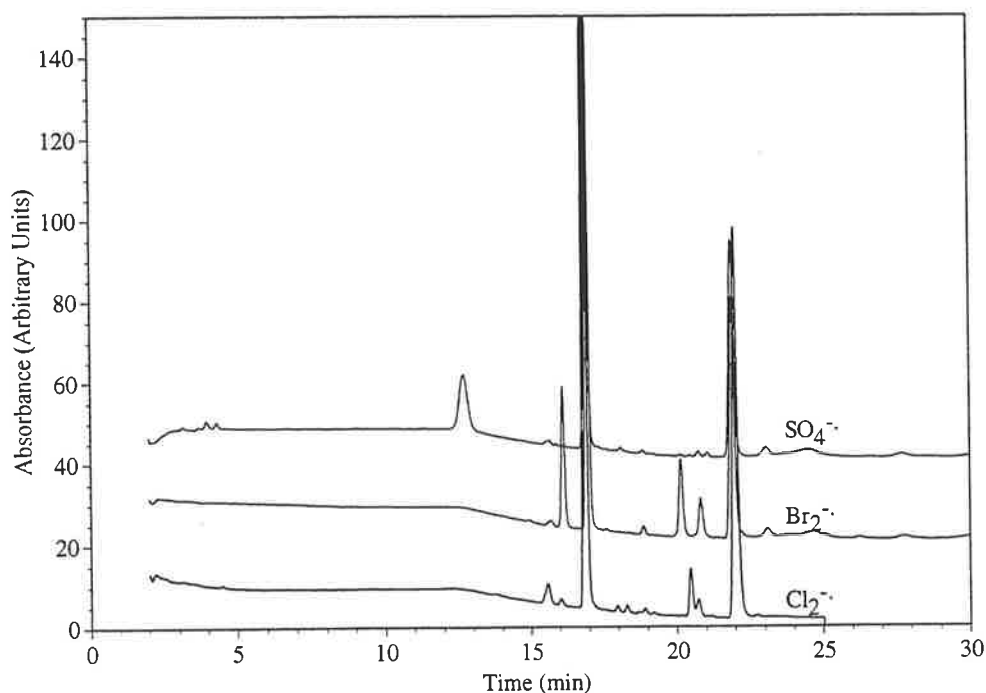
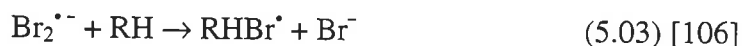


Figure 5.12. Comparison of the HPLC traces produced by the reaction of dichloride, dibromide, and the sulfate radical anion with Ioxynil (1×10^{-4} M). Experimental conditions are as follows; $\text{Br}_2^{\bullet-}$; pH 6.8, 0.02 M NaBr, oxygen saturated. $\text{SO}_4^{\bullet-}$; pH 6.8, 0.02 M $\text{S}_2\text{O}_8^=$, 0.1 M *t*-butyl alcohol, nitrogen saturated. $\text{Cl}_2^{\bullet-}$; pH 2, 0.02 M NaCl, oxygen saturated. The traces indicate the differences in products produced from the reaction of radical anions with Ioxynil. See text for discussion on the identification of specific products.

The precursor for the formation of the sulfate radical anion ($\text{S}_2\text{O}_8^=$) is known to thermally oxidise a variety of compounds. Over the time scale of the reaction Ioxynil was shown to be stable to thermal oxidation by testing a non-irradiated sample of the sulfate radical anion mixture. The sulfate radical anion's HPLC trace was reproducible at both pH 2 and 6.8. A major product was observed at 22 minutes as a result of the irradiation. This is the same retention time for the predominate compound produced by the reaction of Ioxynil with hydroxyl radicals. Electrospray mass spectrometry confirms this is the same species with an identical parent ion mass to charge ratio and fragmentation pattern recorded. A minor compound was observed at 15.7 minutes, this product was not observed in other radical reactions with Ioxynil. Attempts to determine the structure of this compound using

electrospray mass spectrometry were unsuccessful due to interference from the ion pairing reagent TFA.

The dibromide radical anion's HPLC trace shows the same predominate compound at 20 minutes that has previously been observed. Minor products different to any previously determined are also present in the chromatogram. Electrospray mass spectrometry revealed the compound at 20 minutes, to have two parent ions of equal intensity at 439 and 441. Two isotopes of equal intensity indicate the presence of a bromine atom in the molecule. The parent ion corresponds to the formation of an Ioxynil dimer with the loss of three iodine atoms and the addition of a bromine atom. The compound observed at 21 minutes in the dibromide radical anion's trace also produces two peaks of equal intensity with the parent ions being recorded at 437 and 439 Daltons. The compound's mass to charge ratio is two hydrogens less than the compound at 20 minutes. The addition of bromide to a molecule during a reaction with the dibromide radical anion has been reported by Cruco *et al.* [106]. The dibromide radical can add to unsaturated bonds and can be symbolised by the following reaction scheme.



The transient produced in reaction 5.03 must then eliminate an iodine atom to form the corresponding phenoxy radical. This radical must then combine to form the two compounds observed in the HPLC chromatogram. The two compounds resulting from the combination reaction must be similar to the products observed for the hydroxyl radical reaction since their parent ion corresponds to that of the hydroxyl radical with a bromine atom replacing an iodine. Formation of the minor products might pose a possible explanation for the different pulse radiolysis spectra recorded, since their formation requires a different transient to the minor species.

Ab initio calculations were performed on the Ioxynil anion and neutral Ioxynil with one electron missing from its full electron set. [The compounds were optimised as a doublet at HF/LanL2DZ (HF/6-31G** was not used because the atomic number of the iodine was too large for the basis set).] Ioxynil anion's spin is distributed largely over the carbon attached to the oxygen. The remaining spin is delocalised over the carbons ortho and para to the oxygen atom as expected by the resonance structures. Neutral Ioxynil produced a completely different spin surface, with the majority of the spin being located over one of the iodine atoms and the carbons which are meta and ipso to the oxygen atom. The spin surface calculations were carried out on the optimised structure of the radical, the resulting geometry is asymmetrical.

This explains why the resulting spin surface is also asymmetrical. The spin surface suggests that electron loss would come from the iodine since the spin on the carbons is located on the ortho and para positions to the iodine with the large spin surface located on it.

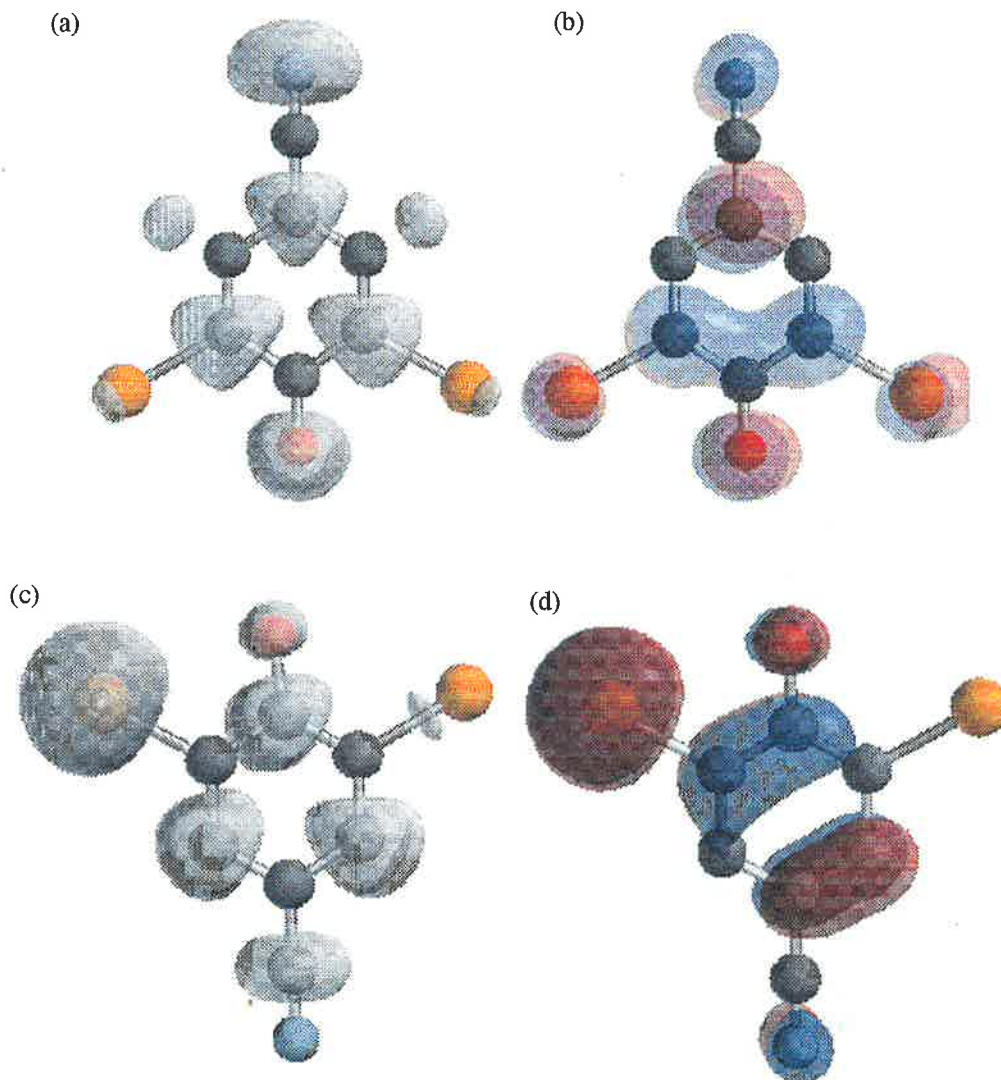


Figure 5.13. Plots of the electron spin density surface (a and c), HOMO (b and d), of Ioxynil (bottom) and Ioxynil anion (top) as determined by *ab initio* molecular orbital theory. Calculations were performed at the HF/LanL2DZ level of theory. Plot (a) was determined with a neutral molecule and a multiplicity of 2. Plot (b) was determined for a molecular charge of -1 possessing a corresponding multiplicity of +1. Plot (c) was determined with a molecular charge of +1 and a multiplicity of 2. Plot (d) was determined for the neutral molecule possessing a corresponding multiplicity of +1.

The spin surface for the Ioxynil anion is contained within the HOMO surface of the parent compound, suggesting the electron was taken from this orbital. The result is not unexpected since this is the orbital of highest energy. The spin surface for neutral Ioxynil was substantially, but not completely contained within the HOMO. The same argument that was used for the Ioxynil anion can still be used here.

5.6 REACTION OF IOXYNIL WITH THE HYDRATED ELECTRON

Absorbance of the hydrated electron at 640 nm was observed to increase in the presence of small amounts of Ioxynil (1×10^{-4} M) at pH 7.0 (phosphate buffer and NaOH). This indicates a reaction between the hydrated electron and Ioxynil is occurring. TDA spectrum obtained upon the pulse radiolysis of an aqueous Ioxynil (1×10^{-4} M) solution containing *t*-butyl alcohol (0.1 M) saturated with nitrogen gas at pH 7.0 (phosphate buffer and NaOH) is displayed in Figure 5.14. This spectrum exhibits a large negative peak in the region between 265 and 330 nm. There is only a small positive absorbance in the region from 330 to 450 nm. The negative absorbance is due to the large ground state absorbance of the Ioxynil anion in this region.

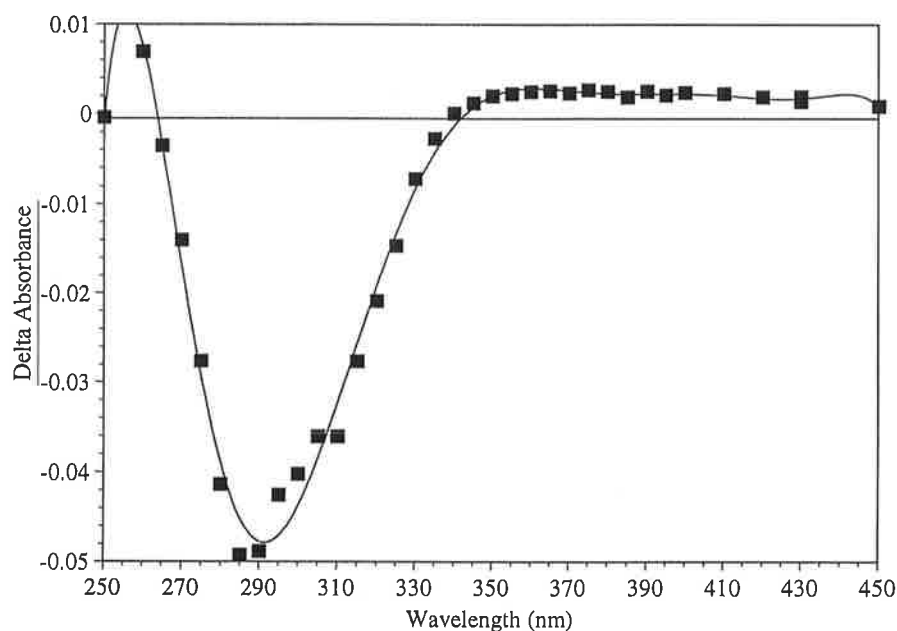


Figure 5.14. TDA spectrum obtained upon the pulse radiolysis of an aqueous Ioxynil (1×10^{-4} M) solution containing *t*-butyl alcohol (0.1 M) saturated with nitrogen gas at pH 7.0 (phosphate buffer and NaOH). Spectrum recorded directly after the 2.5 μ s pulse.

The bimolecular rate constant for the reaction of the hydrated electron with the Ioxynil anion was determined from the slope of a plot of the decay rate of the hydrated electron at 640 nm against the concentration of Ioxynil (25 to 50 μ M). The rate constant was determined to be $7.5 \times 10^9 \text{ M}^{-1} \text{ s}^{-1}$. Though this is the first reported rate constant for the reaction of the hydrated electron with the Ioxynil anion, rate constants for compounds with similar functional groups have been reported and are reproduced below.

Iodobenzene	$1.2 \times 10^{10} \text{ M}^{-1} \text{ s}^{-1}$ [129]
para-Cyanophenoxide anion	$2.0 \times 10^9 \text{ M}^{-1} \text{ s}^{-1}$ [129]

3,5-Diiodotyrosine

 $8.3 \times 10^9 \text{ M}^{-1} \text{ s}^{-1}$ [130]

From these rate constants, it can be concluded the presence of Iodine in Ioxynil increases the rate at which the hydrated electron reacts with the para cyanophenoxide anion. The rate constant obtained here is similar to that of 3,5-diiiodotyrosine. The molecule 3,5-diiiodotyrosine is similar to Ioxynil in that it is a phenol with two iodines in both the ortho positions and hydrogens in both the meta positions. It differs from 3,5-diiiodotyrosine by the presence of the electron withdrawing cyano group in the position para to the hydroxyl group. Comparison of the rate constants for the reaction of the Ioxynil anion with the 3,5-diiiodotyrosine anion indicates that changing the group in the para position had little effect.

Decay of the transient produced by the reaction of Ioxynil with the hydrated electron is observed to be slow at 290 nm. Time resolved studies out to 1000 μs produced only a minimal decrease in the absorbance at 290 nm, suggesting the transient reacts very quickly to form stable compounds that do not decay any further and do not absorb in the 290 nm region, or that the transient absorbance in this region is similar to the final products.

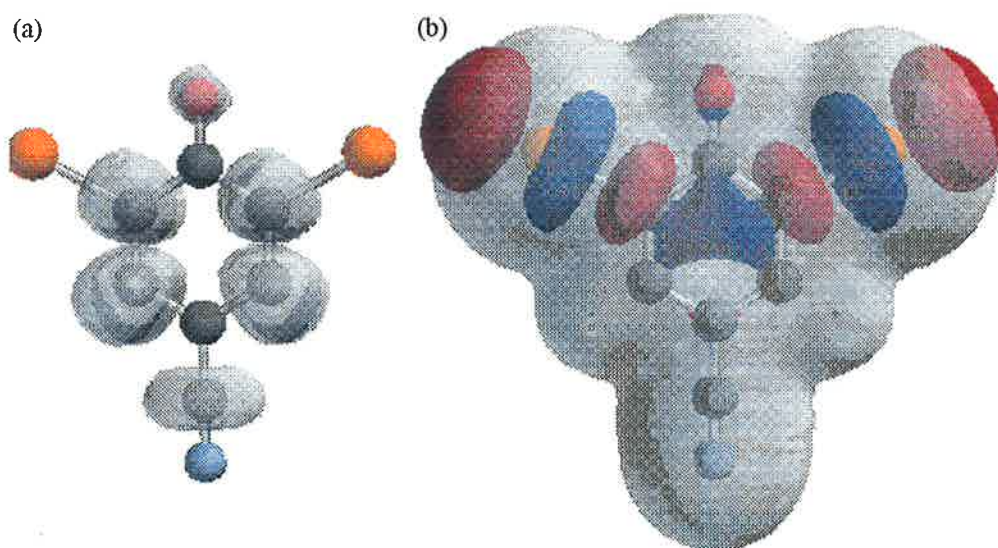


Figure 5.15. Plots of the electron spin density surface (a), and LUMO with the density surface superimposed on the LUMO (b), of Ioxynil as determined by *ab initio* molecular orbital theory. Calculations were performed at the HF/LanL2DZ level of theory. Plot (a) was determined with a molecular charge of -2 and a multiplicity of 2. Plot (b) was determined with a molecular charge of -1 possessing a corresponding multiplicity of +1. (Hydrogens not shown).

From the *ab initio* and population analysis calculations reported in appendix 1 it can be observed that the most electron deficient carbons are those next to the oxygen in the ring and the carbon of the nitrile group. Figure 5.15 (b) displays an illustration of the LUMO of the Ioxynil anion and indicates that this molecular orbital is located over the iodines and the aromatic ring. Overlaying the density surface of the same molecule indicates that the iodine

atoms are the most exposed for nucleophilic attack. The spin surface resulting from the optimised structure of the Ioxynil anion with an electron added (charge -2, multiplicity 2) produced the spin density delocalised over the ring, oxygen and carbon of the nitrile group. No resonance structures could be drawn to encompass all the positions of the spin surface. The spin surface does not resemble the LUMO suggesting that the molecular orbitals have undergone substantial rearrangement due to the addition of an electron.

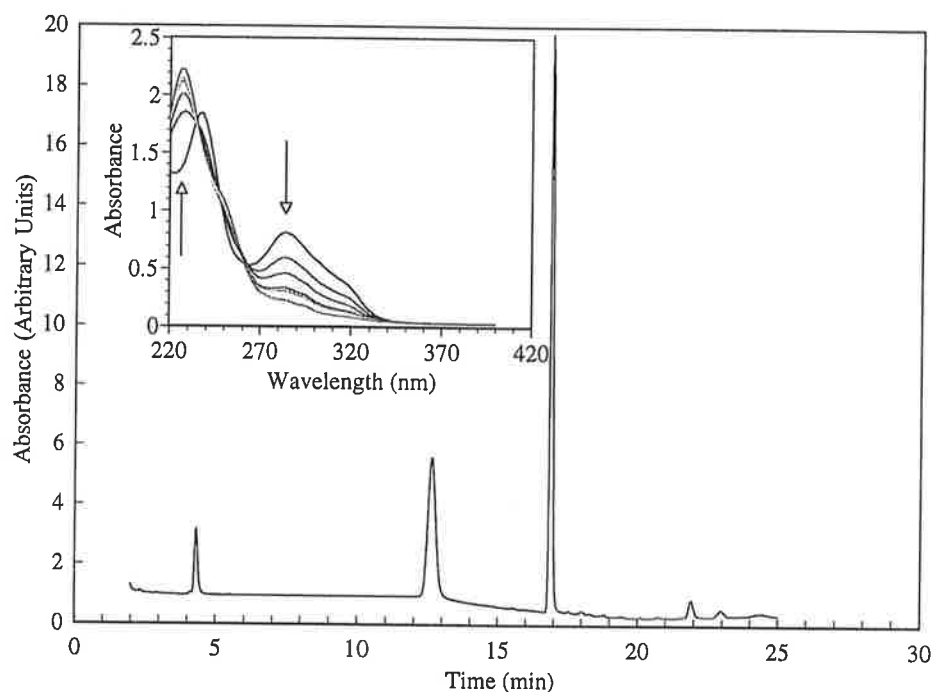


Figure 5.16. HPLC analysis following the gamma irradiation of an aqueous Ioxynil (1×10^{-4} M) solution containing, *t*-butyl alcohol (0.1 M) (pH 7.0 phosphate buffer and NaOH) and saturated with nitrogen. The traces displays the products formed from the reaction of Ioxynil with the Hydrated electrons. See text for discussion on product identification. Inset. Observed change in optical absorbance of the same solution (0 to 350 Gray). Arrows indicate the direction of absorbance change with radiation dose. Dose rate 80 Gray/hr.

Gamma irradiation of an aqueous Ioxynil (1×10^{-4} M) solution containing, *t*-butyl alcohol (0.1 M) (pH 7.0 phosphate buffer and NaOH) and saturated with nitrogen produced the HPLC trace reported in Figure 5.16. The effect on optical absorbance was to decrease the absorbance maxima at 280 nm and at 238 nm, forming a new maximum at 230 nm. The HPLC trace shows the formation of a major peak at 12 minutes with a minor peak at 4.5 minutes. The loss of Ioxynil calculated by HPLC was the same percentage as that observed in the U.V. spectra at 290 nm, indicating that pulse radiolysis did result in permanent loss of Ioxynil at 290 nm.

Electrospray mass spectrometry on the two predominate compounds proved unsuccessful due to interference from the ion pairing reagent TFA required as part of the chromatographic conditions to ensure reproducible peaks in the HPLC trace.

5.7 REACTION OF IOXYNIL WITH THE HYDROGEN ATOM

Figure 5.17 shows the TDA spectrum obtained upon the pulse radiolysis of an aqueous Ioxynil (1×10^{-4} M) solution containing *t*-butyl alcohol (0.1 M) saturated with nitrogen (pH 2, HClO_4). The spectrum itself is small when compared to the hydroxyl radical transient at the same pH, indicating that the effect on the absorbance observed for that spectrum is minimal. This spectrum is different from that observed for the reaction of the hydrated electron with Ioxynil. Corrections made to the spectra to account for the differences in the ground state did not form a match between the two spectra below 350 nm, but above this wavelength the two spectra did match. This would suggest that the transient^s produced are different.

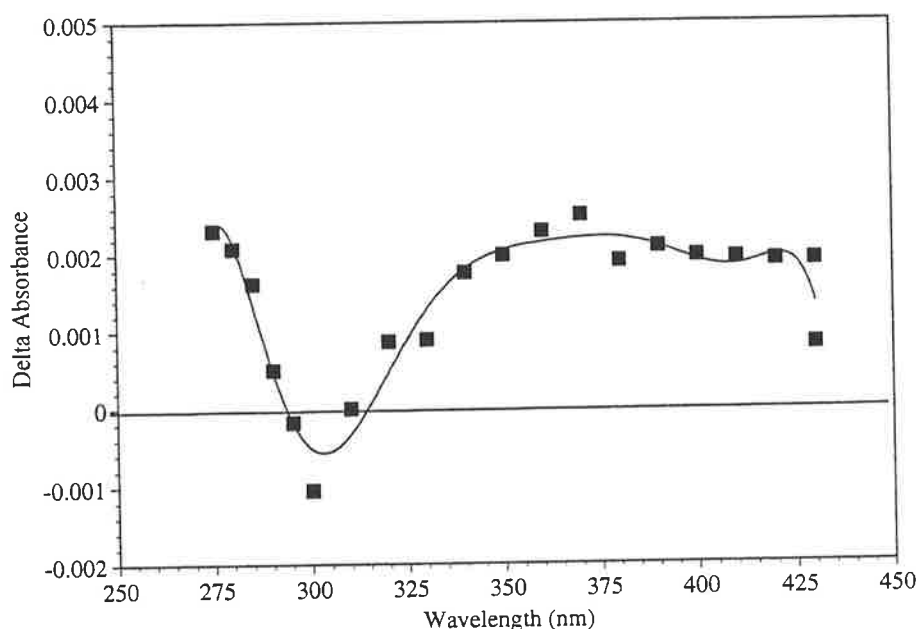


Figure 5.17. TDA spectrum obtained upon the pulse radiolysis of an aqueous Ioxynil (1×10^{-4} M) solution containing *t*-butyl alcohol (0.1 M) saturated with nitrogen (pH 2, HClO_4). Spectrum recorded 10 μs after the pulse.

Formation kinetics were conducted on this maximum by obtaining the slope of a plot of the pseudo first order rate constant against the concentration of Ioxynil at 360 nm. The kinetic study produced a bimolecular rate constant for the reaction of $8.4 \times 10^8 \text{ M}^{-1} \text{ s}^{-1}$. Comparison of the reaction rate of 3,5-Diiodotyrosine with the hydrogen atom ($3.4 \times 10^9 \text{ M}^{-1} \text{ s}^{-1}$) [130] is significantly higher than that recorded for the reaction with Ioxynil. This can be rationalised using the same argument used to account for the reaction with the hydroxyl

radical. The electrophilic nature of the hydrogen atom [66] is affected by the change of an electron donating group to a strong electron withdrawing group.

Transient species arising from the reaction of Ioxynil with hydrogen atoms should result from the addition of a hydrogen atom to the double bonds within the aromatic ring. The transient observed in Figure 5.17 is therefore assigned to the H-adduct.

The HPLC analysis (Figure 5.18) following gamma irradiation of an aqueous Ioxynil (1×10^{-4} M) solution containing *t*-butyl alcohol (0.1 M) saturated with nitrogen (pH 2, HClO₄) showed the presence of one major product at 238 nm. The predominate compound had a similar retention time to that of the major product from the reaction of Ioxynil with the hydrated electron. At pH 2 it is unlikely that any of the hydrated electron would react with Ioxynil before it reacted with the hydrogen ions. Electrospray mass spectral data of this compound also could not be determined from the noise created by the background signal due to the TFA. Though direct evidence through mass spectral analysis for the two compounds in the hydrated electron and hydrogen atom experiments could not be obtained, the similarity of retention times suggests it is likely they are the same compound. Differences in the TDA spectra recorded between the hydrated electron and the hydrogen atom must therefore result from either the presence of the second compound observed in the HPLC trace or the differences caused by the protonation-deprotonation of the hydroxyl group.

The H-adduct resulting from the addition of the hydrogen atom to Ioxynil can either react to form a dimer or react with the *t*-butyl alcohol to form the hydrogenated product. Decay of the transient produced by reaction with the hydrated electron is rapid. This would suggest a reaction with *t*-butyl alcohol since it is in such high concentration. Dimerisation would produce a second order decay, which was not observed in our experiment. Addition of the hydrated electron to the Ioxynil anion could potentially result in the elimination of an iodide ion from the molecule as this is common for the reaction of hydrated electrons with halogenated compounds [51, 52, 62]. Das *et al.* [130] found that with the structurally similar molecule 3,5-Diiodotyrosine the hydrated electron did not eliminate iodide.

Differences recorded in the pulse radiolysis experiment occurs because of the protonation of the transient producing different spectra. No attempt was made to determine the pK_a of the transient because of the large difference in ground state absorbance for the two forms of Ioxynil in the region that the transients absorbed.

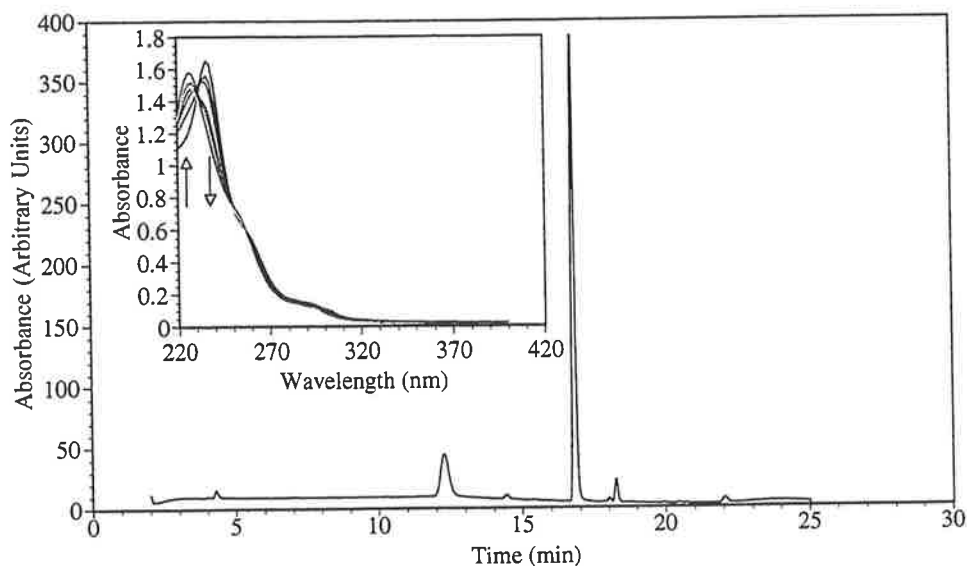


Figure 5.18. HPLC analysis following the gamma irradiation of an aqueous Ioxynil (1×10^{-4} M) solution containing *t*-butyl alcohol (0.1 M) saturated with nitrogen (pH 2, HClO_4). The trace displays products formed from the reaction of Ioxynil with hydrogen atoms. Inset, Observed change in optical absorbance of the same solution (0 to 350 Gray). Arrows indicate the direction of absorbance change with radiation dose. Dose rate 80 Gray/hr.

5.8 REACTION OF IOXYNIL WITH REDUCING RADICALS.

Pulse radiolysis of a nitrous oxide saturated solution containing sodium formate (0.02 M) and Ioxynil (1×10^{-4} M) produced a maximum below 250 nm with no other absorbance maxima observed. Absorbance observed was due to the formation of the carbon dioxide radical. Time resolved studies indicated the presence of no new absorption in the range of 250 nm to 600 nm out to 1.3 milliseconds. This ~~proposes~~^{suggests} that the carbon dioxide radical does not react with Ioxynil. The redox potential of the carbon dioxide radical has been determined to be -2.0 V (versus NHE) [43, 111] implying the redox potential for the $\text{Iox}/\text{Iox}^{\bullet -}$ is more negative than -2.0 V. Therefore, $\text{Iox}^{\bullet -}$ is a strong reducing agent with a reduction potential between -2.0 and -2.9 V (versus NHE).

5.9 OVERVIEW OF THE RADIATION CHEMISTRY OF IOXYNIL

This study has allowed for the first time the elucidation of the radiation chemistry of aqueous Ioxynil. The new chemistry for Ioxynil is summarised in Figure 5.19.

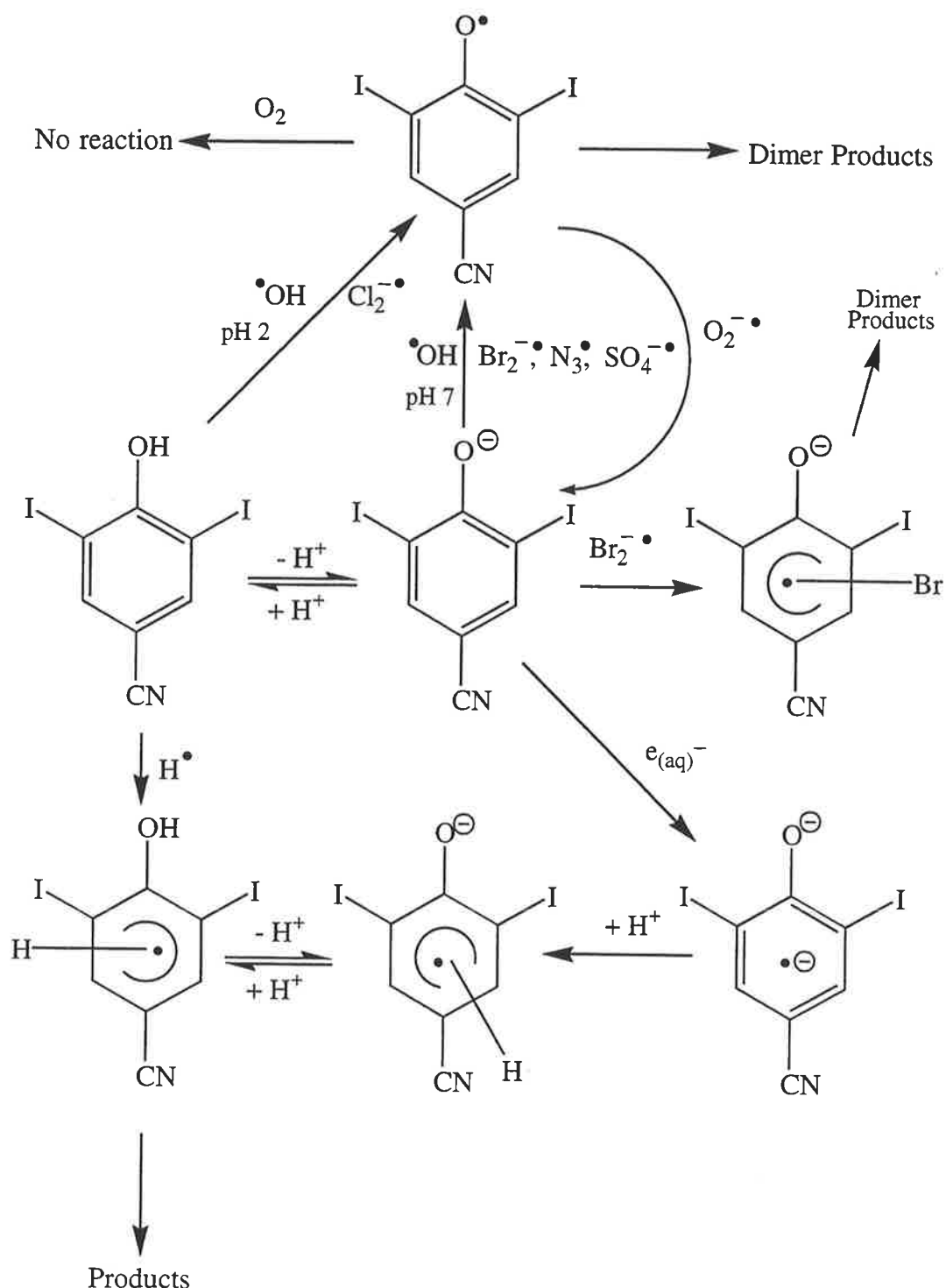


Figure 5.19. Overview of the radiation chemistry characterised in this study.

The TDA spectrum obtained from the reaction of Ioxynil with hydroxyl radicals did not suggest the formation of a OH-adduct as an intermediate. A large ground state absorbance for Ioxynil is responsible for the negative delta absorbance observed. Correction for the ground state absorbance of Ioxynil produced a spectrum which correlated to the phenoxyl radical of 3,5-diiodotyrosine. It is observed that the rate constant obtained for the reaction of Ioxynil with the hydroxyl radical is similar to that of 3,5-diiodotyrosine [122]. Reaction of 3,5-diiodotyrosine with the hydroxyl radical is known to predominantly proceed through a

phenoxy type radical, supporting the transfer of an electron to the hydroxyl radical from Ioxynil. The decay rate of the phenoxy type radical showed no dependence on the ionic strength of the solution, therefore the transient is neutral. The transient decays by second order kinetics, indicating that degradation products are formed by radical-radical reactions. HPLC characterisation of compounds formed by the reaction of Ioxynil with the hydroxyl radical through steady state irradiation showed that these compounds have a retention time greater than Ioxynil. This suggests the newly formed products are less polar than Ioxynil. Mass spectrometric studies determined that the major product had a mass equivalent to the dimer of Ioxynil minus two iodine atoms. This is in agreement with what we have determined through the pulse radiolysis studies. The rate of Ioxynil loss and the formation of products from the reaction of Ioxynil with the hydroxyl radical is initially linear under steady state irradiation. As the amount of hydroxyl radicals is increased past 50% of Ioxynil's concentration, the loss of Ioxynil and the formation of products follows a higher order kinetic mechanism. This result suggests that the products of the initial reaction also react with the hydroxyl radical to form (uncharacterised) compounds.

The TDA spectrum obtained upon the reaction of the hydroxyl radical with Ioxynil at pH 2 differs from that obtained from the same reaction at neutral pH. Correction for the ground state absorbance of Ioxynil produced a spectrum which matched the phenoxy type radical obtained at neutral pH. The rate constant for the reaction of Ioxynil with the hydroxyl radical at pH 2 is lower than that obtained at neutral pH. Qualitatively, this can be explained as follows: in the phenoxide form of Ioxynil the electron density is expected to be more accessible than in the case of the phenolic form. Since the hydroxyl radical behaves as an electrophile, its reaction with the electron rich phenoxide form is faster. Gamma irradiation coupled with HPLC of Ioxynil at pH 2, has shown that the compounds observed for the reaction of Ioxynil are those observed at neutral pH. Mass spectral fragmentation data indicated that this product is the same compound.

The transient produced from the reaction of Ioxynil with the hydroxyl radical has shown to be unreactive with oxygen as no change is observed in the decay of the transient. Gamma irradiation coupled with HPLC shows formations of the same products as in the deoxygenated solution. The major product's concentration is observed to decrease in the presence of the superoxide radical anion. Variation of the major product's concentration with pH indicated a dependence typical of an acid-base equilibria. Previous studies on the reactions of phenoxy radicals with the superoxide radical anion have produced conflicting

results on whether addition takes place in preference to electron transfer [103] [125]. Our results indicate that electron transfer is the preferential mechanism.

The TDA spectrum obtained from the reaction of Ioxynil with one electron oxidants is similar to that obtained for the phenoxyl radical of Ioxynil. The transient for the reaction of the one electron oxidants is therefore assigned as a phenoxyl radical. Rate constants for the bimolecular reaction of Ioxynil with one electron oxidising agents decrease with the redox potential of the oxidising agents, with the exception of the azide radical, which has a higher self exchange rate. Ioxynil is not observed to react with the diiodide radical anion and therefore the phenoxyl radical of Ioxynil is a powerful one electron oxidant with a redox potential between 1.4 and 1.0 V. Gamma irradiation coupled with HPLC for the one electron oxidising agents shows that the major product is that observed in the hydroxyl radical experiments. This is in agreement with what we have determined through pulse radiolysis studies. Minor products observed differed to those obtained for the hydroxyl radical experiment. Ioxynil's reaction with the dibromide radical anion produced a product which resulted in the addition of a bromide atom to Ioxynil.

Ab initio calculations indicate that the HOMO of Ioxynil is located over the aromatic ring in both the phenolic and a phenoxide forms. It is suspected that the electron loss occurs from this orbital, which is in agreement with the experimental results. The spin density surface is also located on the aromatic ring and the oxygen, and can be described by resonance theory.

The TDA spectrum obtained for the reaction of Ioxynil with the hydrated electron produced a large negative absorbance. The rate constant obtained for the reaction of Ioxynil with the hydrated electron is similar to that of 3,5-diiodotyrosine [130]. It is known that 3,5-diiodotyrosine reacts with the hydrated electron by addition to the aromatic ring, followed by the addition of a hydrogen ion to form a H-adduct. Decay of the transient is slow with little decrease in the absorbance of the transient observed. This suggests that the transient reacts quickly to form products that do not absorb in the 290 nm region. Steady state irradiation found a large loss in absorbance in this region for the parent compound. Gamma irradiation coupled with HPLC revealed the formation of one major product. Mass spectral analysis of the product did not identify a conclusive parent ion, precluding the structure from being determined. The radical anion of Ioxynil has been shown to be a strong reducing agent with a redox potential between -2.0 and -2.9 V.

Ab initio calculations indicate that the LUMO of Ioxynil is located over the aromatic ring and the iodines of Ioxynil. It is suspected the electron gain would initially occur in this orbital. The spin density surface is also located on the ring, which is in agreement with the experimental results.

The TDA spectrum recorded for the reaction of Ioxynil with hydrogen atoms differs from that recorded for the hydrated electron. Gamma irradiation coupled with HPLC shows the formation of one major product. This product is at the same retention time observed for the hydrated electron's major product. The radical anion produced by the reaction of Ioxynil with the hydrated electron must therefore undergo addition of a hydrogen ion to form the same products as observed for the hydrogen atom. Corrections made to the spectra accounting for the differences in ground state absorbance did not match the spectra, suggesting that the transient species' absorbance is effected by pH.

Ioxynil will degrade upon the reaction with a number of free radicals produced in natural and treated industrial discharge water, however, upon formation of the phenoxy type radical of Ioxynil, it can react via electron transfer to regenerate Ioxynil.

6.0 Radiation Chemistry of Aqueous Chlorsulfuron Solution

6.1 CHLORSULFURON

Chlorsulfuron (2-chloro-N-[[[4-methoxy-6-methyl-1,3,5, triazine-2-yl)-amino] carbonyl] benzenesulfonamide) (Figure 6.01) was first synthesised by Ulrich *et al.* in 1966 [131]. It is a white solid with a melting point of 174-178 °C. The maximum solubility in water is 125 ppm [131].

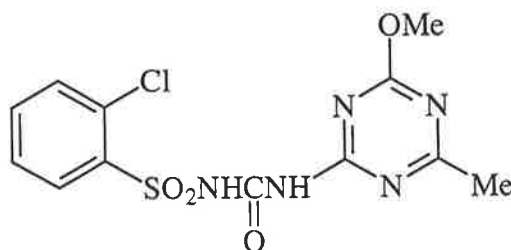


Figure 6.01. Chemical structure of Chlorsulfuron.

Chlorsulfuron was first released as a herbicide by the Du Pont company in 1981 [131]. Since then, it has been shown to provide control of a large number of weed species. The great advantage of Chlorsulfuron is that only small quantities are required to give the desired results, typically between 4 and 27 g/ha [132] depending on the type of soil. The effective quantity is 100 times less than that of the herbicides used previously [133].

The application rate required is low due to Chlorsulfuron's selectivity for weeds [134]. Weeds are poisoned specifically because Chlorsulfuron has the ability to inhibit the enzyme acetolactate synthetase, which is involved in the biosynthesis of valine and isoleucine [134]. Cereal crops (including wheat and corn) possess an enzyme which effectively deactivate the herbicide to harmless conjugates for example, the O-glucose conjugates [135].

Despite the relatively large number of advantages that Chlorsulfuron possesses, there are also disadvantages to its use. The most negative aspect of Chlorsulfuron is its ability to remain in the soil for periods longer than one crop rotation [136, 137]. This can be detrimental to cereal crops which do become susceptible at higher concentrations of the herbicide [138]. The other disadvantage of Chlorsulfuron is its potential to leach deep into the soil, where microbiological activity is low [138]. Chlorsulfuron residues can therefore persist for much longer periods of time, and ultimately reach the water table.

Normal degradation of Chlorsulfuron occurs via two primary routes. The first is through hydrolysis of the compound in slightly acidic environments. The second mechanism is through microbiological degradation. However, when the pH rises above 7.5, both chemical hydrolysis and microbiological degradation are restricted. Chlorsulfuron has a pK_a of 3.3; at higher pH it deprotonates one of the nitrogens in the sulfonurea bridge [139], with the negative charge created by the deprotonation of the nitrogen resonance stabilised over the carbonyl. In the hydrolysis of Chlorsulfuron, water attacks the carbonyl, as shown in Figure 6.02. When the carbonyl is resonance stabilising the negative charge at high pH it becomes unavailable for this type of reaction. Chlorsulfuron is therefore more persistent in alkaline environments [131, 140, 141].

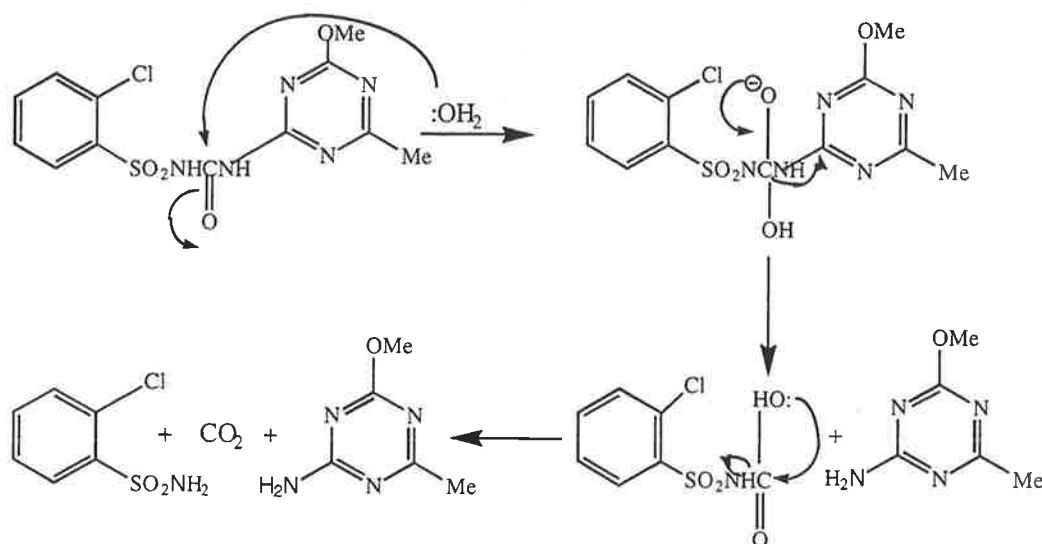


Figure 6.02. Reaction scheme for the hydrolysis of Chlorsulfuron.

6.2 REACTION OF CHLORSULFURON WITH THE HYDROXYL RADICAL

Figure 6.03 shows the time resolved TDA spectra obtained upon pulse radiolysis of an aqueous Chlorsulfuron (1×10^{-4} M) solution saturated with nitrous oxide (pH 6.8, phosphate buffer). It exhibits an absorption band with maxima at 310 nm and 350 nm.

In the presence of *t*-butyl alcohol (0.1 M), an effective hydroxyl radical scavenger but a weak hydrogen atom scavenger, the absorption spectrum was considerably reduced. The high $G(\cdot\text{OH})$ yield and appreciable decrease in the transient absorption suggests the transient absorption spectrum in Figure 6.03 is due mainly to the reaction of the hydroxyl radical with Chlorsulfuron.

No negative absorbance was detected in the TDA spectrum recorded between the hydroxyl radical and Chlorsulfuron. This is because the Chlorsulfuron anion does not have a large ground state absorbance in the region of 250 to 450 nm. The TDA spectrum can be corrected for the small ground state absorbance by using the formula 3.14 and the assumption that the yield of hydroxyl radicals is equal to the yield of the transient radical. Since the ground state absorbance in this region is not significant when compared to the absorbance of the radical, the molar delta optical absorbance spectrum of the radical does not vary considerably in shape from the delta absorbance spectra observed in Figure 6.03.

Reducing the dose (and hence the amount of transient radical) produced an increase in the half life of the transient species at these wavelengths. The radical therefore decays by second order kinetics. When the decay curves were fitted to second order kinetics they produced a fit with decay rates of $2k/\epsilon l = 1.1 \times 10^5 \text{ s}^{-1}$ and $1.8 \times 10^5 \text{ s}^{-1}$ at 310 nm and 350 nm respectively. Assuming that all the hydroxyl radicals react with Chlorsulfuron and the G value of the hydroxyl radical is equal to that of the transient (ie. 5.5), the molar absorbance of the maxima are $1600 \text{ M}^{-1} \text{ cm}^{-1}$ and $1700 \text{ M}^{-1} \text{ cm}^{-1}$ for 310 nm and 350 nm, respectively. Using the molar absorbance values, it was determined that $2k = 1.8 \times 10^8 \text{ M}^{-1} \text{ s}^{-1}$ and $3.1 \times 10^8 \text{ M}^{-1} \text{ s}^{-1}$ respectively. Differences in the decay rates suggests that the absorbance maxima at 310 nm and 350 nm may be due to the formation of two different species.

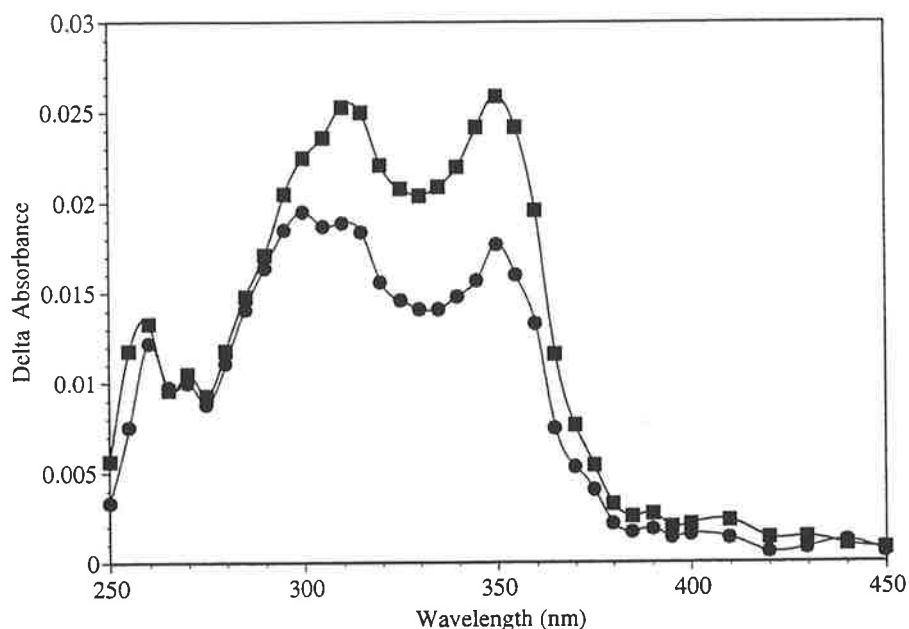


Figure 6.03. Time resolved TDA spectra obtained upon the pulse radiolysis of an aqueous Chlorsulfuron ($1 \times 10^{-4} \text{ M}$) solution saturated with nitrous oxide (pH 6.8, phosphate buffer). Spectra recorded at, ■ $10 \mu\text{s}$ after the pulse, ● $100 \mu\text{s}$ after the pulse.

Radiation chemistry studies on sulphone urea compounds and 1,3,5-triazines have not been extensively studied in the past, however some molecules containing similar functionality have been reported in the literature. This includes Sulphacetamide [142] and several 1,3,5-triazine [143, 144] derivatives. Sulphacetamide showed the formation of a OH-adduct when reacted with the hydroxyl radical; the reactions of 1,3,5-triazines with the hydroxyl radical were dependent on the other functional groups present. Since Chlorsulfuron is an unsaturated aromatic system, the spectrum observed in Figure 6.03 is most likely due to the formation of a OH-adduct from the addition of the hydroxyl radical to Chlorsulfuron. Carbons on the 1,3,5-triazine ring are electron deficient and can be thought of as positively charged. This has been described by Quirke [145] using the polar conical representation of 1,3,5-triazine presented in Figure 6.04. This makes the 1,3,5-triazine ring resistant to electrophilic reaction and suggests the hydroxyl radical would add to the benzenesulfonamide ring. The presence of two maxima decaying at different rates indicates the OH-adducts formed produce absorbances at different regions of the spectrum.

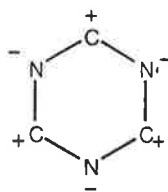


Figure 6.04. Polar canonical form of 1,3,5-triazine [145].

Adjusting the ionic strength of the solution by addition of NaClO_4 (1 M) produced an increase in the decay rate of both maxima. This suggests that the transient formed by reaction of the hydroxyl radical with Chlorsulfuron possesses a charge. At pH 6.8 Chlorsulfuron is a negatively charged species, and the transient resulting from the addition of the hydroxyl radical to Chlorsulfuron is expected to be negative and therefore observed result is in agreement with the postulated mechanism.

Competition kinetics produced a bimolecular rate constant for the reaction of the hydroxyl radical with the Chlorsulfuron anion of $2.4 \times 10^9 \text{ M}^{-1}\text{s}^{-1}$. This rate constant indicates that the Chlorsulfuron anion reacts with hydroxyl radicals at slightly less than diffusion controlled rates.

Though this is the first reported rate constant for the reaction of the hydroxyl radical with the Chlorsulfuron anion, rate constants for molecules that contain similar functional groups have been determined. These rate constants are:

Sulphacetamide	$k=9.2 \times 10^9 \text{ M}^{-1} \text{ s}^{-1}$ [142]
\8N,\8N'-Diethyl-6-methoxy-1,3,5-triazine-2,4-diamine	$k=4.7 \times 10^9 \text{ M}^{-1} \text{ s}^{-1}$ [144]
\8N,\8N'-Diethyl-6-(methylthio)-1,3,5-triazine-2,4-diamine	$k=2.6 \times 10^9 \text{ M}^{-1} \text{ s}^{-1}$ [144]
6-Chloro-\8N'-(1,1-dimethylethyl)-\8N-ethyl-1,3,5-triazine-2,4-diamine	$k=2.8 \times 10^9 \text{ M}^{-1} \text{ s}^{-1}$ [143]
\8N-Ethyl-\8N'-(1-methylethyl)-6-(methylthio)-1,3,5-triazine-2,4-diamine	$k=2.6 \times 10^{10} \text{ M}^{-1} \text{ s}^{-1}$ [144]
\8N-Ethyl-6-methoxy-\8N'-(1-methylethyl)-1,3,5-triazine-2,4-diamine	$k=3.3 \times 10^9 \text{ M}^{-1} \text{ s}^{-1}$ [144]
6-Chloro-\8N-ethyl-1,3,5-triazine-2,4-diamine	$k=1.8 \times 10^9 \text{ M}^{-1} \text{ s}^{-1}$ [143]
2-Chloro-4,6-diamino-1,3,5-triazine	$k=5 \times 10^7 \text{ M}^{-1} \text{ s}^{-1}$ [143]
6-Chloro-\8N-isopropyl-1,3,5-triazine-2,4-diamine	$k=1.2 \times 10^9 \text{ M}^{-1} \text{ s}^{-1}$ [143]
6-Hydroxy-\8N-ethyl-\8N'-isopropyl-1,3,5-triazine-2,4-diamine	$k=2.6 \times 10^9 \text{ M}^{-1} \text{ s}^{-1}$ [144]

From the rate constant data for the reaction of the hydroxyl radical with a 1,3,5-triazine ring, it can be observed that the rate constants are highly dependent on the functional group attached to the ring. The electron withdrawing chloro group generally produces a lower rate constant than of the electron donating alkyl and methoxy groups.⁴ Studies conducted by De Laat *et al.* [143, 144] did not elaborate on possible mechanisms for the reaction of the hydroxyl radical with the 1,3,5-triazine rings. It can, however, be observed from their results that the 2-Chloro-4,6-diamino-1,3,5-triazine molecule is similar to melamine and is not highly reactive as predicted by the polar canonical diagram.

Sulfacetamide has a relatively high rate constant with hydroxyl radicals when compared to the equivalent rate constant for Chlorsulfuron. This is explained by the presence of the amino group attached in the para position in Sulphacetamide, which would be electron donating therefore accelerating the electrophilic reaction. In Chlorsulfuron, the chloro group in the ortho position decreases the rate of reaction with the hydroxyl radical because it is electron withdrawing.

Steady state irradiation of an aqueous Chlorsulfuron (58 μM) solution saturated with nitrous oxide (Dose 80 Grays per hour) produced only a small decrease in absorbance due to the Chlorsulfuron anion at 236 nm (Figure 6.06). The spectrum varied slightly over the range of the dose radiation added to the system. The decrease in absorbance was less than expected according to dosimetry, suggesting that either the products must absorb in this region, or the transients formed by the reaction of the hydroxyl radical with the Chlorsulfuron react to reform the starting material, or a combination of both.

HPLC of a Chlorsulfuron (1×10^{-4} M) solution saturated with nitrous oxide (pH 6.8, phosphate buffer) and irradiated with gamma irradiation showed the formation of new species

and a decrease in the concentration of Chlorsulfuron (Figure 6.07), at 236 nm. No change in product distribution was observed at either 220 or 254 nm. Two predominate compounds (A & B) were detected in this trace along with three other minor products (C, D & E). All compounds were at a retention time less than Chlorsulfuron suggesting that all products were more polar. This is consistent with the addition of the hydroxyl radical to Chlorsulfuron to form hydroxylated species.

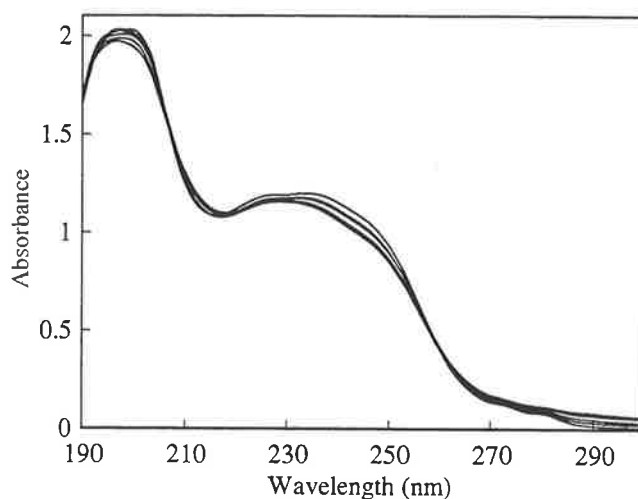


Figure 6.05. Observed change in optical absorbance of an aqueous Chlorsulfuron ($58 \mu\text{M}$) solution saturated with nitrous oxide and irradiated with gamma radiation (0 to 120 Gray). Dose rate 80 Grays/hr.

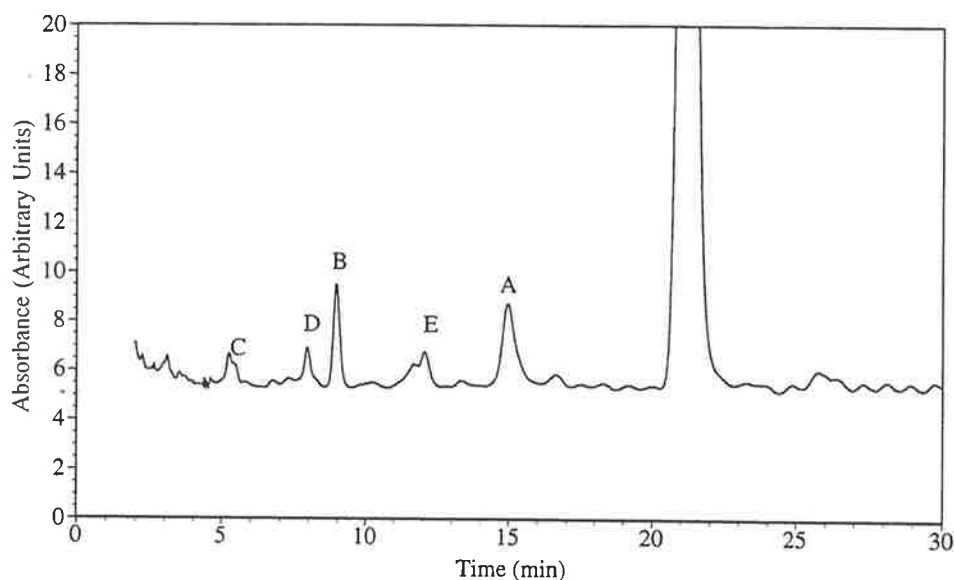


Figure 6.06. HPLC analysis following gamma irradiation of Chlorsulfuron ($1 \times 10^{-4} \text{ M}$) solution saturated with nitrous oxide (pH 6.8, phosphate buffer). The trace displays the products formed from the reaction of Ioxynil with hydroxyl radicals (A and E). See Figure 6.08 for product identification.

The area of the products formed at 236 nm does not equal the decrease in Chlorsulfuron concentration. The G value for the loss of Chlorsulfuron (after 20% of Chlorsulfuron had reacted) is 4.9. If second order reaction kinetics is controlling the decay of

the OH-adduct to form the hydroxylated product then a G value of about 2.8 is expected for the loss of Chlorsulfuron. The result suggests the transient formed is reacting through a pseudo first order mechanism with Chlorsulfuron. The reaction transpires because steady state irradiation produces a concentration of the transient that is many orders of magnitude less than the pulse radiolysis study. This effectively allows the pseudo first order reaction of the OH-adduct with Chlorsulfuron to compete with the second order decay. The result of this reaction is high molecular weight compounds that do not elute off the column readily.

A linear rate of Chlorsulfuron loss against concentration of hydroxyl radicals added to the system (calculated using Frickie Dosimetry) was observed, until approximately 30% of the Chlorsulfuron anion had reacted. The appearance of the products was also followed by HPLC and found to be initially linear, suggesting the compounds formed from the initial reaction also react with hydroxyl radicals. This is important in determining whether or not Chlorsulfuron undergoes full degradation in the environment. Further reactions of the initial products is required to breakdown the product to base constituents.

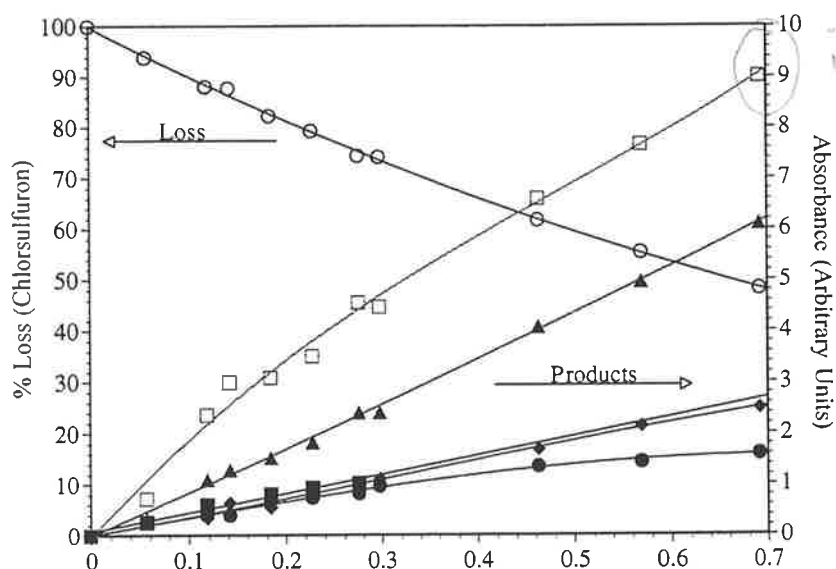


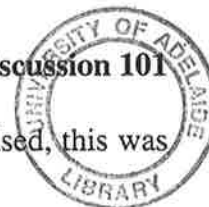
Figure 6.07. Loss of Chlorsulfuron anion (left axis) and the formation of the products (right axis) from the gamma irradiation of an aqueous Chlorsulfuron (1×10^{-4} M) solution saturated with nitrous oxide (pH 6.8, phosphate buffer). The products are A= \square , B= \blacktriangle , C= \blacksquare , D= \bullet , E= \blacklozenge .

Structures of the compounds created from the reaction of the hydroxyl radical with Chlorsulfuron were determined by electrospray mass spectrometry and reported in Figure 6.09. Chlorsulfuron produced a parent ion with a mass of 358/360 (3:1) Daltons ($M+H^+$) and a fragmentation pattern (using MS^2 experiment) that consisted of two daughter ions at 167 and 141 Daltons. This spectrum matches the previous recorded electrospray mass spectrum of Chlorsulfuron [146]. The predominate compounds A and B both produced a parent ion at

374/376 (3:1) Daltons . This mass corresponds to the addition of 16 Daltons or an oxygen atom to Chlorsulfuron. The 3:1 isotope pattern observed for the major compounds indicates that the chlorine atom is still located in the molecule. Fragmentation of the parent ion at 374 Daltons produced two daughter ions at 167 and 141 Daltons. These are the same two daughter ions observed in the fragmentation of Chlorsulfuron. Since the two daughter ions formed are from the triazine part of Chlorsulfuron, it is reasonable to assume the hydroxyl radical did not add to this part of the molecule, adding instead to the benzenesulfonamide ring. The exact position of the hydroxyl group on the benzenesulfonamide ring cannot be determined from the mass spectrometric analysis, however the position of the hydroxyl group must be in a different position to affect the polarity of the molecules and therefore displaying them in a different position in the HPLC chromatogram.

The minor products D and E also showed the same mass spectra patterns observed for A and B. Compounds D and E must also be Chlorsulfuron with the addition of a hydroxyl group onto the benzenesulfonamide. The four products place a hydroxyl group on each of the non sterically hindered carbons on the benzene ring. The amount of each compound formed suggests that either the molar absorbance of the species varies widely with the position of the hydroxyl group and/or the addition of the hydroxyl radical shows some selectivity to its position in the ring. It is known that the hydroxyl radical shows some selectivity when adding to aromatic systems. Schuler [101] demonstrated that the partial rate constants for addition of the hydroxyl radical to the ortho and para positions of biphenyl is greater than for the addition to benzene. Addition of the hydroxyl radical to the meta position was found to be less rapid. The electrophilic hydroxyl radical will react with an electron rich site more rapidly than an electron poor site.

Ab initio calculations performed on Chlorsulfuron for the deprotonated form (with one proton missing from the triazine side of the sulphone urea bridge) showed the most electron dense ring to be the benzenesulfonamide. The triazine ring produced natural populations similar to that described in Figure 6.04. On the benzenesulfonamide ring the non sterically hindered carbons show varying natural populations. Carbons in both the meta positions to the sulphone group produced the highest electron density, suggesting the hydroxyl radical would preferentially react at these positions. The two remaining non sterically hindered carbons (ortho and para to the sulphone group) show significantly less electron density in comparison. As stated earlier, it is impossible from the mass spectra to determine the position of the hydroxyl group. To determine the exact position of the hydroxyl group on the ring the molecule would have to be obtained and then matched to the retention time in the trace. Since



these compounds are not commercially available they would have to be synthesised, this was considered beyond the scope of this project and therefore was not attempted.

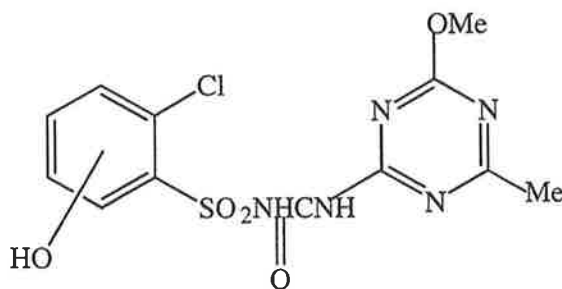


Figure 6.08. Compounds (A, B, D and E) of the gamma radiolysis of an aqueous Chlorsulfuron in nitrous oxide saturated solution as determined by the analysis of electrospray mass spectrometric fragmentation data. Location of the hydroxyl groups are not unambiguously assignable in the structures. See text for discussion.

6.3 REACTION OF CHLORSULFURON WITH THE HYDROXYL RADICAL IN ACIDIC SOLUTION

The corrected TDA spectrum obtained from pulse radiolysis of Chlorsulfuron (1×10^{-4} M) in acidic solution (pH 2, HClO_4) saturated with nitrous oxide was identical to that observed in Figure 6.03 for the neutral pH experiment ($10 \mu\text{s}$). A correction to the spectrum was made to take into account the lower G value at pH 2 due to formation of hydrogen atoms from the reaction of hydrated electrons with the hydrogen ions. The maxima at 310 nm and 350 nm decayed by second order kinetics with $2k/\epsilon l = 2.5$ and $3.2 \times 10^8 \text{ M}^{-1}\text{s}^{-1}$ respectively. The values are slightly higher than the figures reported in section 6.2. This evidence suggests that the transient produced is the same as that observed at neutral pH. The higher decay rate results because Chlorsulfuron has a pK_a of 3.3, [139] and at low pH the transient will be neutral and therefore will decay faster because it does not have to overcome electrostatic repulsion.

The transient produced by the reaction of Chlorsulfuron with hydroxyl radicals is independent of the pH of solution (pH 2.0 to 6.8), indicating that the protonation state of Chlorsulfuron had no effect on the absorbing chromophore of the radical. The protonation-deprotonation sites are the nitrogens of the sulphone urea bridge. The negative charge created by the deprotonation is resonance stabilised by the carbonyl and the sulphone groups. This is in agreement with the experimental results, since it was determined in section 6.2 that addition of the hydroxyl radical took place on the benzenesulfonamide ring, which is electronically isolated from the protonation-deprotonation point.

Competition kinetics were used to determine a bimolecular rate constant for the reaction of the hydroxyl radical with Chlorsulfuron of $1.7 \times 10^9 \text{ M}^{-1}\text{s}^{-1}$ at pH 2 (HClO_4). The rate constant indicates that neutral Chlorsulfuron reacts with hydroxyl radicals at a rate slightly less than the anion. This result is expected due to the electrophilic nature of the hydroxyl radical.

At low pH Chlorsulfuron undergoes hydrolysis as shown in Figure 6.02. This process is catalysed by the presence of the hydrogen ions [147]. Since steady state irradiations were performed at dose rates of 60 to 80 Grays per hour, hydrolysis of Chlorsulfuron is not insignificant over the reaction time scale. For this reason no steady state reactions of Chlorsulfuron at pH 2 were conducted. Pulse radiolysis performed on solutions at pH 2 were made fresh before the experiment with the experiment conducted over a short time scale so as to avoid interference effects from the competing hydrolysis (determined by UV).

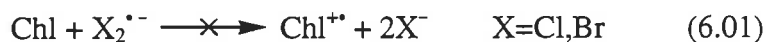
6.4 REACTION OF CHLORSULFURON WITH THE HYDROXYL RADICAL IN THE PRESENCE OF OXYGEN

Decay of the transient produced by the reaction of hydroxyl radicals with the Chlorsulfuron anion (pH 6.8, phosphate buffer), in a solution saturated with nitrous oxide/oxygen (4:1 v/v), showed no observable change in the rate of decay of the transient at 310 nm and 350 nm. Carbon centred radicals are known to react quickly with oxygen, however the reaction of cyclohexadienyl type radicals is documented to be slower than other carbon centred radicals [100]. The observation that there is no increase in the decay rate indicates that ^{NO}if a reaction between the transient and oxygen is occurring, then the reverse reaction is faster. Delocalisation of the unpaired electron on the sulphone group would make the reaction with oxygen unfavourable.

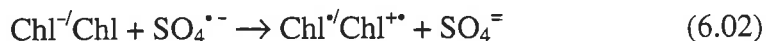
Steady state irradiation of a Chlorsulfuron solution saturated with nitrous oxide/oxygen (4:1 v/v) (pH 6.8, phosphate buffer) produced no change in the product distribution from that observed in the nitrous oxide saturated solution. This result is consistent with the pulse radiolysis data. Electrospray mass spectrometry confirmed that the five species collected in the experiment were the same as those reported in section 6.2, as they displayed the same parent ions and fragmentations patterns.

6.5 REACTION OF CHLORSULFURON WITH ONE ELECTRON OXIDANTS

The dichloride radical anion formed in the pulse radiolysis of oxygen saturated sodium chloride (0.02 M) Chlorsulfuron solution (1×10^{-4} M) at pH 2 (HClO_4) reacts as a strong one electron oxidant with a potential of 2.09 V (versus NHE) [43]. Reaction of the dichloride radical anion with Chlorsulfuron was studied by following the decay of the dichloride radical anion absorption band of 340 nm. It was observed that in the presence of Chlorsulfuron (1×10^{-4} M) this band still decayed by second order kinetics, therefore indicating that a reaction between Chlorsulfuron and the dichloride radical anion had not resulted. When sodium chloride was replaced with sodium bromide (0.02 M) (pH 6.8 and 2.0) no effect on the decay of the dibromide radical anion at 360 nm was observed. This implies that the following reaction is not occurring and therefore no electron is being transferred from Chlorsulfuron to the dihalide radical anions.



The sulfate radical anion formed in the pulse radiolysis of nitrogen saturated potassium persulfate (0.02 M), *t*-butyl alcohol (0.1 M), Chlorsulfuron solution (1×10^{-4} M) at pH 6.8 and 2.0 (phosphate buffer and HClO_4 respectively) reacts as a strong one electron oxidant with a potential of 2.43 V (versus NHE) [43, 86, 148]. Reaction of the sulfate radical anion with Chlorsulfuron was studied by observing the decay of the sulfate radical anion absorption band at 460 nm. It was observed that in the presence of Chlorsulfuron (1×10^{-4} M) this band decayed faster than without the Chlorsulfuron, indicating a reaction between Chlorsulfuron and the sulfate radical anion occurred. Since Chlorsulfuron reacts with the sulfate radical anion and not the dichloride radical anion, it implies that the $\text{Chl}^{+}/\text{Chl}$ (Chlorsulfuron is mainly protonated at pH 2) redox potential must lie between that of the sulfate and dichloride radical anions. i.e. between 2.43 to 2.09 V (versus NHE).



Using the pseudo first order rate constants of the decay of the sulfate radical anion at 460 nm it was determined that 13.5 μs after the pulse more than 90% of the sulfate radical anion had reacted with Chlorsulfuron. The TDA spectrum obtained at this time is reported in Figure 6.09. This spectrum shows two very broad peaks at 310 and 440 nm. The spectrum is different to that obtained from the reaction of the hydroxyl radical with Chlorsulfuron and is therefore not assigned to the OH-adduct. The recorded spectrum indicates that Chlorsulfuron

does not react with the sulphate radical anion to form a transient which then transforms into a OH-adduct.

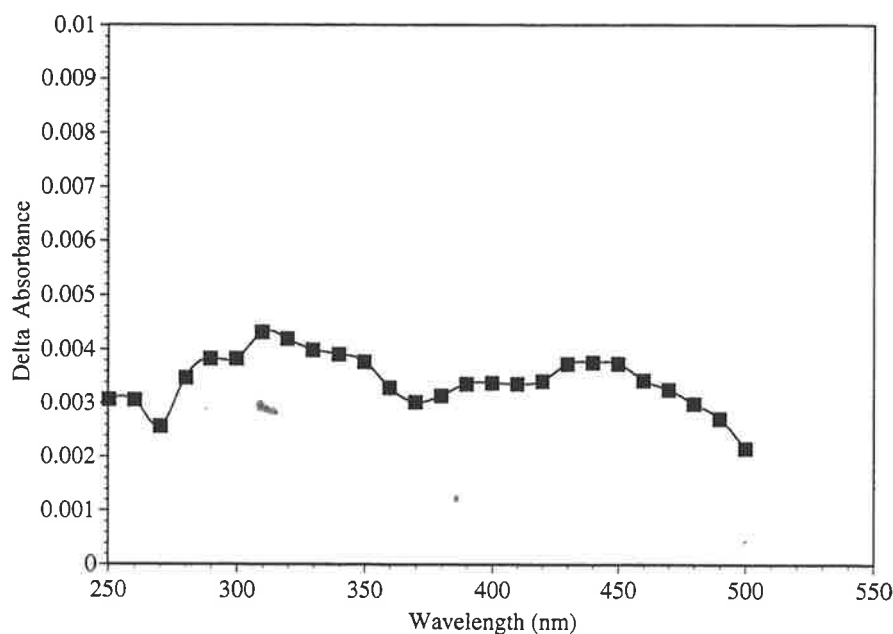


Figure 6.09. TDA spectrum obtained upon pulse radiolysis of an aqueous Chlorsulfuron solution (1×10^{-4} M) containing potassium persulfate (0.02 M), *t*-butyl alcohol (0.1 M) saturated with nitrogen (pH 6.8, phosphate buffer). Spectrum recorded 13.5 μ s after the pulse.

The rate constant for the reaction of Chlorsulfuron with the sulfate radical anion was determined from the slope of a plot of the pseudo first order rate constant of the decay of the sulfate radical anion at 460 nm against the concentration of Chlorsulfuron. This produced a bimolecular rate constant of $3.8 \times 10^8 \text{ M}^{-1} \text{ s}^{-1}$. It should be noted that the value recorded here might show some effects from the absorbance of the transient at 460 nm. Sulfacetamide in its protonated and deprotonated states has been reacted with a number of one electron oxidants including the sulfate radical anion, the dichloride and dibromide radical anions. Rate constants determined by Sunil *et al.* [142] were observed to vary widely with the type of oxidising radical used and the protonation state of Sulphacetamide. While Chlorsulfuron produced no reaction with the less powerful one-electron oxidants the Sulphacetamide molecule did. The difference in results between the compounds occurs because of the triazine ring of Chlorsulfuron. 1,3,5 Triazine or any of its derivatives have not been reported to react with one electron oxidants and thus little information is available [149]. It is postulated that they would be unreactive toward the triazine ring for the reasons given in section 6.2 and Figure 6.04. That is, the nitrogen in the ring has the greatest share of the electron density, making it unsuitable for electrophilic reactions. The sulphone is the fully oxidised form of sulphur and it is reasonable to assume that it will not readily donate an electron.

Steady state irradiation of a Chlorsulfuron solution (1×10^{-4} M) containing potassium persulfate (0.02 M), *t*-butyl alcohol (0.1 M) and saturated with nitrogen (pH 6.8, phosphate buffer) produced a loss of Chlorsulfuron and the formation of new species at 11 (A) and 14 (B) minutes in the HPLC trace (Figure 6.10). A non-irradiated sample of the above solution displayed no loss of Chlorsulfuron therefore indicating the reaction products were not due to thermal oxidation of Chlorsulfuron by the persulfate ion [43]. Compounds formed by the reaction of Chlorsulfuron with the sulfate radical anion are at a retention time less than that of Chlorsulfuron. This indicates that the compounds A and B are more polar than Chlorsulfuron.

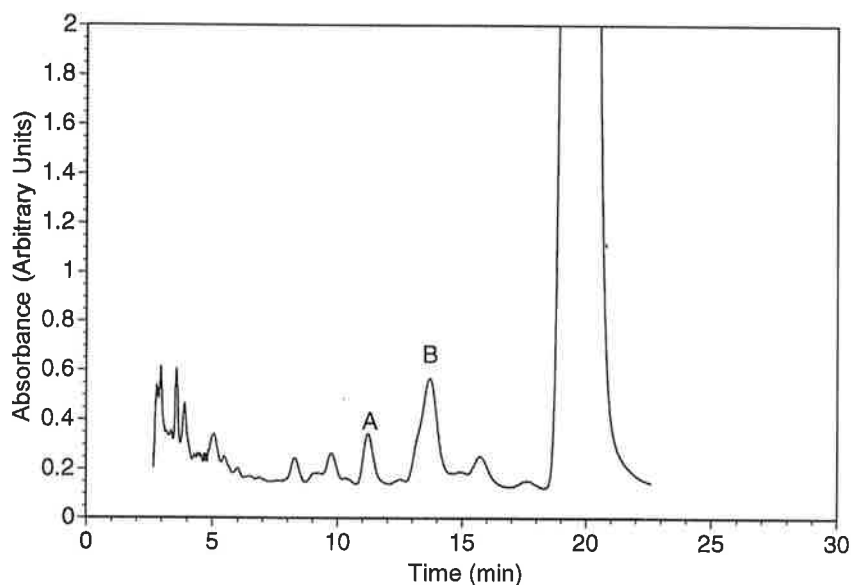


Figure 6.10. HPLC analysis following gamma irradiation of an aqueous Chlorsulfuron solution (1×10^{-4} M) containing potassium persulfate (0.02 M), *t*-butyl alcohol (0.1 M) and saturated with nitrogen (pH 6.8, phosphate buffer). The trace displays the products formed from the reaction of Chlorsulfuron with the sulfate radical anion (A and B). See text for details.

Electrospray mass spectrometry on the compounds produced the mass of 251/253 (3:1) and 323/325 (3:1) Daltons for A and B respectively. Isotope patterns of 3:1 for both compounds suggest the chlorine atom is still present in the molecule, since in both cases the first peak is three times the size of the next peak. MS^n experiments on A displayed the loss of 18 Daltons (OH_2), followed by another 57 Daltons (C_4H_9) and then a further 35 Daltons (a chlorine atom). The fragmentation pattern indicates loss of a *t*-butyl group from compound A. The parent ion corresponds to the benzenesulfonamide ring with one double bond saturated with hydrogen and the addition of *t*-butyl alcohol. Analysis of the products indicates that the transient produced by the reaction of Chlorsulfuron with the sulphate radical anion reacts with *t*-butyl alcohol. Compound B produced a daughter ion at 167 (the triazine ring to the carbonyl) and at 153 Daltons (minus a further nitrogen). A subsequent MS^3 fragmentation experiment on the 153 daughter ion produced a loss of 28 Daltons (CO). The fragmentation

pattern indicates that compound B still has the triazine ring intact. The total difference in mass to charge ratio from that of Chlorsulfuron is 8 Daltons. No reasonable structure can be determined from the data obtained for compound B. It does however indicate that the triazine ring has remained unaffected by the one electron loss from Chlorsulfuron. This is to be expected because the triazine ring does not contain electron density that is available to the oxidant.

No steady state reaction was performed using the dichloride radical anion since it required low pH for its formation. This would produce significant hydrolysis of Chlorsulfuron over the time span of the experiment.

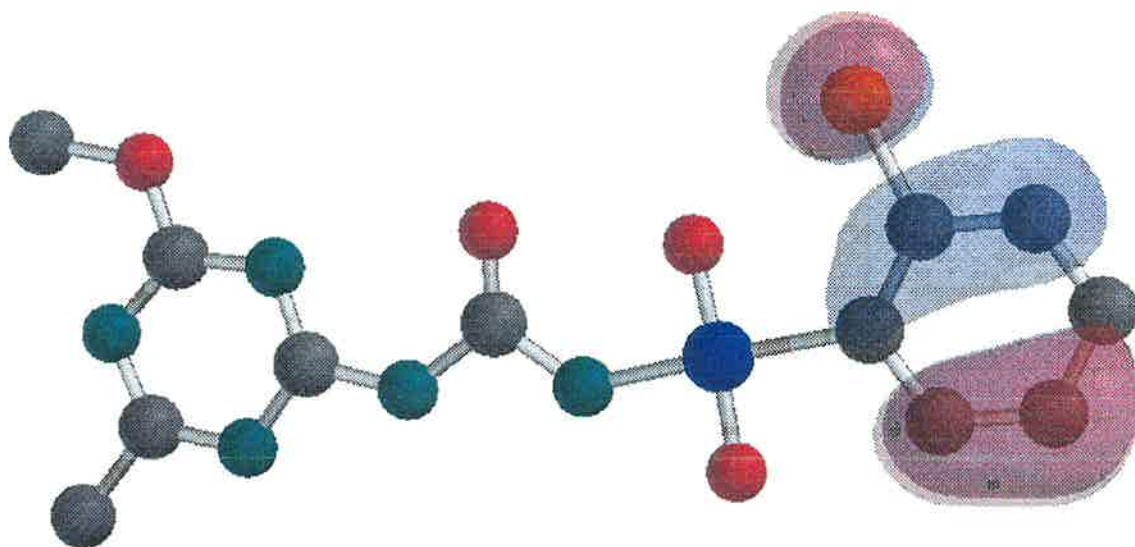


Figure 6.11. Plot of the HOMO of Chlorsulfuron as determined by *ab initio* molecular orbital theory. Calculations were performed at the HF/6-31G** level of theory. The plot was determined for the neutral molecule possessing a corresponding multiplicity of +1.

Ab initio calculations on the Chlorsulfuron anion failed to optimise successfully with the molecule falling apart at the sulphone group during the calculations. Using a less computationally expensive basis set like HF/STO-3G did not effect this fragmentation. The failure meant calculations were confined to neutral Chlorsulfuron. Figure 6.11 displays the HOMO for neutral Chlorsulfuron. It is observed from this diagram that the HOMO is located over the benzene ring attached to the sulphonamide group. The position of the HOMO is in agreement with the polar conical diagram presented in figure 6.04. It also agrees with the experimental observations that the triazine ring remained unaffected by the oxidation, since the electron would be expected to be removed from this orbital. Optimisation of

Chlorsulfuron's radical cation also failed with the molecule falling apart during calculations, thus no spin surface could be generated for this transient

6.6 REACTION OF CHLORSULFURON WITH THE HYDRATED ELECTRON

The rate of decay of the hydrated electron's absorbance at 640 nm was observed to increase in the presence of small amounts of Chlorsulfuron (1×10^{-4} M) at pH 7.0 (phosphate buffer and NaOH). This indicates that a reaction between the hydrated electron and Chlorsulfuron anion is occurring. The TDA spectrum obtained upon pulse radiolysis of an aqueous Chlorsulfuron (1×10^{-4} M) solution containing *t*-butyl alcohol (0.1 M) saturated with nitrogen gas (pH 7.0, phosphate buffer and NaOH) is reproduced in Figure 6.12. This spectrum exhibits a small absorbance in the region between 250 and 400 nm. The maximum of the spectrum was recorded at 330 nm, with what seems to resemble a small shoulder at 290 nm. No significant absorbance was recorded in the region between 400 and 640 nm. Comparing the TDA spectrum recorded here with the equivalent reaction of the hydrated electron with sulphanilamide shows a different TDA spectrum [150], indicating that a different mechanism is occurring between the two compounds. Sulphanilamide is known to react with the hydrated electron to produce a transient with the radical residing on the sulfur. The transient obtained for Chlorsulfuron's reaction with the hydrated electron therefore cannot be of a similar nature.

The bimolecular rate constant for the reaction of the hydrated electron with Chlorsulfuron was determined from the slope of a plot of the decay rate of the hydrated electron at 640 nm against the concentration of Chlorsulfuron (20 to 50 μ M). The rate constant determined was $1.7 \times 10^{10} \text{ M}^{-1} \text{ s}^{-1}$. Though this is the first reported rate constant for the reaction of the hydrated electron with the Chlorsulfuron anion, rate constants for compounds with similar functional groups have been reported and can be observed below.

Chlorobenzene	$k=5.0 \times 10^8 \text{ M}^{-1} \text{ s}^{-1}$ [129]
Sulphanilamide	$k=2.4 \times 10^{10} \text{ M}^{-1} \text{ s}^{-1}$ [150]
Benzenesulphamide	$k=9.8 \times 10^9 \text{ M}^{-1} \text{ s}^{-1}$ [150]

No rate constants on 1,3,5-triazine or any derivative have been recorded with the hydrated electron [149]. The rate constant for the reaction of Chlorsulfuron is closer to the benzenesulphamide than chlorobenzene, suggesting a reaction similar to that of benzenesulphamide.

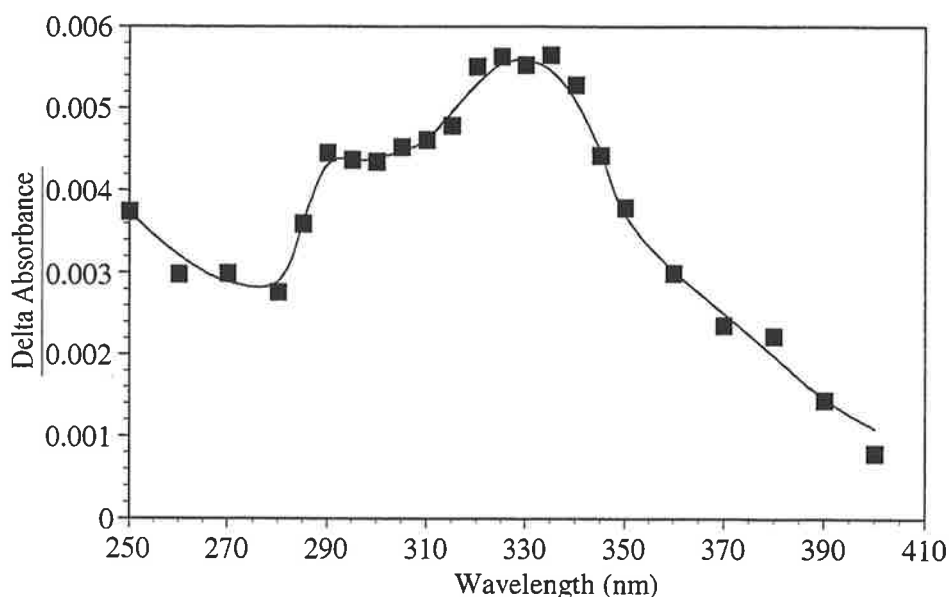


Figure 6.12. TDA spectrum obtained upon the pulse radiolysis of an aqueous Chlorsulfuron (1×10^{-4} M) solution containing *t*-butyl alcohol (0.1 M) saturated with nitrogen gas (pH 7.0, phosphate buffer and NaOH). The spectrum was recorded 5 μ s after the pulse.

A study by Phillips *et al.* [150] on the reaction of hydrated electron with benzenesulphamide and its derivatives found the end result of the reaction to be highly dependent on the other functional groups present in the molecule. In all cases the reaction of hydrated electrons with the benzenesulphamide resulted in the addition of the electron to the molecule, usually to the sulphone group.

Reaction of the hydrated electron with Chlorsulfuron should initially result in addition of an electron to Chlorsulfuron to form the Chlorsulfuron radical di-anion (ie. $\text{Chl}^{\cdot-2}$). The site of the addition of the electron should be to the sulphone group. Once the sulphone group has captured the electron, it is likely that the radical will be stabilised into the benzenesulfonamide ring. This would then be expected to result in the dissociation of a chloride ion from the parent molecule.

Ab initio calculations performed on neutral Chlorsulfuron indicated that the sulphur atom was the most electron poor atom in the molecule. Spin calculations on the Chlorsulfuron radical anion could not be completed because the molecule fragmented in much the same way as was observed for the radical cation. The LUMO is displayed in Figure 6.13 with the density surface map superimposed on it. The diagram indicates that the LUMO is located over the sulfur atom with part of this orbital protruding out of the density map, indicating that this is the most likely spot for nucleophilic attack. This result is in agreement with the experimental results.

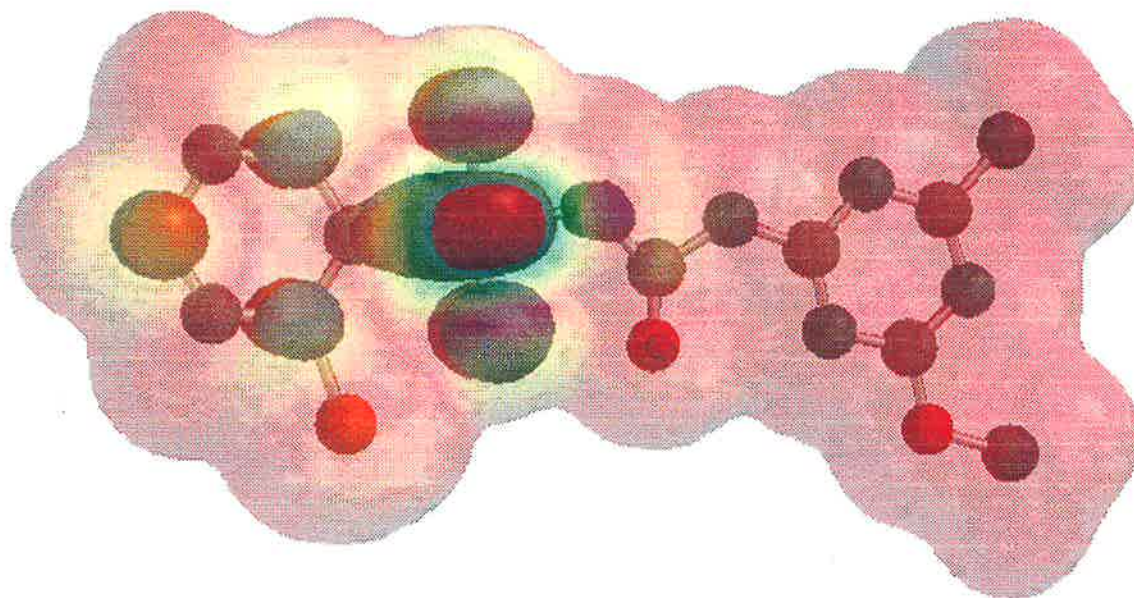


Figure 6.13. Plot of the LUMO with the superimposed density surface of the LUMO of Chlorsulfuron as determined by *ab initio* molecular orbital theory. Calculations were performed at the HF/6-31G** level of theory. The plot was determined for the neutral molecule possessing a corresponding multiplicity of +1.

Time resolved studies out to 1000 μs showed no formation of any new peaks in the region of 250 to 600 nm, suggesting that the reaction forms stable products which do not absorb in this region.

Gamma irradiation of an aqueous Chlorsulfuron ($8.4 \times 10^{-5} \text{M}$) solution containing *t*-butyl alcohol (0.1 M) and saturated with nitrogen (pH 7.0, phosphate buffer and NaOH) produced the HPLC trace observed in Figure 6.14. The effect on optical absorbance was to decrease the absorbance maximum at 236 nm and to form a new maximum at 230 nm. The HPLC trace of the same solution indicated the formation of a major species at 15 minutes. Mass spectrometry on this compound produced a mass to charge ratio at 324 Daltons. Loss of the isotope pattern indicates the chlorine atom is no longer present in the molecule. The mass to charge ratio of 324 Daltons is 34 Daltons less than that of Chlorsulfuron, or minus one chlorine atom, plus one hydrogen atom. MS^2 fragmentation of the 324 peak produced the familiar daughter ion of 161 and 141 Daltons which are formed from the triazine ring when the same experiment is performed on Chlorsulfuron. The exact mechanism for the reaction of the hydrated electrons with Chlorsulfuron would be initial electron capture, followed by ejection of a chloride ion leaving an alkyl radical. This radical would then extract an hydrogen atom from the *t*-butyl alcohol to form the observed compound. These observations allow for the postulation of the mechanism in Figure 6.15.

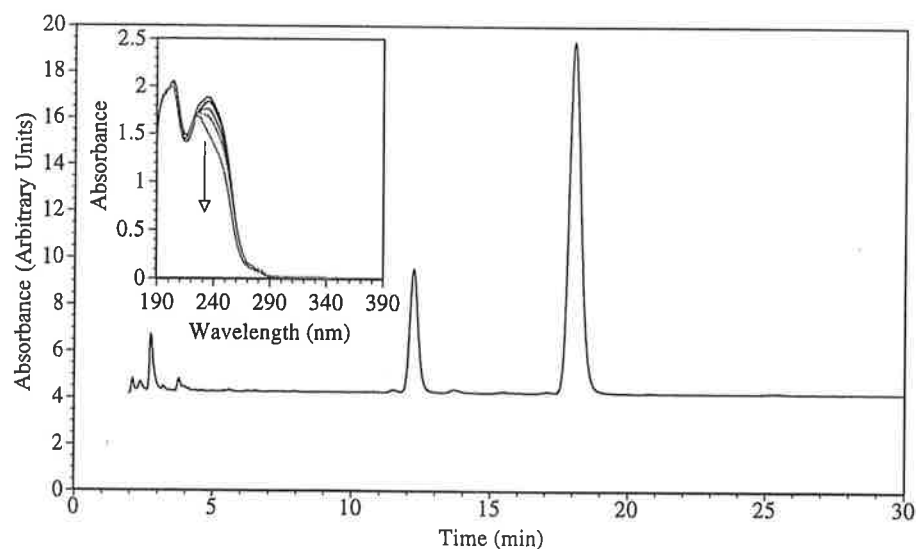


Figure 6.14. HPLC analysis following the gamma irradiation of an aqueous Chlorsulfuron ($8.4 \times 10^{-5} \text{M}$) solution containing *t*-butyl alcohol (0.1 M) and saturated with nitrogen (pH 7.0, phosphate buffer and NaOH). The arrow indicates the direction of absorbance change. Inset. Observed change in optical absorbance of the same solution (0 to 400 Gray).

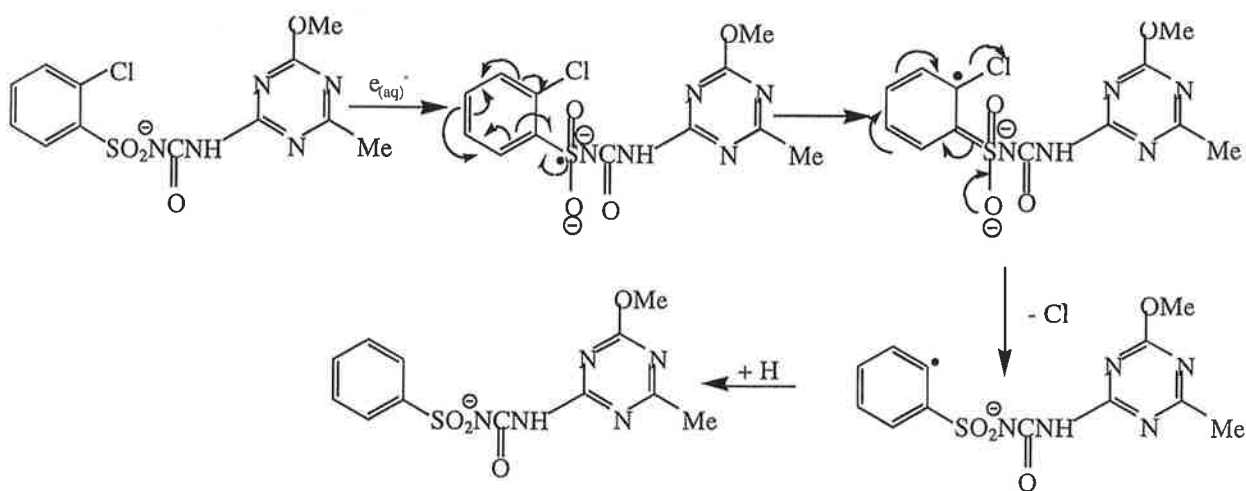


Figure 6.15. Proposed scheme for the reaction of the hydrated electron with Chlorsulfuron. See text for discussion.

Analysis of the above solution after steady state irradiation indicated the presence of chloride ion. The G value determined for the production of the chloride ion was 0.75, and the G value for the loss of chloride ion is the same value as determined for the destruction of Chlorsulfuron. This indicates the chloride anion is being eliminated quantitatively from the molecule as a result of the hydrated electron's reaction with Chlorsulfuron.

6.7 REACTION OF CHLORSULFURON WITH THE HYDROGEN ATOM

Figure 6.16 shows the TDA spectrum obtained upon the pulse radiolysis of an aqueous Chlorsulfuron (1×10^{-4} M) solution containing *t*-butyl alcohol (0.1 M) saturated with nitrogen (pH 2, HClO_4). It exhibits an absorption peak with a maximum at 340 nm. The TDA spectrum is similar in shape to that obtained for the H^{\bullet} -adduct, therefore the absorbance observed from this reaction probably results from the addition of the hydrogen atom to the benzene ring.

Formation kinetics conducted from the slope of a plot of the pseudo first order rate constant against the concentration of Chlorsulfuron at 340 nm, produced a bimolecular rate constant for the reaction of $1.4 \times 10^9 \text{ M}^{-1} \text{ s}^{-1}$. This rate is fast for a hydrogen atom, but is still slower than that of the reaction with hydroxyl radicals at the same pH. No direct comparison could be made with the reactions of similar functional groups as none have been reported in the literature [149].

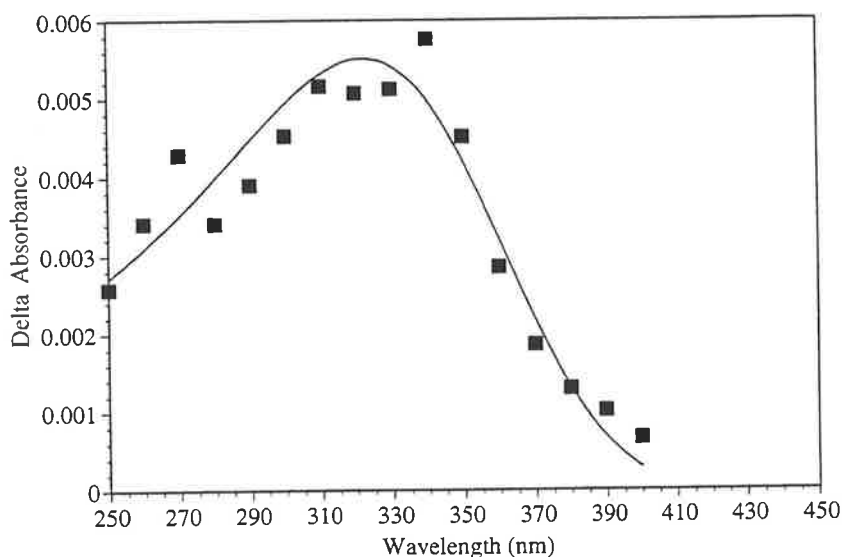


Figure 6.16. TDA spectrum obtained upon the pulse radiolysis of an aqueous Chlorsulfuron (1×10^{-4} M) solution containing 0.1 M *t*-butyl alcohol saturated with nitrogen (pH 2, HClO_4). Spectrum recorded 10 μs after the pulse.

Hydrolysis of Chlorsulfuron is significant at the low pH values required for the formation of the hydrogen atom, thus the steady state reaction could not be carried out. The formation of the H-adduct can therefore not be confirmed comprehensively,

6.8 REACTION OF CHLORSULFURON WITH REDUCING RADICALS.

Pulse radiolysis of a nitrous oxide saturated solution containing sodium formate (0.02 M) and Chlorsulfuron (1×10^{-4} M) (pH 6.8, phosphate buffer) produced a maximum below 250 nm with no other absorbance maxima observed. Absorbance observed was due to the formation of the carbon dioxide radical anion. Time resolved studies out to 1000 μ s indicated the presence of no new absorption in the range of 250 nm to 600 nm. This suggests that the carbon dioxide radical does not react with Chlorsulfuron. The redox potential of the carbon dioxide radical has been determined to be -2.0 V (versus NHE) [43, 111] suggesting that the redox potential of the $\text{Chl}^-/\text{Chl}^{\bullet 2-}$ is more negative than -2.0 V. Therefore, $\text{Chl}^{\bullet 2-}$ is a strong reducing agent with a reduction potential between -2.0 and -2.9 V (versus NHE).

Gamma irradiation of the same solution showed no loss of Chlorsulfuron when sufficient radical was placed into the matrix to react with 50% of the available starting compound. This confirms results obtained in the pulse radiolysis experiments. In natural and industrial waste water the elimination of the chloride ion would stop the radical anion reforming Chlorsulfuron, thus allowing for its breakdown.

6.9 OVERVIEW OF THE RADIATION CHEMISTRY OF CHLORSULFURON

This study has allowed for the first time elucidation of the radiation chemistry of aqueous Chlorsulfuron. The new chemistry is summarised in figure 6.17.

The TDA spectrum obtained from the reaction of Chlorsulfuron with the hydroxyl radical suggests formation of a OH-adduct as an intermediate. Two maxima were observed in the TDA spectrum, suggesting that the OH-adducts formed absorb in different regions of the spectrum. *Ab initio* calculations indicate that the triazine ring of Chlorsulfuron is unfavourable for electrophilic addition of the hydroxyl radical. The rate constant for the reaction of Chlorsulfuron with the hydroxyl radical is significantly slower than that of Sulphacetamide's reaction with the hydroxyl radical [142]. This is attributed to the electron withdrawing affect of the chlorine atom on the benzenesulfonamide ring. The decay rate of the OH-adduct showed dependence on the ionic strength of the solution, therefore the transient is charged. The transient decayed by second order kinetics, indicating the degradation products are formed from radical-radical reactions. HPLC characterisation of the compounds formed by the reaction of Chlorsulfuron with the hydroxyl radical showed that all

of these species have retention times less than Chlorsulfuron. This suggests that the newly formed compounds are more polar than Chlorsulfuron. Mass spectrometric studies determined that the four major species each have masses equivalent to the addition of one oxygen atom to the Chlorsulfuron molecule. Comparison of the mass spectral fragmentation data collected for Chlorsulfuron with that of the newly formed compounds, indicate that the oxygen atom is attached to the benzenesulfonamide ring. This is agreement with what we determined through the pulse radiolysis and *ab initio* studies. The rate of Chlorsulfuron loss and the formation of products from the reaction of Chlorsulfuron with the hydroxyl radical is initially linear under steady state irradiation. As the amount of hydroxyl radicals is increased past 30% of Chlorsulfuron's concentration, the loss of Chlorsulfuron and the formation of products follows a higher order kinetic mechanism. This result suggests that the products of the initial reaction also react with the hydroxyl radical to form (uncharacterised) compounds.

The corrected TDA spectrum obtained upon the reaction of the hydroxyl radical with Chlorsulfuron at pH 2 matches that obtained from the same reaction at neutral pH. The rate constant for the reaction of Chlorsulfuron with the hydroxyl radical at pH 2 is lower than that obtained at neutral pH. Qualitatively, this can be explained as follows: in the anion form of Chlorsulfuron the electron density is greater than in the case of the neutral form. Since the hydroxyl radical behaves as an electrophile in its reactions, reaction with the electron rich species is faster. Steady state irradiations of Chlorsulfuron at pH 2 were not carried out because the degradation of the starting compound is no longer insignificant.

The OH-adduct produced by the reaction of Chlorsulfuron with the hydroxyl radical was shown to be unreactive with oxygen. It is postulated this occurred because of the delocalisation of the radical over the sulphone group. Identical compounds were identified using gamma irradiation coupled with HPLC as were produced in the de-oxygenated study.

The TDA spectra obtained from the reaction of Chlorsulfuron with the sulfate radical anion differs from that obtained for the reaction OH-adduct of Chlorsulfuron, thus the transient produced does not transform into a OH-adduct. Chlorsulfuron is not observed to react with the dichloride radical anion and therefore the resulting radical of Chlorsulfuron is a powerful one electron oxidant with a redox potential between 2.43 to 2.09 Volts (versus NHE). Gamma irradiation coupled with HPLC for the sulphate radical anion shows that newly formed compounds are more polar than Chlorsulfuron. We have determined that one of the products formed from the reaction of Chlorsulfuron with the sulfate radical anion arises following the reaction of the transient with the *t*-butyl alcohol required for the study.

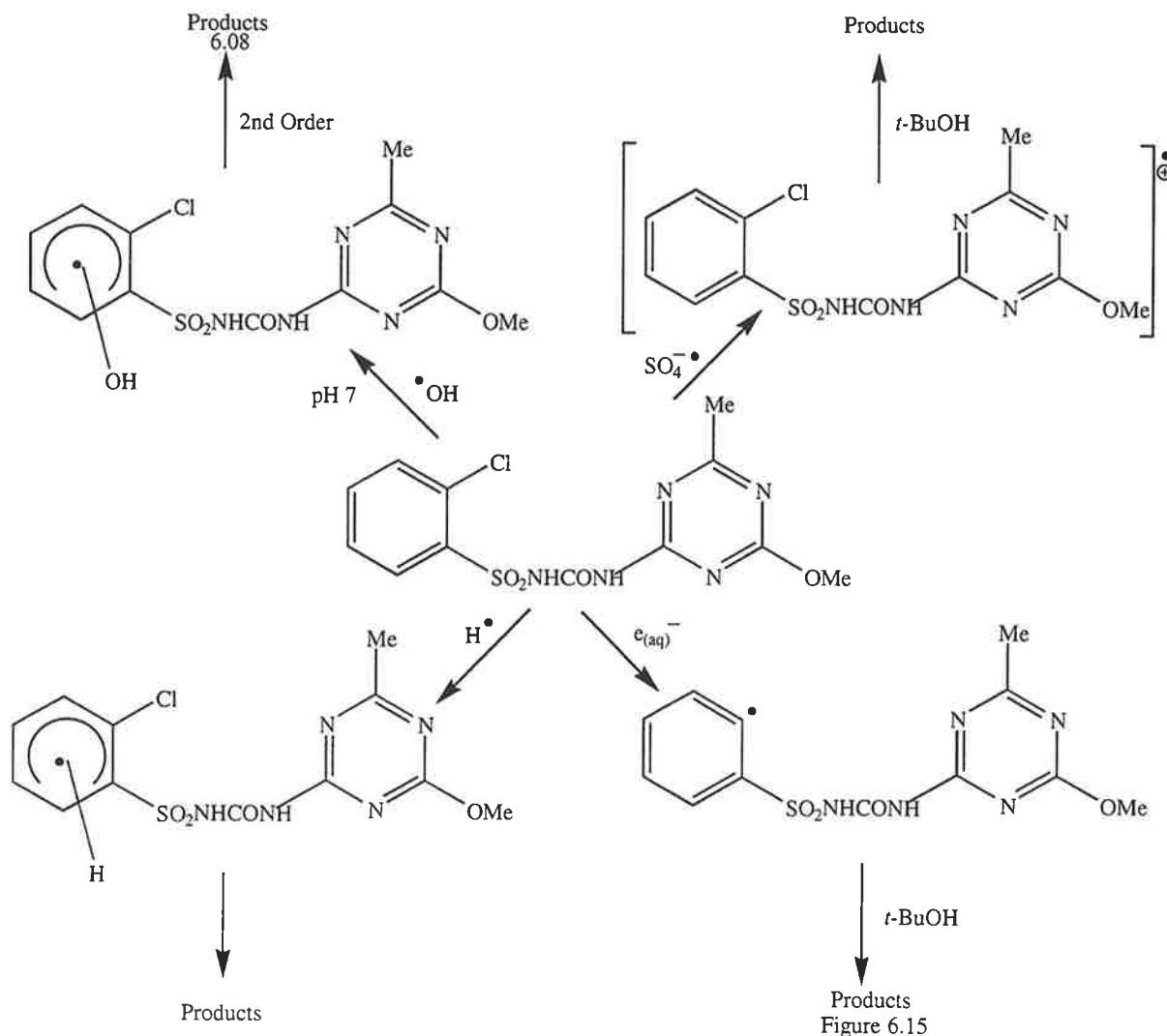


Figure 6.17. Overview of the radiation chemistry characterised in this study.

Ab initio calculations indicate that the HOMO of Chlorsulfuron is located over the benzenesulfonamide ring. It is suspected that the electron lost occurs from this orbital, which is in agreement with the experimental results. The spin density surface could not be calculated.

The TDA spectrum for the reaction of Chlorsulfuron with the hydrated electron differs from that obtained for sulphanilamide. The rate constant for the reaction of Chlorsulfuron with the hydrated electron is similar to that of sulphanilamide [150]. Reaction of the two compounds therefore might proceed via similar mechanisms, but result in different transients. It is known for sulphanilamide that the radical resides on the sulfur, but the difference in TDA spectra indicates this is not true of the transient obtained from Chlorsulfuron, thus another part of the Chlorsulfuron molecule must affect the transient.

Gamma irradiation coupled with HPLC found one major product for the reaction of the hydrated electron with Chlorsulfuron. Using mass spectral fragmentation we have

determined that the product is the dehalogenated form of Chlorsulfuron. The different TDA spectrum is accounted for by the formation of the benzyl radical on the elimination of the chloride ion. The radical anion of Chlorsulfuron is a strong reducing agent with a redox potential of between -2.0 and -2.9 V. In natural and industrial waste water the elimination of the chloride ion would stop the radical anion reforming Chlorsulfuron, thus allowing for its breakdown.

Ab initio calculations indicate the LUMO of Chlorsulfuron is located over the sulfur atom. An overlaid density surface suggests this is the most accessible site for nucleophilic attack. It is suspected that the electron gain would initially occur in this orbital, which is in agreement with our experimental results.

The TDA spectrum for the reaction of Chlorsulfuron with hydrogen atoms is similar to that expected for a H-adduct. Steady state irradiations of Chlorsulfuron at pH 2 were not carried out because the degradation of the starting compound is no longer insignificant.

Chlorsulfuron will degrade upon the reaction with a number of free radicals produced in natural and treated industrial discharge. Upon reduction by free radical processes chloride ion elimination will occur.

7.0 Radiation Chemistry of Aqueous Dichlorophen Solution

7.1 DICHLOROPHEN

Dichlorophen (4,4'-dichloro-2,2'-methylene-diphenol) (Figure 7.01) is a white solid with a melting point of 176-177 °C [151]. The maximum solubility of Dichlorophen is 30 ppm, though this increases when the pH rises above the first pK_a . The two pK_a s of Dichlorophen are 7.5 and 11.5 [152]. The first pK_a value when compared to that of 4-chlorophenol ($pK_a=10$) is low. This is most likely attributable to the intermolecular hydrogen bonding between the two hydroxyl groups.

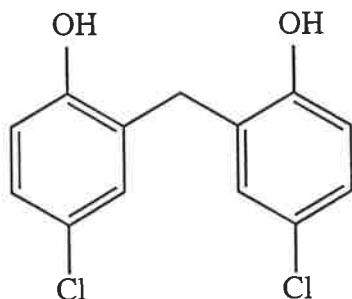


Figure 7.01. Chemical structure of Dichlorophen.

Dichlorophen is an algicide, fungicide and bactericide with contact action. In particular, it is used to protect horticultural benches, textiles and equipment from moulds and algae. The compound is known to be slowly oxidised by air but undergoes photo-transformation in direct sunlight [152]. Photo-transformation has previously been postulated to cause its degradation in natural water. Dichlorophen is also a photo-allergic compound to skin due to its photo-labile carbon-chlorine bond. This photoallergy has been postulated to be due to the formation of free radicals interacting with skin after irradiation with U.V. light [153].

Irradiation of Dichlorophen with U.V. light has been studied by Grabner *et al.* [154]. Results of their study demonstrated the formation of a carbene as an intermediate. This intermediate then reacts with water, oxygen and Dichlorophen itself to form benzoquinone, hydroquinone and coupling products.

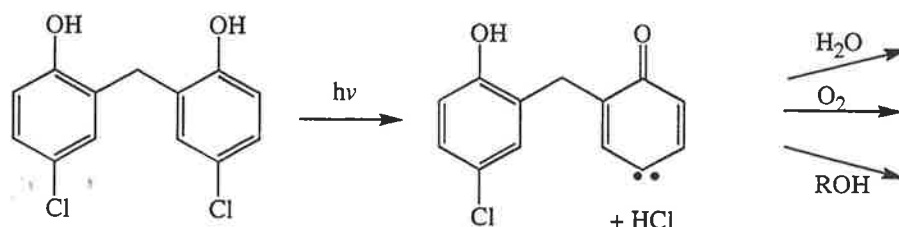


Figure 7.02. Reaction mechanism for the photolysis of Dichlorophen as proposed by Evans *et al.* [152].

7.2 REACTION OF DICHLOROPHEN WITH THE HYDROXYL RADICAL

Figure 7.03 shows the time resolved TDA spectrum obtained upon pulse radiolysis of an aqueous Dichlorophen (1×10^{-4} M) solution saturated with nitrous oxide (pH 9.2, NaOH). It exhibits an absorption band with a maximum at 310 nm. Figure 7.03 is similar to that recorded by Getoff *et al.* [94] for the reaction of the hydroxyl radical with 4-chlorophenol.

In the presence of *t*-butyl alcohol (0.1 M), an effective hydroxyl radical scavenger but a weak hydrogen atom scavenger, the absorption spectrum was considerably reduced. The high G ($\cdot\text{OH}$) yield and appreciable decrease in the transient absorption suggests the spectrum in Figure 7.03 is mainly due to the reaction of hydroxyl radicals with Dichlorophen.

No negative absorbance was detected in the TDA spectrum between the hydroxyl radical and Dichlorophen. This is despite the Dichlorophen anion having a ground state absorbance in the region of 250 to 500 nm (maximum at 300 nm). The TDA spectrum can be corrected for the small ground state absorbance by using formula 3.14 and the assumption that the yield of hydroxyl radicals is equal to that of the transient radical. The corrected spectrum is presented in Figure 7.04. Since the yield of transient radicals is not known for certain the result should not be over interpreted.

Reducing the radiation dose (and hence the amount of transient radical) produced an increase in the half life of the transient species at 310 nm. The radical therefore decays by second order kinetics. When the decay curve at 310 nm was fitted to second order kinetics it produced a decay rate of $2k/\epsilon l = 1.8 \times 10^5 \text{ s}^{-1}$. Assuming that all hydroxyl radicals react with Dichlorophen and the G value of the hydroxyl radical is equal to that of the transient, (ie. 5.5) the molar absorbance of the maxima is $9100 \text{ M}^{-1}\text{cm}^{-1}$ for 310 nm (Figure 7.04). Using this molar absorbance value, the second order decay constant was determined to be $2k = 1.6 \times 10^9 \text{ M}^{-1}\text{s}^{-1}$.

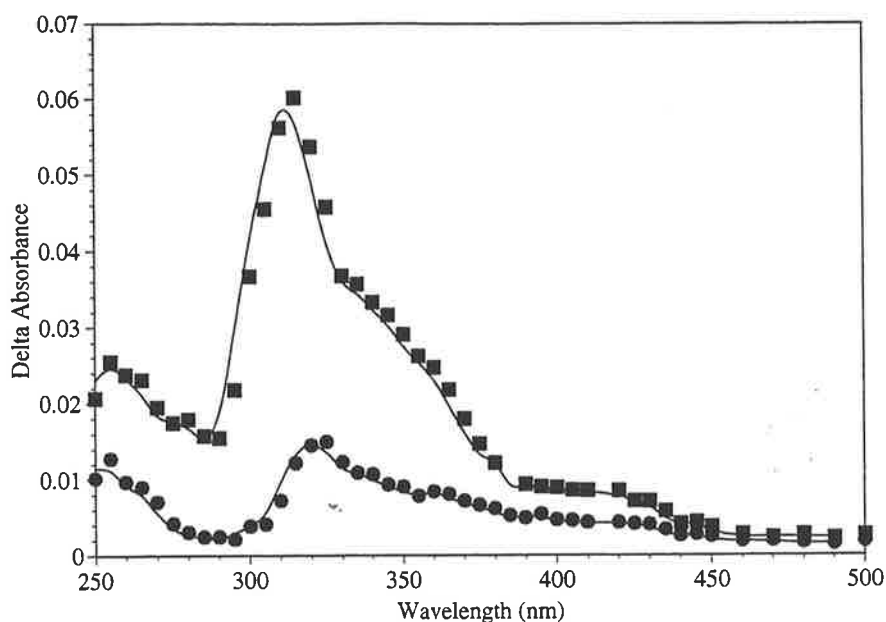


Figure 7.03. Time resolved TDA spectrum obtained upon the pulse radiolysis of an aqueous Dichlorophen (1×10^{-4} M) solution saturated with nitrous oxide pH (9.2 NaOH). (■ 5 μ s after the pulse, ● 1000 μ s after the pulse).

Reactions of chlorinated aromatic compounds have been extensively studied in the past. These compounds include chlorobenzene, 3-chlorotoluene, 2, 3 and 4-chlorophenol and 2, 3 and 4-chlorophenoxide anion. The neutral compounds all react with the hydroxyl radical to form OH-adduct intermediates as the major transient. Phenoxide ions have been reported to form the phenoxyl radical. Since the spectrum recorded here appears similar to that of the OH-adduct of 4-chlorophenol, [118] it is reasonable to assume that the hydroxyl radical also reacts with Dichlorophen to form the same type of intermediate. At pH 9.2 Dichlorophen possesses one ring which will be phenolic and another which will be a phenoxide ion. Since the spectrum does not resemble the phenoxyl radical spectrum, and resembles the spectrum for a OH-adduct, it can be concluded that the hydroxyl radical reacts with the phenol ring in preference to the phenoxide ring. The small absorbance at 400 nm would be due to the phenoxyl radical resulting from the oxidation of the phenoxide ring.

Adjusting the ionic strength of a solution by the addition of NaClO_4 (1 M) produced a change in the rate of decay of the transient at 310 nm (pH 9.2). This suggests the transient species is charged, consistent with the OH-adduct assignment.

Competition kinetics produced a bimolecular rate constant for the reaction of hydroxyl radicals with the Dichlorophen anion of $3.1 \times 10^9 \text{ M}^{-1}\text{s}^{-1}$. The rate constant indicates the Dichlorophen anion reacts with hydroxyl radicals at slightly less than diffusion controlled rates.

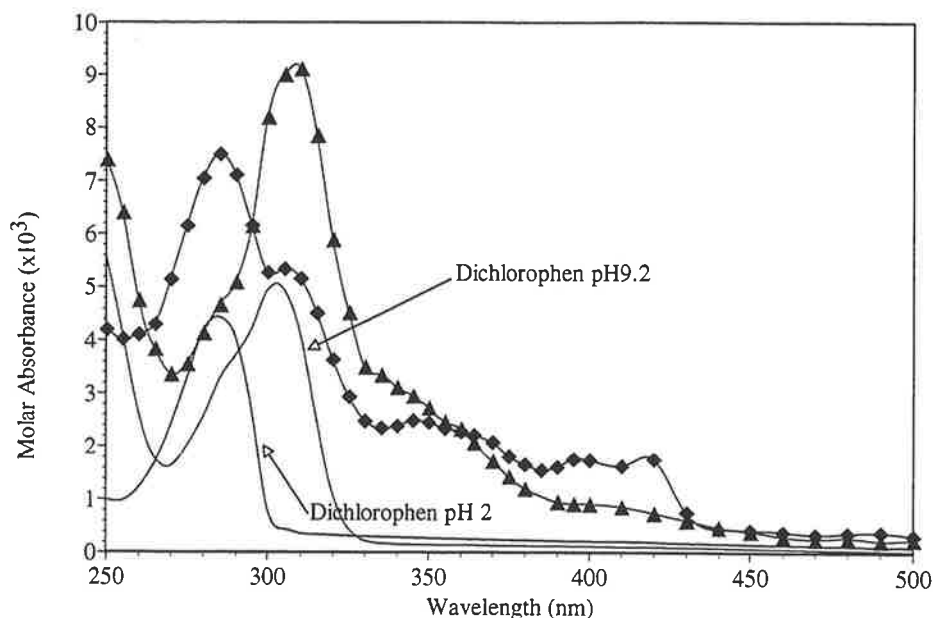


Figure 7.04. Molar Absorbance spectra of Dichlorophen at pH 2 and 9.2 (solid lines) and the transients arising from the reaction of Dichlorophen with hydroxyl radicals (\blacktriangle pH 9.2, \blacklozenge pH 2). Spectra recorded 5 μ s after the pulse.

Though this is the first reported rate constant for the reaction of the hydroxyl radical with the Dichlorophen anion, rate constants for molecules that contain similar functional groups have been determined. These rate constants are:

Chlorobenzene	$k=5.6 \times 10^9 \text{ M}^{-1} \text{ s}^{-1}$ [155]
4-Chlorophenol	$k=7.6 \times 10^9 \text{ M}^{-1} \text{ s}^{-1}$ [156]
3-Chlorotoluene	$k=3.5 \times 10^9 \text{ M}^{-1} \text{ s}^{-1}$ [157]
4-Chlorophenoxide anion	$k=4.6 \times 10^9 \text{ M}^{-1} \text{ s}^{-1}$ [158]

The rate constant determined for the reaction of Dichlorophen with the hydroxyl radical is a similar magnitude to that obtained for both phenolic and phenoxide forms of 4-chlorophenol.

Steady state irradiation of an aqueous Dichlorophen (58 μ M) solution saturated with nitrous oxide using cobalt 60 (Dose 60 Grays per hour) resulted in only a small change in absorbance due to the Dichlorophen anion at 300 nm (Figure 7.05). The spectrum varied slightly over the range of the dose of radiation, with only a small increase in the absorbance at 265 nm. The stability of the absorbance spectrum of Dichlorophen inferred that either the products absorb in this region, or the transients formed by the reaction of the hydroxyl radical with Dichlorophen react to reform the starting material, or a combination of both.

HPLC of a Dichlorophen (1×10^{-4} M) solution saturated with nitrous oxide (pH 9.2 (NaOH) and irradiated with gamma irradiation indicates the formation of new species and a

decrease in the concentration of Dichlorophen at 254 nm (Figure 7.06). No change in the product distribution was observed by altering the analysing wavelength to either 220 or 254 nm. One predominate compound (A) was detected in the trace along with two other minor products (B & C), no other species were observed out to 40 minutes. All compounds produced were at retention times less than Dichlorophen, suggesting all the products were more polar than the starting compound. This is consistent with the addition of the polar hydroxyl group to Dichlorophen. Re-running of the solution using a steep acetonitrile gradient indicated that there were no compounds at longer retention time and therefore dimer formation was not likely. Merga *et al.* [100] found the opposite for chlorobenzene, that is, the preferential formation of dimers. Differences between the results suggest the lower dose rate employed in this study affected the type of second order reactions occurring to form products.

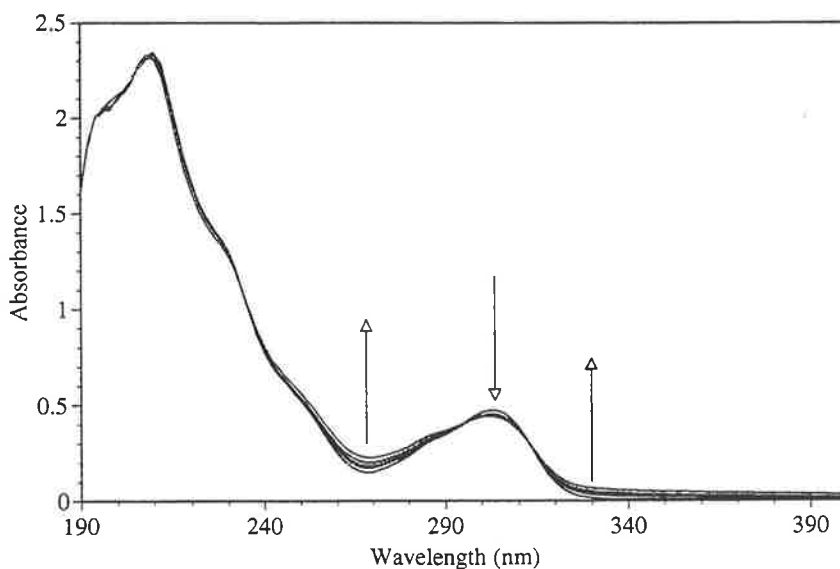


Figure 7.05. Observed change in optical absorbance of an aqueous Dichlorophen ($58 \mu\text{M}$) solution saturated with nitrous oxide and irradiated with gamma irradiation (0 to 120 Gray). Arrows indicate the direction of absorbance change with radiation dose. Dose rate 66 Gray/hr.

The rate of Dichlorophen loss against the concentration of hydroxyl radicals added to the system (calculated using Frickie Dosimetry), was difficult to determine quantitatively using HPLC. The experiment was unsuccessful due to an absence of reproducibility in the HPLC quantitative measurements. This was most likely due to the low solubility of Dichlorophen. The experimental failure makes it impossible to put forward any suggestions on the further reactions of the products from the initial reaction with the hydroxyl radical.

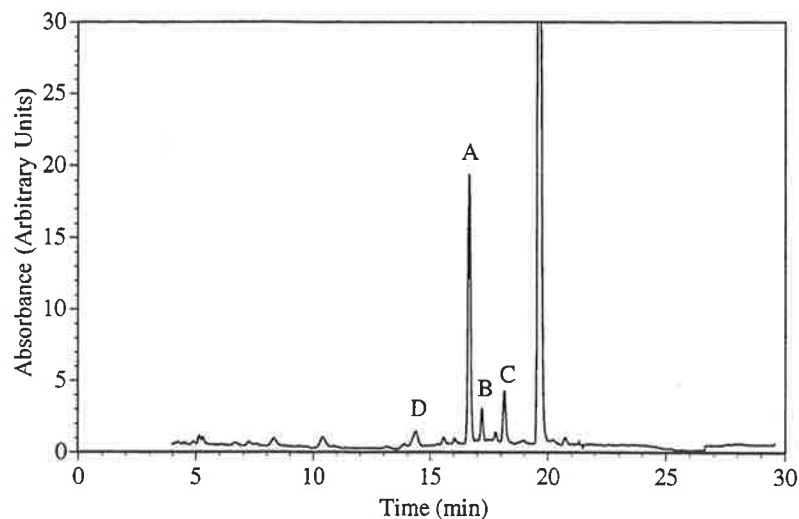


Figure 7.06. HPLC analysis following the gamma irradiation of a Dichlorophen (1×10^{-4} M) solution saturated with nitrous oxide (pH 9.2 (NaOH)). The trace displays the products formed from the reaction of Dichlorophen with hydroxyl radicals (A to D). See Figure 7.07 for product identification.

Structures of the compounds created from this reaction were determined by electrospray mass spectrometry and are reported in Figure 7.07. Dichlorophen produced a parent ion mass to charge ratio of 267/269/271 (4:3:1) Daltons ($M-H^+$) with a fragmentation pattern (using MS^2 experiment) that consisted of a single daughter ion at 127 Daltons. The isotope pattern of 4:3:1 is consistent with two chlorine atoms being present in the molecule [159]. The major compound A produced parent ions at 247/249 (3:1) Daltons. This mass to charge ratio corresponds to the addition of a hydroxyl group and loss of a chlorine atom. Change in the isotope pattern to 3:1 also indicates the presence of only one chlorine atom in the molecule. Fragmentation of the parent ion at 247 Daltons produced a daughter ion at 219 Daltons (minus CO). Replacement of the chlorine atom by a hydroxyl group has previously been observed for chlorobenzene by Merga *et al.* [100]. The reaction mechanism postulated by Merga *et al.* [100] involved addition of the hydroxyl radical to the aromatic system to form the OH-adduct. The disproportionation reaction of the OH-adduct produced one hydroxylated product and a mono saturated version of the starting compound. The thermodynamically more favoured aromatic species is then formed by elimination of HCl to produce the observed compound. A chloride test produced a G value of 1.3 for chloride ion production. Comparison of the G value for the production of the chloride ion to the loss of Dichlorophen could not be made because of the aforementioned solubility reasons. This result is consistent with the results produced by mass spectrometry.

The minor product B produced a mass spectrum with the parent ions at 283/285/287 (4:3:1) Daltons. The parent ion corresponds to the addition of 16 Daltons or an oxygen to the starting compound. The isotope pattern of 4:3:1 is consistent with two chlorine atoms being

present in the molecule [159]. A MS^2 fragmentation experiment on the parent ion at 283 Daltons produced a single daughter ion peak at 127 Daltons, the same daughter ion as observed for Dichlorophen. Compound B is therefore assigned as Dichlorophen with a hydrogen atom replaced by a hydroxyl group. Compound C produced a parent ion with a complex isotope pattern of 535/537/539 Daltons. The parent ion corresponds to double the mass to charge ratio of Dichlorophen, while the complex isotope pattern indicates that more than two chlorine atoms are present in the molecule. This compound must be formed from the phenoxy radical which subsequently reacts with another phenoxy radical to form the dimer observed in the HPLC trace. Generally dimers are less polar than the starting compound, however, in this situation the dimer is shown to be more polar than the starting compound (from the relative retention times in the HPLC trace). The dimer has four hydroxyl groups compared to the monomer's two, explaining the increase in polarity observed. The variety of each product formed suggests the addition of the hydroxyl radical showed some selectivity to the position in the ring and therefore affected the chemistry of the products. It is known that the hydroxyl radical does show some selectivity when adding to aromatic systems. Schuler [101] reported that the partial rate constants for the addition of the hydroxyl radical to the ortho and para positions of biphenyl is greater than the addition to benzene, while the addition to the meta position was found to be less rapid. The electrophilic hydroxyl radical reacts with an electron rich site more rapidly than an electron poor site.

Ab initio calculations showed the greatest electron density on the aromatic carbons to be on the carbon ortho to the O^- and meta to the CH_2 bridging group on the deprotonated ring. To determine the exact position of the hydroxyl group on the ring, the molecule would have to be obtained and matched to the retention time in the trace. Since these compounds are not commercially available they would have to be synthesised. This was beyond the scope of this project and therefore not attempted.

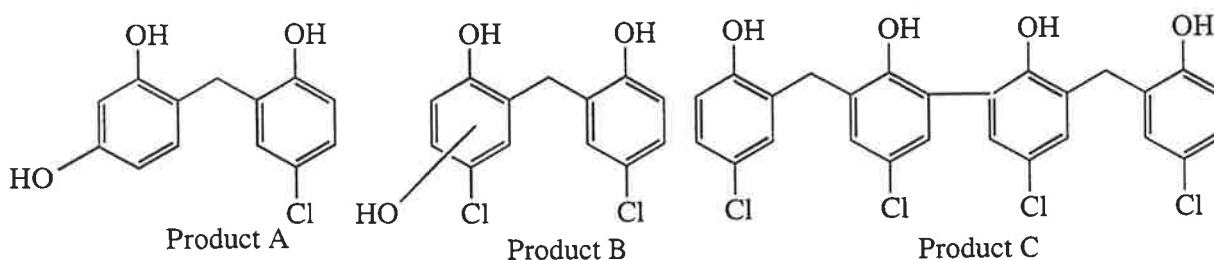


Figure 7.07. Products (A to C) of the gamma radiolysis of aqueous Dichlorophen in nitrous oxide saturated solution as determined by the analysis of electrospray mass spectrometric fragmentation data. Location of the new functional groups are not unambiguously assignable in structures A to C. See text for discussion.

7.3 REACTION OF DICHLOROPHEN WITH THE HYDROXYL RADICAL IN ACIDIC SOLUTION

Time resolved TDA spectra obtained upon the pulse radiolysis of an aqueous Dichlorophen (1×10^{-4} M) solution saturated with nitrous oxide (pH 2, HClO_4) is different to the spectrum recorded at pH 9.2 (Figure 7.08). The spectrum has maxima at 300 nm with a shoulder out to 400 nm. When the decay curve at 295 nm is fitted to second order kinetics it produces a fit with a decay rate of $2k/\epsilon l = 2.2 \times 10^5 \text{ s}^{-1}$. Using the molar absorbance of the radical determined at 295 nm from Figure 7.04, $2k$ was determined to be $1.2 \times 10^9 \text{ M}^{-1} \text{ s}^{-1}$. The decay rate observed here is similar to that observed for the reaction conducted at pH 9.2.

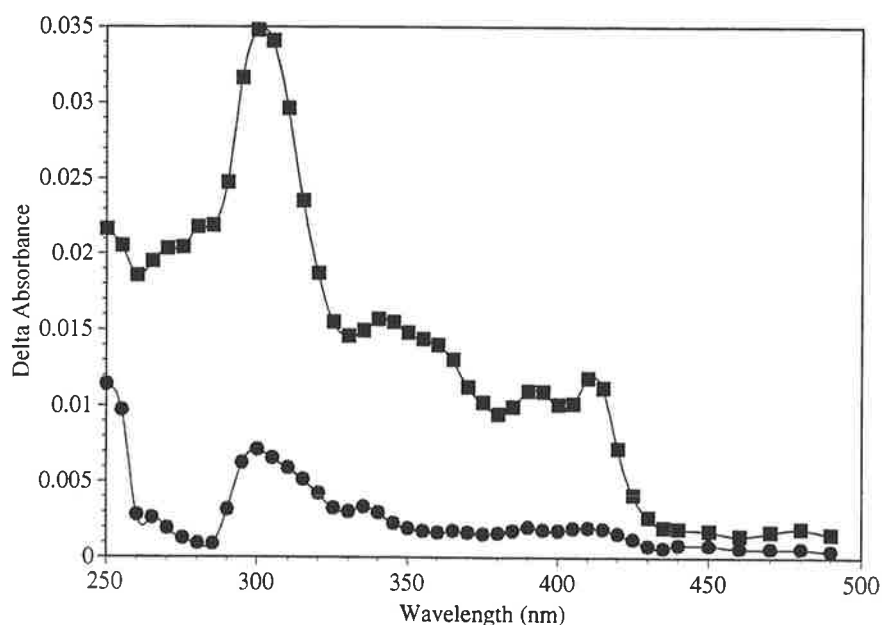


Figure 7.08. Time resolved TDA spectra obtained upon the pulse radiolysis of an aqueous Dichlorophen (1×10^{-4} M) solution saturated with nitrous oxide (pH 2, HClO_4). (■ 5 μs after the pulse, ● 1000 μs after the pulse).

The spectrum is similar to that observed for 4-chlorophenol by Stafford *et al.* [118] and Getoff *et al.* [100] and therefore assigned as the OH-adduct. The absorbance at 400 nm is assigned to the formation of small amounts of phenoxy radicals formed through the known acid catalyst splitting process of the OH-adduct [100].

Effect of pH on the TDA spectra can be observed more effectively in the molar absorbance spectra (Figure 7.04) because it takes into account the lower G value of the hydroxyl radical, the difference in ground state absorbance between Dichlorophen and the Dichlorophen anion and the contribution to the spectra made by the hydrogen atom adduct. Since neutral Dichlorophen has both hydroxyl groups protonated, the electron density oxygens have to donate into the ring is less than that of the deprotonated form. Therefore the U.V.

absorbance maximum of neutral Dichlorophen moves to a lower wavelength. This is observed in Figure 7.04 with the absorbance maxima of the anionic form being at 301 nm while the neutral form it is at 281 nm [123].

Spectral difference between the transients produced at high and low pH can be attributed to the deprotonation of one of the phenol groups in much the same way as is observed for Dichlorophen. pK_a determination was not attempted because of the change in absorbance of the parent compound in the region of the absorbance of the transients. The isosbestic points could not be used because of the similarity in the absorbance of the two transients at these points.

The bimolecular rate constant determined for the reaction of hydroxyl radicals with Dichlorophen by competition kinetics (pH 2, $HClO_4$) was $3.5 \times 10^9 M^{-1}s^{-1}$. This rate constant indicates that Dichlorophen reacts with hydroxyl radicals at a similar rate to that of the Dichlorophen anion. Considering the electrophilic nature of the hydroxyl radical, the absence of any change in the rate constant suggests addition is occurring on the phenolic ring in the pH 9.2 experiment. If addition of the hydroxyl radical was occurring on the phenoxide ring then protonation of the hydroxyl group at pH 2 should lead to a decrease in the observed rate constant because of the reduction in the electron density being donated into the ring.

Gamma irradiation coupled with HPLC revealed that only one major species was formed when Dichlorophen was reacted with hydroxyl radicals in the presence of excess hydrogen ions. The compound was at the same retention time as the product observed at pH 9.2 (Figure 7.06). Electrospray mass spectrometry on this compound revealed it was the same product as compound A (Figure 7.07). The compound had the same parent ion and fragmentation pattern (using MS^2) for the pH 9.2 experiment. Minor species (B and C) observed in the pH 9.2 experiment were also present at pH 2, these compounds were also consistent with the products observed previously. Formation of the same species at different pH values is consistent with the hypothesis that the different TDA spectra observed in Figure 7.04 were due to the protonation of the phenol group since the formation of structurally different transients would produce different compounds in the HPLC trace. The HPLC running solvent is at a pH of approximately 3 and therefore the products of the reaction whether conducted at high or low pH have the same chromatogram.

7.4 REACTION OF DICHLOROPHEN WITH THE HYDROXYL RADICAL IN THE PRESENCE OF OXYGEN

Time resolved TDA spectrum obtained upon the pulse radiolysis of an aqueous Dichlorophen (1×10^{-4} M) solution saturated with nitrous oxide/oxygen (4:1 v/v) (pH 9.2, NaOH) can be observed in Figure 7.09. The TDA spectrum is different to that observed in Figure 7.03, with new absorbance peaks observed at 285 and 420 nm. Comparison of the decay rates of transient species illustrates a deviation from second order kinetics (Figure 7.10) with the addition of oxygen (310 nm). A deviation in the kinetics indicates that transients produced by the reaction of Dichlorophen with the hydroxyl radical react through pseudo first order kinetics with oxygen. Reaction of the transient with oxygen is consistent with the OH-adduct mechanism, as carbon centred radicals are known to react with oxygen [48, 82, 84, 102, 103].

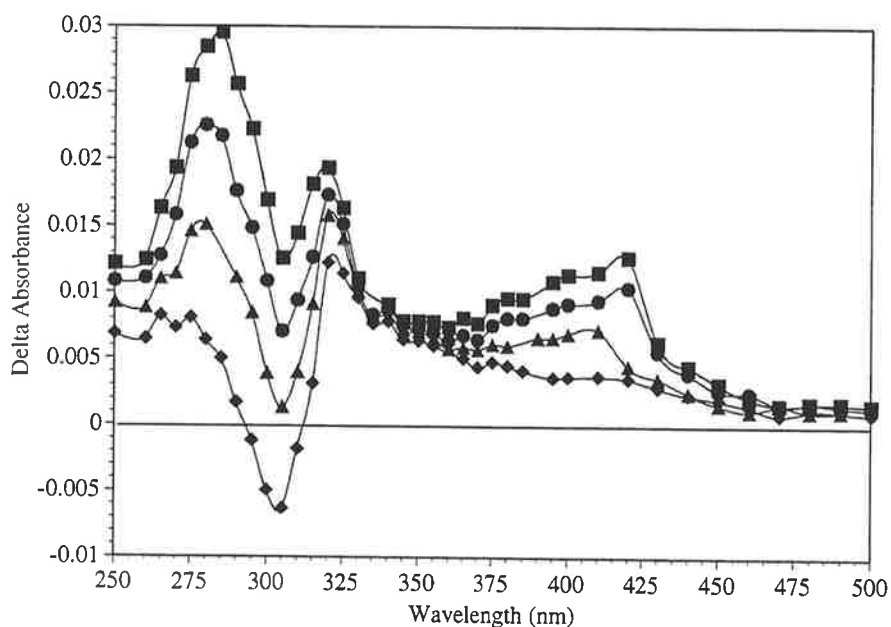


Figure 7.09. Time resolved TDA spectrum obtained upon pulse radiolysis of an aqueous Dichlorophen (1×10^{-4} M) solution saturated with nitrous oxide/oxygen (4:1 v/v) (pH 9.2, NaOH). (■ 20 μ s, ● 50 μ s, ▲ 100 μ s, ◆ 500 μ s after the pulse).

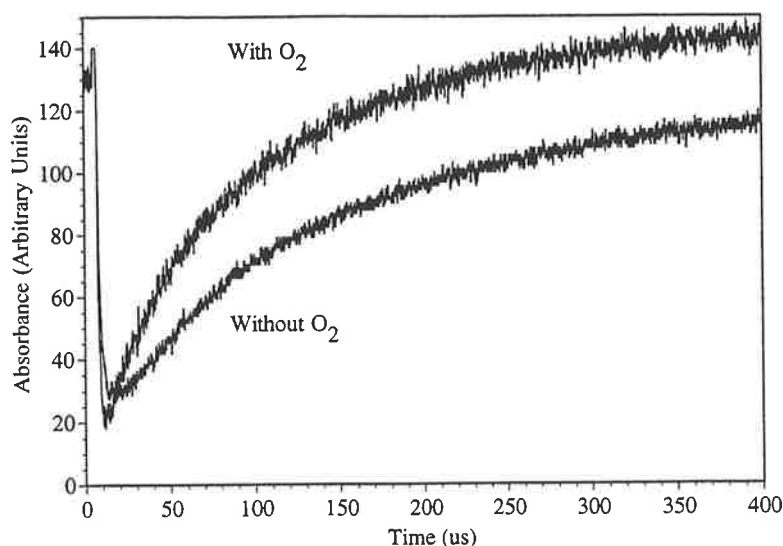


Figure 7.10. Comparison of the pulse radiolysis traces obtain from a solution of Dichlorophen (1×10^{-4} M) saturated with nitrous oxide and nitrous oxide/oxygen (4:1 v/v). Absorbance data were collected at 310 nm. Traces are normalised. Both radiation pulses are $2.5 \mu\text{s}$ long with a dose of 10.0 Gray per pulse.

Change in absorbance of a Dichlorophen (1×10^{-4} M) solution at pH 9.2, saturated with nitrous oxide/oxygen after gamma irradiation can be observed in the inset of Figure 7.11. The maximum at 310 nm was replaced with a new maximum at 285 nm. Change observed in this experiment was different to that observed in the de-oxygenated experiment, therefore the presence of oxygen is producing an effect on the products of the reaction between the hydroxyl radical and Dichlorophen.

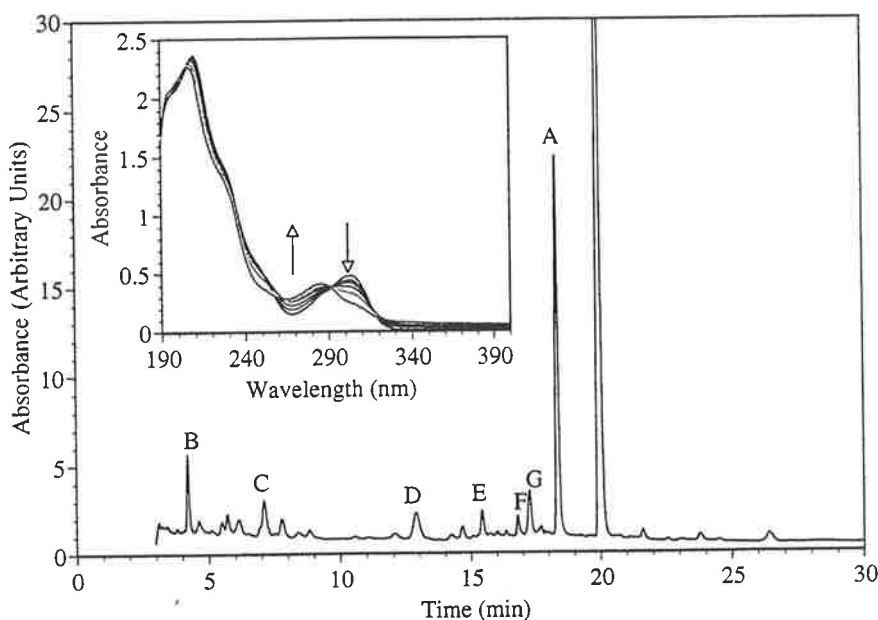


Figure 7.11. HPLC analysis following the gamma irradiation of an aqueous Dichlorophen (1×10^{-4} M) solution saturated with nitrous oxide/oxygen. The trace displays the products formed from the reaction of the Dichlorophen with hydroxyl radicals in the presence of oxygen. Inset. Observed change in optical absorbance of the same solution (0 to 180 Gray). Arrows indicate the direction of absorbance change.

The HPLC trace recorded following gamma irradiation of an aqueous Dichlorophen (1×10^{-4} M) solution saturated with nitrous oxide/oxygen (displayed in Figure 7.11) indicates the formation of one major species at 18.5 minutes (A) along with several other minor compounds. The main peak in the de-oxygenated system at 16.5 minutes was observed to be absent from this HPLC trace. Mass spectral analysis of the major product A produced a parent ion of 283/285/287 (4:3:1) Daltons. The mass to charge ratio corresponds to the addition of an oxygen atom to the Dichlorophen. An isotope ratio of 4:3:1 indicates there are two chlorine atoms present in the molecule. A similar mass to charge ratio was observed with the reaction of the hydroxyl radical in de-oxygenated solution, however, this compound possessed a different retention time from the species observed here, therefore the positioning of the hydroxyl group must be different. MS² fragmentation of the major peak also produced a different pattern from the compound observed in the de-oxygenated system. Daughter ions were observed at 145 Daltons, 16 Daltons more than that observed for Dichlorophen. Product E was also observed to have a parent ion of 283/285/287 Daltons and therefore must be a similar type of compound as product A.

Product F recorded a mass to charge ratio of 299/301/303 (4:3:1) Daltons corresponding to the addition of two oxygens to the starting compound. The isotope ratio of 4:3:1 indicates the presence of two chlorine atoms in the molecule. MS² fragmentation of the parent ion produced a base peak daughter ion of 143 and another ion at 267 Daltons. This type of reaction was discussed in chapter 4 and results from the addition of an oxygen molecule to the OH-adduct followed by a disproportionation reaction to form a product with two hydroxyl groups added to the aromatic ring [82].

Product G's parent ion was observed at 297/299/301 (4:3:1) Daltons which is two Daltons less than compound F and results from the addition of two oxygen atoms and the elimination of two hydrogen atoms. The exact structure of the compound cannot be determined from the mass spectrometric data, but it is suspected that either a benzoquinone or epoxide type compounds are forming. The product is not the result of the addition of four oxygen and the elimination of a chlorine atom since the isotope pattern still indicates the presence of two chlorine atoms in the compound. The mechanism for the formation of this compound could not be determined.

Products B, C and D all produced the same parent ion of 307/309 Daltons. MS² and MS³ fragmentation of this peak produced a daughter and grand daughter ion at 287 (-20) and

267 (-20) Daltons, respectively. No structure could be assigned to these species from the available mass spectral data.

Reaction of benzene with hydroxyl radicals under steady state conditions in the presence of oxygen have previously been shown to form phenol in yields of between 50 to 90%, depending on the conditions [82]. No quantitative results were obtained from the percentage of phenol derivatives formed from this reaction. Qualitatively however, results obtained for Dichlorophen are in agreement with this observation as the predominate compound results from the addition of the hydroxyl group.

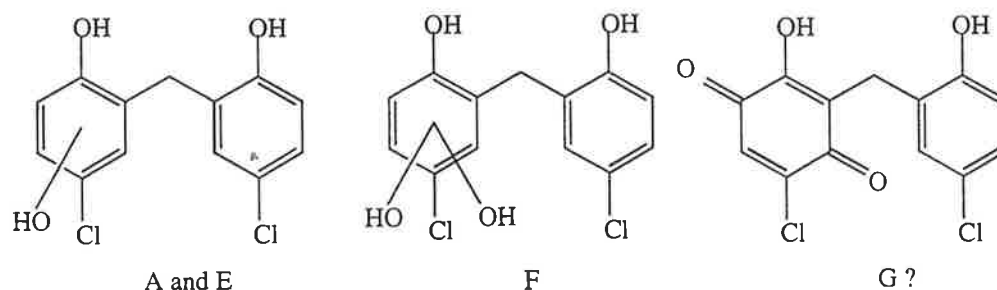


Figure 7.12. Products (A, E, F and G) of the gamma radiolysis of an aqueous Dichlorophen solution as determined by analysis of electrospray mass spectrometric fragmentation data. Location of the new functional groups are not ambiguously assignable in the structures A, E, F and G. See text for discussion.

7.5 REACTION OF DICHLOROPHEN WITH ONE ELECTRON OXIDANTS

The dichloride radical anion formed in the pulse radiolysis of oxygen saturated sodium chloride (0.02 M) Dichlorophen solution (1×10^{-4} M) at pH 2 (HClO_4) reacts as a strong one electron oxidant with a potential of 2.09 V (versus NHE) [43]. Reaction of the dichloride radical anion with Dichlorophen was studied by following the decay of the dichloride radical anion absorption band at 340 nm. It was observed that in the presence of Dichlorophen (1×10^{-4} M) the band decayed faster and by first order kinetics instead of second order kinetics (Figure 7.13) indicating a reaction between Dichlorophen and the dichloride radical anion had resulted.



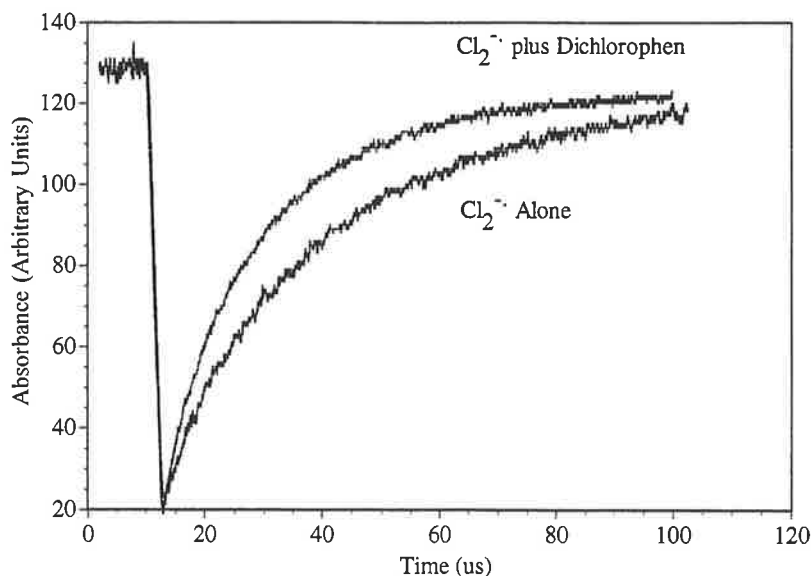


Figure 7.13. Comparison of the pulse radiolysis traces produced at 340 nm, with and without the presence of Dichlorophen (1×10^{-4} M) containing NaCl (0.02 M) in an oxygen saturated solution (pH 2, HClO_4), indicating a reaction between the dichloride radical anion and Dichlorophen had occurred.

The bimolecular rate constant was determined to be $4.2 \times 10^8 \text{ M}^{-1} \text{ s}^{-1}$ from the slope of a plot of the pseudo first order rate constant against the concentration of Dichlorophen (5 to $10 \times 10^{-5} \text{ M}$) at 340 nm. Time resolved studies initially produced a broad absorbance with λ_{max} at 340 nm due to the formation of the dichloride radical anion. Using the pseudo first order rate constant it was determined that more than 95% of the dichloride radical anion had reacted 50 μs after the pulse. The spectrum at 50 μs produced absorbance maxima at 300 nm and 400 nm. Since the dichloride radical anion is a specific one electron oxidant, it should react by electron transfer and be followed by deprotonation to form the phenoxyl radical.

Steady state irradiation of a sodium chloride (0.02 M), oxygen saturated solution containing Dichlorophen (1×10^{-4} M) at pH 2 (HClO_4) produced a HPLC trace which resulted in the formation of one major compound (Figure 7.16). This product appeared at the same retention time as that observed for the hydroxyl radical reaction. Electrospray mass spectrometry on the predominate compound produced a mass to charge ratio of 535/335/339 Daltons with a complex isotope pattern. This corresponds to double the mass to charge ratio of Dichlorophen, indicating formation of the phenoxide ion which subsequently reacts with a similar radical to form a dimer.

Studies of the reactions of other specific one electron oxidants such as the sulfate, dibromide radical anions and the azide radical with Dichlorophen were also conducted. The TDA spectra that resulted from these reactions are shown in Figure 7.15. Graphs presented illustrate the spectra recorded after 90% of the reaction had proceeded.

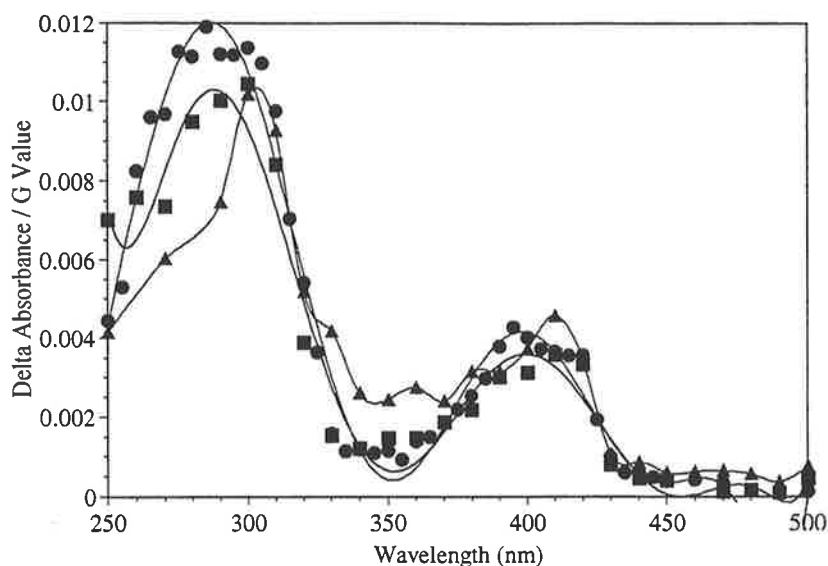
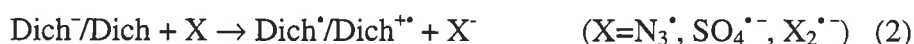


Figure 7.15. TDA spectra recorded for the reaction of Dichlorophen (1×10^{-4} M) with \blacktriangle $\text{Cl}_2^{\bullet -}$, \bullet N_3^{\bullet} , and \blacksquare $\text{SO}_4^{\bullet -}$. Experimental conditions are as follows; $\text{SO}_4^{\bullet -}$, 0.02 M $\text{S}_2\text{O}_8^{2-}$, 0.1 M *t*-butyl alcohol (pH 9.2 NaOH), nitrogen saturated. $\text{Cl}_2^{\bullet -}$, 0.02 M NaCl, oxygen saturated (pH 2, HClO_4). N_3^{\bullet} ; 0.02 M NaN_3 , nitrous oxide saturated (pH 9.2 NaOH).

The TDA spectrum of the sulfate radical anion appears similar to that of the azide radical. It is known that the azide radical reacts with the phenoxide ion to form the phenoxyl radical, these radicals are known to absorb at approximately 400 nm. The spectra shown here for the azide radical and sulfate radical anion are therefore assigned as the corresponding phenoxyl radical of Dichlorophen. The phenoxyl radical recorded at the isosbestic point of Dichlorophen (290 nm) at pH 9.2 (N_3^{\bullet} , $\text{SO}_4^{\bullet -}$) is different to that recorded at pH 2 ($\text{Cl}_2^{\bullet -}$). Since only one of the phenol rings forms the phenoxyl radical, the other ring can still participate in acid-base equilibria. Difference in absorbance at the isosbestic point is attributed to the acid-base behaviour of the second phenol group. Spectrum recorded for the reaction of Dichlorophen with the azide radical at pH 6, matched that of the dichloride radical anions (data not shown). Thus the pK_a for this acid-base equilibrium is between pH 9.2 and 6.

The dibromide radical anion produced on the pulse radiolysis of NaBr (0.02 M), did not exhibit any increase in decay rate when a small amount of Dichlorophen (1×10^{-4} M) was added. The azide radical has a redox potential less than the dibromide radical anion, so the dibromide radical anion would be expected to show a reaction with Dichlorophen. Absence of evidence for this reaction indicates that the reaction is too slow to be measured by the pulse radiolysis techniques as the competing second order self disproportionation is faster. The reaction between the dichloride radical anion and Dichlorophen was observed to occur in the mid $10^8 \text{ M}^{-1} \text{ s}^{-1}$. At pH 9.2 Dichlorophen carries a single negative charge as does the bromide radical anion, causing repulsion between the compounds as they approach each other to react,

thus slowing the reaction rate. Since the azide radical is neutral, it is not repelled by the negative Dichlorophen and thus a reaction can occur. The azide radical also has a higher self exchange rate with the azide ion when compared to the dihalide radical anions [44], explaining the difference in rate of reaction of the dichloride radical and azide radical. Attempts to react Dichlorophen with the dithiosulfate and diiodide radical anions both proved unsuccessful as no increase in the rate of decay of these ion was detected at 475 and 380 nm, respectively. The diiodide radical anion is an one electron oxidant with redox potential of 1.0 V (versus NHE) while the azide radical has a redox potential of 1.4 V (versus NHE). Since Dichlorophen reacts with the azide radical and not the diiodide radical anion the redox potential of the $\text{Dich}^{\bullet}/\text{Dich}^-$ couple in reaction 7.02 must be between 1.4 and 1.0 Volts (versus NHE).



Rate constants determined from the slope of a plot of the pseudo first order decay rate (formation for N_3^{\bullet}) against the concentration of Dichlorophen (50 to 100 μM) for the reactions with the specific one electron oxidants are given in Table 7.01.

Radical	pH	Rate of reaction with Dichlorophen ($\text{M}^{-1}\text{s}^{-1}$)	Wavelength of Determination (nm)
$\text{Cl}_2^{\bullet-}$	2.0	4.2×10^8	340
$\text{SO}_4^{\bullet-}$	9.2	1.2×10^9	460
N_3^{\bullet}	9.2	6.2×10^9	400

Table 7.01. Bimolecular rate constants determined for the reaction of Dichlorophen with one electron oxidants. Rates were determined from the slope of a plot of the pseudo first order rate constant against the concentration of Dichlorophen (50 to 100 μM).

Rate constants decreased with the corresponding one electron oxidant's redox potential, with the exception of the azide radical. The azide radical reacts at close to a diffusion controlled rate. This phenomenon can be explained by the same reasoning used to explain why the azide radical reacts with the Dichlorophen anion and the bromide radical cannot (ie. because the azide radical has no charge while the radical anion possesses a single negative charge). Electrostatic repulsion between the negative charge of the phenoxide anion and the radical anions is thought to slow the reaction rates down. For the reaction of the chloride radical anion with the neutral form of Dichlorophen, the electron density available for the one electron transfer is less due to the protonation of the oxygen.

Comparison of the oxidation of phenol and Dichlorophen by the dichloride radical anion indicated that the rate constant for the oxidation of phenol is of a similar magnitude ($3.8 \times 10^8 \text{ M}^{-1} \text{ s}^{-1}$) [160]. Reaction of 4-chlorophenol and 4-chlorophenoxide anion with one electron oxidants has not been widely studied. The only rate constant that could be found after a comprehensive literature search [149] was the reaction with the azide radical. The rate constant for the reaction of the azide radical with 4-chlorophenol was determined to be $4 \times 10^7 \text{ M}^{-1} \text{ s}^{-1}$.

Reaction of the chlorophenoxide anion with the azide radical has not previously been recorded. Rate constants for the reaction of the dibromide, diiodide and dithiocyanide radical anion have been reported [127]. Reactions for the latter two radicals were not observed with Dichlorophen, and a rate constant could not be determined for the dibromide radical anion.

HPLC chromatograms obtained from the reactions of the dichloride, dibromide radical anions and the azide radicals generated by steady state gamma irradiation with Dichlorophen are shown in Figure 7.16.

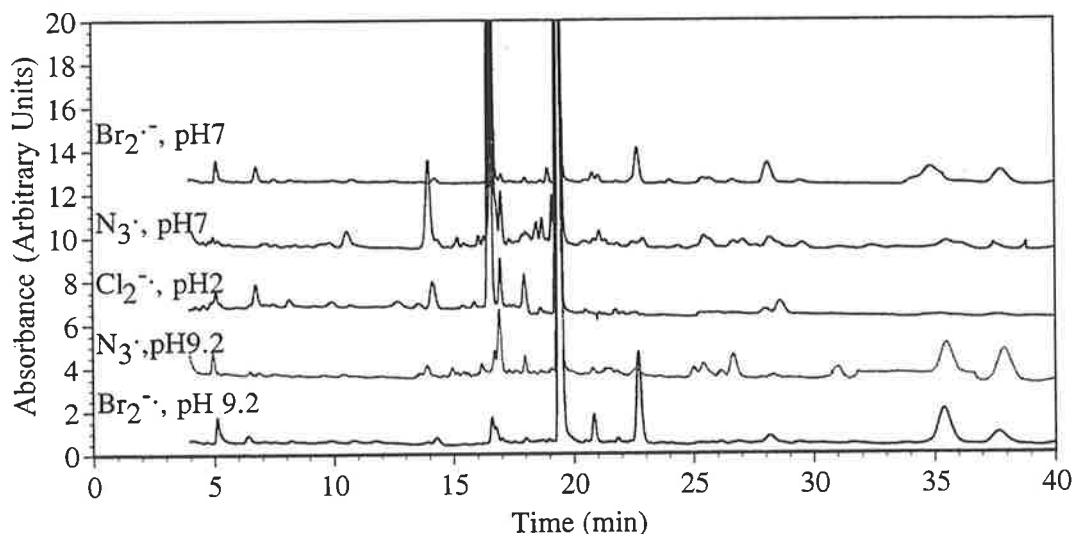


Figure 7.16. Comparison of the HPLC traces produced by the reaction of dichloride, dibromide radical anion, and the azide radical with Dichlorophen ($1 \times 10^{-4} \text{ M}$). Experimental conditions are as follows; $\text{Br}_2^{\bullet -}$; pH 9.2 and pH 2, 0.02 M NaBr, oxygen saturated. N_3^{\bullet} ; pH 9.2 and pH 6.2, 0.02 M N_3^- , nitrous oxide saturated. $\text{Cl}_2^{\bullet -}$; pH 2, 0.02 M NaCl, oxygen saturated. The traces indicate the differences in products produced from the reaction of radical anions with Ioxynil. See text for discussion on the identification of specific products.

Dibromide radical anion formed on the steady state irradiation of a NaBr (0.02 M), nitrous oxide saturated Dichlorophen ($1 \times 10^{-4} \text{ M}$) solution produced a decrease in the concentration of Dichlorophen as well as the formation of new products in the HPLC trace. In

the pulse radiolysis experiments no reaction was observed. The reaction was observed using a steady state method because the concentration of the dibromide radical anion is less than in the pulsed experiment. In a pulse radiolysis experiment the concentration of the radical^s are in the order of micro-molar, where as in the steady state reaction the concentration is many orders of magnitude^s lower. The end effect is that the disproportionation reaction of the dibromide radical anion becomes less favourable and it therefore reacts with the solute [101].

It can be observed from the HPLC traces in Figure 7.16 that the product distribution from the reaction with oxidising radicals is highly dependent on pH. The azide radical at pH 7 produces a peak at 16.5 minutes, while at pH 9.2 this peak decreases with new peaks observed at 35 and 36 minutes. This same phenomenon is also observed with the dibromide radical anion. The dichloride radical anion can only be formed at low pH and produced the same HPLC trace as observed for the pH 9.2. A plot of the peak area at 16.5 minutes, produced by the reaction of the azide radical with Dichlorophen at different pH's, can be observed in Figure 7.17. The graph presented displays a pK_a of 8.0, suggesting that Dichlorophen's protonation state is not involved in the change in product distribution observed since Dichlorophen has a pK_a of 7.5 [152]. This is in agreement with the pulse radiolysis data suggesting the second phenolic group in the phenoxyl type radical possessed a pK_a between pH 9.2 and 6. The protonation state of the transient is therefore controlling the resulting product distribution. The difference in area of the major products between the two pH's is large, suggesting that in basic solutions the second order reaction might be over shadowed by the pseudo first order reaction between the transient and Dichlorophen. These products would be of higher molecular weight and might not readily elute off the column.

Electrospray mass spectrometry was used to determine the structure of the newly formed compounds. A peak observed at 16.5 minutes produced a mass to charge ratio of 535/335/339 Daltons with a complex isotope ratio. The mass to charge ratio and isotope pattern corresponds to the same compound observed for the dichloride radical anion's major species. The compound at 35 minutes produced a mass to charge ratio of 497/499/501 (4:3:1) Daltons. This compound is also formed from the phenoxyl radical. The radical then reacts to again form the dimer, but this time the position of one of the radicals must be in the para position while the other must be in the ortho position. This positioning would allow for elimination of the HCl and formation of a compound with a mass to charge ratio of 497 Daltons ($498-1H = 497$).

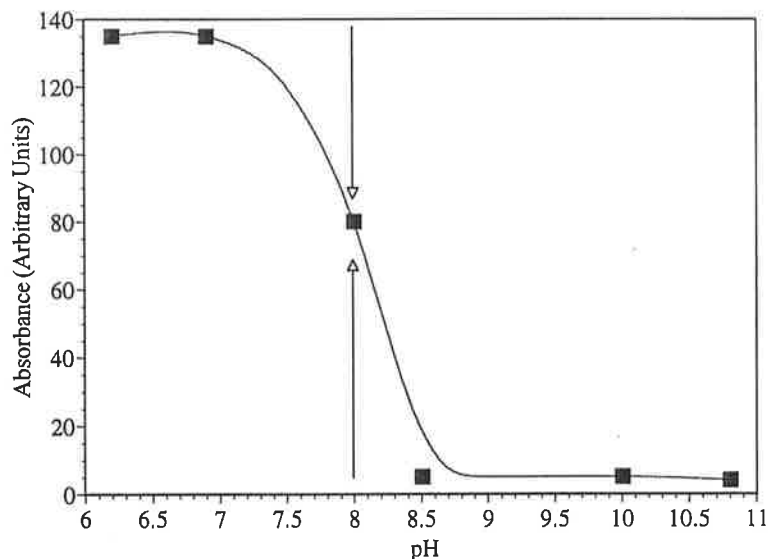


Figure 7.17. Variation of the area of the product at 16.5 minutes with solution pH of aqueous Dichlorophen (1×10^{-4} M) solution containing 0.02 M NaN_3 saturated with nitrous oxide. pH adjusted using phosphate buffers and NaOH. $\text{pK}_a(254\text{nm}) = 7.8$. Arrows indicate point of inflection.

Ab initio calculations were performed on Dichlorophen in both its neutral and mono-deprotonated forms. These compounds were optimised at HF/6-31G** both for the radical (minus one electron from its full electron set) and the starting compound. The spin surfaces generated from the calculations are reported in Figure 7.18.

The spin surface for the deprotonated Dichlorophen indicates the radical is located over the oxygen and the carbons ortho and para to the oxygen on that ring. As expected, the spin is on the deprotonated ring with only a small spin surface also being observed over the other ring. The HOMO of the parent compound can be observed to be located over the deprotonated ring. The spin surface can be accounted for by resonance theory (Figure 7.19)

Neutral Dichlorophen has a similar spin surface to the deprotonated molecule, except that the carbon attached to the oxygen also has a spin surface over it. The reason for the difference between the two molecules is that the electron must be removed from the ring instead of the oxygen as described by the resonance structures shown in Figure 7.19. In both cases the spin surface can be observed to be located within the HOMO of the parent ion. As discussed previously this is to be expected since this is the first orbital that the one electron oxidant would encounter.

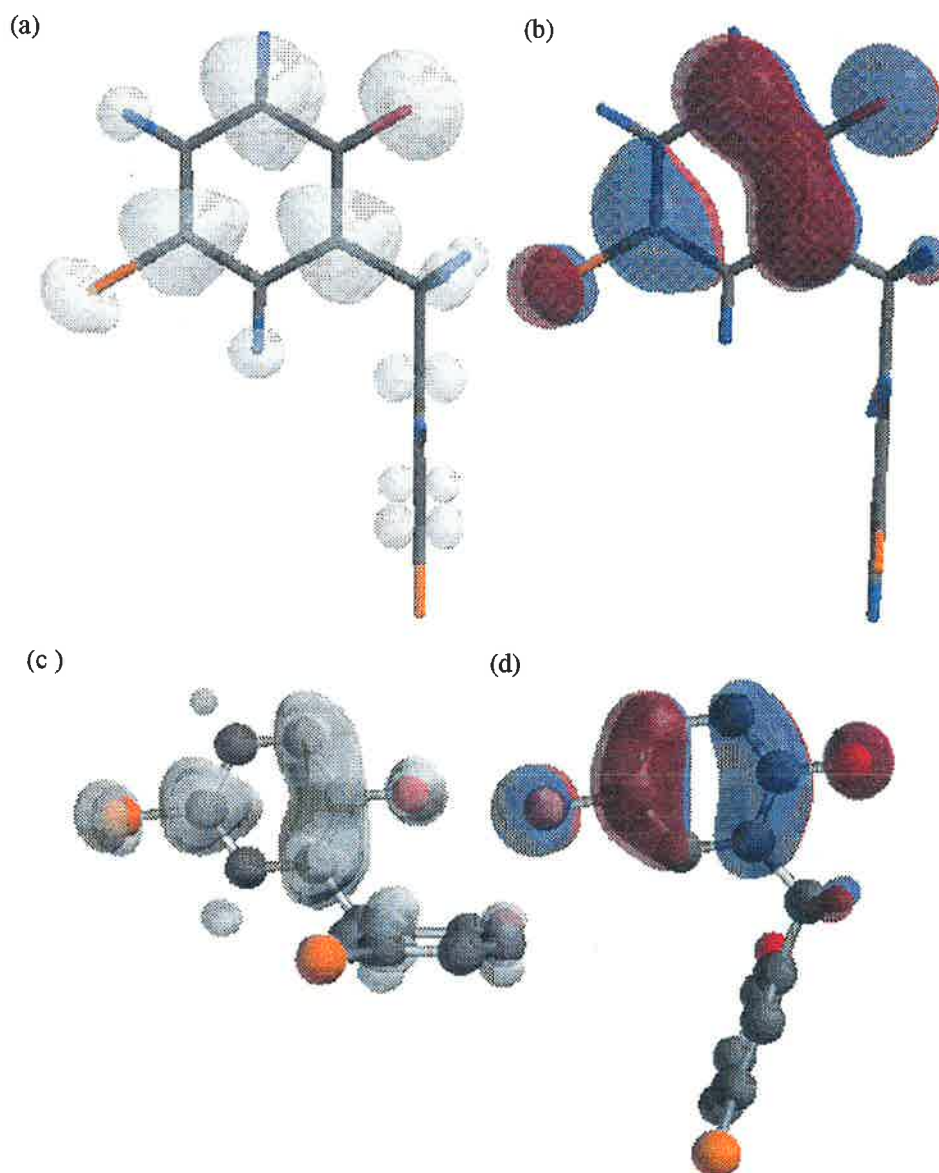


Figure 7.18. Plots of the electron spin density surface (a and c), and HOMO (b and d), of Dichlorophen as determined by *ab initio* molecular orbital theory. Calculations were performed at the HF/6-31G** level of theory. Plot (a) was determined with a neutral molecule and a multiplicity of 2. Plot (b) was determined for a molecular charge of -1 possessing a corresponding multiplicity of +1. Plot (c) was determined with a molecular charge of +1 and a multiplicity of 2. Plot (d) was determined for the neutral molecule possessing a corresponding multiplicity of +1.

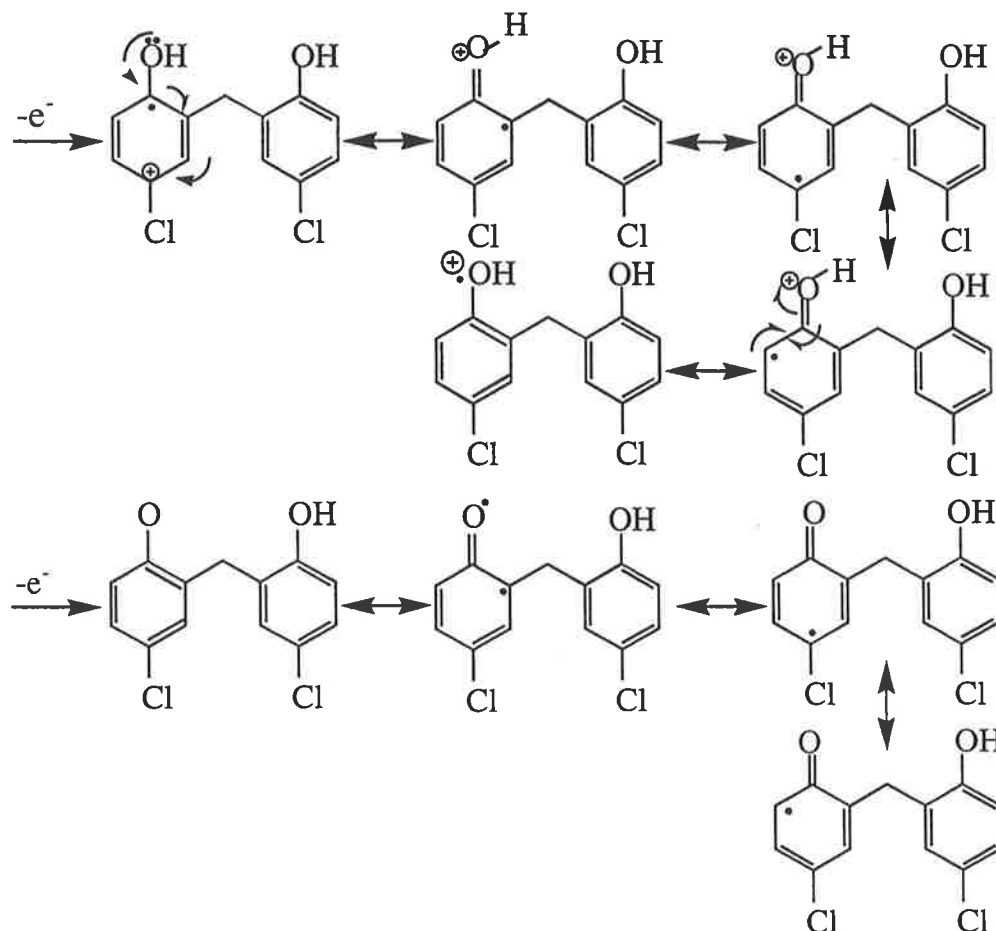


Figure 7.19. Resonance structures accounting for the calculated difference in electron spin density for a and c electrons for the Dichlorophen radical cation and the Dichlorophen phenoxyl type radical. The difference in electron spin density was illustrated in Figure 7.18.

7.6 REACTION OF DICHLOROPHEN WITH THE HYDRATED ELECTRON

The decay of the hydrated electron's absorbance at 640 nm increased in the presence of small amounts of Dichlorophen (1×10^{-4} M) at pH 9.2 (NaOH). This indicates that a reaction between the hydrated electron and Dichlorophen is occurring. Time resolved TDA spectra obtained upon pulse radiolysis of a Dichlorophen (1×10^{-4} M) solution containing *t*-butyl alcohol (0.1 M) saturated with nitrogen gas (pH 9.2, NaOH) is shown in Figure 7.20. The spectrum exhibits a small absorbance in the region between 250 nm and 450 nm. Maxima of the spectra varied with time indicating the reaction was not instantaneous when compared with the 2.5 μ s pulse. Initially maxima were observed at 280 nm and 450 nm. The maximum at the wavelength greater than 450 nm was due to the absorbance of the hydrated electron and quickly disappeared to show the formation of a new maximum at 365 nm. In addition to the positive absorbance, the spectrum also shows a negative absorbance in the

region between 290 and 320 nm. This negative absorbance is due to the ground state absorbance of Dichlorophen in this region (Figure 7.04).

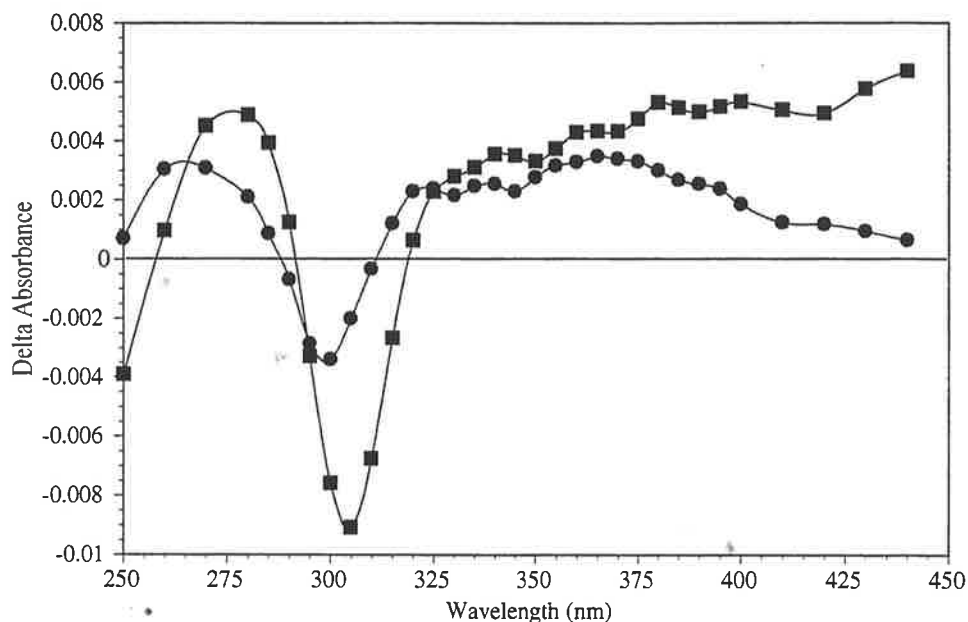


Figure 7.20. Time resolved TDA spectra obtained upon pulse radiolysis of a Dichlorophen (1×10^{-4} M) solution containing *t*-butyl alcohol (0.1 M) saturated with nitrogen gas (pH 9.2, NaOH). (■ Directly after Pulse, ● 10 μ s).

The bimolecular rate constant for the reaction of the hydrated electron with Dichlorophen was calculated from the slope of a plot of the decay rate of the hydrated electron at 640 nm against the concentration of Dichlorophen (20 to 50 μ M). The rate constant determined was $2.0 \times 10^9 \text{ M}^{-1} \text{ s}^{-1}$. Though this is the first reported rate constant for the reaction of the hydrated electron with the Dichlorophen anion, rate constants for compounds with similar functional groups have been reported and are:

Chlorobenzene	$k = 5.0 \times 10^8 \text{ M}^{-1} \text{ s}^{-1}$ [161]
4-Chlorophenol	$k = 1.5 \times 10^9 \text{ M}^{-1} \text{ s}^{-1}$ [162]
3-Chlorotoluene	$k = 8.8 \times 10^8 \text{ M}^{-1} \text{ s}^{-1}$ [163]
4-Chlorophenoxide anion	$k = 6.5 \times 10^8 \text{ M}^{-1} \text{ s}^{-1}$ [162]

The rate constant for the reaction of Dichlorophen with the hydrated electron recorded here is similar to that observed for the same reaction with 4-chlorophenol. The rate constant for the reaction of the hydrated electron is less for the phenoxide anion when compared to the corresponding phenol. Since the rate constant is similar to the 4-chlorophenol it is probable the hydrated electron will add to the protonated ring of Dichlorophen resulting in the transient $\text{Dich}^{\bullet 2-}$. The transient would then be expected to result in the dissociation of a chloride ion from the parent molecule.

Ab initio calculations performed on the Dichlorophen anion showed that the carbon atom attached to the chlorine atom on the protonated ring is the most electron deficient in the molecule. This would, in theory, make it the most favourable for electron attack which is consistent with the rate constant data obtained on Dichlorophen.

No new absorbance maxima were detected in the region 250 to 600 nm in time resolved studies out to 1000 μs , suggesting the reaction forms stable compounds that do not absorb in this region.

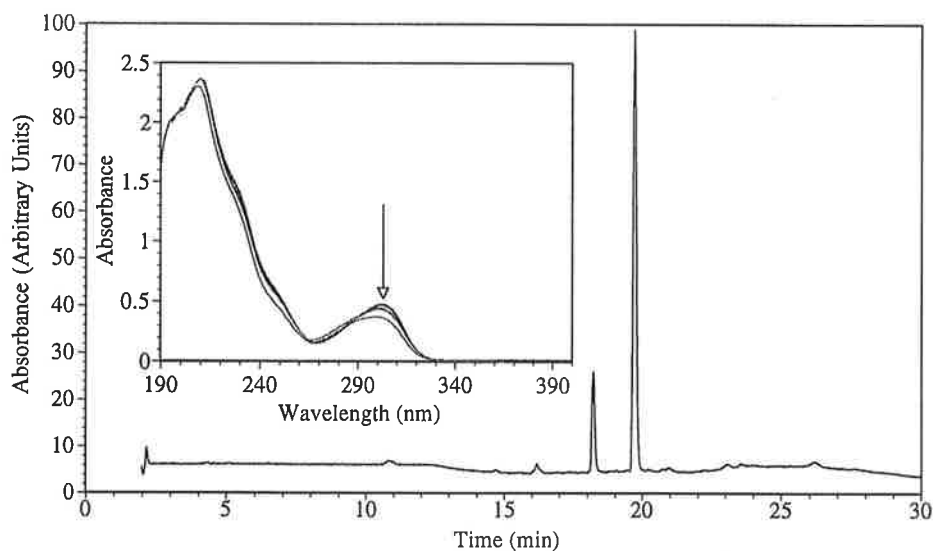


Figure 7.21. HPLC analysis following the gamma irradiation of an aqueous Dichlorophen ($8.4 \times 10^{-5} \text{M}$) solution containing *t*-butyl alcohol (0.1 M) saturated with nitrogen (pH 9.2, NaOH). The trace displays the product formed from the reaction of Dichlorophen with the hydrated electron. Inset. Change in optical absorbance of the same solution (0 to 400 Gray). The arrow indicates the direction of change with radiation dose.

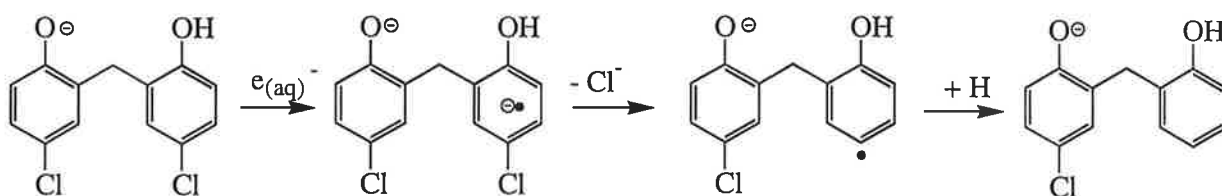


Figure 7.22. Reaction pathway for the reaction of the hydrated electron with Dichlorophen.

Gamma irradiation of an aqueous Dichlorophen ($8.4 \times 10^{-5} \text{M}$) solution containing *t*-butyl alcohol (0.1 M) saturated with nitrogen (pH 9.2, NaOH) followed by HPLC produced the trace in Figure 7.21. The effect on optical absorbance was a decrease in the absorbance maximum at 300 nm with no new maximum observed throughout the irradiation period. The HPLC trace shows the formation of a major peak at 18 minutes. Mass spectrometry on this peak produced a double mass to charge ratio at 233/235 (3:1) Daltons. A change in the isotope pattern from 4:3:1 to 3:1 indicates that one chlorine atom is missing when compared

to the parent molecule. The mass to charge ratio of 235 Daltons is 34 Daltons less than that of Dichlorophen (minus one chlorine, plus one hydrogen). MS^2 fragmentation of the 233 Daltons ion produced a daughter ion at 127 and 93 Daltons. The 127 peak has been observed previously and assigned in Dichlorophen, the 93 mass unit daughter ion is the 127 ion minus 35 Daltons (one chlorine). The exact mechanism for the reaction of the hydrated electron with Dichlorophen would be initial electron capture, followed by ejection of a chloride ion leaving an alkyl radical. This radical would then extract a hydrogen atom from the *t*-butyl alcohol to form the final stable product [94]. These observations allow the postulation of the mechanism in Figure 7.22.

The G value for the production of the chloride ion was determined to be 1.0. No comparison with the loss of Dichlorophen could be made because of the solubility problems mentioned in section 7.2.

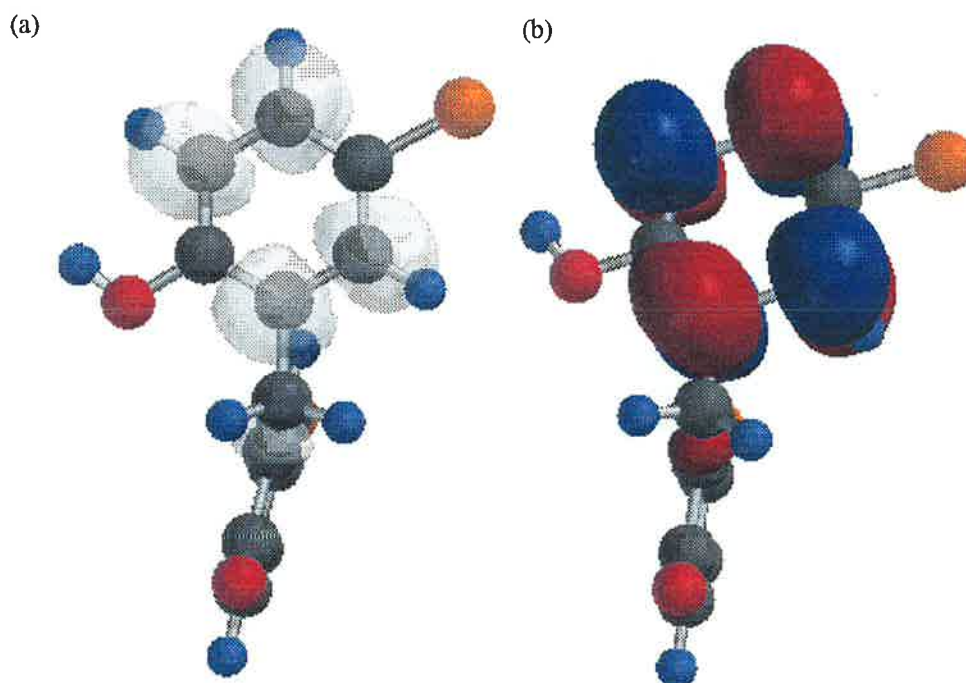


Figure 7.23. Plots of the electron spin density surface (a), and the LUMO (b), of Dichlorophen as determined by *ab initio* molecular orbital theory. Calculations were performed at the HF/6-31G** level of theory. Plot (a) was determined with a molecular charge of -2 and a multiplicity of 2. Plot (b) was determined for a molecular charge of -1 possessing a corresponding multiplicity of +1.

Ab initio calculations were carried out on Dichlorophen, in its mono phenoxide form, with an extra electron in its full electron set. Structures that resulted from the optimisation at HF/6-31G** (as a doublet) produced the spin surface observed in Figure 7.23. The deprotonated Dichlorophen produces a spin surface located over the neutral ring. This result is consistent with the nucleophilic nature of the hydrated electron.

The LUMO of the neutral Dichlorophen molecule is located over all of the carbons ortho and meta to the oxygen on the phenolic ring. This is a different site suggested by electron density calculation (natural population analysis).

7.7 REACTION OF DICHLOROPHEN WITH THE HYDROGEN ATOM

Figure 7.24 shows the TDA spectrum obtained upon the pulse radiolysis of an aqueous Dichlorophen (1×10^{-4} M) solution containing *t*-butyl alcohol (0.1 M) saturated with nitrogen (pH 2, HClO₄). It exhibits absorption with maxima at 355 nm and 305 nm. The spectrum also exhibits a small negative absorbance in the region of 280 nm to 290 nm. This is due to the ground state absorbance of Dichlorophen at this pH. The spectrum is similar to the spectra recorded by Getoff *et al.* [94] for the reaction of the hydrogen atom with 4-chlorophenol. The 4-chlorophenol transient produced by the reaction with hydrogen atoms was assigned to a H-adduct. We can therefore assign the transient observed for the reaction of Dichlorophen with hydrogen atoms to the same type of transient.

Formation kinetics were performed on the maximum at 340 nm by obtaining the slope of a plot of the pseudo first order rate constant against the concentration of Dichlorophen. This produced a bimolecular rate constant for the reaction of $3.0 \times 10^9 \text{ M}^{-1} \text{ s}^{-1}$. The rate constant for the reaction of hydrogen atoms with 2-chlorophenol was measured at $1.5 \times 10^9 \text{ M}^{-1} \text{ s}^{-1}$ by Getoff *et al.* [94]. As expected the rate constant is similar to Dichlorophen due to the similarities between the two compounds.

Steady state irradiation of an aqueous Dichlorophen (1×10^{-4} M) solution containing *t*-butyl alcohol (0.1 M) saturated with nitrogen (pH 2, HClO₄) produced a decrease in absorbance area of the peak in the HPLC trace corresponding to Dichlorophen. Formation of three compounds in the HPLC trace was also observed. The products had retention times of 4, 5.5 and 8 minutes (data not shown). Absorbance of the species was small suggesting the molar absorbance of the product was not large at 254 nm. All attempts at trying to determine the mass to charge ratio of the compounds using electrospray mass spectrometry failed due to interference from the ion pairing reagent TFA. From the pulse radiolysis result it can be assumed that the compounds are the result of an addition of the hydrogen atom to the starting compound.

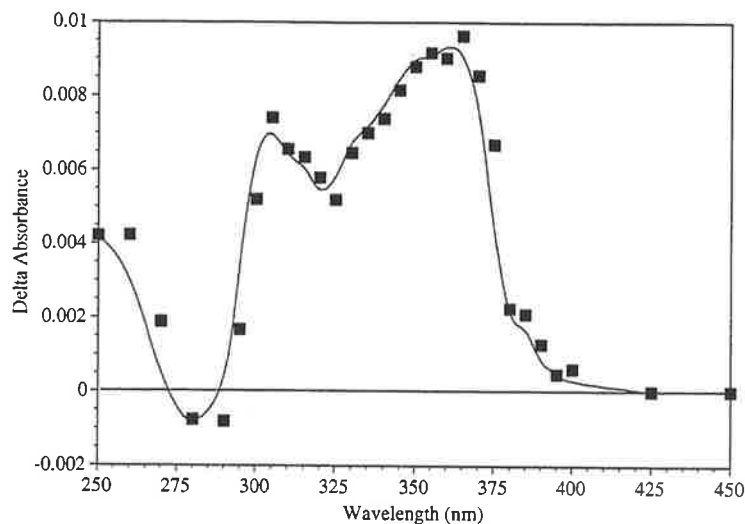


Figure 7.24. TDA spectrum obtained upon the pulse radiolysis of an aqueous Dichlorophen (1×10^{-4} M) solution containing *t*-butyl alcohol (0.1 M) saturated with nitrogen (pH 2, HClO_4). Spectrum recorded 10 μs after the pulse.

7.8 REACTION OF DICHLOROPHEN WITH REDUCING RADICALS.

Pulse radiolysis of a nitrous oxide saturated solution containing sodium formate (0.02 M) and Dichlorophen (1×10^{-4} M) (pH 9.2, NaOH) produced a maximum below 250 nm with no other absorbance observed. This maximum observed was due to the formation of the carbon dioxide radical anion. Time resolved studies out to 1000 μs indicated the presence of no new absorption in the range of 250 to 600 nm. This suggests the carbon dioxide radical does not react with Dichlorophen. The redox potential of the carbon dioxide radical has been determined to be -2.0 V (versus NHE) [43, 111]. The redox potential of $\text{Dich}^-/\text{Dich}^{\bullet 2-}$ must therefore be more negative than -2.0 V. Therefore, $\text{Dich}^{\bullet 2-}$ is a strong reducing agent with a reduction potential between -2.0 and -2.9 V (versus NHE).

Gamma irradiation of the same solution showed no loss of Dichlorophen when sufficient radical was added into the matrix to react with 50% of the available starting compound. This result confirms those obtained in the pulse radiolysis experiments.

7.9 OVERVIEW OF THE RADIATION CHEMISTRY OF DICHLOROPHEN

This study has allowed for the first time the elucidation of the radiation chemistry of aqueous Dichlorophen. The new chemistry for Dichlorophen is summarised in Figure 7.25.

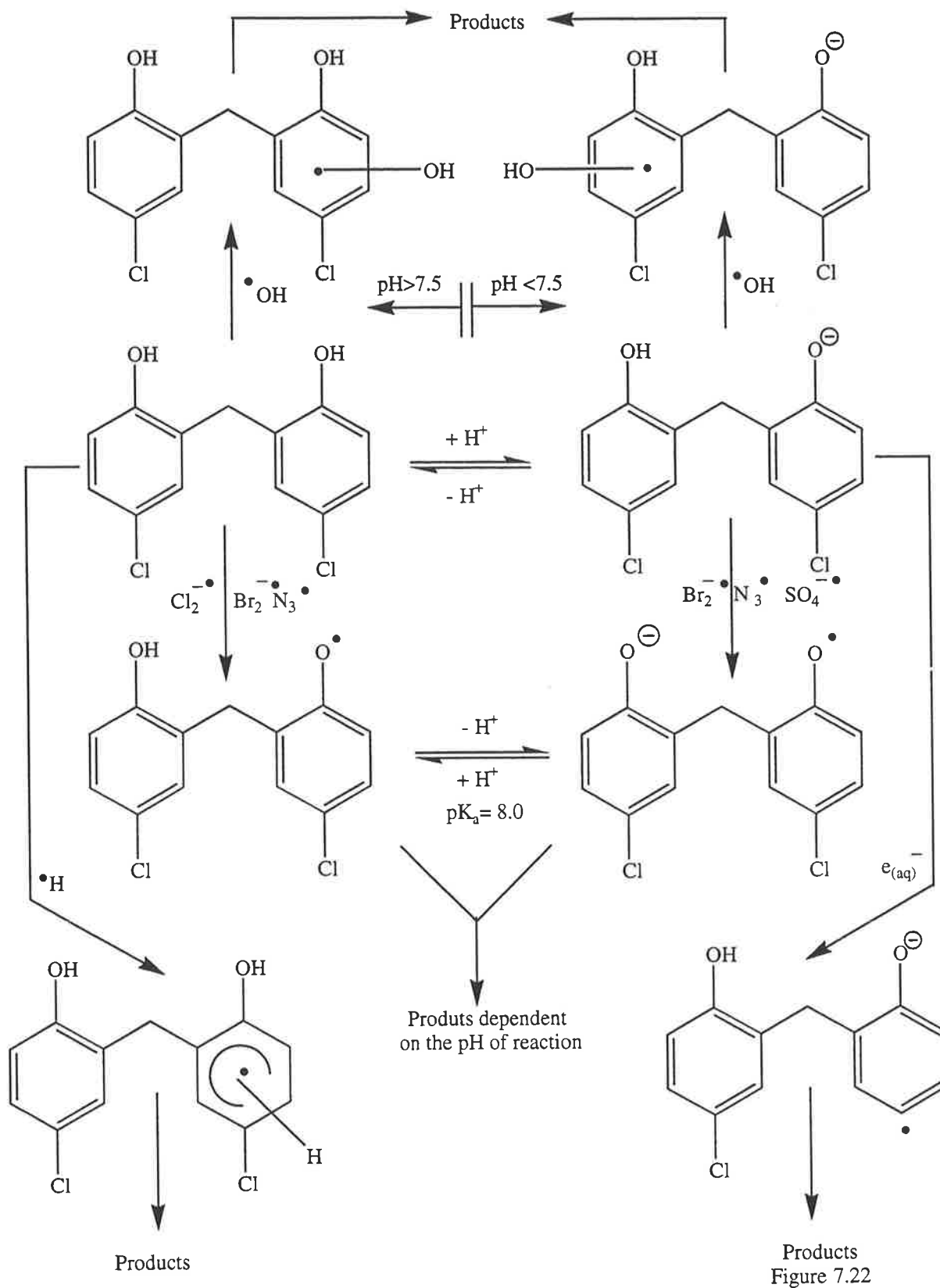


Figure 7.25 Overview of the radiation chemistry for Dichlorophen characterised in this report.

The TDA spectrum obtained from the reaction of Dichlorophen with hydroxyl radicals suggests the formation of a OH-adduct as an intermediate. The transient spectrum is compared to that from the reaction of the hydroxyl radical with 4-chlorophenol and the 4-chlorophenoxide ion, it is observed that the transient resembles that obtained for the 4-

chlorophenol. Reaction of 4-chlorophenol is known to proceed through a OH-adduct intermediate, supporting our hypothesis [118]. The decay rate of the OH-adduct shows a dependence on the ionic strength of the solution, therefore the transient possesses a charge. The transient decays by second order kinetics, indicating the degradation products are formed by radical-radical reactions. HPLC characterisation of the compounds formed by the reaction of Dichlorophen with the hydroxyl radical showed that these compound have a retention time less than Dichlorophen. Mass spectrometric studies determined the predominate compound is the hydroxylated, mono dehalogenated form of Dichlorophen. Minor products were characterised as the hydroxylated form of Dichlorophen as well as a dimer. This is in agreement with what we have determined through pulse radiolysis. The rate of loss of Dichlorophen and the formation of products from the reaction with the hydroxyl radical could not be studied under steady state conditions because of the low solubility of Dichlorophen.

The TDA spectrum obtained upon the reaction of Dichlorophen with the hydroxyl radical at pH 2 differs from that obtained for the same reaction at neutral pH. The spectrum obtained still resembled a OH-adduct. Correction for the ground state absorbance of Dichlorophen produced a spectrum different to that of the neutral pH experiment, suggesting the OH-adduct possesses a pK_a between pH 2 and 9.2. Ground state absorbance of Dichlorophen is such that it is not possible to determine the pK_a of the OH-adduct. The rate constant for the reaction of Dichlorophen with the hydroxyl radical at pH 2 is similar to that obtained at neutral pH. Considering the electrophilic nature of the hydroxyl radical this implies that its addition to the mono phenoxide form of Dichlorophen occurs on the phenolic ring. Gamma irradiation coupled with HPLC of Dichlorophen at pH 2, has shown that the predominate compound for the reaction of Dichlorophen is that observed at pH 9.2. Mass spectral fragmentation data indicates that this compound is the same product.

The transient produced from the reaction of Dichlorophen with the hydroxyl radical has been shown to be reactive with oxygen. Gamma irradiation coupled with HPLC reveals the formation of different compounds than those obtained for the de-oxygenated experiment. Mass spectral fragmentation data indicates that the major products results from the addition of molecular oxygen to the transient. The newly produced transient then reacts to form a major compound corresponding to the addition of a hydroxyl group to Dichlorophen. This is in agreement with a previous study which found that addition of a single oxygen atom to the starting compound was the most prevalent product for the reaction of benzene with the hydroxyl radical in the presence of oxygen [82].

The TDA spectrum obtained from the reaction of Dichlorophen with one electron oxidants is similar to that obtained for the phenoxyl radical of 4-chlorophenol. The transient for the reaction of the one electron oxidants is therefore assigned as a phenoxyl radical. Rate constants for the bimolecular reaction of Dichlorophen with one electron oxidising agents decrease with the redox potential of the oxidising agents, with the exception of the azide radical, which has a higher self exchange rate. Dichlorophen is not observed to react with the diiodide radical anion and therefore the phenoxyl radical of Dichlorophen is a powerful one electron oxidant with a redox potential between 1.4 and 1.0 V. Gamma irradiation coupled with HPLC for the one electron oxidising agents shows a pH dependence on the type of products formed. The pK_a determined for the control of the formation of the major product is observed to be different to that of Dichlorophen (using the azide radical as the oxidant), suggesting the phenoxyl type radical resulting from the oxidation has a different pK_a . The protonation state of the phenoxyl radical of Dichlorophen controls the product distribution.

Ab initio calculations indicate that the HOMO of Dichlorophen is located over the phenoxide ring. It is suspected that electron loss occurs from this orbital, which is in agreement with the experimental results. The spin density surface is also located on the aromatic ring and the oxygen, and can be accounted for by resonance theory.

The TDA spectrum for the reaction of Dichlorophen with the hydrated electron produces a negative absorbance due to the ground state of the starting compound. The rate constant obtained for the reaction of Dichlorophen with the hydrated electron is similar to that of 4-chlorophenol [162], suggesting the hydrated electron reacts with the phenolic ring. Gamma irradiation coupled with HPLC found one major product for the reaction of the hydrated electron with Dichlorophen. Using mass spectral fragmentation we have determined that the compound is the dehalogenated form of Dichlorophen. The radical anion of Dichlorophen is a strong reducing agent with a redox potential of between -2.0 and -2.9 V. In natural and industrial waste water the elimination of the chloride ion would prevent the radical anion from reforming Dichlorophen, thus allowing for its breakdown.

Ab initio calculations indicate that the LUMO of Dichlorophen is located on phenolic ring. It is suspected that the electron gain would initially occur in this orbital, which is in agreement with experimental results.

The TDA spectrum for the reaction of Dichlorophen with hydrogen atoms is similar to that observed for the H-adduct obtained upon the reaction of 4-chlorophenol with hydrogen

atoms [94]. Steady state irradiations of Dichlorophen at pH 2 produced three compounds in the HPLC chromatogram, but no structures could be determined.

Dichlorophen will degrade upon reaction with a number of free radicals produced in natural and treated industrial discharge water. Chloride ion elimination will occur for the reaction of Dichlorophen with one electron oxidising agents (pH greater than 8), the hydrated electron and the hydroxyl radical.

8.0 Radiation Chemistry of Aqueous Cyromazine Solution

8.1 CYROMAZINE

Cyromazine (N-cyclopropyl-1,3,5-triazine 2,4,6 triamine) (Figure 8.01) is a white solid with a melting point of 220-222 °C. The maximum solubility in water is 11 g/L at pH 7.5 [164].

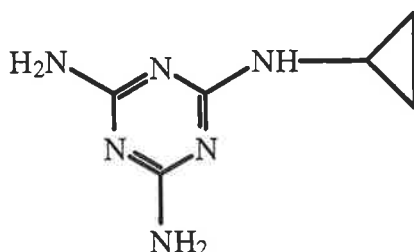


Figure 8.01. Chemical structure of Cyromazine.

The Ciba-Giegy Chemical Company released Cyromazine as a systemic insecticide. It is an insect growth regulator, which is effective against fly larvae and leaf miners [165]. Unlike most triazines, Cyromazine exhibits no herbicidal activities.

The major dealkylation product of Cyromazine (melamine (Figure 8.02)) is a suspected carcinogen even though it gives negative results as a mutagenic in an Ames test [166]. The suspected carcinogenic properties of melamine has caused the US Environmental Protection Agency to issue stringent guidelines for the analysis of food that has been exposed to Cyromazine [165].

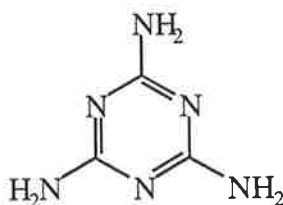


Figure 8.02. Cyromazine major degradation product Melamine [165].

Degradation of Cyromazine occurs in plants where it is readily metabolised to its principal metabolite melamine [165]. Cyromazine degradation has been shown to utilise the bacteria *Pseudomonas* spp. (strains A and D). This bacterium is known to degrade Cyromazine down to carbon dioxide and ammonia [167]. Cyromazine is not expected to undergo direct photolysis since it does not absorb light above 290 nm.

In addition, Cyromazine has two reported pK_a values, one at 5.3 and the other at 1.7, making it a weak base [168].

8.2 REACTION OF CYROMAZINE WITH THE HYDROXYL RADICAL

Figure 8.03 shows the time resolved TDA spectra obtained upon pulse radiolysis of an aqueous Cyromazine (1×10^{-4} M) solution saturated with nitrous oxide (pH 6.8, phosphate buffer). It exhibits an absorption band with a maximum at 275 nm with a shoulder at 350 nm. The spectrum does not match that obtained for a cyclohexadienyl type radical, thus addition of the hydroxyl radical to Cyromazine is not occurring.

In the presence of *t*-butyl alcohol (0.1 M), an effective hydroxyl radical scavenger but a weak hydrogen atom scavenger, the absorption spectrum was considerably reduced. The high G ($\cdot\text{OH}$) yield and appreciable decrease in the transient absorption suggests the transient absorption spectrum in Figure 8.03 is due mainly to the reaction of the hydroxyl radical with Cyromazine.

No negative absorbance was detected in the TDA spectrum recorded from the reaction of the hydroxyl radical with Cyromazine. This is because Cyromazine does not have a large ground state absorbance in the region of 250 nm to 450 nm. The TDA spectrum can be corrected for the small ground state absorbance by using equation 3.14, and the assumption that the yield of the hydroxyl radical is equal to the yield of the transient radical. Since Cyromazine does not absorb strongly in the region of 250 to 450 nm, the molar absorbance spectrum of the transient does not vary considerably in shape from that of the delta absorbance spectrum.

Reducing the dose (and hence the amount of transient radical) produced an increase in the half-life of the transient species at 275 nm. The radical therefore decays by second order kinetics. When the decay curves were fitted to second order kinetics they produced fits with decay rates of $2k/\epsilon l = 6.8 \times 10^4 \text{ s}^{-1}$ and $8.4 \times 10^5 \text{ s}^{-1}$ at 275 and 350 nm, respectively. Assuming that all the hydroxyl radicals react with Cyromazine and the G value of the hydroxyl radical is equal to that of the transient (ie. 5.5), the molar absorbance of the maxima are 4580 and 1140 $\text{M}^{-1}\text{cm}^{-1}$ for 275 and 350 nm, respectively. Using these molar absorbance values, it was determined that $2k = 5.1 \times 10^8 \text{ M}^{-1}\text{s}^{-1}$ and $9.5 \times 10^8 \text{ M}^{-1}\text{s}^{-1}$, respectively. Differences in the decay rates at the maximum and shoulder indicate they are formed by different radicals. The second order decay of the transient indicates that products are formed through radical-radical reactions.

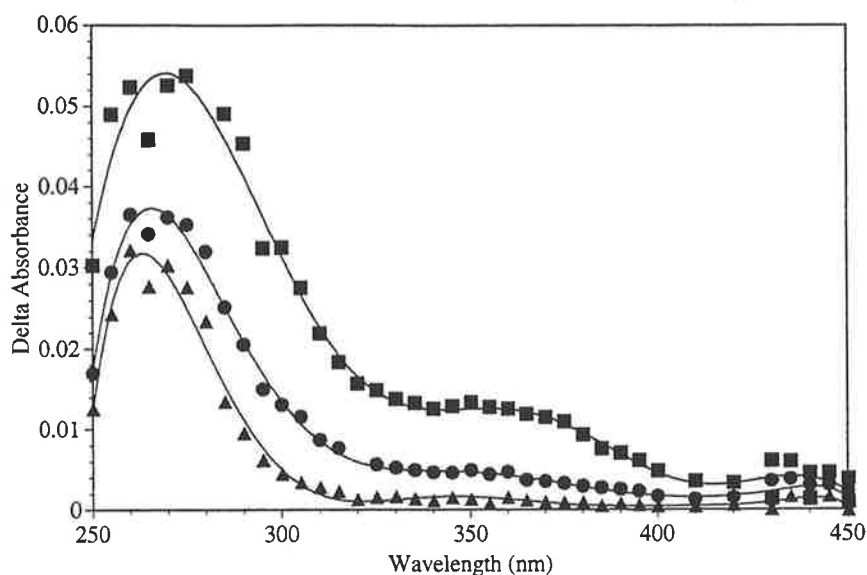


Figure 8.03. Time resolved TDA spectra obtained upon the pulse radiolysis of an aqueous Cyromazine (1×10^{-4} M) solution saturated with nitrous oxide (pH 6.8, phosphate buffer). (■ Directly after the pulse, ● 200 μ s after the pulse, ▲ 1000 μ s after the pulse).

Reactions of 1,3,5-triazines and cyclopropane with hydroxyl radicals has not been extensively studied in the past, however, some molecules containing this functionality have been reported in the literature. Reaction of 1,3,5-triazines with the hydroxyl radical [143, 144] were dependent on the other functional groups present. Cyromazine is an unsaturated aromatic system, however, carbons on the 1,3,5-triazine ring are electron deficient and can be thought of as positively charged (as described by Quirke [145] and observed in Figure 6.04). This makes the 1,3,5-triazine ring unsuitable for electrophilic reactions, suggesting the hydroxyl radical does not react with the 1,3,5-triazine ring. Absorbance maximum at 275 nm is not consistent with the formation of a OH-adduct as these types of radicals tend to have a maximum in the region of 300 to 340 nm. It is therefore likely that the transient is from hydrogen abstraction from the cyclopropane ring.

Adjusting ionic strength of the solution by the addition of NaClO_4 (1 M) produces no change in the decay of the transient, indicating the transient is not charged. This result suggests electron transfer is not occurring between the hydroxyl radical and Cyromazine, since at pH 6.8 Cyromazine is neutral and electron transfer to the hydroxyl radical would result in a charged species.

Competition kinetics were used to determine the bimolecular rate constant for the reaction of the hydroxyl radical with Cyromazine. The rate constant obtained was $4.3 \times 10^9 \text{ M}^{-1}\text{s}^{-1}$ indicating that Cyromazine reacts with the hydroxyl radical at slightly less than diffusion controlled rates. This is the first reported rate constant for the reaction of the

hydroxyl radical with Cyromazine. Reactions of hydroxyl radicals with 1,3,5-triazine were summarised in chapter six. To date the reaction of the hydroxyl radical with cyclopropane has not been studied, however reactions with cyclopentane and cyclohexane have. The rate constants for these reactions are:

$$\text{cyclopentane} \quad k=4.9 \times 10^9 \text{ M}^{-1}\text{s}^{-1} \quad [169]$$

$$\text{cyclohexane} \quad k=6.1 \times 10^9 \text{ M}^{-1}\text{s}^{-1} \quad [170]$$

It can be concluded from these rate constants for the reaction of the hydroxyl radical with the given cyloalkanes are similar in magnitude to that of Cyromazine's reaction with hydroxyl radicals.

Steady state irradiation of an aqueous Cyromazine (48 μM) solution saturated with nitrous oxide at pH 6.8 using cobalt 60 (Dose 80 Grays per hour) produced only a small decrease in the absorbance due to the Cyromazine at 208 nm (Figure 8.04). The spectrum varied slightly over the range of the radiation dose added to the system with the maximum shifting to the slightly lower wavelength of 206 nm. Decrease in absorbance was less than expected by the dosimetry. This implies that either the products must absorb in the region between 190 nm and 250 nm, or the transients formed by the reaction of the hydroxyl radical with Cyromazine reacts to reform the starting material, or a combination of both. Since absorbance does not vary greatly with dose, the chromophore (the 1,3,5-triazine) is not affected by reaction with the radical.

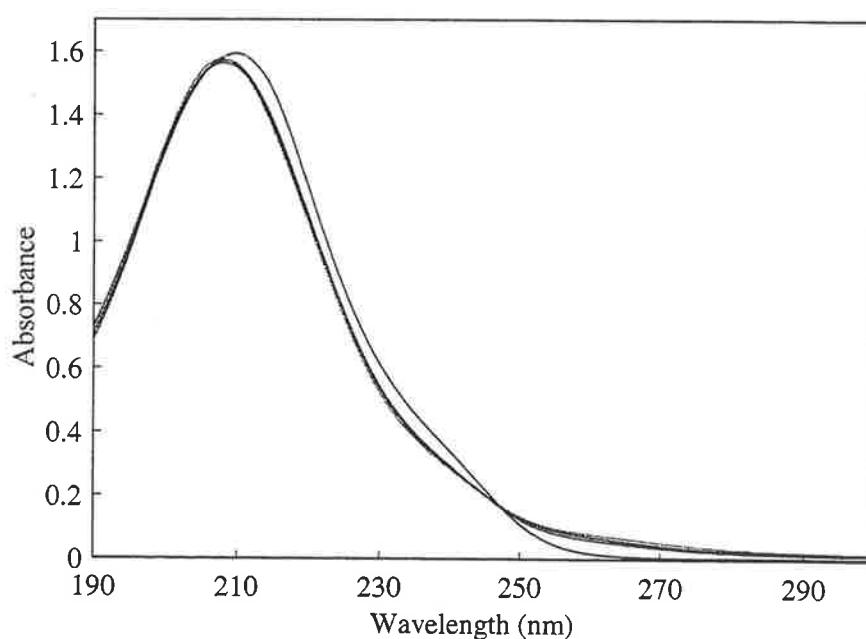


Figure 8.04. Observed change in optical absorbance resulting from the gamma irradiation of an aqueous Cyromazine (48 μM) solution saturated with nitrous oxide at pH 6.8 (0 to 100 Gray). Dose rate 80 Gray/hr.

High Performance Liquid Chromatography of a Cyromazine (1×10^{-4} M) solution saturated with nitrous oxide (pH 6.8, phosphate buffer) and irradiated with gamma irradiation showed formation of new products and a decrease in the concentration of Cyromazine (Figure 8.05), at 240 nm. Loss of Cyromazine was followed at 240 nm because the ion-pairing reagent required in the chromatography absorbed strongly at lower wavelengths. No change in the product distribution was observed at 254 nm. All six products were of varying intensities in the trace (A to F) with all products possessing a retention time less than Cyromazine, suggesting that they were more polar than the starting compound.

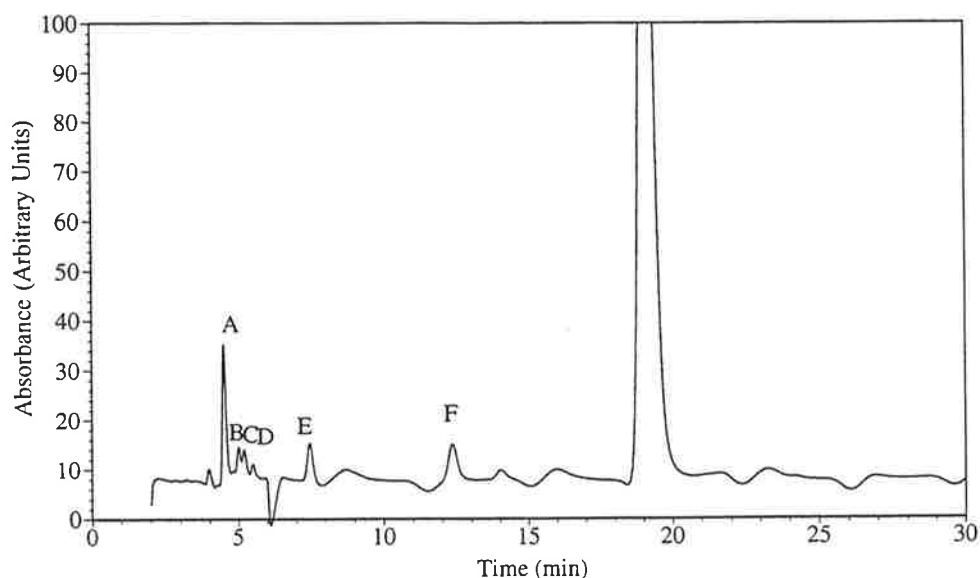


Figure 8.05. HPLC analysis following the gamma irradiation of Cyromazine (1×10^{-4} M) solution saturated with nitrous oxide (pH 6.8, phosphate buffer). The trace displays the product formed from the reaction of Cyromazine with hydroxyl radicals (A to F). See Figure 8.07 for product identification.

The rate of Cyromazine loss was linear against the concentration of hydroxyl radicals added to the system (calculated using Frickie Dosimetry), until approximately 30% of the Cyromazine had reacted. Appearance of the products was also followed by HPLC and found to be initially linear. This suggests that the products of the initial reaction also react with hydroxyl radicals to form new products and thus continue the degradation of the pesticide.

Absorbance of the products (A to F) is small compared to the loss of absorbance for the Cyromazine. When compared to the change in U.V. spectrum reported in Figure 8.04, it is observed that all products of the reaction are not detected in the HPLC trace. Due to the low concentration of the transient produced by steady state irradiation, it is possible that the second order reaction observed in the pulse radiolysis is being over shadowed by a pseudo first order reaction with Cyromazine. The G value for the loss of Cyromazine (after 20% loss) is 5.0, slightly less than the G value for the hydroxyl radical. However, it is anticipated that

the second order reaction would reform one Cyromazine molecule as well as one product. The G value for this reaction process is 2.8. This result suggests that a pseudo first order reaction is occurring and the products formed from the reaction are of a high molecular weight which do not readily elute off the column.

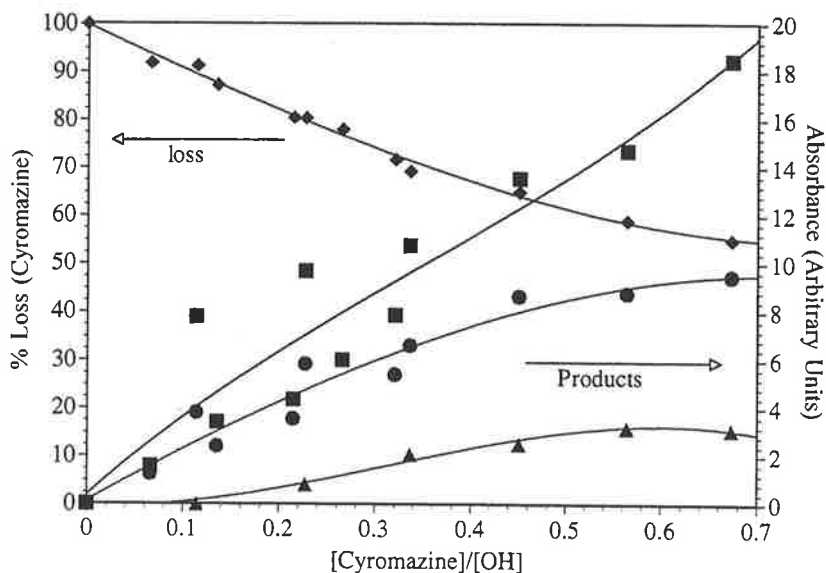


Figure 8.06. Loss of Cyromazine (left axis) and the formation of the products (right axis) from the gamma irradiation of aqueous Cyromazine (1×10^{-4} M) solution saturated with nitrous oxide (pH 6.8, phosphate buffer). Products are A=■, E=▲, F=●, B, C, and D not shown.

The structures of the products from this reaction were determined by electrospray mass spectrometry and are shown in Figure 8.07. Cyromazine produced a parent ion with a mass to charge ratio of 167 Daltons ($M+H^+$) and a fragmentation pattern (using MS^2) that consisted of daughter ions at 140 and 125 Daltons. The ions correspond to the triazine ring missing two carbons of the cyclopropane ring (140 Daltons) and missing the whole cyclopropane ring (125 Daltons). The major peak, A, produced a parent ion of 127 Daltons. This corresponds to the product melamine, therefore the transient must fragment to lose cyclopropane. A non-irradiated sample over the same time period displayed no loss of Cyromazine and no formation of any products, indicating their presence was due to irradiation of the solution. Products E and F both produced the same parent ion of 183 Daltons. The mass to charge ratio of the parent ion for E and F is 16 Daltons more than the starting compound and therefore corresponds to the addition of an oxygen atom to Cyromazine. Fragmentation of the parent compound produced daughter ions at 165 and 127 Daltons. The daughter ion at 127 Daltons is the 1,3,5-triazine ring alone which implies oxygen must have added to the ring. It is suspected from the pulse radiolysis that Cyromazine reacts with the hydroxyl radical to form an alkyl radical on the cyclopropane ring. It would be expected that this radical would disproportionate to form an unsaturated bond in the cyclopropane ring. The unsaturated bond

would be highly strained in a cyclopropane ring and consequently be highly reactive. Solvent water must therefore add across the unsaturated bond resulting in the addition of a hydroxyl group to the cyclopropane group. This reaction would be catalysed by the electrophilic addition of a hydrogen ion (from the ion pairing reagent BFA) across the double bond followed by the addition of water. Compounds B and C produced a parent ion of 165 Daltons which is two hydrogens less than the starting compound Cyromazine. Products B and C can consequently be postulated to be the precursor to the products E and F. Attempts to determine the mass to charge ratio of compound D using the electrospray technique failed and thus no information pertaining to this compound can be gained.

Ab initio calculations performed on Cyromazine produced a natural population similar to that described in Figure 6.04. Natural population analysis consequently agrees with the hypothesis that the 1,3,5-triazine ring is unsuitable for addition of the electrophilic hydroxyl radical. Carbons on the cyclopropane ring do show an excess of electron density when compared to the other atoms in the molecule.

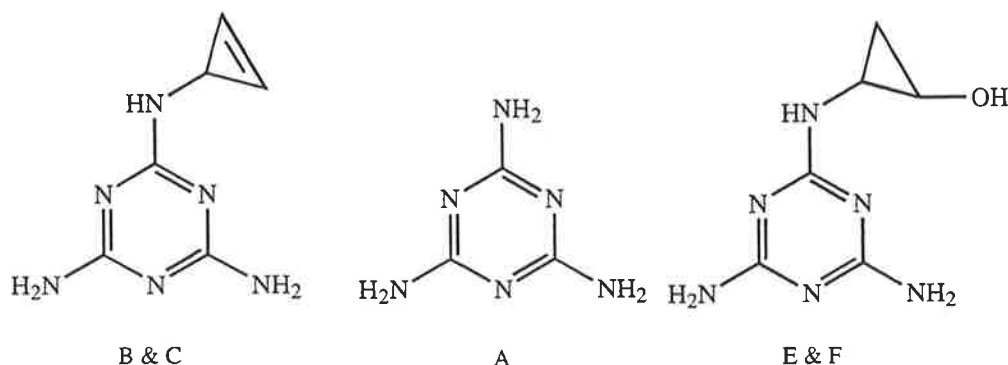


Figure 8.07. Products (A, B, C, D, F) of the gamma radiolysis of aqueous Cyromazine (1×10^{-4} M) solution saturated with nitrous oxide as determined by the analysis of electrospray mass spectrometric fragmentation data. Location of the new functional groups are not unambiguously assignable in structures B, C E and F.

8.3 REACTION OF CYROMAZINE WITH THE OXIDE RADICAL

The TDA spectrum obtained on pulse radiolysis of a nitrous oxide saturated solution of Cyromazine (1×10^{-4} M) at pH 13.2 (NaOH) exhibits an absorption band with a maximum at 275 nm with a shoulder at 350 nm. At this pH the hydroxyl radical formed by the pulse radiolysis experiment deprotonates to form the oxide radical as described in section 2.1.6. Stability of the Cyromazine molecule at this pH was established by U.V. spectroscopy and was found to be stable over the time period of both the pulsed and steady state experiments. The oxide radical reacts through hydrogen abstraction to form the hydroxide ion and an alkyl radical [171]. The spectrum is identical within experimental error to that observed in Figure

8.03. Since the spectrum in Figure 8.03 was also attributed to the abstraction of a hydrogen atom from Cyromazine, it is reasonable to assume that both arise from the same transient. Therefore this data further supports the hypothesis given in section 8.2.

Oxide radicals are known to react with substrates at approximately an order of magnitude less than the corresponding reaction with a hydroxyl radical. This allows the rate constant for the reaction of the oxide radical to be measured directly from the build up of the transient absorbance at 275 nm. A plot of the pseudo first rate constant of the reaction against the concentration of Cyromazine produced a bimolecular constant for the reaction of the oxide radical with the substrate of $k=7.0 \times 10^8 \text{ M}^{-1} \text{ s}^{-1}$. No rate constant data is available on molecules similar to the 1,3,5-triazine. This value is reasonable for the abstraction of hydrogen from an unsaturated ring. Rate constants for the abstraction of a hydrogen atom from methanol and ethanol have been recorded at 7.5 and $12 \times 10^8 \text{ M}^{-1} \text{ s}^{-1}$, respectively [44]. The rate constant for the hydrogen abstraction from cyclopentene has been reported at approximately $7 \times 10^8 \text{ M}^{-1} \text{ s}^{-1}$. This rate constant is similar to that recorded for the abstraction of hydrogen from the cyclopropane ring of Cyromazine [172].

Steady state irradiation of a $1 \times 10^{-4} \text{ M}$ Cyromazine solution at pH 13.2 saturated with nitrous oxide proved unsuccessful. The HPLC trace produced a large change in retention time for the Cyromazine molecule. A non-irradiated sample at this pH also exhibited this shift in retention time, suggesting the change was due to the high pH of the solution. For this reason no quantitative data could be taken from the experiment. However, while the trace did show peaks at different retention times, these appeared equivalent to those observed in the hydroxyl radical experiment. Mass spectral analysis was not performed on the products because the pH of the solution would result in damage to the HPLC column and affect the resulting chromatography, thus making any comparison impossible.

8.4 REACTION OF CYROMAZINE WITH THE HYDROXYL RADICAL IN ACIDIC SOLUTION

The corrected TDA spectrum obtained from pulse radiolysis of Cyromazine ($1 \times 10^{-4} \text{ M}$) in acidic solution (pH 2, HClO_4) saturated with nitrous oxide was identical (within experimental error) to that observed in Figure 8.03 for the neutral pH experiment (10 μs). A correction to the spectrum was made to take into account the lower G value for hydroxyl radicals [52] at pH 2, due to formation of hydrogen atoms from the reaction of the hydrated electrons with extra hydrogen ions. The maxima at 275 and 350 nm decayed by second order kinetics with $2k/\epsilon l = 2.8$ and $37.0 \times 10^4 \text{ s}^{-1}$, respectively. These values are in a similar ratio to

that reported in section 7.2, but the absolute values are approximately half that recorded at neutral pH. The absorbance spectra suggests the transient produced was the same as observed at neutral pH, however decay of the resulting transients was affected by the pH of the solution. Cyromazine has pK_a values of 5.3 and 1.7 [168] with the protonation-deprotonation site being the nitrogens, the positive charge created by the protonation being resonance-stabilised across the ring. Therefore at pH 2 the transient should be charged and the resulting electrostatic repulsion would be responsible for the slower decay rate observed. The transient produced by the reaction of Cyromazine with hydroxyl radicals is independent of the pH of the solution (pH 2.0 to 6.8), so the protonation state of Cyromazine and the point of protonation has no effect on the absorbing chromophore of the transient.

Competition kinetics determined a bimolecular rate constant for the reaction of the hydroxyl radical with Cyromazine of $1.4 \times 10^9 \text{ M}^{-1}\text{s}^{-1}$. This rate constant indicates that the protonated form of Cyromazine reacts at a slower rate to that observed for the neutral form.

Steady state irradiation of the same solution produced an identical HPLC trace to that of the reaction conducted at neutral pH. This result is in agreement with the pulse radiolysis data, which also implies that the protonation state or the presence of excess hydrogen ion (pH 2 to 7) does not affect the reaction. Products observed in the HPLC trace were collected and analysed by electrospray mass spectrometry. This produced the same result as that described in section 8.2.

8.5 REACTION OF CYROMAZINE WITH THE HYDROXYL RADICAL IN THE PRESENCE OF OXYGEN

The TDA spectrum obtained upon the pulse radiolysis of Cyromazine ($1 \times 10^{-4} \text{ M}$) saturated with nitrous oxide/oxygen (4:1 v/v) is illustrated in Figure 8.08. The TDA spectrum appears different from that observed in Figure 8.03, with absorbance at 275 nm no longer present. Comparison of the decay rates of the transient species indicates a change from second order kinetics to initial first order kinetics (Figure 8.09) with the addition of oxygen. This implies that the transients produced by the reaction of Cyromazine with hydroxyl radicals reacts with oxygen initially through pseudo first order kinetics. This is consistent with the hydrogen abstraction mechanism since alkyl carbon centred radicals are known to react rapidly with oxygen [48, 82, 84, 102, 103]. Figure 8.09 also indicates that the transient produced by the reaction of the hydroxyl radical with Cyromazine reacts rapidly compared to the transients previously discussed. It is known that OH-adducts react much more slowly (and through a reversible reaction) than other carbon centred radicals [85, 173]. The rate of the

reaction observed in Figure 8.09 agrees with the hypothesis that the hydroxyl radical reacts through hydrogen abstraction and not addition. Following the rapid first order reaction, the reaction then undergoes a slower process which can be observed to be taking place between 20 and 400 μs in Figure 8.09.

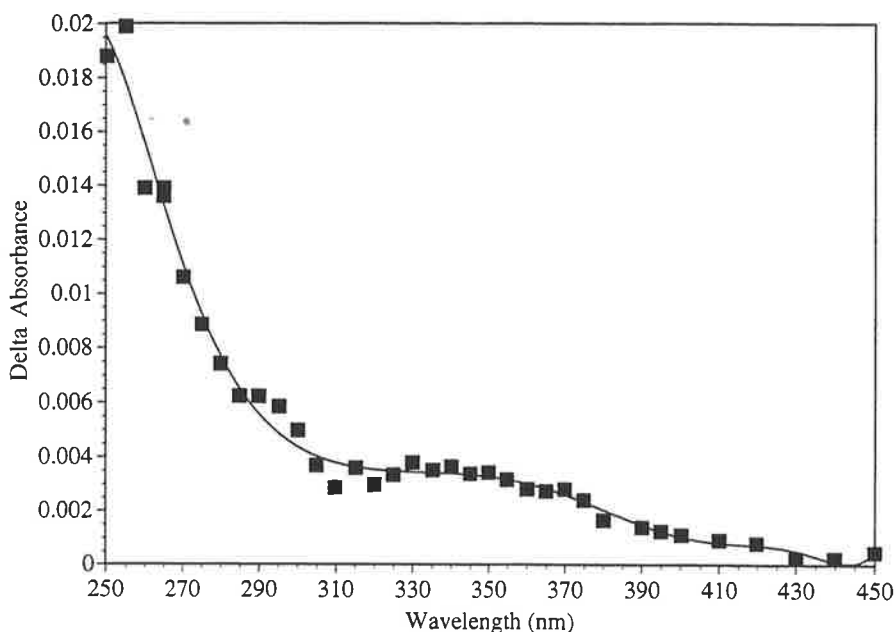


Figure 8.08. TDA spectrum obtained upon the pulse radiolysis of Cyromazine (1×10^{-4} M) saturated with nitrous oxide/oxygen (4:1 v/v). Spectrum recorded 10 μs after the pulse.

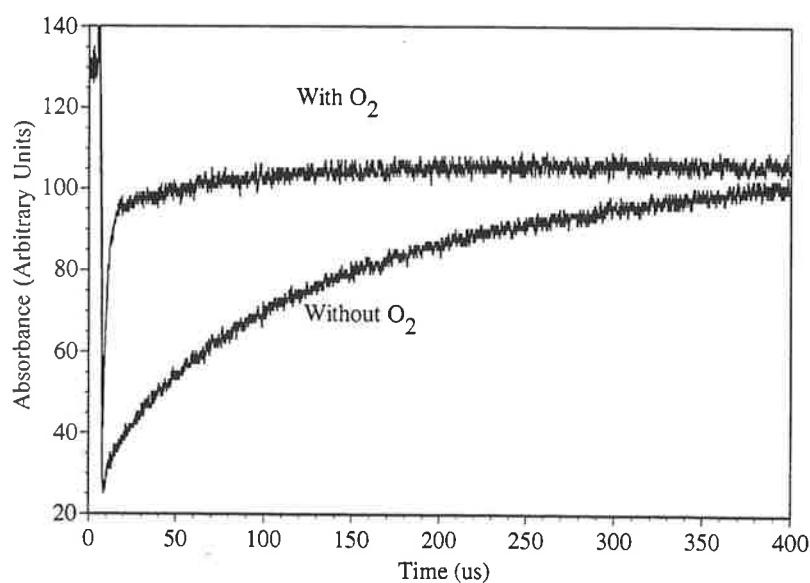


Figure 8.09. Comparison of the pulse radiolysis traces obtained from a solution of Cyromazine (1×10^{-4} M) saturated with nitrous oxide and nitrous oxide/oxygen (4:1 v/v). Absorbance data were collected at 280 nm. Traces are normalised. Both radiation pulses are 2.5 μs long with a dose of 10.0 Gray per pulse.

The inset of Figure 8.10 demonstrates the change in the ultra violet spectrum upon gamma irradiation of the Cyromazine (22 μM) solution saturated with nitrous oxide/oxygen. This is different from that observed for the de-oxygenated system. This spectrum exhibits a

small decrease in absorbance at 208 nm with no new absorbance at lower wavelengths. This suggests that the products should absorb strongly in the region of 190 to 250 nm.

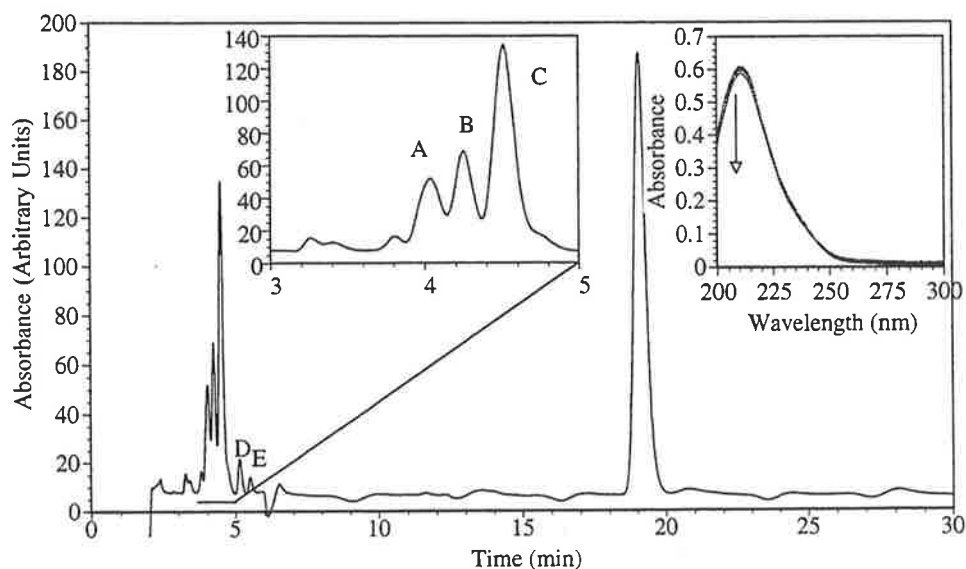


Figure 8.10. HPLC analysis following the gamma irradiation of a Cyromazine (1×10^{-4} M) solution saturated with nitrous oxide/oxygen. The trace displays the products formed from the reaction of hydroxyl radicals with Cyromazine in the presence of oxygen (A to E). See Figure 8.11 for reaction mechanism. Inset. Change in optical absorbance of the Cyromazine (22 μ M) solution saturated with nitrous oxide/oxygen produced by gamma irradiation (0 to 40 Gray). Arrow indicates the direction of absorbance change with radiation dose.

HPLC analysis of a gamma irradiated Cyromazine (1×10^{-4} M) solution saturated with nitrous oxide/oxygen can be observed to be different to that recorded for the de-oxygenated solution (Figure 8.10). Products previously observed at 7.5 and 12.5 minutes have disappeared from the trace. In addition, peaks at the beginning of the trace have increased in size compared with the de-oxygenated experiment. This indicates that these compounds are different from those observed in the hydroxyl experiment, even though they have a similar retention time. Collection of the products allowed for mass spectrometric determination of the species observed in Figure 8.11. Compounds B, D and E all possessed the same parent ion with a mass to charge ratio of 199 Daltons. This mass to charge ratio is 32 Daltons greater than the starting compound, Cyromazine, and corresponds to the addition of two oxygens to the Cyromazine molecule. MS^2 fragmentation of the peak at 199 Daltons produced a daughter ion at 181 Daltons (minus OH_2). Further fragmentation of this ion produced a peak at 127 Daltons. The 127 Daltons ion corresponds to the triazine ring, indicating the additional oxygens were attached to the cyclopropane ring. Initially the reaction results in the addition of oxygen to the radical to form the RHO_2^{\bullet} transient. The RHO_2^{\bullet} radical further reacts with the perhydroxyl radical to form the corresponding organic hydroperoxide (RHO_2H). Compounds A & C produced a parent ion of 215 Daltons. This equates to the addition of 3 oxygens to the starting Cyromazine molecule. The MS^2 fragmentation pattern shows a peak at 197 Daltons

(minus OH_2). A further fragmentation demonstrated a daughter ion at 143 (minus 54 Daltons). As the daughter ion of 127 Daltons was not observed in these experiments no data is available to determine the position of the extra oxygens in the new molecule. It is therefore impossible to assign structures for the molecules A and C.

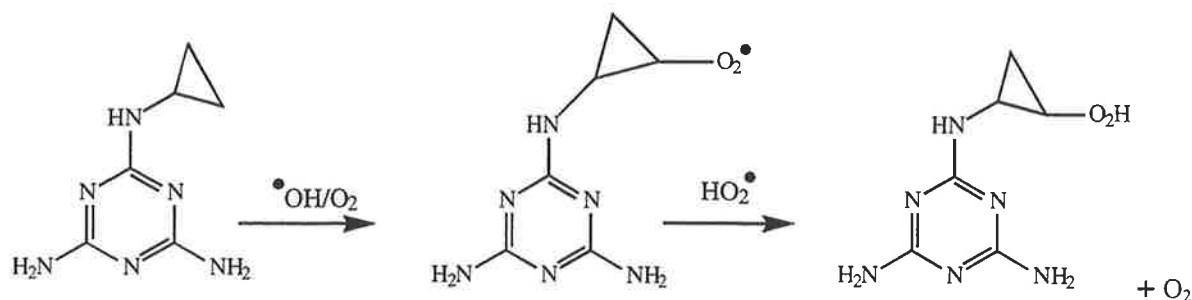


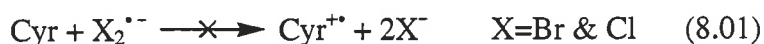
Figure 8.11. Proposed scheme for the reaction of hydroxyl radicals with Cyromazine in the presence of oxygen for products B, D and E. The exact location of the new functional group in the above scheme is arbitrary as the mass spectra data is unable to determine the exact site of addition.

Comparison of the size of the absorbance of the products indicates that the pseudo first order reaction between the transient and Cyromazine under steady state conditions is occurring in the de-oxygenated solution. Since the change in optical absorbance of the two solutions is similar, it would be expected that for the same decrease in Cyromazine concentration, the same total area in products should be observed. It is, however, observed that the area of the products in the HPLC chromatogram for the de-oxygenated experiment is less than a quarter of that of the oxygenated experiment. Difference in the results occur because the transient reacts faster with oxygen than it does with Cyromazine to form compounds more polar than those postulated in section 8.2 for the pseudo first order reaction between the cyclopropyl radical and Cyromazine, thus all the products are detected in the oxygenated trace.

8.6 REACTION OF CYROMAZINE WITH ONE ELECTRON OXIDANTS

The dichloride radical anion formed in the pulse radiolysis of oxygen saturated sodium chloride (0.02 M) Cyromazine solution (1×10^{-4} M) at pH 2 (HClO_4) reacts as a strong one electron oxidant with a potential of 2.09 V (versus NHE) [43]. Reaction of the dichloride radical anion with Cyromazine was studied by following the decay of the dichloride radical anion absorption at 340 nm. It was observed that in the presence of Cyromazine (1×10^{-4} M) this band still decayed by second order kinetics indicating a reaction between Cyromazine and the dichloride radical anion had not resulted. When sodium chloride was replaced with sodium bromide (0.02 M) (pH 6.8 and 2.0), no effect was observed on the decay of the

dibromide radical anion at 360 nm. This implied that no reaction occurred with the dibromide radical anion either, ie. the electron transfer reaction from Cyromazine to the dihalide radical anions does not occur.



The sulfate radical anion formed upon the pulse radiolysis of a nitrogen saturated potassium persulfate (0.02 M), *t*-butyl alcohol (0.1 M), Cyromazine solution (1×10^{-4} M) at pH 6.8 (phosphate buffer) reacts as a strong one electron oxidant with a potential of 2.43 V (versus NHE) [43, 86, 148]. Reaction of the sulfate radical anion with Cyromazine was studied by following the decay of the sulfate radical anion absorption at 460 nm. It was observed that in the presence of Cyromazine (5×10^{-4} M) this band decay was accelerated when compared to the solution without Cyromazine. The change in decay rate indicates that a reaction between Cyromazine and the sulfate radical anion had resulted. Since Cyromazine reacts with the sulfate radical anion and not the dichloride radical anion, it implies that the $\text{Cyr}^{++}/\text{Cyr}$ redox potential must lie between that of the sulfate and dichloride radical anions, ie. between 2.43 to 2.09 V (versus NHE).

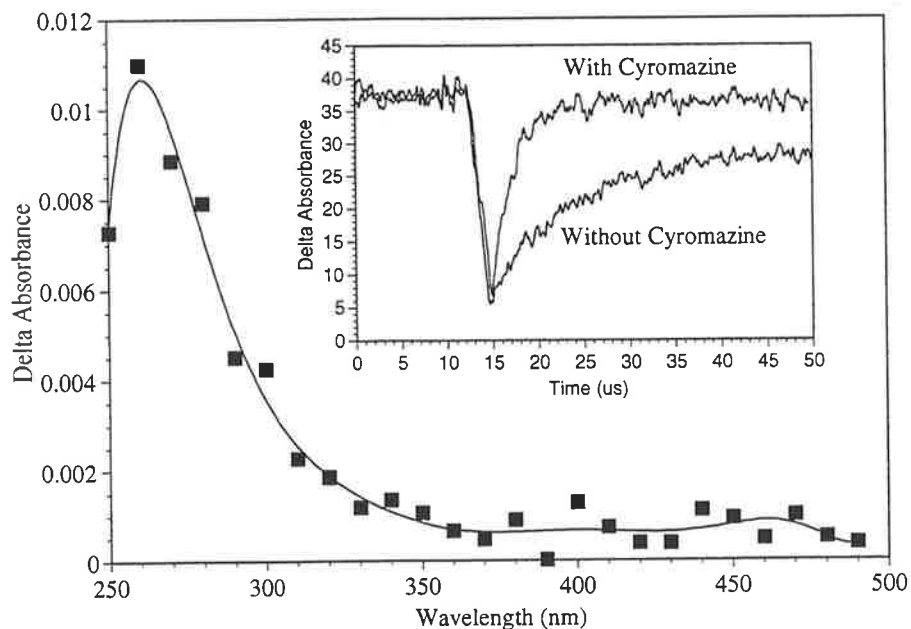
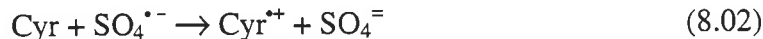


Figure 8.12. TDA spectrum obtained 10 μs after the pulse of a nitrogen saturated potassium persulfate (0.02 M), *t*-butyl alcohol (0.1 M), Cyromazine (1×10^{-4} M) solution at pH 6.8 (phosphate buffer). Inset, Comparison of the pulse radiolysis traces produced at 460 nm, with and with the presence of Cyromazine (5×10^{-4} M) in a nitrogen saturated potassium persulfate (0.02 M), *t*-butyl alcohol (0.1 M) solution. The traces indicate that a reaction has occurred between Cyromazine and the sulfate radical anion.

Using pseudo first order rate constants of the decay it was determined that 10 μs after the pulse more than 90% of the sulfate radical anion had reacted with Cyromazine. The TDA spectrum obtained at this time is shown in Figure 8.12. The spectrum has one peak at 260 nm. This spectrum is different from that obtained from the reaction of the hydroxyl radical with Cyromazine and so therefore is not assigned to the same type of transient observed for this reaction.

The rate constant for the reaction of Cyromazine with the sulfate radical anion was determined by a plot of the pseudo first order rate constant against the concentration of Cyromazine. This produced a bimolecular rate constant of $6.0 \times 10^9 \text{ M}^{-1} \text{ s}^{-1}$. Reactions of 1,3,5 triazine or any of its derivatives have not been studied with one electron oxidants and thus little information is available [149]. It is postulated that the sulfate radical anion would have diminished reactivity towards the triazine ring for the reasons given in section 6.2 and Figure 6.04. That is, the nitrogen in the ring has the greatest share of the electron density, making it unsuitable for electrophilic reactions.

Steady state irradiation of a nitrogen saturated potassium persulfate (0.02 M), *t*-butyl alcohol (0.1 M), Cyromazine solution (1×10^{-4} M) at pH 6.8 (phosphate buffer) resulted in the complete loss of Cyromazine from the HPLC trace (Figure 8.13). A non-irradiated sample of the above solution displayed no loss of Cyromazine, indicating the products were due to the radical reaction and not due to the thermal oxidation of Cyromazine by the persulfate ion [43].

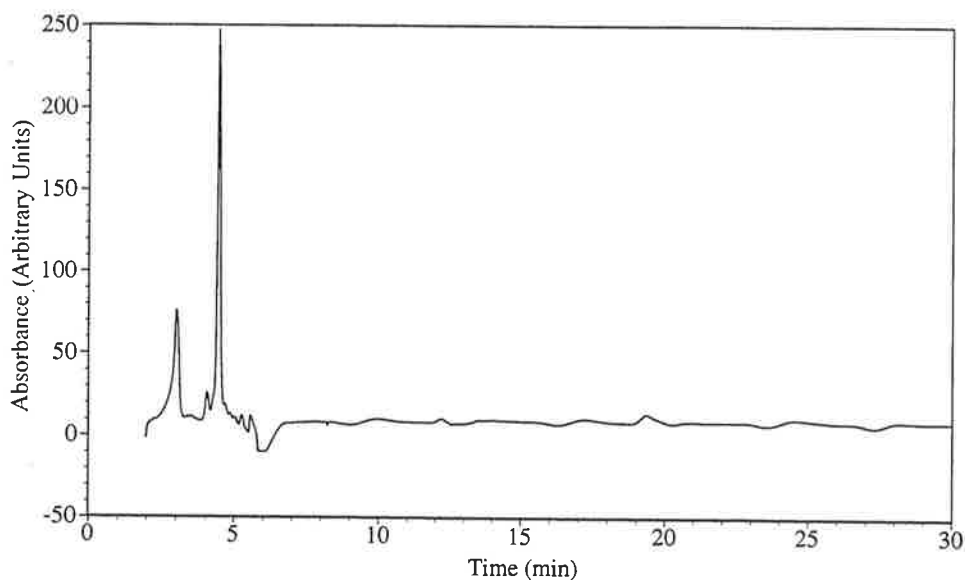


Figure 8.13. HPLC analysis following the gamma irradiation of a Cyromazine (1×10^{-4} M) containing potassium persulfate (0.02 M), *t*-butyl alcohol (0.1 M) saturated with nitrogen (pH 6.8, phosphate buffer).

Electrospray mass spectrometry on the products found a mass to charge ratio of 167 Daltons, which is equivalent to the mass to charge ratio of Cyromazine. Previously it was stated that a non-irradiated sample of Cyromazine produced no thermal degradation, therefore it can be assumed that the presence of the persulfate anions has not affected the chromatography of the HPLC trace in Figure 8.13. The resulting ion observed must therefore result from the breakdown of the parent ion during the ionisation process.

Steady state reactions performed using the dichloride radical anion at low pH produced no significant degradation of Cyromazine over the radiation dose. This is in agreement with the pulse radiolysis results.

Ab initio calculations were carried out on Cyromazine minus one electron from its full electron set at HF/6-31G** (with a doublet multiplicity) to determine the spin surface. The surface (shown in Figure 8.14 (a)) displayed an even spin distribution over the nitrogens in the triazine ring and the nitrogen connected to the cyclopropane ring. The spin surface is also located over the cyclopropane ring. These observations can be reconciled by resonance structures for the ring, but not the cyclopropane ring, since the spin surface does not seem to be located over any particular atom. The HOMO surface is also displayed in Figure 8.14 (b) and when compared to the spin surface it is observed that the spin surface is nearly contained within the HOMO, suggesting that the electron is removed from this orbital by the one electron oxidant.

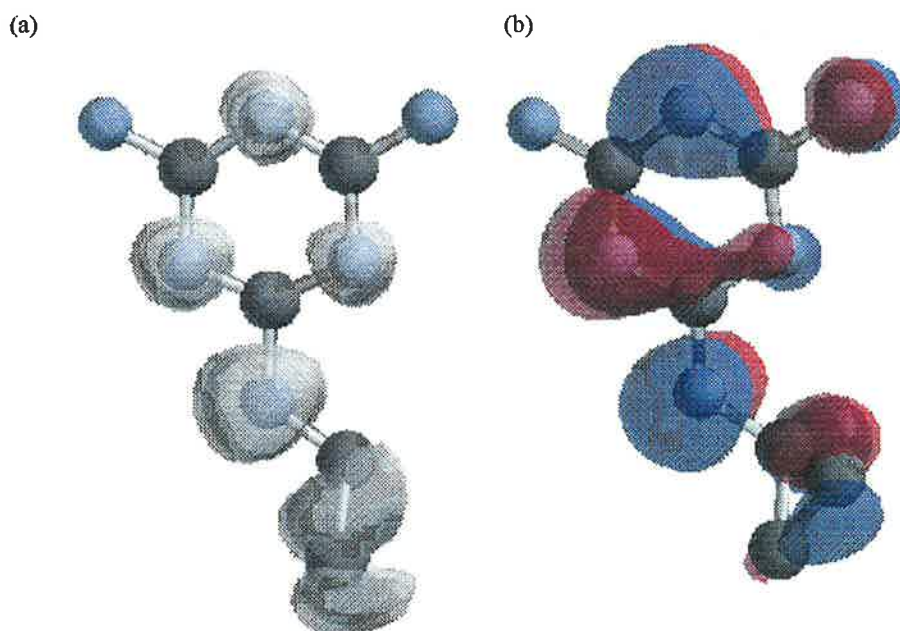


Figure 8.14. Plots of the electron spin density surface (a), and HOMO (b), of Cyromazine as determined by *ab initio* molecular orbital theory. Calculations were performed at the HF/6-31G** level of theory. Plot (a) was determined with a molecular charge of +1 and a multiplicity of 2. Plot (b) was determined for the neutral molecule possessing a corresponding multiplicity of +1.

8.7 REACTION OF CYROMAZINE WITH THE HYDRATED ELECTRON

Decay of the hydrated electron's absorbance at 640 nm (generated in a *t*-butyl alcohol (0.1 M) nitrogen saturated solution) was observed to be independent of small amounts of Cyromazine added to the solution (10 to 1×10^{-4} M) at pH 7.0 (phosphate buffer and NaOH) even up to a concentration of 10 mM Cyromazine. This indicates that a reaction between the hydrated electron and Cyromazine does not occur.

As mentioned in section 6.6, no reaction on 1,3,5-triazine or any derivatives have been recorded with the hydrated electron [149]. It was also determined in chapter 6 that the hydrated electron did not react with the triazine part of the Chlorsulfuron molecule but instead reacted with the other ring. This result and the absence of any reported reactions in the literature suggests that hydrated electrons are unreactive towards 1,3,5-triazine rings.

Gamma irradiation of an aqueous Cyromazine (1×10^{-4} M) solution containing *t*-butyl alcohol (0.1 M) saturated with nitrogen (pH 7.0 NaOH and phosphate buffer) produced no change in the optical absorbance over the dose range. The solution revealed no loss of Cyromazine when the peak area of the compound was measured and compared to the area of a non-irradiated sample. In addition, the HPLC trace revealed the formation of no new products. These results are consistent with the pulse radiolysis results and indicate that Cyromazine does not react with the hydrated electron.

Pulse radiolysis of a solution containing Cyromazine (1×10^{-4} M) in sodium formate (0.02 M) and saturated with nitrous oxide produced a peak below 250 nm. Time resolved studies showed the formation out to 1000 μ s after the pulse. Steady state irradiation of the same solution produced no loss of Cyromazine when measured by HPLC over the range of the dose. This result is expected as the carbon dioxide radical resulting from the irradiation is a less powerful reducing agent than the hydrated electron.

Ab initio calculations performed on Cyromazine with an extra electron above its full electron set allow for the generation of the spin surface [75] recorded in Figure 8.15 (a). The spin can be observed to be located over the ring in a pattern which is not reconcilable with resonance structures. The LUMO of the starting compound is also presented in Figure 8.15 (b) and indicates that the LUMO is mainly located over the ring. The spin surface is slightly different but nearly contained within the LUMO suggesting that the electron would add to this orbital. The structure of the triazine ring makes nucleophilic addition of the hydrated electron

difficult. The position of the LUMO over the ring suggests this might be the reason for no observable reaction between Cyromazine and the hydrated electron.

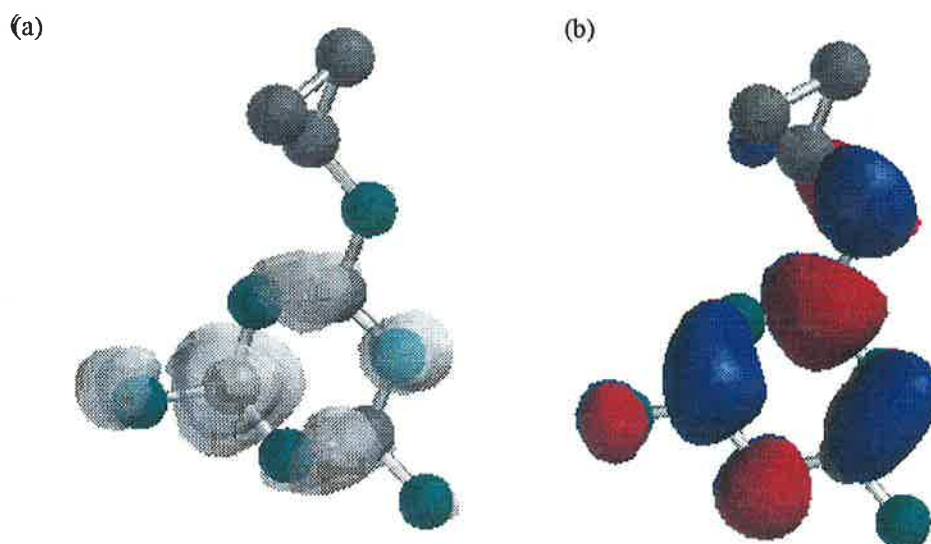


Figure 8.15. Plots of the electron spin density surface (a), and LUMO (b), of Cyromazine as determined by *ab initio* molecular orbital theory. Calculations were performed at the HF/6-31G** level of theory. Plot (a) was determined with a molecular charge of -1 and a multiplicity of 2. Plot (b) was determined for the neutral molecule possessing a corresponding multiplicity of +1.

8.8 OVERVIEW OF THE RADIATION CHEMISTRY OF CYROMAZINE

This study has allowed for the first time the elucidation of the radiation chemistry of aqueous Cyromazine. The new chemistry for Cyromazine is summarised in Figure 8.15.

The TDA spectrum obtained from the reaction of Cyromazine with hydroxyl radicals does not suggest the formation of an OH-adduct as an intermediate. *Ab initio* calculations indicate the triazine ring of Cyromazine is unfavourable to electrophilic addition of the hydroxyl radical. Reaction of Cyromazine with the oxide anion (a known hydrogen atom abstractor) produces the same spectrum as observed for the hydroxyl radical, suggesting a cyclopropanyl radical as the transient. When the rate constant obtained for the reaction of Cyromazine with the hydroxyl radical is compared to that of cyclohexane and cyclopentane [169][170], it is observed that the rate constants are similar. The decay rate of the cyclopropanyl radical showed no dependence on the ionic strength of the solution, therefore the transient is neutral. The transient decays by second order kinetics, indicating degradation products are formed by radical-radical reactions. HPLC characterisation of the compounds formed by the reaction of Cyromazine with the hydroxyl radical showed that all of these species have retention times less than Cyromazine. This suggests that the newly formed compounds are more polar than

Cyromazine. Mass spectrometric studies determined that the two major species each have masses equivalent to the addition of an oxygen atom to the Cyromazine molecule. Comparison of the mass spectral fragmentation data collected for Cyromazine with that of the newly formed compounds indicate that the oxygens are on the cyclopropane ring. This is in agreement with what we determined through the pulse radiolysis and *ab initio* studies. The rate of Cyromazine loss and the formation of products from the reaction of Cyromazine with the hydroxyl radical is initially linear under steady state irradiation. As the amount of hydroxyl radicals is increased past 30% of Cyromazine's concentration, the loss of Cyromazine and the formation of products follows a higher order kinetic mechanism. This result suggests that the products of the initial reaction also react with the hydroxyl radical to form (uncharacterised) compounds.

The corrected TDA spectrum obtained upon the reaction of the hydroxyl radical with Cyromazine at pH 2 matches that obtained from the same reaction at neutral pH. The rate constant for the reaction of Cyromazine with the hydroxyl radical at pH 2 is lower than that obtained at neutral pH. Qualitatively, this can be explained as follows: in the neutral form of Cyromazine the electron density is greater than in the case of the cation form. Since the hydroxyl radical behaves as an electrophile, reaction with the electron rich species is faster. Steady state irradiations of Cyromazine at pH 2 reproduced the results obtained at neutral pH.

The transient produced from the reaction of Cyromazine with the hydroxyl radical has been shown to be reactive with oxygen. Gamma irradiation coupled with HPLC shows the formation of different compounds than those obtained for the de-oxygenated experiment. Mass spectral fragmentation data indicate that the products result from the addition of molecular oxygen to the transient. The newly produced secondary intermediates then react to form the observed products.

The TDA spectra obtained from the reaction of Cyromazine with the sulfate radical anion differs from that obtained for the cyclopropanyl radical of Cyromazine, thus the transient produced does not transform into a cyclopropanyl type radical. Cyromazine is not observed to react with the dichloride radical anion indicating that the resulting radical cation of Cyromazine is a powerful one electron oxidant with a redox potential between 2.43 to 2.09 Volts (versus NHE). Gamma irradiation coupled with HPLC for the sulphate radical anion shows the complete loss of Cyromazine, indicating a chain reaction has occurred. Mass spectral data of the product produced a mass to charge ratio the same as Cyromazine, suggesting the parent ion breaks down during the ionisation process.

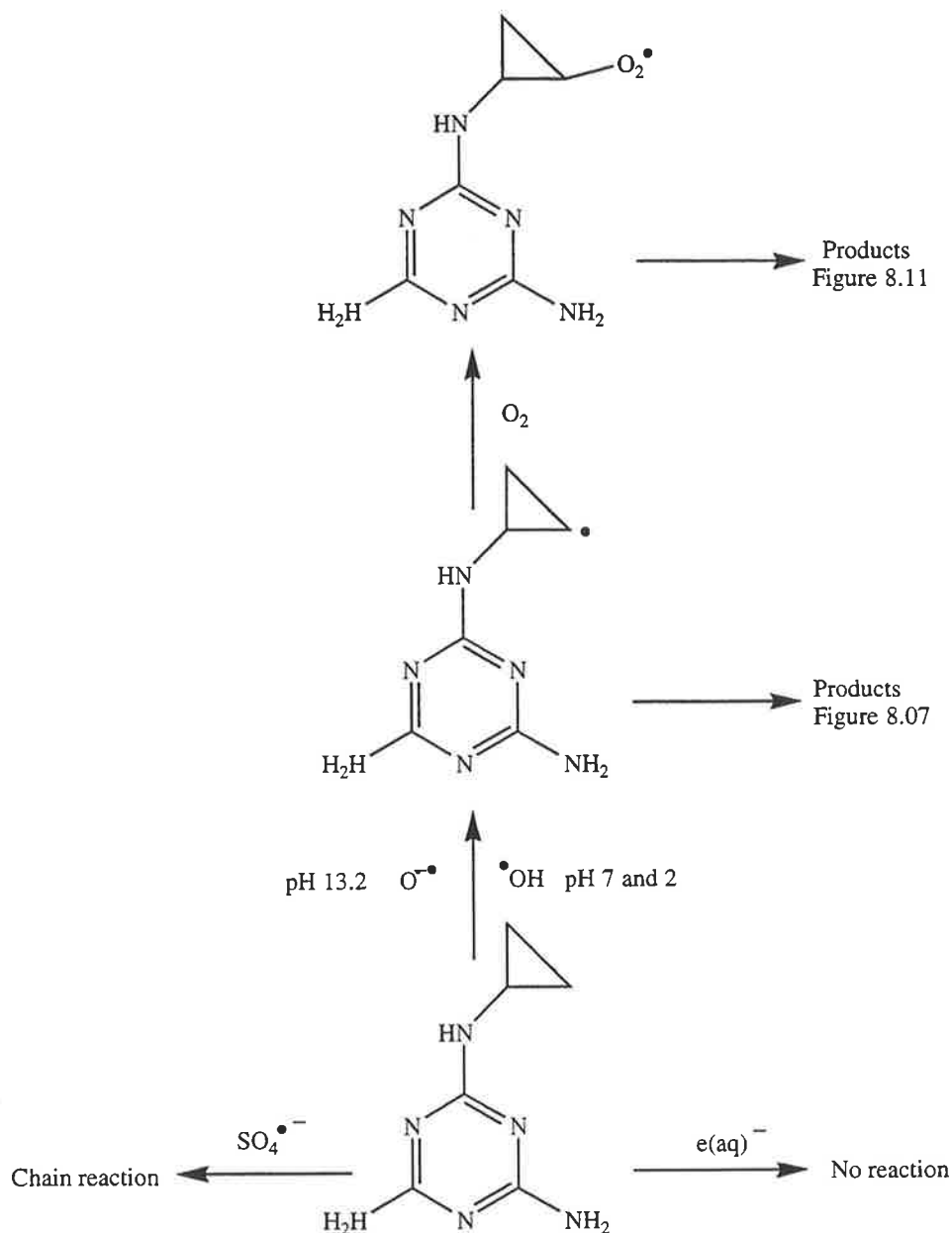


Figure 8.15. Overview of the radiation chemistry characterised in this study.

Ab initio calculations indicate that the HOMO of Cyromazine is located over the triazine ring. It is suspected that the electron lost in the one electron oxidation occurs from this orbital. The spin density surface shows the radical of the cation evenly distributed over the nitrogens of the triazine ring and the nitrogen connected to the cyclopropane ring. The spin density surface can be accounted for in part by resonance theory.

Cyromazine was shown to be unreactive towards the hydrated electron both through pulse radiolysis and steady state studies. This is due to the triazine ring of Cyromazine being unsuitable for addition of an electron.

Ab initio calculations indicate that the LUMO of Cyromazine is located above the ring and it is expected that if one electron gain was to transpire then addition would occur in this orbital. The structure of the triazine ring makes nucleophilic addition of the hydrated electron difficult. Positioning of the LUMO over the ring suggests this is the reason for no observable reaction between Cyromazine and the hydrated electron.

Cyromazine will degrade upon the reaction of hydroxyl radicals produced in natural and treated industrial discharge water. Reduction of Cyromazine through free radical processes, however, will not occur.

9.0 Radiation Chemistry of Aqueous Dimethrimiol Solution

9.1 DIMETHRIMIOL

Dimethrimiol (5-butyl-2-dimethylamino-6-methylpyrimidin-4-ol) (Figure 9.01) is a white solid with a melting point of 102°C. The maximum solubility of Dimethrimiol in water is 1.2 g/L [174].

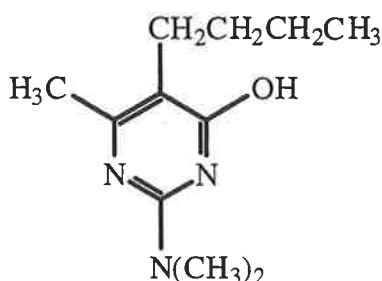


Figure 9.01. Chemical Structure of Dimethrimiol.

Dimethrimiol has been released by ICI Crop Care as a systemic fungicide. After application it is absorbed by the plant through its roots and is then translocated into the xylem where it controls Powdery Mildew [174] on cucurbits [175].

Dimethrimiol is reportedly stable in both alkaline and acidic environments [174]. Metabolism of Dimethrimiol in plants is known to involve dealkylation of the dimethylamino group [174]. It is also expected that significant amounts of Dimethrimiol will undergo direct photolysis as it absorbs at wavelengths greater than 290 nm at neutral pH. A study involving the photochemical reactions of Dimethrimiol was conducted by Cavel *et al.* [175]. This study determined the quantum yield for photo-reaction of Dimethrimiol to be 0.09 for an excitation wavelength between 290 and 330 nm. The products were determined to be the photo-dimerised products of Dimethrimiol.

9.2 REACTION OF DIMETHRIMIOL WITH THE HYDROXYL RADICAL

Figure 9.02 displays the time resolved TDA spectra obtained upon the pulse radiolysis of an aqueous Dimethrimiol (1×10^{-4} M) solution saturated with nitrous oxide (pH 6.8, phosphate buffer). It exhibits absorption bands with maxima at 330 nm and 490 nm. In the presence of *t*-butyl alcohol (0.1 M), an effective hydroxyl radical scavenger but a weak hydrogen atom scavenger, the absorption spectrum was considerably reduced. The high

$G(\cdot\text{OH})$ yield and appreciable decrease in the transient absorption suggests the spectrum in Figure 9.02 arises mainly from the reaction of the hydroxyl radical with Dimethrimiol.

The spectrum of the transient produced in the reaction of Dimethrimiol and the hydroxyl radical shows no negative absorbance in the region between 250 nm and 600 nm, despite there being a ground state absorbance in the region of 250 nm to 350 nm. The ground state corrected spectrum (Figure 9.03) exhibits an absorption maximum at 275 nm. The extinction coefficient of this maximum is $5500 \text{ M}^{-1}\text{cm}^{-1}$.

The maximum at 330 nm gives way to a new maximum at 320 nm, 50 μs after the pulse, indicating the formation of a new species. This maximum remains until all absorbance decays back to the base line. The 490 nm peak does not decay away to produce the formation of a new maxima.

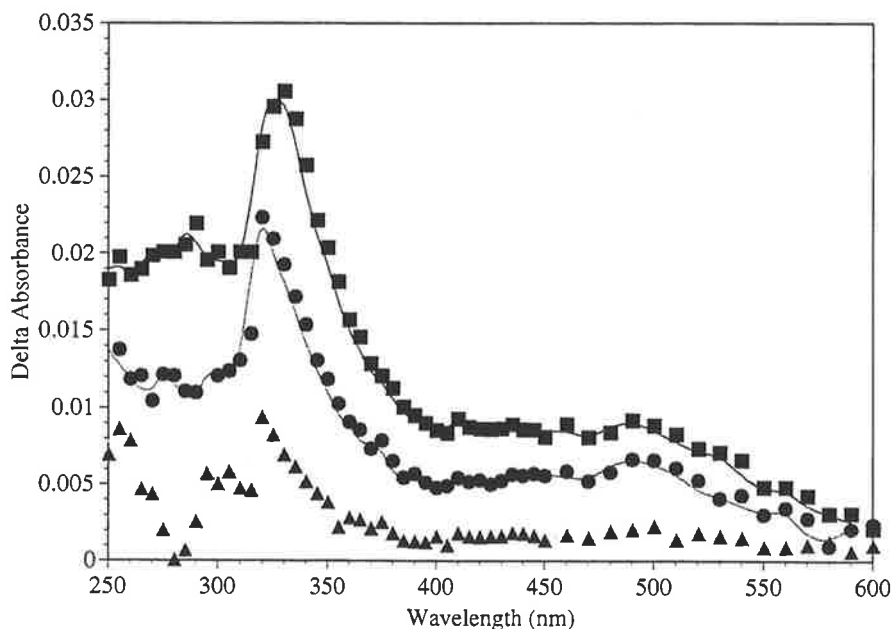


Figure 9.02. Time resolved TDA spectra obtained upon the pulse radiolysis of an aqueous Dimethrimiol ($1 \times 10^{-4} \text{ M}$) solution saturated with nitrous oxide (pH 6.8, phosphate buffer). (■ Directly after the pulse, ● 50 μs , ▲ 500 μs).

Reducing the dose (and hence the amount of transient radical) produced an increased half life of the transient species at this wavelength. The radical therefore decays by second order kinetics. When the curve was fitted to second order kinetics it produced decay rates of $2k/\epsilon l = 3.1$ and $16.5 \times 10^5 \text{ s}^{-1}$ respectively for 330 and 490 nm. Using the molar absorbance value in Figure 9.03, it was determined that $2k = 8.2 \times 10^8 \text{ M}^{-1}\text{s}^{-1}$ and $1.2 \times 10^9 \text{ M}^{-1}\text{s}^{-1}$. Our experimental error of 10% shows the decay rates are similar, but not identical. This suggests that the maxima observed in the spectra are formed from different transient species. The

second order rate constant indicates that the transients decay by radical-radical interactions to form products.

Reactions of phenol, pyrimidine, toluene and aniline derivatives have been studied previously [49, 116, 117]. All react through addition of the hydroxyl radical to the aromatic ring to form the OH-adduct. The resulting OH-adducts have an absorbance maximum in the region of 300 to 340 nm. Though the nitrogens on pyrimidine are the most electron rich, addition to these atoms has not been observed. This phenomenon has been studied previously by Anthony *et al.* [176]. *Ab initio* calculations, showed that for pyrimidine the electron density was not the only factor to control the selectivity of the addition of the hydroxyl radical to the heterocyclic ring. Energy of the resulting transient also controlled the addition process. In the case of pyridine the transient resulting from the addition of the hydroxyl radical to the nitrogen atom was found to be energetically unfavourable (and hence is not observed experimentally). Addition of the hydroxyl radical to other nitrogen containing heterocyclic atoms has been observed with the reaction of the neutral 2,2'-bipyridine with the hydroxyl radical to form the nitrogen addition cyclohexadienyl radical. Protonation of one of the available nitrogens results only in the addition of the hydroxyl radical to the carbons in the ring. Addition of the hydroxyl radical to nitrogen has been shown to produce a maximum around 370 nm, while attack on the carbon produces a maximum at 305 nm. Absence of any maxima in the 370 nm region coupled with the transient of this reaction producing a maxima at 330 nm makes it reasonable to assume that this maximum is due to the formation of a OH-adduct by addition onto one of the carbons. All four carbons on the aromatic ring possess another functional group, this means all positions will be sterically hindered and therefore no site of attack should be favoured over any other on steric reasons alone.

Ab initio calculations showed that only the carbon attached to the butyl group is electron rich. The other three carbons in the ring are all adjacent to electron withdrawing nitrogens, making them unfavourable for the addition of the electrophilic hydroxyl radical. Comparisons of the calculated energies of all the possible transients produced by the addition of the hydroxyl radical to the aromatic ring can be observed in table 9.01. This table indicates that addition of the hydroxyl group to the nitrogens produces transients which are higher in energy than the corresponding transient were the hydroxyl group is attached to a carbon atom. This is in agreement with the pulse radiolysis data which suggested that a carbon centred OH-adduct was formed. The lowest energy transient formed was at the HO-C-Me position with the second lowest being HO-C-OH position.

TRANSIENT	ENERGY (Hartrees)
HO-C-Bu	-741.2701364
HO-C-Me	-741.2766520
HO-N	-741.2001286
HO-C-NMe ₂	-741.2709887
HO-N	-741.1983637
HO-C-OH	-741.2732916
Dimethrimiol Alone	-665.877155
OH Alone	-75.388331

Table 9.01. Energy as determined by *ab initio* molecular orbital theory of the six possible isomers for the hydroxyl radical addition to Dimethrimiol. Calculations were performed at the HF/6-31G** level of theory.

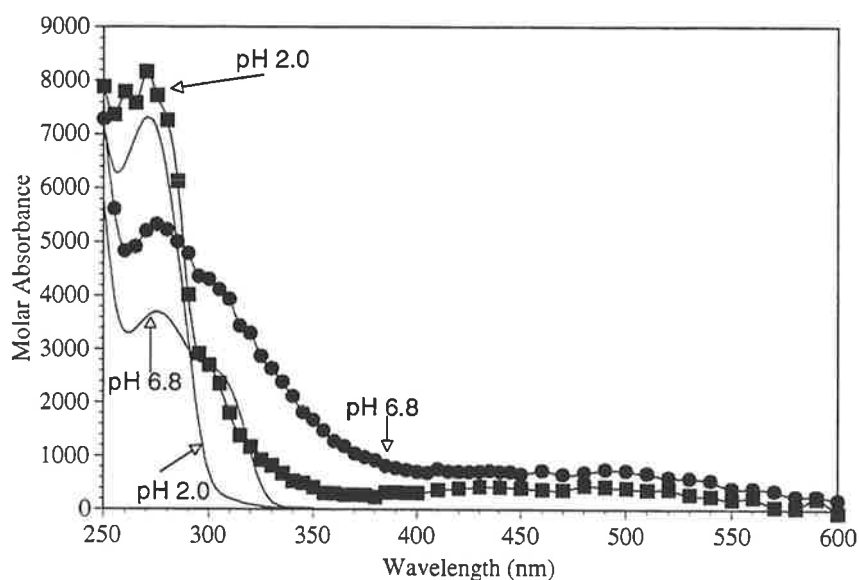


Figure 9.03. Molar Absorbance spectra of Dimethrimiol at pH 2 and 6.8 (solid lines) and the transient arising from the reaction of Dimethrimiol with hydroxyl radicals (pH 2.0 ■, pH 6.8 ●). Transient spectra recorded directly after the pulse.

Adjusting the ionic strength of the solution by the addition of NaClO₄ (1 M) at pH 6.8, produced a change in the observed rate of decay of the transient at 330 nm. This implies that the transient is charged which is not consistent with the formation of a neutral OH-adduct. This result therefore suggests the transient radical formed undergoes a reaction resulting in a charged species.

The rate constant for the reaction of the hydroxyl radical with Dimethrimiol determined by competition kinetics was $4.7 \times 10^9 \text{ M}^{-1}\text{s}^{-1}$. This rate constant shows that Dimethrimiol reacts with hydroxyl radicals at less than diffusion controlled rates.

Though this is the first reported rate constant for the reaction of the hydroxyl radical with Dimethrimiol, rate constants for the reaction of the hydroxyl radical with molecules that contain similar functional groups have been studied. These rate constants are:

Pyrimidine	$k=1.6 \times 10^8 \text{ M}^{-1}\text{s}^{-1}$ [177]
Phenol	$k=1.4 \times 10^{10} \text{ M}^{-1}\text{s}^{-1}$ [119]
Aniline	$k=1.5 \times 10^{10} \text{ M}^{-1}\text{s}^{-1}$ [89]
Toluene	$k=5.1 \times 10^9 \text{ M}^{-1}\text{s}^{-1}$ [178]

These values show that pyrimidine has the slowest recorded rate constant. The other three compounds all have high rate constants because of their electron donating substituents. The rate constant reported here for that of Dimethrimiol with the hydroxyl radical is therefore higher than that observed for pyrimidine because of the electron donating substituents on Dimethrimiol.

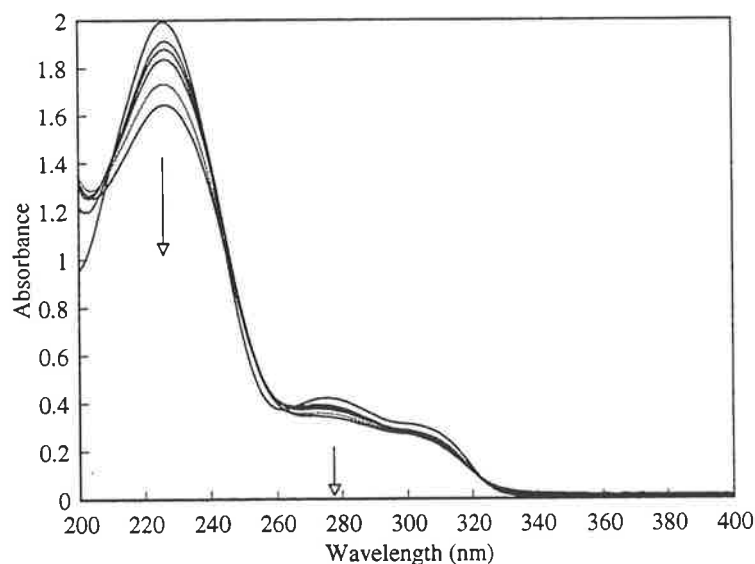


Figure 9.04. Observed change in optical absorbance of an aqueous Dimethrimiol ($60 \mu\text{M}$) solution saturated with nitrous oxide and irradiated with gamma irradiation (pH 6.8, phosphate buffer) (0 to 200 Gray). Arrow indicates the direction of absorbance change with radiation dose. Dose rate 80 Gray/hr.

Steady state irradiation of an aqueous Dimethrimiol ($60 \mu\text{M}$) solution saturated with nitrous oxide and irradiated with gamma irradiation (pH 6.8, phosphate buffer) using cobalt 60 (80 Grays per hour) produced a decrease in the absorbance due to the Dimethrimiol at 228 nm (Figure 9.04). The decrease in absorbance was less than expected by dosimetry. The

products must therefore absorb in this region, or the transient formed by the reaction of the hydroxyl radical with Dimethrimiol reacts to reform the starting compound.

HPLC analysis of a Dimethrimiol (1×10^{-4} M) solution saturated with nitrous oxide (pH 6.8, phosphate buffer) after irradiation with gamma radiation produced the formation of new products and a decrease in the concentration of Dimethrimiol (Figure 9.05) at 228 nm. No change in the product distribution was observed when the detection wavelength was changed to 280 nm. One major product was detected in this trace (Product A). Four other minor products were also formed. All the products were at a retention times less than Dimethrimiol suggesting that the products of the reaction of Dimethrimiol with the hydroxyl radical are more polar than the starting compound. This result is consistent with the formation of the OH-adduct, as the products resulting from addition of the hydroxyl radical to Dimethrimiol would be expected to be more polar than Dimethrimiol and therefore at a retention time less than Dimethrimiol.

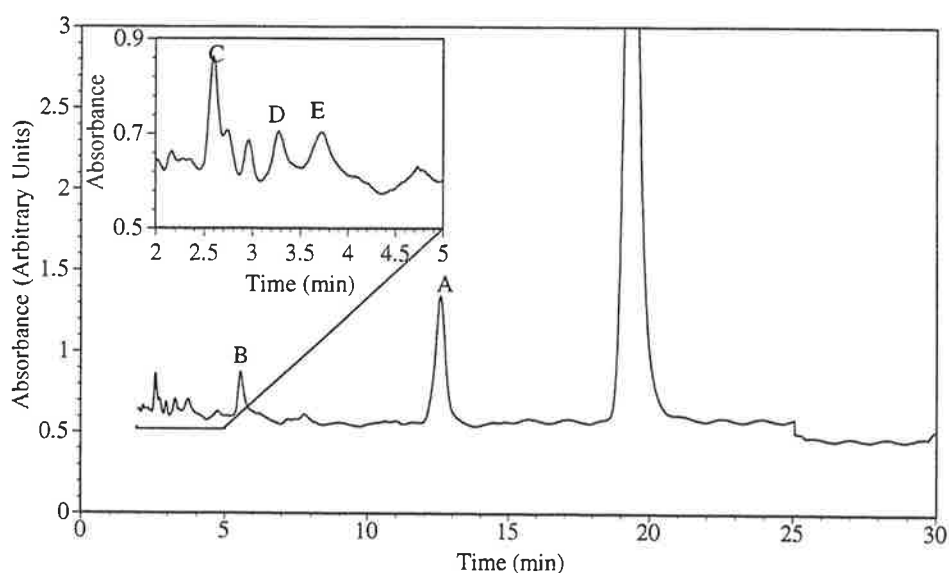


Figure 9.05. HPLC analysis following the gamma irradiation of a Dimethrimiol (1×10^{-4} M) solution saturated with nitrous oxide (pH 6.8, phosphate buffer). The trace displays the products formed from the reaction of Dimethrimiol with hydroxyl radicals (A to E). See Figure 9.07 for product identification.

The solution was re-run through the HPLC column, this time with a steep acetonitrile gradient to determine if any non-polar products were bonded to the column. No compounds were observed to elute off the column at a longer retention time. The area of the products formed at 228 nm does not equal the decrease in Dimethrimiol concentration. The G value for the loss of Dimethrimiol (after 20% of Dimethrimiol had reacted) is 5.5. This value is the same as the G value for the hydroxyl radical. If second order reactions kinetics is controlling the decay of the OH-adduct to form hydroxylated products then a G value of approximately

2.8 would be expected for the loss of Dimethrimiol. The result suggests the transient formed is reacting through a pseudo first order mechanism with Dimethrimiol also. This reaction transpires because steady state irradiation produces a concentration of the transient that is many orders of magnitudes less than the pulse radiolysis study. This effectively allows the pseudo first order reaction between Dimethrimiol and the transient to compete with the second order decay. The result of this reaction is high molecular weight compounds that do not elute off the column readily.

The rate of Dimethrimiol loss was linear against the concentration of the hydroxyl radical added to the system (calculated using Frickie Dosimetry) until approximately 30% of the Dimethrimiol had reacted. Product formation was also observed to be initially linear. After approximately 30% of Dimethrimiol had reacted, the rate of loss of the starting compound and the formation of products lost their linearity, suggesting that the initial species of the reaction also react with the hydroxyl radical.

The structures of the products observed in this trace were determined by electrospray mass spectrometry and are shown in Figure 9.07. Dimethrimiol produced a parent ion of 210 Daltons (Dim+H) and a fragmentation pattern using a MS² experiment consisted of a base peak at 140 Daltons with less intense daughter ions at 150 and 167 Daltons. The daughter ions correspond to the loss of 70 Daltons (minus NCNMe₂), 60 Daltons (minus a butyl group) and 43 Daltons (minus HOCN). The second major product (B) produced a parent ion at 226 Daltons. This mass to charge ratio corresponds to the addition of an oxygen atom to the Dimethrimiol molecule. The fragmentation pattern of this product using MS² experiments, showed the formation of only one peak at 208 Daltons (minus OH₂). Further fragmentation of the first daughter ion produced another ion at 166 Daltons (minus CNO). No further fragmentation was achieved on this ion. The fragmentation pattern reveals very little concerning the position of the new oxygen atom in the molecule. In the addition of the hydroxyl radical to benzene the hydrogen on the ring is replaced by the hydrogen attached to the oxygen, thus the end result is just the addition of 16 Daltons. Unlike benzene, Dimethrimiol has no hydrogens on the actual ring to be replaced by the hydroxyl group. This suggests that a hydrogen must be lost elsewhere (like the methyl or butyl groups) for the molecule to produce the addition of 16 Daltons.

Minor products C, D and E also produced a parent ion at 226 Daltons. The fragmentation pattern for C and D was, however, different from that of B. Fragmentation of the 226 parent ion produced a single daughter ion at 114 (or the formation of the ion

MeC(OH)NCNMe_2 or MeCNC(OH)NMe_2). The loss of 112 Daltons (minus BuCC(OH)N) indicates that this part of the molecule did not receive any additional oxygen. The last product (E) was in low concentration and so could not have its fragmentation pattern determined. The parent ion does, however, correspond to the addition of 16 Daltons or an extra oxygen.

The major product A produced a parent ion at 196 Daltons. It was determined from the isotope pattern that this compound was singularly charged. The product is 14 Daltons lighter than the starting compound Dimethrimiol and must correspond to either the loss of a nitrogen atom or the loss of a methyl group and the gain of one hydrogen. Since it is impossible for any molecule to be formed with a parent ion of 196 Daltons from just the loss of nitrogen alone the compound must correspond to Dimethrimiol with a methyl group replaced by a hydrogen. Fragmentation of the parent ion produced a base peak daughter ion of 140. This ion has been previously recorded for the fragmentation ion of Dimethrimiol. In Dimethrimiol it corresponded to the loss of the NCNMe_2 fragment. In the case of product A it corresponds to the loss of NCNHMe , thus indicating that the major product of A has had one of its methyl groups replaced from the NMe_2 group by a hydrogen.

The reaction mechanism for the formation of the products B through to E is the addition of the hydroxyl radical to Dimethrimiol to form the OH-adduct followed by the disproportionation reaction to reform the starting material and the hydroxylated product. Formation of product A is more complex. Loss of an alkyl group from a compound has been observed before in this study. In section 4.3 the major product observed between Napropamide and the hydroxyl radical at pH 2 resulted in the formation of a compound which had an ethyl group replaced by a hydrogen. In that section, the product resulting from the reaction of the hydroxyl radical with Napropamide was attributed to the formation of the OH-adduct, followed by conversion to a radical cation. This cation then reacted to form the end product. In the Napropamide example the formation of the radical cation was due to a shift in equilibrium brought about by the excess hydrogen ions present in solution, the Dimethrimiol experiment however was performed at close to neutral pH. The driving mechanism for the formation of a radical cation from the Dimethrimiol's OH-adduct must be the steric strain caused by the other functional groups present in the molecule. The addition of the hydroxyl radical to sterically hindered benzene derivatives like hexachlorobenzene and Idopentafluorobenzene results in the formation of the OH-adduct followed by the elimination of a good leaving group (such as the iodide or chloride ion) to give a phenoxyl radical [90]. Dimethrimiol does not possess any good leaving groups as substituents on the pyrimidine ring. Addition of the hydroxyl radical to the pyrimidine ring effectively makes the newly

added hydroxyl group the best leaving group in the molecule. Donation of a lone pair of electrons from a nitrogen atom into the ring can eject the hydroxyl group from the transient to form a radical cation. The resulting radical cation then decays to form the final product observed. The relative size of the peak observed in the HPLC trace compared with the other products indicates that this is the major reaction pathway. Formation of the other products which are simply the hydroxylated products, indicates that the radical cation is not an exclusive reaction pathway.

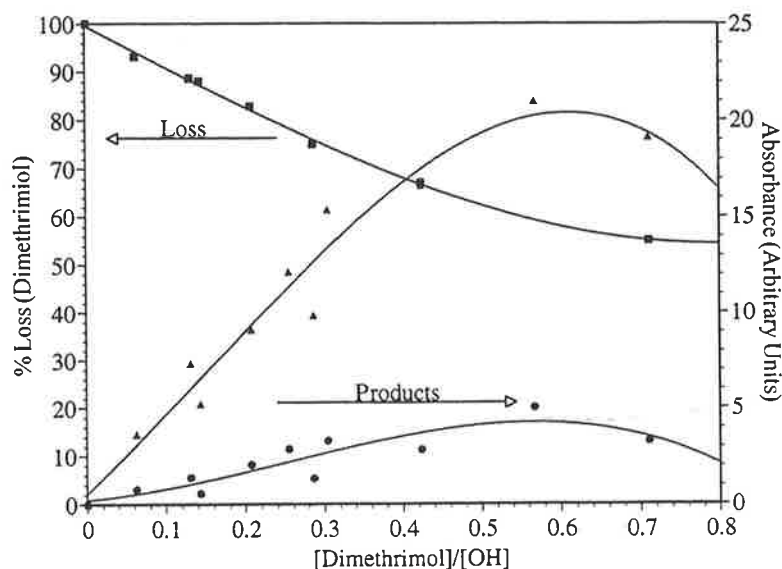


Figure 9.06. Loss of the Dimethrimiol (left axis) and the formation of the products (right axis) from the gamma irradiation of aqueous Dimethrimiol (1×10^{-4} M) solution saturated with nitrous oxide (pH 6.8, phosphate buffer) as determined by HPLC. The products are A=▲, B=●. C, D and E are not shown.

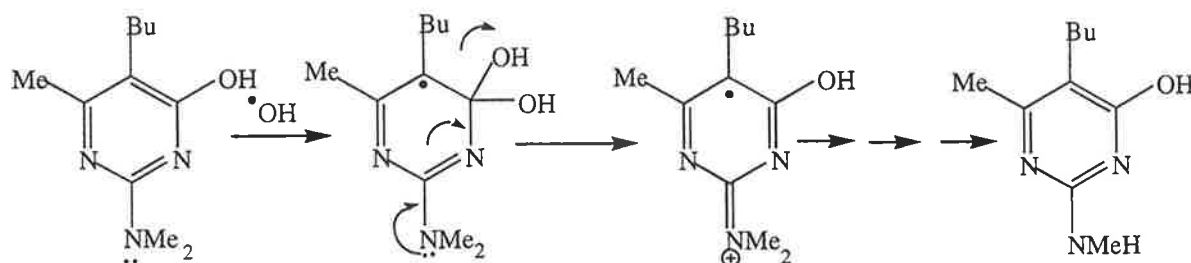


Figure 9.07. Proposed reaction pathway for the reaction of the hydroxyl radical with Dimethrimiol to form the major product observed in the HPLC trace (A).

9.3 REACTION OF DIMETHRIMIOL WITH THE HYDROXYL RADICAL IN ACIDIC SOLUTION

The TDA spectrum obtained upon by pulse radiolysis of an aqueous Dimethrimiol (1×10^{-4} M) solution saturated with nitrous oxide (pH 2, HClO_4) is different from the spectrum recorded at neutral pH (Figure 9.08). The spectrum has maxima at 305 nm and a less intense

absorbance at 490 nm. Reducing the dose produced an increase in the half life of the transient species at 305 nm. The radical therefore decays by second order kinetics. When the curve is fitted to second order kinetics it produces a decay rate of $2k/εl = 1.7 \times 10^5$ and $1.2 \times 10^6 \text{ M}^{-1}\text{s}^{-1}$ for 305 nm and 490 nm, respectively. Comparing the decay rates for the 490 nm maximum of the neutral and low pH transients shows that the rates of decay are similar, therefore the transients that produced the absorbance at 490 nm are probably due to the same species.

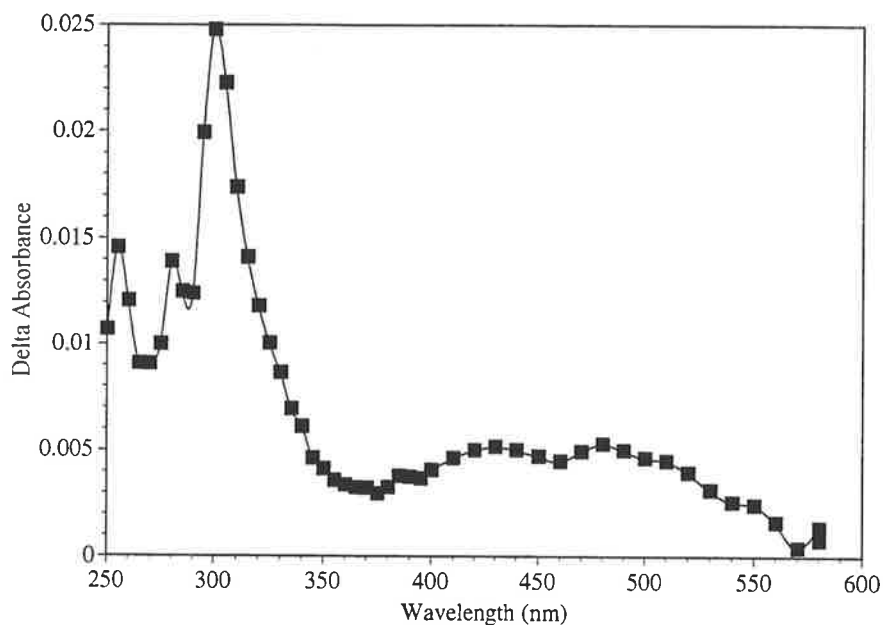


Figure 9.08. TDA spectrum obtained upon by pulse radiolysis of an aqueous Dimethrimiol ($1 \times 10^{-4} \text{ M}$) solution saturated with nitrous oxide (pH 2, HClO_4). Spectrum recorded $5 \mu\text{s}$ after the pulse.

Effect of pH on the transient species can be observed more effectively in the molar absorbance spectra (Figure 9.03) because it takes into account the lower G value of the hydroxyl radical and the difference in ground state absorbance between Dimethrimiol and the Dimethrimiol cation. Since the cationic form of Dimethrimiol has a protonated nitrogen atom, the electron density it has available to donate into the ring is less than for neutral Dimethrimiol. This results in a change in the ground state absorbance of the parent compound and for reasons described in section 3.5.3 any change in the ground state absorbance will effect the resulting TDA spectrum. It is therefore necessary to make a correction for this effect. The result of this correction is the formation of two molar absorbance spectra for the reaction of the cationic and neutral forms. Comparison of these spectra in Figure 9.03 indicates that the transients are different. Transients produced from the reaction of the cationic and neutral forms of Dimethrimiol are either different transients or the same transient but with a spectrum that varies with pH. The TDA spectrum is similar to that of a

cyclohexadienyl type radical so it is plausible that the OH-adduct is still formed at low pH, and like Dimethrimiol it has a pK_a in the region between pH 2 and 6.8.

A literature value for the pK_a of Dimethrimiol could not be found by the author and so was determined by a plot of the absorbance of Dimethrimiol (1.1×10^{-4} M) at 230 nm against the pH of the solution. The pK_a of the Dimethrimiol molecule in aqueous solution was determined to be 4.7 using this procedure.

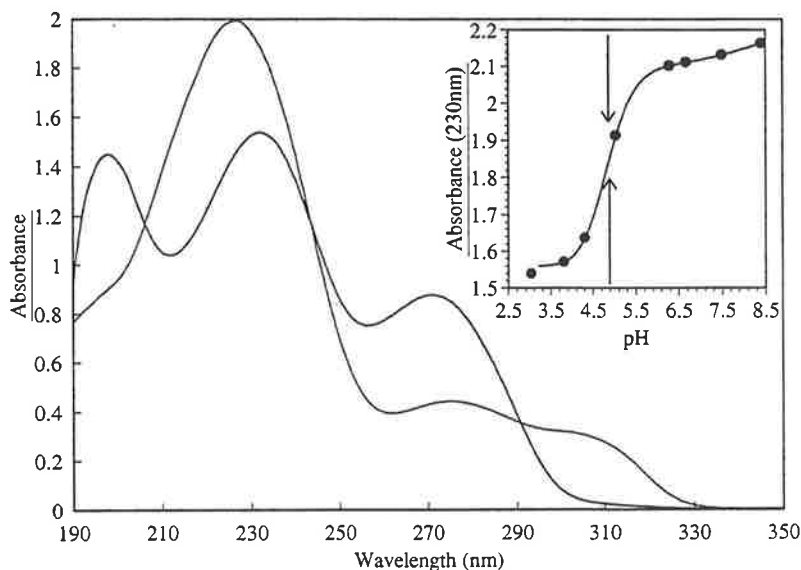


Figure 9.09. Observed change in absorbance of Dimethrimiol at pH 5.0 and 8.4. Inset. Variation of the absorbance of Dimethrimiol with solution pH. (pH adjusted using phosphate buffers, $HClO_4$ and $NaOH$). Data were measured at 230 nm. Arrows indicate point of inflection.

A plot of the change in molar absorbance of the transient with pH at 340 nm, is shown in Figure 9.10. This graph produces a pK_a for the transient of 4.8. This value is close to the value of the parent compound. It therefore could correspond to the same deprotonation-protonation point that is observed in Dimethrimiol.

The bimolecular rate constant determined for the reaction of the hydroxyl radical with Dimethrimiol using competition kinetics (pH 2, $HClO_4$) was $2.3 \times 10^9 M^{-1}s^{-1}$. This rate constant indicates that the Dimethrimiol cation reacts with the hydroxyl radical at a slightly slower rate than the neutral form. This effect has also been observed for the aniline/aniline cation system [89, 179]. The effect is due to the protonated aniline reducing the amount of electron density that is available for donation to the aromatic ring. This therefore affects the rate at which the electrophilic hydroxyl radical adds to the aromatic ring. The measured rate constants for the addition of a hydroxyl radical to aniline and the aniline cation are 1.5 and $0.48 \times 10^{10} M^{-1}s^{-1}$ respectively [89, 179].

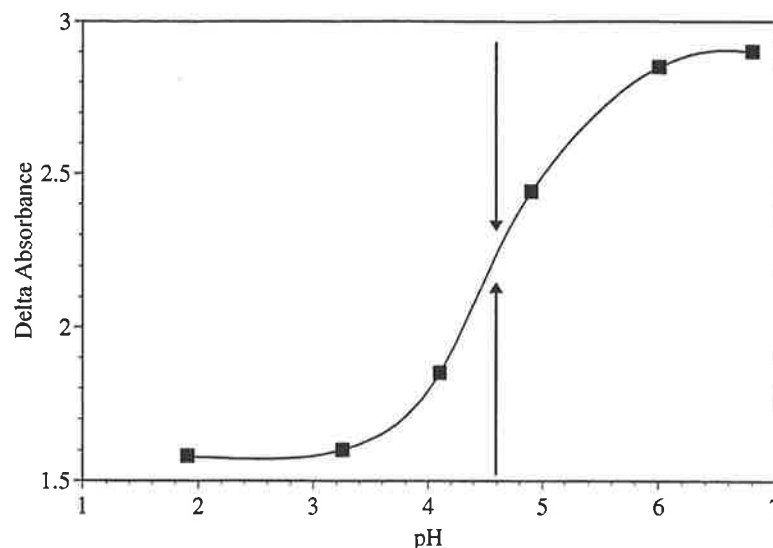


Figure 9.10. Variation of the transient absorbance with solution pH of an aqueous Dimethrimiol (1×10^{-4} M) solution saturated with nitrous oxide (pH adjusted using phosphate buffers and HClO_4). Data were measured at 340 nm. Arrows indicate the inflection point.

Comparison of the HPLC traces generated by gamma irradiation of a Dimethrimiol (1×10^{-4} M) solution saturated with nitrous oxide at pH 2.0 and 6.8 can be observed in Figure 9.11. Comparisons revealed that the major product formed when Dimethrimiol was reacted in the presence of hydroxyl radicals at neutral pH was not formed at low pH. The minor products of the neutral pH experiment were still observed in the chromatograms. Loss of the major product suggests that protonation of Dimethrimiol affects the resulting radiation chemistry. In the previous section it was postulated that the major product was created through the formation and subsequent decay of a radical cation. Formation of the radical cation relied on the lone pair of electrons from the nitrogen feeding into the aromatic ring to expel the hydroxyl group. The cationic form of Dimethrimiol has the electron pair from the nitrogen unavailable for donation because it is bonded to the hydrogen ion. The transient formed by the addition of the hydroxyl radical to Dimethrimiol therefore does not have the available electron density to displace the hydroxyl group from the ring to form the radical cation and transient observed at pH 6.8. The transient therefore has to react to form the hydroxylated products.

Comparison of the area of minor products formed in the HPLC chromatogram indicates no substantial increase in the concentration of these compounds. Loss of the intramolecular reaction to form the major compound at neutral pH should result in the creation of more minor products at low pH. This observation is in agreement with the hypothesis postulated in section 9.2, that is, the transient is proceeding through a pseudo first

order reaction with Dimethrimiol instead of second order kinetics because of the low concentration of the transient produced by steady state irradiation.

Mass spectral analysis of the compound observed in the HPLC trace showed that compounds A, B, D and E all possess a parent ion with a mass to charge ratio of 226 Daltons, compound C had a parent ion of 417.4 Daltons. The fragmentation pattern of compound A and B were similar with a major daughter ion at 114 Daltons. This fragmentation pattern has been observed in the previous section and thus no further discussion is needed. The first daughter ion for compounds D and E had an initial peak at 208 Daltons (minus OH_2), further fragmentation produced a daughter at 166 Daltons (minus CNO). Compound E was observed in the equivalent neutral pH experiment. The small absorbance at 12 minutes (Compound F) had a parent ion of 196 Daltons and thus is the same compound as that observed in the neutral experiment at the same retention time. Formation of this compound indicates that some of the radical cation still forms at this pH.

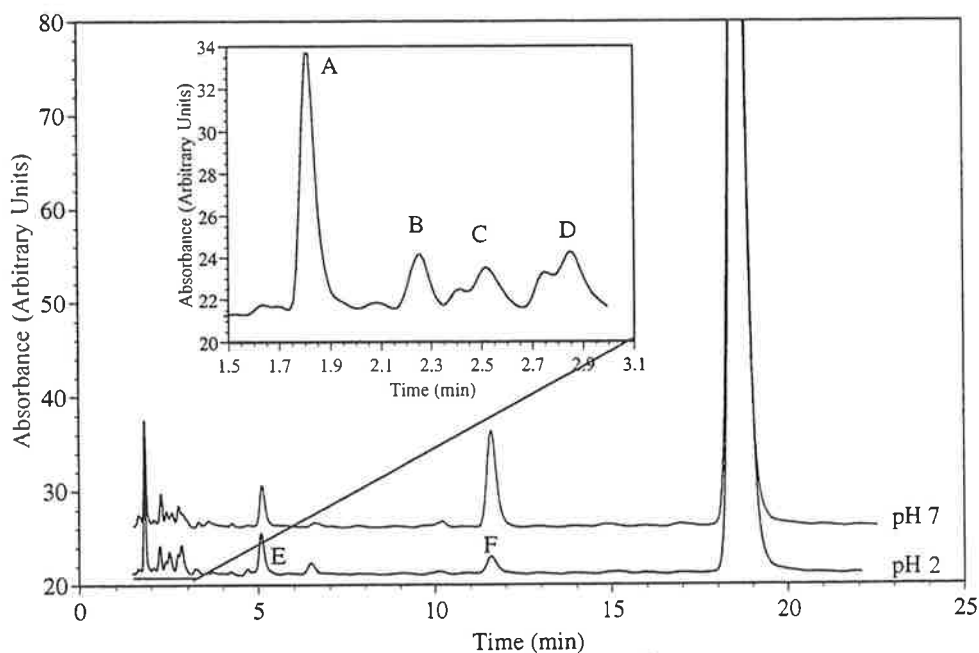


Figure 9.11. Comparison of the HPLC traces following the gamma irradiation of a Dimethrimiol (1×10^{-4} M) solution saturated with nitrous oxide at pH 2 and 7. Inset. The initial section of the pH 2 HPLC trace.

Variation of the area of the peak at 12 minutes with pH produced a curve displaying an inflection point at 4.6 pH units. This value is close to the pK_a of Dimethrimiol, further supporting the radical cation hypothesis for its formation.

9.4 REACTION OF DIMETHRIMIOL WITH THE HYDROXYL RADICAL IN THE PRESENCE OF OXYGEN

The TDA spectrum obtained upon the pulse radiolysis of an aqueous Dimethrimiol (1×10^{-4} M) solution saturated with nitrous oxide/oxygen (4:1 v/v) is shown in Figure 9.12. The TDA spectrum is different from that observed in Figure 9.03; the absorbance at 330 nm and the maximum at 490 nm are no longer present. Comparison of the decay rates of the transient species indicates a change from second order kinetics to initial first order kinetics (Figure 9.13) with the addition of oxygen at 330 nm. This indicates that the transients produced by the reaction of Dimethrimiol with hydroxyl radicals reacts through pseudo first order kinetics with oxygen. This is consistent with the addition mechanism, as carbon centred radicals are known to react rapidly with oxygen [48, 82, 84, 102, 103]. After the rapid first order reaction a slower reaction can be observed to be occurring between 20 and 400 μ s (Figure 9.13).

As stated in the previous chapters, OH-adducts react relatively slowly (and reversibly) with oxygen when compared to other carbon centred radicals. Figure 9.13 indicates the reaction of the transient produced by hydroxyl radicals and Dimethrimiol occurs quickly. This result indicates that the OH-adduct must be transformed into another carbon centred radical which then undergoes the observed fast reaction with oxygen.

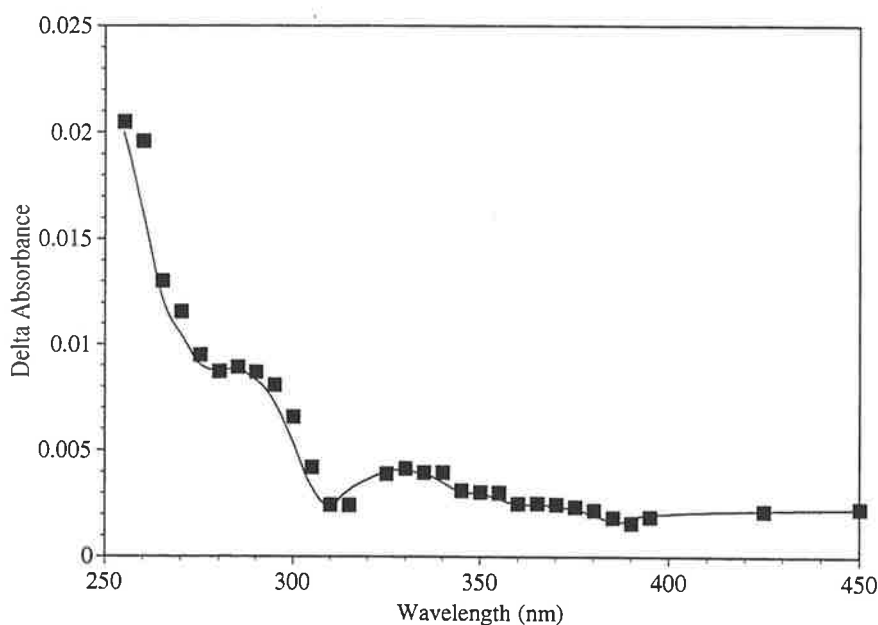


Figure 9.12. TDA spectrum obtained upon the pulse radiolysis of an aqueous Dimethrimiol (1×10^{-4} M) solution saturated with nitrous oxide/oxygen (4:1 v/v). Spectrum recorded 10 μ s after the pulse.

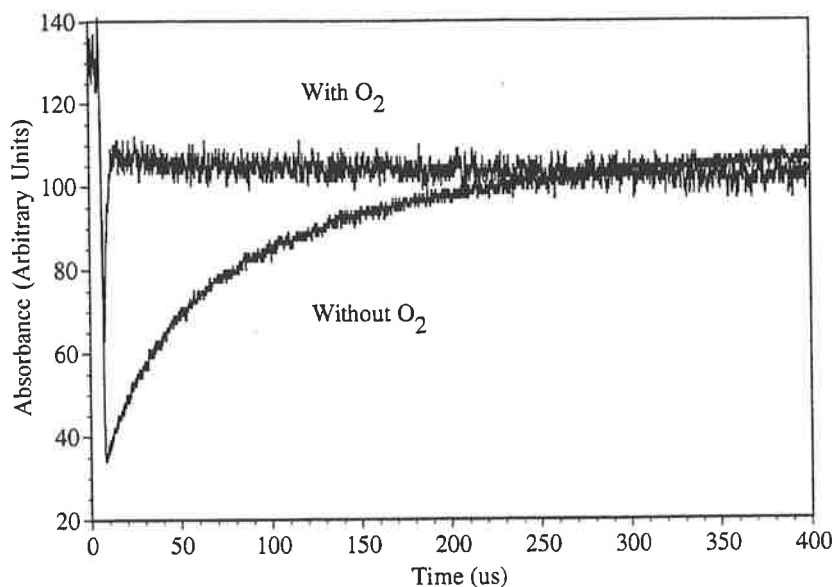


Figure 9.13. Comparison of the pulse radiolysis traces obtain from a solution of Dimethrimiol (1×10^{-4} M) with nitrous oxide and nitrous oxide/oxygen (4:1 v/v). Absorbance data were collected at 330 nm. Traces are normalised. Both radiation pulses are $2.5 \mu\text{s}$ long with a dose of 10.5 Gray per pulse.

Figure 9.14 indicates the observed change in optical absorbance of an aqueous Dimethrimiol ($72 \mu\text{M}$) solution saturated with nitrous oxide/oxygen and irradiated with gamma radiation. This is different from that observed for the de-oxygenated system. This spectrum shows a decrease in absorbance at 228 nm. This loss of absorbance at 228 nm was still less than expected and therefore the products should absorb strongly at 228 nm.

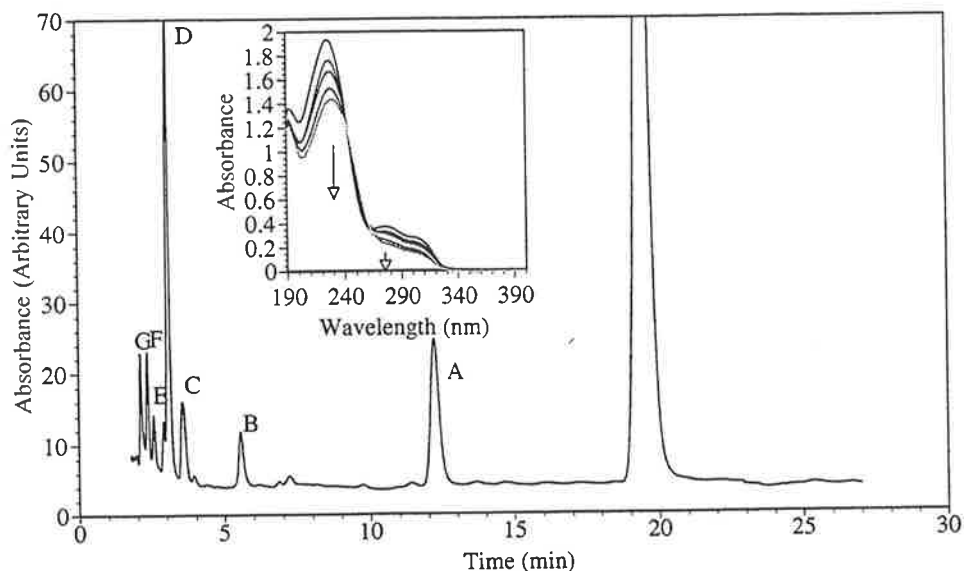


Figure 9.15. HPLC analysis following the gamma irradiation of an aqueous Dimethrimiol (1×10^{-4} M) solution saturated with nitrous oxide/oxygen. The trace displays the products formed from the reaction of Dimethrimiol with hydroxyl radicals in the presence of oxygen. Inset. Observed change in optical absorbance of an aqueous Dimethrimiol ($72 \mu\text{M}$) solution saturated with nitrous oxide/oxygen and irradiated with gamma irradiation (0 to 173 Grays). Arrows indicate the direction of absorbance change with radiation dose.

The HPLC trace recorded following the gamma irradiation of an aqueous Dimethrimiol (1×10^{-4} M) solution saturated with nitrous oxide/oxygen produced a different trace from that observed for the de-oxygenated solution (Figure 9.15). It can be observed that the products previously seen at 5.5 and 12 minutes remain in the trace while there is the formation of new peaks at the beginning of the chromatogram.

The area for the products is consistent with the change observed for the U.V. spectrum at 228 nm. This result is in agreement with the hypothesis postulated in section 4.2, that is, a pseudo first order reaction is transpiring between the transient and Dimethrimiol. Oxygen reacts with the transient to form compounds which are more polar than those postulated in section 9.2 for the pseudo first order reaction between the OH-adduct and Dimethrimiol, thus all the products are detected in this trace. The area of the major product at 12 minutes is not influenced by the presence of oxygen. The radical cation that leads to its formation does not react with oxygen.

Collection of the products allowed for the determination of the products reported in Figure 9.16. Products A and B produced a parent ion the same as those observed in the de-oxygenated experiment. MS^2 fragmentation of the parent ions of compound A and B produced the same fragmentation pattern as that observed for the de-oxygenated products. This indicates that these compounds are the same as those observed for the de-oxygenated experiment. The major product D produced a mass spectrum with a parent ion of 244 Daltons. Fragmentation of the 244 Dalton parent ion produced a daughter ion at 226 (minus OH_2) and 114 Daltons. Further fragmentation on the 226 Daltons ion produced a grand-daughter ion at 208 Daltons (or minus OH_2). The parent ion corresponds to the addition of O_2H_2 to the Dimethrimiol molecule. Product C produced a similar spectrum to that of D, except that this compound was two Daltons less than D with a parent ion of 242 Daltons and thus corresponds to the addition of only two oxygens. The fragmentation pattern showed the formation of a daughter ion at 225, 195 and 181 with the base peak recorded at 195 Daltons. Further MS^3 fragmentation on the 225 Daltons daughter ion produced a grand-daughter ion of 195 Daltons. The fragmentation pattern therefore corresponds to the loss of OH, followed by a ON or COH_2 group. The structure of this compound could not be determined from the data presented here. The formation of carbonyl groups is not possible because this would require the elimination of one of the other functional groups. The formation of an epoxide is however possible, though no mechanism could be determined for its production.

Compound E (Figure 9.16) had a parent ion of 226 Daltons indicating the presence of a species that had an oxygen atom added to the Dimethrimiol molecule. A fragmentation pattern could not be determined for this ion. The last two products F and G had parent ions of 244 and 242 Daltons, respectively. Compound F corresponds to the addition of O_2H_2 , while compound G corresponds to the gain of two oxygens. These products are similar to compounds D and C of this experiment respectively.

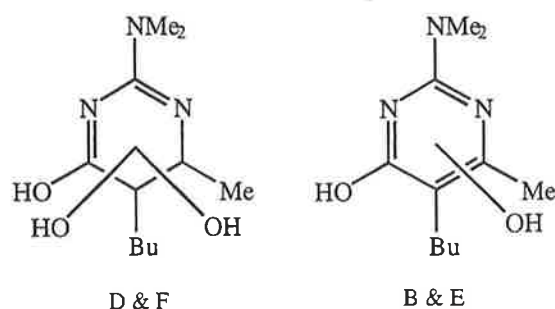


Figure 9.16. Products (B, D, E, F) of the gamma irradiation of a Dimethrimiol (1×10^{-4} M) solution saturated with nitrous oxide/oxygen as determined by the analysis of electrospray mass spectrometric fragmentation data. Location of the hydroxyl groups are not ambiguously assignable in the structures B, D, E, F.

9.5 REACTION OF DIMETHRIMIOL WITH ONE ELECTRON OXIDANTS

The dichloride radical anion formed in the pulse radiolysis of oxygen saturated sodium chloride (0.02 M) Dimethrimiol solution (1×10^{-4} M) at pH 2 ($HClO_4$) reacts as a strong one electron oxidant with a potential of 2.09 V (versus NHE). Reaction of the dichloride radical anion with Dimethrimiol was studied by following the decay of the dichloride radical anions absorbance band at 340 nm. It was observed that in the presence of Dimethrimiol (1×10^{-4} M) this band decayed faster and by first order kinetics instead of second order kinetics (Figure 9.17), indicating that a reaction between Dimethrimiol and the dichloride radical anion had resulted.

The change in the decay rate of the dichloride radical anion indicates the following reaction has taken place:



The bimolecular rate constant was determined to be $1.1 \times 10^8 \text{ M}^{-1} \text{ s}^{-1}$ from the slope of a plot of the pseudo first order rate constant against the concentration of Dimethrimiol (2 to 10×10^{-4} M). Time resolved studies produced an initial broad absorbance with λ_{max} at 340 nm due to the formation of the dichloride radical anion. Using the pseudo first order rate constant it

was determined that more than 90% of the dichloride radical anion had reacted 20 μs after the pulse. The spectrum at 20 μs displayed similar maxima to that of Dimethrimiol's reaction with hydroxyl radicals at pH 2, ie. absorbance maxima were recorded at 305 nm and 490 nm.

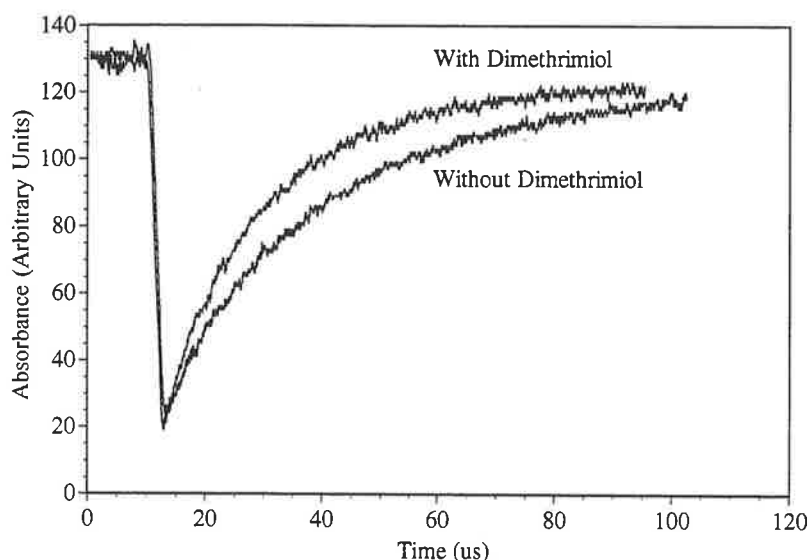


Figure 9.17. Comparison of the pulse radiolysis traces produced at 340 nm, with and without the presence of Dimethrimiol (1×10^{-4} M) in oxygen saturated solution NaCl (0.02 M) solution (pH 2, HClO_4). The traces indicate that a reaction between Dimethrimiol and the dichloride radical anion had occurred.

Since the dichloride radical anion is a specific one electron oxidant, it should react by electron transfer. The resulting product should therefore be a dication radical anion or a phenoxy radical. Since the spectra exhibits the same maxima as the hydroxyl radical transient, then the reaction with the dichloride radical anion probably forms the radical cation which then reacts with water and eliminates a hydrogen ion to form a OH-adduct.

Steady state irradiation of a Dimethrimiol (1×10^{-4} M) solution containing sodium chloride (0.02 M) and saturated with nitrous oxide at pH 2 (HClO_4) produced a HPLC trace with the formation of one major product at 5.5 minutes (Figure 9.16). This product was at the same retention time as that observed for one of the minor products of the hydroxyl radical reaction. Electrospray mass spectrometry revealed that this was the same product with the same mass fragmentation pattern as that reported in section 9.2. The size of the HPLC peak is larger than that observed for the hydroxyl experiment, suggesting that the dichloride radical anion formed a predominant transient that reacted to form the OH-adduct and the observed product. Formation of the major product from the neutral pH hydroxyl experiment was not observed because the nitrogen was protonated.

Studies of the reactions of other specific one electron oxidants such as the sulfate, dibromide, diiodide radical anions and the azide radical with Dimethrimiol were also

conducted. The TDA spectra that resulted from these reactions are displayed in Figure 9.18. Graphs presented display the spectra recorded after 90% of the reaction had proceeded (determined from the resulting pseudo first order rate constants). At low pH a reaction was observed with the sulfate and dichloride radical anions only. Spectra obtained from the sulfate radical anion and the dichloride radical anion exhibit the same maxima but with different relative heights. The same was observed at neutral pH, with the transient produced by the sulfate radical anion and the azide radical producing different sized maxima at 305 and 490 nm. This is in agreement with the two maxima formed by different transient species as suggested in section 9.2.

The dibromide radical anion was observed to react with neutral Dimethrimiol but at low pH no reaction was observed with the protonated form of Dimethrimiol. The difference in the reactivity between the neutral and protonated forms can be explained by the decrease in electron density explained in section 9.3.

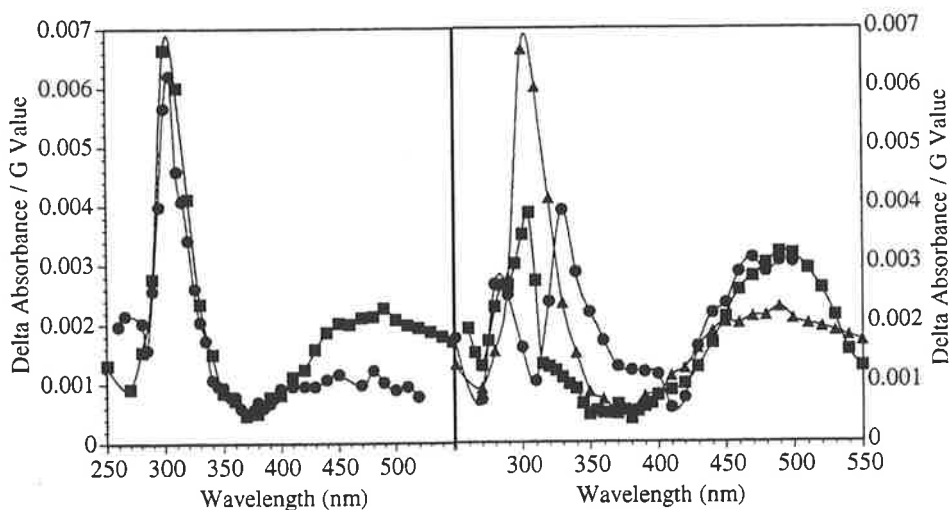


Figure 9.18. TDA spectra recorded for the reaction of Dimethrimiol (1×10^{-4} M) with Left hand side, pH 2 (HClO_4) \bullet $\text{Cl}_2^{\bullet -}$, \blacksquare $\text{SO}_4^{\bullet -}$ and right hand side, pH 6.8 (phosphate buffer) \blacktriangle $\text{N}_3^{\bullet -}$, \blacksquare $\text{SO}_4^{\bullet -}$, \bullet $\text{Br}_2^{\bullet -}$. Experimental conditions are as follows; $\text{Br}_2^{\bullet -}$; 0.02 M NaBr, oxygen saturated. $\text{SO}_4^{\bullet -}$; 0.02 M $\text{S}_2\text{O}_8^{2-}$, 0.1 M *t*-butyl alcohol, nitrogen saturated. $\text{Cl}_2^{\bullet -}$; pH 2, 0.02 M NaCl, oxygen saturated. $\text{N}_3^{\bullet -}$; 0.02 M NaN_3 , nitrous oxide saturated.

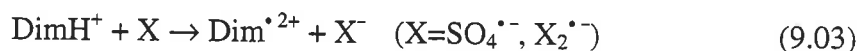
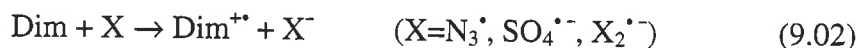
The rate constant determined from the slope of a plot of the pseudo first order decay rate (formation for $\text{N}_3^{\bullet -}$) against the concentration of Dimethrimiol (50 to 100 μM) for the reactions with the one electron oxidants can be observed in Table 9.02.

Radical	pH	Rate of reaction with Dimethrimiol ($M^{-1}s^{-1}$)	Wavelength of Determination (nm)
$Cl_2^{\bullet-}$	2.0	1.1×10^8	340
$Br_2^{\bullet-}$	2.0	No reaction	360
$Br_2^{\bullet-}$	6.8	2.5×10^8	360
$SO_4^{\bullet-}$	6.8	1.7×10^9	460
N_3^{\bullet}	6.8	3.9×10^8	360

Table 9.02. Bimolecular rate constants determined for the reaction of Ioxynil with one electron oxidants. Rates were determined from the slope of a plot of the pseudo first order rate constant against the concentration of Ioxynil (50 to 100 μM).

At pH 6.8 Dimethrimiol has the phenol group protonated and is therefore neutral. The reaction of the one electron oxidants does not react with Dimethrimiol to form phenoxy radicals, but in preference removes the electron from the ring. The rate constant for the reaction of Dimethrimiol with the azide radical is an order of magnitude higher than that reported for phenol [160]. The large difference in rate constants suggests that the azide radical does not react with Dimethrimiol to form a phenoxy radical as it does with phenol.

The diiodide radical anion formed on the pulse radiolysis of a nitrous oxide saturated solution containing iodide anion (0.02 M) was not observed to decay faster in the presence of a small concentration of Dimethrimiol (1×10^{-4} M). The diiodide radical anion is a one electron oxidant with redox potential of 1.0 V (versus NHE) [43] while the azide radical has a redox potential of 1.4 V (versus NHE) [43]. Since Dimethrimiol reacts with the azide radical and not the diiodide radical anion the redox potential of the $Dim^{\bullet+}/Dim$ couple in reaction 9.02 must be between 1.4 and 1.0 Volts (versus NHE).



The redox potential for the protonated form of Dimethrimiol must be between that of the dichloride and dibromide radical anions. Thus the redox potential for reaction 9.03 is between 2.09 and 1.7 Volts using the same reasoning.

The spin surface generated from the *ab initio* calculations on Dimethrimiol with a electron missing from its full electron set is shown in Figure 9.19. The spin can be

rationalised using resonance stabilisation structures, with the absence of four spin sites in the ring suggesting the electron was not lost from the ring but from the nitrogen in the NMe₂ group. The spin surface can be observed to be located within the HOMO of the starting compound. The spin surface does not indicate the spin pattern that would be expected for a phenol, which is in agreement with the pulse radiolysis results.

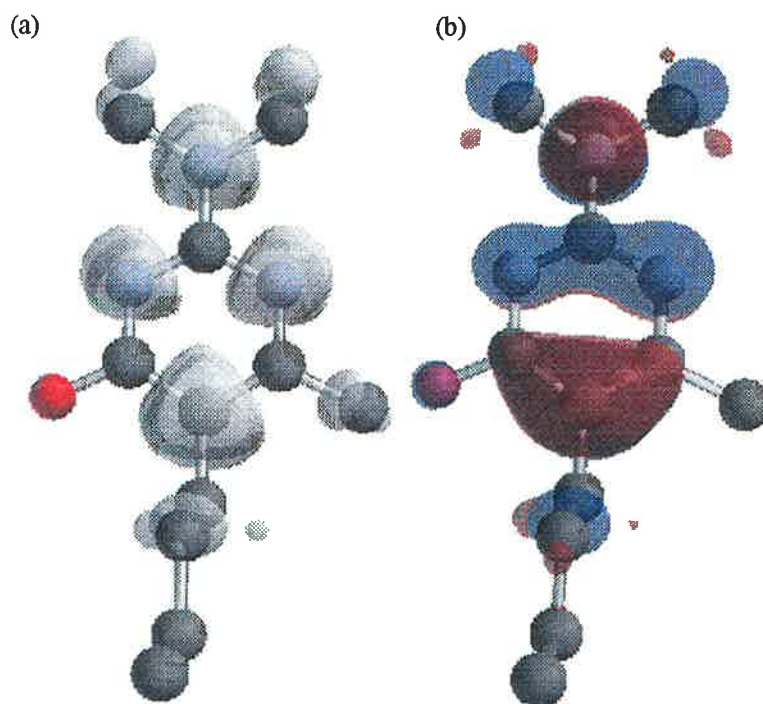


Figure 9.19. Plots of the electron spin density surface (a), HOMO (b), of Dimethrimiol as determined *ab initio* molecular orbital theory. Calculations were performed at the HF/6-31G** level of theory. Plot (a) was determined with a molecular charge of +1 and a multiplicity of 2. Plot (b) was determined for the neutral molecule possessing a corresponding multiplicity of +1.

HPLC traces obtained from the reactions of Dimethrimiol with the dichloride, dibromide radical anions and the azide radicals generated by steady state gamma irradiation are displayed in Figure 9.20.

The precursor ($S_2O_8^-$) for the formation of the sulfate radical anion is known to thermally oxidise a variety of compounds. Over the time scale of the reaction it was shown that small amounts of the starting compound did undergo thermal oxidation. The HPLC trace of a non-irradiated sample of Dimethrimiol (1×10^{-4} M) containing persulfate anion (0.02 M), *t*-butyl alcohol (0.1 M) at pH 6.8 (phosphate buffer) indicated that the total loss through this reaction was approximately 5%. The HPLC trace of an irradiated sample displayed almost the complete loss of Dimethrimiol, despite the presence of only enough radical to react with 50% of the starting compound, suggesting that the transient produced by the reaction of Dimethrimiol undergoes a chain reaction (data not shown). The sulfate radical anion's HPLC

trace differed with pH with both pH 2 and 6.8 having slightly different product distributions. Mass spectral analysis on the products was not attempted.

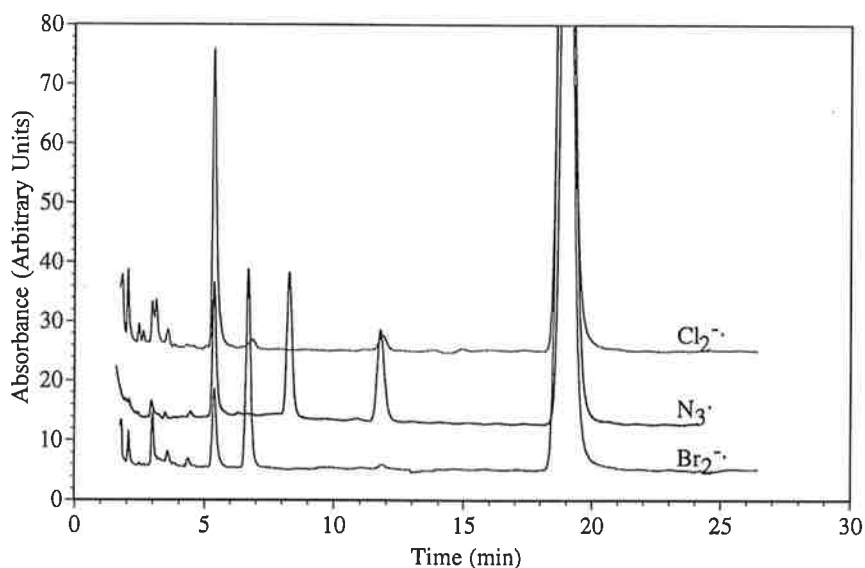


Figure 9.20. Comparison of the HPLC traces produced by the reaction of dichloride, dibromide radical anions, and the azide radical with Dimethrimiol (1×10^{-4} M). Experimental conditions are as follows; $\text{Br}_2^{\cdot-}$; pH 6.8, 0.02 M NaBr, oxygen saturated. $\text{N}_3^{\cdot-}$; pH 6.8, 0.02 M N_3^- , nitrous oxide saturated. $\text{Cl}_2^{\cdot-}$; pH 2, 0.02 M NaCl, oxygen saturated. The traces indicate the differences in products produced from the reaction of radical anions with Ioxynil. See text for discussion on the identification of specific products

The dichloride, dibromide radical anions and azide radical all produced different product distributions. This is in agreement with the pulse radiolysis results which produced no consistency in the spectra between the one electron oxidants. The azide radical displayed the formation of three major products at 5.5, 8 and 12 minutes. The mass spectral data on these compounds indicated that the parent ions were 226, 291 and 196 Daltons, respectively. The compounds with parent ions of 226 and 196 Daltons have been previously observed in section 9.2 and since they have the same retention times and fragmentation pattern, it is probable that these are the same compounds. The compound with a parent ion of 291 Daltons did not produce a MS^2 fragmentation pattern and thus no information could be determined concerning its structure.

The major product in the dichloride radical anion experiment was the compound with retention time of 5.5 minutes. The mass spectral analysis found the parent ion of this peak to be 226 Daltons which is identical to that of the other compounds with the same retention time. The dibromide radical anion also showed the formation of the compound with a retention time of 5.5 minutes and a parent ion of 226 Daltons. The major product however was at 7 minutes, this produced a parent ion of 417 Daltons. This ion corresponds to the coupling product of Dimethrimiol formed from a phenoxy type radical. The formation of this product must

therefore result from one electron loss from the hydroxyl group, followed by coupling with a similar transient. MS² fragmentation of the 417 Daltons parent ion produced a daughter ion of 304 Daltons (minus 113 Daltons), further fragmentation produced a 247 Daltons grand-daughter ion.

Results observed from the reaction of the one electron oxidants with Dimethrimiol using steady state and pulse radiolysis techniques indicated that this type of reaction is highly dependent on the type of oxidant used. The results of both the pulse radiolysis and steady state experiments suggest that the oxidation power of the radical may be a determining factor in what transient is created and thus what final product will form.

9.6 REACTION OF DIMETHRIMIOL WITH THE HYDRATED ELECTRON

Absorbance of the hydrated electron at 640 nm was observed to increase in the presence of small amounts of Dimethrimiol (1×10^{-4} M) at pH 7.0 (phosphate buffer and NaOH). This indicates a reaction between the hydrated electron and Dimethrimiol is occurring. The TDA spectrum obtained upon the pulse radiolysis of an aqueous Dimethrimiol (1×10^{-4} M) solution containing *t*-butyl alcohol (0.1 M) saturated with nitrogen (pH 7.0, phosphate buffer and NaOH) is shown in Figure 9.21. The spectrum recorded directly after the pulse exhibits a maximum at 330 nm. Time resolved studies out to 1000 μ s showed the formation of no new peaks, thus suggesting the compound reacts to form the product directly. The small absorbance out to 500 nm is a combination of the absorbance of the hydrated electron and the transient species. This absorbance is observed to ^{have} disappeared 10 μ s after the pulse.

The bimolecular rate constant for the reaction of the hydrated electron with Dimethrimiol was determined from the slope of a plot of the decay rate of the hydrated electron at 640 nm against the concentration of Dimethrimiol (25 to 50 μ M). The rate constant determined was $5.0 \times 10^9 \text{ M}^{-1} \text{ s}^{-1}$. Though this is the first reported rate constant for the reaction of the hydrated electron with Dimethrimiol, rate constants for reactions of compounds with similar functional groups have been reported previously and are shown below:

Pyrimidine	$k = 2.0 \times 10^{10} \text{ M}^{-1} \text{ s}^{-1}$ [180]
Phenol	$k = 2.0 \times 10^7 \text{ M}^{-1} \text{ s}^{-1}$ [109]

Toluene	$k=1.1 \times 10^7 \text{ M}^{-1} \text{ s}^{-1}$ [109]
Aniline	$k=3.0 \times 10^7 \text{ M}^{-1} \text{ s}^{-1}$ [89]
2-Aminopyrimidine	$k=7.6 \times 10^7 \text{ M}^{-1} \text{ s}^{-1}$ [181]

The above rate constants show that the pyrimidine molecule had the fastest rate constant, with toluene, phenol and aniline all reacting approximately two to three orders of magnitude slower. Because the functional groups present on these molecules are all electron donating, the end effect is the deceleration of the nucleophilic reaction between the hydrated electron and the substrate. Functional groups attached to the pyrimidine ring of Dimethrimiol are all electron donating, thus it would be expected that the rate constant for the reaction of the nucleophilic hydrated electron with Dimethrimiol would be less than that of pyrimidine. This effect has also been observed for the 2-aminopyrimidine molecule which is similar to Dimethrimiol [181].

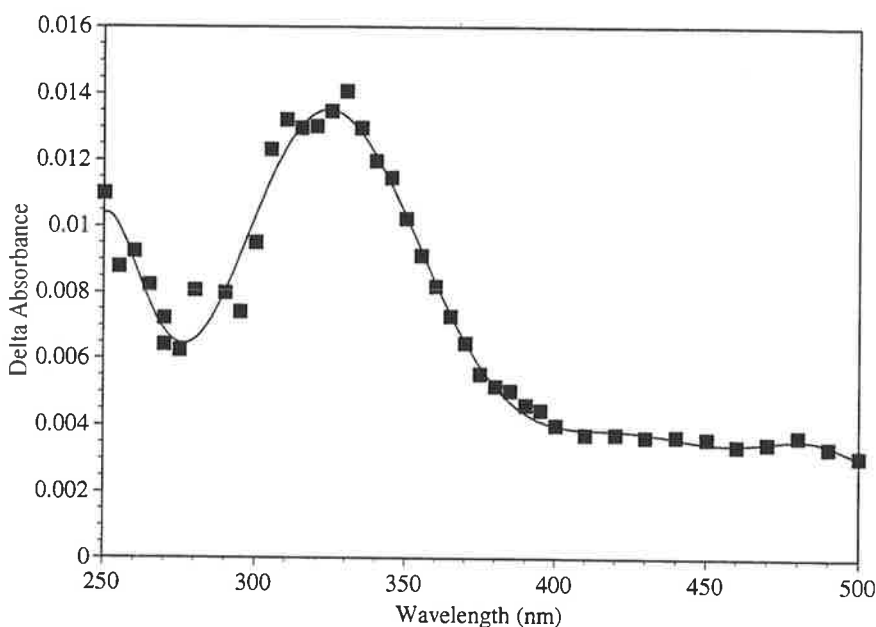


Figure 9.21. TDA spectrum obtained upon the pulse radiolysis of an aqueous Dimethrimiol ($1 \times 10^{-4} \text{ M}$) solution containing *t*-butyl alcohol (0.1 M) saturated with nitrogen (pH 7.0, phosphate buffer and NaOH). The spectrum was recorded 5 μs after the pulse.

Reaction of the hydrated electron with Dimethrimiol should proceed initially by the addition of an electron, resulting in the formation of a Dimethrimiol radical anion. (ie. Dim^-). The site of addition of the electron should be the ring due to the electron deficient nature of the carbons next to the nitrogens (as observed in the *ab initio* calculations). The resulting radical anion then must react to form the two major products which were observed in the steady state reaction (Figure 9.23).

Ab initio calculations on Dimethrimiol using natural population analysis [74] indicated that the atom with the least amount of electron density is located on the carbon between the three electron withdrawing nitrogens. The spin surface displayed in Figure 9.22 (a) indicates that the spin of the molecule is located over three of the atoms in the ring and between a nitrogen and a carbon. The mechanism postulated in Figure 9.24 suggests that the hydrated electron adds to the ring and a negative charge results on the nitrogen, with the radical on the carbons adjacent to the nitrogens. This is in agreement with the spin density pattern observed, in particular the largest spin density is observed on the carbons directly adjacent to the nitrogens. The only discrepancy with Figure 9.24 (a) is that radical character would also be expected to be located on the carbon between the two nitrogens and this was not observed. It might be expected that this resonance is unstable and therefore does not form. The LUMO is located over all of the ring, indicating the most likely place for nucleophilic addition to be on the aromatic ring.

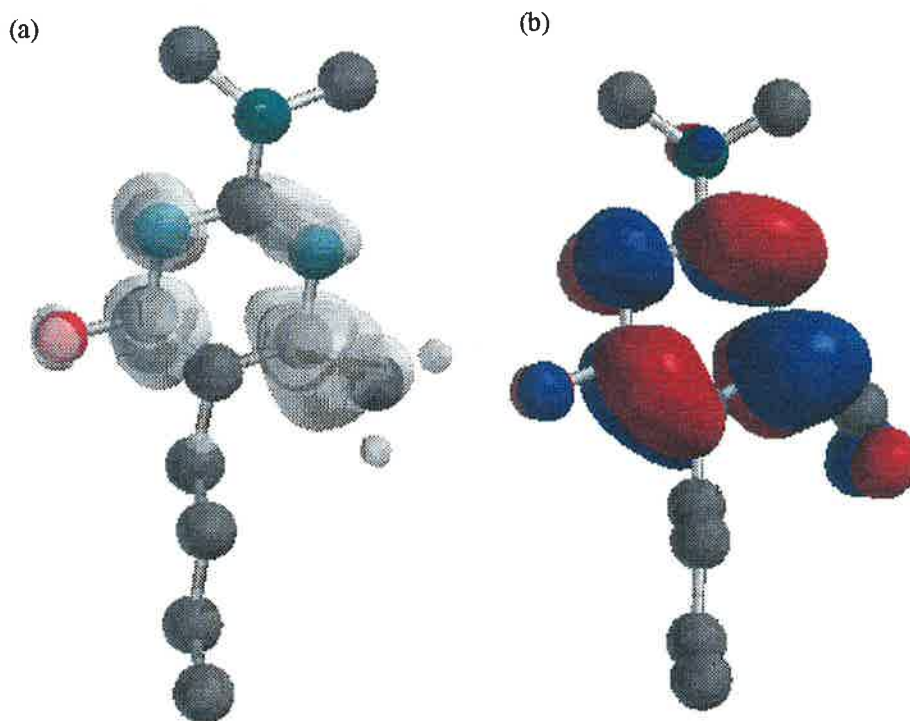


Figure 9.22. Plots of the electron spin density surface (a), and the LUMO (b), of Dimethrimiol as determined by *ab initio* molecular orbital theory. Calculations were performed at the HF/6-31G** level of theory. Plot (a) was determined with a molecular charge of -1 and a multiplicity of 2. Plot (b) was determined for the neutral molecule possessing a corresponding multiplicity of 1.

Gamma irradiation of a Dimethrimiol (1×10^{-4} M) solution containing, *t*-butyl alcohol (0.1 M) saturated with nitrogen (pH 7.0, phosphate buffer and NaOH) produced the HPLC trace reported in Figure 9.23. The effect on optical absorbance was to decrease the absorbance maximum at 228 nm and the formation of a new maximum at 232 nm. The HPLC

trace showed the formation of two major compounds of roughly equal intensity at 5 and 7 minutes with a minor absorbance at 16.5 minutes. Mass spectrometry on the compounds produced identical parent ion of 212 Daltons. This mass to charge ratio is that of Dimethrimiol plus two hydrogen atoms, suggesting that the end product of the reaction of Dimethrimiol with the hydrated electron is the saturation of a double bond. MS² fragmentation of both parent ions resulted in formation of three daughter ions at 142, 124 and 88 Daltons. While the last two ions were not detected in the fragmentation of Dimethrimiol, the 142 Daltons ion had a similar ion observed before. The fragmentation of Dimethrimiol lead to the formation of a daughter ion at 140 Daltons, the 142 Daltons peak observed in this experiment is the 140 Daltons ion plus two hydrogens. In the fragmentation of Dimethrimiol the 140 ion was assigned to the fragment NCNMe_2 , thus the 142 Daltons ion is assigned $(\text{NCNMe}_2)\text{H}_2$. The reaction of the hydrated electron must proceed through the addition of the hydrated electron to the carbon between the three nitrogen atoms (the most electron deficient shown by the Gaussian calculations) or the carbon attached to the methyl groups (as predicted by the LUMO), resulting in the formation of a radical on that carbon and a negative charge on one of the nitrogens. The negatively charged nitrogen then acquires a hydrogen ion from water while the carbon centred radical abstracts a hydrogen from the *t*-butyl alcohol to form a stable product with a mass to charge ratio of 212 Daltons.

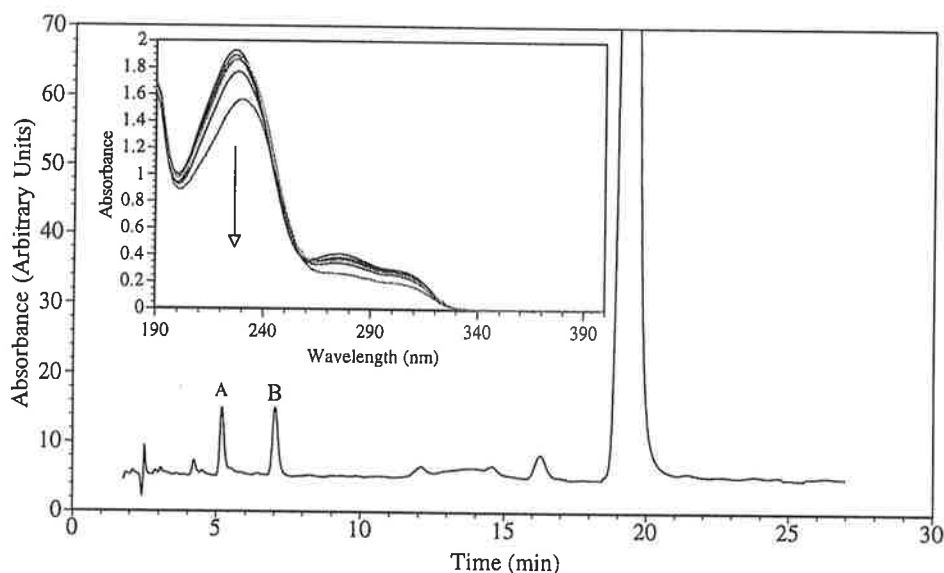


Figure 9.23. HPLC analysis following the gamma irradiation of a Dimethrimiol (1×10^{-4} M) solution containing, *t*-butyl alcohol (0.1 M) saturated with nitrogen (pH 7.0, phosphate buffer and NaOH). The trace displays the formation of the products of the reaction of the hydrated electron with Dimethrimiol. See Figure 9.24 for proposed mechanism of reaction. Inset. Change in optical absorption of the same solution (0 to 460 Gray). Arrow indicates the direction of absorbance change.

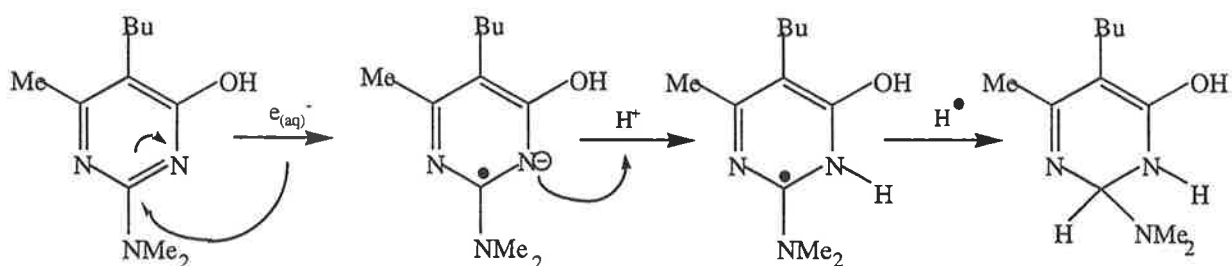


Figure 9.24. Reaction mechanism for the reaction of the hydrated electron with Dimethrimiol.

9.7 REACTION OF DIMETHRIMIOL WITH THE HYDROGEN ATOM

Figure 9.25 displays the TDA spectrum obtained upon the pulse radiolysis of an aqueous Dimethrimiol (1×10^{-4} M) solution containing *t*-butyl alcohol (0.1 M) saturated with nitrogen (pH 2, HClO_4). It exhibits absorbance maxima at 300 and 500 nm. The spectrum is different from that of the hydrated electron and thus cannot be assigned to the same radical observed in that experiment.

Formation kinetics were carried out on the maximum from the slope of a plot of the pseudo first order rate constant against the concentration of Dimethrimiol at 300 nm. This produced a bimolecular rate constant for the reaction of $5.3 \times 10^8 \text{ M}^{-1} \text{ s}^{-1}$. This rate constant for reaction with hydrogen atoms is an order of magnitude slower than the corresponding reaction of Dimethrimiol with hydroxyl radicals at the same pH.

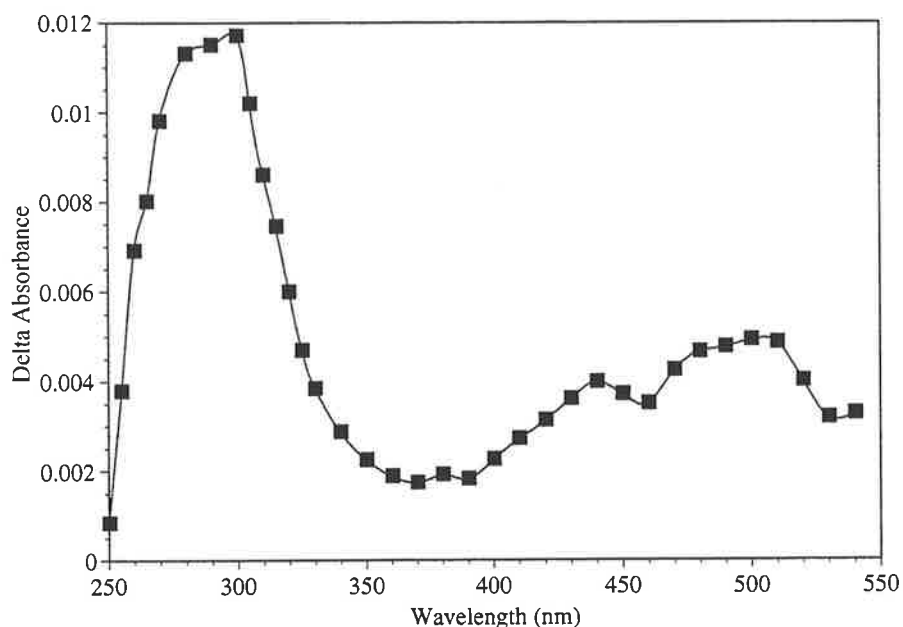


Figure 9.25. TDA spectrum obtained upon the pulse radiolysis of an aqueous Dimethrimiol (1×10^{-4} M) solution containing *t*-butyl alcohol (0.1 M) saturated with nitrogen (pH 2, HClO_4). Spectrum recorded 10 μs after the pulse.

Steady state irradiation of a Dimethrimiol (1×10^{-4} M) solution containing, *t*-butyl alcohol (0.1 M) saturated with nitrogen (pH 2.0, HClO_4) produced a decrease in the absorbance of the area in the HPLC trace which corresponded to Dimethrimiol. Two new products were observed to form after the irradiation period. It can be seen from the graph that the retention times of these products are identical to those of the products of the hydrated electron experiment. Mass spectrometric analysis confirms that the products of this reaction are they same as those reported for the reaction with the hydrated electron.

Pulse radiolysis experiments indicated that the transients produced by the reaction of the hydrated electron and hydrogen atom are different while the steady state results indicated that the products of the reactions are the same. The explanation for this apparent contradiction can be explained by the different mechanisms by which the radicals react. The reaction scheme for the hydrated electron can be observed in Figure 9.24, and results in the formation of a carbon centred radical adjacent the nitrogen atoms. The reaction of the hydrogen atom results in the addition to this same carbon resulting in the formation of a nitrogen centred radical. This nitrogen centred radical must then abstract a hydrogen from the *t*-butyl alcohol to form a stable product which is identical to that observed for the hydrated electron. This mechanism is recorded in Figure 9.27.

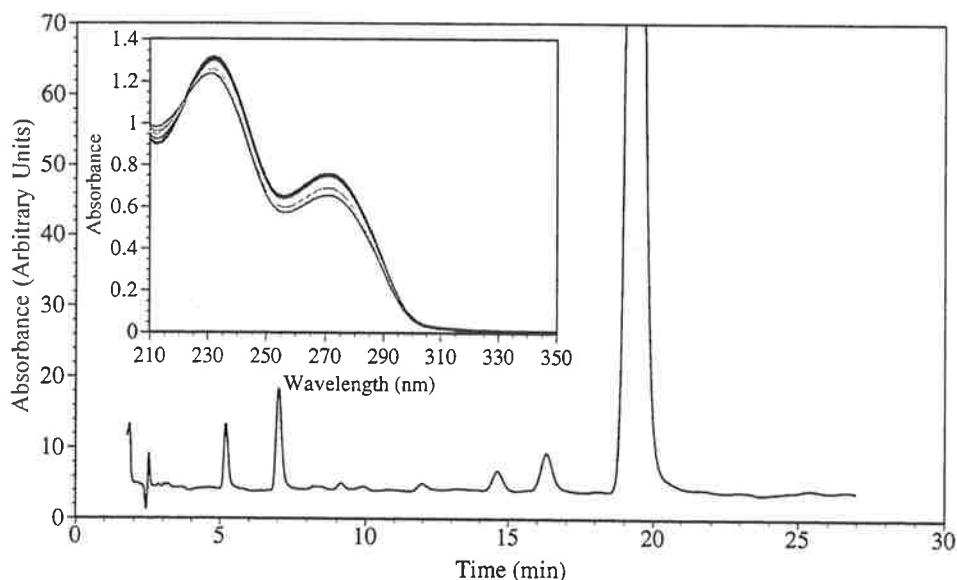


Figure 9.26. HPLC analysis following the gamma irradiation of a Dimethrimiol (1×10^{-4} M) solution containing, *t*-butyl alcohol (0.1 M) saturated with nitrogen (pH 2.0, HClO_4). The trace indicates the products formed from the reaction of Dimethrimiol with hydrogen atoms. Inset. Change in optical absorption of the same solution (0 to 240 Gray). Arrows indicate the direction of absorbance change with radiation dose.

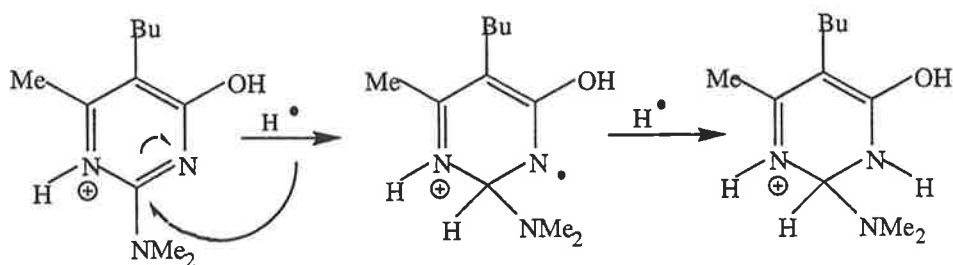


Figure 9.27. Reaction mechanism for the reaction of hydrogen atoms with Dimethrimiol.

9.8 REACTION OF DIMETHRIMIOL WITH REDUCING RADICALS.

Pulse radiolysis of a nitrous oxide saturated solution of sodium formate (0.02 M) and Dimethrimiol (1×10^{-4} M) (pH 6.8, phosphate buffer) produced a maximum below 250 nm with no other absorbance maximum observed. Absorbance detected was due to the formation of the carbon dioxide radical anion. Time resolved studies out to 1000 μ s found no new absorption in the range of 250 to 600 nm. This suggests that the carbon dioxide radical does not react with Dimethrimiol. The redox potential of the carbon dioxide radical has been determined to be -2.0 V (versus NHE) [43, 111], suggesting that the redox potential for the Dim/Dim $^{\bullet-}$ is more negative than -2.0 V. Therefore, Dim $^{\bullet-}$ is a strong reducing agent with a reduction potential between -2.0 and -2.9 V (versus NHE).

Gamma irradiation of the same solution showed no loss of Dimethrimiol when sufficient radical was placed into the matrix to react with 50% of the available starting compound. This result confirms those obtained in the pulse radiolysis experiments.

9.9 OVERVIEW OF THE RADIATION CHEMISTRY OF DIMETHRIMIOL

This study has allowed for the first time the elucidation of the radiation chemistry of aqueous Dimethrimiol. The new chemistry for Dimethrimiol is summarised in Figure 9.28.

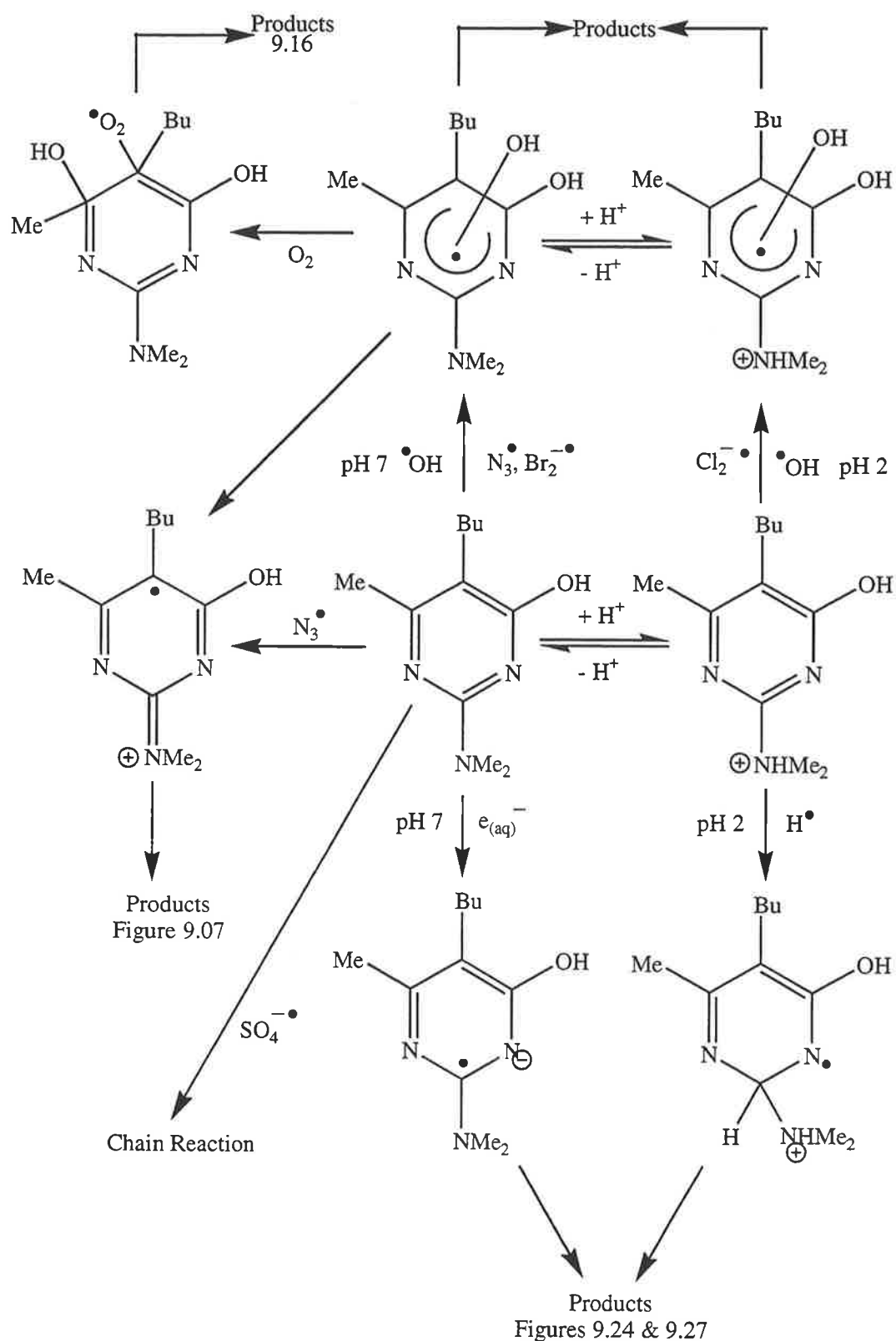


Figure 9.28. Overview of the radiation chemistry characterised in this study.

The TDA spectrum obtained from the reaction of Dimethrimiol with hydroxyl radicals suggests the formation of the OH-adduct and another type of radical as intermediates. The rate constant obtained for the reaction of Dimethrimiol with the hydroxyl radical ranges between that determined for the reaction of the hydroxyl radical with the electron deficient

pyrimidine and the electron donating functional groups. The reaction of these compounds with the hydroxyl radical is known to proceed through a OH-adduct intermediate, supporting our hypothesis.

Decay of the OH-adduct shows dependence on the ionic strength of the solution, indicating the transient is charged. This disagrees with what would be expected from the OH-adduct which should be neutral, suggesting the transient must undergo a transformation to become charged. *Ab initio* calculations indicated that the transients with the lowest energies are the OH-adducts with the hydroxyl group located on the ortho position of the nitrogens in the ring. Positioning of the hydroxyl radical in this location allows for the nitrogen to eliminate the hydroxyl group forming a radical cation. The intermediate decayed by second order kinetics, indicating that degradation products are formed by radical-radical interactions. HPLC characterisation of the compounds formed by the reaction of Dimethrimiol with the hydroxyl radical showed that these compounds have retention times less than that of Dimethrimiol. This suggests that the degradation products are more polar than Dimethrimiol. Mass spectrometric studies have determined that the major product is equivalent to the replacement of a methyl group with a hydrogen atom. Comparison of the mass spectrometric fragmentation data collected for Dimethrimiol with the major degradation product indicates that the methyl group replaced came from the NMe₂. Minor products were determined to be the hydroxylated form of Dimethrimiol. This is in agreement with what we have determined through pulse radiolysis. The rate of Dimethrimiol loss and the formation of products from the reaction of Dimethrimiol with the hydroxyl radical is initially linear under steady state irradiation. As the amount of hydroxyl radicals is increased past 30% of Dimethrimiol's concentration, the loss of Dimethrimiol and the formation of products follows a higher order kinetic mechanism. This result suggests that the products of the initial reaction also react with the hydroxyl radical to form (uncharacterised) compounds.

The TDA spectrum obtained upon the reaction of the hydroxyl radical with Dimethrimiol at pH 2 differs from that obtained for the same reaction at neutral pH. As such, transients formed from the two reactions could not be assigned as the same species. The rate constant for the reaction of Dimethrimiol with the hydroxyl radical at pH 2 is approximately half that determined from the addition of the hydroxyl radical to Dimethrimiol at neutral pH. Qualitatively, this can be explained as follows: in the neutral form of Dimethrimiol the electron density is expected to be more accessible than in the case of the cation form. Since the hydroxyl radical behaves as an electrophile, its reaction with the electron poor cation is slower. The effect of the variation of pH on the transient absorbance at 340 nm for the

reaction of the hydroxyl radical with Dimethrimiol showed a pH dependence typical of an acid-base equilibria. The pK_a of the transient was shown to be similar to that of Dimethrimiol. Gamma irradiation coupled with HPLC of Dimethrimiol at pH 2, has shown that the major compound observed for the reaction of Dimethrimiol with the hydroxyl radical at neutral pH is no longer formed. Formation of the minor products did not increase in concentration indicating that under steady state conditions the transient formed reacts with Dimethrimiol through a pseudo first order mechanism to form products.

The transient produced from the reaction of Dimethrimiol with the hydroxyl radical has been shown to be reactive with oxygen. Gamma irradiation coupled with HPLC shows the formation of different compounds to those obtained for the de-oxygenated experiment. Mass spectral fragmentation data indicate that the products result from the addition of molecular oxygen to the transient. The newly produced transient then reacts to form the observed products. A previous study found that addition of a single oxygen atom to the starting compound was the most prevalent product for the reaction of benzene with the hydroxyl radical in the presence of oxygen [82]. Dimethrimiol reacts to produce compounds with the addition of two oxygen atoms.. Gamma irradiation coupled with HPLC shows the formation of new compounds as well as the major product obtained for the de-oxygenated experiment. Mass spectral fragmentation data indicates the products result from the addition of molecular oxygen to the transient. The newly produced transient then reacts to form the observed products.

The TDA spectrum obtained from the reaction of Dimethrimiol with one electron oxidants is a similar shape to that obtained for the transient produced by the reaction of Dimethrimiol with the hydroxyl radical, however, the intensities of the maxima vary with the oxidant used. Rate constants for the bimolecular reaction of Dimethrimiol with one electron oxidising agents decrease with the redox potential of the oxidising agents. Dimethrimiol is not observed to react with the diiodide radical anion at neutral pH and the dibromide radical anion at low pH. The Dimethrimiol radical cation is a powerful one electron oxidant with a redox potential between 1.4 and 1.0 V, while the dication has a redox potential between 1.7 and 1.4 V. Gamma irradiation coupled with HPLC for the one electron oxidising agents shows that the product distribution varies with the oxidising agent. This is in agreement with what we have determined through the pulse radiolysis studies. In all cases the hydroxylated product was formed.

Ab initio calculations indicate that the HOMO of Dimethrimiol is located over the aromatic ring and the nitrogen. It is suspected that the electron loss occurs from this orbital, which is in agreement with the experimental results. The spin density surface is also located on the aromatic ring and the nitrogen.

The TDA spectrum obtained for the reaction of Dimethrimiol with the hydrated electron suggests the formation of a H-adduct as the transient. The rate constant obtained for the reaction of Dimethrimiol with the hydrated electron lies between that determined for the reaction of the hydrated electron with the electron deficient pyrimidine and the electron donating substituent. It is known that the pyrimidine reacts with the hydrated electron by addition to the aromatic ring, followed by the addition of a hydrogen ion to form a H-adduct, further supporting our hypothesis.

Gamma irradiation coupled with HPLC found the formation of two major products. Mass spectral analysis of the products identified the compounds as mono-saturated forms of Dimethrimiol. The radical anion of Dimethrimiol has been shown to be a strong reducing agent with a redox potential of between -2.0 and -2.9 V.

Ab initio calculations indicate that the LUMO of Dimethrimiol is located over the aromatic ring. It is suspected that the electron gain would initially occur in this orbital, which is in agreement with the experimental results. The spin density surface is also located on the ring.

The TDA spectrum for the reaction of Dimethrimiol with hydrogen atoms differs to the TDA spectrum obtained for Dimethrimiol's reaction with the hydrated electron. This suggests that the transient formed from the reaction of Dimethrimiol with the hydrogen atom is a different radical to the H-adduct produced by the hydrated electron. Gamma irradiation coupled with HPLC shows the formation of two major products. Using mass spectral fragmentation data the products were determined to be the same compound as for the hydrated electron. Thus addition of the hydrogen atom to Dimethrimiol forms a different H-adduct than the hydrated electron.

Dimethrimiol will degrade upon reaction with a number of free radicals produced in natural and treated industrial discharge water.

10.0 Radiation Chemistry of Aqueous Hexazinone Solution

10.1 HEXAZINONE

Hexazinone (3-cyclohexyl-6-dimethylamino-1-methyl-1,3,5-triazine-2,4-dione) (Figure 10.01) is a white solid with a melting point of 115-117°C. The maximum solubility of Hexazinone in water is 33g/l [182], which when compared to other triazine pesticides is high. The pK_a as reported by Thompson *et al.* is 1.09 [183]. Thus Hexazinone at pH 2 and above Hexazinone is primarily neutral.

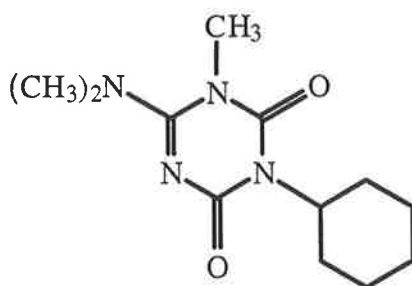


Figure 10.01. Chemical structure of Hexazinone.

Hexazinone (Du Pont) is a triazine herbicide used for the control of annual and biennial weeds as well as unwanted hardwood trees in pine plantations [184]. Typical application rate for the forestry industry is 4kg/ha [2, 185]. Hexazinone is a systemic herbicide that works on inhibiting photosynthesis in the target plant. Rainfall or irrigation is needed to activate the pesticide .

Hexazinone has been reported to be stable in aqueous environments between the pH values of 4 and pH 9. Microbial degradation is thought to be responsible for the breakdown of Hexazinone. Degradation proceeds through the breaking of the triazine ring resulting in the liberation of carbon dioxide. Photodegradation has also been postulated for the loss of Hexazinone [186]. The amount of loss is thought to be dependent on the light intensity and depth of incorporation in the soil. Hexazinone's degradation rate in soil is also dependent on soil type and climate [184]. Hexazinone does not evaporate to any appreciable extent from the soil, it does however leach and has been found in the ground water in several states of the USA. Products of the primary soil and metabolites degradation have been determined previously [187, 188]. These consist of the addition of a hydroxyl group to the cyclohexane, as well as the loss of the -NMe₂ group.

10.2 REACTION OF HEXAZINONE WITH THE HYDROXYL RADICAL

Figure 10.02 displays the time resolved TDA spectra obtained upon the pulse radiolysis of an aqueous Hexazinone (1×10^{-4} M) solution saturated with nitrous oxide (pH 6.8, phosphate buffer). It exhibits an absorption band with a maximum at 280 nm with a less intense maximum at 440 nm. The spectrum does not resemble that of a OH-adduct, therefore the transient does not result from the addition of the hydroxyl radical to Hexazinone.

In the presence of *t*-butyl alcohol (0.1 M), an effective hydroxyl radical scavenger but a weak hydrogen atom scavenger, the absorption spectrum was considerably reduced. The high G (OH \cdot) yield and appreciable decrease in the transient absorption suggests that the transient absorption spectrum in Figure 10.03 is due mainly to the reaction of hydroxyl radicals with Hexazinone.

No negative absorbance was detected in the TDA spectrum recorded between the hydroxyl radical and Hexazinone. This is because Hexazinone does not have a large ground state absorbance in the region of 250 to 450 nm. The TDA spectrum can be corrected for the small ground state absorbance by using formula 3.14 and the assumption that the yield of hydroxyl radicals is equal to the yield of the transient radical. Since the yield of transient radicals is not known for certain the result should not be over interpreted. The molar absorbance spectrum of the transient does not vary considerably in shape from that of the delta absorbance spectrum.

Reducing the dose (and hence the amount of transient radical) produced an increase in the half-life of the transient species at 280 nm and 440 nm. The radical therefore decays by second order kinetics. When the decay curves were fitted to second order kinetics they produced decay rates of $2k/\epsilon l = 9.3 \times 10^5 \text{ s}^{-1}$ and $3.3 \times 10^6 \text{ s}^{-1}$ for 280 nm and 440 nm, respectively. Assuming that all the hydroxyl radicals react with Hexazinone and the G value of the hydroxyl radical is equal to the G value of the transient (i.e. 5.5) the molar absorbance of the maxima is 970 and 340 $\text{M}^{-1}\text{cm}^{-1}$ for 280 and 440 nm, respectively. Using the molar absorbance values, it was determined that $2k = 9.0 \times 10^8 \text{ M}^{-1}\text{s}^{-1}$ and $1.1 \times 10^9 \text{ M}^{-1}\text{s}^{-1}$ for 280 nm and 440 nm, respectively. The two-absorbance maxima decay at similar rates indicating that they may be due to the same transient species.

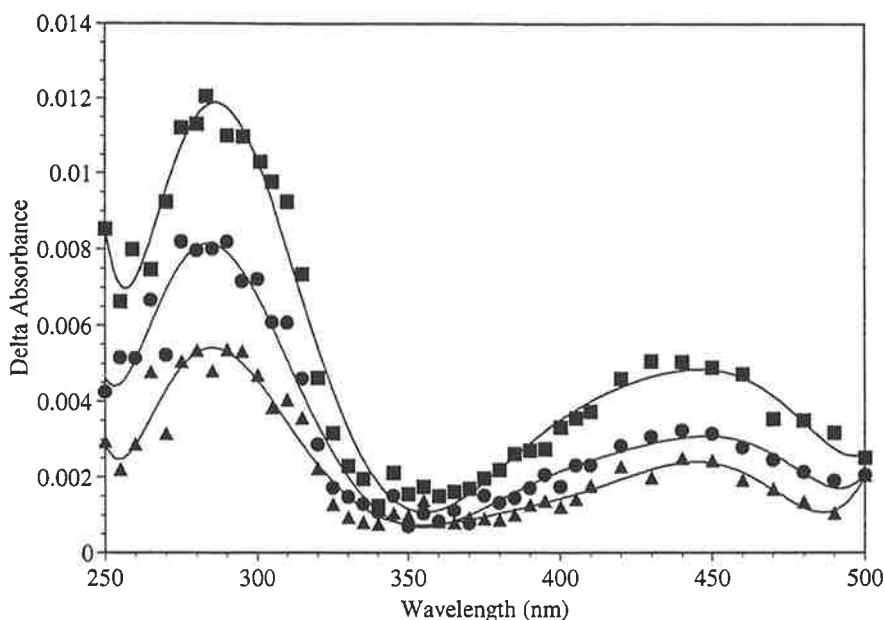


Figure 10.02. Time resolved TDA spectra obtained upon the pulse radiolysis of an aqueous Hexazinone (1×10^{-4} M) solution saturated with nitrous oxide (pH 6.8, phosphate buffer). (■ Directly after the pulse, ● 50 μ s after the pulse, ▲ 100 μ s after the pulse).

As stated in chapters 6 and 8 the reactions of the 1,3,5-triazines with hydroxyl radicals has not been extensively studied in the past. 1,3,5-Triazine reactions with the hydroxyl radical that have been studied [143, 144] and were found to be dependent on the other functional groups. Hexazinone is an unsaturated aromatic system, however the carbons on the 1,3,5-triazine ring are electron deficient and can be thought of as positively charged, as described by Quirke [145] and observed in Figure 6.04. This makes the 1,3,5-triazine ring unlikely to be involved in an electrophilic addition reaction and therefore suggests that the hydroxyl radical does not add to the 1,3,5-triazine ring of the Hexazinone. Absorbance maxima at 280 nm is also not consistent with the formation of a OH-adduct as these types of radicals tend to have a maximum in the region of 300 nm to 340 nm. The reaction of hydroxyl radicals with cyclohexane has been studied previously by Sauer and Mani [189]. They reported that the hydroxyl radical reacts with cyclohexane in aqueous solution through hydrogen abstraction. The absorbance maximum for the resulting cyclohexanyl radical was recorded at 240 nm. The Hexazinone transient displays a 40 nm red shift when compared to the transient of cyclohexane. Since addition of the hydroxyl radical is unlikely, the reaction must therefore proceed through hydrogen abstraction. There are three potential sites for hydrogen abstraction from the molecule, at the NMe_2 , Me or cyclohexane groups. If the hydroxyl radical is reacting with the cyclohexane ring then the shift in absorbance maximum observed when compared to the cyclohexanyl radical results because of the rest of the molecule.

Decay of the absorbance maximum at 280 nm was not affected by the addition of NaClO₄ (1 M), suggesting the transient species is neutral. This result is in agreement with the abstraction of a hydrogen from the Hexazinone molecule, as the resulting transient is neutral.

Competition kinetics produced a bimolecular rate constant determined for the reaction of the hydroxyl radical with Hexazinone of $5.1 \times 10^9 \text{ M}^{-1}\text{s}^{-1}$. This rate constant indicates that Hexazinone reacts with the hydroxyl radical at slightly less than diffusion controlled rates.

This is not the first reported rate constant for the reaction of the hydroxyl radical with Hexazinone. Mabury and Crosby [190] reported a rate constant for the reaction of the hydroxyl radical with Hexazinone as $6.2 \times 10^8 \text{ M}^{-1}\text{s}^{-1}$. The rate constant Mabury and Crosby reported is nearly 10 times slower than the rate constant determined here. The reason for this discrepancy may be due to the method of determination for the rate constants. Mabury and Crosby used steady state irradiation competition kinetics to determine their rate constant. Experiments performed to compare their reported value with pulse radiolysis indicated that this method produced results that are up to five times slower. However, this does not explain the ten fold difference between the two values.

The reactions of hydroxyl radicals with 1,3,5-triazines were summarised in section 6.2. Rate constants for the reactions of hydroxyl radicals with cyclopentane and cyclohexane are:

cyclopentane $k=4.9 \times 10^9 \text{ M}^{-1}\text{s}^{-1}$ [169]

cyclohexane $k=6.1 \times 10^9 \text{ M}^{-1}\text{s}^{-1}$ [189]

It can be observed that the rate constant for the reaction of the hydroxyl radical with cyclohexane is slightly higher than that of the Hexazinone. This is consistent with hydrogen abstraction from the cyclohexane group of Hexazinone.

Attempts to react Hexazinone with the oxide radical (which is a known hydrogen atom abstractor) proved unsuccessful due to the instability of Hexazinone molecule at the pH required to form the desired radical. Ultraviolet absorbance indicated the degradation of Hexazinone as there was a change in the absorbance maximum over the time scale of the experiment at pH 13.2 (NaOH).

Steady state irradiation of a Hexazinone (80 μM) solution saturated with nitrous oxide using cobalt 60 (Dose 80 Grays per hour) produced only a small decrease in the absorbance due to the Hexazinone at 246 nm (Figure 10.03). Over the radiation dose the shape of the obtained spectra does not vary greatly. The decrease in absorbance was less than expected by

the dosimeter, implying that either the products absorb in this region, the transients formed by the reaction with the hydroxyl radical react to reform the starting material, or a combination of both. The absence of any change in the general shape of the spectra suggests that the hydroxyl radical is not affecting the chromophore in the molecule. This result is consistent with the formation of the cyclohexanyl type radical and formation of products from that radical, as the cyclohexane ring is not part of the conjugated chromophore.

A HPLC trace recorded following the gamma irradiation of an aqueous Hexazinone (1×10^{-4} M) solution saturated with nitrous oxide (pH 6.8, phosphate buffer) displays the formation of new products and a decrease in the concentration of Hexazinone at 246 nm (Figure 10.04). No change in the product distribution was observed at either 220 or 254 nm. In all, seven products of varying intensities were collected from the trace (A to G). All products were of a retention time less than Hexazinone suggesting they were more polar than the starting compound.

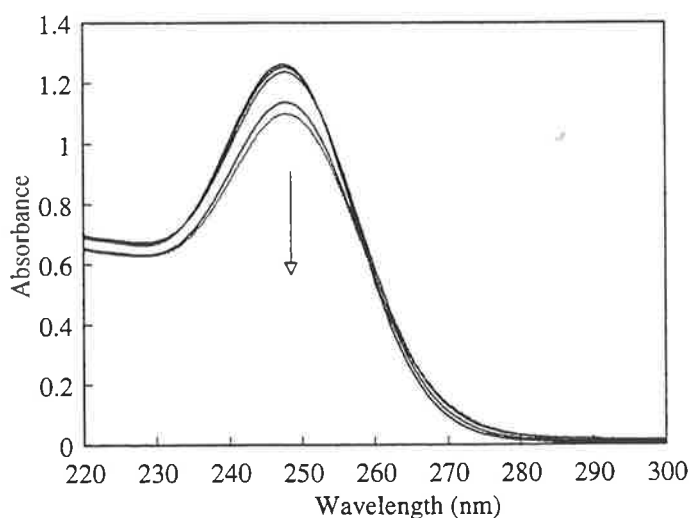


Figure 10.03. Observed change in optical absorbance of a Hexazinone ($80 \mu\text{M}$) solution saturated with nitrous oxide and irradiated with gamma irradiation (0 to 200 Gray). Arrow indicates the direction of absorbance change with radiation dose.

The rate of Hexazinone loss was linear against the concentration of hydroxyl radicals added to the system (calculated using Frickie Dosimetry), until approximately 20% of the Hexazinone had reacted. Appearance of the products was also followed by HPLC and found to be initially linear. After this both the loss of Hexazinone and the gain of products curved suggesting that the products of the initial reaction also react with hydroxyl radicals. The major products A and B were observed to react with the hydroxyl radical because at higher doses it can be observed that their formation slows down and actually decreases. The solution

was re-run with a steep acetonitrile gradient. No products were observed at longer retention times. The area of the products formed at 246 nm does not equal the decrease in Hexazinone concentration. The G value for the loss of Hexazinone (after 20% of Hexazinone had reacted) is 4.7. If second order reaction kinetics is controlling the decay of the cyclohexanyl type radical then a G value of approximately 2.8 would be expected for the loss of Hexazinone. The result suggests that the transient formed is reacting through a pseudo first order mechanism with Hexazinone. This reaction transpires because steady state irradiation produces a concentration of the transient that is many orders of magnitudes less than the pulse radiolysis study. This effectively allows the slower pseudo first order reaction to compete with the second order decay. The result of this reaction is high molecular weight compounds that do not elute off the column readily.

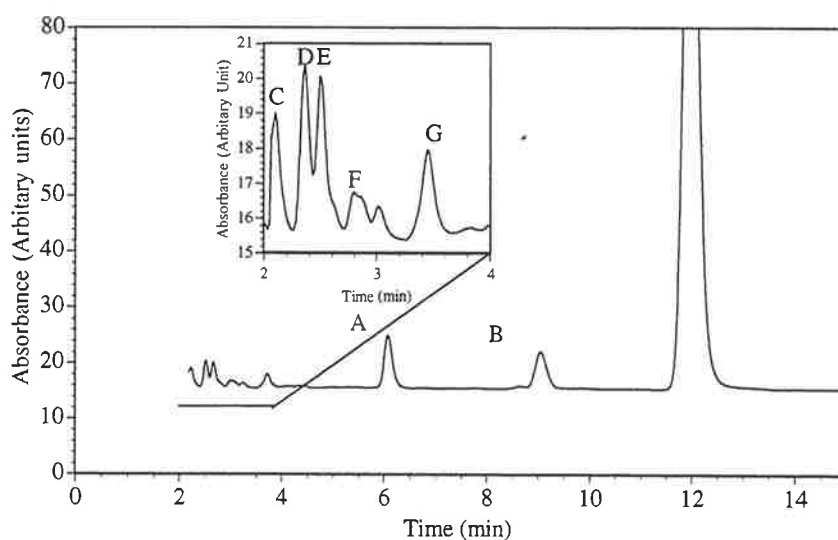


Figure 10.04. HPLC analysis following the gamma irradiation of an aqueous Hexazinone (1×10^{-4} M) solution saturated with nitrous oxide (pH 6.8, phosphate buffer). The trace displays the products formed from the reaction of Hexazinone with hydroxyl radicals (A to G). See Figure 10.06 for product identification.

The major products A and B were collected and their U.V. spectra recorded. The spectra are nearly identical in shape to the one recorded for Hexazinone. This indicates that the product's chromophore must be similar to that of Hexazinone. The structures of the products of this reaction were determined by electrospray mass spectrometry and can be observed in Figure 10.06. Hexazinone produced a mass to charge ratio of 253 ($M+H^+$) with a fragmentation pattern (using MS^2 experiment) that consisted of a daughter ion at 171 Daltons. This ion corresponds to the triazine ring missing the whole cyclohexane ring (C_6H_{10}). Further fragmentation of this peak produced grand-daughter ions at 128, 85 and 71 Daltons. These

peaks correspond to the loss of NMe_2 , and the formation of $\text{N}_2\text{C}_2\text{O}_2$ and NCNMe_2 ions, respectively. The major peaks, A and B, showed identical mass spectra with a parent ion of 251 Daltons, which corresponds to Hexazinone minus two protons. Fragmentation of this compound produced a daughter ion at 171 Daltons, which is identical to that of the first daughter ion of Hexazinone. Further fragmentation of the 171 Daltons ion produced the same daughter ion as previously mentioned for Hexazinone. Since the 171 Daltons daughter ion had been assigned to the daughter ion of Hexazinone minus the cyclohexane ring, the two protons must have been lost from the cyclohexane ring. The loss of 80 Daltons corresponds to the loss of a cyclohexene ring. Therefore products A and B must be Hexazinone with an unsaturated bond in the cyclohexane ring. Product G also displays the same mass spectra as observed for A and B. The actual position of the formation of the double bond in the cyclohexane ring cannot be determined by mass spectrometry, however it must be in a different position for A, B and G to have different retention times in the HPLC trace. Products C, D and F all produced the same parent ion of 269 Daltons in the mass spectral analysis. This mass to charge ratio is 16 Daltons more than Hexazinone. It therefore corresponds to Hexazinone plus oxygen. Fragmentation of the parent ion produced a daughter ion at 251 Daltons (minus OH_2). Further fragmentation of the daughter ion produced another ion at 171 Daltons. Fragmentation of the grand-daughter ion produced the same ions produced for the equivalent fragmentation of Hexazinone. Addition of an oxygen would normally correspond to the addition of the hydroxyl radical to an unsaturated part of the molecule. However the fragmentation pattern indicates that the oxygen is attached to the cyclohexane ring. It is impossible for a hydroxyl radical to be added to a saturated bond. The only explanation available for the formation of this product is the presence of trace amounts of oxygen in the solution during the irradiation. This will be discussed at greater lengths in section 10.4. Solvent water is not expected to add across the unsaturated bond resulting in the addition of a hydroxyl group to the cyclohexene ring (as observed for cyclopropene ring of Cyromazine). This reaction would not occur because hydrogen ions were not present in the HPLC eluent because an ion pairing reagent was not used. The last peak (E) produced a parent ion at 267 Daltons. This mass to charge ratio is two hydrogens less than the products C, D and F. Fragmentation of E produced the daughter ion at 171 Daltons, and then followed the equivalent fragmentation pattern observed for Hexazinone. Product E must result from the formation of a carbonyl product on the ring. Again this could only be formed in the presence of oxygen. Its formation will be discussed at length in section 10.4.

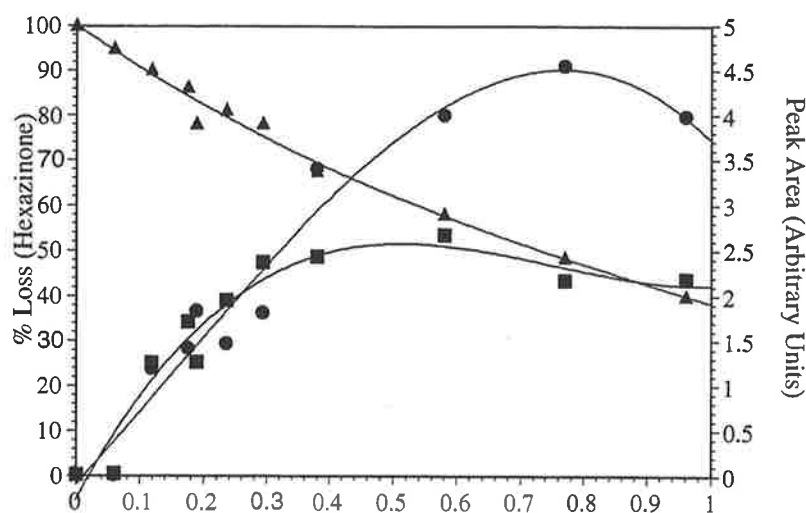


Figure 10.05. Loss of Hexazinone (left axis) and the formation of the products (right axis) from the gamma irradiation of aqueous Hexazinone (1×10^{-4} M) solution saturated with nitrous oxide (pH 6.8, phosphate buffer). The products are A=●, B=■, C,D,E,F,G not shown.

Ab initio calculations performed on Hexazinone produced a natural population similar to that described in Figure 6.04 for the 1,3,5-triazine. This agrees with the hypothesis that the hydroxyl radical would not add to the 1,3,5-triazine ring. The carbons on the cyclohexane ring do show an excess of electron density when compared to the other carbon atoms in the molecule.

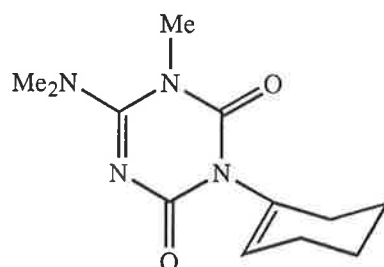


Figure 10.06. Products (A, B and G) of the gamma radiolysis of an aqueous Hexazinone solution saturated with nitrous oxide as determined by the analysis of electrospray mass spectrometric data. Location of the double bond is not unambiguously assignable in structures A, B and G. See text for discussion.

10.3 REACTION OF HEXAZINONE WITH THE HYDROXYL RADICAL IN ACIDIC SOLUTION

The corrected TDA spectrum obtained from the pulse radiolysis of Hexazinone (1×10^{-4} M) in acidic solution (pH 1.0, HClO_4) saturated with nitrous oxide was identical to that observed in Figure 10.02 for the neutral pH experiment. A correction to the spectrum was made to take into account the lower G value at pH 2 due to the formation of hydrogen atoms from the reaction of hydrated electrons with the extra hydrogen ions. The maxima at 280 and 440 nm decayed by second order kinetics with $2k/\epsilon I = 1.1$ and $1.5 \times 10^9 \text{ M}^{-1}\text{s}^{-1}$,

respectively. The values are similar to that reported in section 10.2. This evidence suggests that the transient produced is the same as observed at neutral pH. Hexazinone has a pK_a of 1.09 [183] with the protonation-deprotonation site being the nitrogens. The positive charge created by the protonation is resonance-stabilised on the ring. At pH 1, Hexazinone will be in approximately a 50-50 mix of both the protonated and deprotonated states. The transient produced by the reaction of Hexazinone with hydroxyl radicals is independent of the pH of solution (pH 1.0 to 6.8).

Competition kinetics produced a bimolecular rate constant for the reaction of hydroxyl radicals with Hexazinone of $4.9 \times 10^9 \text{ M}^{-1}\text{s}^{-1}$. The rate constant shows that a mixture of the protonated and deprotonated forms of Hexazinone reacts at a slightly slower rate than that observed for neutral Hexazinone alone. Since the hydroxyl radical reacts primarily through hydrogen abstraction, protonation of the 1,3,5 triazine ring would not be expected to influence the rate of reaction.

Steady state irradiation of an aqueous Hexazinone ($1 \times 10^{-4} \text{ M}$) solution saturated with nitrous oxide (pH 2, HClO_4) produced the same HPLC trace as observed in the reaction of hydroxyl radicals with Hexazinone at neutral pH. This result is in agreement with the pulse radiolysis data, which also implies that the protonation state or the presence of excess hydrogen ion (pH 1 to 7) does not affect the reaction. Products observed in the HPLC trace were collected and analysed by electrospray mass spectrometry. This produced the same result as that reported in section 9.2.

10.4 REACTION OF HEXAZINONE WITH THE HYDROXYL RADICAL IN THE PRESENCE OF OXYGEN

The TDA spectrum obtained upon the pulse radiolysis of an aqueous Hexazinone ($1 \times 10^{-4} \text{ M}$) solution saturated with nitrous oxide/oxygen (4:1 v/v) is displayed in Figure 10.07. The TDA spectrum does not appear similar to that observed in Figure 10.02, the maxima absorbance at 280 and 440 nm had disappeared. Comparison of the decay rates of the transient species indicates a change from second order kinetics to initial first order kinetics (Figure 10.08) with the addition of oxygen. This indicates that the transients produced by the reaction of Hexazinone with hydroxyl radicals react through pseudo first order kinetics with oxygen. This is consistent with the hydrogen abstraction mechanism as carbon centred radicals are known to react rapidly with oxygen [48, 82, 84, 102, 103]. The reaction rate is relatively fast, indicating that the carbon centred radical is not a OH-adduct [85]. This observation is in agreement with hydroxyl radicals reacting with Hexazinone through

hydrogen abstraction instead of addition. After the initial rapid first order process a much slower reaction can be observed to be taking place between 20 and 400 μs in Figure 10.08.

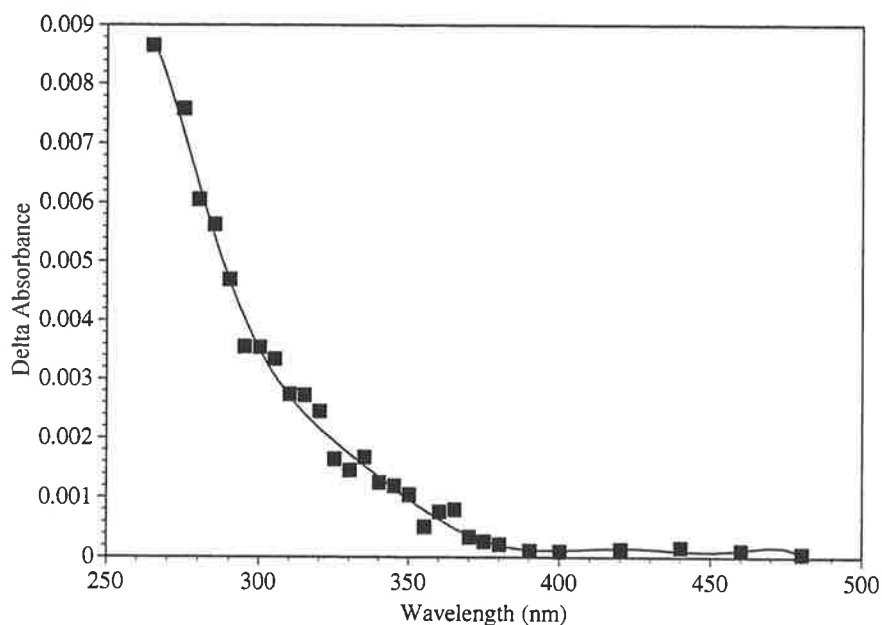


Figure 10.07. TDA spectrum obtained upon the pulse radiolysis of an aqueous Hexazinone (1×10^{-4} M) solution saturated with nitrous oxide/oxygen (4:1 v/v). Spectrum recorded 10 μs after the pulse. *at > 50 μs post?*

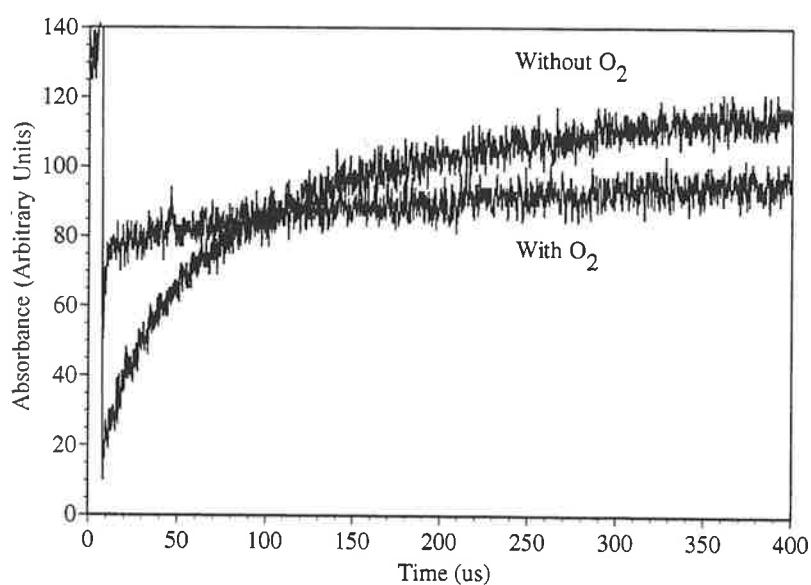


Figure 10.08. Comparison of the pulse radiolysis traces obtained from a solution of Hexazinone (1×10^{-4} M) saturated with nitrous oxide and nitrous oxide/oxygen (4:1 v/v). Absorbance data were collected at 280 nm. Traces are normalised. All radiation pulses are 2.5 μs long with a radiation dose of 11.3 Gray per pulse.

Figure 10.09 displays the change in the ultra violet spectrum following gamma irradiation of an aqueous Hexazinone (79 μM) solution saturated with nitrous oxide/oxygen. This is different from that for the de-oxygenated system. This spectrum indicates a larger decrease in absorbance at 246 nm when compared to the same experiment performed without

oxygen. The loss of absorbance at 246 nm was still less than expected and therefore the products should absorb at 246 nm.

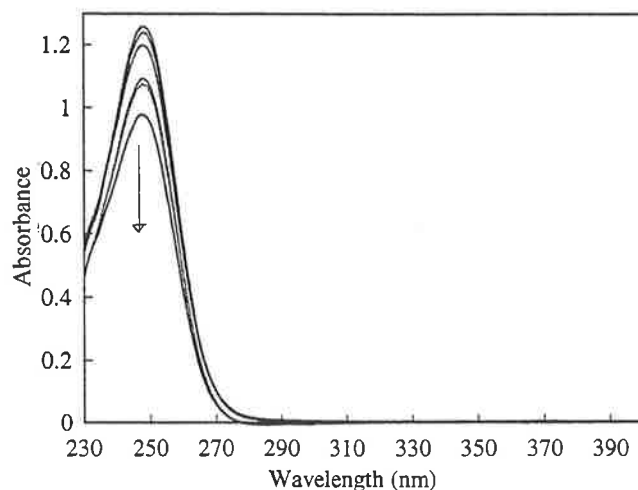


Figure 10.09. Observed change in optical absorbance of an aqueous Hexazinone ($79 \mu\text{M}$) solution saturated with nitrous oxide/oxygen and irradiated with gamma irradiation (0 to 200 Gray). Arrow indicates the direction of absorbance change with radiation dose. Dose rate of 80 Gray per hours.

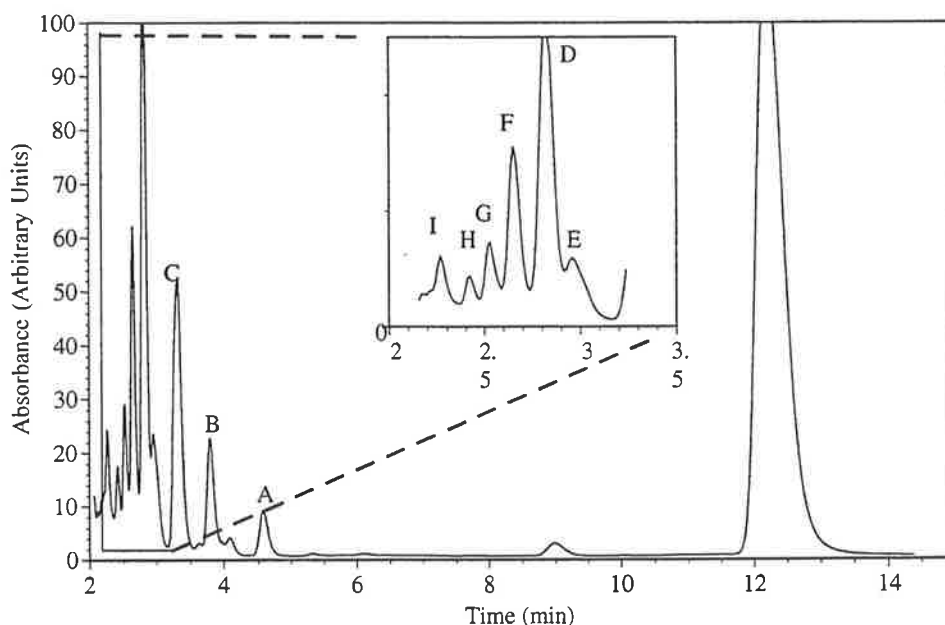
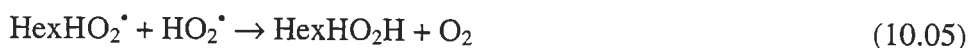
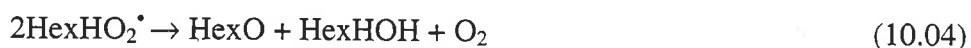
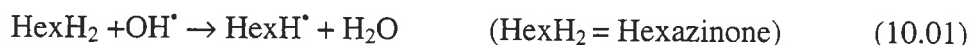


Figure 10.10. HPLC analysis following the gamma irradiation of an aqueous Hexazinone ($1 \times 10^{-4} \text{ M}$) solution saturated with nitrous oxide/oxygen. The trace displays products formed from the reaction of the hydroxyl radical with Hexazinone in the presence of oxygen (A to H). See Figure 10.11 for product identification.

The HPLC trace of an aqueous Hexazinone ($1 \times 10^{-4} \text{ M}$) solution saturated with nitrous oxide/oxygen produced a different trace from that observed for the de-oxygenated solution (Figure 10.10). Products previously observed at 5 and 8 minutes have disappeared. Also peaks at the beginning of the trace have increased in size when compared to the de-

oxygenated hydroxyl radical experiment. Collected products had their structures determined using electrospray mass spectrometry and are shown in Figure 10.11. Products A and E produced a parent ion of 285 Daltons. This is 32 Daltons more than Hexazinone, or equivalent to the addition of two oxygens to the Hexazinone molecule. MS² fragmentation of the parent ion at 285 Daltons produced a daughter ion with a base peak of 171 Daltons along with other daughter ions at 267 (minus OH₂) and 251 Daltons (minus O₂H₂). This fragmentation pattern indicates that two oxygens must be on the cyclohexane ring as would be expected from the de-oxygenated study. Further fragmentation of the daughter ion produced a grand-daughter ion at 267 Daltons as well as the base peak grand-daughter ion at 171 Daltons (minus the cyclohexane ring from Hexazinone). The reaction to form products A and E would initially result in the addition of oxygen to the cyclohexanyl radical to form the RHO₂[•] transient. The RHO₂[•] radical would then react with the perhydroxyl radical to form the corresponding organic hydroperoxide (RHO₂H). Compounds B, G, H, I produced a parent ion of 269 Daltons. This equates to the addition of an oxygen to the starting Hexazinone molecule. The MS² fragmentation pattern produced a peak at 251 Daltons (minus OH₂). Further fragmentation produced a daughter ion at 171 Daltons (the formation of Hexazinone minus the cyclohexane ring). The products are Hexazinone with an additional oxygen on the cyclohexane ring. Products C, D and F all had parent ions with mass to charge ratio of 267 Daltons. This mass to charge ratio corresponds to the formation of a product that is plus one oxygen and minus two hydrogens from the starting compound. MS² fragmentation of this ion produced a daughter ion at 171 Daltons. As previously stated this is Hexazinone minus the cyclohexane ring. The products must therefore result from the formation of a carbonyl compound. The product with mass of 269 and 267 Daltons must be formed from the addition of the hydrogen abstracted Hexazinone radical to oxygen followed by the disproportionation of the resulting radical to form the products observed (Reaction 10.04).



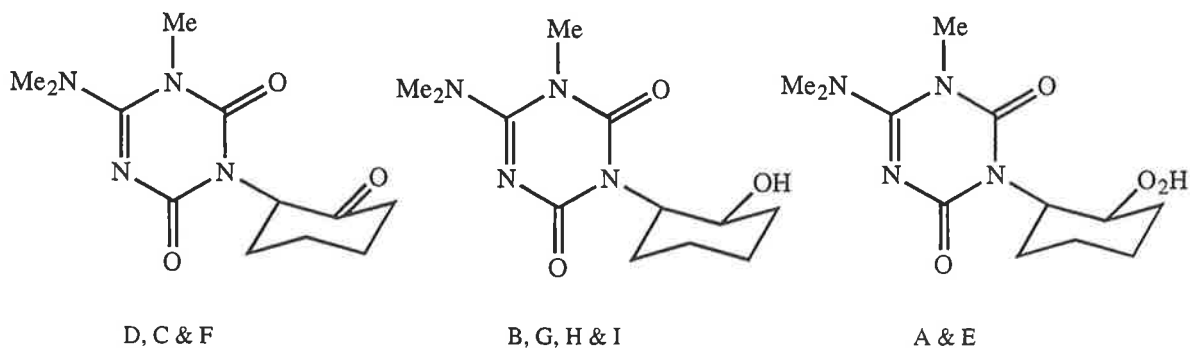


Figure 10.11. Products (A to I) of the gamma radiolysis of aqueous Hexazinone (1×10^{-4} M) separated saturated with nitrous oxide/oxygen as determined by the analysis of electrospray mass spectrometric fragmentation data. Location of the hydroxyl group are not ambiguously assignable in structures A to I. See text for discussion.

It was observed in the de-oxygenated experiment that some of the products could only be formed in the presence of oxygen. It was suggested in section 10.2 that formation of these products might be due to trace amounts of oxygen still remaining in the solution. Comparison of the products between the two experiments confirmed that the products at the beginning of the HPLC trace are identified here and are observed in the de-oxygenated experiment. It was also observed that the size of the peaks are substantially greater than that of the same peaks detected in the de-oxygenated experiments. Figure 10.11 also revealed that the reaction of the hydrogen abstracted Hexazinone radical with oxygen is rapid when compared to the bimolecular decay of the same radical. It is therefore likely that products C to G are formed by the reaction of the cyclohexanyl radical with trace amounts of oxygen in the de-oxygenated experiment.

The area for the products is consistent with the change observed for the U.V. spectrum at 246 nm. This result is in agreement with the hypothesis postulated in section 10.2, that is, a pseudo first order reaction is transpiring between the cyclohexanyl type radical and Hexazinone. Oxygen reacts with the transient to form compounds which are more polar than those postulated to form in section 10.2 for the pseudo first order reaction between the cyclohexanyl radical and Hexazinone, thus all the products are detected in this trace.

10.5 REACTION OF HEXAZINONE WITH ONE ELECTRON OXIDANTS

The dichloride radical anion formed in the pulse radiolysis of oxygen saturated sodium chloride (0.02 M), Hexazinone solution (1×10^{-3} M) at pH 2 (HClO_4) reacts as a strong one electron oxidant with a redox potential of 2.09 V (versus NHE) [43]. The reaction of the dichloride radical anion with Hexazinone was studied by following the decay of the dichloride radical anion absorption at 340 nm. It was observed that in the presence of Hexazinone (1×10^{-3}

³M) this band still decayed by second order kinetics indicating that no reaction between Hexazinone and the dichloride radical anion had resulted. When sodium chloride was replaced with sodium bromide (0.02 M) (pH 6.8 and 2.0) no effect was observed on the decay of the dibromide radical anion at 360 nm. This implies that no reaction occurred with the dihalide radical anions and therefore no electron was transferred from Hexazinone to the dihalide radical anions.

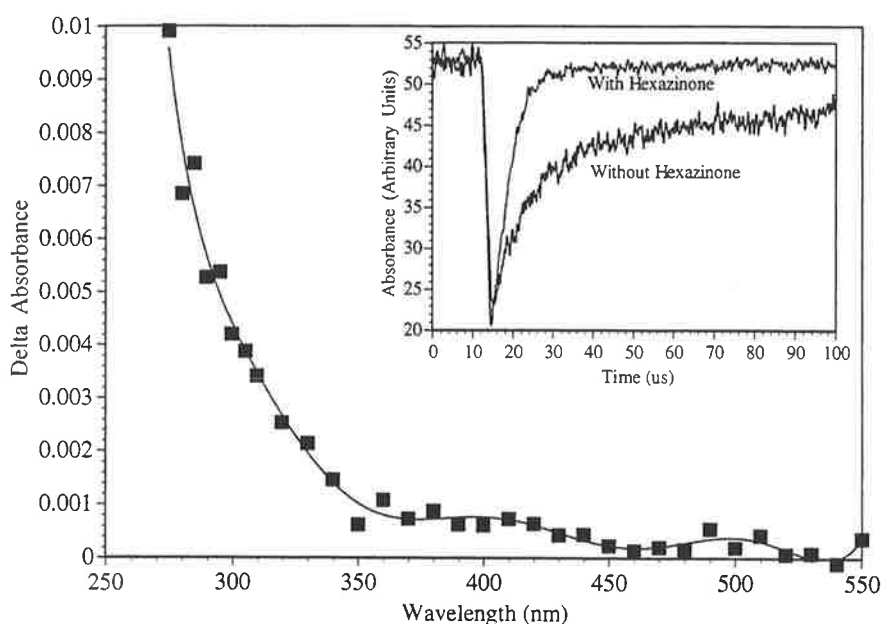
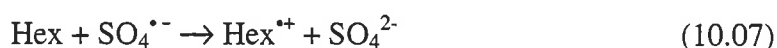
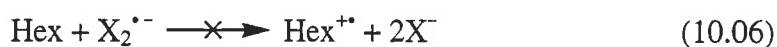


Figure 10.12. TDA spectrum obtained 20 μs after the pulse of a nitrogen saturated potassium persulfate (0.02 M), 0.1 M *t*-butyl alcohol, Hexazinone solution (2×10^{-4} M) at pH 6.8 (phosphate buffer). Inset, Comparison of the pulse radiolysis traces produced at 460 nm, with and with the presence of Hexazinone (2×10^{-4} M) in a nitrogen saturated potassium persulfate (0.02 M), *t*-butyl alcohol (0.1 M) solution. The traces indicate that a reaction has occurred between Hexazinone and the sulfate radical anion.

The sulfate radical anion formed in the pulse radiolysis of a nitrogen saturated potassium persulfate (0.02 M), *t*-butyl alcohol (0.1 M), Hexazinone (2×10^{-4} M) solution at pH 6.8 (phosphate buffer) and 2.0 (HClO_4) also reacts as a strong one electron oxidant with a potential of 2.43 V (versus NHE) [43, 86, 148]. The reaction of the sulfate radical anion with Hexazinone was studied by following the decay of the sulfate radical anion absorbance at 460 nm. It was observed that in the presence of Hexazinone (2×10^{-4} M) this band decayed faster than without Hexazinone. The result indicates that a reaction between Hexazinone and the sulfate radical anion had resulted. Since Hexazinone reacts with the sulfate radical anion and

not the dichloride radical anion, it implies that the Hex^{•+}/Hex redox potential must lie between that of the sulfate and dichloride radical anions. i.e. between 2.43 to 2.09 V (versus NHE). This would make the Hexazinone radical cation a strong one electron oxidant.

Using the pseudo first order rate constant for the decay of the sulfate radical anion it was determined that 20 μs after the pulse more than 95% of the sulfate radical anion had reacted with Hexazinone. The TDA spectrum of a nitrogen saturated potassium persulfate (0.02 M), *t*-butyl alcohol (0.1 M), Hexazinone (2x10⁻⁴ M) solution at pH 6.8 (phosphate buffer) obtained at this time can be observed in Figure 10.12. The spectrum exhibits a maximum below 260 nm. The spectrum recorded for this reaction is different from that obtained for the cyclohexanyl radical and so is not assigned to the same type of radical.

The rate constant for the reaction of Hexazinone with the sulfate radical anion was determined by the slope of a plot of the pseudo first order rate constant against the concentration of Hexazinone. This produced a bimolecular rate constant of 3.4x10⁸ M⁻¹s⁻¹. Reactions of 1,3,5 triazine or any of its derivatives with the sulphate radical anion have not been studied and little to no information on their reaction kinetics is available [149]. It is postulated that oxidising radicals would exhibit diminished reactivity toward the triazine ring for the reasons given in section 6.2, Figure 6.04. That is, the nitrogen in the ring has the greatest share of the electron density, making it unsuitable for electrophilic reaction. However, the electron density value produced by the natural population analysis on the nitrogens is large, potentially making them available for an electron to be removed by the sulfate radical anion.

Ab initio calculations displaying the spin surface of the optimised structure of Hexazinone minus one electron from its full electron set at HF/6-31G** indicates the radical is located over the oxygen of the carbonyl, the nitrogen of the amine and the nitrogen of the triazine ring between the two previously mentioned functional groups. The HOMO of Hexazinone is also observed to be a similar shape to the spin surface. This would imply that the electron is being removed from the HOMO orbital of Hexazinone and has not been resonance stabilised around the ring (Figure 10.13).

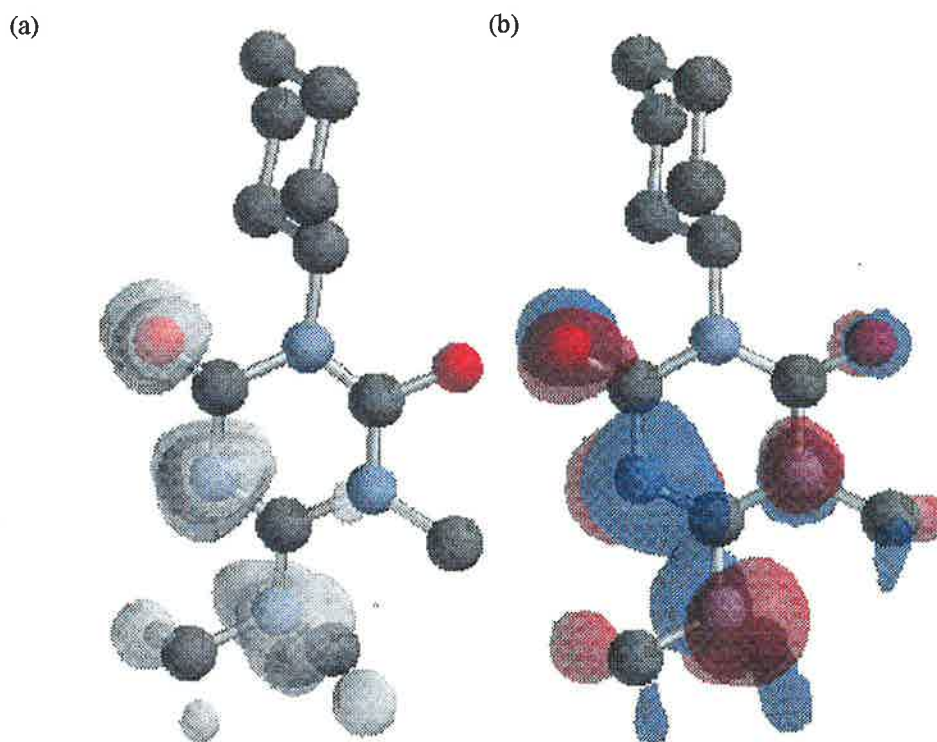


Figure 10.13. Plots of the electron spin density surface (a), and HOMO (b), of Hexazinone as determined by *ab initio* molecular orbital theory. Calculations were performed at the HF/6-31G** level of theory. Plot (a) was determined with a molecular charge of +1 and a multiplicity of 2. Plot (b) was determined for the neutral molecule possessing a corresponding multiplicity of +1.

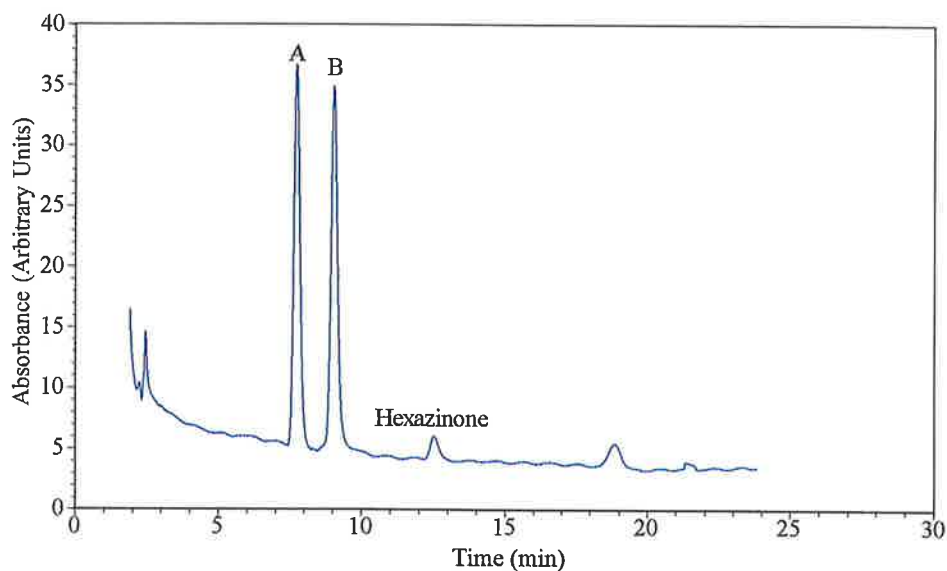


Figure 10.14. HPLC analysis following the gamma irradiation of an aqueous Hexazinone (1×10^{-4} M) solution containing potassium persulfate (0.02 M), *t*-butyl alcohol (0.1 M) and saturated with nitrogen (pH 6.8, phosphate buffer). The trace displays the products of the reaction of the sulfate radical anion with Hexazinone (A and B). See text for discussion.

Steady state irradiation of a nitrogen saturated potassium persulfate (0.02 M), *t*-butyl alcohol (0.1 M), Hexazinone solution (1×10^{-4} M) at pH 6.8 (phosphate buffer) produced almost the complete loss of Hexazinone in the HPLC trace (Figure 10.16). A non-irradiated

sample of the above solution displayed no loss of Hexazinone over the same time period therefore indicating the observed products result from radiation chemistry and were not due to the thermal oxidation of Hexazinone by the persulfate ion [43]. This suggests the transient produced by the reaction of Hexazinone with the sulfate radical anion initiated a chain reaction with Hexazinone. This effect has been previously observed by Vinchurlar *et al.* [191].

Electrospray mass spectrometry on the product A produced a mass to charge ratio of 710 Daltons. This is almost three times the mass to charge ratio of the original starting compound. Fragmentation of the parent ion produced the daughter ions (all consecutive MSⁿ experiments) 518, (minus 192), 448 (minus 70), 225 (minus 225.6), 143 (minus 82), 126 (minus 17) Daltons. The mass spectral data presented here does not allow for the structure of product to be determined. It was determined that product B had a mass to charge ratio of 239. This is 14 Daltons less than Hexazinone. MSⁿ fragmentation of the parent ion produced a peak at 157 Daltons, which is again 14 Daltons less than that observed for the equivalent fragmentation of Hexazinone. Fragmentation of the 157 ion produced more ions at 114, 85 and 71 Daltons. The last two daughter ions were also recorded for the equivalent fragmentation of Hexazinone, however the 128 Daltons ion is missing and has been replaced by the 114 daughter ion which is 14 Daltons less than the 128 Daltons ion. The 128 Daltons ion in Hexazinone was determined to be the basic triazine ring structure with only both the oxygens and methyl group attached to it. The replacement of this ion by a new daughter ion at 114 Daltons suggests that Product B must be the replacement of the methyl group attached to the nitrogen in the triazine ring with a hydrogen atom. This effect has previously been observed with the radical cations in chapters 4 and 9.

The steady state reaction performed using the dichloride radical anion at low pH produced no significant degradation of Hexazinone over the time span of the experiment. This is in agreement with the pulse radiolysis results.

10.6 REACTION OF HEXAZINONE WITH THE HYDRATED ELECTRON

Decay of the hydrated electron's absorbance at 640 nm was observed to increase in the presence of small amounts of Hexazinone (1×10^{-4} M) at pH 7.0 (phosphate buffer and NaOH). This indicates that a reaction between the hydrated electron and Hexazinone is occurring. The transient optical spectrum obtained on pulse radiolysis of a solution containing Hexazinone (1×10^{-4} M), *t*-butyl alcohol (0.1 M) saturated with nitrogen gas is shown in Figure 10.15.

This spectrum initially exhibited a large absorbance at wavelengths longer than 500 nm, which quickly disappeared to display a small absorbance at 275 nm.

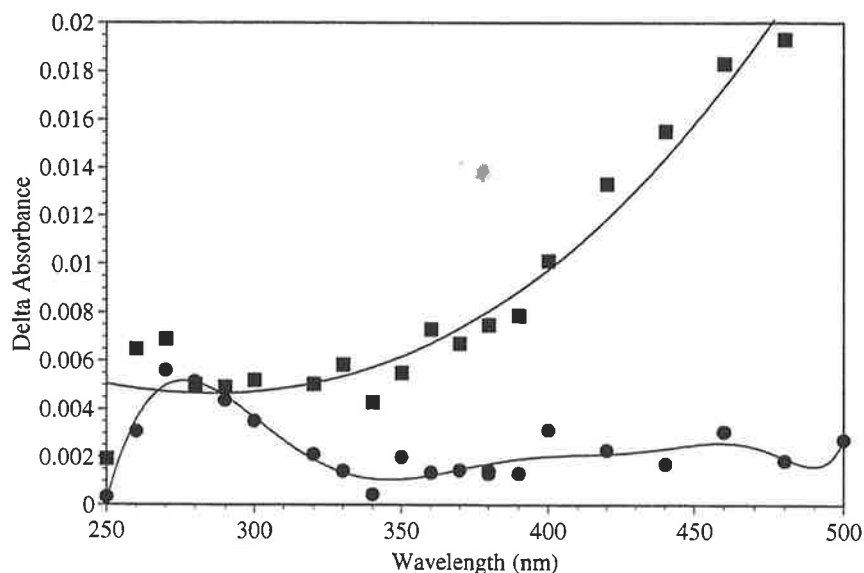
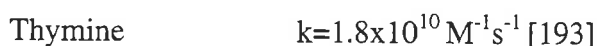
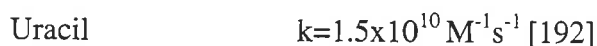


Figure 10.15. Time resolved TDA spectra obtained upon the pulse radiolysis of an aqueous Hexazinone (1×10^{-4} M) solution containing, *t*-butyl alcohol (0.1 M) saturated with nitrogen (pH 7.0, phosphate buffer and NaOH). (■ Directly and ● 15 μ s after pulse).

The bimolecular rate constant for the reaction of the hydrated electron with the Hexazinone was determined from the slope of a plot of the decay rate of the hydrated electron at 640 nm against the concentration of Hexazinone (20 to 50 μ M). The determined rate constant is $5.9 \times 10^9 \text{ M}^{-1} \text{ s}^{-1}$. Hexazinone as well as being a triazine also contains two carbonyl groups making it structurally similar to compounds like Uracil and Thymine. Carbonyl groups are known to be highly reactive towards the hydrated electron as can be observed from the rate constants given below:



No rate constants on 1,3,5-triazine or any derivatives have been recorded with the hydrated electron [149]. The rate constant for the reaction with Hexazinone is approximately half that of Thymine and Uracil, suggesting the presence of an additional nitrogen is affecting the rate of reaction with Hexazinone.

It is expected that the hydrated electron will react initially with Hexazinone at one of the carbonyl groups. This would result in the formation of a $\cdot\text{C-O}^-$ radical anion that can potentially be protonated at the oxygen. No attempt was made to determine the pK_a of this radical. It would be expected that this would then react to form either monomeric or dimeric

products. Hayon [194] determined the optical absorbance of ketyl radicals and radical anions generated from a number of pyrimidines and found that the absorbance maxima varied with the substituents on the ring between 260 and 330 nm. The molar absorbance of these maxima were determined to be between 1000 and 6000 $M^{-1}cm^{-1}$, dependent on the substituents. Molar absorbance at the absorption maximum of 275 nm was determined to be 950 $M^{-1}s^{-1}$, and is of a similar magnitude to that recorded by Hayon. The result is consistent with the formation of either a ketyl or radical anion from the reaction of the hydrated electron with Hexazinone.

Ab initio calculations performed on Hexazinone found the lowest electron density on the carbons of the carbonyl groups. This would make them the most favourable for the addition of a nucleophile. This agrees with the mechanism postulated earlier in this section.

Time resolved studies out to 1000 μs found no new peaks in the region of 250 to 600 nm suggesting that the reaction proceeds to form stable products that do not absorb in this region.

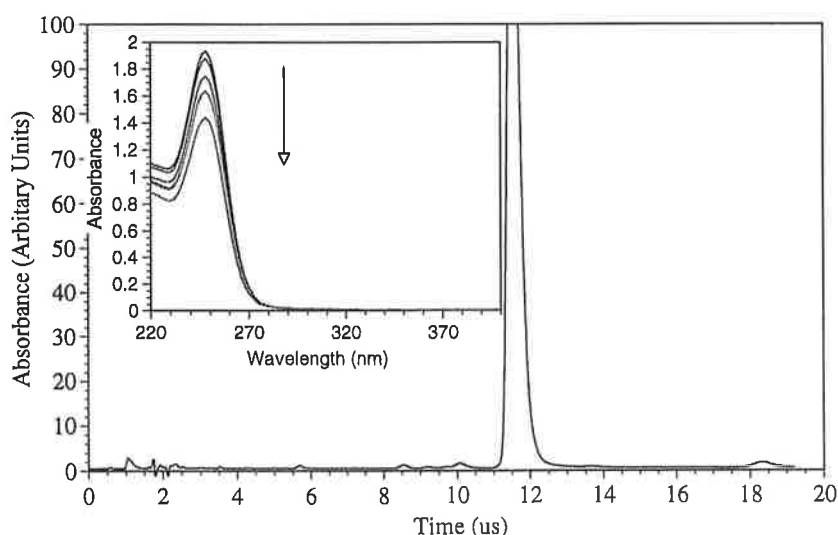


Figure 10.16. HPLC analysis following the gamma irradiation of a Hexazinone (1.1×10^{-4} M) solution containing, *t*-butyl alcohol (0.1 M) saturated with nitrogen (pH 7.0, phosphate buffer and NaOH). The trace displays no observable products for the reaction of the hydrated electron with Hexazinone. Inset. Change in optical absorption of the same solution (0 to 400 Gray). Arrow indicates the direction of absorbance change.

Gamma irradiation of a nitrogen saturated solution containing only Hexazinone and *t*-butyl alcohol (0.1 M) produced the HPLC trace observed in Figure 10.16. The HPLC trace displayed the formation of no new major peaks at 246 nm. A 1 mL injection of the irradiated solution did not produce any compounds in the trace, indicating that no products were being masked by the base line. The irradiated solution was also allowed to run out to longer retention times (60 minutes) using a steep acetonitrile gradient to determine if any non-polar

products were produced. This experiment also found no products at longer retention times. Only 50% of the expected loss of Hexazinone predicted by the dosimetry was observed, suggesting that transient radicals resulting from the reaction of Hexazinone with the hydrated electrons react to reform the starting compound. The effect on optical absorbance was to decrease the absorbance maximum at 246 nm with no new maximum forming. This indicates the chromophore is being affected by the reaction. Loss of the 246 nm maximum was less than predicted by the dosimetry, producing only a 15% decrease in the maximum while for the equivalent dose 25% of Hexazinone was observed by HPLC to disappear. Comparison of these experiments suggested there should be some products observed, however their absorbance would be small. It is possible that compounds of high molecular weight are forming which do not readily elute off the column.

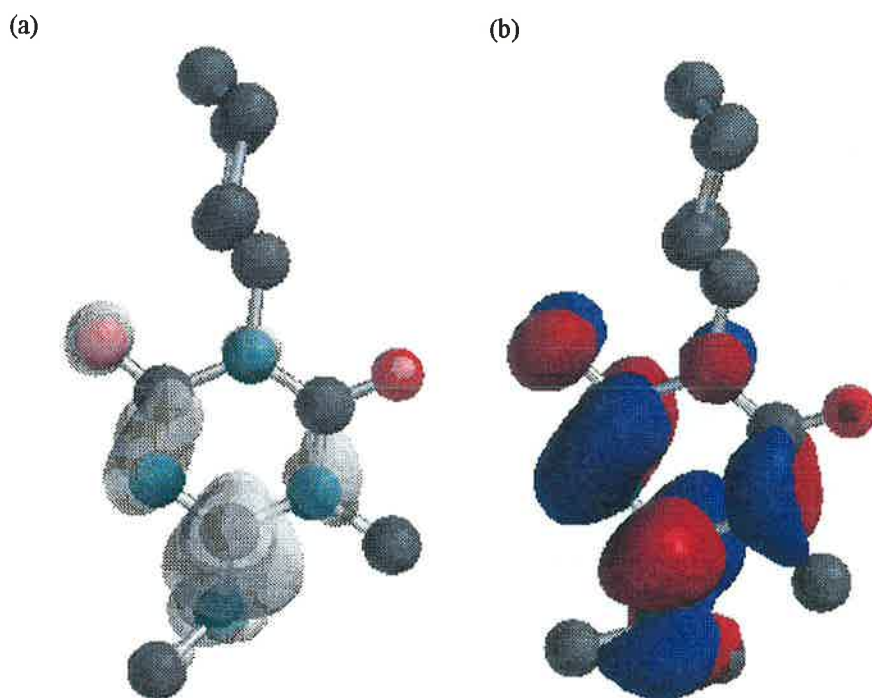


Figure 10.18. Plots of the electron spin density surface (a), and the LUMO (b), of Hexazinone as determined by *ab initio* molecular orbital theory. Calculations were performed at the HF/6-31G** level of theory. Plot (a) was determined with a molecular charge of -1 and a multiplicity of 2. Plot (b) was determined for the neutral molecule possessing a corresponding multiplicity of 1.

The results of *ab initio* calculations can be observed in Figure 10.18 which shows both the spin surface and LUMO for the Hexazinone radical anion and Hexazinone. The spin surface is prominent over the carbon attached to the $-NMe_2$. This is not the carbon where the extra electron was expected to attack, however the end result would be the same with a negative charge resulting on the carbonyl. The spin surface suggests that the radical on the carbon attached to the $-NMe_2$ is not resonance stabilised to any great extent. This is an unexpected result because it was expected that the radical would be delocalised. The LUMO

is located over the ring with the largest lobe on the carbon with the $-NMe_2$ group attached to it making it the most accessible for electron addition. The LUMO and the spin surface are similar in shape suggesting that the electron is added to the LUMO of Hexazinone and not delocalising.

10.7 REACTION OF HEXAZINONE WITH THE HYDROGEN ATOM

Pulse radiolysis of a nitrogen saturated, *t*-butyl alcohol (0.1 M) solution containing Hexazinone (1×10^{-4} M) at pH 2 ($HClO_4$) produced only a small absorbance in the region of 250 to 500 nm. Hydrogen atoms would be expected to abstract a hydrogen atom from the cyclohexane ring in much the same way as the hydroxyl radical. The absorbance of the transient suggests that the cyclohexanyl must somehow reform Hexazinone. It is possible that the transient species is actually abstracting hydrogen from the *t*-butyl alcohol present in the solution to reform the starting compound.

Steady state irradiation of a nitrogen saturated, *t*-butyl alcohol (0.1 M) solution containing Hexazinone (1×10^{-4} M) at pH 2 ($HClO_4$) produced less than a 5% loss of Hexazinone over the entire dose (200 Grays). The HPLC trace showed that no new products were formed during the radiation. This is consistent with the transient species abstracting hydrogen from the *t*-butyl alcohol present in the solution and reforming the starting compound.

10.8 REACTION OF HEXAZINONE WITH REDUCING RADICALS

Pulse radiolysis of a nitrous oxide saturated solution containing sodium formate (0.02 M) and Hexazinone (1×10^{-4} M) (pH 6.8, phosphate buffer) produced a maximum below 250 nm with no other absorbance maxima being observed. Absorbance observed was due to the formation of the carbon dioxide radical anion. Time resolved studies out to 1000 μs indicated the presence of no new absorption in the range of 250 to 600 nm. This suggests that the carbon dioxide radical does not react with Hexazinone. The redox potential of the carbon dioxide radical has been determined to be -2.0 V (versus NHE) [43, 111] indicating the redox potential of the Hex/Hex $^{\bullet-}$ is more negative than -2.0 V. Therefore, Hex $^{\bullet-}$ is a strong reducing agent with a reduction potential between -2.0 and -2.9 V (versus NHE).

Gamma irradiation of the same solution produced no loss of Hexazinone when sufficient radical was placed into the matrix to react with 50% of the available starting compound. This result confirms those obtained in the pulse radiolysis experiments.

10.8 OVERVIEW OF THE RADIATION CHEMISTRY OF HEXAZINONE

This study has allowed for the first time the elucidation of the radiation chemistry of aqueous Hexazinone. The new chemistry for Hexazinone is summarised in Figure 10.19.

The TDA spectrum obtained from the reaction of Hexazinone with hydroxyl radicals did not suggest the formation of an OH-adduct as an intermediate. *Ab initio* calculations indicate that the triazine ring of Hexazinone is unfavourable towards electrophilic addition of the hydroxyl radical, thus a cyclohexanyl radical is proposed as the intermediate. Reaction of Hexazinone with the oxide anion (a known hydrogen atom abstractor) could not be achieved because the high pH required to generate the radical resulted in destruction of the starting material. The rate constant obtained for the reaction of Hexazinone with the hydroxyl radical is similar to that determined for cyclohexane and cyclopentane's reaction with the hydroxyl radical [169][170]. Decay rate of the cyclohexanyl radical showed no dependence on the ionic strength of the solution, therefore the transient is neutral. The transient decays by second order kinetics, indicating that degradation products are formed by radical-radical reactions. HPLC characterisation of the compounds formed by the reaction of Hexazinone with the hydroxyl radical showed that all of these species have retention times less than Hexazinone. This suggests that the newly formed compounds are more polar than Hexazinone. Mass spectrometric studies determined that the two major species each have masses equivalent to the loss of two hydrogen atoms from the Hexazinone molecule. Comparison of the mass spectral fragmentation data collected for Hexazinone with that of the newly formed compounds, indicate that the hydrogens were lost from the cyclohexane ring. This is in agreement with what we determined through the pulse radiolysis and *ab initio* studies. The rate of Hexazinone loss and the formation of products from the reaction of Hexazinone with the hydroxyl radical is initially linear under steady state irradiation. As the amount of hydroxyl radicals is increased past 25% of Hexazinone's concentration, the loss of Hexazinone and the formation of products follows a higher order kinetic mechanism. This result suggests that products of the initial reaction also react with the hydroxyl radical to form (uncharacterised) compounds.

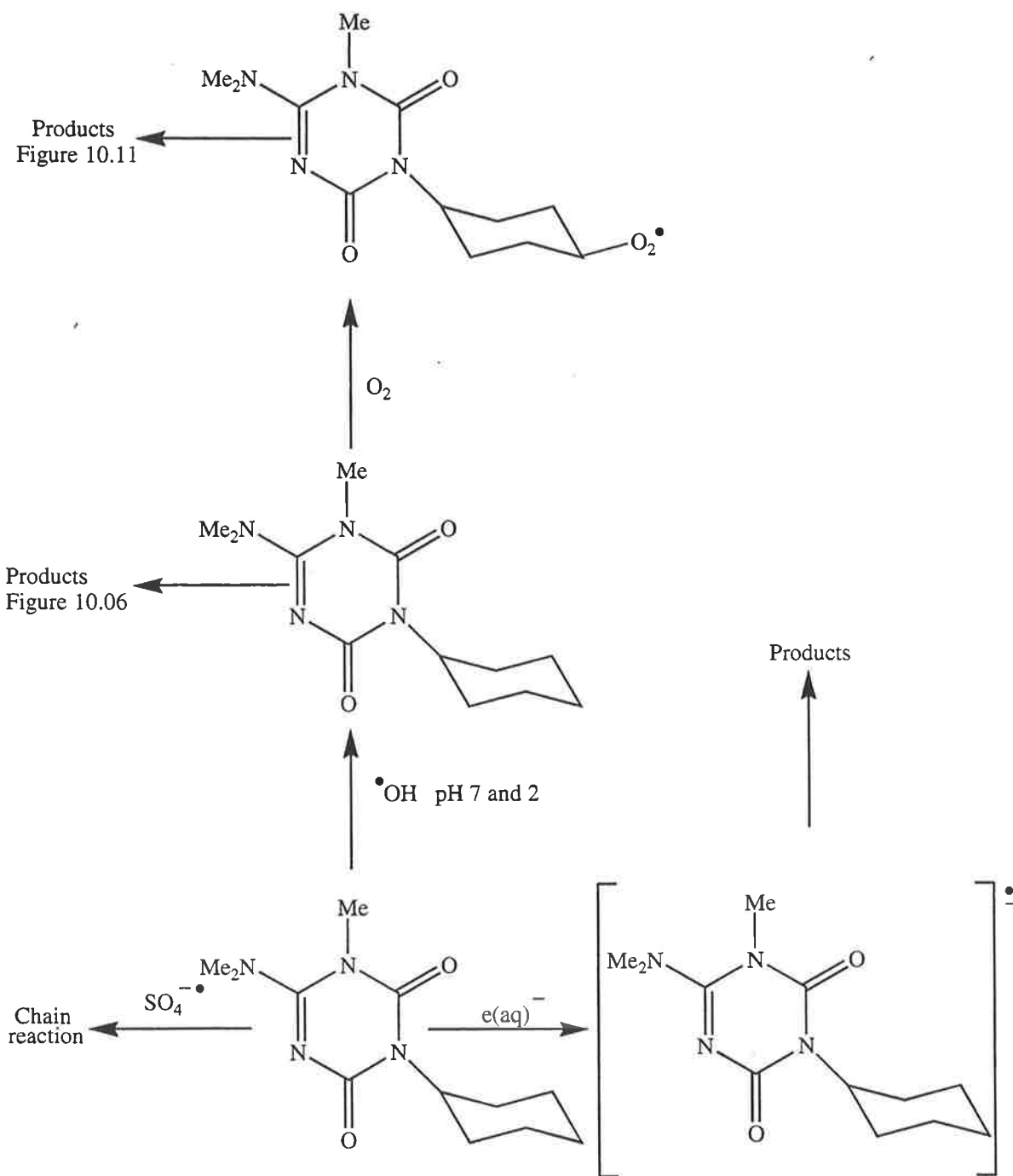


Figure 10.19. Overview of the radiation chemistry characterised in this study.

The corrected TDA spectrum obtained upon the reaction of the hydroxyl radical with Hexazinone at pH 2 matches that obtained from the same reaction at neutral pH. The rate constant for the reaction of Hexazinone with the hydroxyl radical at pH 2 is slightly lower than that obtained at neutral pH. Steady state irradiations of Hexazinone at pH 2 reproduced the results obtained at neutral pH.

The transient produced from the reaction of Hexazinone with the hydroxyl radical has been shown to be reactive with oxygen. Gamma irradiation coupled with HPLC shows the formation of different compounds to those obtained for the de-oxygenated experiment. Mass

spectral fragmentation data indicates that the products result from the addition of molecular oxygen to the transient. The newly produced transients then react to form the observed products.

The TDA spectra obtained from the reaction of Hexazinone with the sulfate radical anion differs from that obtained for the cyclohexanyl radical of Hexazinone, thus the transient produced does not transform into a cyclohexanyl type radical. Hexazinone is not observed to react with the dichloride radical anion and therefore the resulting radical cation of Hexazinone is a powerful one electron oxidant with a redox potential between 2.43 to 2.09 Volts (versus NHE). Gamma irradiation coupled with HPLC for the sulphate radical anion shows the complete loss of Hexazinone, indicating a chain reaction occurred. Mass spectral data of the products shows the formation of a compound three times the mass to charge ratio to that of Hexazinone. The other product was similar to Hexazinone with a methyl group replaced by a hydrogen atom.

Ab initio calculations indicate that the HOMO of Hexazinone is located only over certain atoms in the triazine ring. It is suspected that the electron lost in the one electron oxidation occurs from this orbital. The spin density surface shows the radical of the cation has not been delocalised from the HOMO as it is a similar shape.

The TDA spectrum obtained from the reaction of Hexazinone with the hydrated electron did not allow for a definite assignment to any known radical type, however, from Hexazinone's structure and the transient spectra, it is suspected that either a ketyl or a radical anion is forming. Steady state irradiation showed a loss in Hexazinone's absorbance at 254 nm suggesting that the conjugated ring structure is affected by the addition of the hydrated electron. HPLC shows no products in the chromatogram, indicating that compounds of high molecular weight are being formed. The radical anion of Hexazinone has been shown to be a strong reducing agent with a redox potential of between -2.0 and -2.9 V. No comments can be made on the fate of the transient in the presence of an oxidising agent as it is not known if any transformations are occurring once the radical is formed.

Ab initio calculations indicate that the LUMO of Hexazinone is located over the triazine ring. It is suspected that the electron gained in the one electron reduction would initially enter this orbital. The spin density surface shows the radical of the anion has not been delocalised from the LUMO as it is of a very similar shape.

Hexazinone will degrade upon the reaction of hydroxyl radicals produced in natural and treated industrial discharge water.

11.0 Radiation Chemistry of Aqueous MCPA Solution

11.1 METHYL CHLORO PHENOXY ACETIC ACID

MCPA ((4-chloro-2-methylphenoxy) acetic acid) (Figure 11.01), is a white solid with a melting point of 118-119°C. The maximum solubility of MCPA in water is 0.82 gm/L [195].

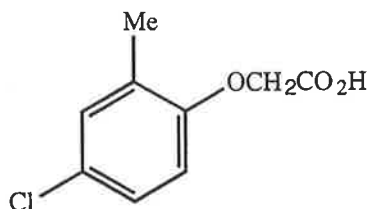


Figure 11.01. Chemical Structure of MCPA.

MCPA was released nearly 50 years ago by Rhone-Poulenc as a systemic herbicide for the control of perennial weeds in cereals, grasslands, trees and turf [196]. The herbicide works by concentrating itself in the meristematic tissue (actively growing tissue) where it interferes with protein synthesis, cell division and ultimately plant growth. MCPA has been used extensively since its release, with annual application rates being recorded in the Netherlands at approximately 800 tonnes [197].

MCPA has been determined to be very stable in water, with a half life of 3 weeks being reported for the degradation of MCPA through the photolysis by sunlight in pure water. Micro-organism such as *Achromobacter* and *Pseudomonas spp* have been observed to degrade MCPA in an aquatic environment with a half life of two weeks [195, 196]. The major metabolite of this type of degradation is 2-methyl-4-chlorophenol. Degradation in soil results in the formation of 2-methyl-4-chlorophenol (through the same micro-organisms), but in soil the breakdown continues via the hydroxylation of the ring followed by its fragmentation [195].

MCPA is highly mobile in soil with its ability to leach increasing inversely with the concentration of dissolved organic matter. The compound has been discovered in well water of areas where it is used in large quantities and has been listed by the (American) EPA as a potential ground water contaminant [198].

11.2 REACTION OF MCPA WITH THE HYDROXYL RADICAL

Figure 11.02 displays the time resolved TDA spectra obtained upon the pulse radiolysis of an aqueous MCPA (1×10^{-4} M) solution saturated with nitrous oxide (pH 6.8, phosphate buffer). It exhibits an absorption band with a maximum at 310 nm. In the presence of *t*-butyl alcohol (0.1 M), an effective hydroxyl radical scavenger but a weak hydrogen atom scavenger, the absorption spectrum was considerably reduced. The high $G(\cdot\text{OH})$ yield and appreciable decrease in the transient absorption suggests that the transient absorption spectrum in Figure 11.02 is mainly due to the reaction of the hydroxyl radical with MCPA. The absorbance spectrum resembles that of a OH-adduct, and thus the transient is assigned to the intermediate formed by the addition of the hydroxyl radical to MCPA.

Spectrum of the transient produced in the reaction of MCPA and the hydroxyl radical showed no negative absorbance in the region between 250 and 500 nm, because the ground state absorbance of MCPA in the region of 250 to 500 nm is small. The ground state corrected spectrum exhibits the same absorption maximum at 310 nm. The extinction coefficient of this maximum is $6900 \text{ M}^{-1} \text{ cm}^{-1}$.

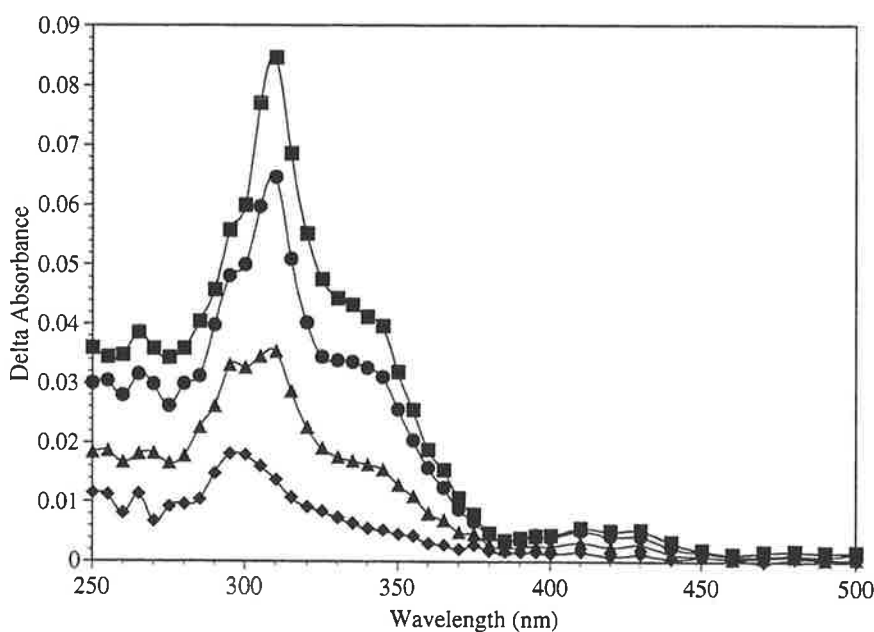


Figure 11.02. Time resolved TDA spectra obtained upon the pulse radiolysis of an aqueous MCPA (1×10^{-4} M) solution saturated with nitrous oxide (pH 6.8, phosphate buffer). (■ Directly after the pulse, ● 20 μs , ▲ 100 μs , ◆ 500 μs).

Reducing the dose (and hence the amount of transient radical) produced an increased half life of the transient species at 310 nm. The radical therefore decays by second order kinetics. When the curve was fitted to second order kinetics it produced a decay rate of $2k/\epsilon l = 1.2 \times 10^5 \text{ s}^{-1}$ at 310 nm. Using the molar absorbance value determined for the maximum at

310 nm, it was determined that $2k = 8.3 \times 10^8 \text{ M}^{-1}\text{s}^{-1}$. The transient therefore decays to products by radical-radical reactions.

The reactions of chlorobenzene, toluene, acetic acid and anisole have been studied previously [8, 44, 93, 178]. All benzene derivatives react through the addition of the hydroxyl radical to the aromatic ring to form the OH-adduct. Resulting OH-adducts all have characteristic absorbance maximum in the region of 300 to 340 nm. Since the transient observed in the reaction of MCPA with hydroxyl radicals had an absorbance maximum in this region, it is reasonable to assume that MCPA's reaction with the hydroxyl radical also results in an addition reaction with the formation of a OH-adduct.

Adjusting the ionic strength of the solution by addition of NaClO_4 (1 M) at pH 6.8, produced an increase in the observed rate of decay of the transient at 310 nm. This implies the transient is charged. This is expected from the formation of the cyclohexadienyl radical which would be negatively charged at pH 6.8 due to the acetate functional group of MCPA having a pK_a of 3.1 [199].

Determination of a bimolecular rate constant for the reaction of the hydroxyl radical with MCPA by competition kinetics produced a rate constant of $8.3 \times 10^9 \text{ M}^{-1}\text{s}^{-1}$. This rate constant indicates that MCPA reacts with hydroxyl radicals at close to diffusion controlled rates.

This is not the first reported rate constant for the reaction of the hydroxyl radical with MCPA. Mabury and Crosby [190] reported a rate constant for the reaction of the hydroxyl radical with MCPA at $2.3 \times 10^9 \text{ M}^{-1}\text{s}^{-1}$. The rate constant reported by Mabury and Crosby is nearly 4 times slower than the rate constant determined here. The reason for the discrepancy between the two results have been discussed in section 10.2. Mabury and Crosby used steady state irradiation competition kinetics to determine their rate constant. Experiments performed by to compare their techniques to that of the pulse radiolysis study indicates that the steady state method produces results that are up to 5 times slower than the analogous pulse radiolysis determined rate constant. The rate constant reported here is less than 4 times faster than the rate constant reported by Mabury and Crosby and therefore the difference between the two can be explained by differences in the methodology used to determine them.

Rate constants for the reaction of structurally similar molecules to MCPA are shown below. It can be seen that rate constants for the reaction of hydroxyl radicals with acetic acid is more than two orders of magnitude less than the rate constant for the reaction of hydroxyl

radicals with MCPA. Chlorobenzene, anisole and toluene rate constants are slightly less than that of MCPA. No information could be found on the reaction rate constant for phenoxy acetic acid [149]. The rate constant data presented here is in good agreement with the rate constant determined for MCPA.

Toluene	$k=5.1 \times 10^9 \text{ M}^{-1} \text{ s}^{-1}$ [178]
Chlorobenzene	$k=5.6 \times 10^9 \text{ M}^{-1} \text{ s}^{-1}$ [155]
Anisole	$k=5.4 \times 10^9 \text{ M}^{-1} \text{ s}^{-1}$ [93]
Acetic acid	$k=6.7 \times 10^7 \text{ M}^{-1} \text{ s}^{-1}$ [8]

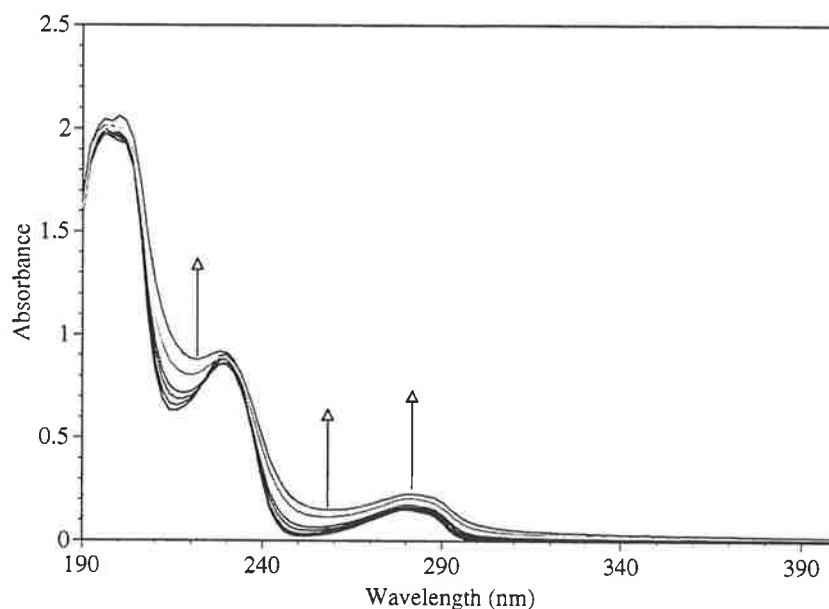


Figure 11.03. Observed change in optical absorbance of an aqueous MCPA (1×10^{-4} M) solution saturated with nitrous oxide and irradiated with gamma irradiation (0 to 165 Gray). Arrows indicate the direction of absorbance change with radiation dose. Dose rate 66 Gray/hr

Steady state irradiation of an aqueous MCPA (1×10^{-4} M) solution saturated with nitrous oxide using cobalt 60 (66 Grays per hour) produced a small increase in the absorbance due to the MCPA at 232 nm (Figure 11.03). Towards the end of the irradiation period, an increase in the absorbance at 215 and 255 nm was also observed. The increase in absorbance suggests the products absorb in this region.

A HPLC trace recorded following the gamma irradiation of an aqueous MCPA (1×10^{-4} M) solution saturated with nitrous oxide (pH 6.8, phosphate buffer) indicated the formation of new products and a decrease in the concentration of MCPA (Figure 11.04) at 232 nm. One major product was detected in this trace (A). Three other minor compounds were also formed. The major product's retention time was slightly longer than that observed for MCPA indicating that it was less polar than the starting material. This suggests that the

predominant species of the reaction of the hydroxyl radical with MCPA is the formation of a dimer. Two of the three minor products were also observed at longer retention times than MCPA. One product was observed at a retention time less than MCPA.

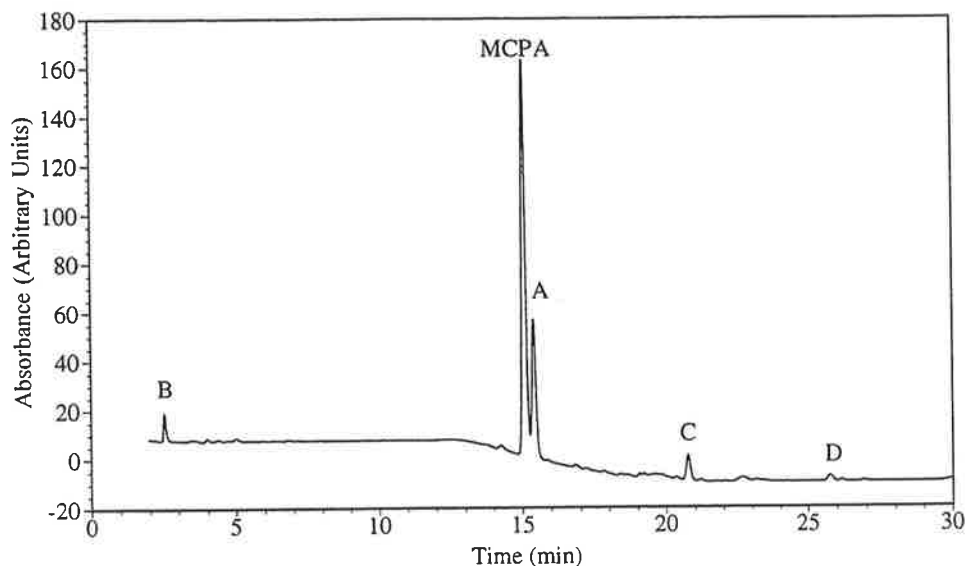


Figure 11.04. HPLC analysis following the gamma irradiation of an aqueous MCPA (1×10^{-4} M) solution saturated with nitrous oxide (pH 6.8, phosphate buffer). The trace displays the products formed from the reaction of MCPA with hydroxyl radicals (A). See text for discussion.

Rate of MCPA loss was linear against the concentration of the hydroxyl radical added to the system (calculated using Frickie Dosimetry), until approximately 35% of the MCPA had reacted. Appearance of the products (followed by HPLC) was also observed to be initially linear. After approximately 35% of MCPA had reacted, the rate of loss of the starting compound and the formation of products lost their linearity suggesting that the initial products of the reaction also react with the hydroxyl radical.

Structures of the products observed in this trace were determined by electrospray mass spectrometry and are recorded in Figure 11.06. MCPA produced a parent ion of 199 and 201 (3:1) Daltons (M-H). MS^2 fragmentation of the parent ion produced daughter ions at 155 and 141 Daltons. The daughter ions correspond to the loss of the CO_2^- and $CH_2CO_2^-$ groups. This spectrum matches the previously recorded electrospray ionisation mass spectrum [197].

The major product (A) of the reaction of the hydroxyl radical with MCPA produced a parent ion at 403/405/407 (4:3:1) Daltons. The mass isotope pattern of 4:3:1 indicates the presence of two chlorine atoms in the molecule and thus the formation of a dimer is confirmed. The parent ion mass to charge ratio is equal to a dimer formed from two OH-adducts minus a carbon and an oxygen atom. MS^2 fragmentation of the 403 Daltons parent ion produced a daughter ion at 215 Daltons. This ion corresponds to the presence of a MCPA

molecule with an additional oxygen atom therefore confirming the presence of a OH-adduct as an intermediate. Dimer formation through the OH-adduct should produce parent ions of (M-H) 431/433/435 (4:3:1) Daltons. Formation of the observed parent ions instead of the expected ions indicates the product must breakdown before the mass to charge ratio measurements are made. Breakdown of the product could either occur in solution or in the mass spectrometer during the ionisation process. A HPLC trace of the irradiated solution which was allowed to sit for 24 hours produced an identical result to the earlier chromatographic run. Hence if the compound is breaking down it occurs prior to the HPLC analysis. The possibility of the breakdown of the compound to produce an observed parent ion in the mass spectrometer has not been eliminated either. Though electrospray ionisation is a soft ionisation technique [70], the possibility of complete fragmentation of the parent ion cannot be discounted.

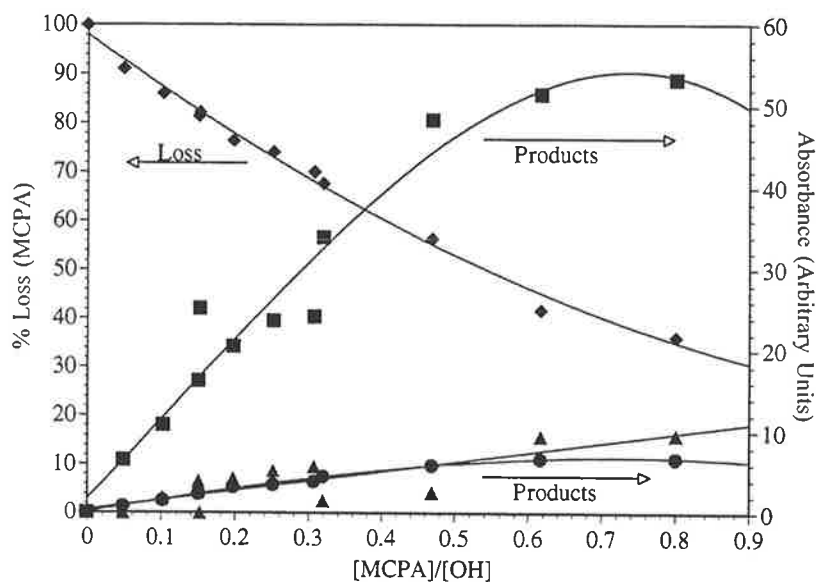


Figure 11.05. Loss of the MCPA (left axis) and the formation of the products (right axis) from the gamma irradiation of aqueous MCPA (1×10^{-4} M) solution saturated with nitrous oxide (pH 6.8, phosphate buffer), determined by HPLC. The products are A=▲, B=●, C=▲.

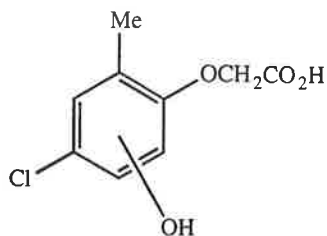


Figure 11.06. Minor product (at 2.5 minutes) of the gamma radiolysis of an aqueous MCPA solution saturated with nitrous oxide as determined by the analysis of electrospray mass spectrometric fragmentation data. Location of the hydroxyl group is not unambiguously assignable in the structure.

The product observed at two and a half minutes generated a parent ion of 215/217 (3:1) Daltons. This parent ion equates to the addition of an oxygen atom to the starting compound. This reaction would proceed through the formation of OH-adduct to products. MSⁿ fragmentation of the product produced daughter ions at 151 and 157 Daltons. The daughter ions correspond to the loss of CH₂CO₂ and OCH₂CO₂ from the parent ion.

The two remaining minor products at longer retention times (21 and 26 minutes) did not produce a parent ion that could be distinguished from the base line and thus their structures remain undetermined.

Ab initio calculations using natural [73] population analysis indicated the most electron rich carbon in the ring is the sterically unhindered carbon ortho to the OAc group. Addition to the ring by the hydroxyl radical would be expected to occur preferentially to the site with the most electron density and, therefore, on the basis of the calculations the hydroxyl radical would be expected to add to this site. The other carbons in the ring all have substantially less electron density, making them unfavourable for the addition of the electrophilic hydroxyl radical.

11.3 REACTION OF MCPA WITH THE HYDROXYL RADICAL IN ACIDIC SOLUTION

The corrected TDA spectrum obtained from the pulse radiolysis of MCPA (1×10^{-4} M) in acidic solution (pH 2.0, HClO₄) saturated with nitrous oxide was similar to that observed in Figure 11.02 for the neutral pH experiment. A correction to the spectrum was made to take into account the lower G value at pH 2 due to the formation of hydrogen atoms from the reaction of the hydrated electrons with the extra hydrogen ions. This implies that the protonation state of MCPA or the point of protonation has no effect on the absorbing chromophore. MCPA has a pK_a of 3.1 [199] with the protonation-deprotonation site on the acid which is isolated from the ring. It is therefore not unexpected that addition of the hydroxyl group to the aromatic ring has no effect on the transient species spectra. The maximum at 305 nm decayed by second order kinetics with $2k = 1.8 \times 10^9 \text{ M}^{-1} \text{ s}^{-1}$. This value is approximately twice that reported in section 11.2, suggesting decay of the transient produced by the reaction of MCPA with hydroxyl radicals is affected by the presence of extra hydrogen ions in solution. The increase in decay rate results because at pH 2 the transient would be neutral, and the bimolecular decay would not experience the same repulsion from the negative charge.

Steady state irradiation of a MCPA (1×10^{-4} M) solution saturated with nitrous oxide at pH 2 produced the same HPLC trace as observed in the reaction of hydroxyl radicals with MCPA at neutral pH. The result is in agreement with the pulse radiolysis data, which also implied that the protonation state or the presence of excess hydrogen ion (pH 1 to 7) does not affect the reaction. Products observed in the HPLC trace were collected and analysed by electrospray mass spectrometry. This produced the same result that as previously mentioned in section 11.2.

11.4 REACTION OF MCPA WITH THE HYDROXYL RADICAL IN THE PRESENCE OF OXYGEN

The time resolved TDA spectra obtained upon the pulse radiolysis of an aqueous MCPA (1×10^{-4} M) solution saturated with nitrous oxide/oxygen (4:1 v/v) is shown in Figure 11.07. The TDA spectrum appears similar to that observed in Figure 11.02. Comparison of the decay rates of transient species indicated a change from second order kinetics to initial first order kinetics (Figure 11.08) with the addition of oxygen. This indicates that transients produced by the reaction of MCPA with the hydroxyl radical react through pseudo first order kinetics with oxygen. This was then followed by a slower decay as can be observed in Figure 11.08. This is consistent with the OH-adduct mechanism, as carbon centred radicals are known to react with oxygen [48, 82, 84, 102, 103].

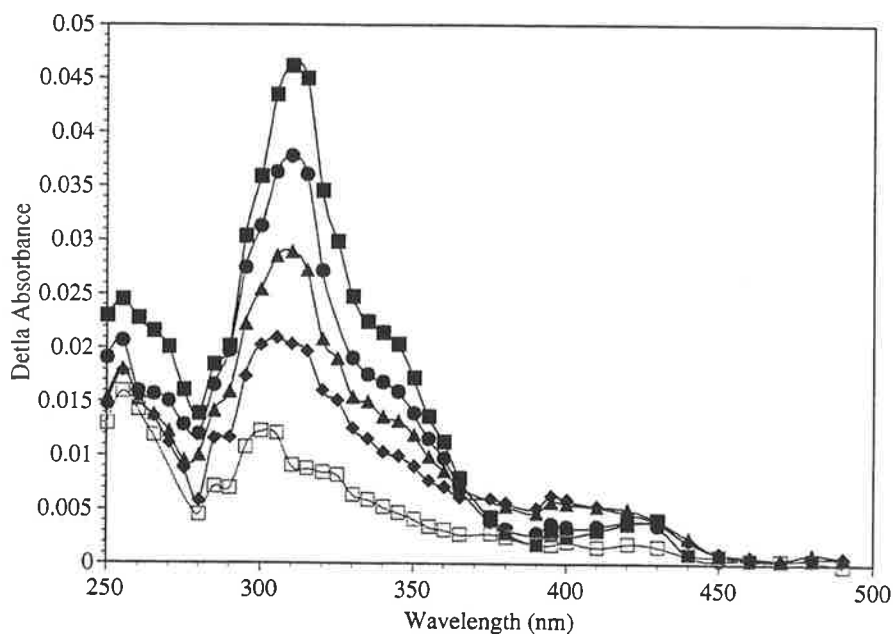


Figure 11.07. Time resolved TDA spectra obtained upon the pulse radiolysis of an aqueous MCPA (1×10^{-4} M) solution saturated with nitrous oxide/oxygen (4:1 v/v). (■ 20 μ s, ● 50 μ s, ▲ 100 μ s, ◆ 500 μ s after the pulse).

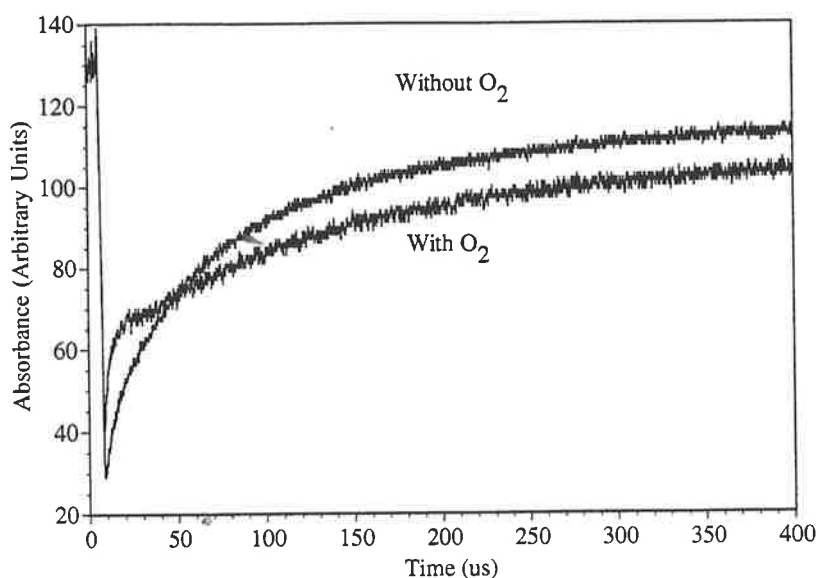


Figure 11.08. Comparison of the pulse radiolysis traces obtain from a solution of MCPA (1×10^{-4} M) saturated with nitrous oxide and nitrous oxide/oxygen (4:1 v/v). Absorbance data were collected 305 nm. Traces are normalised. Both radiation pulses are $2.5 \mu\text{s}$ long with a dose of 10.7 Gray per pulse.

Change in optical absorbance after the gamma irradiation of an aqueous MCPA (1×10^{-4} M) solution saturated with nitrous oxide/oxygen is shown in the inset of Figure 11.09. The maximum at 232 nm is observed to decrease, while the region around 250 nm increases slightly. The change observed in this experiment is different from that observed in the de-oxygenated experiment, therefore the addition of oxygen to the solution produced an effect on the product distribution of the reaction between the hydroxyl radical and MCPA.

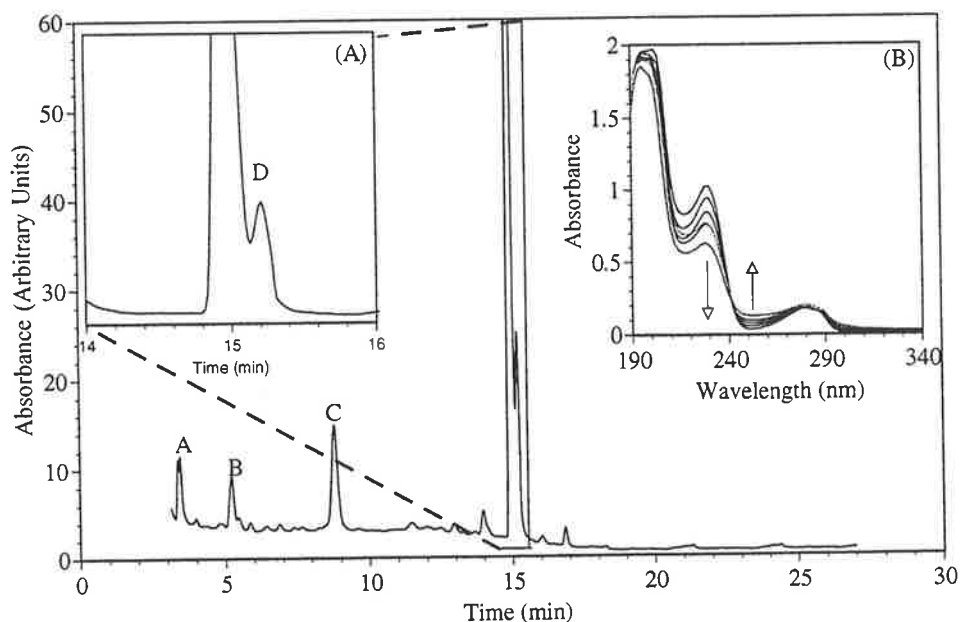


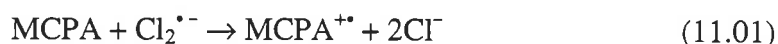
Figure 11.09. HPLC analysis following the gamma irradiation of an aqueous MCPA (1×10^{-4} M) solution saturated with nitrous oxide/oxygen. The trace displays the products formed from the reaction of the hydroxyl radical with MCPA in the presence of oxygen (A to D). Inset B. Change in optical absorbance of the same solution (0 to 180 Gray). Arrows indicate the direction of absorbance change with radiation dose.

The HPLC trace recorded following gamma irradiation of an aqueous MCPA (1×10^{-4} M) solution saturated with nitrous oxide/oxygen in Figure 11.09 indicates the formation of the four products (A-D). The compounds A and D have been previously observed in Figure 11.04 and were confirmed by mass spectrometry. Concentration of compound D (as determined by its area in the HPLC trace) was considerably reduced when compared to the de-oxygenated sample, indicating a competing reaction with oxygen. Mass spectrometry on the remaining compounds indicated that compound B also has a mass to charge ratio of 215/217 (3:1) Daltons, and therefore has a similar structure to compound A. MS² fragmentation of the parent ion produced a daughter ion at 157 Daltons. This fragmentation has also been previously recorded, indicating that the new hydroxyl group is located on the ring.

Compound C produced a similar mass spectrum to B, except that the parent ion was two Daltons less at 213/215 (3:1) Daltons. MS² fragmentation of the parent ion produced a daughter ion at 155 Daltons (minus CH₂CO₂), further fragmentation produced a granddaughter ion at 127 Daltons (minus CO). This product corresponds to the gain of an oxygen and the loss of two hydrogens. This type of product formation was previously observed for Dichlorophen, Napropamide and Dimethrimiol and was attributed to the formation of either a carbonyl group or an epoxide.

11.5 REACTION OF MCPA WITH OXIDISING RADICALS

The dichloride radical anion formed in the pulse radiolysis of oxygen saturated sodium chloride (0.02 M) MCPA solution (1×10^{-4} M) at pH 2 (HClO₄) reacts as a strong one electron oxidant with a potential of 2.09 V (versus NHE) [43]. The reaction of the dichloride radical anion with MCPA was studied by following the decay of the dichloride radical anion absorption band at 340 nm. It was observed that in the presence of MCPA (1×10^{-4} M) this band decayed faster and by first order kinetics instead of second order kinetics (Figure 11.10), indicating a reaction between MCPA and the dichloride radical anion had resulted.



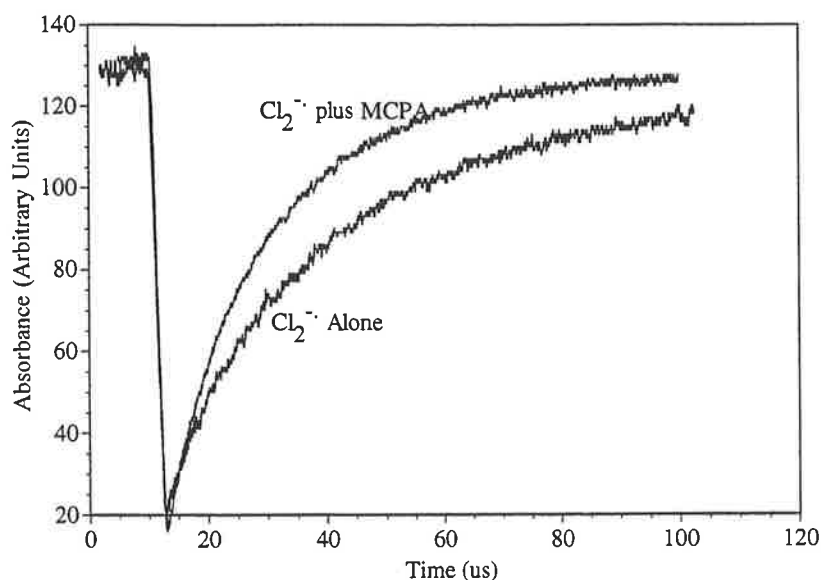


Figure 11.10. Comparison of the pulse radiolysis traces produced at 340 nm, with and without the presence of MCPA (1×10^{-4} M) in oxygen saturated NaCl (0.02 M) solution (pH 2, HClO_4). The traces indicate that a reaction between Dimethylthiomol and the dichloride radical anion had occurred.

The bimolecular rate constant was determined to be $2.6 \times 10^8 \text{ M}^{-1} \text{ s}^{-1}$ from the slope of a plot of the pseudo first order rate constant against the concentration of MCPA. Time resolved studies initially produced a broad absorbance with λ_{max} at 340 nm due to the formation of the dichloride radical anion. Rate constants of other structurally similar molecules have not previously been determined [149], except for acetic acid ($k < 10^4 \text{ M}^{-1} \text{ s}^{-1}$ [200]). Reaction of the dichloride radical anion with phenol derivatives show the electrophilic nature of this radical, thus a reaction is expected with MCPA due to its electron donating substituents. There is insufficient data published to draw conclusions on the magnitude of the rate constant.

Figure 11.11 shows the time resolved TDA spectra obtained upon the pulse radiolysis of an aqueous MCPA (1×10^{-4} M) solution containing NaCl (0.02 M) saturated with nitrous oxide (pH 2, HClO_4). Using the pseudo first order rate constant it was determined that more than 90% of the dichloride radical anion had reacted 20 μs after the pulse. The spectrum at 20 μs is similar to that observed for the MCPA reaction with hydroxyl radicals at pH 2, with an absorbance maximum at 305 nm and a shoulder out to approximately 350 nm. Since the dichloride radical anion is a specific one electron oxidant, it should react by electron transfer. The resulting product must then undergo rapid addition of water and simultaneous elimination of a hydrogen ion to form the cyclohexadienyl type radical which would produce a spectrum similar to that observed in Figure 11.02.

The maximum observed in Figure 11.11, when corrected for the lower G value is within the 10% experimental error of the absorbance maximum observed at 305 nm in Figure 11.02.

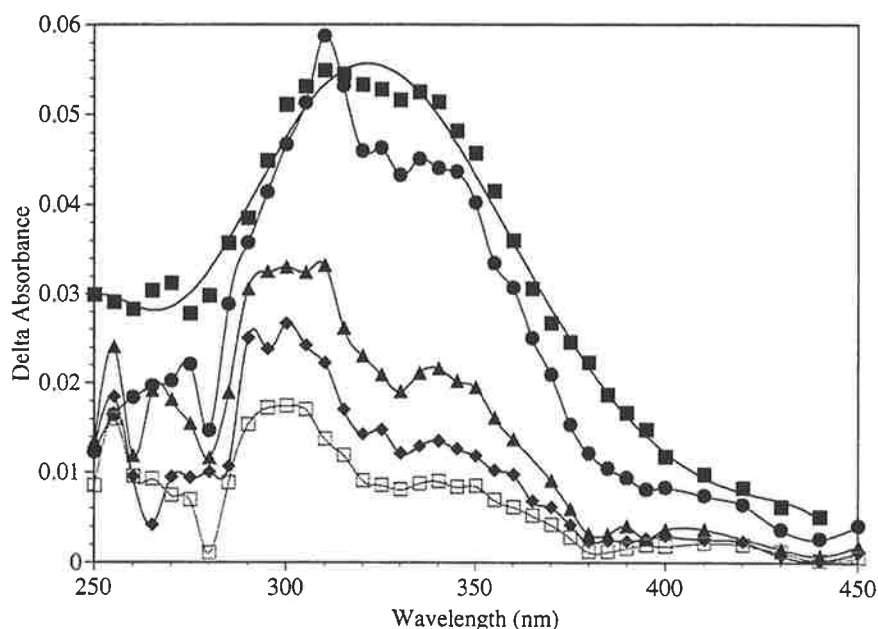


Figure 11.11. Time resolved TDA spectra obtained upon the pulse radiolysis of an aqueous MCPA (1×10^{-4} M) solution containing NaCl (0.02 M) saturated with nitrous oxide (pH 2, HClO_4). (■ Directly after pulse, ● 20 μs , ▲ 50 μs and ◆ 100 μs).

Steady state irradiation of a sodium chloride (0.02 M), nitrous oxide saturated solution containing MCPA (1×10^{-4} M) at pH 2 (HClO_4) produced a HPLC trace which showed the formation of one major product. This product occurred at the same retention time as that observed for the hydroxyl radical reaction. Electrospray mass spectrometry revealed that this is the same product with the same parent ions and mass fragmentation pattern as that reported in section 11.2. Of the minor products, only the compound at 21 minutes was observed to form. Electrospray ionisation on this compound failed to produce a parent ion above the baseline.

The decay rate of the dibromide radical anion produced on the pulse radiolysis of sodium bromide (0.02 M) did not increase when a small amount of MCPA (1×10^{-3} M) was added. Attempts to react MCPA with the dithiosulfate and diiodide radical anion and azide radical all proved unsuccessful as no increase in the rate of decay of these ions was observed at 475, 380 nm or an increase in absorbance in the spectrum for the azide radical. The dibromide radical anion is an one electron oxidant with redox potential of 1.77 V (versus NHE) while the dichloride radical anion has a redox potential of 2.09 V (versus NHE). Since MCPA reacts with the dichloride radical anion and not the dibromide radical anion the redox

potential of the $\text{MCPA}^{\bullet}/\text{MCPA}^-$ couple in reaction 11.02 must be between 2.09 and 1.77 V (versus NHE).



Decay of the absorbance of the sulfate radical anion at 460 nm produced by a nitrogen saturated potassium persulfate (0.02 M), *t*-butyl alcohol (0.1 M) solution at pH 6.8 (phosphate buffer) was observed to decay faster in the presence of MCPA (1×10^{-4} M), suggesting that MCPA reacts with the sulfate radical anion. Time resolved spectra revealed the decay of the 460 nm maximum and the formation of a new maximum at 305 nm. The spectrum recorded was a similar shape to that observed for the hydroxyl radical experiment and the dichloride radical anion experiment, except that the 350 nm side absorbance was missing. A difference was recorded in the relative heights of the absorbance at 305 nm when compared to the hydroxyl radical experiment. After correction for the lower G value (2.7) the Delta absorbance was recorded at 305 nm was approximately half that of the hydroxyl radical experiment. This suggests the sulfate radical anion is reacting through other mechanisms. No other absorbance was recorded out to 500 nm up to 1000 μs after the pulse.

Steady state irradiation of a nitrogen saturated potassium persulfate (0.02 M), *t*-butyl alcohol (0.1 M), MCPA (1×10^{-4} M) solution at pH 6.8 (phosphate buffer) produced a different trace to that observed for the dichloride radical anion and the hydroxyl radical. Near complete loss of MCPA was observed with the formation of one major product at 8.5 minutes. A non-irradiated sample produced a loss of 25% after a six hour period indicating MCPA undergoes a slow thermal oxidation by the persulfate anion. This does not account for the near complete loss of MCPA (measured in a time period less than the blank), indicating that a chain reaction has been initiated by the reaction of MCPA with the sulfate radical anion. This effect has been observed before for Cyromazine, Dimethrimiol and Hexazinone. A mechanism has previously been postulated by Madhavan *et al.* [201] and involves the reaction of the transient produced by the initial reaction reacting with the persulfate ions generating a product and a new sulfate radical anion.

Mass spectrometry on the product produced a parent ion at 251/253 (3:1) Daltons. Isotope patterns indicate the presence of a chlorine atom in the molecule. Overall the compound has gained 52 Daltons more than the starting compound. MS^2 fragmentation of the parent ion produced a daughter ion at 221 Daltons (minus 30, or CO), further fragmentation of the daughter ion produced an ion at 141 Daltons (minus 80 Daltons). The 141 fragmentation

peak has been previously recorded for MCPA and corresponds to the MCPA minus the CH_2CO_2 group. It would be reasonable to assume that the ring structure has remained intact. The actual structure of this product could not be determined from the mass spectrometric data.

Ab initio calculations performed on the MCPA when neutral and in its deprotonated form (minus one electron from its full electron set) produced the spin surfaces observed in Figure 11.12. The neutral form of MCPA had a spin surface similar to that observed for the neutral form of Dichlorophen, with the radical mainly located over the ring and the oxygen. The spin pattern can therefore be rationalised using similar resonance structures to those observed in Figure 7.19. This spin surface would agree with the experimental results that indicated the reaction of the one electron oxidant with MCPA resulted in formation of a radical cation within the ring. Comparison of the HOMO of MCPA indicates a similarity between the two surfaces, suggesting the electron would be removed by the one electron oxidant from this orbital.

The spin surface for deprotonated MCPA is located over the oxygen of the carboxyl group. This result is not in agreement with experimental results. Further theoretical investigations using phenyl acetate produced the same result as MCPA. Madhavan *et al.* [201] used esr spectroscopy to determine that phenyl acetate reacted with the sulfate radical anion to form a radical cation on the benzene ring.

Single point and spin surface calculations on the optimised geometry of deprotonated MCPA (singlet) as a neutral molecule and a multiplicity of 2 produced a spin pattern located over the three carbons in the ortho and para positions to the OAc group as well as one of the oxygens of the carboxylic acid. As expected, there is an increase in energy of approximately 10 kcal/mol between the optimised and non optimised geometries, indicating that it is not as favourable to have the radical located over the ring as it is to have it over the carboxylic acid group. It can therefore be concluded that the calculations do not produce the desired spin pattern within the ring because there is a global minimum of lower energy than was accessed in the theoretical experiment. As calculations are performed on molecules in the gas phase, it is plausible that the calculations have achieved an energy level attainable for the radical cation in the gas phase, but that is not available in aqueous solution due to subsequent reaction with the solvent.

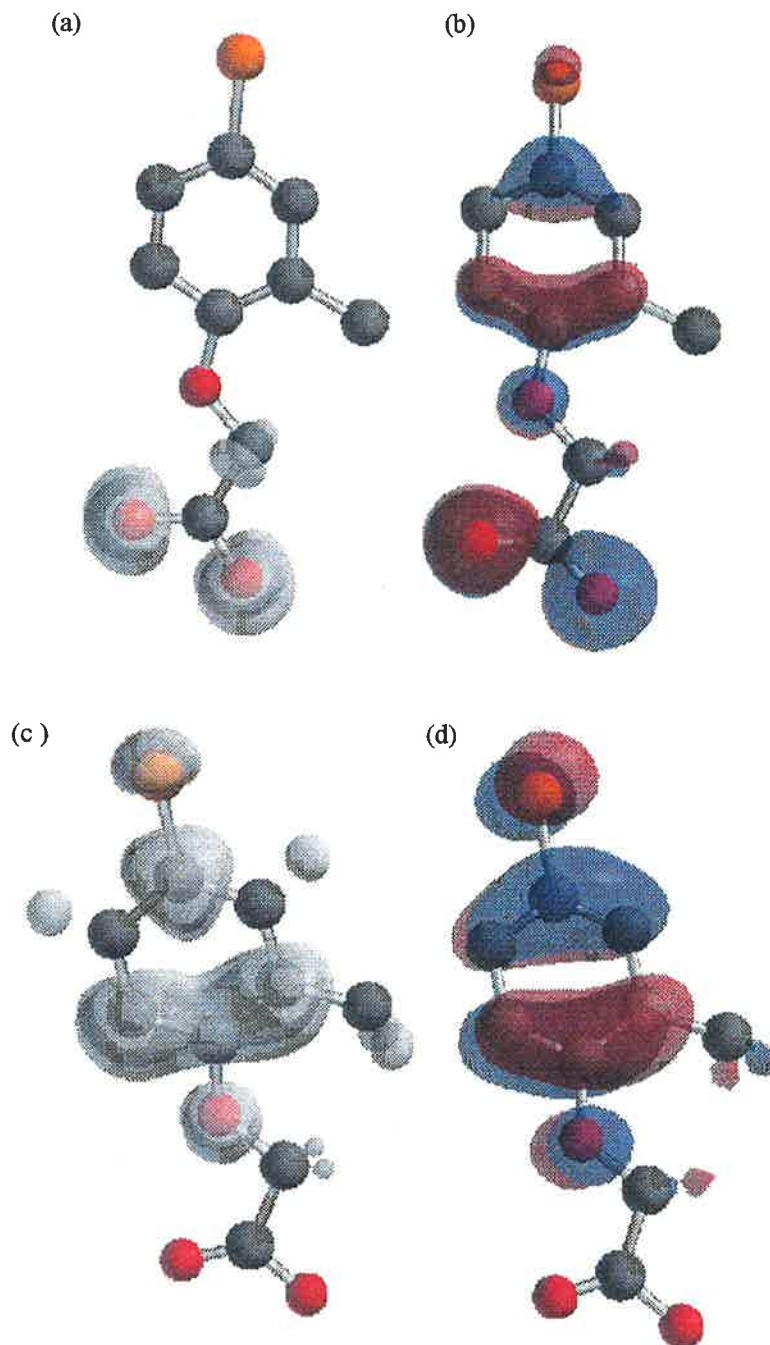


Figure 11.12. Plots of the electron spin density surface (a and c), HOMO (b and d), of Ioxynil as determined by *ab initio* molecular orbital theory. Calculations were performed at the HF/6-31G** level of theory. Plot (a) was determined with a neutral molecule and a multiplicity of 2. Plot (b) was determined for a molecular charge of -1 possessing a corresponding multiplicity of +1. Plot (c) was determined with a molecular charge of +1 and a multiplicity of 2. Plot (d) was determined for the neutral molecule possessing a corresponding multiplicity of +1.

11.6 REACTION OF MCPA WITH THE HYDRATED ELECTRON

Decay of the hydrated electron's absorbance at 640 nm was observed to increase in the presence of small amounts of MCPA (1×10^{-4} M) at pH 6.8 (NaOH), indicating a reaction between the hydrated electron and MCPA is occurring. The time resolved TDA spectrum obtained on pulse radiolysis of a solution containing MCPA (1×10^{-4} M) and *t*-butyl alcohol (0.1 M) saturated with nitrogen gas is shown in Figure 11.13. This spectrum exhibits a small

absorbance in the region between 250 nm and 450 nm. The maximum of the spectra varied with time indicating that the reaction was not instantaneous when compared with the 2.5 μ s pulse. Initially a maximum was observed at wavelengths longer than 500 nm which was due to the absorbance of the hydrated electron, and quickly disappeared to show no new maximum.

Time resolved studies out to 1000 μ s found no new absorbance in the region of 250 to 500 nm, suggesting that the reaction forms stable products that do not absorb in this region.

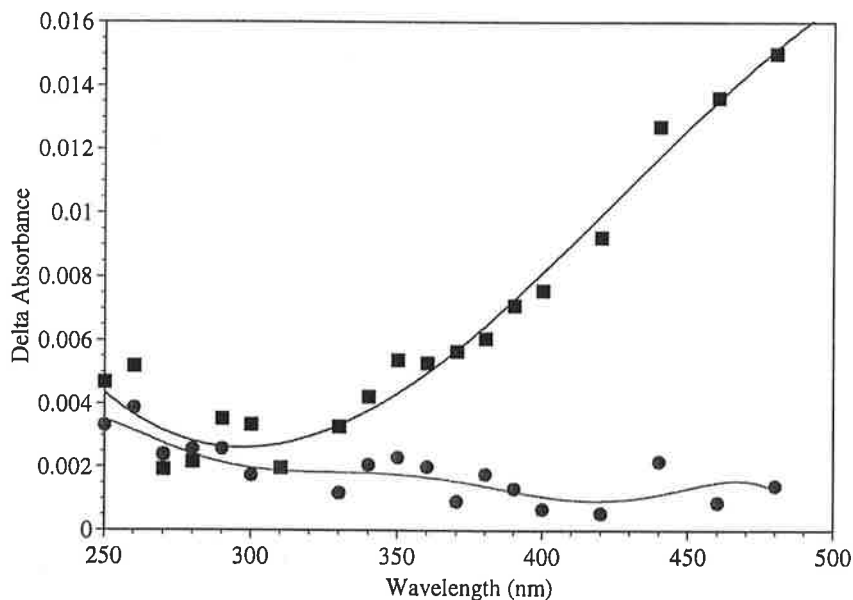


Figure 11.13. Time resolved TDA spectra obtained upon the pulse radiolysis of an aqueous MCPA (1×10^{-4} M) solution containing *t*-butyl alcohol (0.1 M) saturated with nitrogen gas (pH 6.8, phosphate buffer). (■ directly after the pulse, ● 20 μ s).

The bimolecular rate constant for the reaction of the hydrated electron with MCPA was determined from the slope of a plot of the decay rate of the hydrated electron at 640 nm against the concentration of MCPA (20 to 50 μ M). The determined rate constant was 1.5×10^9 $M^{-1}s^{-1}$. Though this is the first reported rate constant for the reaction of the hydrated electron with the MCPA anion, rate constants for compounds with similar functional groups have been determined and are:

Chlorobenzene	$k=9.8 \times 10^8 M^{-1}s^{-1}$ [162]
Benzoate anion	$k=3.1 \times 10^9 M^{-1}s^{-1}$ [202]
Acetate anion	$k=1.1 \times 10^6 M^{-1}s^{-1}$ [202]
Chlorobenzoate	$k=4.1 \times 10^9 M^{-1}s^{-1}$ [162]

The hydrated electron's reaction with MCPA should initially result in the addition of an electron to the MCPA radical (i.e. $\text{MCPA}^{\cdot-}$). It can be observed that the rate constant for the reaction of MCPA with the hydrated electron is similar to that of chlorobenzene. It is therefore probable that the hydrated electron reacts with MCPA in a similar method to its reaction with chlorobenzene.

The HPLC trace of a MCPA (1×10^{-4} M) solution containing, *t*-butyl alcohol (0.1 M) and saturated with nitrogen (pH 6.8, phosphate buffer and NaOH) following gamma irradiation is shown in Figure 11.14. Effect on optical absorbance is a decrease in the absorbance maximum at 232 nm with no new maximum observed throughout the irradiation period. The maximum at 280 nm was not affected by the reaction of the hydrated electron with MCPA. The HPLC trace indicated the formation of a major peak at 11 minutes. Mass spectrometry on this peak produced no observable parent ion above base line. MS^2 fragmentation at 165 Daltons (± 1 Dalton) produced a daughter ion at 121 Daltons. The difference between the two ions equates to the loss of a CH_2CO_2 group from the product. The parent ion chosen for the MS^2 experiment is MCPA with a chlorine atom replaced by a hydrogen atom. Therefore this is the same fragmentation as observed for MCPA. Though the observation of a parent ion at 165 Daltons would have been conclusive evidence for the dehalogenation reaction of MCPA, the MS^2 fragmentation pattern does indicate that the formation of this product is probable and its parent ion was not observable above the base line. The exact mechanism for the reaction of the hydrated electron with MCPA would be initial electron capture, followed by ejection of a chloride ion leaving an alkyl radical. This radical would then extract a hydrogen atom from the *t*-butyl alcohol to form the final stable product [94]. These observations allowed the postulation of the mechanism in Figure 11.15.

Analysis of the above solution after steady state irradiation for the chloride ion indicated its presence. The G value for the production of the chloride ion was determined to be 0.50. For the loss of a chloride ion this G value is slightly less than that for the loss of MCPA (0.66). This indicates the chloride anion is being eliminated from the molecule as a result of the hydrated electron's reaction with MCPA.

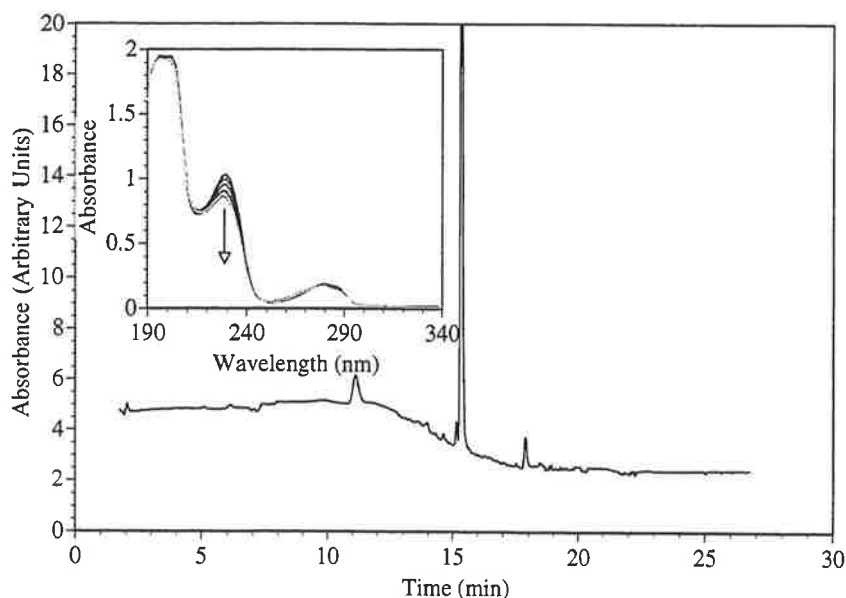


Figure 11.14. HPLC analysis following the gamma irradiation of a MCPA (1×10^{-4} M) solution containing, *t*-butyl alcohol (0.1 M) and saturated with nitrogen (pH 7.0, phosphate buffer and NaOH). The trace displays the products formed from the reaction of the hydrated electron with MCPA. See text for details. Inset. Change in optical absorption of the same solution (0 to 400 Gray). Arrow indicates direction of absorbance change with radiation dose.

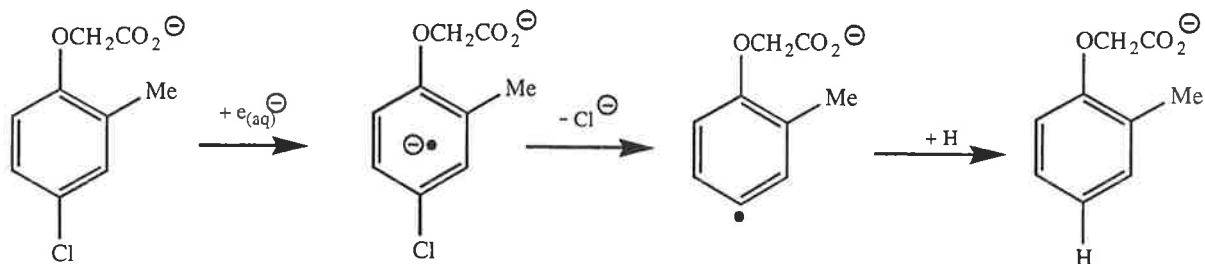


Figure 11.15. Reaction mechanism for the reaction of the hydrated electron with MCPA.

Ab initio calculations performed on the deprotonated form of MCPA revealed the carbon atom attached to the oxygen atom of the OAc group to be the most electron deficient in the molecule with the second most electron deficient the carbon attached to the chlorine atom. This would in theory make these sites the most favourable for electron addition.

Ab initio calculations were performed on the deprotonated form of MCPA when neutral and in its deprotonated form (with the addition of an extra electron to its full electron set) and optimised at HF/6-31G** as a doublet. During the optimisation process it was observed that the chlorine atom fragmented from the molecule and moved away from the remaining fragment of MCPA (Figure 11.16). The spin surface of the final optimised structure was located on the carbon where the chlorine had been attached and on the carbons in the meta positions. No spin surface was calculated on the chlorine atom (Figure 11.17). The LUMO was determined to be located over four carbons in the aromatic ring.

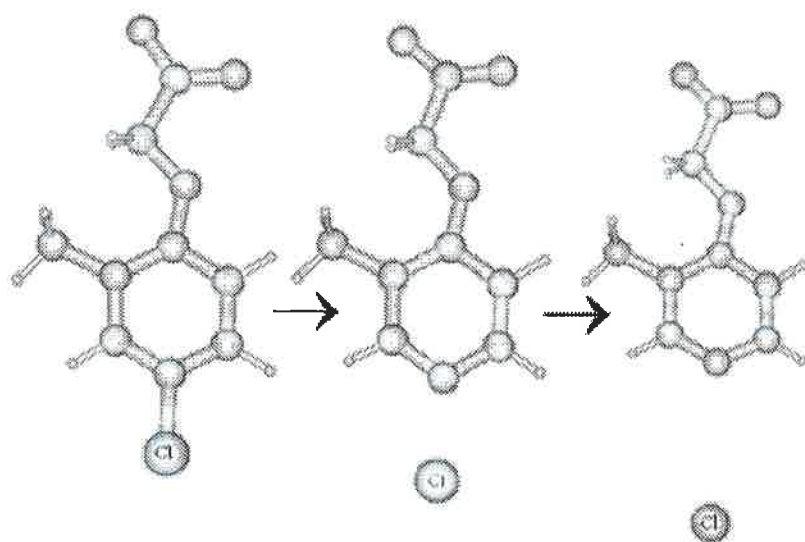


Figure 11.16. Starting, middle and final geometry of the deprotonated form of MCPA as determined by *ab initio* molecular orbital theory. Calculations were performed at the HF/6-31G** level of theory. The geometries displayed indicate the departure of the chlorine atom from the molecule.

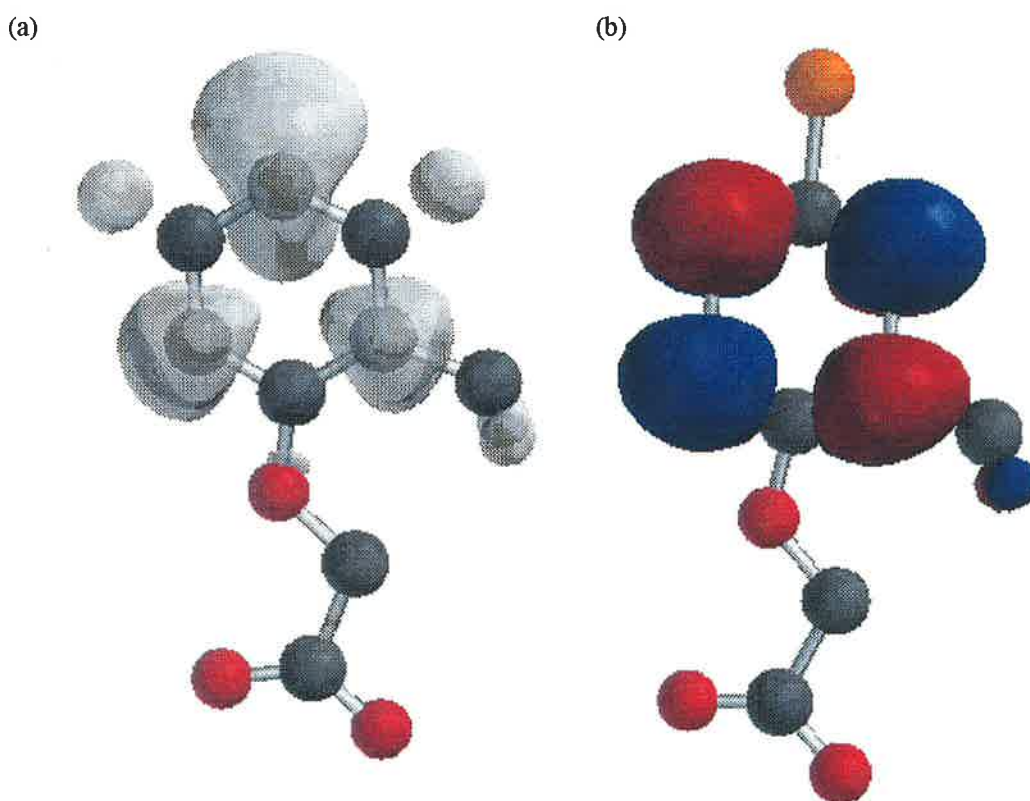


Figure 11.17. Plots of the electron spin density surface minus the departed chlorine atom (a), and LUMO (b), of MCPA as determined by *ab initio* molecular orbital theory. Calculations were performed at the HF/6-31G** level of theory. Plot (a) was determined with a molecular charge of -2 and a multiplicity of 2. Plot (b) was determined with a molecular charge of -1 possessing a corresponding multiplicity of +1. (Hydrogens not shown).

11.7 REACTION OF MCPA WITH THE HYDROGEN ATOM

Figure 11.18 shows the TDA spectrum obtained upon the pulse radiolysis of an aqueous MCPA (1×10^{-4} M) solution containing *t*-butyl alcohol (0.1 M) saturated with nitrogen

(pH 2, HClO₄). It exhibits absorption maxima at 305 and 345 nm. The spectrum is similar to the spectra recorded by Getoff *et al.* [94] for the reaction of the hydrogen atom with 4-chlorophenol and what we have determined for Dichlorophen. Since the TDA spectrum is similar in shape to the 4-chlorophenol transient spectrum produced by the reaction with hydrogen atoms, and this was assigned to a H-adduct, then the transient observed for the reaction of MCPA with hydrogen atoms can also be assigned to the same type of transient.

Formation kinetics were performed on the maximum from the slope of a plot of the pseudo first order rate constant against the concentration of MCPA at 345 nm. The result indicates a bimolecular rate constant for the reaction of $2.6 \times 10^9 \text{ M}^{-1} \text{ s}^{-1}$. The rate constant for the benzene derivatives are of a similar magnitude to that of MCPA. Benzene derivatives mentioned below all react with hydrogen atoms through addition to form a H-adduct. Similarity of the rate constants below also strengthens the argument that hydrogen atoms add to MCPA.

Toluene	$k=2.6 \times 10^9 \text{ M}^{-1} \text{ s}^{-1}$ [203]
Chlorobenzene	$k=1.4 \times 10^9 \text{ M}^{-1} \text{ s}^{-1}$ [204]
Anisole	$k=1.2 \times 10^9 \text{ M}^{-1} \text{ s}^{-1}$ [66]
Acetic acid	$k=7.7 \times 10^4 \text{ M}^{-1} \text{ s}^{-1}$ [205]

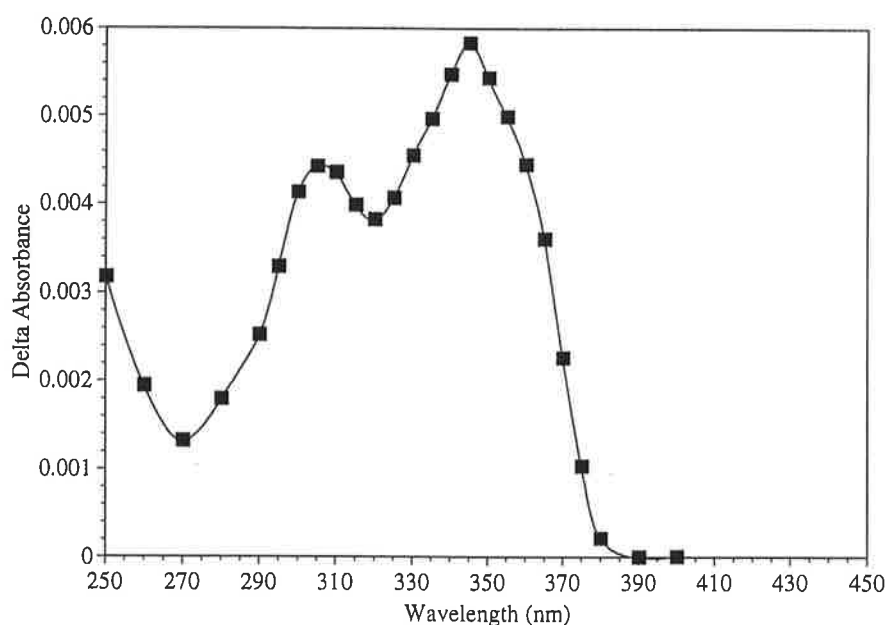


Figure 11.18. TDA spectrum obtained upon the pulse radiolysis of an aqueous MCPA ($1 \times 10^{-4} \text{ M}$) solution containing *t*-butyl alcohol (0.1 M) saturated with nitrogen (pH 2, HClO₄). Spectrum recorded 10 μs after the pulse.

Steady state irradiation of an aqueous MCPA (1×10^{-4} M) solution containing *t*-butyl alcohol (0.1 M) saturated with nitrogen (pH 2, HClO₄) produced a decrease in the absorbance area of the peak in the HPLC trace corresponding to MCPA. Formation of three products in the HPLC trace was also observed at 6, 8 and 10 minutes (data not shown). Absorbance of the products was small, suggesting the molar absorbance of the product was not large at 232 nm. All attempts to determine the mass to charge ratio of these compounds using electrospray mass spectrometry failed. From the pulse radiolysis results it can be presumed the products produced from the reaction are the result of an addition of the hydrogen atom to the starting compound.

11.8 REACTION OF MCPA WITH REDUCING RADICALS.

Pulse radiolysis of a nitrous oxide saturated solution containing sodium formate (0.02 M) and MCPA (1×10^{-4} M) (pH 6.8, phosphate buffer) produced a maximum below 250 nm with no other absorbance maxima observed. The absorbance observed was due to the formation of the carbon dioxide radical anion. Time resolved studies out to 1000 μ s did not find any new absorption in the range of 250 nm to 600 nm. This suggests the carbon dioxide radical does not react with MCPA. The redox potential of the carbon dioxide radical has been determined to be -2.0 V (versus NHE) [43, 111]. Redox potential of MCPA⁻/MCPA^{* 2-} must therefore be more negative than -2.0 V. This means that MCPA^{* 2-} is a strong reducing agent with a reduction potential between -2.0 and -2.9 V (versus NHE).

Gamma irradiation of the same solution produced no loss of MCPA when sufficient radical was added into the matrix to react with 50% of the available starting compound. This result confirms those obtained in the pulse radiolysis experiments.

11.9 OVERVIEW OF THE RADIATION CHEMISTRY OF MCPA

This study for the first time has allowed elucidation of the radiation chemistry of aqueous MCPA. The new chemistry for MCPA is summarised in Figure 11.19.

The TDA spectrum obtained from the reaction of MCPA with hydroxyl radicals suggests the formation of a OH-adduct as an intermediate. The rate constant obtained for the reaction of MCPA with the hydroxyl radical is similar to that of compounds with the same functionality with the hydroxyl radical. Reaction of these compound with the hydroxyl radical is known to proceed through a OH-adduct intermediate, supporting our hypothesis.

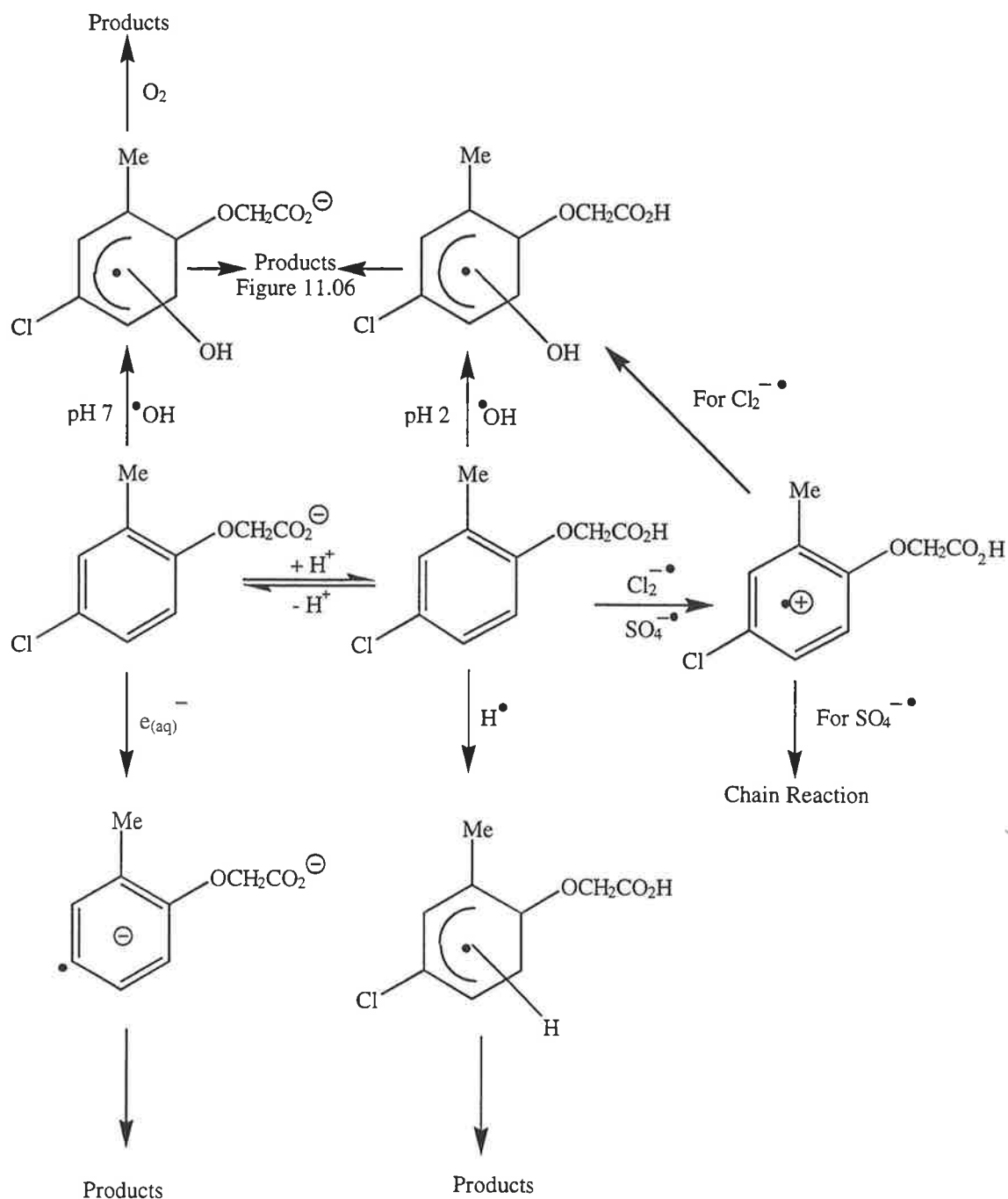


Figure 11.19. Overview of the radiation chemistry discovered in this study.

The decay rate of the OH-adduct shows dependence on the ionic strength of the solution, therefore the transient is charged. The transient decays by second order kinetics, indicating that degradation products are formed by radical-radical reactions. HPLC characterisation of the compounds formed by the reaction of MCPA with the hydroxyl radical shows the major product had a retention time greater than MCPA. This suggests that the degradation major product is less polar than MCPA. Mass spectrometric studies determined through isotope patterns that the major product is a dimer. This is in agreement with what we have determined through the pulse radiolysis studies. Minor products were determined to be the hydroxylated form of MCPA. The rate of MCPA loss and the formation of products from

the reaction of MCPA with the hydroxyl radical is initially linear under steady state irradiation. As the amount of hydroxyl radicals is increased past 35% of MCPA's concentration, the loss of MCPA and the formation of products follows a higher order kinetic mechanism. This result suggests products of the initial reaction also react with the hydroxyl radical to form (uncharacterised) compounds.

Corrected TDA spectrum obtained upon reaction of the hydroxyl radical with MCPA at pH 2 matches that obtained from the same reaction at neutral pH. Steady state irradiation of MCPA at pH 2 reproduced the results obtained at neutral pH.

The transient produced from the reaction of MCPA with the hydroxyl radical has been shown to be reactive with oxygen. Gamma irradiation coupled with HPLC shows the formation of the major product obtained for the de-oxygenated experiment as well as new species. Mass spectral fragmentation data indicates that the predominate species results from the addition of molecular oxygen to the transient.

The TDA spectrum obtained from the reaction of MCPA with the dichloride radical anion is similar to that obtained for the OH-adduct of MCPA, thus the radical cation produced transforms into a OH-adduct via the addition of water and the elimination of a hydrogen ion. MCPA is not observed to react with the dibromide radical anion and therefore the resulting radical of MCPA is a powerful one electron oxidant with a redox potential between 2.09 to 1.71 Volts (versus NHE). Gamma irradiation coupled with HPLC for the dichloride radical anion shows that newly formed compounds are the same as those observed for the addition of the hydroxyl radical to MCPA. The sulfate radical anion was observed to react through a chain reaction mechanism under steady state conditions.

Ab initio calculations indicate that the HOMO of neutral MCPA is located over the benzene ring. It is suspected that the electron lost to the oxidant occurs from this orbital, which is in agreement with the experimental results. The spin density surface is also located on the ring, and can be accounted for by resonance theory. The HOMO of the deprotonated form is located on the aromatic ring and the oxygen of the carboxylic group. The spin density surface locates the radical over the oxygens, which is not in agreement with experimental results. The surface produced indicates that the optimisation process has found a lower energy state available for the radical cation in the gas phase than is available in aqueous solution.

The TDA spectrum for the reaction of MCPA with the hydrated electron produces a small absorbance spectrum. The rate constant obtained for the reaction of MCPA with the

hydrated electron is similar to that of chlorobenzene [162], suggesting that the hydrated electron reacts with aromatic ring. Gamma irradiation coupled with HPLC found one major product for the reaction of the hydrated electron with MCPA. Using mass spectral fragmentation we have determined that the compound is the dehalogenated form of MCPA. This was confirmed by a positive chloride ion determination experiment. The radical anion of MCPA is a strong reducing agent with a redox potential between -2.0 and -2.9 V. In natural and industrial waste water the elimination of the chloride ion would prevent the radical anion from reforming MCPA, thus allowing for its breakdown.

Ab initio calculations indicate that the LUMO of MCPA is located on the aromatic ring. Geometry optimisation of the radical anion resulted in the chlorine atom departing from the rest of the molecule. The spin density surface of the radical indicates the chlorine atom has no radical character, while the aromatic ring shows radical character that is described by resonance theory.

The TDA spectrum for the reaction of MCPA with hydrogen atoms is similar to that observed for the H-adduct of Dichlorophen and 4-chlorophenol [94]. Steady state irradiations of MCPA at pH 2 produced three products in the HPLC trace, however none of the structures could be characterised.

MCPA will degrade following reaction with a number of free radicals produced in natural and treated industrial discharge water. Chloride ion elimination will occur for the reaction of MCPA with one electron reducing agents.

12.0 Radiation Chemistry of Aqueous Acifluorfen Solution

12.0 ACIFLUORFEN

Acifluorfen (5-[2-chloro-4-(trifluoromethyl)phenoxy]-2-nitrobenzoic acid) (Figure 12.01) is a white solid with a melting point of 142-160°C [206]. The maximum solubility of Acifluorfen is 120mg/L, though its solubility increases markedly in its deprotonated state.

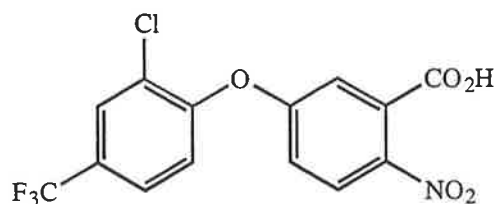


Figure 12.01. Chemical Structure of Acifluorfen.

Acifluorfen is a contact herbicide used to control broad leaf weeds and grasses in crops like soybeans, peanuts and peas [207]. Application can be both pre and post emergent. Acifluorfen's activity is known to increase markedly when exposed to sunlight. This is due to its ability to form singlet oxygen and the superoxide radical anion [208, 209] when photochemically excited. Susceptible plants absorb Acifluorfen through their roots and leaves, with no resulting translocation. The result of no translocation is the inhibition of one of the plants critical enzymes called pyrotoporphyrinogen oxidase. Resistant plants like soybeans metabolise Acifluorfen into harmless non-toxic forms [210, 211].

Acifluorfen is a moderately persistent herbicide with detectable levels lasting from four to six weeks in soil. Microbial action is thought to be responsible for the majority of Acifluorfen degradation in the environment [207, 212]. Leaching of Acifluorfen does not occur since no detectable levels are found more than three inches below the soil surface. Presence of Acifluorfen has never been recorded in well water [212].

Acifluorfen is stable to hydrolysis from water, with no observable degradation occurring over a 28 day period. When Acifluorfen is exposed to sunlight the degradation is greatly enhanced. The half life of Acifluorfen has been reported at 92 hours with continuous irradiation [212]. Photodecomposition produces non-herbicidal products which tend to vaporise into the atmosphere [206].

12.2 REACTION OF ACIFLUORFEN WITH THE HYDROXYL RADICAL

Figure 12.02 shows the time resolved TDA spectra obtained upon the pulse radiolysis of an aqueous Acifluorfen (1×10^{-4} M) solution saturated with nitrous oxide (pH 6.8, phosphate buffer). It exhibits an absorption band with maxima at 350 nm and 440 nm. In the presence of *t*-butyl alcohol (0.1 M), an effective hydroxyl radical scavenger but a weak hydrogen atom scavenger, the absorption spectrum was considerably reduced. The high G ($\cdot\text{OH}$) yield and appreciable decrease in the transient absorption suggests the transient absorption spectrum in Figure 12.02 is mainly due to the reaction of hydroxyl radicals with Acifluorfen.

A negative absorbance was detected in the TDA spectrum recorded between the hydroxyl radical and Acifluorfen with the minimum being recorded at 295 nm. This is because the Acifluorfen anion possesses a ground state absorbance in the region of 250 to 450 nm. It is observed that this absorbance continues to decrease with time producing a more negative absorbance at 295 nm. The TDA spectrum can be corrected for the small ground state absorbance by using formula 3.14 and the assumption that the yield of hydroxyl radicals is equal to the yield of the transient radical. The resulting spectrum exhibits a maximum at 300 nm, with the molar absorbance of $9100 \text{ M}^{-1}\text{cm}^{-1}$.

Reducing the dose (and hence the amount of transient radical) produced an increase in the half life of the transient species at both wavelengths. The radical therefore decays by second order kinetics. When the decay curves were fitted to second order kinetics they produced decay rates of $2k/\epsilon l = 5.3 \times 10^4 \text{ s}^{-1}$ and $2.4 \times 10^5 \text{ s}^{-1}$ at 350 and 440 nm, respectively. Assuming that all the hydroxyl radicals react with Acifluorfen and the G value of the hydroxyl radical is equal to the G value of the transient (ie. 5.5) the molar absorbance of the maxima were calculated to be 2870 and $418 \text{ M}^{-1}\text{cm}^{-1}$ for 350 and 440 nm, respectively. Using these molar absorbance values, it was determined that $2k = 1.6 \times 10^8 \text{ M}^{-1}\text{s}^{-1}$ and $1.0 \times 10^8 \text{ M}^{-1}\text{s}^{-1}$ respectively. Similarity in the decay rates suggests that the absorbance maxima at 350 and 440 nm may be due to the formation of the same species. The transient therefore decays to products via radical-radical reactions.

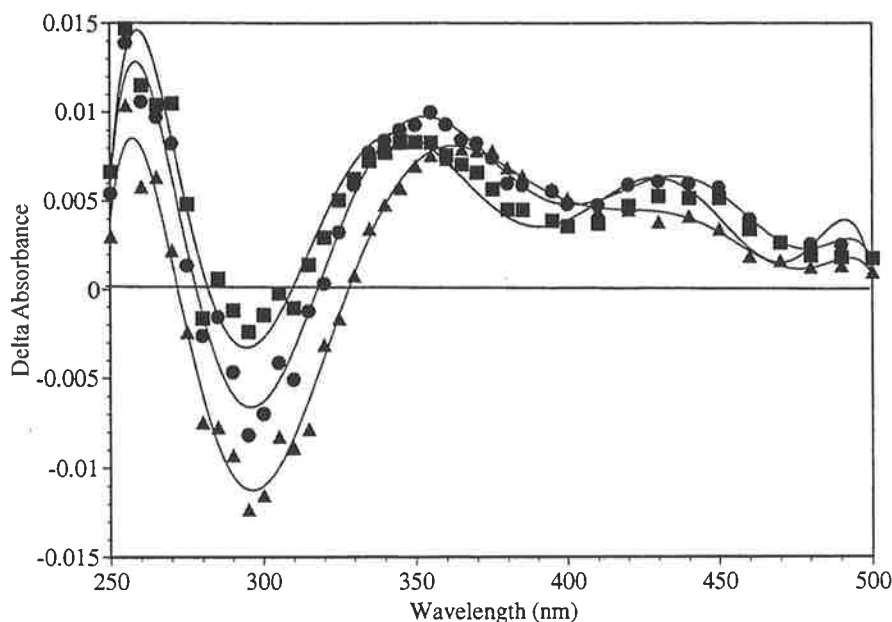


Figure 12.02. Time resolved TDA spectra upon the pulse radiolysis of an aqueous Acifluorfen (1×10^{-4} M) solution saturated with nitrous oxide (pH 6.8, phosphate buffer). (■ Directly after the pulse, ● 10 μ s after the pulse, ▲ 100 μ s after the pulse).

The reactions of chlorobenzene, nitrobenzene, benzoate anion and 1,4-nitrobenzoate anion with the hydroxyl radical have all been previously studied. All these compounds react with the hydroxyl radical through an addition reaction to form the OH-adduct. It is therefore assumed that Acifluorfen also reacts through this type of mechanism. The reaction of $\alpha\alpha\alpha$ -trifluorotoluene with hydroxyl radicals had not been previously studied [149], thus no information could be obtained from this reaction.

Adjusting the ionic strength of the solution at pH 6.8 with NaClO_4 (1 M) caused an increase in the rate of decay of the transient at 350 nm, indicating the transient is charged. A charged transient is consistent with addition of the hydroxyl radical to Acifluorfen, as the intermediate resulting at pH 6.8 would possess a negative charge.

Competition kinetics determined a bimolecular rate constant for the reaction of hydroxyl radicals with the Acifluorfen anion of $2.7 \times 10^9 \text{ M}^{-1}\text{s}^{-1}$. This rate constant indicates that the Acifluorfen anion reacts with hydroxyl radicals at slightly less than diffusion controlled rates.

Though the rate constant is the first reported for the reaction of the hydroxyl radical with the Acifluorfen anion, rate constants for molecules that contain similar functional groups have been determined. These rate constants are;

Nitrobenzene

$4.0 \times 10^9 \text{ M}^{-1}\text{s}^{-1}$ [155]

1,4 Nitrobenzoate	$2.6 \times 10^9 \text{ M}^{-1} \text{ s}^{-1}$ [44]
1,4 Nitrophenol	$3.8 \times 10^9 \text{ M}^{-1} \text{ s}^{-1}$ [213]
Chlorobenzene	$5.8 \times 10^8 \text{ M}^{-1} \text{ s}^{-1}$ [155]

It is observed from the data presented above that the rate constant obtained for Acifluorfen with the hydroxyl radical is similar to the reactions with compounds containing the same functional groups. The relatively slow rate constant of Acifluorfen is due to the electron withdrawing nature of all the substituents on both aromatic rings.

Steady state irradiation of an aqueous Acifluorfen ($1 \times 10^{-4} \text{ M}$) solution saturated with nitrous oxide and irradiated gamma irradiation using cobalt 60 (Dose 66 Grays per hour) produced only a small decrease in the absorbance due to the Acifluorfen anion at 300 nm (Figure 12.03). Small increases in absorbance were also observed at 260 and 390 nm.

HPLC analysis following gamma irradiation of an Acifluorfen ($1 \times 10^{-4} \text{ M}$) solution saturated with nitrous oxide (pH 6.8, phosphate buffer) found the formation of new products and a decrease in the concentration of Acifluorfen (Figure 12.04) at 228 nm. One major product (E) was detected in the trace along with other minor products (A to D & F to J). All products were of a retention time less than Acifluorfen suggesting all the products were more polar than the starting compound which is consistent with the addition of the hydroxyl radical to Acifluorfen. Products A and B were at a retention time significantly less than that of the rest of the products, suggesting that when compared to the remainder of the products, A and B are appreciably more polar. Apart from the labelled compounds (A to J) the formation of an appreciable amount of minor products was observed in the region between 15 and 19 minutes.

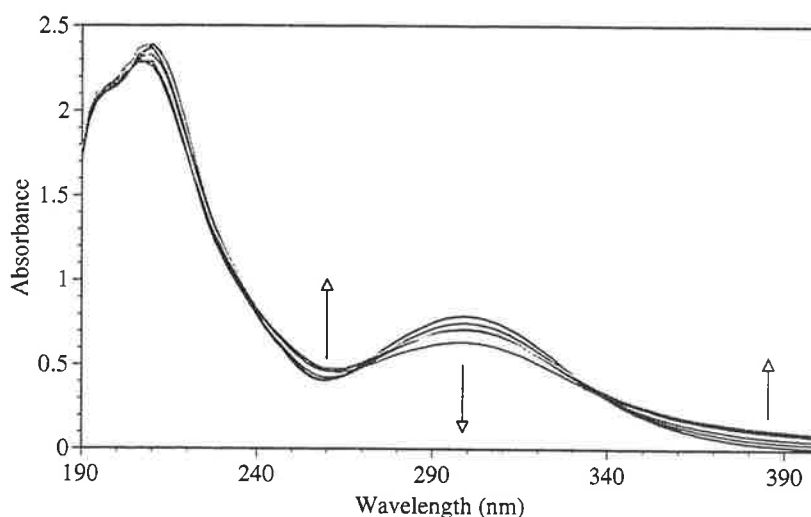


Figure 12.03. Observed change in optical absorbance of an aqueous Acifluorfen ($1 \times 10^{-4} \text{ M}$) solution saturated with nitrous oxide and irradiated gamma irradiation (0 to 180 Gray). Arrows indicate the direction of absorbance change with radiation dose.

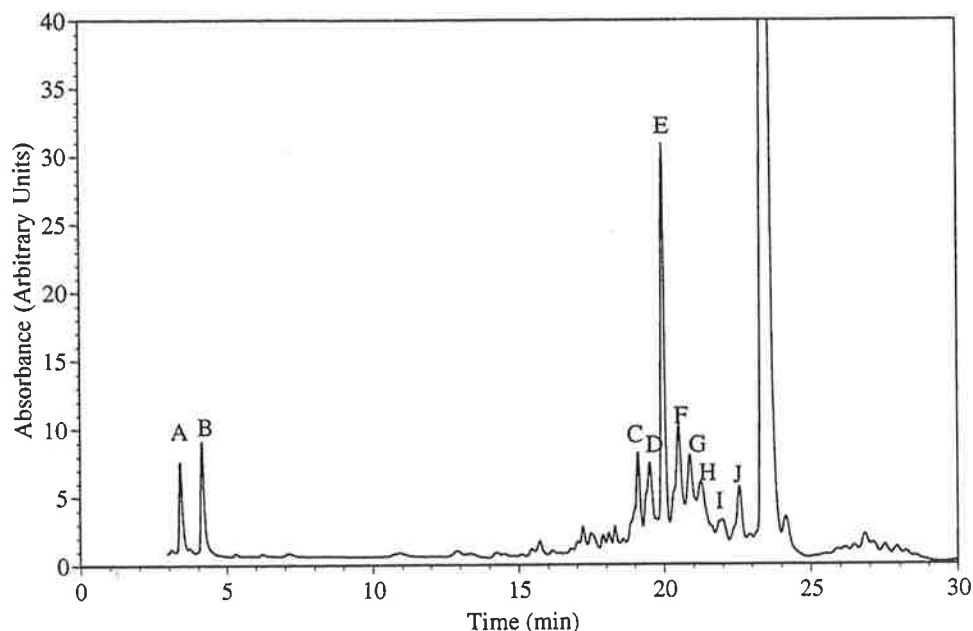


Figure 12.04. HPLC analysis following the gamma irradiation of Acifluorfen (1×10^{-4} M) solution saturated with nitrous oxide (pH 6.8, phosphate buffer). The trace displays the products formed from the reaction of Acifluorfen with hydroxyl radicals (A to J). See Figure 12.08 for product identification.

Rate of Acifluorfen loss was linear against the concentration of hydroxyl radicals added to the system (calculated using Frickie Dosimetry), until approximately 30% of the Acifluorfen anion had reacted. Appearance of the products was also followed by HPLC and found to be initially linear. This suggests the products of the initial reaction also react with hydroxyl radicals.

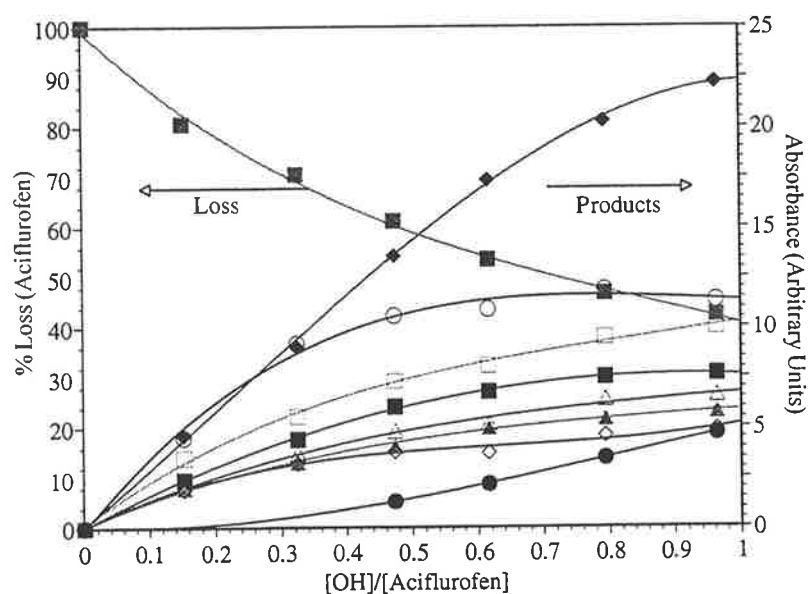


Figure 12.05. Loss of Acifluorfen anion (left axis) and the formation of the products (right axis) from the gamma irradiation of the aqueous Acifluorfen (1×10^{-4} M) solution saturated with nitrous oxide (pH 6.8 (phosphate buffer)). Products are B=■, C=●, D=▲, E=◆, F=○, G=□, H=△, J=◇. (A and I not shown).

Structures of the products from the reaction of the hydroxyl radical with Acifluorfen were determined by electrospray mass spectrometry and are recorded in Figure 12.06. Acifluorfen produced a parent ion with a mass to charge ratio of 360/362 (3:1) Daltons ($M-H^+$) with a fragmentation pattern (using MS^2 experiment) that consisted of two daughter ions at 316 and 165 Daltons. The fragmentation pattern corresponds to the loss of CO_2 and $Ph(NO_2)(CO_2)$ from Acifluorfen, respectively. Further fragmentation of the 316 Daltons daughter ion produced a grand-daughter ion at 286 Daltons (minus NO). Though it might be expected that NO_2 would be lost instead of NO, fragmentation of this type for NO_2 is common [159].

The major product E produced a parent ion at 376/378 (3:1) Daltons. This mass to charge ratio corresponds to the addition of 16 Daltons or an oxygen atom to the original Acifluorfen. Fragmentation of the parent ion at 376 Daltons produced two daughter ions at 340 (minus HCl) and 296 Daltons (minus $HClCO_2$). Fragmentation produced by this experiment is different from that observed for Acifluorfen and does not allow for any structural information to be obtained concerning the position of the hydroxyl group. Further fragmentation of the 296 Dalton ion produced a loss of 30 Daltons (NO) followed by a number of grand-daughter ions, including 176 Daltons which corresponds to $CF_3Ph(OH)O$. This allows for the tentative assignment of product E as the hydroxylated product of Acifluorfen with the OH group on the chlorobenzene ring.

Compound D also produced a parent ion at 376/378 (3:1) Daltons. The fragmentation pattern of this product was different from that observed for the major product. MS^2 fragmentation produced a daughter ion which was minus 44 Daltons (CO_2) from the parent ion. Further fragmentation produced the loss of the NO atoms. No information could be obtained concerning the position of the hydroxyl group in the compound.

Compounds G, H, I, J all produced the same parent ion of 755/757/759 (4:3:1) Daltons. The mass corresponded to the dimerisation of the OH-adducts. The isotope pattern of 4:3:1 indicates there are two chlorine atoms in the molecule which is consistent with dimer formation. MS^2 fragmentation in all cases produced a base peak daughter ion of 376, which corresponds to the monomer. Small variations between compounds were detected in the minor daughter ions observed in this fragmentation. The fragmentation pattern in all cases did not allow for any further structural information to be obtained on the product. The mass of the dimer suggests the product does not eliminate water to reform the more thermodynamically stable aromatic species.

Compound C produced a single parent ion of 342 Daltons. Absences of the 3:1 isotope pattern indicates that the chlorine atom is not present in the molecule. Product C corresponded to the addition of a hydroxyl group and the loss of a chlorine atom. The formation of a similar type of product has been observed for Dichlorophen. Addition of the hydroxyl group occurs on the carbon ortho or para to the carbon attached to the chlorine atom. Following the disproportionation reaction of the transient, the resulting species that has a double bond from the aromatic ring saturated undergoes elimination of HCl to reform the more thermodynamically stable aromatic product.

Products A and B both failed to produce parent ions which were above the base line, thus no information can be ascertained concerning their structures. The polarity of the two compounds when compared to the other compounds in the HPLC chromatogram suggests that they are not structurally similar to the remaining products.

Ab initio calculations performed on the deprotonated form of Acifluorfen (with one proton missing from the carboxylic acid) indicated that the chlorobenzene ring had more electron density than the other ring. The total natural charge of the carbon in the chlorobenzene ring is 0.13 of an electron greater than that of the other ring. The carbon with the highest natural population is the sterically unhindered carbon ortho to the oxygen in the chlorobenzene ring. The next two highest are both on the nitrobenzoate ring. These results suggest that the distribution of the hydroxyl radical addition would be evenly spread over both rings.

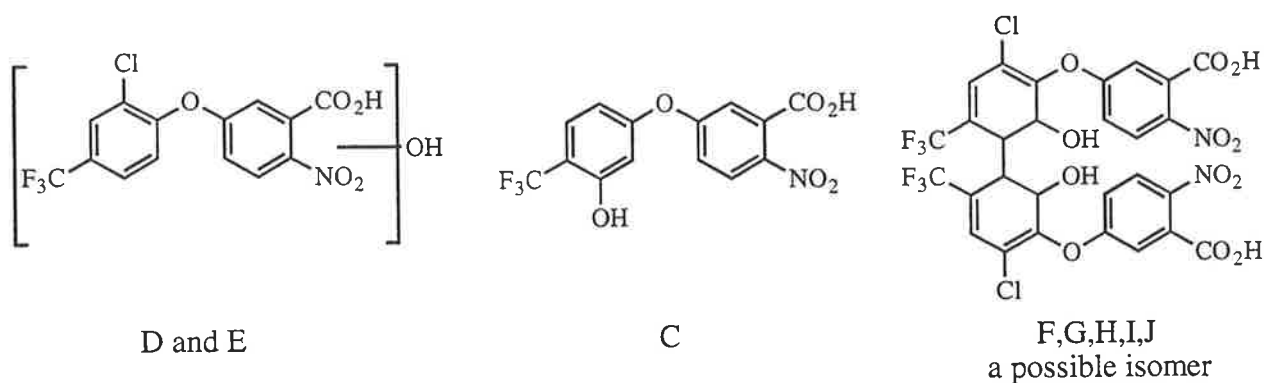


Figure 12.06. Products (C to J) of the gamma radiolysis of an aqueous Acifluorfen in nitrous oxide saturated solution as determined by the analysis of electrospray mass spectrometric fragmentation data. Location of the hydroxyl groups in structure D and E are not unambiguously assignable. Location of the bridge and the hydroxyl group in F to J are not unambiguously assignable.

12.3 REACTION OF ACIFLUORFEN WITH THE HYDROXYL RADICAL IN ACIDIC SOLUTION

The corrected TDA spectrum obtained from the pulse radiolysis of Acifluorfen (1×10^{-4} M) in acidic solution (pH 2, HClO_4) saturated with nitrous oxide was the same as that determined for the neutral pH experiment. A correction to the spectrum was made to take into account the lower G value at pH 2 due to formation of the hydrogen atoms from the hydrated electron with extra hydrogen ions.

Competition kinetics determined a bimolecular rate constant for the reaction of hydroxyl radicals with Acifluorfen of $1.6 \times 10^9 \text{ M}^{-1} \text{ s}^{-1}$. This rate constant indicates that the neutral form of Acifluorfen reacts at approximately half the rate of the anion. The decrease in the rate constant is expected because the available electron density of the neutral form is less than that of the anion. This decreases the rate at which the electrophilic hydroxyl radical reacts.

Steady state irradiation of Acifluorfen at pH 2.0 was attempted but no results could be obtained because the Acifluorfen precipitated out of solution over the time scale of irradiation.

Ab initio calculations were repeated with the neutral form of Acifluorfen. Natural population analysis revealed a change in the order of the atoms with the highest natural charge. The most electron dense carbons were the two carbons ortho to the carbon attached to the oxygen on the nitrobenzoate ring (Appendix 1). Natural populations of both rings were observed to decrease overall when compared to the anion. The reaction of Acifluorfen with hydroxyl radicals occurs at less than diffusion-controlled rates. There is also an observable change in the natural population of Acifluorfen suggesting the electrophilic nature of the hydroxyl radical may result in changes altering the position of the hydroxyl radical addition.

12.4 REACTION OF ACIFLUORFEN WITH THE HYDROXYL RADICAL IN THE PRESENCE OF OXYGEN

Decay of the transient produced by the reaction of hydroxyl radicals with the Acifluorfen anion (pH 6.8, phosphate buffer) in a solution saturated with nitrous oxide/oxygen (4:1 v/v), produced no observable change in the rate at 350 nm. It is known that all but cyclohexadienyl carbon centred radicals react quickly with oxygen [94]. OH-adducts are also known to react reversibly with oxygen [94]. It is possible that the OH-adduct formed reacts with oxygen too slowly to be observed by pulse radiolysis.

Steady state irradiation of a Acifluorfen (1×10^{-4} M) solution saturated with nitrous oxide/oxygen (pH 6.8, phosphate buffer) produced a change in the product distribution from that observed in the de-oxygenated solution (Figure 12.07). This result is consistent with the reaction of oxygen with the transient being slow when compared to the bimolecular reaction of the transient with itself. The steady state irradiation concentration of the transient is orders of magnitude lower than pulse radiolysis, [101] making the pseudo first order reaction with oxygen more favourable than the bimolecular reaction with itself.

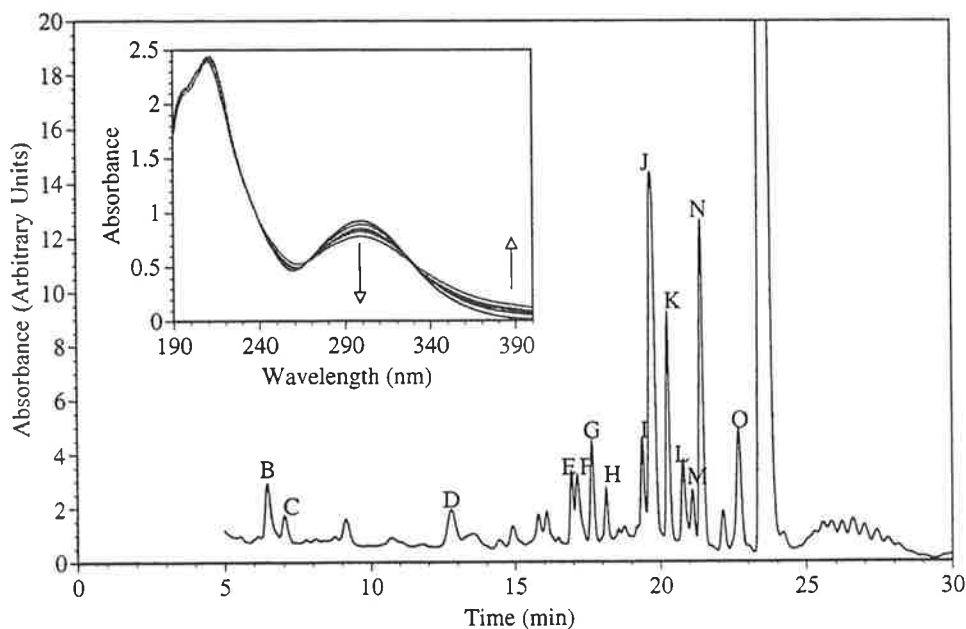
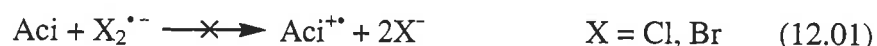


Figure 12.07. HPLC analysis following the gamma irradiation of a Acifluorfen (1×10^{-4} M) solution saturated with nitrous oxide/oxygen (pH 6.8, phosphate buffer). The trace displays the products formed from the reaction of Acifluorfen with hydroxyl radicals in the presence of oxygen (B to O). See text for discussion. Inset, Observed change in optical absorbance of an aqueous Acifluorfen (1×10^{-4} M) solution saturated with nitrous oxide/oxygen and irradiated gamma irradiation (0 to 180 Gray). Arrows indicate the direction of absorbance change with radiation dose.

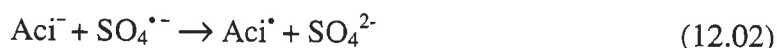
Electrospray mass spectrometry on all of the minor products (B, C, D, E, F, G, H and O) proved unsuccessful in producing a parent ion that was above the baseline because of interference from the ion pairing reagent TFA used in the chromatography. Compounds J, K, L, M and N all produced the same parent ion of 376/378 (3:1) Daltons, indicating they are all the hydroxylated products. After addition of the hydroxyl radical to Acifluorfen, oxygen adds to the OH-adduct which then reacts to form the corresponding hydroxylated product through a mechanism described by Pan *et al.* [82]. Fragmentation patterns of some products varied slightly indicating no contamination had occurred between the collection of eluent.

12.5 REACTION OF ACIFLUORFEN WITH ONE ELECTRON OXIDANTS

The dichloride radical anion formed in the pulse radiolysis of oxygen saturated sodium chloride (0.02 M) Acifluorfen solution (1×10^{-4} M) at pH 2 (HClO_4) reacts as a strong one electron oxidant with a redox potential of 2.09 V (versus NHE) [43]. The reaction of the dichloride radical anion with Acifluorfen was studied by following the decay of the dichloride radical anion absorption band at 340 nm. It was observed that in the presence of Acifluorfen (1×10^{-4} M) this band still decayed by second order kinetics, indicating that no reaction between Acifluorfen and the dichloride radical anion had occurred. When sodium chloride was replaced with sodium bromide (0.02 M) (pH 6.8 and 2.0) no effect was observed on the decay on the dibromide radical anion at 360 nm. This implies that no electron is being transferred from Acifluorfen to the dihalide radical anions.



The sulfate radical anion formed in the pulse radiolysis an aqueous Acifluorfen (1×10^{-4} M) solution containing $\text{K}_2\text{S}_2\text{O}_8$ (0.02 M), *t*-butyl alcohol (0.1 M) and saturated with nitrogen (pH 6.8, phosphate buffer) reacts as a strong one electron oxidant with a potential of 2.43 V (versus NHE) [43, 86, 148]. The reaction of the sulfate radical anion with Acifluorfen was studied by following the decay of the sulfate radical anion absorption band at 460 nm. It was observed that in the presence of Acifluorfen (1×10^{-4} M) this band decayed faster than without Acifluorfen. The change in kinetics indicates that a reaction between Acifluorfen and the sulfate radical anion has occurred. Since Acifluorfen reacts with the sulfate radical anion and not the dichloride radical anion, it implies that the $\text{Aci}^{\bullet}/\text{Aci}^-$ (Acifluorfen is mainly deprotonated at pH 6.8) redox potential must lie between that of the sulfate and dichloride radical anions. ie. between 2.43 and 2.09 V (versus NHE)



Using the pseudo first order rate constants of the decay of the sulfate radical anion at 500 nm it was determined that 13.5 μs after the pulse more than 90% of the sulfate radical anion had reacted with Acifluorfen. The TDA spectrum obtained at this time is shown in Figure 12.08. The spectrum shows two very broad peaks at 360 and 440 nm. This spectrum is a similar shape to that obtained by the reaction of hydroxyl radicals with Acifluorfen at the same pH. The intensity of the signal is not as strong when compared to the hydroxyl radical experiment (taking into account the lower G value of the sulfate radical anion). This result

implies that formation of a OH-adduct might be resulting from the reaction of the sulfate radical with Acifluorfen.

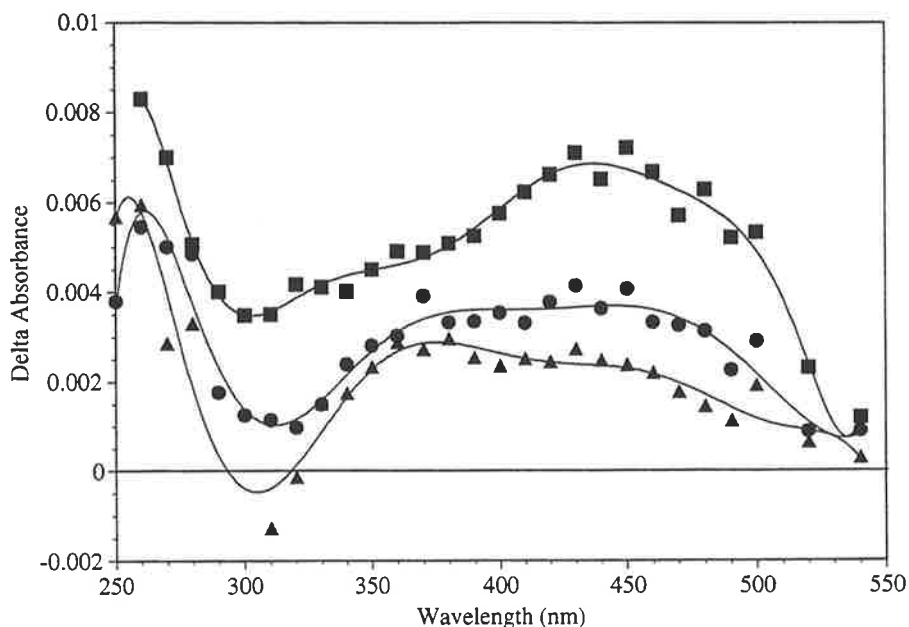


Figure 12.08. Time resolved TDA spectra obtained upon the pulse radiolysis of an aqueous Acifluorfen (1×10^{-4} M) solution containing $K_2S_2O_8$ (0.02 M), *t*-butyl alcohol (0.1 M) and saturated with nitrogen (pH 6.8, phosphate buffer). (■ Directly after pulse, ● 10 μ s, ▲ 14 μ s).

The rate constant for the reaction of Acifluorfen with the sulfate radical anion was determined from the slope of a plot of the pseudo first order rate constant at 500 nm against the concentration of Acifluorfen (the experiment was performed at 500 nm to minimise the interference from the resulting transient). The slope of the graph produced a bimolecular rate constant of $8.8 \times 10^9 \text{ M}^{-1} \text{ s}^{-1}$. The rate constant for the reaction of the structurally similar para-nitrobenzoic acid has been previously reported at less than $10^6 \text{ M}^{-1} \text{ s}^{-1}$ [68]. The authors explained that the slow rate constant for this reaction was due to the electron withdrawing effects of the nitro group. The same would be expected for the nitrobenzoate ring of Acifluorfen. Thus it would be expected that the removal of the electron would occur from the chlorobenzene ring.

Ab initio studies on the resulting radical produced a spin surface which is located over both rings. The spin surface located on the nitrobenzoate is similar to that found for the benzoate radical cation. The spin located on the chlorobenzene ring is similar to that of the phenoxyl radical. As a molecule, the spin pattern could not be rationalised using resonance theory. The HOMO of Acifluorfen was located over the two oxygens of benzoate. Zemel *et al.* [214] found that direct removal of electrons from the oxygens of the carboxylic acid was slow and inefficient. The experimental results contradict what is predicted from the

calculations and therefore either the HOMO generated from the calculations is wrong, or the electron is not removed from the HOMO and thus predicting the position of electron loss via the HOMO is incorrect in this example.

Steady state irradiation of an Acicfluorfen (1×10^{-4} M) solution containing potassium persulfate (0.02 M), *t*-butyl alcohol (0.1 M) and saturated with nitrogen (pH 6.8, phosphate buffer) produced a loss of Acicfluorfen and the formation of new products at 19.5 (A) 20.0 (B) and 22.5 (C) minutes in the HPLC trace (Figure 12.03). A non-irradiated sample of the above solution displayed no loss of Acicfluorfen therefore indicating that products of the reactions were not due to the thermal oxidation of Acicfluorfen by the persulfate ion [43].

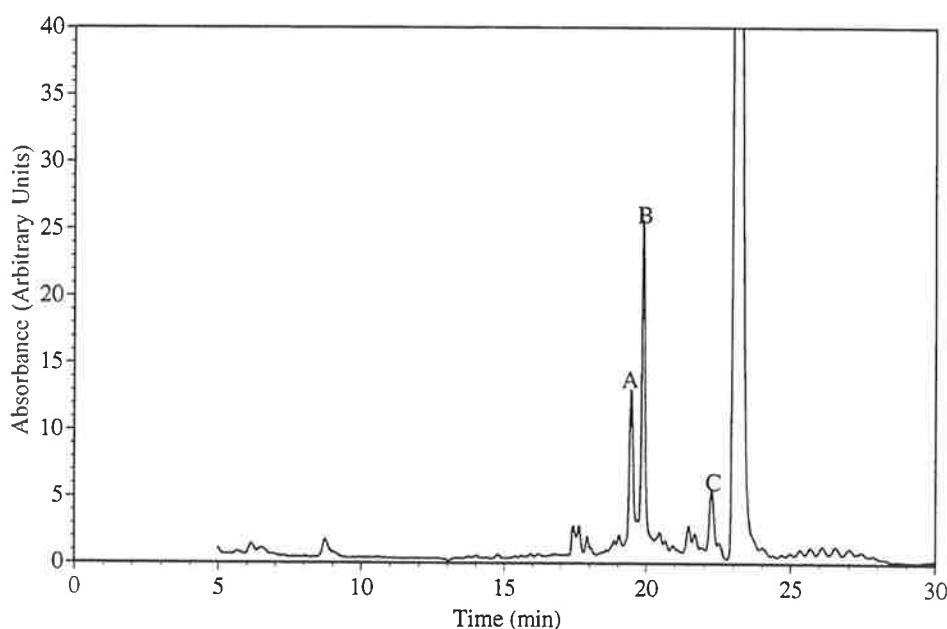


Figure 12.09. HPLC analysis following the gamma irradiation of a Acicfluorfen (1×10^{-4} M) solution containing potassium persulfate (0.02 M), *t*-butyl alcohol (0.1 M) and saturated with nitrogen (pH 6.8, phosphate buffer). The trace displays the products formed from the reaction of Acicfluorfen with the sulfate radical anion (A to C). See text for discussion.

Electrospray mass spectrometry on the products produced a parent ion of 376/378 (3:1) Daltons for the product A. This must be the hydroxylated product observed in the hydroxyl radical experiment. The MS^2 fragmentation pattern of the parent ion and retention times were identical to that observed for product E for the reaction with hydroxyl radicals suggesting that it is the same product. Product B produced a parent ion at 309/311 (3:1) Daltons. The isotope pattern of 3:1 indicates the chlorine atom is still present in the molecule. The parent ion corresponds to the addition of a hydroxyl group and the loss of the CF_3 group. MS^2 fragmentation of the parent ion produced daughter ions which correspond to the loss of NO and CO_2 , indicating these functional groups are still present in the molecule. No parent ion could be observed above the base line for product C.

Formation of product A is in agreement with what was expected from the pulse radiolysis results. Formation of product B however was not expected. The mechanism for its formation would be the loss of one electron from the chlorobenzene ring followed by addition of water to form the OH-adduct of Acifluorfen. This transient must then undergo a disproportionation reaction to form the mono unsaturated product, which then eliminates CF_3 to reform the more thermodynamically stable aromatic ring. Elimination of CF_3 was not observed in the hydroxyl radical experiment and is not expected in this reaction. CF_3 would be expected to be a stable leaving group, through it would not be as good as the hydroxyl group or chlorine atom.

No steady state reaction was performed using the dichloride radical anion since it required low pH for its formation which would result in the precipitation of Acifluorfen from the solution.

12.6 REACTION OF ACIFLUORFEN WITH THE HYDRATED ELECTRON

The decay of the hydrated electron's absorbance at 640 nm was observed to increase in the presence of small amounts of Acifluorfen (1×10^{-4} M) at pH 7.0 (phosphate buffer and NaOH). Change in the decay rate of hydrated electron indicated that a reaction with the Acifluorfen anion had occurred. The TDA spectrum produced upon the pulse radiolysis of an aqueous Acifluorfen (1×10^{-4} M) solution containing *t*-butyl alcohol (0.1 M) saturated with nitrogen gas (pH 7.0, phosphate buffer and NaOH) is shown in Figure 12.10. The maximum of the spectrum was recorded at 300 nm, with a less intense maximum at 420 nm. The maximum at 420 nm did not decay away quickly with time and thus was due to the transient and not the hydrated electron.

The maximum observed at 300 nm is similar to that reported for the reaction of ortho-nitrobenzoate [215] with the carbon dioxide radical anion. No maximum was observed at 450 nm suggesting that a slight difference existed between transients of the two reactions. Transients produced by the reaction of o-nitrobenzoate with the carbon dioxide radical anion was determined to be the $\text{NO}_2^{\bullet -}$ adduct [215]. Molar absorbance of the transient at 293 nm was determined to be approximately $16000 \text{ M}^{-1}\text{cm}^{-1}$. The molar absorbance of the electron adduct with Acifluorfen was determined to be $13400 \text{ M}^{-1}\text{cm}^{-1}$. Assuming that all of the Acifluorfen adduct was in the $\text{NO}_2^{\bullet -}$ form, the molar absorbance is similar to that of ortho-nitrobenzoate at the end of the pulse.

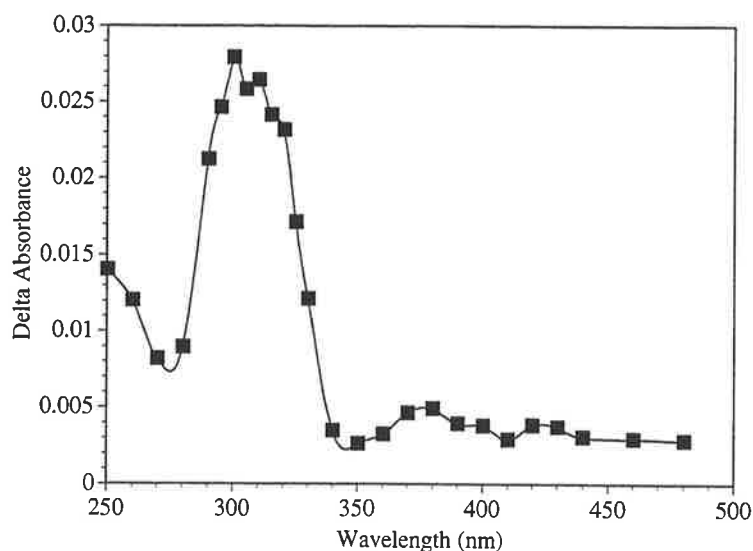


Figure 12.10. TDA spectrum produced upon the pulse radiolysis of an aqueous Acifluorfen (1×10^{-4} M) solution containing *t*-butyl alcohol (0.1 M) saturated with nitrogen gas (pH 7.0, phosphate buffer and NaOH).

The bimolecular rate constant for the reaction of the hydrated electron with Acifluorfen was determined from the slope of a plot of the decay rate of the hydrated electron at 640 nm against the concentration of Acifluorfen (10 to 35.5 μ M). The determined rate constant was $2.7 \times 10^{10} \text{ M}^{-1} \text{ s}^{-1}$. Though this is the first reported rate constant for the reaction of the hydrated electron with the Acifluorfen anion, rate constants for the reaction of the hydrated electron with compounds with similar functional groups have been reported and are displayed below.

Chlorobenzene	$k = 9.1 \times 10^8 \text{ M}^{-1} \text{ s}^{-1}$ [162]
Nitrobenzene	$k = 3.8 \times 10^{10} \text{ M}^{-1} \text{ s}^{-1}$ [216]
Benzoate anion	$k = 3.0 \times 10^9 \text{ M}^{-1} \text{ s}^{-1}$ [202]
4-Nitrobenzoate	$k = 3.4 \times 10^{10} \text{ M}^{-1} \text{ s}^{-1}$ [92]
$\alpha\alpha\alpha$ Trifluorotoluene	$k = 1.8 \times 10^9 \text{ M}^{-1} \text{ s}^{-1}$ [129]

Data presented here indicate that the nitro group is involved in the fastest reaction with the hydrated electron. This is due to its strong electron withdrawing power making it accessible for nucleophilic addition. The rate constant determined for Acifluorfen is of a similar magnitude to that of the nitrobenzene, suggesting they are undergoing similar types of reactions.

Ab initio calculations performed on the Acifluorfen anion indicate that the most electron deficient atom is the carbon attached to the three fluorine atoms. This is followed by the carbon of the carboxyl group and the nitrogen of the NO_2 group. The rate constant data

indicates that the hydrated electron should react with the nitro group, thus implying the site of radical attack of the hydrated electron with Acifluorfen is controlled by more than just the most electron deficient atom.

Optimisation calculations on Acifluorfen after one electron gain proved too computationally expensive at HF/6-31G** and therefore were optimised at the less computationally less expensive basis set of HF/STO-3G. The spin surface was determined after the optimisation of Acifluorfen at HF/STO-3G at the basis set of HF/6-31G**. The spin surface revealed that the radical is located over both rings. Resonance structures of the spin pattern could only be rationalised through formation of a three membered ring. Possibility of the formation of this three membered ring is minimal since the calculated bond distance (2.47 Å) is too long for bond formation.

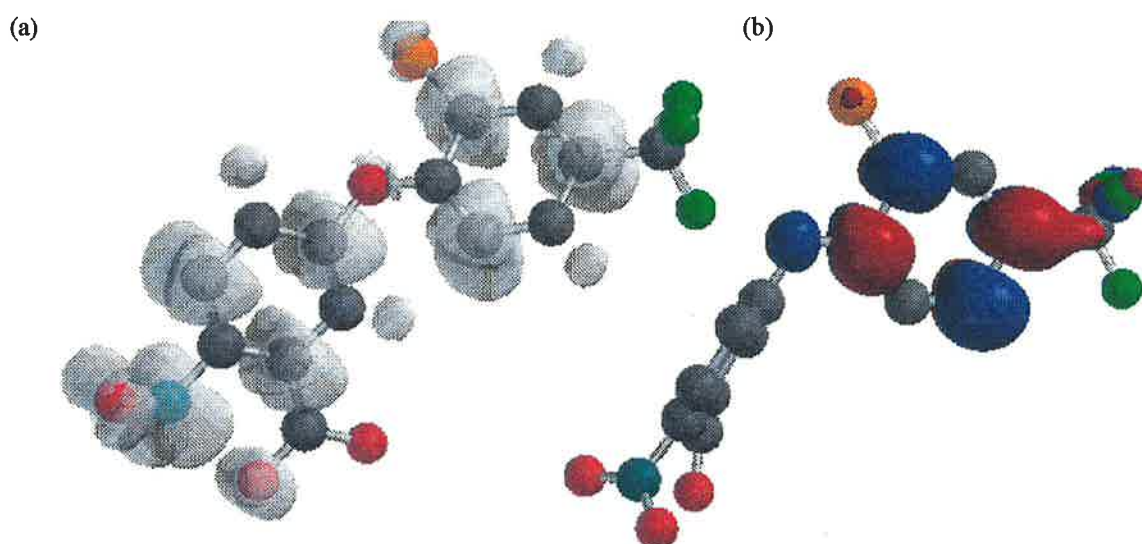


Figure 12.11. Plots of the electron spin density surface (a), and LUMO (b), of Acifluorfen as determined by *ab initio* molecular orbital theory. Calculations were performed at the HF/6-31G** level of theory. Plot (a) was determined with a molecular charge of -2 and a multiplicity of 2. Plot (b) was determined with a molecular charge of -1 possessing a corresponding multiplicity of +1. (Hydrogens not shown).

Time resolved studies out to 1000 μ s showed no new peaks in the region of 250 to 600 nm, suggesting the reaction reacts to form stable products which do not absorb in this region.

Gamma irradiation of an Acifluorfen (1×10^{-4} M) solution containing, *t*-butyl alcohol (0.1 M) and saturated with nitrogen (pH 7.0, phosphate buffer and NaOH) produced the HPLC trace shown in Figure 12.12. The HPLC trace shows the formation of four major compounds, all of which are more polar than the starting compound. Electrospray mass spectrometry produced no parent ions above the baseline and thus no information was obtained on the products structure.

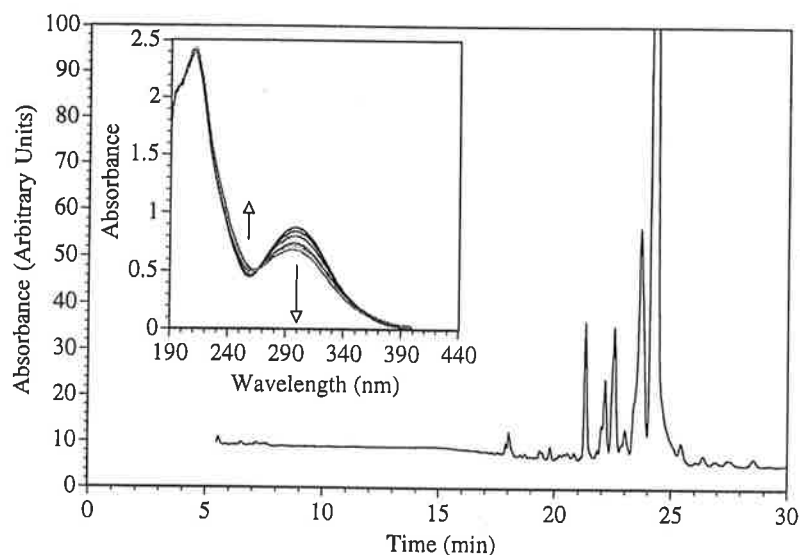


Figure 12.12. HPLC analysis following the gamma irradiation of a Acifluorfen (1×10^{-4} M) solution containing, *t*-butyl alcohol (0.1 M) and saturated with nitrogen (pH 7.0, phosphate buffer and NaOH). Trace displays the products formed from the reaction of Acifluorfen with the hydrated electron. Inset. Change in optical absorption of the same solution (0 to 400 Gray). Arrows indicate the direction of absorbance change with radiation dose. Dose rate 66 Gray/hr.

12.7 REACTION OF ACIFLUORFEN WITH THE HYDROGEN ATOM

Figure 12.13 shows the TDA spectrum obtained upon the pulse radiolysis of an aqueous Acifluorfen (1×10^{-4} M) solution containing *t*-butyl alcohol (0.1 M) saturated with nitrogen (pH 2, HClO_4). It exhibits an absorption peak with maxima at 340 nm and 440 nm. Formation kinetics performed on this maximum from the slope of a plot of the pseudo first order rate constant against the concentration of Acifluorfen at 340 nm produced a rate constant for the bimolecular reaction between the hydrogen atom and the Acifluorfen of $7.7 \times 10^8 \text{ M}^{-1} \text{ s}^{-1}$.

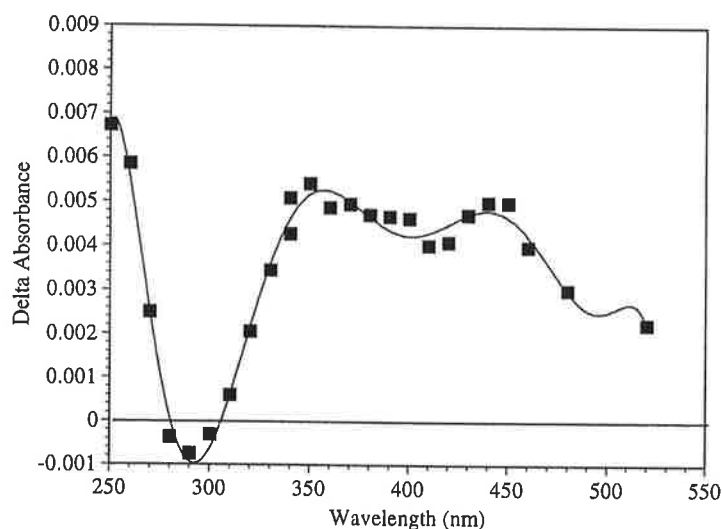


Figure 12.13. TDA spectrum obtained upon the pulse radiolysis of an aqueous Acifluorfen (1×10^{-4} M) solution containing *t*-butyl alcohol (0.1 M) saturated with nitrogen (pH 2, HClO_4) Spectrum recorded 10 μs after the pulse.

The TDA spectrum is similar in shape to the OH-adduct formed by the addition of the hydroxyl radical to Acifluorfen, the absorbance observed from this reaction probably results from the addition of the hydrogen atom to one of the benzene rings to form the H-adduct.

Precipitation of Acifluorfen is significant at low pH and formation of the hydrogen atom requires a low pH, therefore the steady state reaction failed. Formation of the H-adduct of Acifluorfen can therefore not be concluded comprehensively.

12.8 REACTION OF ACIFLUORFEN WITH REDUCING RADICALS.

Pulse radiolysis of a nitrous oxide saturated solution containing sodium formate (0.02 M) and Acifluorfen (1×10^{-4} M) (pH 6.8, phosphate buffer) initially produced a maxima at approximately 250 nm with no other absorbance maximum being observed. Absorbance observed was due to the formation of the carbon dioxide radical anion. Time resolved studies out to 1000 μ s indicate the formation of a new maximum at 300 nm. This suggests that the carbon dioxide radical reacts with Acifluorfen. The absorbance maximum is at a similar wavelength to that of the transient produced by the hydrated electron's reaction with Acifluorfen. The carbon dioxide radical anion is known to undergo one electron transfer with ortho-nitrobenzoate to form a transient that absorbs at 300 nm. The maximum at 300 nm was determined to have molar absorbance of $13300 \text{ M}^{-1}\text{s}^{-1}$, this value is a similar size to that recorded for the reaction of the carbon dioxide radical anion with ortho-nitrobenzoate, indicating that an analogous reaction has taken place.

The rate of formation of the transient was determined by the slope of the pseudo first order rate constant against the concentration of Acifluorfen and produced a bimolecular rate constant of $1.6 \times 10^8 \text{ M}^{-1}\text{s}^{-1}$. The rate constant for the reaction of the carbon dioxide radical with ortho-benzoic acid was reported by Neta *et al.* [215] to be $3.0 \times 10^8 \text{ M}^{-1}\text{s}^{-1}$. This rate constant is of the same order of magnitude as that reported here for the reaction of the carbon dioxide radical with Acifluorfen.

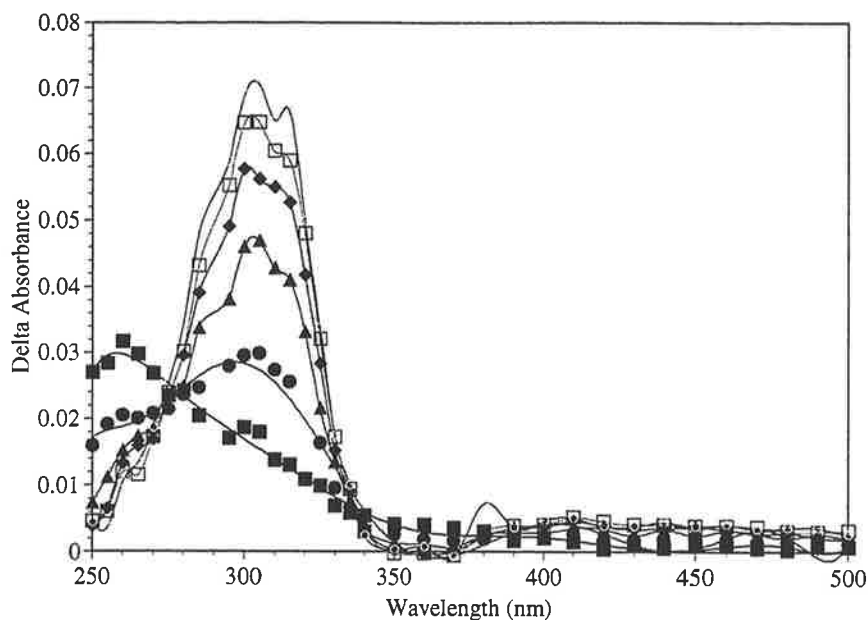


Figure 12.14. Time resolved TDA spectra obtained upon the pulse radiolysis of an aqueous Acifluorfen (1×10^{-4} M) solution containing sodium formate (0.02 M) and saturated with nitrous oxide (pH 6.8, phosphate buffer). (■ Directly after the pulse, ● 10 μ s, ▲ 20 μ s, ◆ 50 μ s, □ 100 μ s, ○ 500 μ s).

Steady state irradiation of an aqueous Acifluorfen (1×10^{-4} M) solution containing sodium formate (0.02 M) and saturated with nitrous oxide (pH 6.8, phosphate buffer) produced the HPLC trace observed in Figure 12.15. The chromatogram indicates the formation of products at similar retention times to that of the hydrated electron. However, concentration of the species was different suggesting that radicals reacting to produce the transient may influence the product distribution (Figure 12.15).

Electrospray mass spectrometry on the predominate compound at 22.5 minutes produced a parent ion at 346/348 (3:1) Daltons. The parent ion for the compound at 22.5 minutes is 14 Daltons less than that recorded for the parent ion, and therefore must correspond either to the loss of a nitrogen or the loss of an oxygen and the addition of two hydrogen atoms. MS^2 fragmentation of the 246 parent ion produced daughter ions at 302 (or minus CO_2) and 266 Daltons. Further fragmentation of the 266 Daltons ion produced a granddaughter ion at 236 Daltons (minus NO). The fragmentation pattern indicates that the nitrogen has not been lost and the latter of the two proposed accounts for the production of the parent ion.

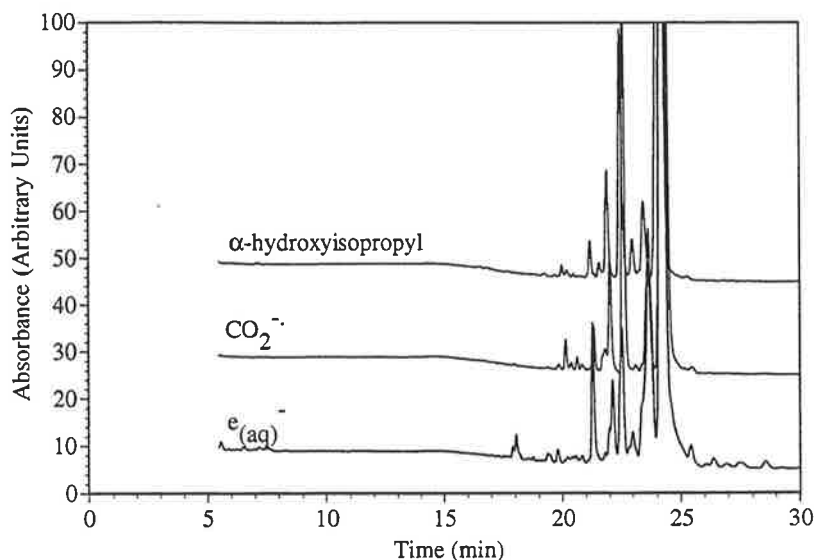


Figure 12.15. Comparison of the HPLC traces produced by the reaction of hydrated electron, carbon dioxide radical anion and α -hydroxyisopropyl radical with Acifluorfen (1×10^{-4} M). Experimental conditions are as follows: $\text{CO}_2^{\bullet -}$; 0.02 M sodium formate, nitrous oxide saturated. $e_{(aq)}^{\bullet -}$; 0.1 M *t*-butyl alcohol, nitrogen saturated. α -hydroxyisopropyl radical; 0.1 M 2-propanol, nitrous oxide saturated. All experiments were performed at pH 6.8 (phosphate buffer). See text for discussion.

Pulse radiolysis of a nitrous oxide saturated solution containing 2-propanol (0.1 M) and Acifluorfen (1×10^{-4} M) (pH 6.8, phosphate buffer) produced an absorbance maximum at 300 nm. Time resolved studies out to 1000 μs did not find any new absorption in the range of 250 to 600 nm. The redox potential of the α -hydroxyisopropyl radical has been determined to be -1.1 V (versus NHE) [90]. This suggests that the redox potential of the for the $\text{Aci}^-/\text{Aci}^{\bullet -}$ is more than -1.1 V. Therefore, $\text{Aci}^{\bullet -}$ is a reducing agent with a reduction potential greater than -1.1 V (versus NHE).

Gamma irradiation of the same solution produced a product distribution similar to that observed for the hydrated electron experiment and the carbon dioxide radical anion. Determination of the products by electrospray mass spectrometry proved unsuccessful in producing parent ions above the base line, thus no structural information could be obtained on the products.

12.9 OVERVIEW OF THE RADIATION CHEMISTRY OF ACIFLUORFEN

This study has allowed for the first time the elucidation of the radiation chemistry of aqueous Acifluorfen. The new chemistry for Acifluorfen is summarised in Figure 12.16

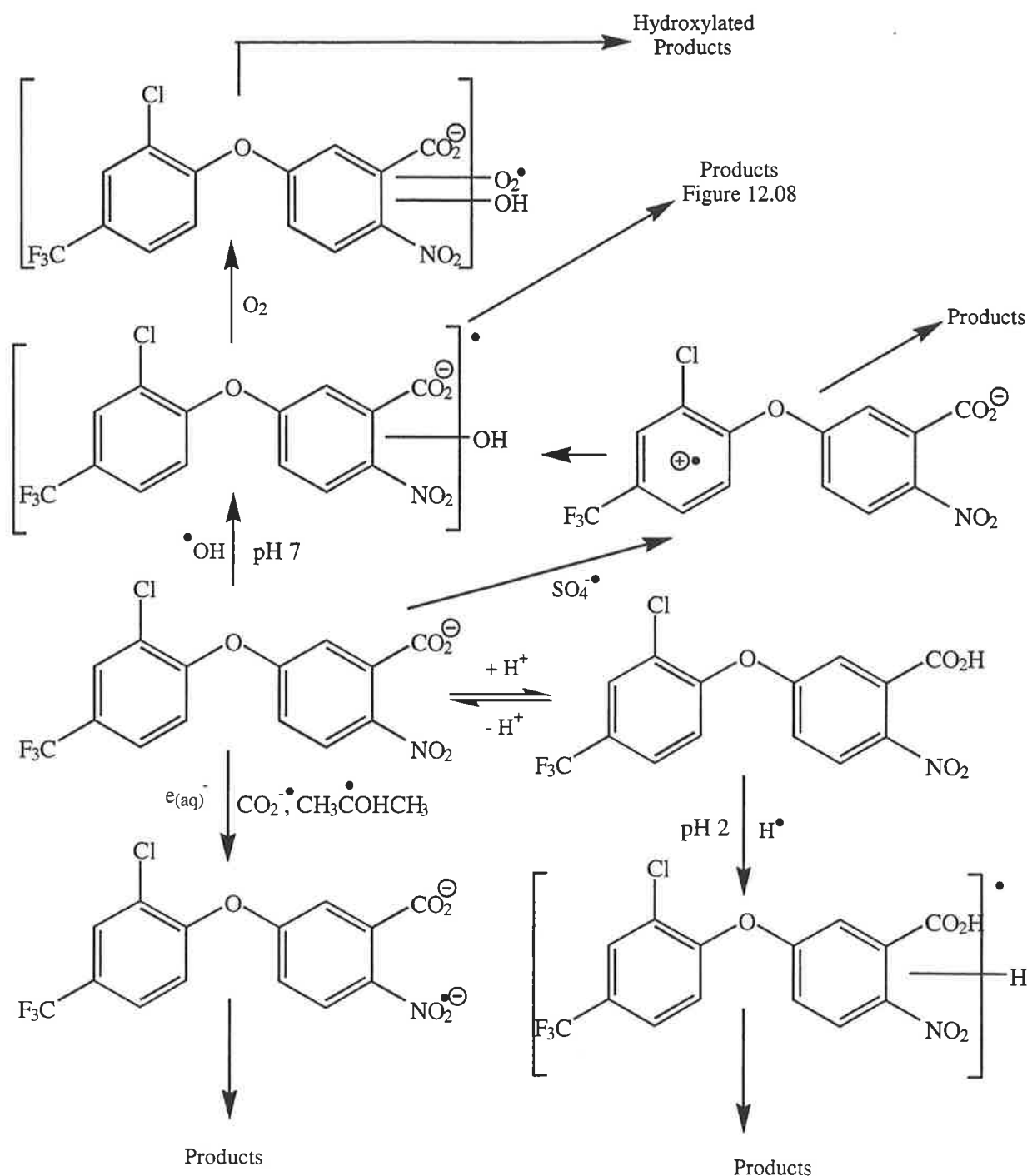


Figure 12.16. Overview of the radiation chemistry characterised in this study

The TDA spectrum obtained from the reaction of Acicfluorfen with the hydroxyl radical is affected by the ground state absorbance of the starting compound. The rate constant obtained for the reaction of Acicfluorfen with the hydroxyl radical is similar to that of nitrobenzoate's reaction with the hydroxyl radical [44]. The reaction of nitrobenzoate with the hydroxyl radical is known to proceed through a OH-adduct intermediate, suggesting a similar type of reaction for Acicfluorfen.

The decay rate of the transient radical shows dependence on the ionic strength of the solution, therefore the transient is charged. The transient decays by second order kinetics,

indicating that degradation products are formed by radical-radical reactions. HPLC characterisation of the compounds formed by the reaction of Acifluorfen with the hydroxyl radical showed that these compounds have a retention time less than Acifluorfen. This suggests that the newly formed compounds are more polar than Acifluorfen. Mass spectrometric studies have determined that the major products were a mixture of the hydroxylated, dimer and dehalogenated products. The rate of Acifluorfen loss and the formation of products from the reaction of Acifluorfen with the hydroxyl radical is initially linear under steady state irradiation. As the amount of hydroxyl radicals is increased past 30% of Acifluorfen's concentration, the loss of Acifluorfen and the formation of products follows a higher order kinetic mechanism. This result suggests that products of the initial reaction also react with the hydroxyl radical to form (uncharacterised) compounds.

The corrected TDA spectrum obtained upon the reaction of the hydroxyl radical with Acifluorfen at pH 2 matches that obtained from the same reaction at neutral pH. The rate constant for the reaction of Acifluorfen with the hydroxyl radical at pH 2 is lower than that obtained at neutral pH. Qualitatively, this can be explained as follows: in the anion form of Acifluorfen the electron density is greater than in the case of the neutral form. Since the hydroxyl radical behaves as an electrophile in its reactions, reaction with the electron rich species is faster. Steady state irradiation of Acifluorfen at pH 2 was not successful because Acifluorfen precipitated out of solution over the time scale of the reaction.

Pulse radiolysis studies indicate that the OH-adduct generated upon the reaction of Acifluorfen with the hydroxyl radical does not react with oxygen. Gamma irradiation coupled with HPLC shows the formation of different compounds than those obtained for the deoxygenated experiment. This indicates that reaction of the OH-adduct of Acifluorfen is too slow to be observed on the pulse radiolysis time scale. Mass spectral fragmentation data indicates that the products result from the addition of molecular oxygen to the transient. The newly produced transient then reacts to form compounds which correspond to the addition of a hydroxyl group to Acifluorfen.

The TDA spectra obtained from the reaction of Acifluorfen with the sulfate radical anion is similar to that obtained for the OH-adduct of Acifluorfen, thus the radical cation produced transforms into a cyclohexadienyl type radical via the addition of water and the elimination of a hydrogen ion. The rate constant for the reaction of the sulfate radical anion is similar to that of chlorobenzene indicating that this ring is reacting in preference to the nitrobenzoate ring. Acifluorfen is not observed to react with the dichloride radical anion,

therefore the resulting radical of Acifluorfen is a powerful one electron oxidant with a redox potential between 2.43 to 2.09 Volts (versus NHE). Gamma irradiation coupled with HPLC for the sulfate radical anion shows that a newly formed compound is at the same retention time as that observed for the addition of the hydroxyl radical to Acifluorfen.

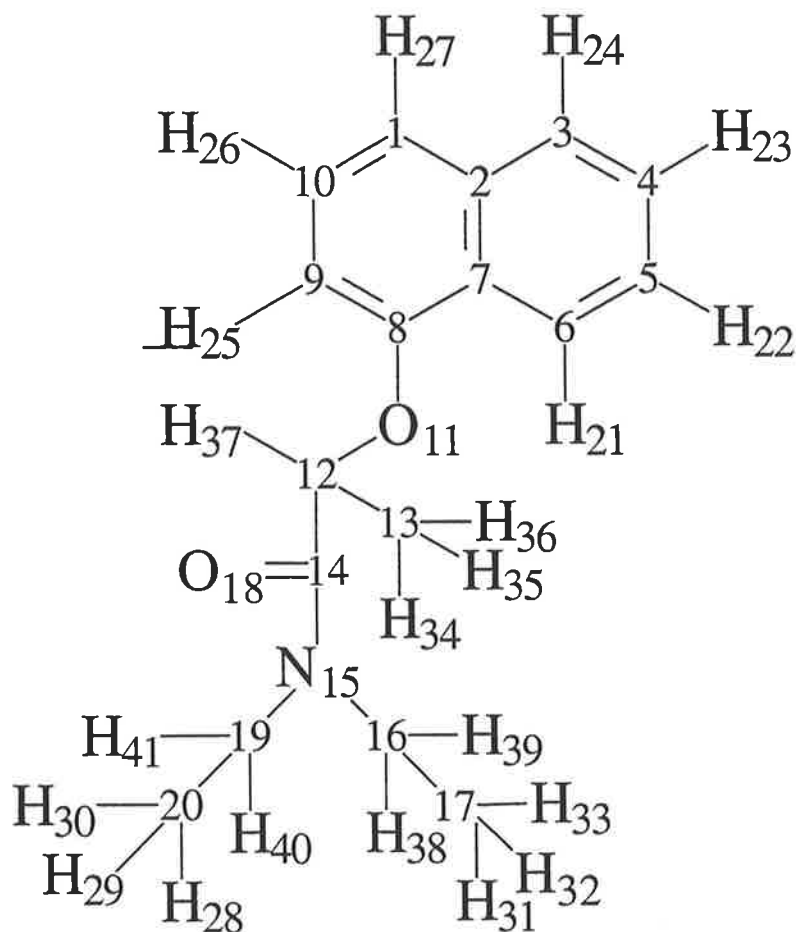
The TDA spectrum for the reaction of Acifluorfen with the hydrated electron is similar to that obtained for the reaction of 2-nitrobenzoate with the same radical [92]. The rate constant obtained for the reaction of Acifluorfen with the hydrated electron is similar to that of 2-nitrobenzoate. It is known that 2-nitrobenzoate reacts with the hydrated electron forming a radical anion on the nitro group [92]. Gamma irradiation coupled with HPLC found the formation of four major products, none of which were identified by mass spectrometric studies (due to interference by TFA). The carbon dioxide radical anion and the α -hydroxyisopropyl radical react with Acifluorfen producing similar transient spectra and HPLC chromatograms to that of the hydrated electron, indicating a similar type of reaction is occurring. The radical anion of Acifluorfen therefore has a redox potential greater than -1.1 V.

The TDA spectrum for the reaction of Acifluorfen with hydrogen atoms is similar to the TDA spectrum obtained for Acifluorfen's reaction with the hydroxyl radical, suggesting the formation of a H-adduct. Steady state irradiations of Acifluorfen at pH 2 were not successful because Acifluorfen precipitated out of solution over the time scale of the reaction.

Acifluorfen will degrade upon the reaction with a number of free radicals produced in natural and treated industrial discharge. Chloride ion elimination will not occur as a major degradation pathway for any free radical processes.

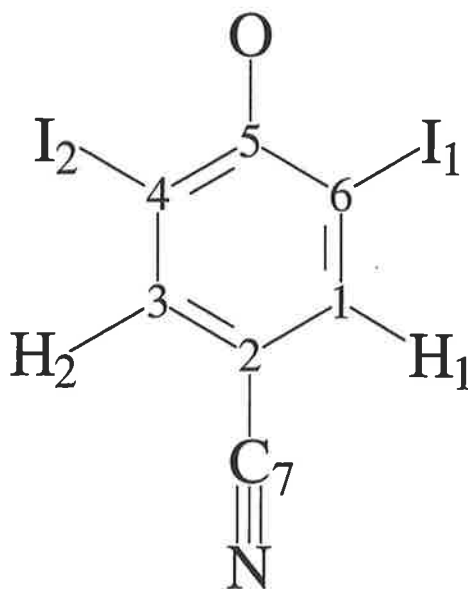
13.0 APPENDIX 1

NPA ON NAPROPAMIDE



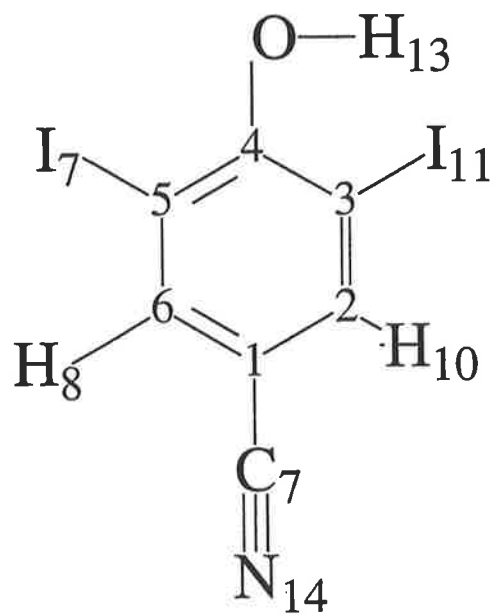
C1	-0.24299	H23	0.23381
C2	-0.03177	H24	0.23157
C3	-0.1038	H25	0.23298
C4	0.41445	H26	0.23438
C5	-0.35174	H27	0.23225
C6	-0.19543	H28	0.21829
C7	-0.21529	H29	0.21233
C8	-0.21653	H30	0.24003
C9	-0.23857	H31	0.22371
C10	-0.19577	H32	0.21455
O11	-0.63273	H33	0.21455
C12	0.07526	H34	0.23788
C13	-0.66672	H35	0.24393
C14	0.83966	H36	0.22515
N15	-0.57992	H37	0.20567
C16	-0.2067	H38	0.21013
C17	-0.65537	H39	0.22383
O18	-0.72738	H40	0.23672
C19	-0.19668	H41	0.20987
C20	-0.65622		
H21	0.25049		
H22	0.23444		

NPA ON DEPROTONATED IOXYNIL



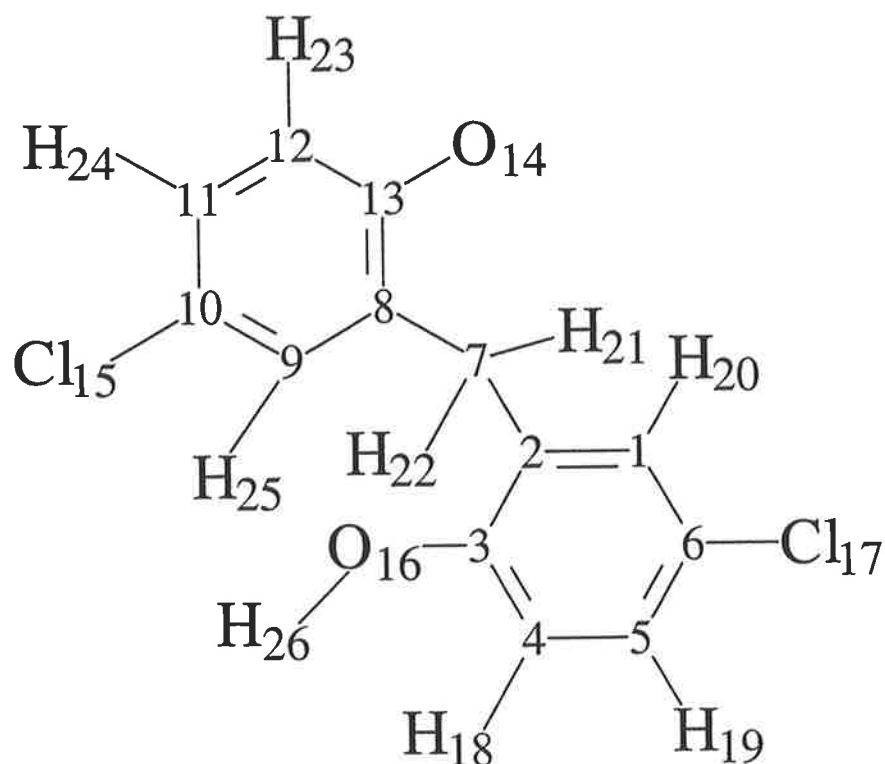
C1	-0.11501
C2	-0.29893
C3	-0.11502
C4	-0.35874
C5	0.51277
C6	-0.35878
C7	0.36523
N	-0.45873
I1	0.09922
O	-0.81799
I2	0.09923
H1	0.22337
H2	0.22338

NPA ON IOXYNIL



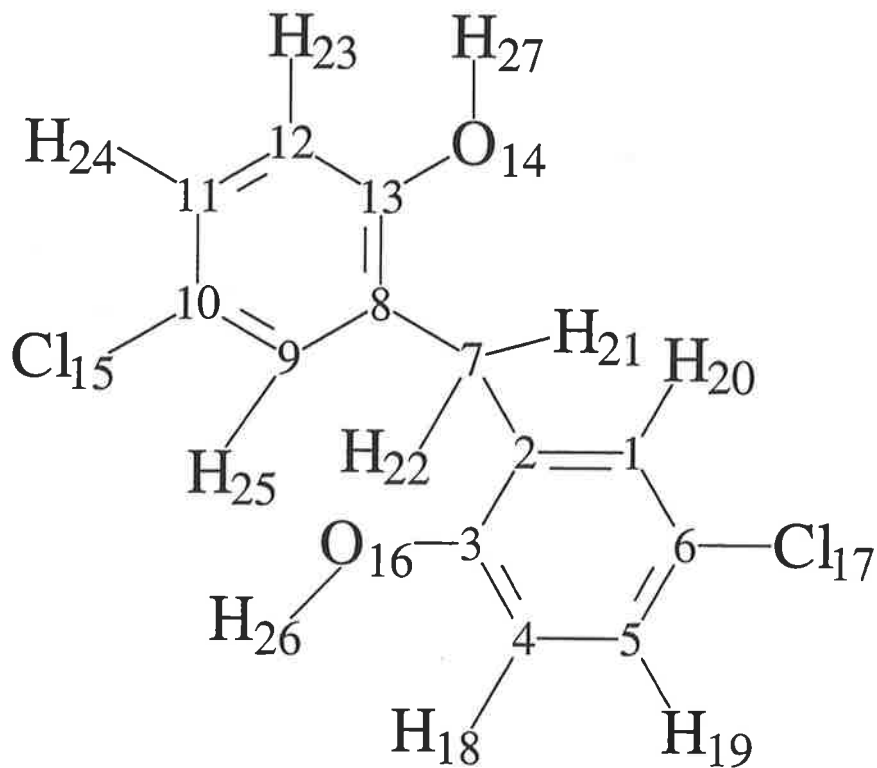
C1	0.41281
C2	-0.30797
C3	-0.12338
C4	-0.19357
C5	-0.11767
C6	-0.33555
I7	0.24441
H8	0.23612
C9	0.35404
H10	0.24071
I11	0.22693
O12	-0.76816
H13	0.5166
N14	-0.39037

NPA ON THE DEPROTONATED DICHLOROPHEN



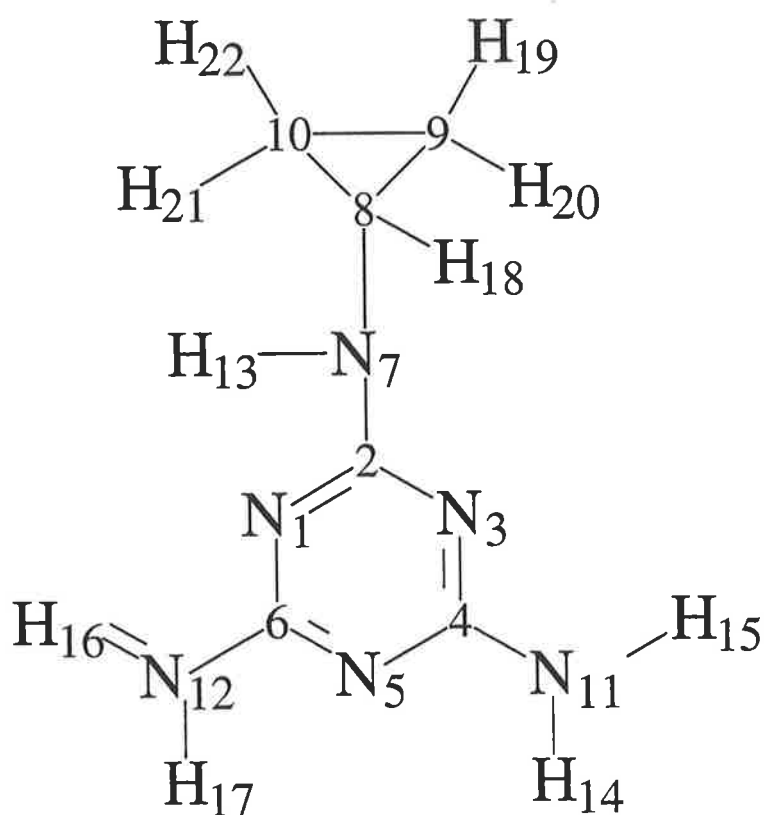
C 1	-0.21142
C 2	-0.17206
C 3	0.52912
C 4	-0.40079
C 5	-0.20981
C 6	-0.15754
C 7	-0.44796
C 8	-0.05335
C 9	0.38711
C 10	-0.31485
C 11	-0.23238
C 12	-0.06283
C 13	-0.21220
O 14	-0.75190
Cl 15	-0.05434
O 16	-0.86252
Cl 17	-0.12304
H 18	0.22326
H 19	0.24295
H 20	0.24906
H 21	0.25179
H 22	0.24067
H 23	0.20719
H 24	0.21332
H 25	0.22537
H 26	0.49712

NPA ON DICHLOROPHEN



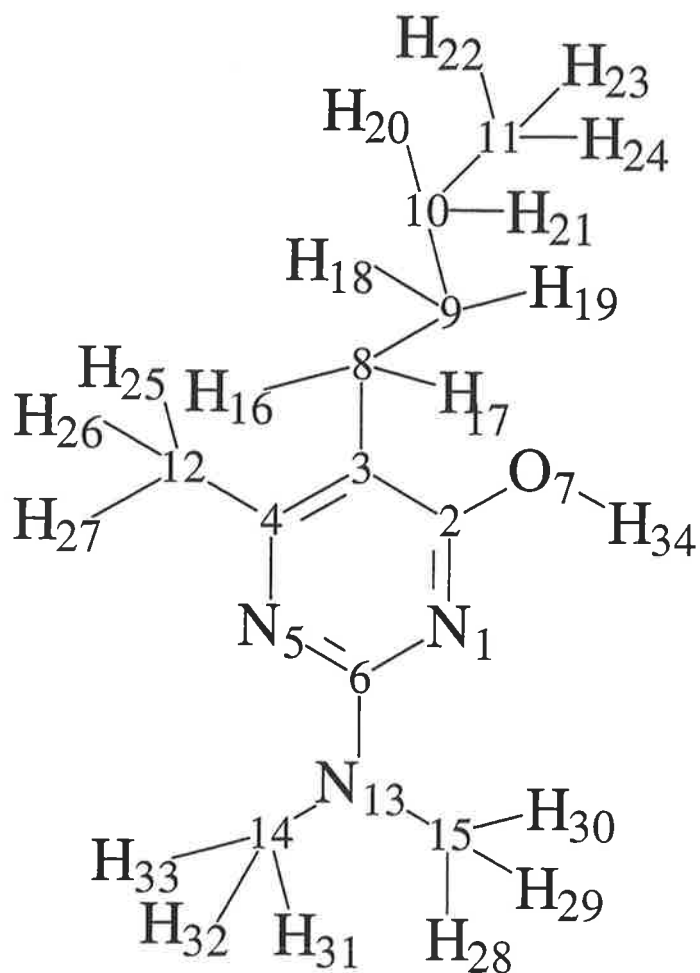
C 1	-0.21326
C 2	-0.06560
C 3	0.39118
C 4	-0.31256
C 5	-0.21676
C 6	-0.06581
C 7	-0.45196
C 8	-0.09191
C 9	0.39537
C 10	-0.31234
C 11	-0.21109
C 12	-0.07112
C 13	-0.20307
O 14	-0.75565
Cl 15	-0.02680
O 16	-0.76038
Cl 17	-0.03145
H 18	0.23370
H 19	0.25152
H 20	0.25057
H 21	0.26804
H 22	0.24790
H 23	0.23179
H 24	0.25034
H 25	0.25552
H 26	0.50724
H 27	0.50659

NPA ON CYROMAZINE



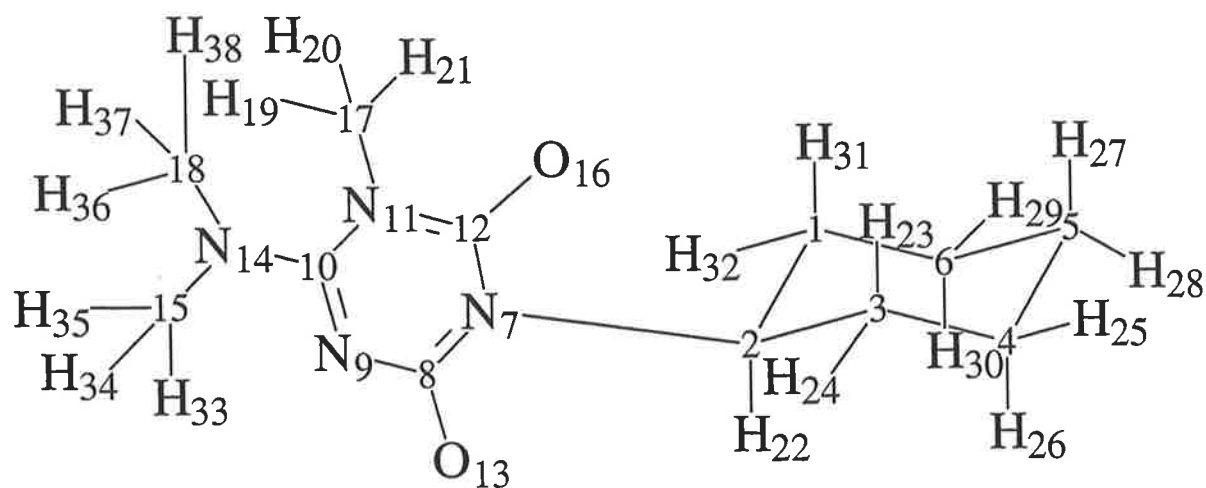
N1	-0.75677
C2	0.80514
N3	-0.75987
C4	0.79054
N5	-0.76078
C6	0.79311
N7	-0.71071
C8	-0.037
C9	-0.43798
C10	-0.45833
N11	-0.88775
N12	-0.88907
H13	0.4327
H14	0.42944
H15	0.43003
H16	0.42847
H17	0.42854
H18	0.22892
H19	0.23106
H20	0.23209
H21	0.23821
H22	0.23001

NPA ON DIMITHERIOL



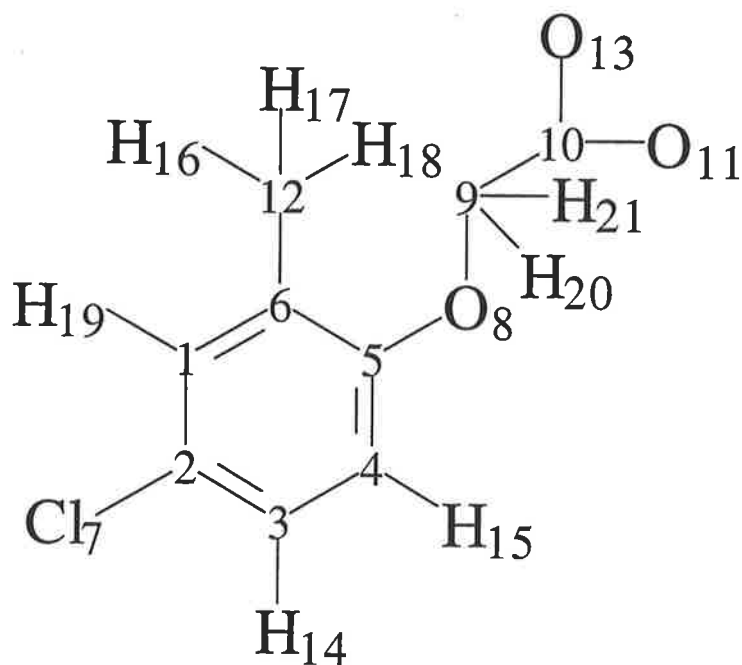
N1	-0.67518	H23	0.22616
C2	0.73883	H24	0.21583
C3	-0.30826	H25	0.25092
C4	0.3766	H26	0.22933
N5	-0.67424	H27	0.23528
C6	0.77199	H28	0.23528
O7	-0.74404	H29	0.20791
C8	-0.4447	H30	0.19749
C9	-0.42656	H31	0.24352
C10	-0.43275	H32	0.2071
C11	-0.64354	H33	0.24938
C12	-0.67829	H34	0.50913
N13	-0.53827		
C14	-0.40664		
C15	-0.40855		
H16	0.23787		
H17	0.2114		
H18	0.22123		
H19	0.21182		
H20	0.21284		
H21	0.21607		
H22	0.22308		

NPA ON HEXAZINONE



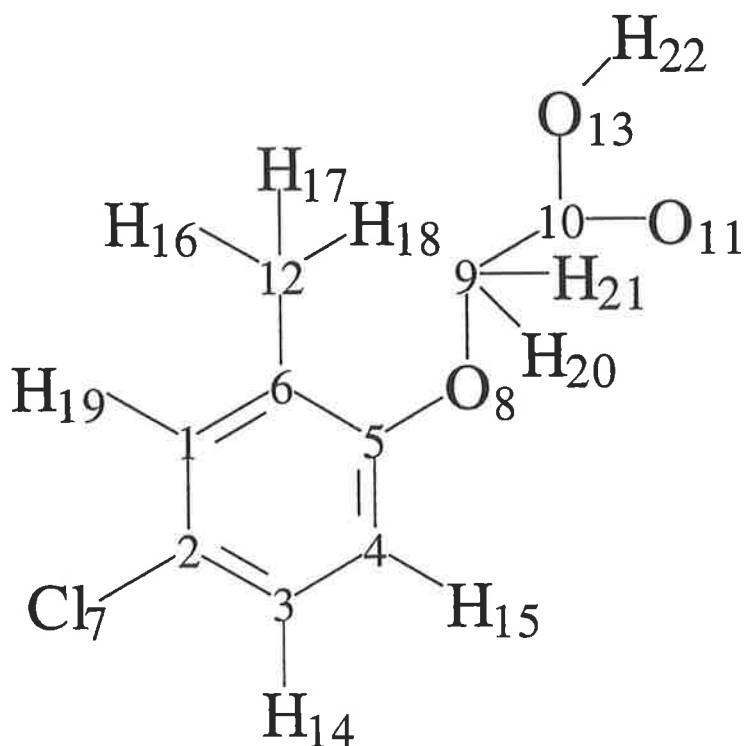
C1	-0.44890	H37	0.22318
C2	-0.02275	H38	0.22245
C3	-0.44882		
C4	-0.43526		
C5	-0.43659		
C6	-0.43422		
N7	-0.62364		
C8	0.99439		
N9	-0.71636		
C10	0.82617		
N11	-0.59795		
C12	1.02667		
O13	-0.69764		
N14	-0.57499		
C15	-0.41058		
O16	-0.72972		
C17	-0.41217		
C18	-0.41387		
H19	0.2463		
H20	0.23485		
H21	0.2246		
H22	0.26037		
H23	0.24449		
H24	0.22487		
H26	0.21274		
H27	0.21796		
H28	0.22474		
H29	0.22894		
H30	0.21161		
H31	0.24667		
H32	0.2233		
H33	0.21453		
H34	0.2126		
H35	0.24219		
H36	0.21103		

NPA ON MCPA DEPROTONATED



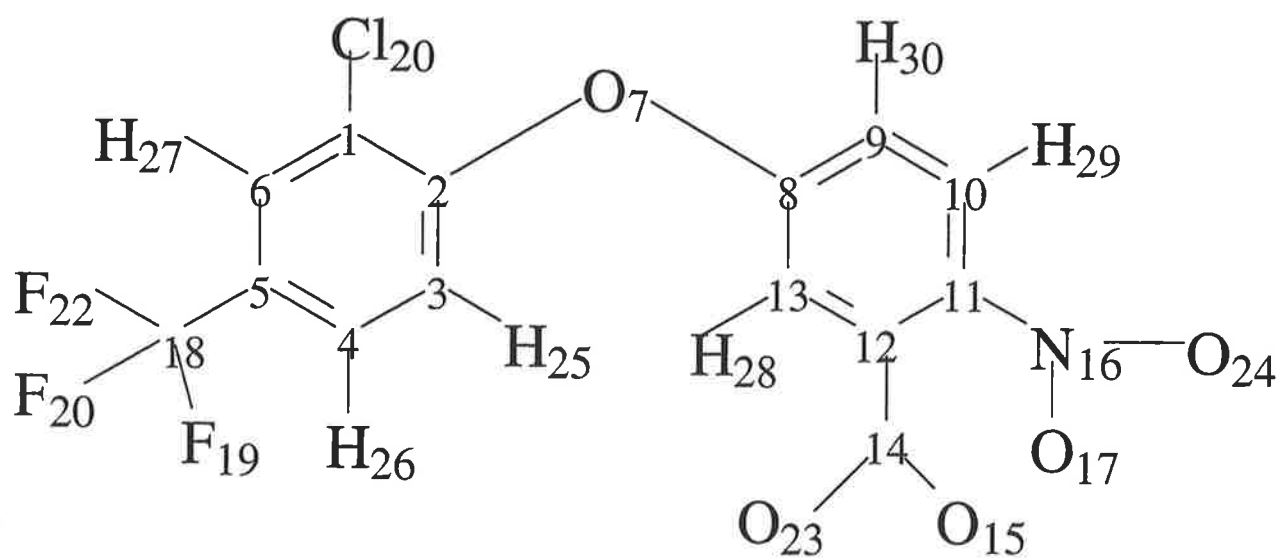
C1	-0.21803
C2	-0.0823
C3	-0.23043
C4	-0.27227
C5	0.43407
C6	-0.12841
Cl7	-0.06962
O8	-0.610723
C9	-0.15915
C10	0.95641
O11	-0.85283
C12	-0.64463
O13	-0.89608
H14	0.23811
H15	0.25452
H16	0.21168
H17	0.23518
H18	0.23518
H19	0.23117
H20	0.18308
H21	0.18308

NPA ON MCPA



C1	-0.21579
C2	-0.06135
C3	-0.22199
C4	-0.25485
C5	0.37842
C6	-0.11059
Cl7	-0.0263
O8	-0.61207
C9	-0.13504
C10	0.97015
O11	-0.6681
C12	-0.65393
O13	-0.79952
H14	0.25223
H15	0.25712
H16	0.23616
H17	0.22925
H18	0.22925
H19	0.24566
H20	0.21879
H21	0.21879
H22	0.52376

NPA ON ACIFLUROFEN



C1	-0.10066
C2	0.41124
C3	-0.31088
C4	-0.66246
C5	-0.22905
C6	-0.18184
O7	-0.58696
C8	0.32089
C9	-0.289
C10	-0.20789
C11	0.07712
C12	-0.08204
C13	-0.25828
C14	0.97254
O15	-0.85417
N16	0.68068
O17	-0.49047
C18	1.29907
F19	-0.42229
Cl20	-0.00602
F21	-0.42415
F22	-0.41968
O23	-0.84407
O24	-0.43569
H25	0.27003
H27	0.25389
H28	0.27614
H29	0.24819
H30	0.23966

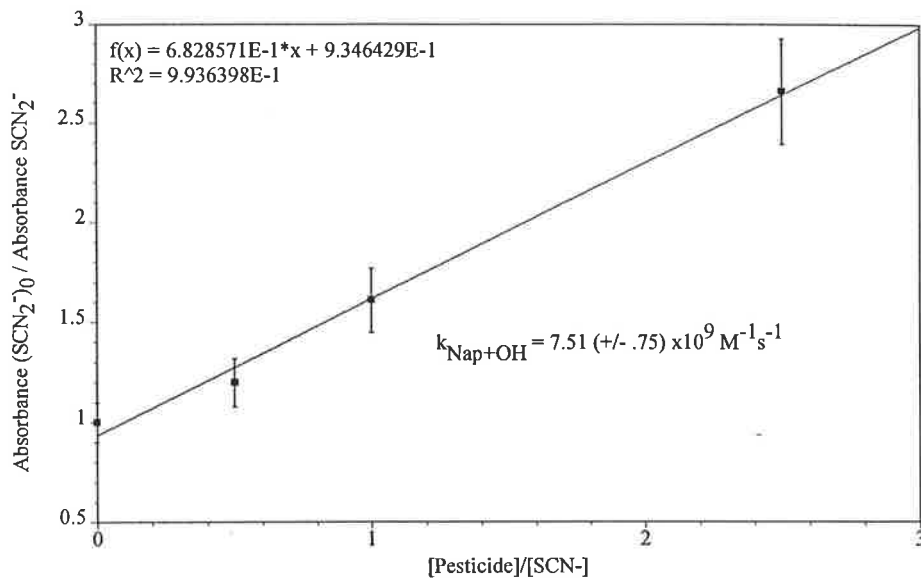


Figure 1. Competition kinetic results from the reaction of Napropamide with the hydroxyl radical.

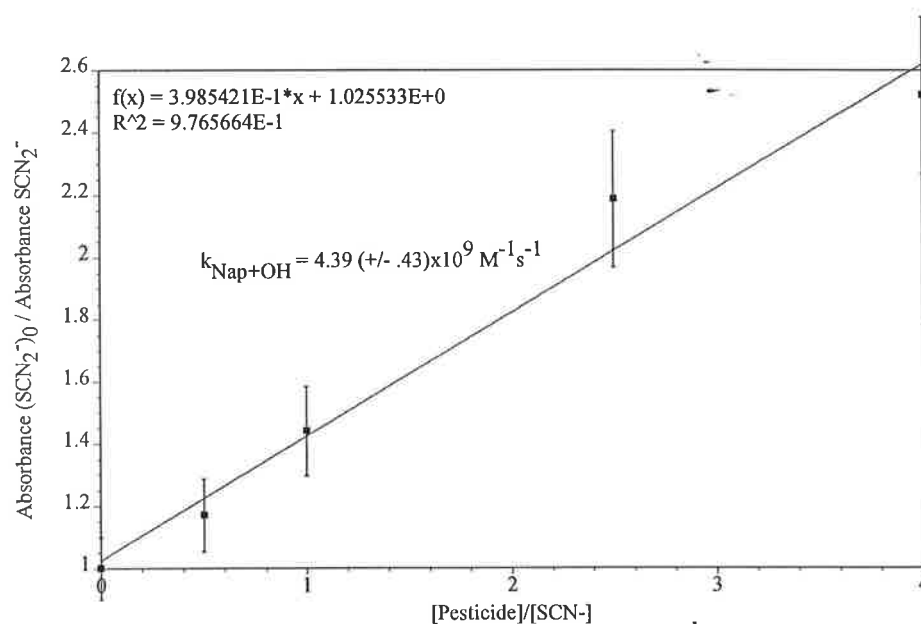


Figure 2. Competition kinetic results from the reaction of Napropamide with the hydroxyl radical at pH 2.3.

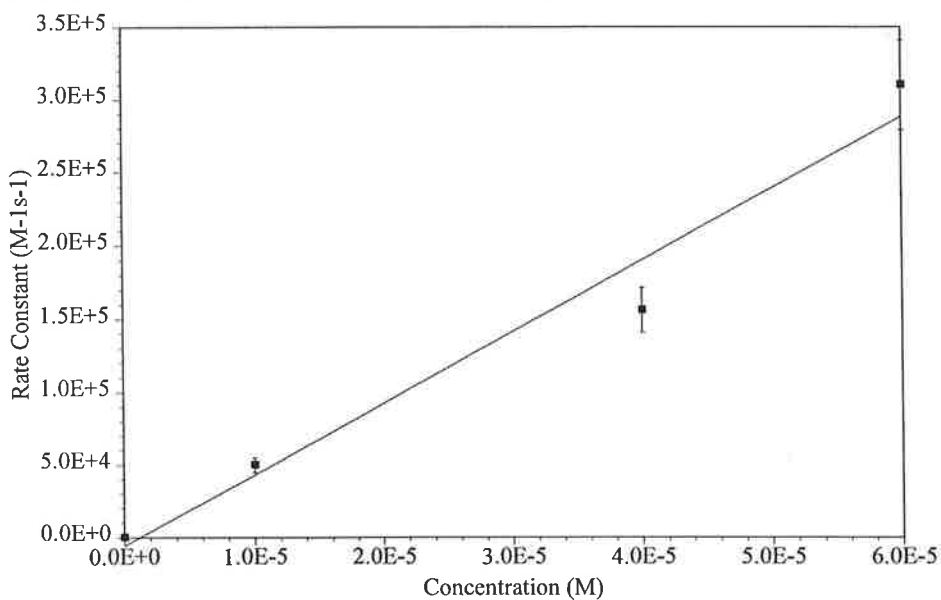


Figure 3. Formation kinetic results from the reaction of Napropamide with the hydrogen atom at pH 2.3.

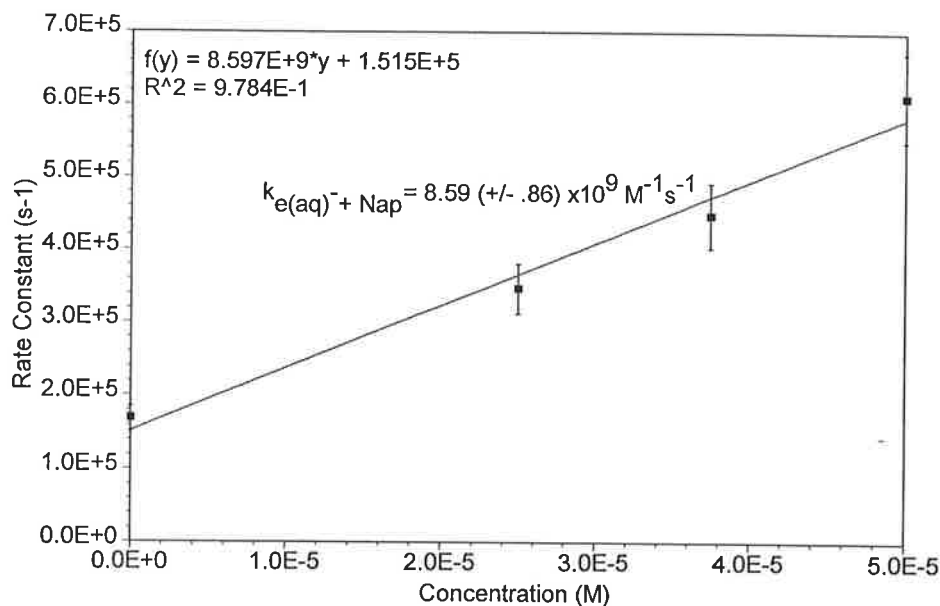


Figure 4. Decay kinetic results from the reaction of Napropamide with the hydrated electron at pH 7.1

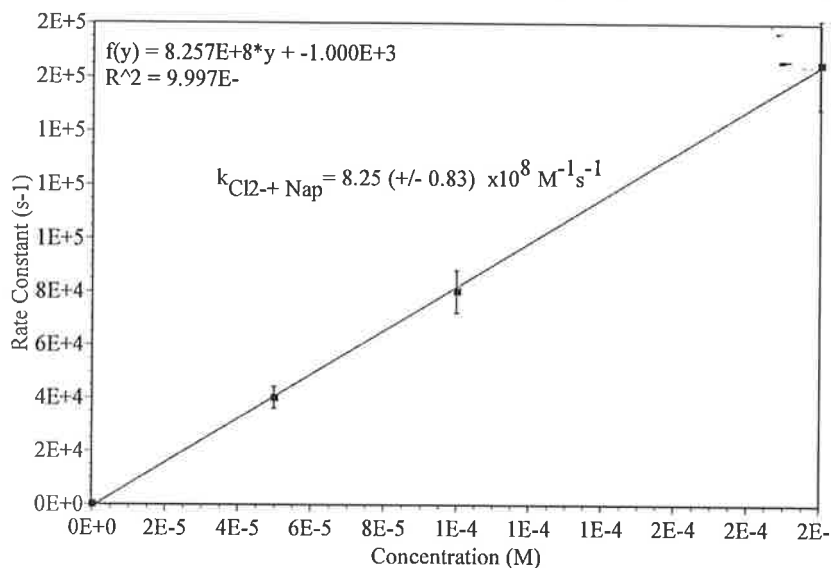


Figure 5. Decay kinetic results from the reaction of Napropamide with the chlorine radical anion at pH 2.3

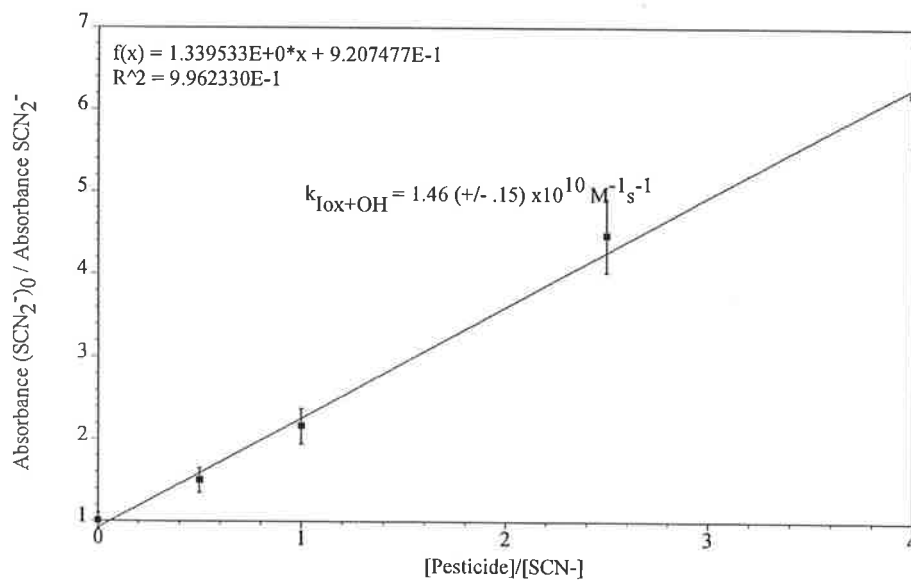


Figure 6. Competition kinetic results from the reaction of Ioxynil with the hydroxyl radical.

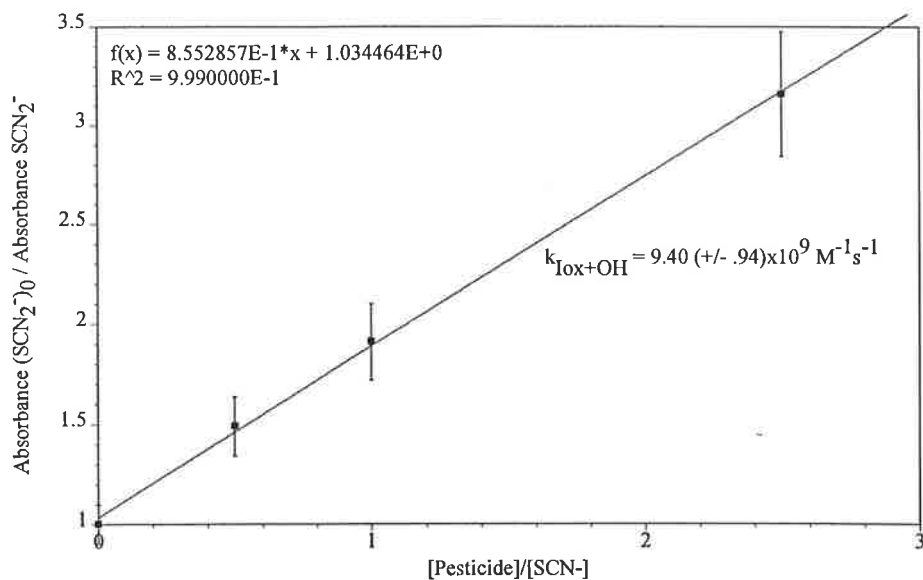


Figure 7. Competition kinetic results from the reaction of Ioxynil with the hydroxyl radical at pH 2.3.

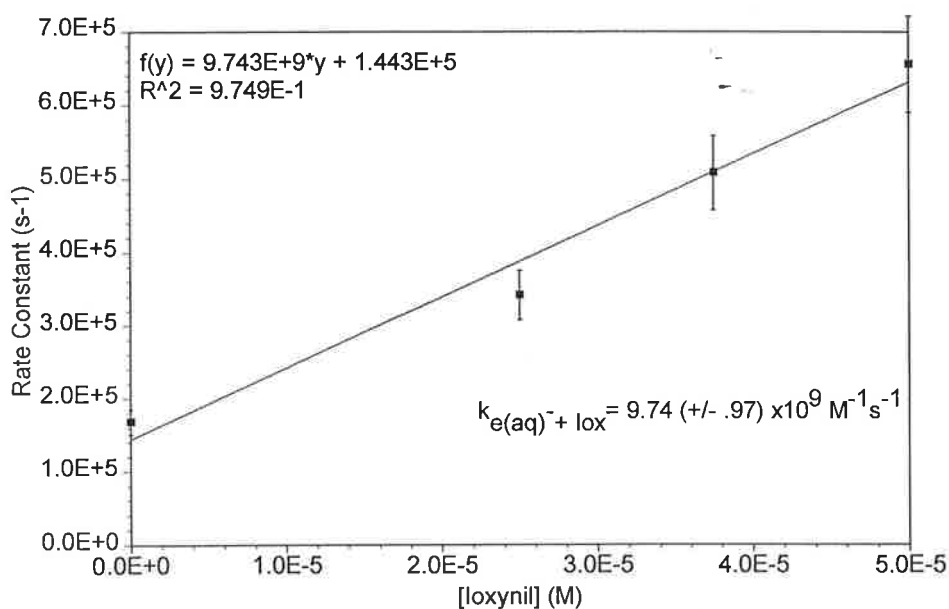


Figure 8. Decay kinetic results from the reaction of Ioxynil with the hydrated electron at pH 7.1.

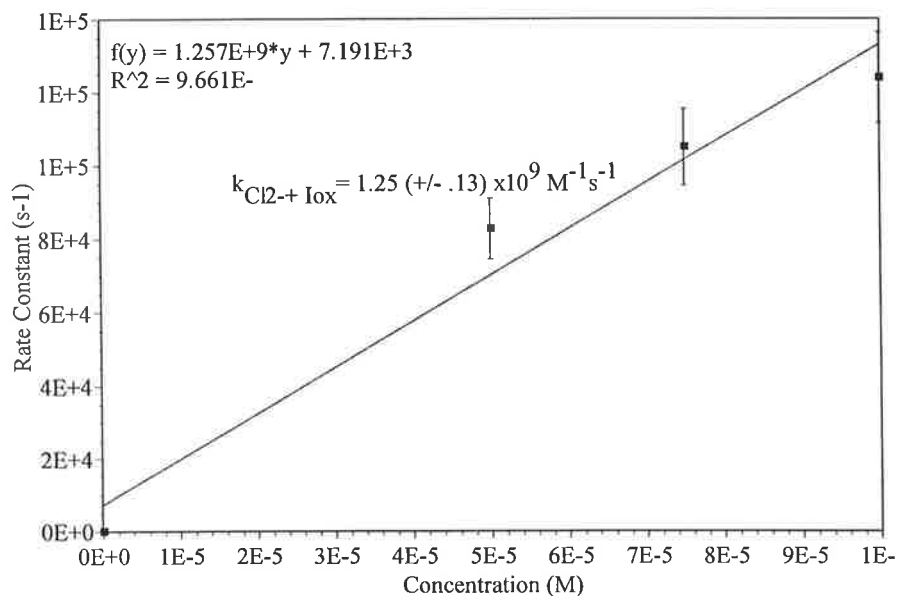


Figure 9. Decay kinetic results from the reaction of Ioxynil with the chloride radical anion at pH 2.3.

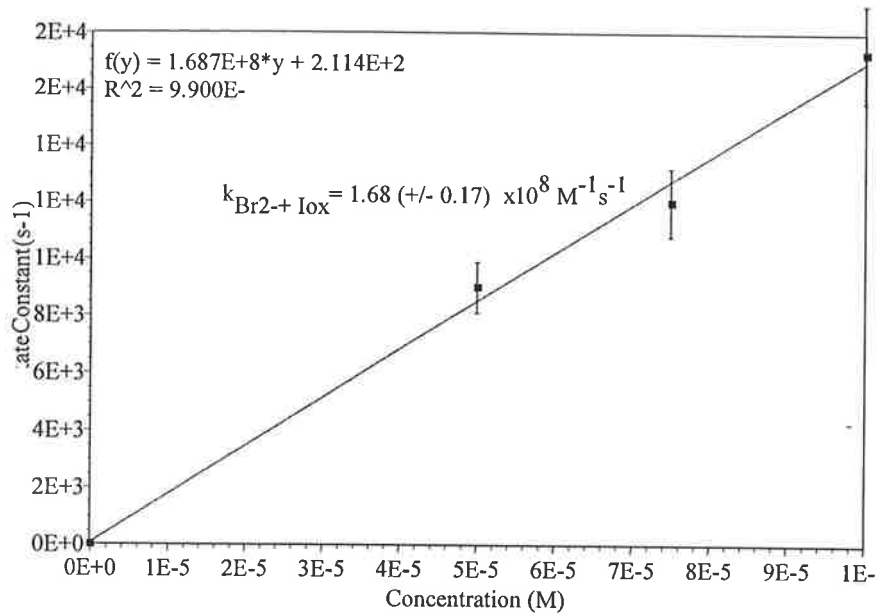


Figure 10. Decay kinetic results from the reaction of Ioxynil with the bromide radical anion at pH 7.2.

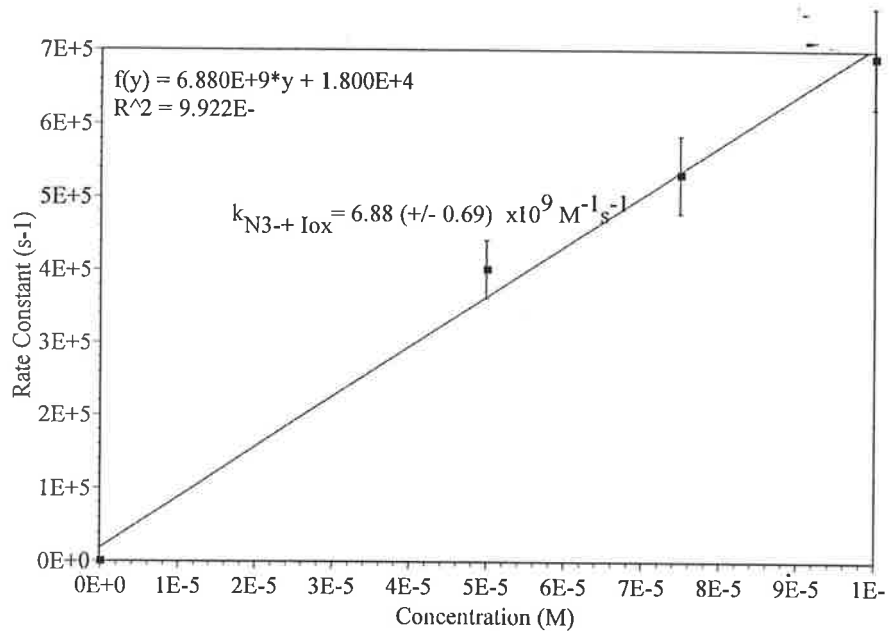


Figure 11. Formation kinetic results from the reaction of Ioxynil with the azide radical at pH 7.2.

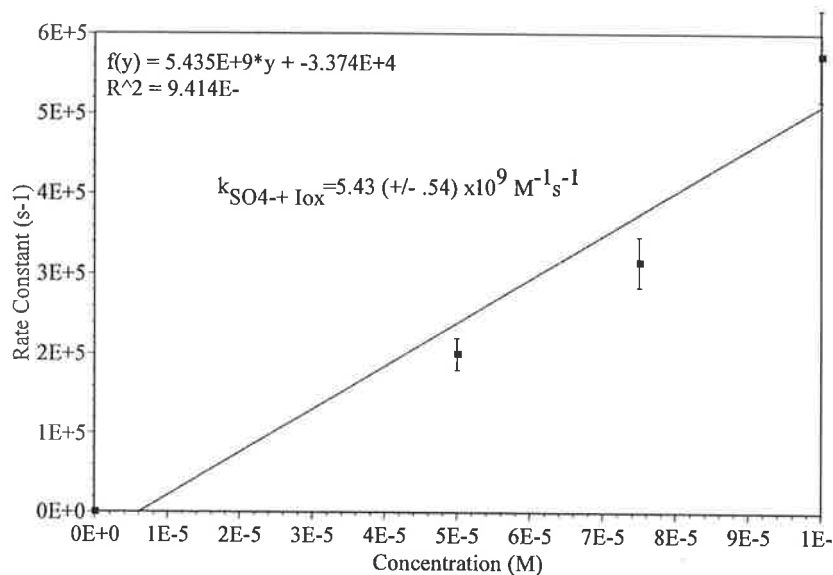


Figure 12. Decay kinetic results from the reaction of Ioxynil with the sulphate radical anion at pH 7.2.

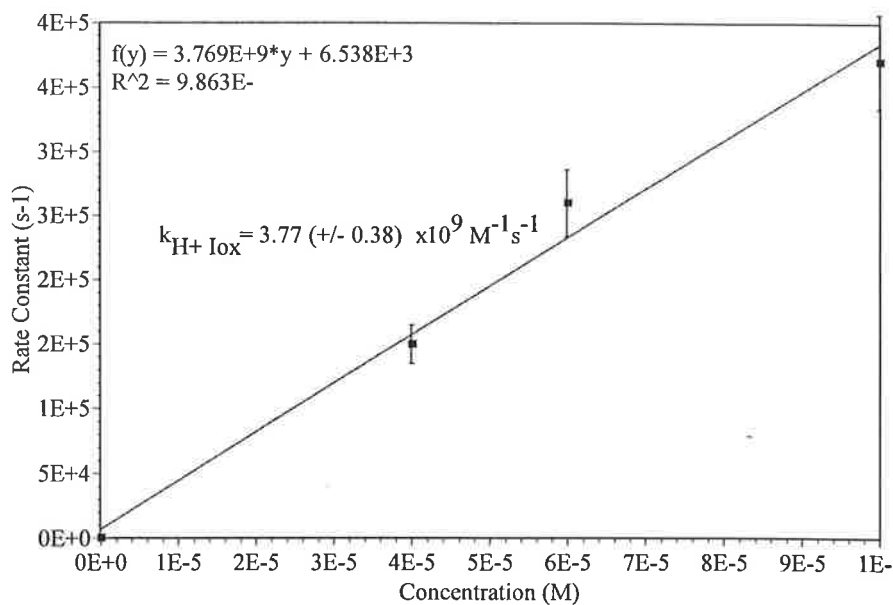


Figure 13. Formation kinetic results from the reaction of Ioxnyl with the hydrogen atom at pH 2.3.

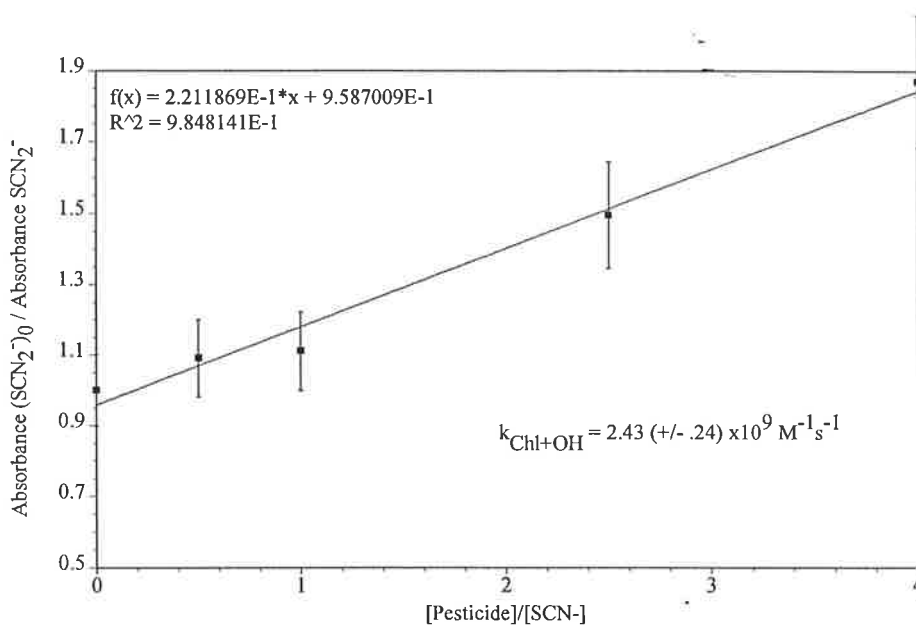


Figure 14. Competition kinetic results from the reaction of Chlorsulfuron with the hydroxyl radical.

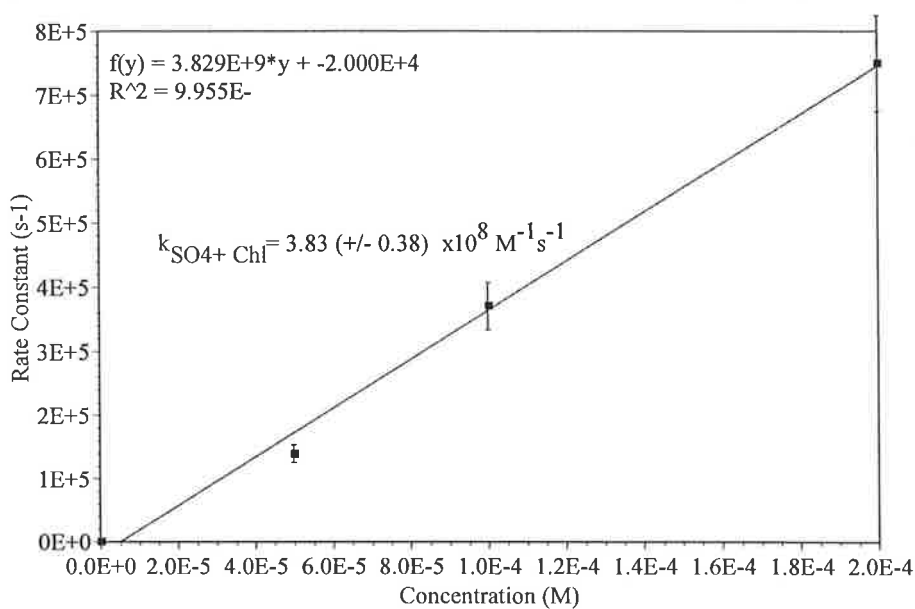


Figure 15. Decay kinetic results from the reaction of Chlorsulfuron with the sulphate radical anion.

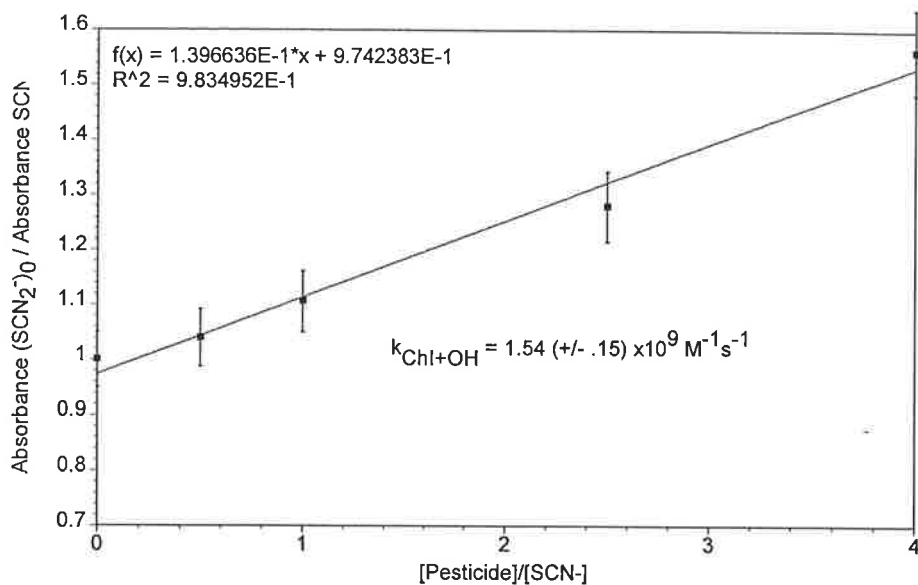


Figure 16. Competition kinetic results from the reaction of Chlorsulfuron with the hydroxyl radical at pH 2.3.

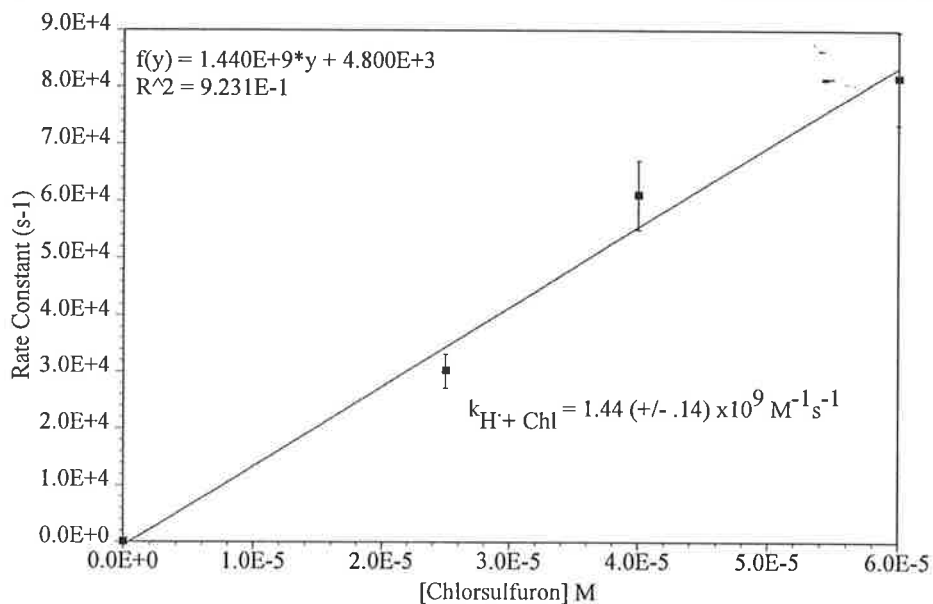


Figure 17. Formation kinetic results from the reaction of Chlorsulfuron with the hydrogen atom at pH 2.3.

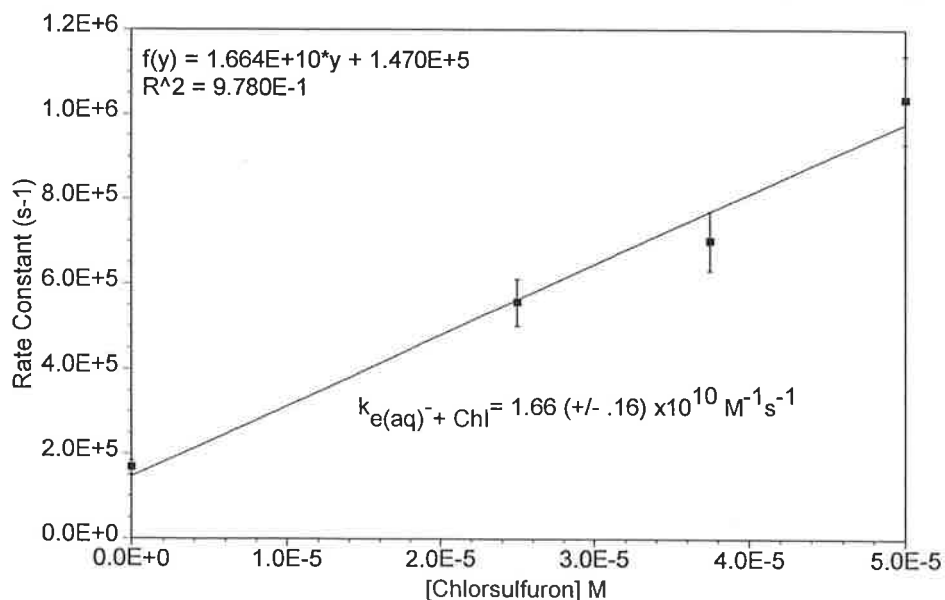


Figure 18. Decay kinetic results from the reaction of Chlorsulfuron with the hydrated electron at pH 7.2.

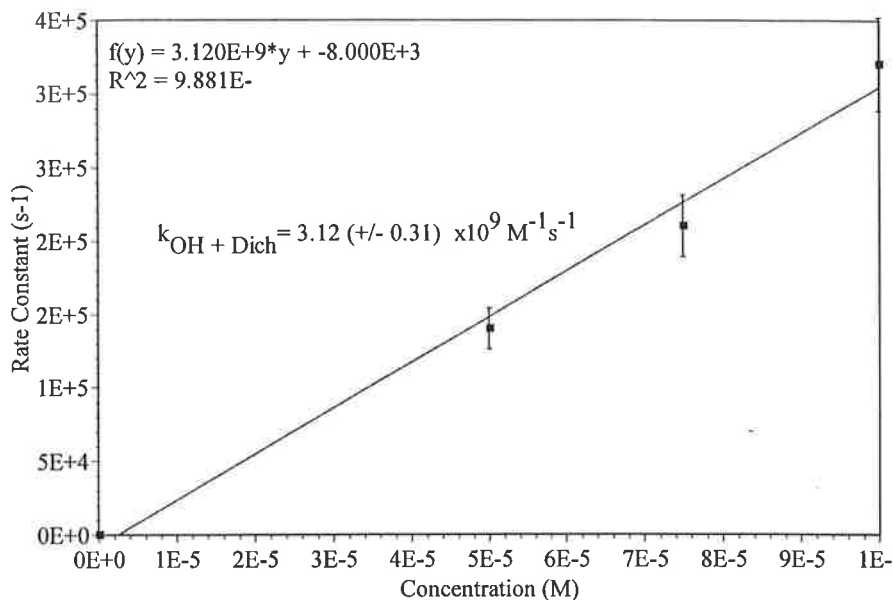


Figure 19. Formation kinetic results from the reaction of Dichlorophen with the hydroxyl radical at pH 9.2.

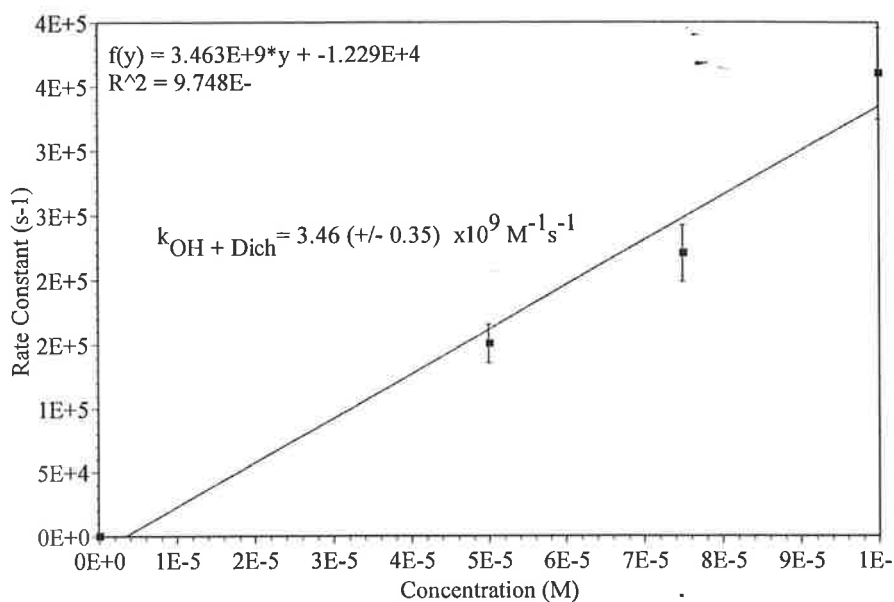


Figure 20. Formation kinetic results from the reaction of Dichlorophen with the hydroxyl radical at pH 2.3.

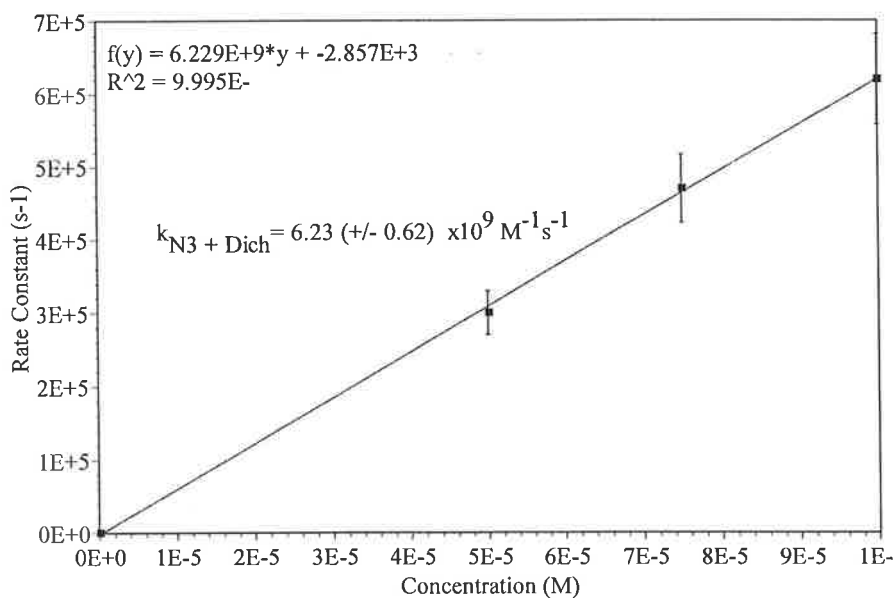


Figure 21. Formation kinetic results from the reaction of Dichlorophen with the azide radical at pH 9.2.

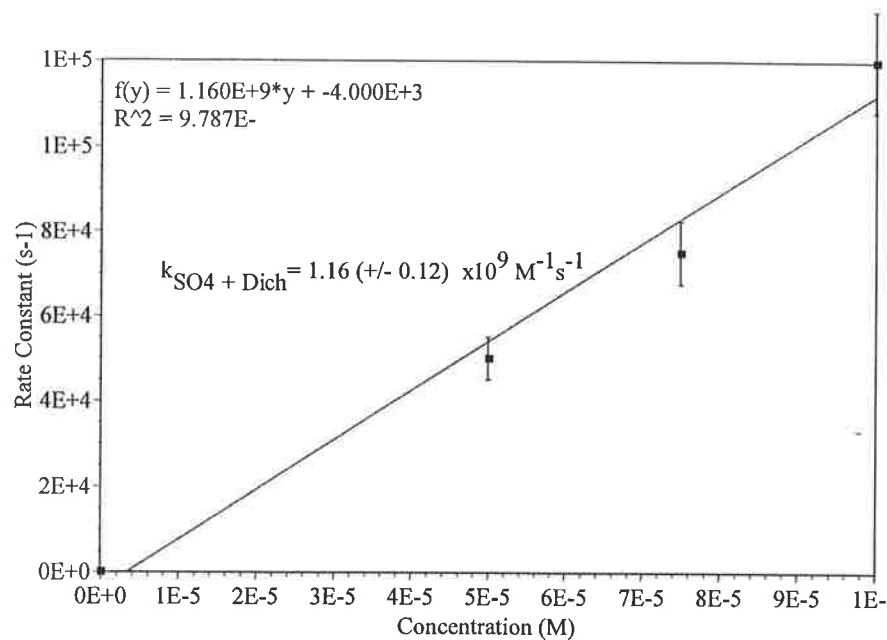


Figure 22. Decay kinetic results from the reaction of Dichlorophen with the sulphate radical radical at pH 9.2.

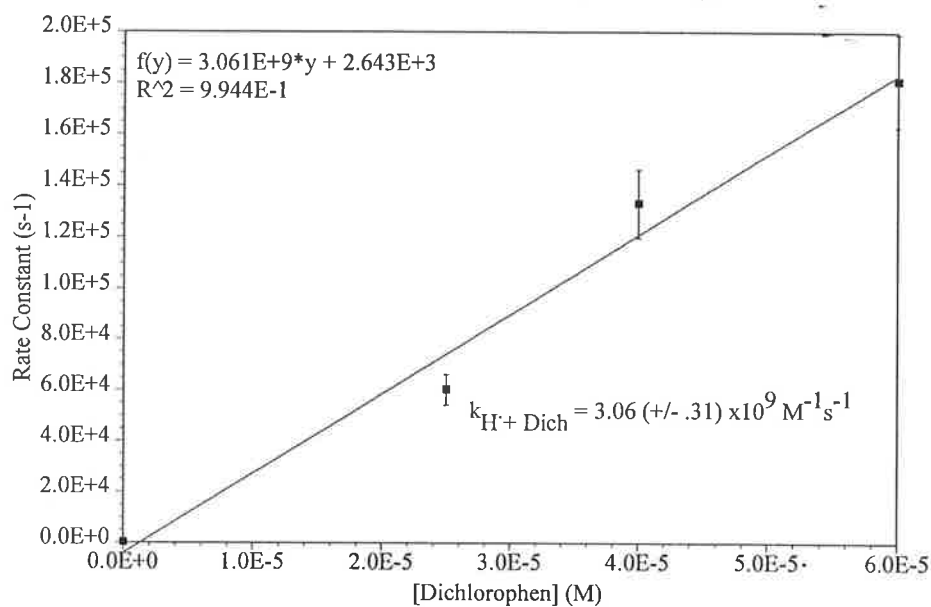


Figure 23. Formation kinetic results from the reaction of Dichlorophen with the hydrogen atom at pH 2.3.

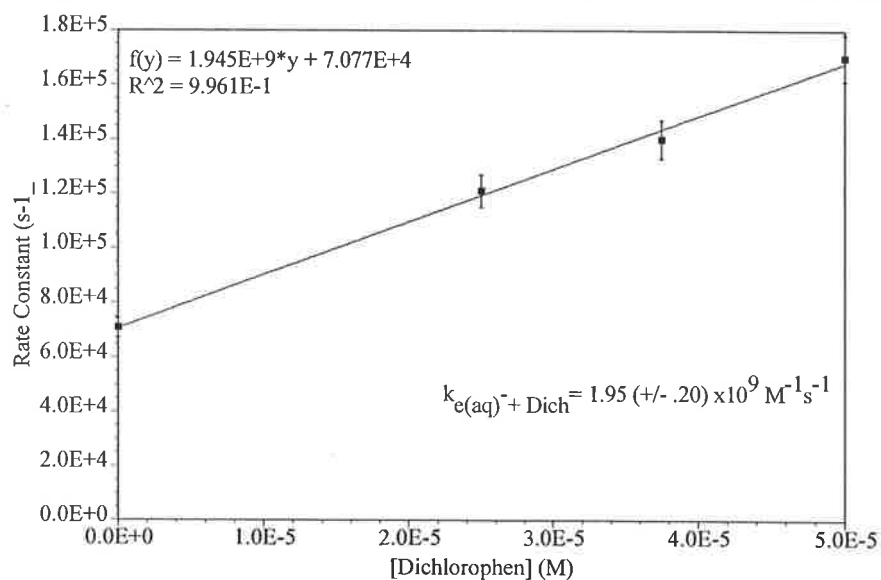


Figure 24. Decay kinetic results from the reaction of Dichlorophen with the hydrated electron at pH 7.2.

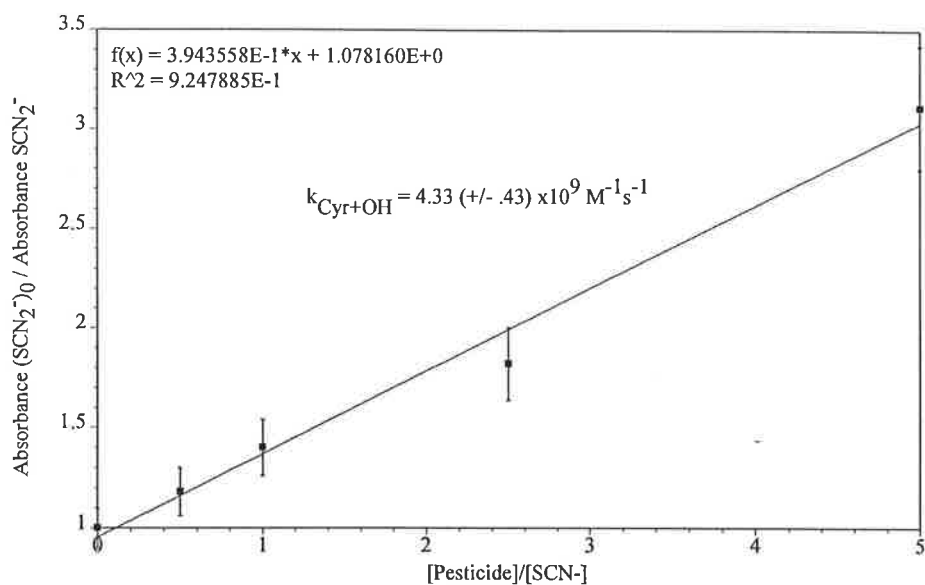


Figure 25. Competition kinetic results from the reaction of Cyromazine with the hydroxyl radical.

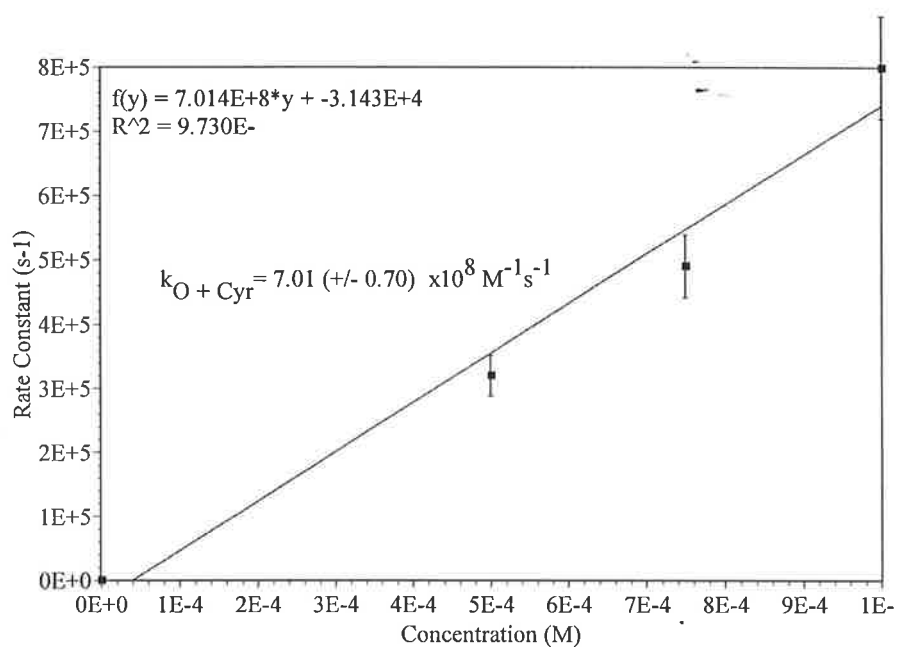


Figure 26. Formation kinetic results from the reaction of Cyromazine with the oxide anion radical at pH 13.2.

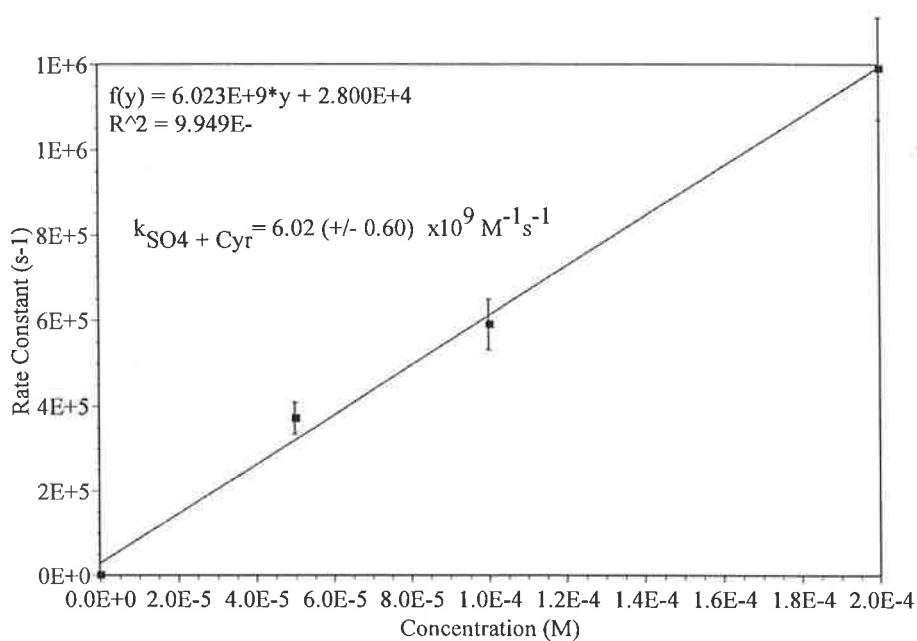


Figure 27. Formation kinetic results from the reaction of Cyromazine with the sulphate radical anion at pH 7.2.

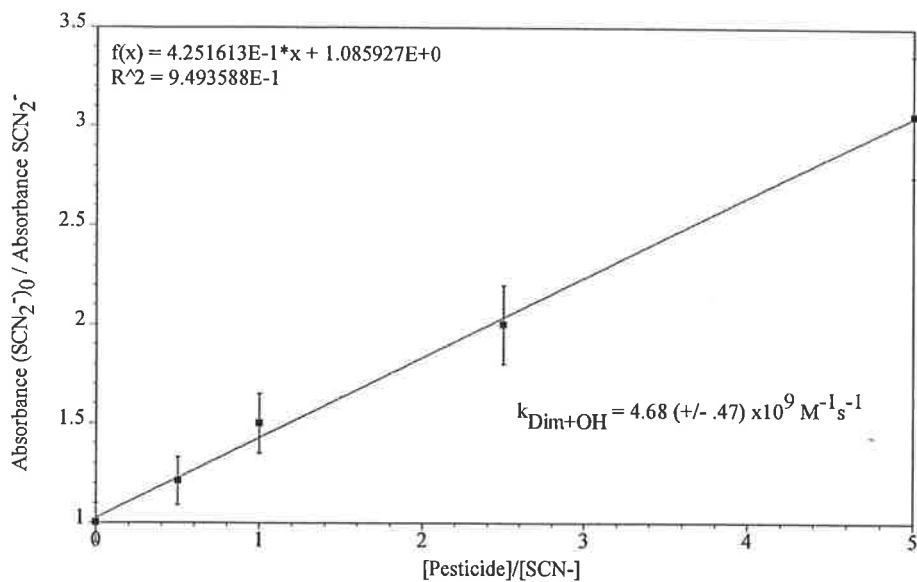


Figure 28. Competition kinetic results from the reaction of Dimethirimol with the hydroxyl radical

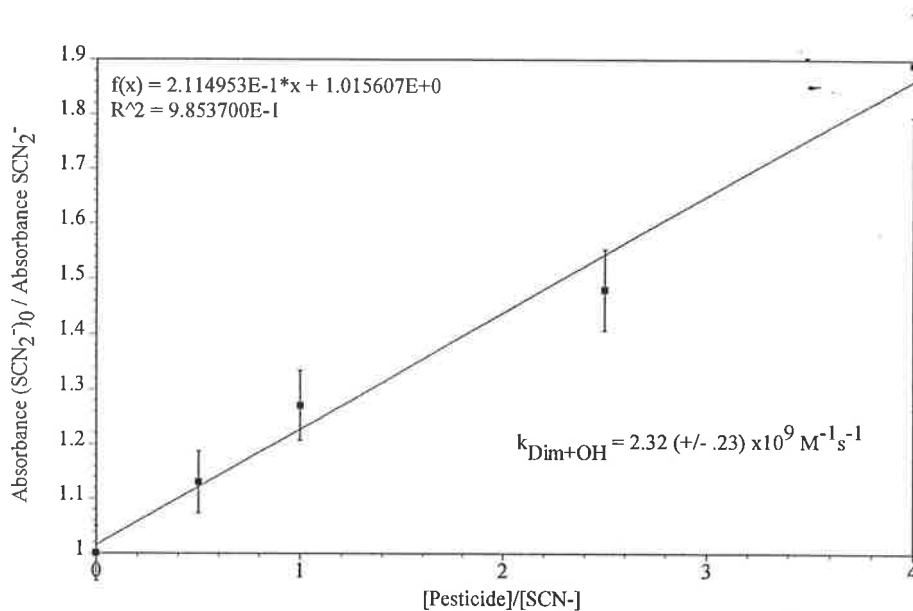


Figure 29. Competition kinetic results from the reaction of Dimethirimol with the hydroxyl radical at pH 2.3.

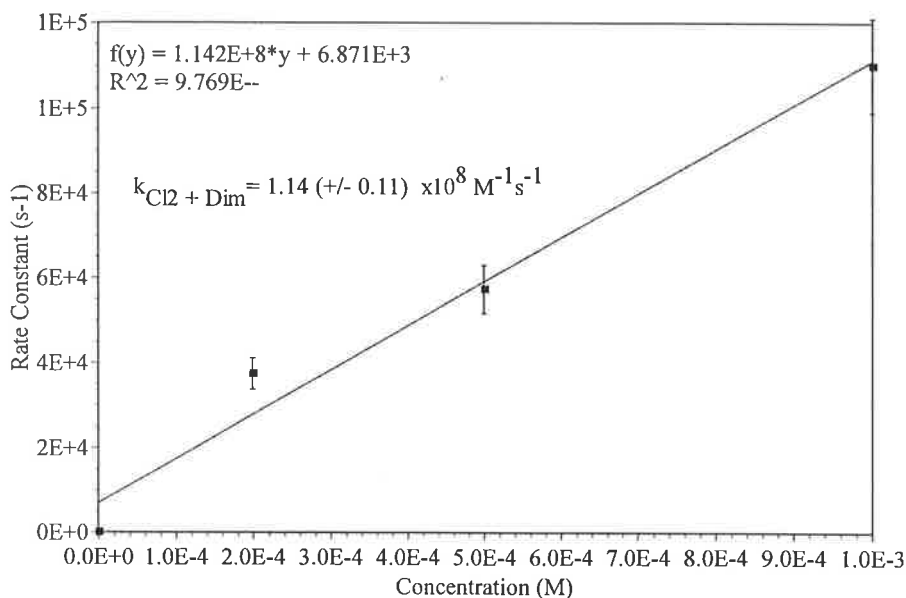


Figure 30. Competition kinetic results from the reaction of Dimethirimol with the chloride radical anion at pH 2.3.

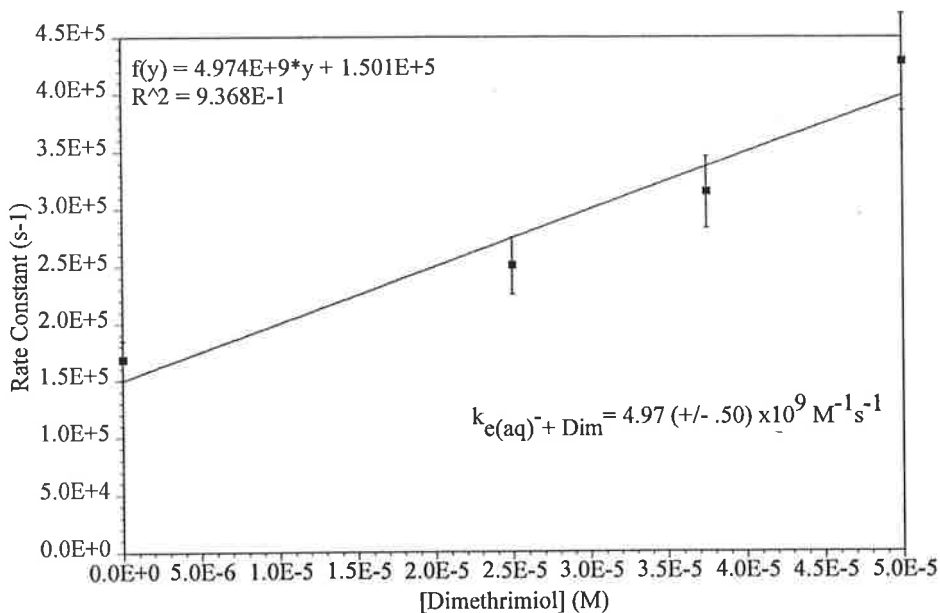


Figure 31. Decay kinetic results from the reaction of Dimethrimiol with the hydrated electron at pH 7.2.

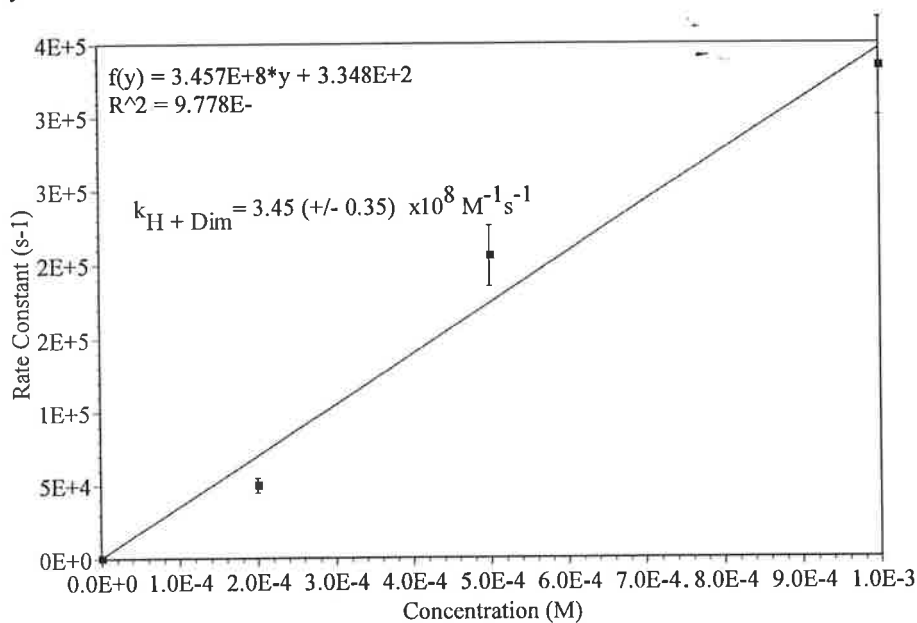


Figure 31. Formation kinetic results from the reaction of Dimethrimiol with the hydrogen atom at pH 2.3..

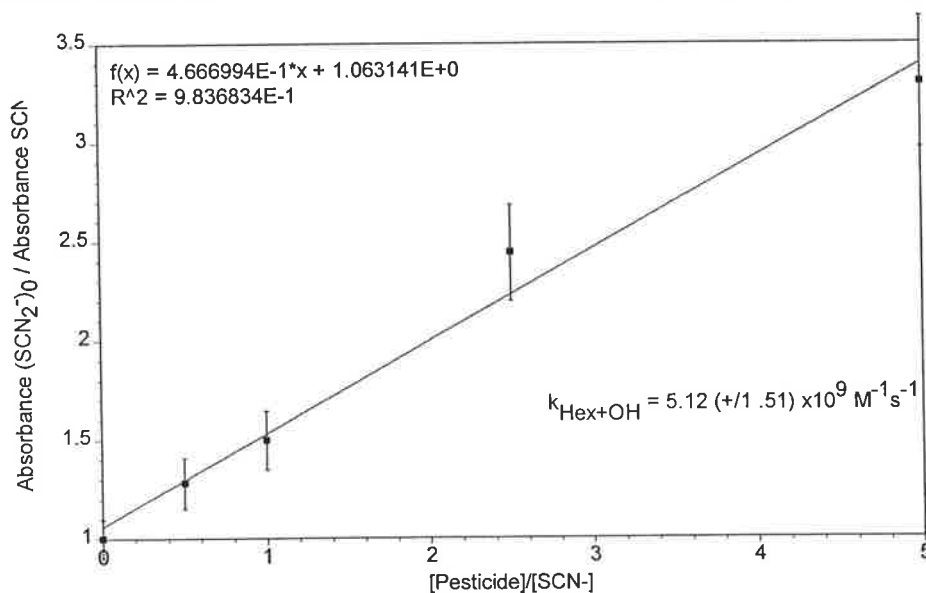


Figure 32. Competition kinetic results from the reaction of Hexazinone with the hydroxyl radical.

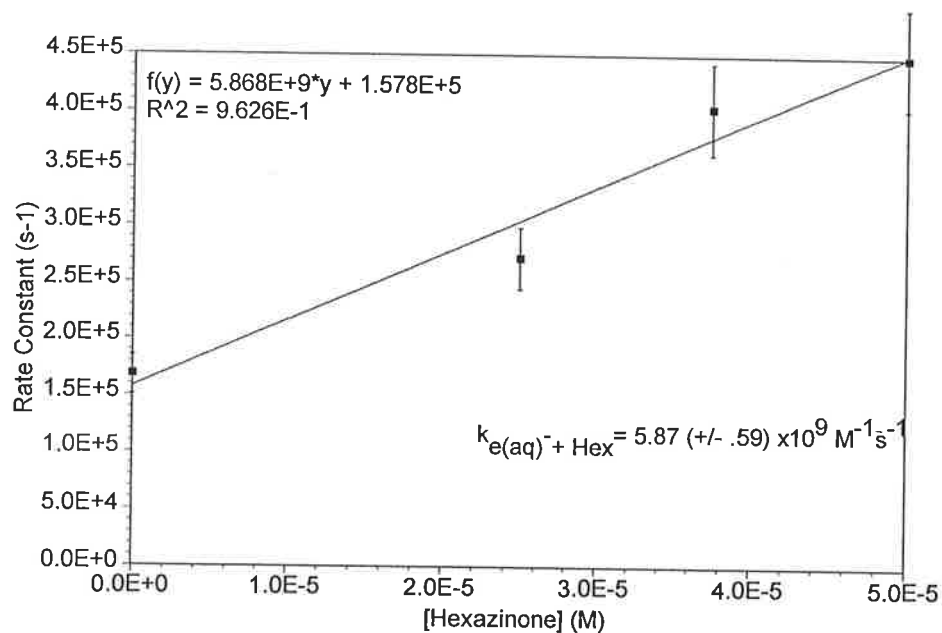


Figure 33. Decay kinetic results from the reaction of Hexazinone with the hydrated electron at pH 7.2.

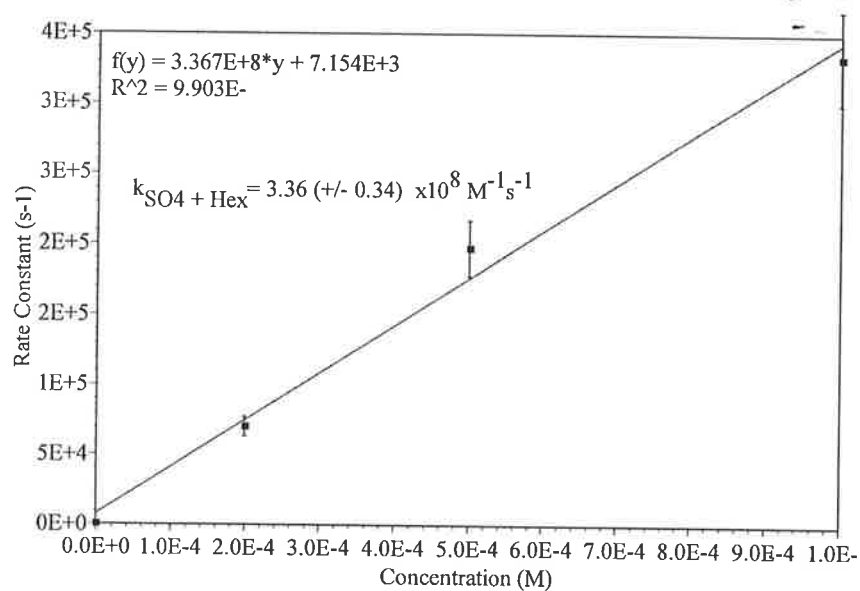


Figure 34. Decay kinetic results from the reaction of Hexazinone with the sulphate radical anion at pH 7.2

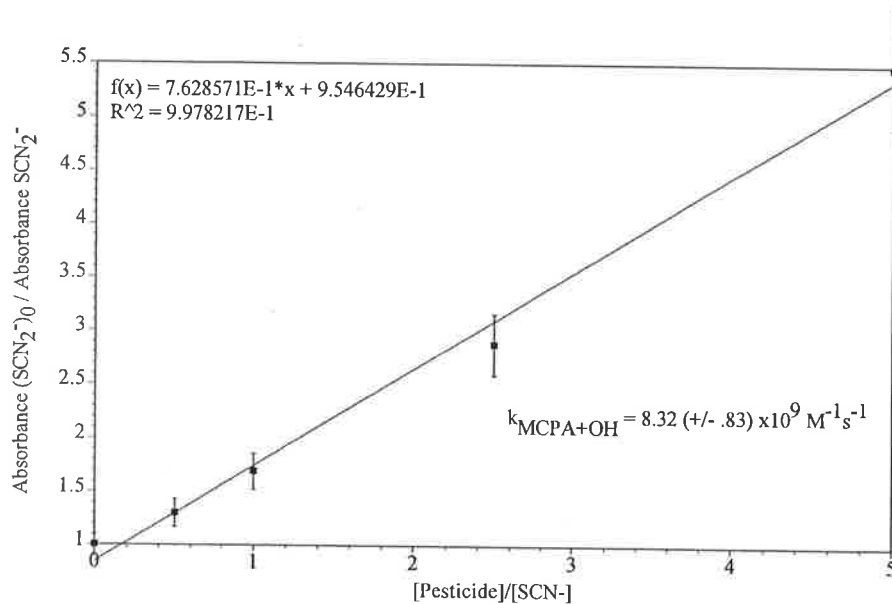


Figure 35. Competition kinetic results from the reaction of MCPA with the hydroxyl radical at pH 7.2..

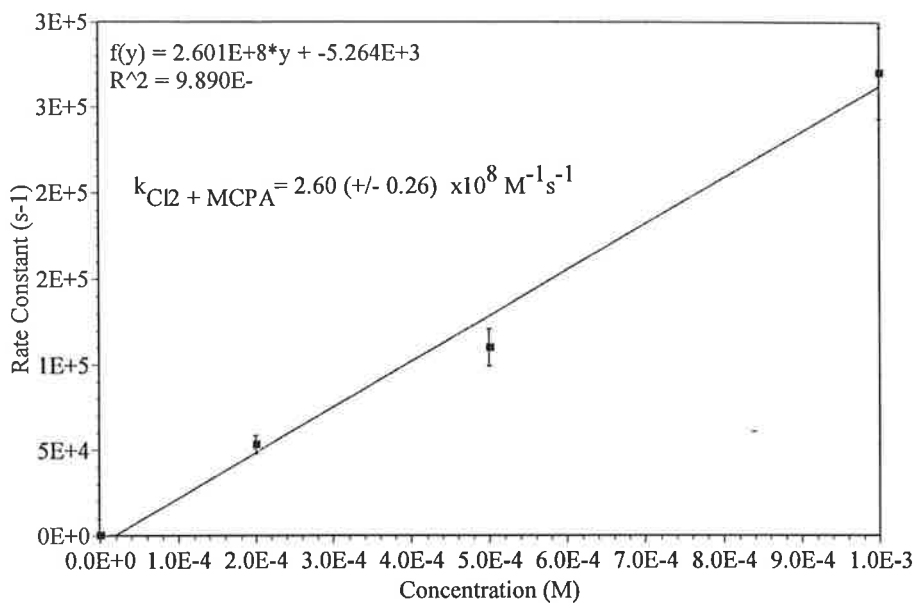


Figure 37. Decay kinetic results from the reaction of MCPA with the chloride radical anion at pH 2.3.

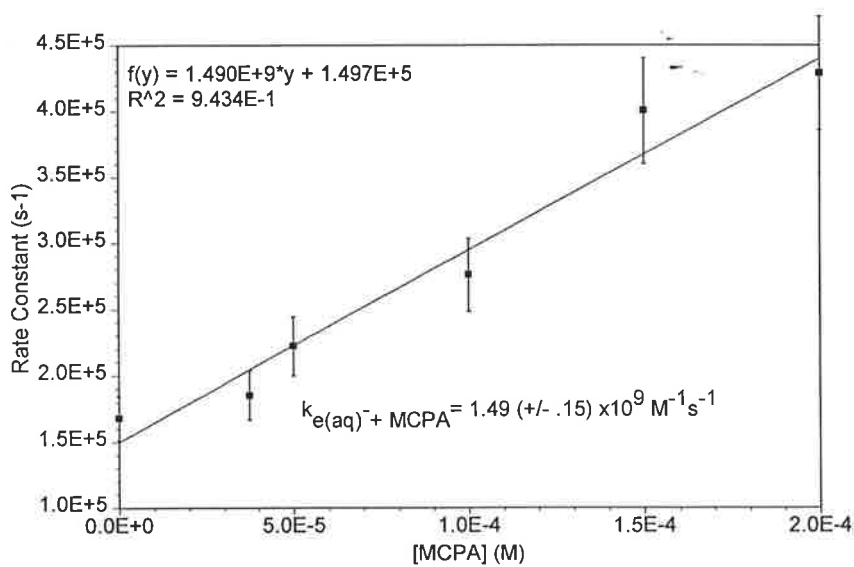


Figure 38. Decay kinetic results from the reaction of MCPA with the hydrated electron at pH 7.2.

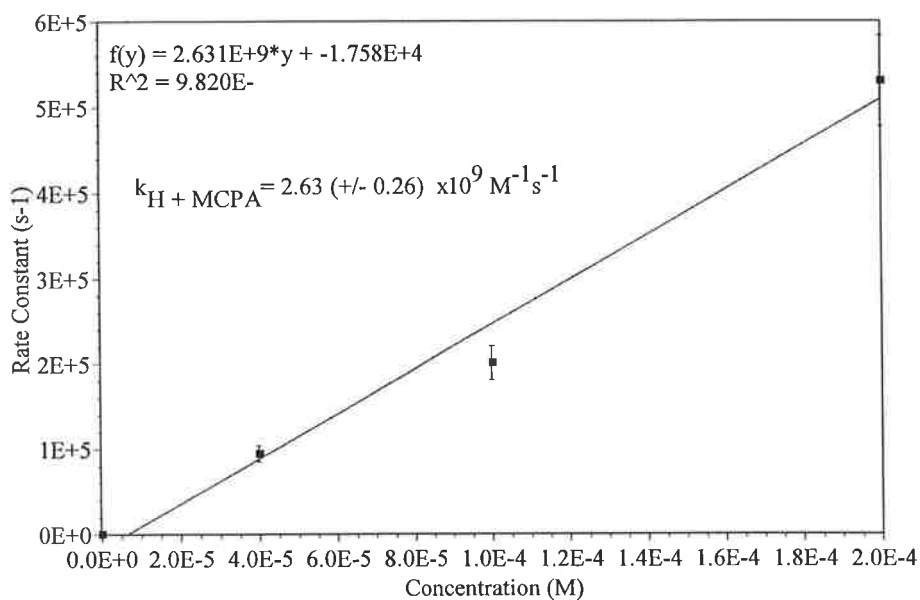


Figure 39. Formation kinetic results from the reaction of MCPA with the hydrogen atom at pH 2.3.

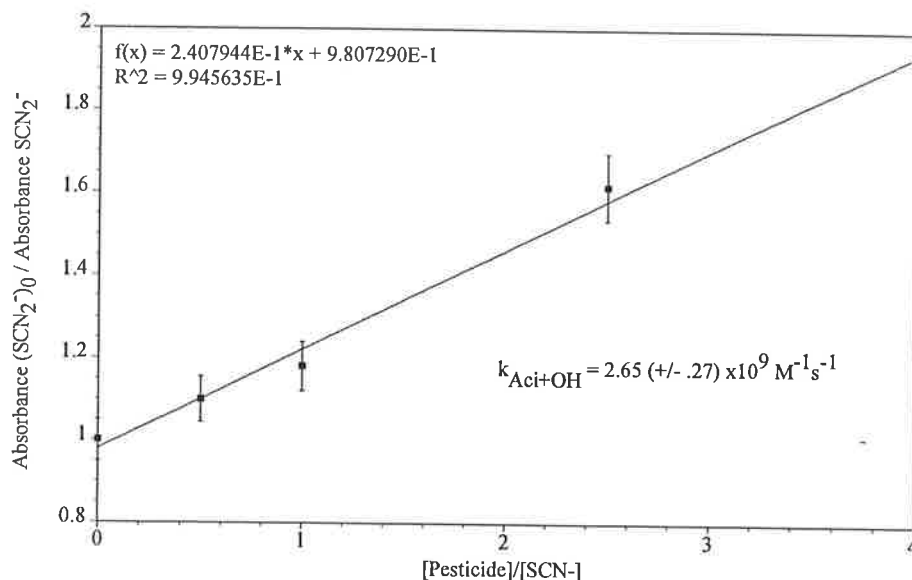


Figure 40. Competition kinetic results from the reaction of Acifluofen with the hydroxyl radical.

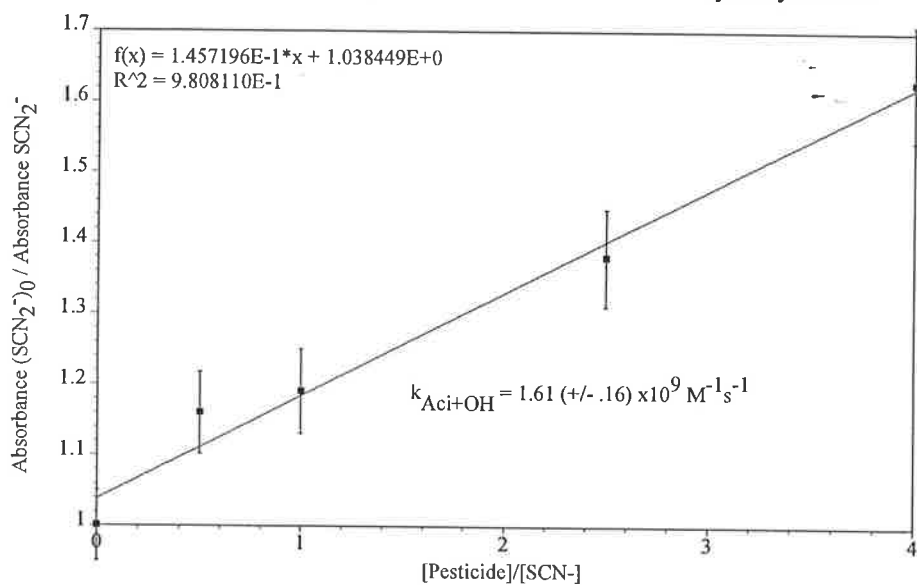


Figure 41. Competition kinetic results from the reaction of Acifluofen with the hydroxyl radical at pH 2.3.

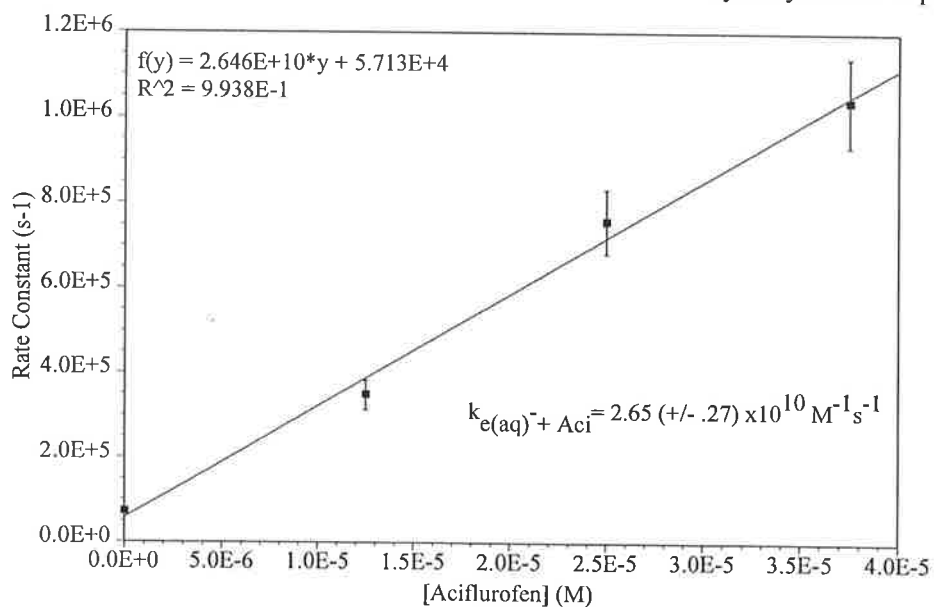


Figure 42. Decay kinetic results from the reaction of Acifluofen with the hydrated electron at pH 7.2.

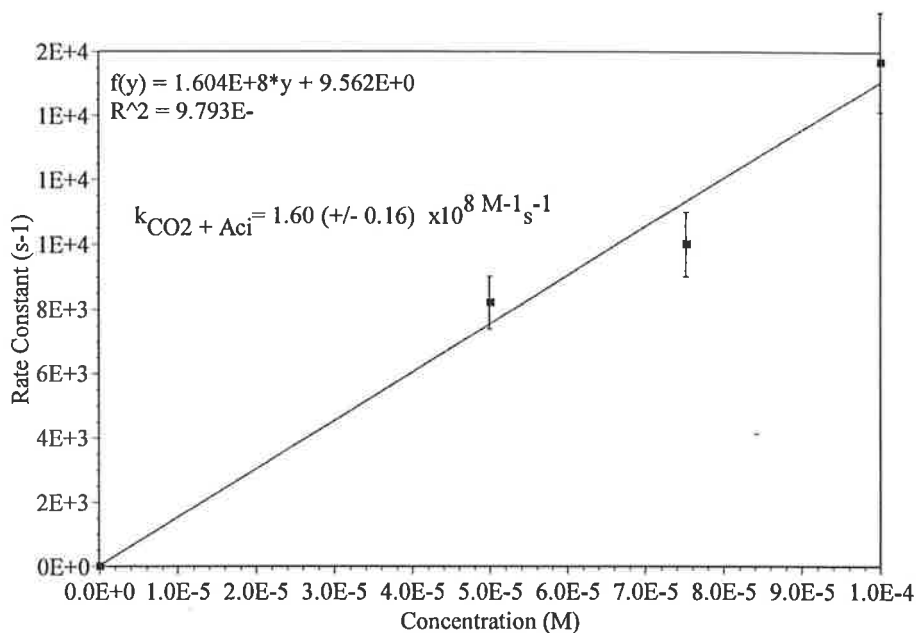


Figure 42. Formation kinetic results from the reaction of Acifluoren with the carbon dioxide radical at pH 7.2.

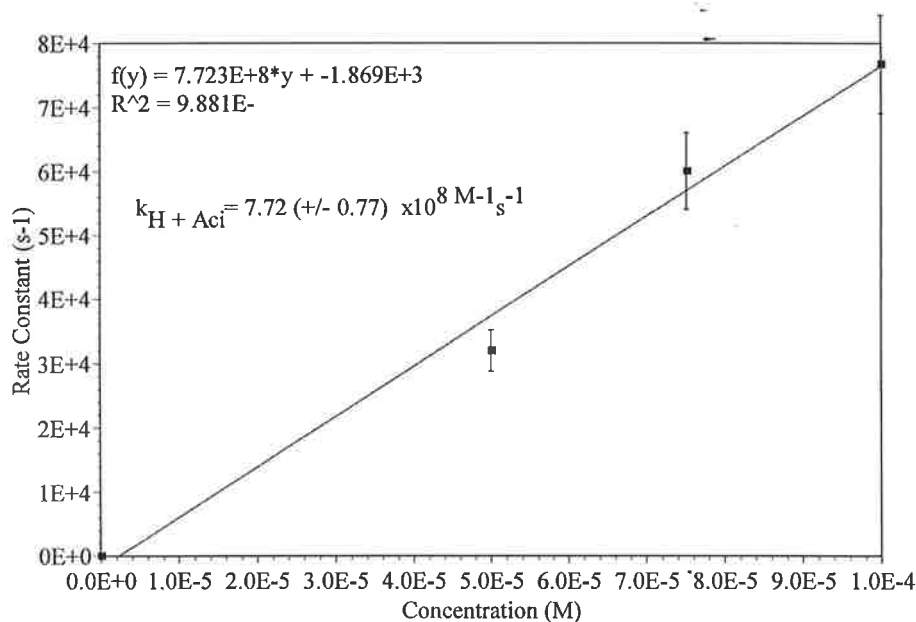


Figure 43. Formation kinetic results from the reaction of Acifluoren with the hydrogen atom at pH 2.3.

14.0 BIBLIOGRAPHY

- 1) Lewis; R. H. L. "16th Report Fresh Water Quality," in the Royal Commission of Environmental Pollution, 1992.
- 2) Peterson HG; Boutin C; Martin PA; Freemark KE; Ruecker NJ; Moody MJ; *Aquatic phyto-toxicity of 23 pesticides applied at expected environmental concentrations: Aquatic Toxicology*, **1994**, 28, p. 275-292.
- 3) Lode O; Elklo OM; Holen B; Svensen A; Johnson AM; *Pesticides in precipitation in Norway: Sci. Total Environ.*, **1995**, 160/161, p. 421-431.
- 4) Loehrer RC; *Pollution Control for Agriculture*; 2nd ed.; Academic Press: London, 1984.
- 5) Gurnham CF; *Industrial Waste Water Control*; Academic Press: London, 1965.
- 6) Burns LA; *Fate of Chemicals in Aquatic Systems: Process Model and Computer Codes*; Burns LA, Ed.; American Chemical Society: Washington D.C., 1983, pp 25-39.
- 7) Zafiriou OC; Jousset-Dubien J; Zepp RG; Zika RG; *Photochemistry of Natural Waters: Environ. Sci & Tech.*, **1984**, 18, p. 358A-371A.
- 8) Helz GR, R Zepp; Crosby DG *Aquatic and Surface Photochemistry*; Lewis Publishers: London, 1994.
- 9) Kochany J; Maguire RJ; *Abiotic transformation of polynuclear aromatic hydrocarbons and polynuclear aromatic nitrogen heterocycles in aquatic environments: Sci. Total Environ.*, **1994**, 144, p. 17-31.
- 10) Mill T; Hendry DG; Richardson H; *Free-Radical Oxidants in Natural Waters: Science*, **1980**, 207, p. 886-887.
- 11) Miller GC; Zepp RG; *Extrapolating photolysis rates from the laboratory to the environment: Res. Reviews*, **1983**, 85, p. 89-110.
- 12) Miller S; *Photochemistry of Natural Water: Environ. Sci & Technol.*, **1983**, 17, p. 568A-570A.
- 13) Zepp RG; Holgne J; Bader H; *Nitrate-Induced Photooxidation of Traced Organic Chemicals in water: Environ. Sci. & Tech.*, **1987**, 21, p. 443-450.
- 14) Legrini D; *Photochemical process for waste water treatment: Chem Rev.*, **1993**, 93, p. 671-698.
- 15) Sutton P; *Chemistry and Light*; Royal Society of Chemistry: Cambridge, 1994.
- 16) Cooper WJ; Zika RG; Petasne RG; Plane JM; *Photochemical Formation of H₂O₂ in natural waters exposed to sunlight: Environ. Sci. & Technol.*, **1988**, 22, p. .
- 17) Draper WM; Crosby DG; *The Photochemical Generation of Hydrogen Peroxide in Natural Waters: Arch. Environ. Contam. Toxicol.*, **1982**, 12, p. 121-126.

- 18) Draper WM; Crosby DG; *Solar Photooxidation of Pesticides in Dilute Hydrogen Peroxide*: J. Agric. Food. Chem., **1984**, 32, p. 231-237.
- 19) Draper, W; Crosby D; *Hydrogen Peroxide and Hydroxyl Radical: Intermediates in Indirect Photolysis Reaction in Water*: J. Agric. Food. Chem., **1981**, 29, p. 699-702.
- 20) Cooper WJ; Zika RG; *Photochemical Formation of Hydrogen Peroxide in Surface and Ground Waters Exposed to Sunlight*: Science, **1983**, 220, p. 711-712.
- 21) Haag WR; Hoigne J; Gassman E; Braun AM; *Singlet Oxygen in surface waters- Part II: Quantum yields of its production by some natural Humic Materials as a function of wavelength*: Chemosphere, **1984**, 13, p. 641-650.
- 22) Haag WR; Hoigne J; Gassman E; Braun AM; *Singlet Oxygen in surface water- Part I: Furfuryl Alcohol as a Trapping Agent*: Chemosphere, **1984**, 13, p. .
- 23) Zepp RG; Wolfe NL; Baughman GL; Hollis RC; *Singlet Oxygen in Natural Waters*: Nature, **1977**, 267, p. 421-423.
- 24) Faust BC; Allen JM; *Aqueous-Phase Photochemical formation of Hydroxyl radicals in Authentic Cloud Water and Fogwater*: Environ. Sci & Tech., **1993**, 27, p. 1221-1224.
- 25) Gierer J; Yang E; Reitberger T; *On the Significance of the Superoxide Radical (O_2^-/HO_2) in Oxidative Delignification, Studies with 4-t-Butylsringol and 4-t-Butylguaiacol Part I: The Mechanism of Aromatic ring opening*: Holzforschung, **1994**, 48, p. 405-414.
- 26) Haag WR; Hoigne J; *Photo-Sensitised Oxidation in Natural Water via OH Radicals*: Chemosphere, **1985**, 14, p. 1659-1671.
- 27) Zepp RG; Faust BC; Hoigne J; *Hydroxyl Radicals Formation in Aqueous Reaction (pH 3-8) of Iron(II) with Hydrogen Peroxide: The Photo-Fenton Reaction*: Environ. Sci. Technol., **1992**, 26, p. 313-319.
- 28) Faust BC; Zepp RG; *Photochemistry of Aqueous Iron(III)-Polycarboxylate Complexes: Roles in the Chemistry of Atmospheric and Surface Waters*: Environ. Sci. Technol., **1993**, 27, p. 2517-2522.
- 29) Lipczynska-Kochany E; Sprah G; Harms S; *Influence of some ground water and surface waters constituents on the degradation of 4-chlorophenol by Fenton Reaction*: Chemosphere, **1995**, 30, p. 9-20.
- 30) Russi H; Kotzaias D; Korte F; *Photoinduierte hydroxylierungsreaktionen organischer chemikalien in naturlischen gewassern - Nitrate als potentielle OH-radikalquellen*: Chemosphere, **1982**, 11, p. 1041-1048.
- 31) Kotzais D; Palar H; Korte F; *Photoreaktivitat organischer chemiakalien in wabrigen system in gegenwart vo nitraten and nitrinen*: Naturwissenschaften, **1982**, 69, p. 3444-5.
- 32) Masten SJ; Davies SHR; *The use of ozonisation to degrade organic contaminants in waste water*: Environ. Sci. Technol., **1994**, 28, p. 180a-185a.

- 33) Pignatello JJ; Chapa G; *Degradation of PCB's by ferric ion, hydrogen peroxide and UV light*: Environ. Tox. Chem., **1994**, *13*, p. 423-427.
- 34) Pignatello JJ; *Dark and photo assisted Fe³⁺ catalysed degradation of Chlorophenoxy herbicides by hydrogen peroxide*: Environ. Sci. Technol., **1992**, *26*, p. 944-951.
- 35) Murphy AP; Boegil WJ; Price MK; Moody CD; *A Fenton-like reaction to neutralise formaldehyde waste solutions*: Environ. Sci. Technol., **1989**, *23*, p. 166-169.
- 36) Pramauro E; Vincenti M; Augugliaro V; Palmisano L; *Photocatalytic degradation of Monuron in aqueous TiO₂ dispersions*: Environ. Sci. Technol., **1993**, *27*, p. 1790-1795.
- 37) Prairie MR; Evans LR; Stange BM; Martinez SL; *An investigation for the treatment of water contaminated with metals and organic chemicals*: Environ. Sci. Technol., **1993**, *27*, p. 1776-1782.
- 38) Zhang Y; Crittenden JC; Hand DW; Perram DL; *Fix-Bed photo catalysts for solar decontamination of water*: Environ. Sci. Technol., **1994**, *28*, p. 435-442.
- 39) Korrman C; Bahnemann DW; Hoffmann MR; *Photocatalytic production of hydrogen peroxide in aqueous suspension of TiO₂, ZnO, and desert sand*: Environ. Sci. Technol., **1988**, *22*, p. 798-806.
- 40) Manouni M; Mansour M; Schmitt P *Chapter 24*; Manouni M; Mansour M; Schmitt P, Ed.; Academic Press: New York, pp 249.
- 41) Hilarides RJ; Gray KA; *Radiolytic degradation of Dioxin on Soil: Optimal Conditions and Economic Considerations*: Environ. Progress, **1994**, *13*, p. 263-267.
- 42) Hilarides RJ; Gray KA; Guzzetta J; Cortellucci N; Sommer C; *Radiolytic degradation of 2,3,7,8-TCDD in Artificially Contaminated Soils*: Environ. Sci. & Tech., **1994**, *28*, p. 2249-2258.
- 43) Neta P; Huie RE; Ross AB; *Rate Constants for the reactions of Inorganic Radicals in Aqueous Solution*: J. Phys. Chem. Ref. Data, **1988**, *17*, p. 1043.
- 44) Buxton GV; Greenstock CL; Helman WP; Ross AB; *Critical Review of Rate Constants for Reaction of Hydrated Electrons, Hydrogen Atoms and Hydroxyl Radicals (OH/O⁻) in Aqueous Solution*: J. Phys. Chem. Ref. Data, **1988**, *17*, p. 513.
- 45) Bielski BHJ; Cabelli DE; Arudi RL; Ross AB; *Reactivity of HO₂/O₂⁻ radicals in aqueous solution*: J. Phys. Chem Ref. Data, **1985**, *14*, p. 1041.
- 46) Bucholtz DL; Lavy TL; *Effects of Cobalt-60 radiation on Herbicides in Aqueous Solutions*: Wees Sci., **1977**, *25*, p. 200-202.
- 47) Solar S; Getoff N; *Radiolysis and Pulse Radiolysis of chlorinated phenols in aqueous solutions*: Radiat. Phys. Lett., **1986**, *28*, p. 443-450.
- 48) Fox MA *The Role of Hydroxyl Radical in the Photocatalyzed Detoxification of Organic Pollutants: Pulse Radiolysis and Time-resolved Diffused Reflectance Measurements*; Fox MA, Ed.; Elsevier Science Publisher, 1993, pp 163-167.

- 49) Terzain R; Serpone N; Fox MA; *Primary radicals in the photo-oxidation of aromatics-reactions of xylenols with OH, N₃ and H radicals and formation and Characterization of dimethylphenoxyl, dihydroxydimethylcyclohexadienyl and hydroxydimethylcyclohexadienyl radicals by pulse radiolysis*: J. Photochem. Photobiol. A, **1995**, 90, p. 125-135.
- 50) Quint RM; Park HR; Krajnik P; Solar S; Getoff N; Shehested K; *Gamma-Radiolysis and Pulse Radiolysis of Aqueous 4-Chloroanisole*: Radiat. Phys. Chem., **1996**, 47, p. 835-845.
- 51) Sangter DF; O'Donnell JH *Principle of radiation chemistry*; Edward Arnild: London, 1970.
- 52) Spinks JWT; Woods RJ *An Introduction to Radiation Chemistry*; 3rd ed.; John Wiley & Son: New York, 1992.
- 53) Allan JT; Scholes G; *Effects of pH and the Nature of the Primary Species in the Radiolysis of Aqueous Solutions*: Nature, **1960**, 187, p. 218-220.
- 54) Ross F; Ross AB *Selected specific rates of reaction of transients from water in aqueous solution III, Hydroxyl radicals*; US Government Printing Office: Washington, 1977.
- 55) Ross AB; *Selected specific rates of reaction of transients from water in aqueous solution I. Hydrated electron*; US Government printing Office: Washington, 1975.
- 56) Neta P; Grodkowski J; Ross AB; *Rate Constants for reactions of Aliphatic Carbon-Centered radicals in Aqueous Solution*: J. Phys. Chem. Ref. Data, **1996**, 25, p. 709.
- 57) Koppenol WH; Leibmann JF; *The oxidising nature of the hydroxyl radical. A comparison with Ferryl Ion (FeO₂⁺)*: J. Phys. Chem., **1984**, 88, p. 99.
- 58) Schwarz HA; Dodson RW; *Equilibrium between hydroxyl radicals and Thallium(II) and the oxidation potential of OH(aq)*: J. Phys. Chem., **1984**, 88, p. 3643.
- 59) Neta P; Hoffman MZ; Simic M.; *Electron Spin Resonance and Pulse Radiolysis Studies of the Reactions of OH and O- Radicals and Olefinic Compounds*: J. Phys. Chem., **1972**, 76, p. 847-853.
- 60) Allen AO; Bielski BHJ *Formation and Disappearance of superoxide radicals in aqueous solutions*; Allen AO; Bielski BHJ, Ed.; Vol. 1, p 125.
- 61) Suzuki YI; Ford GD; *Mathematical model supporting the superoxide theory of oxygen toxicity*: Free Radical Biology and Medicine, **1994**, 16, p. 63-72.
- 62) Swallow AJ *Radiation Chemistry: An introduction*; Wiley: New York, 1973.
- 63) Anabar M; Ross F; Ross AB *Selected specific rates of transients from water in aqueous solution II. Hydrogen atom*; US Government Printing office: Washington, 1975.
- 64) Neta P; Meyerstein D; Anbar M; *Reactivity of Aromatic Compounds towards Hydrogen Atoms*: Nature, **1966**, 208, p. 1348.
- 65) Neta P; Holdern GR; Schuler RH.; *On the Rate Constants for Reaction of Hydrogen Atoms in Aqueous Solutions*: J. Phys. Chem., **1971**, 75, p. 449-454.

- 66) Neta P; Schuler RH; *Rate Constants for the reaction of Hydrogen Atoms with Aromatic and Heterocyclic Compounds. The Electrophilic Nature of Hydrogen Atoms.*: J. Amer. Chem. Soc., **1972**, *94*, p. 1056-1059.
- 67) Schwarz HA; Beliski BHJ; *Reactions of HO₂ and O₂⁻ with Iodine and Bromine and the I₂⁻ and I atom reduction potential*: J. Phys. Chem., **1986**, *90*, p. 1445.
- 68) Neta P; Madhavan V; Zemel H; Fessenden RW; *Rate constants and Mechanisms of Reaction of SO₄⁻ with aromatic compounds*: J. Amer. Chem. Soc., **1977**, *99*, p. 163-164.
- 69) Careri M; Mangia A; Musci M; *Applications of liquid chromatography-mass spectrometry interfacing in food analysis: pesticide, drug and toxic substance residues*: J Chrom. A, **1996**, *727*, p. 153-184.
- 70) Heather RW *LCQ, MS Detector Hardware Manual*; C ed.; Finnigan Corporation: San Jose, 1997.
- 71) Chang R *Chemistry*; 3rd ed.; McGraw-Hill Publishing Company: New York, 1988.
- 72) Schaftenaar G; *MOLDEN*; 3.3 ed.; CAOS/CAMM Centre: Nijmegen, 1997.
- 73) M. J. Frisch; G. W. Trucks; H. B. Schlegel; P. M. W. Gill; B. G. Johnson; M. A. Robb; J. R. Cheeseman; T. Keith; G. A. Petersson; J. A. Montgomery; . Raghavachari; M. A. Al-Laham; V. G. Zakrzewski; J. V. Ortiz; J. B. Foresman; J. Cioslowski; B. B. Stefanov; A. Nanayakkara; M. Challacombe; C. Y. Peng; P. Y. Ayala; W. Chen; M. W. Wong; J. L. Andres; E. S. Replogle; R. Gomperts; R. L. Martin; D. J. Fox; J. S. Binkley; D. J. Defrees; J. Baker; J. P. Stewart; M. Head-Gordon; C. Gonzalez; J. A. Pople *Gaussian 94*; Revision C.3, Gaussian, Inc.: Pittsburgh PA, 1995.
- 74) Glendening ED; Reed AE; Carpenter JE; Weinhold F; *NBO Version 3.1*;
- 75) Deppmeier BA; Driessen AJ; Hehre WJ; Johnson JA; Klunzinger PE; Lou L; Vu J *Spartan*; 4.1.2 x11 ed.; Deppmeier BA; Driessen AJ; Hehre WJ; Johnson JA; Klunzinger PE; Lou L; Vu J, Ed.; Wavefunction: Irvine CA., 1996.
- 76) Patchett GG; Brookman DJ; Rodebush JE; *Devrinol: Analytical methods for pesticides and plant growth regulators*, **1976**, *8*, p. 347-357.
- 77) Kidd H; David JR; *Napropamide in the Agrochemical Handbook*; Royal society of Chemistry: Cambridge, 1991; Vol. 3rd Edition.
- 78) Chan JHH; Walker F; Tseng CK; Baker DR; Arneklev DR; *Synthesis and Herbicidal Activity of N,N-Dimethyl-2-(1-naphthylloxy)propionamide and its optical isomers*: J. Agric. Food Chem., **1975**, *23*, p. 1008-1010.
- 79) Chang LL; Giang BY; Lee KS; Teseng CK.; *Aqueous photolysis of Napropamide*: J. Agric. Food Chem., **1991**, *39*, p. 6117-521.
- 80) Stanger CE; Vargas TC; *The Photodecomposition study of Napropamide*: Proc. Western Soc. of Weed, **1984**, *37*, p. 221-226.
- 81) Gordoin S; Schmidt KH; Hart EJ.; *A Pulse Radiolysis Study of Aqueous Benzene Solution*: J. Phys. Chem.; **1977**, *81*, p. 104-109.

- 82) Pan XM; Schuchmann MN, Sonntag CV.; *Oxidation of Benzene by the OH Radical. A product and Pulse Radiolysis Study in Oxygenated Aqueous Solution*: Chem. Soc. Perkins Trans. 2, **1993**, p. 289-297.
- 83) MacLachlan A; McCarthy RL; *Pulse Radiolysis of Aromatic Compounds*: J. Chem. Phys., **1962**, 84, p. 2519-2524.
- 84) Pan XM; Sonntag CV; *OH-Radical-Induced Oxidation of Benzene in the Presence of Oxygen: $R + O_2 \leftrightarrow RO_2$ Equilibria in Aqueous Solution. A Pulse Radiolysis Study*: Z. Naturforsch, **1990**, p. 1337-1339.
- 85) Merga G; Schuchmann HP; Rao BSM; Sonntag CV; *OH Radical induced oxidation of chlorobenzene in aqueous solution in the presence and absence of oxygen*: J. Chem. Soc. Perkin Trans. 2, **1996**, p. 1097-1103.
- 86) Mohan H; Mittal JP; *Direct Evidence for H^+ -catalysed Dehydration of Fluorohydroxycyclohexadienyl Radicals: A Pulse Radiolysis Study*: J. Chem. Soc. Faraday Trans., **1995**, 91, p. 2121-2126.
- 87) Mohan H; Mittal JP; *Formation of radical cations of chlorobenzene in aqueous solutions. A Pulse Radiolysis study*: Chem. Phys. Lett., **1995**, 2335, p. 444-449.
- 88) Mohan H; Mittal JP; *Formation and Reactivity of the radical Cation of Bromobenzene in Aqueous Solution: A Pulse Radiolysis Study*: J. Phys. Chem., **1995**, 99, p. 6519-6524.
- 89) Solar S; Solar W; Getoff N; *Resolved Multisite OH-Attack on Aqueous Aniline Studied by Pulse Radiolysis*: Radiat. Phys. Chem., **1986**, 28, p. 229-234.
- 90) Mohan H; Mittal. JP; *Formation and Redox Properties of Radical Ions of Idopentafluorobenzene in Aqueous Solution: A Pulse Radiolysis Study*: J. Phys. Chem., **1995**, 99, p. 12559-12563.
- 91) Simic M; Hoffman MZ; Ebert M; *Reaction of OH and O- radicals with Aromatic carboxylate in aqueous solution*: J. Phys. Chem., **1973**, 77, p. 1117-1120.
- 92) Micheal BD; Hart EJ; *The rate constants of Hydrated Electrons, Hydrogen atoms, and Hydroxyl radical Reactions with Benzene, 1,3-Cylohexadiene, 1,4-Cyclohexadiene, and Cyclohexane*: J. Phys. Chem., **1970**, 74, p. 2878-2884.
- 93) O'Neill P; Steenken S; Schulte-Frohlinde D; *Formation of radical cations of methoxylated benzenes by reaction with OH radicals Tl_2^+ , Ag_2^+ , SO_4^- , in aqueous solution. An optical and conductometric pulse radiolysis and in situ radiolysis electron spin resonance study.*: J. Phys. Chem., **1975**, 79, p. 2773-2279.
- 94) Getoff N; Solar S; *Radiolysis and pulse radiolysis of chlorinated phenols in aqueous solution*: Int. J. Radiat. Appl. Instrum. Part C., **1986**, 28, p. 443-450.
- 95) Naik DB; Moorthy PN; *Studies on the Transient Species Formed in the Pulse Radiolysis of Benzotriazole*: Radiat. Phys. Chem., **1995**, 46, p. 353-357.
- 96) Sehested K; Holcman J; *A Pulse Radiolysis Study of the OH Radical induced Autoxidation of Methanesulfinic Acid*: Radiat. Phys. Chem., **1996**, 47, p. 357-360.

- 97) Dey GR; Naik BD; Kishore K; Moorhty PN; *Nature of the Transient Species Formed in the Pulse Radiolysis of Some Thiourea Derivatives*: J. Chem. Soc. Perkin Trans. 2, **1994**, p. 1625-1629.
- 98) Ellison D.H.; Salmon G.A.; Wilkinson F.; *Nanosecond pulse radiolysis of methanolic and aqueous solution*: PROC. ROY. SOC. LONDON SER. A., **1972**, 328, p. 23-36.
- 99) Zevos N; Sehested K; *Pulse Radiolysis of Aqueous Naphthalene Solutions*: J. Phys. Chem., **1978**, 82, p. 138-141.
- 100) Merga G; Schuchmann HP; Rao BSM; Sonntag CV; *Radical induced oxidation of Chlorobenzene in aqueous solution in the absence and presence of oxygen.*: J. Chem. Soc. Perkin Trans. 2, **1996**, p. 1097-1103.
- 101) Schuler RH; *Three decades of spectroscopic studies of radiation produced intermediates*: Radiat. Phys. Chem., **1994**, 43, p. 417-423.
- 102) Pan XM; Schuchmann MN; Sonntag CV; *Hydroxyl-radicals-induced Oxidation of Cyclohexa-1,4-diene by O₂ in Aqueous Solution. A Pulse Radiolysis Study*: J. Chem. Soc. Perkin Trans 2, **1993**, p. 1021-1028.
- 103) Jonsson M; Lind J; Reitberger T; Eriksen TE; Merenyl G; *Free radical combination reactions involving phenoxyl radicals*: J. Phys. Chem., **1993**, 97, p. 8229-8233.
- 104) Ram M.S; Stanbury D.M; *Electron transfer reactions involving the Azidyl radical*: J. Phys. Chem., **1986**, 90, p. 3691.
- 105) Alfassi Z.B, Harriman. A., Huie R.E, Mosseri S, Neta P.; *Redox potential of the Azide/Azidyl radical*: J. Phys. Chem., **1987**, 91, p. 2120.
- 106) Cruco AS; Tilquin BL; Hickel B; *Radical Mechanisms of Cephalosporins: A Pulse Radiolysis Study*: Fre Rad. Biol. Med., **1995**, 18, p. 841-847.
- 107) Kapoor SR; Gopinathan C; *Studies in mixed solvents: Comparison between asolvated electron reaction and quenching of the excited state.*: Int. J. Chem. Kinet., **1995**, 27, p. 535-45.
- 108) Willix RLS; Garrison WM; *Chemistry of the effects on the reactivity of solvated electrons with organic solutes in methanol/water and ethanol/water mixed solvents.*: Radiat. Res., **1967**, 32, p. 452-62.
- 109) Lai CC; Freeman GR; *Solvent effects on the reactivity of solvated electrons with organic solutes in methano/water and ethanol/water mixed solvents.*: J. Phys. Chem., **1990**, 94, p. 302-8.
- 110) Evers EL; Jayson GC; Robb ID; Swallow AJ; *Determination by pulse radiolysis of the distribution of solubilizates between micellar and nonmicellar phase.*: Faraday Trans 1, **1980**, 76, p. 528-36.
- 111) Butler J; Henglein A; *Elementary reactions of the reduction of Tl⁺ in aqueous solution.*: J. Radiat. Phys. Chem., **1980**, 15, p. 603.
- 112) Kidd H; David. JR; *The Agrochemicals Handbook*; 3rd ed.; Ed.; Royal Society of Chemistry: London, 1991.

- 113) Flanagan RJ; Ruprah M; *HPLC Measurement of Chlorophenoxy Herbicides, Bromoxynil, and Ioxynil, in Biological Specimens to aid Diagnosis of Acute Poisoning*: Clin. Chem., **1989**, 35, p. 1342-1347.
- 114) Vosahlova J; Paavlu L; Vosahlo J; Brenner V; *Degradation of Bromoxynil, Ioxynil, Dichlorobenil and their mixtures by Agrobacterium radiobacter 8/4*: Pestic. Sci., **1997**, 49, p. 303-306.
- 115) Savory BM; Hibbitt CJ; Catchpole AH; *Effect of Climatic Factors on the Potency of Ioxynil and Bromoxynil*: Pestic. Sci, **1975**, 6, p. 145-158.
- 116) Shevchuk LG; Zhikharev VS; Vysotaskaya NA; *Kinetics of the reaction of hydroxyl radicals with benzene and pyridine derivatives.*: J. Org. Chem. USSR., **1969**, 5, p. 1606-8.
- 117) Mathews RW; Sangster DF; *Measurement by benzoate radiolytic decarboxylation of relative rate constants for hydroxyl radical reactions.*: J. Phys. Chem., **1965**, 69, p. 1389-46.
- 118) Stanfford U; Gray KA; Kamat PV; *Radiolytic and TiO₂ assisted photocatalytic degradation of 4-chlorophenol. A Comparative study*: J. Phys. Chem., **1994**, 98, p. 6343-6351.
- 119) Field RJ; Raghavan NV; Brummer JG; *A pulse radiolysis investigation of the reactions of BrO₂ with Fe(CN)₆⁴⁻, Mn(II), Phenoxide Ion and Phenol*: J. Phys. Chem., **1982**, 86, p. 2443-2449.
- 120) Guha SN; Moorthy PN; Mittal JP; *Redox reactions of Natural Red. A Pulse Radiolysis Study*: J. Chem. Soc. Perkin Trans 2, **1993**, p. 409-415.
- 121) Neta P; Dortman LM; *Pulse Radiolysis Studies. XIII. Rate constants for the reaction of hydroxyl radicals with aromatic compounds in aqueous solution.*: Advan. Chem. Ser., **1968**, 81, p. 222-30.
- 122) Das TN; Priyadarsini KI; *Characterization of the transients produced in aqueous medium by pulse radiolytic oxidation of 3,5-Diiodotyrosine*: J. Phys. Chem., **1994**, 98, p. 5272-5278.
- 123) Mc Murry J; *Organic Chemistry*; 2nd ed.; Brooks/Cole Publishing: California, 1988.
- 124) Land EJ; Ebert M; *Pulse radiolysis studies of aqueous phenol. Water from dihydroxylcyclohexadienyl radicals to form phenoxyl.*: Faraday Trans., **1967**, 63, p. .
- 125) Jin F; Leitich J; Sonntag CV; *The Superoxide radical Reacts with Tyrosine-derived Phenoxyl Radicals by addition rather than by Electron Transfer*: J. Chem. Soc. Perkin Trans., **1993**, p. 1583-1588.
- 126) Alfassi AB; Schuler RH; *Reaction of Azide radical with aromatic compounds. Azide as a selective oxidant*: J. Phys. Chem., **1985**, 89, p. 3359-3363.
- 127) Kemsley K; Moore JS; Phillips GO; Sosnowski H; *Reaction of radical probes with substituted phenols as models for the investigation of Tyrosine in Aldolase and chemically modified Aldolase.*: Acta Vitaminol Enzymol, **1974**, 28, p. 263-7.

- 128) Alfassi ZB; Neta P; Schoute LCT; *Temperature dependence of the rate constant for reaction of inorganic radicals with organic reductants*: J. Phys. Chem., **1990**, 94, p. 8800-5.
- 129) Anbar M; Hart EJ; *The reactivity of aromatic compounds towards the hydrated electron*: J. Am. Chem. Soc., **1964**, 86, p. 5633.
- 130) Das TN; *Aqueous Medium Pulse and Steady State Radiation Chemical Studies on the Reduction of 3,4-Diiodotyrosine*: J. Phys. Chem., **1994**, 98, p. 11109-11114.
- 131) Levitt G; Ploeg HL; Weigel RC; Fitzgerald DJ; *2-Chloro-N-[(4-methoxy-6-methyl-1,3,5-triazin-2-yl)aminocarbonyl]benzenesulfoamide, a new herbicide*: J. Agric. Food Chem., **1981**, 29, p. 416-418.
- 132) Thirunarayanan K; Zimdahl RL; Smika DE; *Chlorsulfuron Adsorption and Degradation*: Weed Sci., **1985**, 33, p. 558-563.
- 133) Fletcher JS; Pfleeger TG; Ratsch HC; *Potential Environmental risks associated with the new sulfonylurea herbicides*: Envir. Sci. & Tech., **1993**, 27, p. 2250.
- 134) Joshi MM; Brown HM; Romesser JA; *Degradation of Chlorsulfuron by soil Microorganisms*: Weed Sci., **1985**, 33, p. 888-893.
- 135) Chkanikov DI; Makeev; Nazarova TA; Ustimenko NV; *Effect of the antidote 1,8-Naphthalic Anhydride on phytotoxicity and the rate of metabolism of 2,4-dichlorophenoxyacetic acid and chlorosulfuron in plants*: Fiziologiya Rastenii, **1991**, 38, p. 290-296.
- 136) Herrmann M; Kotzais D; Korte F; *Photochemical behaviour of Chlorosulfuron in water in absorbed phase*: Chemosphere, **1985**, 14, p. 3-8.
- 137) Kotoula-Syka E; Eleftherohorinos IG; Gagianas AA; Sficas AG; *Persistence of preemergence applications of chlorosulfuron, Metasulfuron, Triasuluron, and Tribenuron in Three Soils in Greece*: Weed Sci., **1993**, 41, p. 246-250.
- 138) Walker A; Cotterill EG; Welch SJ; *Adsorption and degradation of Chlorosulfuron and Metasulfuron-methyl in soils from different depths*: Weed Res., **1989**, 29, p. 281-287.
- 139) Hemmamda S; Calmon M; Calmon JP; *Kinetics and Hydrolysis Mechanism of Chlorosulfuron and Metasulfuron-Methyl*: Pestic. Sci., **1994**, 40, p. 71-76.
- 140) Sabadie J; *Degradation du Chlorsulfuron et du Metasulfuron methyle en presence d'acides humiques*: Weed Research, **1993**, 33, p. .
- 141) Sabadie J; *Reactivite de l'herbicide chlorosulfuron; synthese et structure de ses produits de degradation*: Weed Res., **1992**, 32, p. 137-142.
- 142) Sabharwal S; Kishore K; Moorthy PN; *Pulse radiolysis of Oxidation reactions of Sulphacetamide in Aqueous Solutions*: Radiat. Phys. Chem., **1994**, 44, p. 499-506.
- 143) DeLaat J; Chramosta N; Dore M; Suty J; Povillot M; *Rate constants for reactions of hydroxyl radicals with some degradation by products of atrazine by O₃ or O₃/H₂O₂*: Environ. Tech., **1994**, 15, p. 419-28.

- 144) DeLaat J; Lebarbier R; Chramosta N; Dore M; *Reactivity of 2-chloro-2-methoxyl and methyl thio s-triazine towards hydroxyl radicals.*: J. Eur. Hydrol., **1994**, 25, p. 185-198.
- 145) Quirke JME *1,3,5-Triazines*; in Comprehensive Heterocyclic Chemistry. Bulton, McKillop, Ed. p 457
- 146) Marek LJ; Koskinen WC; *LC/MS Analysis of 4-Methoxy-6-methyl-1,3,5-triazin-2-yl Conataning Solfonurea Herbicides in Soil*: J.Agric. Food Chem., **1996**, 44, p. 3878-3881.
- 147) Slates RV, Watson R; *Chlorosulfuron: Analytical methods for pesticides and plant growth regulators*, **1988**, 16, p. 53-67.
- 148) Huie RE; Clifton LC; Neta P; *Electron transfer reaction rates and equilibria of the carbonate and sulfate radical anions.*: Radiat. Phys. Chem., **1991**, 38, p. 477.
- 149) Madden KP; *NDRL Radiation: Chemistry Data Center!*, <http://allen.rad.nd.edu>; Madden KP, Ed.; University of Notre Dame: Notre Dame, 1996.
- 150) Phillips GO; Power DM; Sewart MCG; *Effects of Gamma irradiation on Sulphonamides*: Radiat. Res., **1973**, 53, p. 204-215.
- 151) Kidd H; David JR; *Dichlorophen*: in the Agrochemical Handbook; 3rd ed.; Royal Society of Chemistry: Cambridge, 1991.
- 152) Mansfield E; Richards C; *Phototransformation of Dichlorophen in Aqueous Phase*: Pestic. Sci, **1996**, 48, p. 73-76.
- 153) Evans JC; Rowlands CC; Turkson LA; MD, B.; *Radicals formed by ultraviolet irradiation of substituted 4-Chlorophenols*: J. Chem. Soc., Faraday Trans 1, **1988**, 84, p. 3249-3255.
- 154) Grabner G; Richard C; Kohler G; *Formation and reactivity of 4-oxocyclohexa-2,5-dienylidene in the photolysis of 4-chlorophenol in aqueous solution at ambient temperature*: J. Am. Chem. Soc., **1994**, 116, p. 11470-11480.
- 155) Ashton L; Buxton GV; Stuart CR; *Temperature dependence of the rate of reaction of OH with some Aromatic Compounds in Aqueous Solutions*: J. Chem. Soc. Faraday Trans., **1995**, 91, p. 1631-1633.
- 156) Stafford U; Gray KA; Kamat PV; *Radiolytic and TiO₂ assisted photocatalytic degradation of 4-chlorophenol. A Comparative study*: J. Phys. Chem., **1994**, 98, p. 6343-51.
- 157) Mohan H; Mudaliar M; Arauindakumar CT; Rao BSM; Mittal JP; *Studies on structure-reactivity in the reaction of hydroxyl radicals with substituted halobenzene in aqueous solution.*: J. Chem. Soc. Perkins Trans. 2, **1991**, p. 1387-92.
- 158) Ye M; Schuler RH; *Determination of oxidation products in radiolysis of halophenol with pulse radiolysis, HPLC and ion chromatography.*: J. Liq. Chromatog., **1990**, 13, p. 3369-87.

- 159) Williams DH; Fleming I; *Spectroscopic methods in organic chemistry*; 4th ed.; McGraw-Hill: London, 1989.
- 160) Alfassi ZB; Huie RE; Neta P; Shoute LCT; *Temperature Dependence of the rate constants for reaction of Inorganic radicals with organic reductants*: J. Phys. Chem., **1994**, *94*, p. 8800-8805.
- 161) Lichtscheidl J; Getoff N; *Radiolysis of halogenated compounds in aqueous solutions I. Conductrometric pulse radiolysis and steady state studies of the reaction of the hydrated electron*: Int. J. Radiat. Phys. Chem., **1976**, *8*, p. 661-5.
- 162) Ye M; *Ph.D Thesis*; Ye M, Ed.; University of Notre Dame: Notre Dame, 1989, pp 196.
- 163) Mohan H; Midalia M; Rao BSM; Mittal JP; *Reaction of the hydrated electron and alcohol radicals with halogenated aromatic compounds: A pulse radiolysis study*: Radiat. Phys. Chem., **1992**, *40*, p. 513.
- 164) Kidd H; David JR; *Cyromazine*: in the Agrochemical Handbook; Royal society of Chemistry: Cambridge, 1991; Voi. 3rd Edition.
- 165) Lim LO; Scherer SJ; Shuler KD; Toth JP; *Diposition of Cyromazine in plants under environmental conditions*: J. Agric. Food Chem., **1990**, *38*, p. 860-864.
- 166) Melnick RL; Boorman GA; Haseman JK; Montali RJ; Huff J; *Urolithiasis and bladder carcinogenicity of melamine in rodents*: Toxicol. Appl. Pharmacol., **1984**, *72*, p. 292-303.
- 167) Cook AM; Grossenbacher H; Hutter R; *Bacterial degradation of N-cyclopropylmelamine*: Biochem. J., **1984**, *222*, p. 315-320.
- 168) Scasny M, Private Communication. 1997
- 169) Rabani J; Pick M; Simic M; *Pulse radiolysis of cyclopentane in aqueous solution*: J. Phys. Chem., **1974**, *78*, p. 1049-1051.
- 170) Rudakov ES; Volkova LK; Tret'yako VP; *Low selectivity of the reaction of the hydroxyl radical with nucleic and bases and the related compounds in gamma irradiated aqueous solution*: React. Kinet. Catal. Lett., **1981**, *16*, p. 333-7.
- 171) Mezyk S; *Arrhenius parameter determination for the reaction of the oxide radical, hydrated electron and hydroxyl radical with iodate in aqueous solution*: J. Chem Soc. Faraday Trans., **1996**, *92*, p. 2251-2254.
- 172) Soeylemez T; Schuler RH; *Radiolysis of aqueous solutions of cyclopentane and cyclopentene*: J. Phys. Chem., **1974**, *78*, p. 1052-62.
- 173) Fang X; Pan X; Rahmann A; Schuchmann HP; von Sonntag C; *Reversibility in the reaction of cyclohexadienyl radicals with oxygen in aqueous solution*; Chem. Eur. J., **1995**, *1*, p. 125.
- 174) Kidd H; David JR; *Dimethrimiol*: in the Agrochemicals Handbook; Royal society of Chemistry: Cambridge, 1991; Vol. 3rd Edition.

- 175) Cavell BD; Pollard SJ; Wells CH; *Kinetic and Energetic Aspects of the Photodimerisation of Some Systemic Pyrimidine Fungicides*: J. Chem. Soc. Perkins Trans. II, **1977**, p. 216-221.
- 176) Anthony MC; Waltz WL; Mezey PG; *Ab initio SCF MO calculations on the reaction of OH radicals with pyridine and pyridinium ion*: Can J Chem, **1981**, 60, p. 813-819.
- 177) Masuda T; Shinohura H; Kondo M; *Reactions of hydroxyl radicals with nucleic acid bases and the related compounds in gamma irradiated aqueous solution*. J. Radiat. Res., **1975**, 16, p. 153-161.
- 178) Roder M; Wojnarovits L; Foldiak G; *Pulse Radiolysis of Aqueous solutions of aromatic hydrocarbons in the presence of oxygen*: Radiat. Phys. Chem., **1990**, 36, p. 175-176.
- 179) Christensen H; *Intermediates produced from one electron reduction of nitrogen heterocyclic compounds in solution*: Int. J Radiat. Phys. Chem., **1972**, 4, p. 311-33.
- 180) Moorthy PN; Hayon E; *Intermediates produced from the one-electron reduction of nitrogen heterocyclic compounds in solution.*: J. Phys. Chem., **1974**, 75, p. 2615-20.
- 181) Anbar M; Alfassi ZB; Breyman-Reisler H; *Hydrated electron reactions in view of their temperature dependence*: J. Am. Chem. Soc., **1967**, 89, p. 1263-4.
- 182) Kidd H; David JR; *Hexazinone*: in the Agrochemical Handbook; Royal society of Chemistry: Cambridge, 1991; Vol. 3rd Edition.
- 183) Thompson DG; MacDonald LM; Staznik B; *Persistence of Hexazinone and Metasulfuron-methyl in a mixed-wood/ boreal forest lake*: J. Agric. Food Chem., **1992**, 40, p. 1444-1449.
- 184) Bouchard DC; Lavy TL; *HPLC determination of Hexazinone residues in soils and water*: J. of Chromatography, **1983**, 270, p. 396-401.
- 185) Campbell RA; *Silvicultural herbicides in Canada: registration status and research trends.*: For. Chron., **1991**, 67, p. 520-527.
- 186) US Department of Agriculture Forest Services; *Pesticide background statement*; Herbicides ed.; United States Department of Agriculture.; 1984; Vol. 1.
- 187) Sidhu SS; Feng JC; *Hexazinone and its metabolites in Boreal Forest Vegetation*: Weed Sci., **1993**, 41, p. 281-287.
- 188) Fischer JB; Michael JL; *Thermospray ionisation liquid chromatography-mass spectrometry and chemical ionisation gas chromatography-mass spectrometry of Hexazinone metabolites in soil and vegetation extracts*: J. Chrom. A, **1995**, 704, p. 131-139.
- 189) Sauer MC; Mani I; *Pulsed Radiolysis of Liquid cyclohexane and n-Hexane. I. Yield of Hydrogen atoms measured by the cyclohexadienyl radical absorption in solution containing benzene. II. Absorption spectra and reactions of cyclohexyl and Hexyl radicals*: J. Phys. Chem., **1968**, 72, p. 3856-3864.

- 190) Mabury SA; Crosby DG; *Pesticide Reactivity toward hydroxyl and its relationship to field persistence*: J. Agric. Food Chem., **1996**, *44*, p. 1920-1924.
- 191) Vinchurkar MS; Rao BSM; Mohan H; Mittal JP; Schmidt KH; Jonah CD; *Absorption spectra of isomeric OH adducts of 1,3,4-Triethylxanthine*: J. Phys. Chem., **1997**, *101*, p. 2953-2959.
- 192) Greenstock GL; Nume M; Hunt JW; *Pulse radiolysis studies of reaction of primary species in water with nucleic acid and derivatives*. Adv. Chem. Ser., **1968**, *81*, p. 397-417.
- 193) Hart EJ; Gordon S; Thomas JK; *Rate constant of hydrated electron with organic compounds*: J. Phys. Chem., **1964**, *68*, p. 1271-1274.
- 194) Hayon H; *Optical absorption spectra of Ketyl radicals and radical anions of some pyrimidines*: J. Chem. Phys., **1969**, *51*, p. 4881-4892.
- 195) Kidd H; David JR; *MCPA*: in the Agrochemical Handbook; Royal society of Chemistry: Cambridge, 1991; Vol. 3rd Edition.
- 196) Smith AE; Mortensen K; Aubin AJ; Molloy MM; *Degradation of MCPA, 2,4-D, and Other Phenoxyalkanoic Acid Herbicides Using an Isolated Soil Bacterium*: J. Agric Food Chem., **1994**, *42*, p. 401-405.
- 197) Vink M; Van der Poll JM; *Gas Chromatographic determination of acid herbicides in surface water samples with electron-capture detection and mass spectrometric confirmation*: Journal of Chromatography A, **1996**, *733*, p. 361-366.
- 198) US Environmental Protection Agency Health Advisory, Office of Drinking Water, 1987.
- 199) Agriculture Research Service: US Department of Agriculture; *MCPA*; <http://www.arsusda.gov/rsml/ppdb3/MCPA>, 1997.
- 200) Hasegawa K; Neta P; *Rate Constants and Mechanisms of reaction of Cl₂⁻ Radicals*: J. Phys. Chem., **1978**, *82*, p. 854-857.
- 201) Madhavan V; Levanon H; Neta P; *Decarboxylation by SO₄⁻ Radical*: Radiation Res., **1978**, *76*, p. 15-22.
- 202) Kochler G; Solar S; Gettoff N; Notzworth AR; Schaffner K; J. Photochem., **1985**, *28*, p. 383-91.
- 203) Sauer MC; Ward B; *Reaction of hydrogen atoms with benzene and toluene studied by pulse radiolysis: Reaction rate constants and transient spectra in the gas phase and aqueous solution.*: J. Phys. Chem., **1967**, *71*, p. 3971-83.
- 204) Lichtscheidl J; Gettoff N; *Reaktion der H-Radikale mit aromatischen Halogenverbindungen in wässriger Lösung*: Monatsh. Chem., **1979**, *110*, p. 1377-86.
- 205) Neta P; Fessenden RW; Schuler RH; *An electron spin resonance study of the rate constants for reaction of hydrogen atoms with organic compounds in aqueous solution*: J. Phys. Chem., **1971**, *75*, p. 1654-1666.

- 206) Kidd H; David JR; *Acifluorfen*: in the Agrochemical Handbook; Royal Society of Chemistry: Cambridge, 1991; Vol. 3rd Edition.
- 207) Gennari M; Negre M; Ambrosoli R; Andreoni V; Vivventi M; A, A.; *Anaerobic Degradation of Acifluorfen by Different Enrichment Cultures*: J. Agric. Food Chem., **1994**, *42*, p. 1232-1236.
- 208) Lee HJ; Duke SO; *Protoporphyrinogen IX-oxidising Activities Involved in the mode of action of peroxidizing Herbicides*: J. Agric. Food. Chem., **1994**, *42*, p. 26100-2618.
- 209) Bridger GM; Yang W; Falk DE; BD, M.; *Cold acclimation Increases Tolerances of activated oxygen in winter cereals*: J. Plant Physiol., **1994**, *144*, p. 235-240.
- 210) Ritter RL; Coble HD; *Influence of temperature and relative humidity on the activity of Acifluorfen*: Weed Sci., **1981**, *29*, p. 480-485.
- 211) Ritter RL, Coble H; *Penetration, translocation, and metabolism of Acifluorfen in soybean, common ragweed, and common cocklebur*: Weed Sci., **1981**, *29*, p. 474-80.
- 212) US Environmental Protection Agency; *Acifluorfen Health Advisory, Draft Report*: Office of Drinking Water, **1987**.
- 213) Cercek B; Ebert M; *Activation energies for reactions of the hydrated electron.*: Adv. Chem. Ser., **1968**, *81*, p. 210-221.
- 214) Zemel H; Fessenden RW; *The Mechanism of reaction of SO_4^{--} with some Derivatives of Benzoic Acid*: J. Phys. Chem., **1978**, *82*, p. 2670-2676.
- 215) Neta P; Simic MG; Hoffman MZ; *Pulse radiolysis and esr of nitroaromatic radical anions*: J. Phys. Chem., **1976**, *80*, p. 2018-2023.
- 216) Perris SA; Freeman GR; *Solvent structure effects on solvated electron reaction with ions in 2-butanol/water mixed solvents*: Can J Chem, **1991**, *69*, p. 884-92.